

Contrails

FOREWORD

This report presents the results of one segment of an experimental program for the investigation of hypersonic flow separation and control characteristics being conducted by the Research Department of Grumman Aircraft Engineering Corporation, Bethpage, N. Y. Mr. Donald E. Hoak of the Flight Dynamics Laboratory, Research and Technology Division, located at Wright-Patterson Air Force Base, Ohio, is the Air Force Project Engineer for the program, which is being supported primarily under Contract AF 33(616)-8130, Air Force Task 821902.

The experimental data obtained (pressure distributions, aerodynamic heating rates, and six-component force data) are extensive and must be presented in a series of data reports, of which this is one. These data reports are presented without analysis for the purpose of disseminating all the experimental information as rapidly as possible.

The author wishes to express his appreciation to the staff of the von Karman Facility, ARO Inc., for their helpfulness in conducting the tests and particularly to Messrs. Burchfield and Deitering for providing the machine plotted graphs of the experimental data included in this report. The tabulated data, not included herein, are available to qualified Air Force requestors as an Appendix to this report. These Appendices can be obtained on loan from the Flight Dynamics Laboratory (Research and Technology Division, Air Force Systems Command, Wright-Patterson Air Force Base, Ohio).

Contracts

Controls

ABSTRACT

Heat transfer data were obtained at Mach 8 for a winged re-entry configuration with several types of aerodynamic controls. The basic model consisted of a clipped delta wing with an overslung cone-cylinder body. Most of the tests were conducted with partial span trailing edge flaps. The effects of tip fins, a hemisphere-cylinder body, a full span trailing edge flap, and a full span, plug-type, trailing edge spoiler were also investigated. The partial span flap deflection were varied between + 39 degrees in an angle of attack range of ± 20 degrees. Selected configurations were used to examine the angle of attack ranges of -30 degrees to -50 degrees and + 30 degrees to + 50 degrees. The major portion of the program was conducted at a unit test section Reynolds number of $3.3 \times 10^6/\text{ft}$ with limited comparative testing being done at a unit test section Reynolds number of $1.1 \times 10^6/\text{ft}$.

This report has been reviewed and is approved.

for C.R. Bryan
for W. A. SLOAN, Jr.
Colonel, USAF
Chief, Flight Control Division
AF Flight Dynamics Laboratory

Controls

TABLE OF CONTENTS

<u>Item</u>	<u>Page</u>
Introduction	1
Description of Models	2
General	2
Controls and Sign Conventions	2
Model Designation	3
Model Construction and Instrumentation	5
Experimental Data	7
Description of Wind Tunnel and Test Conditions	7
Data Reduction and Accuracy	8
Results and Discussion	10
References	12

Contrails

LIST OF ILLUSTRATIONS

<u>Figure</u>		<u>Page</u>
1	Model Illustration and Photographs	
a)	General Outline of Models and Remarks for Over-all Program	18
b)	Configuration I - Basic Wing-Body	19
c)	Configuration IV - Basic Wing-Body + Tip Fins (for dimensions see Figure 1b)	20
d)	Configuration VII - Wing - Blunt Body + Full Span Plug Spoiler (for dimensions see Figure 1b)	21
e)	Configuration VIII - Wing - Blunt Body + Full Span Plug Spoiler + Tip Fins (for dimensions see Figures 1b, 1c, 1d)	22
f)	Configuration IX - Wing - Blunt Body (for dimensions see Figures 1b, 1d)	23
g)	Configuration X - Wing - Blunt Body + Full Span Flap (showing center flap deflected +20°) (for dimensions see Figures 1b, 1d)	24
h)	Thermocouple Location and Model Coordinate System	25
i)	Top View Photograph - Configuration I	26
j)	Bottom View Photograph - Configuration I	27
k)	Top View Photograph - Configuration IV	28
l)	Rear View Photograph - Configuration IV, Mounted on Actuator Housing in the 50" Hypersonic Mach 8 Wind Tunnel	29
m)	Photograph - Actuator Housing Components (1) Actuator Housing Cover, (2) Actuator Assembly, (3) Water Jacket, (4) Actuator Housing	30
n)	Photograph - Actuator Assembly (1) Electric Motors, (2) Potentiometers, (3) Lead Screws, (4) Control Rods (5) Water Cooled Bulkheads	31
2	Sign Convention for Model Angles and Control Deflection Angles	32
3	Configuration I, $\alpha = 0$	
a)	$Nu/\sqrt{Re_x}$ vs. Y' $\delta_2 = \delta_3 = 0$ lower surface	33
b)	$Nu/\sqrt{Re_x}$ vs. Y' upper surface	
c)	$Nu/\sqrt{Re_x}$ vs. X' lower surface	34
d)	$Nu/\sqrt{Re_x}$ vs. X' upper surface	
e)	$Nu/\sqrt{Re_x}$ vs. Y' $\delta_2 = \delta_3 = +10$ lower surface.....	35
f)	$Nu/\sqrt{Re_x}$ vs. X' lower surface.....	36
g)	$Nu/\sqrt{Re_x}$ vs. Y' upper surface.....	37
h)	$Nu/\sqrt{Re_x}$ vs. X' upper surface.....	38
i)	$Nu/\sqrt{Re_x}$ vs. Y' $\delta_2 = \delta_3 = +20$ lower surface.....	39
j)	$Nu/\sqrt{Re_x}$ vs. X' lower surface.....	40
k)	$Nu/\sqrt{Re_x}$ vs. Y' upper surface.....	41
l)	$Nu/\sqrt{Re_x}$ vs. X' upper surface.....	42

Controls

<u>Figure</u>			<u>Page</u>
3	Configuration I, $\alpha = 0$ (Cont'd)		
m)	$Nu/\sqrt{Re_x}$ vs. Y'	$\delta_2 = \delta_3 = +30$	lower surface..... 43
n)	$Nu/\sqrt{Re_x}$ vs. X'		lower surface..... 44
o)	$Nu/\sqrt{Re_x}$ vs. Y'		upper surface..... 45
p)	$Nu/\sqrt{Re_x}$ vs. X'		upper surface..... 46
q)	$Nu/\sqrt{Re_x}$ vs. Y'	$\delta_2 = \delta_3 = +39$	lower surface..... 47
r)	$Nu/\sqrt{Re_x}$ vs. X'		lower surface..... 48
s)	$Nu/\sqrt{Re_x}$ vs. Y'		upper surface..... 49
t)	$Nu/\sqrt{Re_x}$ vs. X'		upper surface..... 50
4	Configuration I, $\alpha = 0$		
a)	$Nu/\sqrt{Re_x}$ vs. Y'	$\delta_2 = \delta_3 = -10$	upper surface..... 51
b)	$Nu/\sqrt{Re_x}$ vs. X'		upper surface..... 52
c)	$Nu/\sqrt{Re_x}$ vs. Y'	$\delta_2 = \delta_3 = -20$	upper surface..... 53
d)	$Nu/\sqrt{Re_x}$ vs. X'		upper surface..... 54
e)	$Nu/\sqrt{Re_x}$ vs. Y'	$\delta_2 = \delta_3 = -30$	upper surface..... 55
f)	$Nu/\sqrt{Re_x}$ vs. X'		upper surface..... 56
g)	$Nu/\sqrt{Re_x}$ vs. Y'	$\delta_2 = \delta_3 = -39$	upper surface..... 57
h)	$Nu/\sqrt{Re_x}$ vs. X'		upper surface..... 58
i)	$Nu/\sqrt{Re_x}$ vs. Y'	$\delta_2 = \delta_3 = -10$	lower surface..... 59
j)	$Nu/\sqrt{Re_x}$ vs. Y'	$\delta_2 = \delta_3 = -20$	lower surface
k)	$Nu/\sqrt{Re_x}$ vs. Y'	$\delta_2 = \delta_3 = -30$	lower surface
l)	$Nu/\sqrt{Re_x}$ vs. Y'	$\delta_2 = \delta_3 = -39$	lower surface
m)	$Nu/\sqrt{Re_x}$ vs. X'	$\delta_2 = \delta_3 = -10$	lower surface 60
n)	$Nu/\sqrt{Re_x}$ vs. X'	$\delta_2 = \delta_3 = -20$	lower surface
o)	$Nu/\sqrt{Re_x}$ vs. X'	$\delta_2 = \delta_3 = -30$	lower surface
p)	$Nu/\sqrt{Re_x}$ vs. X'	$\delta_2 = \delta_3 = -39$	lower surface
5	Configuration I, $\alpha = +10$		
a)	$Nu/\sqrt{Re_x}$ vs. Y'	$\delta_2 = \delta_3 = 0$	upper surface..... 61
b)	$Nu/\sqrt{Re_x}$ vs. Y'		lower surface
c)	$Nu/\sqrt{Re_x}$ vs. X'		upper surface..... 62
d)	$Nu/\sqrt{Re_x}$ vs. X'		lower surface
e)	$Nu/\sqrt{Re_x}$ vs. Y'	$\delta_2 = \delta_3 = +10$	lower surface..... 63
f)	$Nu/\sqrt{Re_x}$ vs. X'		lower surface..... 64
g)	$Nu/\sqrt{Re_x}$ vs. Y'		upper surface..... 65
h)	$Nu/\sqrt{Re_x}$ vs. X'		upper surface
i)	$Nu/\sqrt{Re_x}$ vs. Y'	$\delta_2 = \delta_3 = +20$	lower surface..... 66
j)	$Nu/\sqrt{Re_x}$ vs. X'		lower surface..... 67

Controls

Figure

Page

5	Configuration I, $\alpha = +10$ (Cont'd)		
	k) $Nu/\sqrt{Re_x}$ vs. Y'	$\delta_2 = \delta_3 = +30$	lower surface..... 68
	l) $Nu/\sqrt{Re_x}$ vs. X'		lower surface..... 69
	m) $Nu/\sqrt{Re_x}$ vs. Y'	$\delta_2 = \delta_3 = +39$	lower surface..... 70
	n) $Nu/\sqrt{Re_x}$ vs. X'		lower surface..... 71
	o) $Nu/\sqrt{Re_x}$ vs. Y'	$\delta_2 = \delta_3 = +20$	upper surface..... 72
	p) $Nu/\sqrt{Re_x}$ vs. Y'	$\delta_2 = \delta_3 = +30$	upper surface
	q) $Nu/\sqrt{Re_x}$ vs. Y'	$\delta_2 = \delta_3 = +39$	upper surface
	r) $Nu/\sqrt{Re_x}$ vs. X'	$\delta_2 = \delta_3 = +20$	upper surface..... 73
	s) $Nu/\sqrt{Re_x}$ vs. X'	$\delta_2 = \delta_3 = +30$	upper surface
	t) $Nu/\sqrt{Re_x}$ vs. X'	$\delta_2 = \delta_3 = +39$	upper surface
6	Configuration I, $\alpha = +10$		
	a) $Nu/\sqrt{Re_x}$ vs. Y'	$\delta_2 = \delta_3 = -10$	lower surface..... 74
	b) $Nu/\sqrt{Re_x}$ vs. X'		lower surface
	c) $Nu/\sqrt{Re_x}$ vs. Y'		upper surface..... 75
	d) $Nu/\sqrt{Re_x}$ vs. X'		upper surface
	e) $Nu/\sqrt{Re_x}$ vs. Y'	$\delta_2 = \delta_3 = -20$	lower surface..... 76
	f) $Nu/\sqrt{Re_x}$ vs. X'		lower surface
	g) $Nu/\sqrt{Re_x}$ vs. Y'		upper surface..... 77
	h) $Nu/\sqrt{Re_x}$ vs. X'		upper surface..... 78
	i) $Nu/\sqrt{Re_x}$ vs. Y'	$\delta_2 = \delta_3 = -30$	lower surface..... 79
	j) $Nu/\sqrt{Re_x}$ vs. X'		lower surface
	k) $Nu/\sqrt{Re_x}$ vs. Y'		upper surface..... 80
	l) $Nu/\sqrt{Re_x}$ vs. X'		upper surface..... 81
	m) $Nu/\sqrt{Re_x}$ vs. Y'	$\delta_2 = \delta_3 = -39$	lower surface..... 82
	n) $Nu/\sqrt{Re_x}$ vs. X'		lower surface
	o) $Nu/\sqrt{Re_x}$ vs. Y'		upper surface..... 83
	p) $Nu/\sqrt{Re_x}$ vs. X'		upper surface..... 84
7	Configuration I, $\alpha = +20$		
	a) $Nu/\sqrt{Re_x}$ vs. Y'	$\delta_2 = \delta_3 = 0$	lower surface 85
	b) $Nu/\sqrt{Re_x}$ vs. X'		lower surface 86
	c) $Nu/\sqrt{Re_x}$ vs. Y'	$\delta_2 = \delta_3 = +10$	lower surface 87
	d) $Nu/\sqrt{Re_x}$ vs. X'		lower surface 88
	e) $Nu/\sqrt{Re_x}$ vs. Y'	$\delta_2 = \delta_3 = +20$	lower surface 89
	f) $Nu/\sqrt{Re_x}$ vs. X'		lower surface
	g) $Nu/\sqrt{Re_x}$ vs. Y'	$\delta_2 = \delta_3 = +30$	lower surface 90
	h) $Nu/\sqrt{Re_x}$ vs. X'		lower surface 91
	i) $Nu/\sqrt{Re_x}$ vs. Y'	$\delta_2 = \delta_3 = +39$	lower surface 92

Contrails

Figure

Page

7	Configuration I, $\alpha = +20$ (Cont'd)		
j)	$Nu/\sqrt{Re_x}$ vs. X'	$\delta_2 = \delta_3 = +39$	lower surface..... 93
k)	$Nu/\sqrt{Re_x}$ vs. Y'	$\delta_2 = \delta_3 = 0$	upper surface..... 94
l)	$Nu/\sqrt{Re_x}$ vs. Y'	$\delta_2 = \delta_3 = +10$	upper surface
m)	$Nu/\sqrt{Re_x}$ vs. Y'	$\delta_2 = \delta_3 = +20$	upper surface
n)	$Nu/\sqrt{Re_x}$ vs. Y'	$\delta_2 = \delta_3 = +30$	upper surface
o)	$Nu/\sqrt{Re_x}$ vs. Y'	$\delta_2 = \delta_3 = +39$	upper surface
p)	$Nu/\sqrt{Re_x}$ vs. X'	$\delta_2 = \delta_3 = 0$	upper surface..... 95
q)	$Nu/\sqrt{Re_x}$ vs. X'	$\delta_2 = \delta_3 = +10$	upper surface
r)	$Nu/\sqrt{Re_x}$ vs. X'	$\delta_2 = \delta_3 = +20$	upper surface
s)	$Nu/\sqrt{Re_x}$ vs. X'	$\delta_2 = \delta_3 = +30$	upper surface
t)	$Nu/\sqrt{Re_x}$ vs. X'	$\delta_2 = \delta_3 = +39$	upper surface
8	Configuration I, $\alpha = +20$		
a)	$Nu/\sqrt{Re_x}$ vs. Y'	$\delta_2 = \delta_3 = -10$	lower surface..... 96
b)	$Nu/\sqrt{Re_x}$ vs. X'		lower surface
c)	$Nu/\sqrt{Re_x}$ vs. Y'	$\delta_2 = \delta_3 = -20$	lower surface..... 97
d)	$Nu/\sqrt{Re_x}$ vs. X'		lower surface
e)	$Nu/\sqrt{Re_x}$ vs. Y'	$\delta_2 = \delta_3 = -30$	lower surface..... 98
f)	$Nu/\sqrt{Re_x}$ vs. X'		lower surface
g)	$Nu/\sqrt{Re_x}$ vs. Y'	$\delta_2 = \delta_3 = -39$	lower surface..... 99
h)	$Nu/\sqrt{Re_x}$ vs. X'		lower surface
i)	$Nu/\sqrt{Re_x}$ vs. Y'	$\delta_2 = \delta_3 = -10$	upper surface..... 100
j)	$Nu/\sqrt{Re_x}$ vs. Y'	$\delta_2 = \delta_3 = -20$	upper surface
k)	$Nu/\sqrt{Re_x}$ vs. X'	$\delta_2 = \delta_3 = -10$	upper surface
l)	$Nu/\sqrt{Re_x}$ vs. X'	$\delta_2 = \delta_3 = -20$	upper surface
m)	$Nu/\sqrt{Re_x}$ vs. Y'	$\delta_2 = \delta_3 = -30$	upper surface..... 101
n)	$Nu/\sqrt{Re_x}$ vs. X'		upper surface..... 102
o)	$Nu/\sqrt{Re_x}$ vs. Y'	$\delta_2 = \delta_3 = -39$	upper surface..... 103
p)	$Nu/\sqrt{Re_x}$ vs. X'		upper surface..... 104
9	Configuration I, $\delta_2 = \delta_3 = 0$		
a)	$Nu/\sqrt{Re_x}$ vs. Y'	$\alpha = +30$	lower surface..... 105
b)	$Nu/\sqrt{Re_x}$ vs. X'		lower surface..... 106
c)	$Nu/\sqrt{Re_x}$ vs. Y'	$\alpha = +35$	lower surface..... 107
d)	$Nu/\sqrt{Re_x}$ vs. X'		lower surface..... 108
e)	$Nu/\sqrt{Re_x}$ vs. Y'	$\alpha = +40$	lower surface..... 109
f)	$Nu/\sqrt{Re_x}$ vs. X'		lower surface..... 110
g)	$Nu/\sqrt{Re_x}$ vs. Y'	$\alpha = +45$	lower surface..... 111
h)	$Nu/\sqrt{Re_x}$ vs. X'		lower surface..... 112

Controls

Figure

Page

9	Configuration I, $\delta_2 = \delta_3 = 0$ (Cont'd)		
	i) $Nu/\sqrt{Re_x}$ vs. Y'	$\alpha = +50$	lower surface..... 113
	j) $Nu/\sqrt{Re_x}$ vs. X'		lower surface..... 114
	k) $Nu/\sqrt{Re_x}$ vs. Y'	$\alpha = +30$	upper surface..... 115
	l) $Nu/\sqrt{Re_x}$ vs. Y'	$\alpha = +35$	upper surface
	m) $Nu/\sqrt{Re_x}$ vs. Y'	$\alpha = +40$	upper surface
	n) $Nu/\sqrt{Re_x}$ vs. Y'	$\alpha = +45$	upper surface
	o) $Nu/\sqrt{Re_x}$ vs. Y'	$\alpha = +50$	upper surface
	p) $Nu/\sqrt{Re_x}$ vs. X'	$\alpha = +30$	upper surface..... 116
	q) $Nu/\sqrt{Re_x}$ vs. X'	$\alpha = +35$	upper surface
	r) $Nu/\sqrt{Re_x}$ vs. X'	$\alpha = +40$	upper surface
	s) $Nu/\sqrt{Re_x}$ vs. X'	$\alpha = +45$	upper surface
	t) $Nu/\sqrt{Re_x}$ vs. X'	$\alpha = +50$	upper surface
10	Configuration I, $\alpha = -10$		
	a) $Nu/\sqrt{Re_x}$ vs. Y'	$\delta_2 = \delta_3 = 0$	lower surface 117
	b) $Nu/\sqrt{Re_x}$ vs. X'		lower surface
	c) $Nu/\sqrt{Re_x}$ vs. Y'		upper surface 118
	d) $Nu/\sqrt{Re_x}$ vs. X'		upper surface 119
	e) $Nu/\sqrt{Re_x}$ vs. Y'	$\delta_2 = \delta_3 = +10$	lower surface 120
	f) $Nu/\sqrt{Re_x}$ vs. X'		lower surface
	g) $Nu/\sqrt{Re_x}$ vs. Y'		upper surface 121
	h) $Nu/\sqrt{Re_x}$ vs. X'		upper surface 122
	i) $Nu/\sqrt{Re_x}$ vs. Y'	$\delta_2 = \delta_3 = +20$	lower surface 123
	j) $Nu/\sqrt{Re_x}$ vs. X'		lower surface 124
	k) $Nu/\sqrt{Re_x}$ vs. Y'		upper surface 125
	l) $Nu/\sqrt{Re_x}$ vs. X'		upper surface 126
	m) $Nu/\sqrt{Re_x}$ vs. Y'	$\delta_2 = \delta_3 = +30$	lower surface 127
	n) $Nu/\sqrt{Re_x}$ vs. X'		lower surface 128
	o) $Nu/\sqrt{Re_x}$ vs. Y'		upper surface 129
	p) $Nu/\sqrt{Re_x}$ vs. X'		upper surface 130
	q) $Nu/\sqrt{Re_x}$ vs. Y'	$\delta_2 = \delta_3 = +39$	lower surface 131
	r) $Nu/\sqrt{Re_x}$ vs. X'		lower surface 132
	s) $Nu/\sqrt{Re_x}$ vs. Y'		upper surface 133
	t) $Nu/\sqrt{Re_x}$ vs. X'		upper surface 134
11	Configuration I, $\alpha = -10$		
	a) $Nu/\sqrt{Re_x}$ vs. Y'	$\delta_2 = \delta_3 = -10$	lower surface 135
	b) $Nu/\sqrt{Re_x}$ vs. Y'	$\delta_2 = \delta_3 = -20$	lower surface
	c) $Nu/\sqrt{Re_x}$ vs. Y'	$\delta_2 = \delta_3 = -30$	lower surface

Controls

<u>Figure</u>			<u>Page</u>
11	Configuration I, $\alpha = -10$ (Cont'd)		
d)	$Nu/\sqrt{Re_x}$ vs. Y'	$\delta_2 = \delta_3 = -39$	lower surface..... 135
e)	$Nu/\sqrt{Re_x}$ vs. X'	$\delta_2 = \delta_3 = -10$	lower surface..... 136
f)	$Nu/\sqrt{Re_x}$ vs. X'	$\delta_2 = \delta_3 = -20$	lower surface
g)	$Nu/\sqrt{Re_x}$ vs. X'	$\delta_2 = \delta_3 = -30$	lower surface
h)	$Nu/\sqrt{Re_x}$ vs. X'	$\delta_2 = \delta_3 = -39$	lower surface
i)	$Nu/\sqrt{Re_x}$ vs. Y'	$\delta_2 = \delta_3 = -10$	upper surface..... 137
j)	$Nu/\sqrt{Re_x}$ vs. X'		upper surface..... 138
k)	$Nu/\sqrt{Re_x}$ vs. Y'	$\delta_2 = \delta_3 = -20$	upper surface..... 139
l)	$Nu/\sqrt{Re_x}$ vs. X'		upper surface..... 140
m)	$Nu/\sqrt{Re_x}$ vs. Y'	$\delta_2 = \delta_3 = -30$	upper surface..... 141
n)	$Nu/\sqrt{Re_x}$ vs. X'		upper surface
o)	$Nu/\sqrt{Re_x}$ vs. Y'	$\delta_2 = \delta_3 = -39$	upper surface..... 142
p)	$Nu/\sqrt{Re_x}$ vs. X'		upper surface
12	Configuration I, $\alpha = -20$		
a)	$Nu/\sqrt{Re_x}$ vs. Y'	$\delta_2 = \delta_3 = 0$	lower surface..... 143
b)	$Nu/\sqrt{Re_x}$ vs. Y'	$\delta_2 = \delta_3 = +10$	lower surface
c)	$Nu/\sqrt{Re_x}$ vs. Y'	$\delta_2 = \delta_3 = +20$	lower surface
d)	$Nu/\sqrt{Re_x}$ vs. X'	$\delta_2 = \delta_3 = 0$	lower surface..... 144
e)	$Nu/\sqrt{Re_x}$ vs. X'	$\delta_2 = \delta_3 = +10$	lower surface
f)	$Nu/\sqrt{Re_x}$ vs. X'	$\delta_2 = \delta_3 = +20$	lower surface
g)	$Nu/\sqrt{Re_x}$ vs. Y'	$\delta_2 = \delta_3 = 0$	upper surface..... 145
h)	$Nu/\sqrt{Re_x}$ vs. X'		upper surface..... 146
i)	$Nu/\sqrt{Re_x}$ vs. Y'	$\delta_2 = \delta_3 = +10$	upper surface..... 147
j)	$Nu/\sqrt{Re_x}$ vs. X'		upper surface..... 148
k)	$Nu/\sqrt{Re_x}$ vs. Y'	$\delta_2 = \delta_3 = +20$	upper surface..... 149
l)	$Nu/\sqrt{Re_x}$ vs. X'		upper surface..... 150
m)	$Nu/\sqrt{Re_x}$ vs. Y'	$\delta_2 = \delta_3 = +30$	lower surface..... 151
n)	$Nu/\sqrt{Re_x}$ vs. X'		lower surface..... 152
o)	$Nu/\sqrt{Re_x}$ vs. Y'		upper surface..... 153
p)	$Nu/\sqrt{Re_x}$ vs. X'		upper surface..... 154
q)	$Nu/\sqrt{Re_x}$ vs. Y'	$\delta_2 = \delta_3 = +39$	lower surface..... 155
r)	$Nu/\sqrt{Re_x}$ vs. X'		lower surface..... 156
s)	$Nu/\sqrt{Re_x}$ vs. Y'		upper surface..... 157
t)	$Nu/\sqrt{Re_x}$ vs. X'		upper surface..... 158
13	Configuration I, $\alpha = -20$		
a)	$Nu/\sqrt{Re_x}$ vs. Y'	$\delta_2 = \delta_3 = -10$	lower surface..... 159
b)	$Nu/\sqrt{Re_x}$ vs. Y'	$\delta_2 = \delta_3 = -20$	lower surface

Contrails

<u>Figure</u>		<u>Page</u>
13	Configuration I, $\alpha = -20$ (Cont'd)	
c)	$Nu/\sqrt{Re_x}$ vs. Y'	$\delta_2 = \delta_3 = -30$ lower surface..... 159
d)	$Nu/\sqrt{Re_x}$ vs. Y'	$\delta_2 = \delta_3 = -39$ lower surface
e)	$Nu/\sqrt{Re_x}$ vs. X'	$\delta_2 = \delta_3 = -10$ lower surface..... 160
f)	$Nu/\sqrt{Re_x}$ vs. X'	$\delta_2 = \delta_3 = -20$ lower surface
g)	$Nu/\sqrt{Re_x}$ vs. X'	$\delta_2 = \delta_3 = -30$ lower surface
h)	$Nu/\sqrt{Re_x}$ vs. X'	$\delta_2 = \delta_3 = -39$ lower surface
i)	$Nu/\sqrt{Re_x}$ vs. Y'	$\delta_2 = \delta_3 = -10$ upper surface..... 161
j)	$Nu/\sqrt{Re_x}$ vs. X'	upper surface..... 162
k)	$Nu/\sqrt{Re_x}$ vs. Y'	$\delta_2 = \delta_3 = -20$ upper surface..... 163
l)	$Nu/\sqrt{Re_x}$ vs. X'	upper surface
m)	$Nu/\sqrt{Re_x}$ vs. Y'	$\delta_2 = \delta_3 = -30$ upper surface..... 164
n)	$Nu/\sqrt{Re_x}$ vs. X'	upper surface
o)	$Nu/\sqrt{Re_x}$ vs. Y'	$\delta_2 = \delta_3 = -39$ upper surface..... 165
p)	$Nu/\sqrt{Re_x}$ vs. X'	upper surface..... 166
14	Configuration I, $\delta_2 = \delta_3 = 0$	
a)	$Nu/\sqrt{Re_x}$ vs. Y'	$\alpha = -30$ lower surface..... 167
b)	$Nu/\sqrt{Re_x}$ vs. Y'	$\alpha = -40$ lower surface
c)	$Nu/\sqrt{Re_x}$ vs. Y'	$\alpha = -50$ lower surface
d)	$Nu/\sqrt{Re_x}$ vs. X'	$\alpha = -30$ lower surface
e)	$Nu/\sqrt{Re_x}$ vs. X'	$\alpha = -40$ lower surface
f)	$Nu/\sqrt{Re_x}$ vs. X'	$\alpha = -50$ lower surface
g)	$Nu/\sqrt{Re_x}$ vs. Y'	$\alpha = -30$ upper surface..... 168
h)	$Nu/\sqrt{Re_x}$ vs. X'	upper surface..... 169
i)	$Nu/\sqrt{Re_x}$ vs. Y'	$\alpha = -40$ upper surface..... 170
j)	$Nu/\sqrt{Re_x}$ vs. X'	upper surface..... 171
k)	$Nu/\sqrt{Re_x}$ vs. Y'	$\alpha = -50$ upper surface..... 172
l)	$Nu/\sqrt{Re_x}$ vs. X'	upper surface..... 173

Contrails

<u>Figure</u>			<u>Page</u>
15	Configuration IV, $\alpha = 0$		
a)	$Nu/\sqrt{Re_x}$ vs. Y'	$\delta_2 = \delta_3 = 0$	lower surface..... 174
b)	$Nu/\sqrt{Re_x}$ vs. X'		lower surface
c)	$Nu/\sqrt{Re_x}$ vs. Y'		upper surface..... 175
d)	$Nu/\sqrt{Re_x}$ vs. X'		upper surface
e)	$Nu/\sqrt{Re_x}$ vs. Y'	$\delta_2 = \delta_3 = +10$	lower surface..... 176
f)	$Nu/\sqrt{Re_x}$ vs. X'		lower surface..... 177
g)	$Nu/\sqrt{Re_x}$ vs. Y'		upper surface..... 178
h)	$Nu/\sqrt{Re_x}$ vs. X'		upper surface..... 179
i)	$Nu/\sqrt{Re_x}$ vs. Y'	$\delta_2 = \delta_3 = +20$	lower surface..... 180
j)	$Nu/\sqrt{Re_x}$ vs. X'		lower surface..... 181
k)	$Nu/\sqrt{Re_x}$ vs. Y'		upper surface..... 182
l)	$Nu/\sqrt{Re_x}$ vs. X'		upper surface..... 183
m)	$Nu/\sqrt{Re_x}$ vs. Y'	$\delta_2 = \delta_3 = +30$	lower surface..... 184
n)	$Nu/\sqrt{Re_x}$ vs. X'		lower surface..... 185
o)	$Nu/\sqrt{Re_x}$ vs. Y'		upper surface..... 186
p)	$Nu/\sqrt{Re_x}$ vs. X'		upper surface..... 187
q)	$Nu/\sqrt{Re_x}$ vs. Y'	$\delta_2 = \delta_3 = +39$	lower surface..... 188
r)	$Nu/\sqrt{Re_x}$ vs. X'		lower surface
s)	$Nu/\sqrt{Re_x}$ vs. Y'		upper surface..... 189
t)	$Nu/\sqrt{Re_x}$ vs. X'		upper surface..... 190
16	Configuration IV, $\alpha = 0$		
a)	$Nu/\sqrt{Re_x}$ vs. Y'	$\delta_2 = \delta_3 = -10$	lower surface..... 191
b)	$Nu/\sqrt{Re_x}$ vs. Y'	$\delta_2 = \delta_3 = -20$	lower surface
c)	$Nu/\sqrt{Re_x}$ vs. Y'	$\delta_2 = \delta_3 = -30$	lower surface
d)	$Nu/\sqrt{Re_x}$ vs. Y'	$\delta_2 = \delta_3 = -39$	lower surface
e)	$Nu/\sqrt{Re_x}$ vs. X'	$\delta_2 = \delta_3 = -10$	lower surface..... 192
f)	$Nu/\sqrt{Re_x}$ vs. X'	$\delta_2 = \delta_3 = -20$	lower surface
g)	$Nu/\sqrt{Re_x}$ vs. X'	$\delta_2 = \delta_3 = -30$	lower surface
h)	$Nu/\sqrt{Re_x}$ vs. X'	$\delta_2 = \delta_3 = -39$	lower surface
i)	$Nu/\sqrt{Re_x}$ vs. Y'	$\delta_2 = \delta_3 = -10$	upper surface..... 193
j)	$Nu/\sqrt{Re_x}$ vs. X'		upper surface..... 194
k)	$Nu/\sqrt{Re_x}$ vs. Y'	$\delta_2 = \delta_3 = -20$	upper surface..... 195
l)	$Nu/\sqrt{Re_x}$ vs. X'		upper surface..... 196
m)	$Nu/\sqrt{Re_x}$ vs. Y'	$\delta_2 = \delta_3 = -30$	upper surface..... 197
n)	$Nu/\sqrt{Re_x}$ vs. X'		upper surface..... 198
o)	$Nu/\sqrt{Re_x}$ vs. Y'	$\delta_2 = \delta_3 = -39$	upper surface..... 199
p)	$Nu/\sqrt{Re_x}$ vs. X'		upper surface

Controls

Figure

Page

17 Configuration IV, $\alpha = +10$

a) $Nu/\sqrt{Re_x}$ vs. Y'	$\delta_2 = \delta_3 = 0$	lower surface..... 200
b) $Nu/\sqrt{Re_x}$ vs. X'		lower surface..... 201
c) $Nu/\sqrt{Re_x}$ vs. Y'	$\delta_2 = \delta_3 = +10$	lower surface..... 202
d) $Nu/\sqrt{Re_x}$ vs. X'		lower surface..... 203
e) $Nu/\sqrt{Re_x}$ vs. Y'	$\delta_2 = \delta_3 = +20$	lower surface..... 204
f) $Nu/\sqrt{Re_x}$ vs. X'		lower surface..... 205
g) $Nu/\sqrt{Re_x}$ vs. Y'	$\delta_2 = \delta_3 = +30$	lower surface..... 206
h) $Nu/\sqrt{Re_x}$ vs. X'		lower surface
i) $Nu/\sqrt{Re_x}$ vs. Y'	$\delta_2 = \delta_3 = +39$	lower surface..... 207
j) $Nu/\sqrt{Re_x}$ vs. X'		lower surface..... 208
k) $Nu/\sqrt{Re_x}$ vs. Y'	$\delta_2 = \delta_3 = 0$	upper surface..... 209
l) $Nu/\sqrt{Re_x}$ vs. X'		upper surface
m) $Nu/\sqrt{Re_x}$ vs. Y'	$\delta_2 = \delta_3 = +10$	upper surface..... 210
n) $Nu/\sqrt{Re_x}$ vs. Y'	$\delta_2 = \delta_3 = +20$	upper surface
o) $Nu/\sqrt{Re_x}$ vs. Y'	$\delta_2 = \delta_3 = +30$	upper surface
p) $Nu/\sqrt{Re_x}$ vs. Y'	$\delta_2 = \delta_3 = +39$	upper surface
q) $Nu/\sqrt{Re_x}$ vs. X'	$\delta_2 = \delta_3 = +10$	upper surface..... 211
r) $Nu/\sqrt{Re_x}$ vs. X'	$\delta_2 = \delta_3 = +20$	upper surface
s) $Nu/\sqrt{Re_x}$ vs. X'	$\delta_2 = \delta_3 = +30$	upper surface
t) $Nu/\sqrt{Re_x}$ vs. X'	$\delta_2 = \delta_3 = +39$	upper surface

18 Configuration IV, $\alpha = +10$

a) $Nu/\sqrt{Re_x}$ vs. Y'	$\delta_2 = \delta_3 = -10$	lower surface..... 212
b) $Nu/\sqrt{Re_x}$ vs. X'		lower surface..... 213
c) $Nu/\sqrt{Re_x}$ vs. Y'		upper surface..... 214
d) $Nu/\sqrt{Re_x}$ vs. X'		upper surface..... 215
e) $Nu/\sqrt{Re_x}$ vs. Y'	$\delta_2 = \delta_3 = -20$	lower surface..... 216
f) $Nu/\sqrt{Re_x}$ vs. X'		lower surface
g) $Nu/\sqrt{Re_x}$ vs. Y'		upper surface..... 217
h) $Nu/\sqrt{Re_x}$ vs. X'		upper surface..... 218
i) $Nu/\sqrt{Re_x}$ vs. Y'	$\delta_2 = \delta_3 = -30$	lower surface..... 219
j) $Nu/\sqrt{Re_x}$ vs. X'		lower surface
k) $Nu/\sqrt{Re_x}$ vs. Y'		upper surface..... 220
l) $Nu/\sqrt{Re_x}$ vs. X'		upper surface..... 221
m) $Nu/\sqrt{Re_x}$ vs. Y'	$\delta_2 = \delta_3 = -39$	lower surface..... 222
n) $Nu/\sqrt{Re_x}$ vs. X'		lower surface
o) $Nu/\sqrt{Re_x}$ vs. Y'		upper surface..... 223
p) $Nu/\sqrt{Re_x}$ vs. X'		upper surface..... 224

Controls

Figure

19 Configuration IV, $\alpha = +20$

a)	$Nu/\sqrt{Re_x}$ vs. Y'	$\delta_2 = \delta_3 = 0$	lower surface.....	223
b)	$Nu/\sqrt{Re_x}$ vs. X'		lower surface.....	226
c)	$Nu/\sqrt{Re_x}$ vs. Y'	$\delta_2 = \delta_3 = +10$	lower surface.....	227
d)	$Nu/\sqrt{Re_x}$ vs. X'		lower surface.....	228
e)	$Nu/\sqrt{Re_x}$ vs. Y'	$\delta_2 = \delta_3 = +20$	lower surface.....	229
f)	$Nu/\sqrt{Re_x}$ vs. X'		lower surface	
g)	$Nu/\sqrt{Re_x}$ vs. Y'	$\delta_2 = \delta_3 = +30$	lower surface.....	230
h)	$Nu/\sqrt{Re_x}$ vs. X'		lower surface.....	231
i)	$Nu/\sqrt{Re_x}$ vs. Y'	$\delta_2 = \delta_3 = +39$	lower surface.....	232
j)	$Nu/\sqrt{Re_x}$ vs. X'		lower surface.....	233
k)	$Nu/\sqrt{Re_x}$ vs. Y'	$\delta_2 = \delta_3 = 0$	upper surface.....	234
l)	$Nu/\sqrt{Re_x}$ vs. Y'	$\delta_2 = \delta_3 = +10$	upper surface	
m)	$Nu/\sqrt{Re_x}$ vs. Y'	$\delta_2 = \delta_3 = +20$	upper surface	
n)	$Nu/\sqrt{Re_x}$ vs. X'	$\delta_2 = \delta_3 = 0$	upper surface.....	235
o)	$Nu/\sqrt{Re_x}$ vs. X'	$\delta_2 = \delta_3 = +10$	upper surface	
p)	$Nu/\sqrt{Re_x}$ vs. X'	$\delta_2 = \delta_3 = +20$	upper surface	
q)	$Nu/\sqrt{Re_x}$ vs. Y'	$\delta_2 = \delta_3 = +30$	upper surface.....	236
r)	$Nu/\sqrt{Re_x}$ vs. X'		upper surface	
s)	$Nu/\sqrt{Re_x}$ vs. Y'	$\delta_2 = \delta_3 = +39$	upper surface.....	237
t)	$Nu/\sqrt{Re_x}$ vs. X'		upper surface	

20 Configuration IV, $\alpha = +20$

a)	$Nu/\sqrt{Re_x}$ vs. Y'	$\delta_2 = \delta_3 = -10$	lower surface.....	238
b)	$Nu/\sqrt{Re_x}$ vs. X'		lower surface.....	239
c)	$Nu/\sqrt{Re_x}$ vs. Y'		upper surface.....	240
d)	$Nu/\sqrt{Re_x}$ vs. X'		upper surface	
e)	$Nu/\sqrt{Re_x}$ vs. Y'	$\delta_2 = \delta_3 = -20$	lower surface.....	241
f)	$Nu/\sqrt{Re_x}$ vs. X'		lower surface	
g)	$Nu/\sqrt{Re_x}$ vs. Y'		upper surface.....	242
h)	$Nu/\sqrt{Re_x}$ vs. X'		upper surface	
i)	$Nu/\sqrt{Re_x}$ vs. Y'	$\delta_2 = \delta_3 = -30$	lower surface.....	243
j)	$Nu/\sqrt{Re_x}$ vs. X'		lower surface	
k)	$Nu/\sqrt{Re_x}$ vs. Y'		upper surface.....	244
l)	$Nu/\sqrt{Re_x}$ vs. X'		upper surface.....	245
m)	$Nu/\sqrt{Re_x}$ vs. Y'	$\delta_2 = \delta_3 = -39$	lower surface.....	246
n)	$Nu/\sqrt{Re_x}$ vs. X'		lower surface	
o)	$Nu/\sqrt{Re_x}$ vs. Y'		upper surface.....	247
p)	$Nu/\sqrt{Re_x}$ vs. X'		upper surface.....	248

Contrails

<u>Figure</u>		<u>Page</u>	
21	Configuration IV, $\delta_2 = \delta_3 = 0$		
a)	$Nu/\sqrt{Re_x}$ vs. Y'	$\alpha = +35$	lower surface..... 249
b)	$Nu/\sqrt{Re_x}$ vs. X'		lower surface..... 250
c)	$Nu/\sqrt{Re_x}$ vs. Y'	$\alpha = +40$	lower surface..... 251
d)	$Nu/\sqrt{Re_x}$ vs. X'		lower surface..... 252
e)	$Nu/\sqrt{Re_x}$ vs. Y'	$\alpha = +35$	upper surface..... 253
f)	$Nu/\sqrt{Re_x}$ vs. Y'	$\alpha = +40$	upper surface
g)	$Nu/\sqrt{Re_x}$ vs. X'	$\alpha = +35$	upper surface
h)	$Nu/\sqrt{Re_x}$ vs. X'	$\alpha = +40$	upper surface
i)	$Nu/\sqrt{Re_x}$ vs. Y'	$\alpha = +45$	lower surface..... 254
j)	$Nu/\sqrt{Re_x}$ vs. X'		lower surface..... 255
k)	$Nu/\sqrt{Re_x}$ vs. Y'		upper surface..... 256
l)	$Nu/\sqrt{Re_x}$ vs. X'		upper surface
m)	$Nu/\sqrt{Re_x}$ vs. Y'	$\alpha = +50$	lower surface..... 257
n)	$Nu/\sqrt{Re_x}$ vs. X'		lower surface..... 258
o)	$Nu/\sqrt{Re_x}$ vs. Y'		upper surface..... 259
p)	$Nu/\sqrt{Re_x}$ vs. X'		upper surface..... 260
22	Configuration IV, $\alpha = -10$		
a)	$Nu/\sqrt{Re_x}$ vs. Y'	$\delta_2 = \delta_3 = 0$	lower surface..... 261
b)	$Nu/\sqrt{Re_x}$ vs. X'		lower surface
c)	$Nu/\sqrt{Re_x}$ vs. Y'		upper surface..... 262
d)	$Nu/\sqrt{Re_x}$ vs. X'		upper surface..... 263
e)	$Nu/\sqrt{Re_x}$ vs. Y'	$\delta_2 = \delta_3 = +10$	lower surface..... 264
f)	$Nu/\sqrt{Re_x}$ vs. X'		lower surface..... 265
g)	$Nu/\sqrt{Re_x}$ vs. Y'		upper surface..... 266
h)	$Nu/\sqrt{Re_x}$ vs. X'		upper surface..... 267
i)	$Nu/\sqrt{Re_x}$ vs. Y'	$\delta_2 = \delta_3 = +20$	lower surface..... 268
j)	$Nu/\sqrt{Re_x}$ vs. X'		lower surface..... 269
k)	$Nu/\sqrt{Re_x}$ vs. Y'		upper surface..... 270
l)	$Nu/\sqrt{Re_x}$ vs. X'		upper surface..... 271
m)	$Nu/\sqrt{Re_x}$ vs. Y'	$\delta_2 = \delta_3 = +30$	lower surface..... 272
n)	$Nu/\sqrt{Re_x}$ vs. X'		lower surface..... 273
o)	$Nu/\sqrt{Re_x}$ vs. Y'		upper surface..... 274
p)	$Nu/\sqrt{Re_x}$ vs. X'		upper surface..... 275
q)	$Nu/\sqrt{Re_x}$ vs. Y'	$\delta_2 = \delta_3 = +39$	lower surface..... 276
r)	$Nu/\sqrt{Re_x}$ vs. X'		lower surface..... 277
s)	$Nu/\sqrt{Re_x}$ vs. Y'		upper surface..... 278
t)	$Nu/\sqrt{Re_x}$ vs. X'		upper surface..... 279

Controls

Figure

Page

23 Configuration IV, $\alpha = -10$

a)	$Nu/\sqrt{Re_x}$ vs. Y'	$\delta_2 = \delta_3 = -10$	lower surface.....	280
b)	$Nu/\sqrt{Re_x}$ vs. Y'	$\delta_2 = \delta_3 = -20$	lower surface	
c)	$Nu/\sqrt{Re_x}$ vs. Y'	$\delta_2 = \delta_3 = -30$	lower surface	
d)	$Nu/\sqrt{Re_x}$ vs. Y'	$\delta_2 = \delta_3 = -39$	lower surface	
e)	$Nu/\sqrt{Re_x}$ vs. X'	$\delta_2 = \delta_3 = -10$	lower surface.....	281
f)	$Nu/\sqrt{Re_x}$ vs. X'	$\delta_2 = \delta_3 = -20$	lower surface	
g)	$Nu/\sqrt{Re_x}$ vs. X'	$\delta_2 = \delta_3 = -30$	lower surface	
h)	$Nu/\sqrt{Re_x}$ vs. X'	$\delta_2 = \delta_3 = -39$	lower surface	
i)	$Nu/\sqrt{Re_x}$ vs. Y'	$\delta_2 = \delta_3 = -10$	upper surface.....	282
j)	$Nu/\sqrt{Re_x}$ vs. X'		upper surface.....	283
k)	$Nu/\sqrt{Re_x}$ vs. Y'	$\delta_2 = \delta_3 = -20$	upper surface.....	284
l)	$Nu/\sqrt{Re_x}$ vs. X'		upper surface	
m)	$Nu/\sqrt{Re_x}$ vs. Y'	$\delta_2 = \delta_3 = -30$	upper surface.....	285
n)	$Nu/\sqrt{Re_x}$ vs. X'		upper surface	
o)	$Nu/\sqrt{Re_x}$ vs. Y'	$\delta_2 = \delta_3 = -39$	upper surface.....	286
p)	$Nu/\sqrt{Re_x}$ vs. X'		upper surface	

24 Configuration IV, $\alpha = -20$

a)	$Nu/\sqrt{Re_x}$ vs. Y'	$\delta_2 = \delta_3 = 0$	lower surface	287
b)	$Nu/\sqrt{Re_x}$ vs. Y'	$\delta_2 = \delta_3 = +10$	lower surface	
c)	$Nu/\sqrt{Re_x}$ vs. X'	$\delta_2 = \delta_3 = 0$	lower surface	
d)	$Nu/\sqrt{Re_x}$ vs. X'	$\delta_2 = \delta_3 = +10$	lower surface	
e)	$Nu/\sqrt{Re_x}$ vs. Y'	$\delta_2 = \delta_3 = 0$	upper surface	288
f)	$Nu/\sqrt{Re_x}$ vs. X'		upper surface	289
g)	$Nu/\sqrt{Re_x}$ vs. Y'	$\delta_2 = \delta_3 = +10$	upper surface	290
h)	$Nu/\sqrt{Re_x}$ vs. X'		upper surface	291
i)	$Nu/\sqrt{Re_x}$ vs. Y'	$\delta_2 = \delta_3 = +20$	lower surface	292
j)	$Nu/\sqrt{Re_x}$ vs. X'		lower surface	293
k)	$Nu/\sqrt{Re_x}$ vs. Y'		upper surface	294
l)	$Nu/\sqrt{Re_x}$ vs. X'		upper surface	295
m)	$Nu/\sqrt{Re_x}$ vs. Y'	$\delta_2 = \delta_3 = +30$	lower surface	296
n)	$Nu/\sqrt{Re_x}$ vs. X'		lower surface	297
o)	$Nu/\sqrt{Re_x}$ vs. Y'		upper surface	298
p)	$Nu/\sqrt{Re_x}$ vs. X'		upper surface	299
q)	$Nu/\sqrt{Re_x}$ vs. Y'	$\delta_2 = \delta_3 = +39$	lower surface	300
r)	$Nu/\sqrt{Re_x}$ vs. X'		lower surface	301
s)	$Nu/\sqrt{Re_x}$ vs. Y'		upper surface	302
t)	$Nu/\sqrt{Re_x}$ vs. X'		upper surface	303

Controls

Figure

Page

25 Configuration IV, $\alpha = -20$

a) $Nu/\sqrt{Re_x}$ vs. Y'	$b_2 = b_3 = -10$	lower surface	304
b) $Nu/\sqrt{Re_x}$ vs. Y'	$b_2 = b_3 = -20$	lower surface	
c) $Nu/\sqrt{Re_x}$ vs. Y'	$b_2 = b_3 = -30$	lower surface	
d) $Nu/\sqrt{Re_x}$ vs. Y'	$b_2 = b_3 = -39$	lower surface	
e) $Nu/\sqrt{Re_x}$ vs. X'	$b_2 = b_3 = -10$	lower surface	305
f) $Nu/\sqrt{Re_x}$ vs. X'	$b_2 = b_3 = -20$	lower surface	
g) $Nu/\sqrt{Re_x}$ vs. X'	$b_2 = b_3 = -30$	lower surface	
h) $Nu/\sqrt{Re_x}$ vs. X'	$b_2 = b_3 = -39$	lower surface	
i) $Nu/\sqrt{Re_x}$ vs. Y'	$b_2 = b_3 = -10$	upper surface	306
j) $Nu/\sqrt{Re_x}$ vs. X'		upper surface	
k) $Nu/\sqrt{Re_x}$ vs. Y'	$b_2 = b_3 = -20$	upper surface	307
l) $Nu/\sqrt{Re_x}$ vs. X'		upper surface	
m) $Nu/\sqrt{Re_x}$ vs. Y'	$b_2 = b_3 = -30$	upper surface	308
n) $Nu/\sqrt{Re_x}$ vs. X'		upper surface	
o) $Nu/\sqrt{Re_x}$ vs. Y'	$b_2 = b_3 = -39$	upper surface	309
p) $Nu/\sqrt{Re_x}$ vs. X'		upper surface	310

26 Configuration IV, $\alpha = -30$

a) $Nu/\sqrt{Re_x}$ vs. Y'	$b_2 = b_3 = 0$	lower surface	311
b) $Nu/\sqrt{Re_x}$ vs. Y'	$b_2 = b_3 = +39$	lower surface	
c) $Nu/\sqrt{Re_x}$ vs. X'	$b_2 = b_3 = 0$	lower surface	
d) $Nu/\sqrt{Re_x}$ vs. X'	$b_2 = b_3 = +39$	lower surface	
e) $Nu/\sqrt{Re_x}$ vs. Y'	$b_2 = b_3 = 0$	upper surface	312
f) $Nu/\sqrt{Re_x}$ vs. X'		upper surface	313
g) $Nu/\sqrt{Re_x}$ vs. Y'	$b_2 = b_3 = +39$	upper surface	314
h) $Nu/\sqrt{Re_x}$ vs. X'		upper surface	315

27 Configuration IV, $\alpha = -40$

a) $Nu/\sqrt{Re_x}$ vs. Y'	$b_2 = b_3 = 0$	lower surface	316
b) $Nu/\sqrt{Re_x}$ vs. Y'	$b_2 = b_3 = +39$	lower surface	
c) $Nu/\sqrt{Re_x}$ vs. X'	$b_2 = b_3 = 0$	lower surface	
d) $Nu/\sqrt{Re_x}$ vs. X'	$b_2 = b_3 = +39$	lower surface	
e) $Nu/\sqrt{Re_x}$ vs. Y'	$b_2 = b_3 = 0$	upper surface	317
f) $Nu/\sqrt{Re_x}$ vs. X'		upper surface	318
g) $Nu/\sqrt{Re_x}$ vs. Y'	$b_2 = b_3 = +39$	upper surface	319
h) $Nu/\sqrt{Re_x}$ vs. X'		upper surface	320

28 Configuration IV, $\alpha = -50$

a) $Nu/\sqrt{Re_x}$ vs. Y'	$b_2 = b_3 = 0$	lower surface	321
b) $Nu/\sqrt{Re_x}$ vs. Y'		upper surface	

Controls

<u>Figure</u>		<u>Page</u>
28	Configuration IV, $\alpha = -50$ (Cont'd)	
c)	$Nu/\sqrt{Re_x}$ vs. X'	$\delta_2 = \delta_3 = 0$
d)	$Nu/\sqrt{Re_x}$ vs. X'	
29	Configuration VII, Spoiler On	
a)	$Nu/\sqrt{Re_x}$ vs. Y'	$\alpha = 0, Re_\infty/ft \times 10^{-6} = 3.3$
b)	$Nu/\sqrt{Re_x}$ vs. X'	
c)	$Nu/\sqrt{Re_x}$ vs. Y'	
d)	$Nu/\sqrt{Re_x}$ vs. X'	
e)	$Nu/\sqrt{Re_x}$ vs. Y'	$\alpha = 0, Re_\infty/ft \times 10^{-6} = 1.1$
f)	$Nu/\sqrt{Re_x}$ vs. X'	
g)	$Nu/\sqrt{Re_x}$ vs. Y'	
h)	$Nu/\sqrt{Re_x}$ vs. X'	
i)	$Nu/\sqrt{Re_x}$ vs. Y'	$\alpha = -10, Re_\infty/ft \times 10^{-6} = 3.3$
j)	$Nu/\sqrt{Re_x}$ vs. X'	
k)	$Nu/\sqrt{Re_x}$ vs. Y'	
l)	$Nu/\sqrt{Re_x}$ vs. X'	
m)	$Nu/\sqrt{Re_x}$ vs. Y'	$\alpha = -20, Re_\infty/ft \times 10^{-6} = 3.3$
n)	$Nu/\sqrt{Re_x}$ vs. X'	
o)	$Nu/\sqrt{Re_x}$ vs. Y'	
p)	$Nu/\sqrt{Re_x}$ vs. X'	
30	Configuration VIII, $\alpha = 0$, Spoiler On, Fins On	
a)	$Nu/\sqrt{Re_x}$ vs. Y'	$Re_\infty/ft \times 10^{-6} = 3.3$
b)	$Nu/\sqrt{Re_x}$ vs. X'	
c)	$Nu/\sqrt{Re_x}$ vs. Y'	
d)	$Nu/\sqrt{Re_x}$ vs. X'	
31	Configuration IX, $\alpha = 0$ $Re_\infty/ft \times 10^{-6} = 3.3$	
a)	$Nu/\sqrt{Re_x}$ vs. Y'	$\delta_2 = \delta_3 = +20$
b)	$Nu/\sqrt{Re_x}$ vs. X'	
c)	$Nu/\sqrt{Re_x}$ vs. Y'	
d)	$Nu/\sqrt{Re_x}$ vs. X'	
e)	$Nu/\sqrt{Re_x}$ vs. Y'	$\delta_2 = \delta_3 = +39$
f)	$Nu/\sqrt{Re_x}$ vs. X'	
g)	$Nu/\sqrt{Re_x}$ vs. Y'	
h)	$Nu/\sqrt{Re_x}$ vs. X'	
32	Configuration IX, $\alpha = 0$ $Re_\infty/ft \times 10^{-6} = 3.3$	
a)	$Nu/\sqrt{Re_x}$ vs. Y'	$\delta_2 = \delta_3 = -20$
b)	$Nu/\sqrt{Re_x}$ vs. X'	
c)	$Nu/\sqrt{Re_x}$ vs. Y'	
d)	$Nu/\sqrt{Re_x}$ vs. X'	

Contrails

<u>Figure</u>		<u>Page</u>
32	Configuration IX, $\alpha = 0$ (Cont'd)	
e)	$Nu/\sqrt{Re_x}$ vs. Y'	$\delta_2 = \delta_3 = -39$ lower surface 348
f)	$Nu/\sqrt{Re_x}$ vs. Y'	upper surface
g)	$Nu/\sqrt{Re_x}$ vs. X'	lower surface
h)	$Nu/\sqrt{Re_x}$ vs. X'	upper surface
33	Configuration IX, $\alpha = +10$ $Re_\infty / ft \times 10^{-6} = 3.3$	
a)	$Nu/\sqrt{Re_x}$ vs. Y'	$\delta_2 = \delta_3 = 0$ lower surface 349
b)	$Nu/\sqrt{Re_x}$ vs. X'	lower surface 350
c)	$Nu/\sqrt{Re_x}$ vs. Y'	upper surface 351
d)	$Nu/\sqrt{Re_x}$ vs. X'	upper surface 352
e)	$Nu/\sqrt{Re_x}$ vs. Y'	$\delta_2 = \delta_3 = +20$ lower surface 353
f)	$Nu/\sqrt{Re_x}$ vs. X'	lower surface 354
g)	$Nu/\sqrt{Re_x}$ vs. Y'	upper surface 355
h)	$Nu/\sqrt{Re_x}$ vs. X'	upper surface 356
i)	$Nu/\sqrt{Re_x}$ vs. Y'	$\delta_2 = \delta_3 = +39$ lower surface 357
j)	$Nu/\sqrt{Re_x}$ vs. X'	lower surface 358
k)	$Nu/\sqrt{Re_x}$ vs. Y'	upper surface 359
l)	$Nu/\sqrt{Re_x}$ vs. X'	upper surface 360
34	Configuration IX, $\alpha = +10$ $Re_\infty / ft \times 10^{-6} = 3.3$	
a)	$Nu/\sqrt{Re_x}$ vs. Y'	$\delta_2 = \delta_3 = -20$ lower surface 361
b)	$Nu/\sqrt{Re_x}$ vs. X'	lower surface
c)	$Nu/\sqrt{Re_x}$ vs. Y'	upper surface 362
d)	$Nu/\sqrt{Re_x}$ vs. X'	upper surface 363
e)	$Nu/\sqrt{Re_x}$ vs. X'	$\delta_2 = \delta_3 = -39$ lower surface 364
f)	$Nu/\sqrt{Re_x}$ vs. Y'	lower surface
g)	$Nu/\sqrt{Re_x}$ vs. Y'	upper surface 365
h)	$Nu/\sqrt{Re_x}$ vs. X'	upper surface 366
35	Configuration IX, $\alpha = +20$ $Re_\infty / ft \times 10^{-6} = 3.3$	
a)	$Nu/\sqrt{Re_x}$ vs. Y'	$\delta_2 = \delta_3 = 0$ lower surface 367
b)	$Nu/\sqrt{Re_x}$ vs. X'	lower surface 368
c)	$Nu/\sqrt{Re_x}$ vs. Y'	upper surface 369
d)	$Nu/\sqrt{Re_x}$ vs. X'	upper surface 370
e)	$Nu/\sqrt{Re_x}$ vs. Y'	$\delta_2 = \delta_3 = +20$ lower surface 371
f)	$Nu/\sqrt{Re_x}$ vs. X'	lower surface
g)	$Nu/\sqrt{Re_x}$ vs. Y'	upper surface 372
h)	$Nu/\sqrt{Re_x}$ vs. X'	upper surface 373
i)	$Nu/\sqrt{Re_x}$ vs. Y'	$\delta_2 = \delta_3 = +39$ lower surface 374
j)	$Nu/\sqrt{Re_x}$ vs. X'	lower surface 375

Controls

<u>Figure</u>		<u>Page</u>
35	Configuration IX, $\alpha = +20$ (Cont'd)	
	k) $Nu/\sqrt{Re_x}$ vs. Y'	$\delta_2 = \delta_3 = +39$ upper surface 376
	l) $Nu/\sqrt{Re_x}$ vs. X'	upper surface 377
36	Configuration IX, $\alpha = +20$ $Re_\infty/ft \times 10^{-6} = 3.3$	
	a) $Nu/\sqrt{Re_x}$ vs. Y'	$\delta_2 = \delta_3 = -20$ lower surface 378
	b) $Nu/\sqrt{Re_x}$ vs. X'	lower surface 379
	c) $Nu/\sqrt{Re_x}$ vs. Y'	upper surface 380
	d) $Nu/\sqrt{Re_x}$ vs. X'	upper surface 381
	e) $Nu/\sqrt{Re_x}$ vs. Y'	$\delta_2 = \delta_3 = -39$ lower surface 382
	f) $Nu/\sqrt{Re_x}$ vs. X'	lower surface 383
	g) $Nu/\sqrt{Re_x}$ vs. Y'	upper surface 384
	h) $Nu/\sqrt{Re_x}$ vs. X'	upper surface 385
37	Configuration IX, $\alpha = 0$ $Re_\infty/ft \times 10^{-6} = 1.1$	
	a) $Nu/\sqrt{Re_x}$ vs. Y'	$\delta_2 = \delta_3 = 0$ lower surface 386
	b) $Nu/\sqrt{Re_x}$ vs. Y'	$\delta_2 = \delta_3 = -20$ lower surface
	c) $Nu/\sqrt{Re_x}$ vs. Y'	$\delta_2 = \delta_3 = -39$ lower surface
	d) $Nu/\sqrt{Re_x}$ vs. X'	$\delta_2 = \delta_3 = 0$ lower surface
	e) $Nu/\sqrt{Re_x}$ vs. X'	$\delta_2 = \delta_3 = -20$ lower surface
	f) $Nu/\sqrt{Re_x}$ vs. X'	$\delta_2 = \delta_3 = -39$ lower surface
	g) $Nu/\sqrt{Re_x}$ vs. Y'	$\delta_2 = \delta_3 = 0$ upper surface 387
	h) $Nu/\sqrt{Re_x}$ vs. X'	upper surface 388
	i) $Nu/\sqrt{Re_x}$ vs. Y'	$\delta_2 = \delta_3 = -20$ upper surface 389
	j) $Nu/\sqrt{Re_x}$ vs. X'	upper surface
	k) $Nu/\sqrt{Re_x}$ vs. Y'	$\delta_2 = \delta_3 = -39$ upper surface 390
	l) $Nu/\sqrt{Re_x}$ vs. X'	upper surface
	m) $Nu/\sqrt{Re_x}$ vs. Y'	$\delta_2 = \delta_3 = +20$ lower surface 391
	n) $Nu/\sqrt{Re_x}$ vs. X'	lower surface
	o) $Nu/\sqrt{Re_x}$ vs. Y'	upper surface 392
	p) $Nu/\sqrt{Re_x}$ vs. X'	upper surface 393
	q) $Nu/\sqrt{Re_x}$ vs. Y'	$\delta_2 = \delta_3 = +39$ lower surface 394
	r) $Nu/\sqrt{Re_x}$ vs. X'	lower surface 395
	s) $Nu/\sqrt{Re_x}$ vs. Y'	upper surface 396
	t) $Nu/\sqrt{Re_x}$ vs. X'	upper surface 397
38	Configuration X, $\delta_1 = \delta_2 = \delta_3 = +20$	
	a) $Nu/\sqrt{Re_x}$ vs. Y'	$\alpha = 0$, $Re_\infty/ft \times 10^{-6} = 3.3$ lower surface 398
	b) $Nu/\sqrt{Re_x}$ vs. X'	lower surface 399
	c) $Nu/\sqrt{Re_x}$ vs. Y'	upper surface 400
	d) $Nu/\sqrt{Re_x}$ vs. X'	upper surface 401

Controls

<u>Figure</u>		<u>Page</u>
38 Configuration X, $\delta_1 = \delta_2 = \delta_3 = +20$ (Cont'd)		
e) $Nu/\sqrt{Re_x}$ vs. Y'	$\alpha = 0, Re_\infty/ft \times 10^{-6} = 1.1$	lower surface 402
f) $Nu/\sqrt{Re_x}$ vs. X'		lower surface 403
g) $Nu/\sqrt{Re_x}$ vs. Y'		upper surface 404
h) $Nu/\sqrt{Re_x}$ vs. X'		upper surface 405
i) $Nu/\sqrt{Re_x}$ vs. Y'	$\alpha = +10, Re_\infty/ft \times 10^{-6} = 3.3$	lower surface 406
j) $Nu/\sqrt{Re_x}$ vs. X'		lower surface 407
k) $Nu/\sqrt{Re_x}$ vs. Y'		upper surface 408
l) $Nu/\sqrt{Re_x}$ vs. X'		upper surface 409
m) $Nu/\sqrt{Re_x}$ vs. Y'	$\alpha = +20, Re_\infty/ft \times 10^{-6} = 3.3$	lower surface 410
n) $Nu/\sqrt{Re_x}$ vs. X'		lower surface 411
o) $Nu/\sqrt{Re_x}$ vs. Y'		upper surface 412
p) $Nu/\sqrt{Re_x}$ vs. X'		upper surface 413

Contrails

LIST OF TABLES

<u>Table</u>		<u>Page</u>
1	Geometric Characteristics	13
2	Description of Test Configurations	15
3	Thermocouple Location and Skin Thickness	16
4	Test Schedule for the 50-inch Hypersonic Wind Tunnel at Mach 8.08	17

Controls

LIST OF SYMBOLS

a	density of skin material ~ lbm/ft ³
b	wing semi-span ~ inches
c	specific heat of skin material ~ BTU/lbm
$c_{\text{Root}}^{\text{(Virtual)}}$	virtual root chord of wing ~ inches
h	heat transfer coefficient $(h = \frac{q_w}{T_o - T_w})$ ~ BTU/ft ² sec ^{0R}
k_{∞}	free stream thermal conductivity of air ~ BTU/ft ² sec ^{0R} /ft
M_{∞}	free stream Mach number
Nu	Nusselt Number $Nu = (\frac{hx}{k_{\infty}})$
P_{∞}	free stream static pressure ~ psia
\dot{q}_w	aerodynamic heating rate ~ BTU/ft ² sec
q_{∞}	free stream dynamic pressure = $\frac{\gamma}{2} P_{\infty} M_{\infty}^2$
Re_x	Reynolds number based on planform distance from virtual apex = $\frac{\rho_{\infty} V_{\infty} x}{\mu_{\infty}}$
Re_{∞}/ft	free stream unit Reynolds number = $\frac{\rho_{\infty} V_{\infty}}{\mu_{\infty}}$
t	time ~ seconds
T_o	stagnation temperature ~ ^{0R}
T_w	wall temperature ~ ^{0R}
V_{∞}	free stream velocity ~ ft/sec
x	planform chordwise coordinate (measured from virtual apex) ~ ft
y	planform spanwise coordinate (measured from model center plane) ~ ft
x'	non-dimensional chordwise coordinate = $x/c_{\text{Root}}^{\text{(Virtual)}}$

Controls

y'	non-dimensional spanwise coordinate = y/b
α	angle of attack ~ degrees
γ	ratio of specific heats = 1.4
δ_1	center flap deflection angle ~ degrees
δ_2	left outboard flap deflection angle ~ degrees
δ_3	right outboard flap deflection angle ~ degrees
μ_∞	free stream viscosity ~ $\frac{\text{slugs}}{\text{ft sec}}$
ρ_∞	free stream density ~ $\frac{\text{slugs}}{\text{ft}^3}$
τ	skin thickness ~ ft
ζ	honeycomb correction factor (=1.00 for $t = 1.00$ seconds)

Contrails

INTRODUCTION

The Fluid Mechanics Section of the Grumman Research Department is currently engaged in a research program directed at determining flow separation effects and the effectiveness of aerodynamic controls on hypersonic flight vehicles. The program consists of theoretical and experimental research on "basic" configurations (flat plates with flap and wedge type separators) and representative hypersonic glide configurations (a clipped delta wing-body combination and a pyramidal body). The configurations to be investigated in the over-all program are shown in Fig. 1a.

This report presents the results of one segment of the experimental program. It treats a winged hypersonic glider configuration consisting, in basic form, of a clipped delta wing with an overslung cone-cylinder body. This configuration was used for obtaining pressure and heat transfer data on various aerodynamic controls at hypersonic Mach numbers. The heat transfer data are presented herein, and the pressure data are presented in another report (Ref. 1). The controls investigated were partial span trailing edge flaps, with a deflection range of -39° to $+39^\circ$; a full span flap with a deflection of $+20^\circ$; a full span, plug-type, trailing edge spoiler and tip fins. An overslung hemisphere-cylinder body was also tested.

The experimental work was done at the AEDC 50-inch Mach 8 Hypersonic Wind Tunnel during July and August of 1963. Descriptions of these test facilities can be found in Ref. 2. Heat transfer data were obtained at a unit Reynolds number of 3.3×10^6 with selected points at a Reynolds number of 1.1×10^6 . This same model was also used to obtain pressure data in the AEDC 40 x 40-inch Supersonic Tunnel at $M_\infty = 5.0$, and in the AEDC 50-inch Hypersonic Tunnel at $M_\infty = 8.0$. A geometrically similar model, instrumented to obtain force and moment data, was tested in this facility at an earlier date. Another geometrically similar model, with limited pressure instrumentation, was tested in AEDC Hotshot 2 Hypervelocity Tunnel. The results of the last four investigations are presented in Refs. 1, 3, 4, and 5.

Manuscript released by the author July, 1964 for publication as an RTD Technical Documentary Report

Controls

DESCRIPTION OF MODELS

General

Six test configurations were built up from a basic model that consisted of a clipped delta wing with an overslung body. The clipped delta wing had a spherically blunted apex, cylindrically blunted leading edges, and a blunt base. Of the control surfaces to be tested, three partial span trailing edge flaps were built into the wing, and attachments were provided for mounting a full span spoiler. The two outboard flaps were of the aileron type, deflectable in the positive and negative direction, while the central flap was of the split flap variety, deflectable only in the positive direction. When all three flaps are deflected in the same direction, and to the same angle, they form a full span flap. The flap-type control surfaces were remotely actuated from outside the tunnel. Three-view drawings of the test configurations are presented in Figs. 1b through 1g. The dimensions of the basic configurations are shown in Fig. 1b and are the same for all other configurations. The other configuration drawings show dimensions only for the components added to the basic configuration. A summary of the geometric properties of the various model components is presented in Table 1.

Two of the heat transfer models tested in this program are geometrically similar to force models which were previously reported (Ref. 4). Four additional models are reported on herein for which force data are not available; they were developed by changing the forebody shape from a half-cone to a half-hemisphere. Pressure data are available for five of the six test configurations (Ref. 3).

Controls and Sign Conventions

Each flap-type control was driven by a 28-volt dc, gear reduced, electrical motor through a 1/2 inch-10 acme thread drive screw which was connected to the flap bell cranks by push-pull rods. Control deflection measurements were obtained through calibrated linear potentiometers. The three motors with their attendant potentiometers and drive screws were located in a water cooled housing immediately behind the model. The drive screws were connected to the flap bell cranks by push-pull rods that passed through

Controls

the front of the actuator housing and into the base of the model. This actuation system produced a deflection rate of 1 degree/sec and permitted the independent operation of each control surface. The control surfaces were calibrated cold, that is, when the model was installed in the tunnel, and checked frequently. The calibrating was done with pre-cut templates varying from 0 degrees to 40 degrees in 5-degree increments. A specially cut template was used to calibrate the 39-degree deflection angle. The potentiometer outputs, used in setting flap angles during the test, were recorded visually from Leeds and Northrup Midget Model D indicators. This calibration was also recorded into the digital computing equipment at AEDC for use of the computer during print-out. We were thus capable of testing asymmetric, as well as symmetric, control configurations.

The sign convention for denoting the angle of attack and the control deflection angle can be obtained from the basic model, a flat plate, clipped delta wing with an overslung body. The definition fixes the flat plate surface of the wing as the lower surface. Thus, the angle of attack is positive when the flat plate surface is the windward surface of the model. The control deflection angles are also defined with respect to the lower (flat plate) surface of the model. If we consider our model at zero angle of attack (flow parallel to the lower flat plate surface), then the positive trailing edge flap deflections are obtained by deflecting the trailing edge down. The outboard, partial span, trailing edge flaps, designed to operate independently of each other, had a maximum travel angle of ± 39 degrees, and could be calibrated to yield any deflection angle in this range. The central flap section, which operated independently of the other flaps, had a maximum travel of 0 to +20 degrees.

Model Designation

All the test configurations consisted basically of a clipped delta wing with an overslung body. The instrumented portion of the overslung body consisted of a half-cylindrical after section and a half-hemispherical foresection. An uninstrumented conical fairing was attached over the foresection of the body to provide a body shape that was geometrically similar to the body shape used in the force tests described in Ref. 4. This wing body combination was one of two major configurations of this test program and

Controls

is referred to as Configuration I. The second major configuration was obtained by adding a set of tip fins to Configuration I and is referred to as Configuration IV. These tip fins were clipped deltas in elevation and were attached in such a way as not to alter the aspect ratio (of the configuration). Configurations I and IV provided the heat transfer data corresponding to the pressure and force data previously obtained (Refs. 1 and 4).

In the force test phase of the program, each of these major configurations was expanded into three additional control models, yielding eight test configurations. It was not feasible to attempt heat transfer testing on such a large scale, due to the operational problems and time limitations. Therefore, the heat transfer tests were limited to the two major configurations previously mentioned and to four additional configurations that would provide useful data on: 1) the effects of a strong shock generator, and 2) trailing edge controls that would induce strong separation effects. The strong shock generator was a blunt forebody section on the overslung body, and the separation inducing trailing edge controls were a full span flap and a full span, plug-type spoiler.

As with the force tests, described in Ref. 4, an adequate comparison point between the partial span flaps and the other trailing edge controls (full span spoiler and flap) would be at a flap deflection angle of +20 degrees. The height of the full span, plug-type, trailing edge spoiler was designed to be equal to the vertical displacement of the trailing edge flaps when they are deflected +20 degrees. This spoiler was attached to the lower, flat plate surface at the trailing edge. The full span flap was developed by building into the model a third, partial span, split flap to fit between the outboard, aileron type flaps. When all three flaps were deflected +20 degrees, they formed a full span flap.

The overslung body was built in two sections. The first was a single, instrumented body consisting of a half-hemispherical forebody and a half-cylindrical afterbody. The second section was an uninstrumented conical fairing that could be attached over the blunt, half-hemispherical, forebody of the first section and simulate, on a smaller scale, the conical forebody used in the force tests.

Working on the assumption that the effects of the blunt body, spoiler, and full span flap would be uncoupled if the body and

Controls

spoiler, or flap, were placed on opposite surfaces of the wing, we developed four configurations. The first model consisted of a wing-body combination with a full span, plug-type, spoiler attached at the trailing edge of the lower surface and an overslung body composed of a half-hemispherical forebody and a half-cylindrical afterbody. The blunt forebody was obtained by removing the conical forebody fairing. This configuration was called Configuration VII. The second model, Configuration VIII, was obtained by adding tip fins to Configuration VII. The third model, a wing-body combination without the spoiler, but with the half-hemispherical forebody was denoted as Configuration IX. Configuration X was obtained from Configuration IX by deflecting all three partial span flaps to +20 degrees. A complete definition of the models is presented in Table 2. The model designation system maintains continuity with the previous experimental work reported in Refs. 1 and 4.

Model Construction and Instrumentation

The wing for these configurations was fabricated of an internal stainless steel frame, which served as the basic load supporting structure, and instrumented surface panels, which served as the data gathering units. The flaps were also fabricated the same way; i.e., an internal frame with attached instrumented panels. The flaps were connected to the wing structure by hinges and actuated from the actuator housing by a system of bell cranks and push-pull rods. All internal frame work was made of 416 stainless steel, and the surface panels were pressure relieved, silver braised, honeycomb sections; the face sheets, core, and frame were of 321 stainless steel. Where a thermocouple was to be spot-welded to the inner surface of the honeycomb face sheet, the back sheet was drilled away and the cell cleansed of solder by washing with concentrated nitric acid. This left a clean, solder-free surface upon which to spot-weld the thermocouple. The body and the conical fairing were fabricated of 321 stainless steel sheet, while fins and spoiler were made of solid 321 stainless steel. The actuator housing, which served as the connection between the model and the sting, as well as the housing for the actuation motors, was made of 17-4PH stainless steel.

The model was instrumented with 38 thermocouples distributed on the upper and lower surface of the wing and on the half-hemisphere cylinder body. The thermocouples were made of 30 gage

Contrails

chromel-alumel wire and were spot-welded to the inner surface of the outside honeycomb face sheet (face sheet exposed to the flow). The location of each thermocouple, the skin thickness at the thermocouple station, and the distance from the virtual apex of the model to each thermocouple are listed in Table 3 and shown in Figure 1h. When the conical forebody fairing was installed, five thermocouples (669-673) were covered; and when the spoiler was installed, four thermocouples (528, 538, 548, 588) were covered. Installation of the fins did not inactivate any instrumentation.

Contrails

EXPERIMENTAL DATA

Description of Wind Tunnels and Test Conditions

This segment of the experimental program was conducted in the 50-inch Mach 8 Hypersonic Wind Tunnel located at the von Karman Facility of the Arnold Engineering Development Center. A complete description of the wind tunnels and their associated measuring, recording, and tabulating equipment is given in Ref. 2. The tests were conducted at a nominal test section Mach number of 8.0 and test section unit Reynolds numbers of 3.3×10^6 per foot and 1.1×10^6 per foot. (Most of the program was conducted at a Reynolds number of 3.3×10^6 per foot and the lower Reynolds number data were used for comparative purposes only.) Due to the tunnel operating conditions, the actual test Mach number was 8.09. The variation in each Reynolds number was less than 1.5 per cent.

The two main configurations (I and IV) were tested most extensively, while experiments with the other configurations were restricted and were used only to provide comparison data with the main configurations. Configurations I and IV were tested through an angle of attack range of -20 to +20 degrees, for symmetric, partial span, flap deflections of -39 to +39 degrees. For zero flap deflection angles, data were gathered through an angle of attack range of -50 to +50 degrees. Configurations VII and VIII yielded data on the effect of a full span, plug-type, trailing edge spoiler; and information on the effect of a strong shock generator on the aerodynamic heating characteristics of deflected, partial span, trailing edge flaps was obtained with Configuration IX. The effect of a full span trailing edge flap was determined using Configuration X. These Configurations (VII-X) also provided the information on the effect of a strong shock generator on the aerodynamic heating characteristics of a flat plate wing panel.

A complete tabulation of the experimental program showing the angle of attack range, control deflection, and flow conditions is presented in Table 4. The angle of attack range was obtained by using two different pre-bend angles on the water-cooled split sting that is standard tunnel equipment. The two pre-bend angles used were 12 degrees and 39 degrees, which provided an angle of attack range of 0 to +50 degrees. The negative angles of attack were obtained by inverting the model.

Contrails

Cooling shoes were installed in the Mach 8 Tunnel in order to obtain aerodynamic heating rates by the thin wall, transient temperature technique. Tunnel conditions were stabilized for the desired free stream Reynolds number; the remotely controlled flaps were set at the desired angles, and the model was pitched to the required angle of attack while inside the cooling shoes. The cooling shoes were then rapidly retracted (full retraction from the tunnel centerline to walls within 0.8 second), and temperature of each thermocouple was recorded for 4 seconds at intervals of 0.05 second. The shoes were then closed, the model cooled to approximately 520° R, the flap angles set, and the model pitched to the next desired angle of attack where the process was repeated. In this manner, all of the heat transfer data were obtained for a given configuration and Re/ft through the angle of attack range, while limiting the amount of heat absorbed by the model. The experimental data are presented graphically, in the form of $Nu/\sqrt{Re_x}$.

Data Reduction and Accuracy

Thin wall approximations were used to obtain the transient aerodynamic heating rates from the recorded temperature-time histories. The equation used for calculating the heating rates was $\dot{q}_w = \zeta a_{rc} \frac{dt_w}{dt}$, and the temperature derivative was obtained

by fitting a polynomial through any 11 consecutive points of the temperature time curve and differentiating the polynomial at the mid-point interval. The very thin wall and the absence of heat sinks at each thermocouple installation (see table), which was made possible by the use of honeycomb sandwich construction of the test panels, allowed a very rapid response to the aerodynamic heat input. This made it possible to reduce the data at $t = 1.00$ second after the start of cooling shoe retraction. At this time interval, the honeycomb correction factor ζ was equal to 1.00. Representative thermocouples were monitored during the heat transfer tests and indicated that all starting effects caused by the opening of the cooling shoes were dissipated prior to the time at which the data were reduced. The aerodynamic heating rates were then nondimensionalized in the form:

Controls

$$\frac{Nu}{\sqrt{Re_x}} = \frac{\frac{d_w}{T_o - T_w} \frac{x}{k_\infty}}{\sqrt{\frac{\rho_\infty V_\infty x}{\mu_\infty}}}$$

The values of x , as well as the skin thickness and non-dimensionalized location of each thermocouple, are tabulated and presented in Table 3. Due to the strict time schedule, it was not possible to provide check-runs to determine the error limits in the measured heating rates and assess the inaccuracies in the calculated values of $Nu/\sqrt{Re_x}$. The discrepancy in the plotted data due to the use of automatic plotting machines should not exceed ± 0.20 per cent of the maximum scale. Each graph has been inspected and questionable points have been checked with the tabulated data.

Controls

RESULTS AND DISCUSSION

This program was designed to provide the heat transfer data needed to complement the controls information previously obtained on a basic type of hypersonic flight vehicle; namely, a clipped delta wing-body combination. Data are presented at positive and negative angles of attack for the case of an overslung body.

This configuration was tested with tip fins on and off, with partial span and full span trailing edge flaps, with a full span trailing edge spoiler, and with a blunt instrumented body as well as the conical body used in the force tests. The experiments were conducted at Mach numbers of 8.08 and 8.09 and with limited Reynolds number comparisons. Due to the tight test schedule, only the symmetric flap deflection cases were tested, whereas the force data of Ref. 4 presents both symmetric and asymmetric cases.

The basic wing-body combination was designed to provide heat transfer data for configurations having either overslung or underslung bodies. For convenience we have chosen the overslung body configuration as our reference, and defined the coordinate system and control deflection angles with reference to this basic configuration. Thus, the positive angle of attack regime for the overslung body provides the data for the underslung body at negative angles of attack. The sign of the flap deflection angles for the underslung body case must be reversed in order that both cases be viewed in the same reference system.

The data are presented in the form of $Nu/\sqrt{Re_x}$ plotted as functions of nondimensionalized chordwise (streamwise), and spanwise, coordinates (X' and Y'). The chordwise coordinate is measured from the virtual apex of the model, and the spanwise coordinate is measured from the vertical centerplane of the model. The data obtained on the upper and lower surfaces of the test configuration are presented separately for each set. Thus, for each test configuration, all the data are presented in four graphs (two graphs for the chordwise plots and two graphs for the spanwise plots).

The data for Configuration I are presented in Figs. 3 through 14; for Configuration IV in Figs. 15 through 28; for Configuration VII in Fig. 29; for Configuration VIII in Fig. 30;

Controls

for Configuration IX in Figs. 31 through 37; and for Configuration X in Fig. 38. The complete test program is tabulated in Table 4 and the specific conditions presented in each figure are noted in the list of illustrations in the front matter.

Controls

REFERENCES

1. Meckler, Lawrence, Pressure Measurements at Mach 8 on an Aerodynamically Controllable Winged Re-entry Configuration, to be published.
2. Arnold Center Test Facilities Handbook, AEDC, Arnold Air Force Station, Tennessee, January 1961.
3. Kaufman, Louis II, Pressure Measurements for Mach 5 Flows Over a Winged Re-entry Configuration with Aerodynamic Controls, Part I: Blunt Cabin, Part II: Conical Cabin, RTD-TDR-63-4179.
4. Meckler, Lawrence, Static Aerodynamic Characteristics at Mach 5 and 8 of an Aerodynamically Controllable Winged Re-entry Configuration, FDL-TDR-64-10.
5. Hartofilis, Stavros A., Pressure Measurements at Mach 19 for a Winged Re-entry Configuration, ASD-TDR-63-319, March 1963.

Contrails

TABLE 1

GEOMETRIC CHARACTERISTICS

Wing:

Clipped Delta Wing with Blunt Apex,
Leading Edges, and Base

Root Chord	12.350 inches actual 13.00 inches virtual
Tip Chord	2.608 inches
Span	12.00 inches
Apex Radius	0.650 inch
Leading Edge Sweep	60 degrees
Leading Edge Radius	0.650 inch
Wing Thickness (Constant)	1.30 inches
Planform Area	93.3 inches ² actual, 97.6 inches ² virtual
Aspect Ratio	1.542
Taper Ratio	0.211
Thickness Ratio (Root)	0.1052
Control Area - Outboard Partial Span Flaps	12.75 inches ²

Body:

Half Cone - Cylinder
(Base Mounted Flush with Wing Trailing Edge)

Cone Angle	13 degrees
Cone Length	5.49 inches
Cone Radius (Maximum at Tangency Point)	1.269 inches
Cylinder Length	4.415 inches
Cylinder Radius	1.30 inches
Fairing (Cone to Cylinder)	
Length	0.292 inch
Radius	1.30 inches
Included Angle	13 degrees
Total Body Length (Half-Cone Cylinder)	10.20 inches
Planform Area (Half-Cone Cylinder)	17.81 inches ²
Hemisphere Radius	1.30 inches
Total Body Length (Half-Hemisphere Cylinder)	5.715 inches
Planform Area (Half-Hemisphere Cylinder)	14.145 inches ²

Tip Fin:

Clipped Delta Wing with Blunt Leading Edge

Root Chord	3.275 inches
Tip Chord	0.990 inch
Span	4.160 inches
Leading Edge Sweep	50 degrees
Leading Edge Radius	0.325 inch
Thickness (Constant)	0.650 inch
Area	9.27 inches ²
Aspect Ratio	1.862
Taper Ratio	0.3025
Thickness Ratio (Fin Root-Wing Center Plane)	0.199

Controls

TABLE 1 (Cont'd)

GEOMETRIC CHARACTERISTICS

Spoiler:

Full Span, Plug Type with Cylindrical Lower Edge	
Chord (Constant)	0.650 inch
Span	10.70 inches
Height	0.611 inch
Planform Area	6.96 inches ²
Bottom Cylinder Radius	0.325 inch

Central Flap:

Split Flap - Central Section of Full Span Trailing Edge Flap	
Chord	2.220 inches
Span	2.600 inches
Planform Area	5.772 inches ²

Controls

TABLE 2

DESCRIPTION OF TEST CONFIGURATIONS

Configuration	Description
I	Basic configuration (wing - body) Wing - clipped delta wing, spherically blunted apex, cylindrically blunted leading edges, blunt base +Body - overslung, half-conical forebody and half-cylindrical afterbody
IV	Basic + Tip Fins (I)
VII	Wing - clipped delta wing, spherically blunted apex, cylindrically blunted leading edges, blunt base +Body - overslung, half-hemispherical forebody and half-cylindrical afterbody +Spoiler - plug type, trailing edge spoiler
VIII	VII + Tip Fins
IX	Wing - clipped delta wing, spherically blunted apex, cylindrically blunted leading edges, blunt base +Body - overslung, half-hemispherical forebody and half-cylindrical afterbody
X	IX + Full Span, lower surface flap ($\delta_1 = \delta_2 = \delta_3 = +20^\circ$)

Controls

TABLE 3
THERMOCOUPLE LOCATION & SKIN THICKNESS

Thermo-couple Number	Lower Surface			Upper Surface		
	X'	Y'	Skin Thickness ft	X'	Y'	Skin Thickness ft
580	0.2308	0	0.00148	0.2500	0.2308	0
583	0.6058	0	0.00150	0.6563	0.3750	0
586	0.7846	0	0.00150	0.8500	0.5192	0
587	0.9173	0.0313	0.00147	0.9937	0.5735	0
588	0.9750	0.0313	0.00146	1.0563	0.6058	0
543	0.6058	0.3125	0.00149	0.6563	0.7846	0.1083
546	0.7846	0.3125	0.00150	0.8500	0.9173	0.1083
547	0.9173	0.3125	0.00147	0.9937	0.6923	0.1877
548	0.9750	0.3125	0.00147	1.0563	0.7846	0.1877
533	0.6058	0.5625	0.00150	0.6533	0.9173	0.1877
536	0.7846	0.5625	0.00148	0.8500	0.6058	0.3125
537	0.9173	0.5625	0.00149	0.9937	0.7846	0.3125
538	0.9750	0.5625	0.00148	1.0563	0.9173	0.3125
526	0.7846	0.8020	0.00148	0.8500	0.9750	0.3125
527	0.9173	0.8020	0.00147	0.9937	0.6058	0.5625
528	0.9750	0.8020	0.00148	1.0563	0.6923	0.5625
					0.9173	0.00146
					0.7846	0.5625
					0.9173	0.00147
					0.7846	0.5625
					0.9173	0.00146
					0.9173	0.00147
					0.8020	0.8020
					0.9750	0.00146
					0.8020	0.8020

NOTE: All thermocouples are located with respect to the virtual apex, and the vertical center plane of the model. Thermocouples 626 - 673 are on the upper surface and thermocouples 526 - 588 are on the lower (flat-plate) surface of the model. Thermocouples 657, 666 inoperative for entire test program. Thermocouples 533, 543 inoperative in high angle of attack conditions for Configurations I and IV.

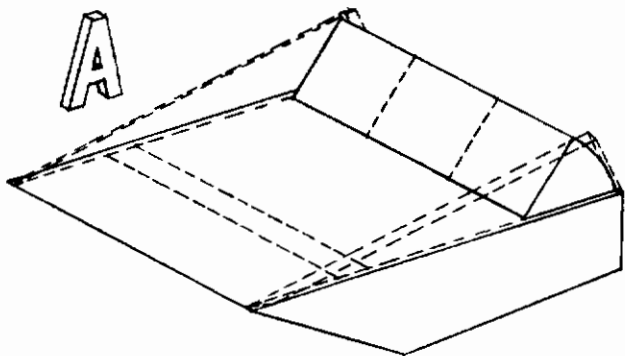
Controls

TABLE 4

TEST SCHEDULE FOR
THE 50-INCH HYPERSONIC WIND TUNNEL
AT MACH 8.08

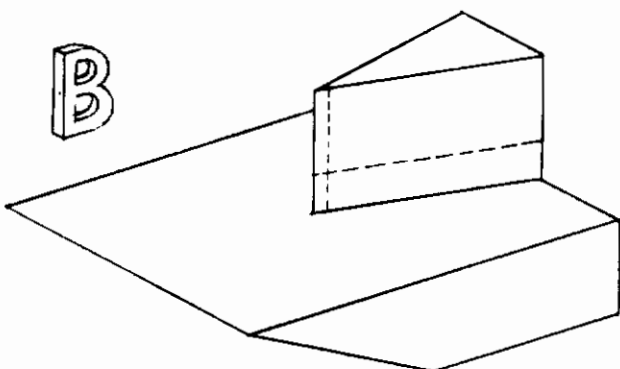
Configuration	Trailing Edge Control			α Range		$Re_\infty / ft \times 10^6$
	Partial Span Flaps					
	δ_1	δ_2	δ_3			
I	0	0	0	-50	+50	
Spoiler off	0	+10	+10	-20	+20	
Conical forebody	0	+20	+20	-20	+20	
Fins off	0	+30	+30	-20	+20	
	0	+39	+39	-20	+20	
	0	-10	-10	-20	+20	
	0	-20	-20	-20	+20	
	0	-30	-30	-20	+20	
	0	-39	-39	-20	+20	
IV	0	0	0	-50	+50	
Spoiler off	0	+10	+10	-20	+20	
Conical forebody	0	+20	+20	-20	+20	
Fins on	0	+30	+30	-20	+20	
	0	+39	+39	-40	+20	
	0	-10	-10	-20	+20	
	0	-20	-20	-20	+20	
	0	-30	-30	-20	+20	
	0	-39	-39	-20	+20	
VII	0	0	0	0	-20	
Spoiler on				0		
Blunt forebody						
Fins off						
VIII	0	0	0	0		
Spoiler on						
Blunt forebody						
Fins on						
IX	0	0	0	0	+20	
Spoiler off	0	0	0	0	+20	
Blunt forebody	0	+20	+20	0	+20	
Fins off	0	+20	+20	0	+20	
	0	+40	+40	0	+20	
	0	+40	+40	0	+20	
	0	-20	-20	0	+20	
	0	-20	-20	0	+20	
	0	-40	-40	0	+20	
	0	-40	-40	0	+20	
X	+20	+20	+20	0	+20	
Spoiler off	+20	+20	+20	0		
Blunt forebody						
Fins off						
Full span flap						

Contrails



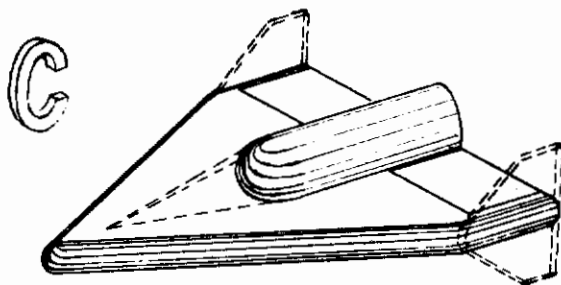
Separated Flows ahead of a Ramp
Fore and aft flaps, end plates
3 separate models:

- 1) Pressure and heat transfer, AEDC Tunnels
A & B, M = 5 & 8
- 2) Controlled wall temperature, pressure,
AEDC Tunnel B, M = 8
- 3) Pressure and heat transfer, Grumman Shock
Tunnel, M ≈ 13 & 19



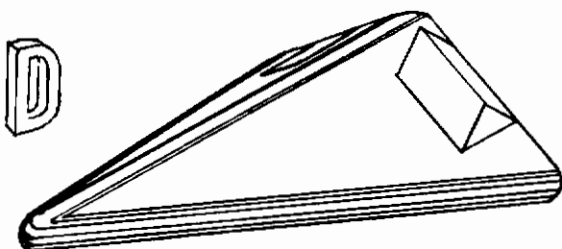
Wedge - Plate Interaction
Small and large fins with sharp
and blunt leading edges
2 separate models:

- 1) Pressure and heat transfer, AEDC Tunnels
A & B, M = 5 & 8
- 2) Pressure and heat transfer, Grumman Shock
Tunnel, M ≈ 13 & 19



Clipped Delta, Blunt L.E.
Center body, T.E. flaps, drooped nose,
spoiler, tip fins
3 separate models:

- 1) Pressure and heat transfer, AEDC Tunnels
A & B, M = 5 & 8
- 2) Pressure, AEDC Hotshot 2,
M ≈ 19
- 3) Six component force, AEDC Tunnels
A & B, M = 5 & 8



Delta, Blunt L.E., Dihedral
T.E. flaps, canard, ventral fin
3 separate models:

- 1) Pressure and heat transfer, AEDC Tunnels
A & B, M = 5 & 8
- 2) Pressure and heat transfer, Grumman Shock
Tunnel, M ≈ 19
- 3) Six component force, AEDC Tunnels
A & B, M = 5 & 8

Fig. 1a General Outline of Models and Remarks for Over-all Program

Contrails

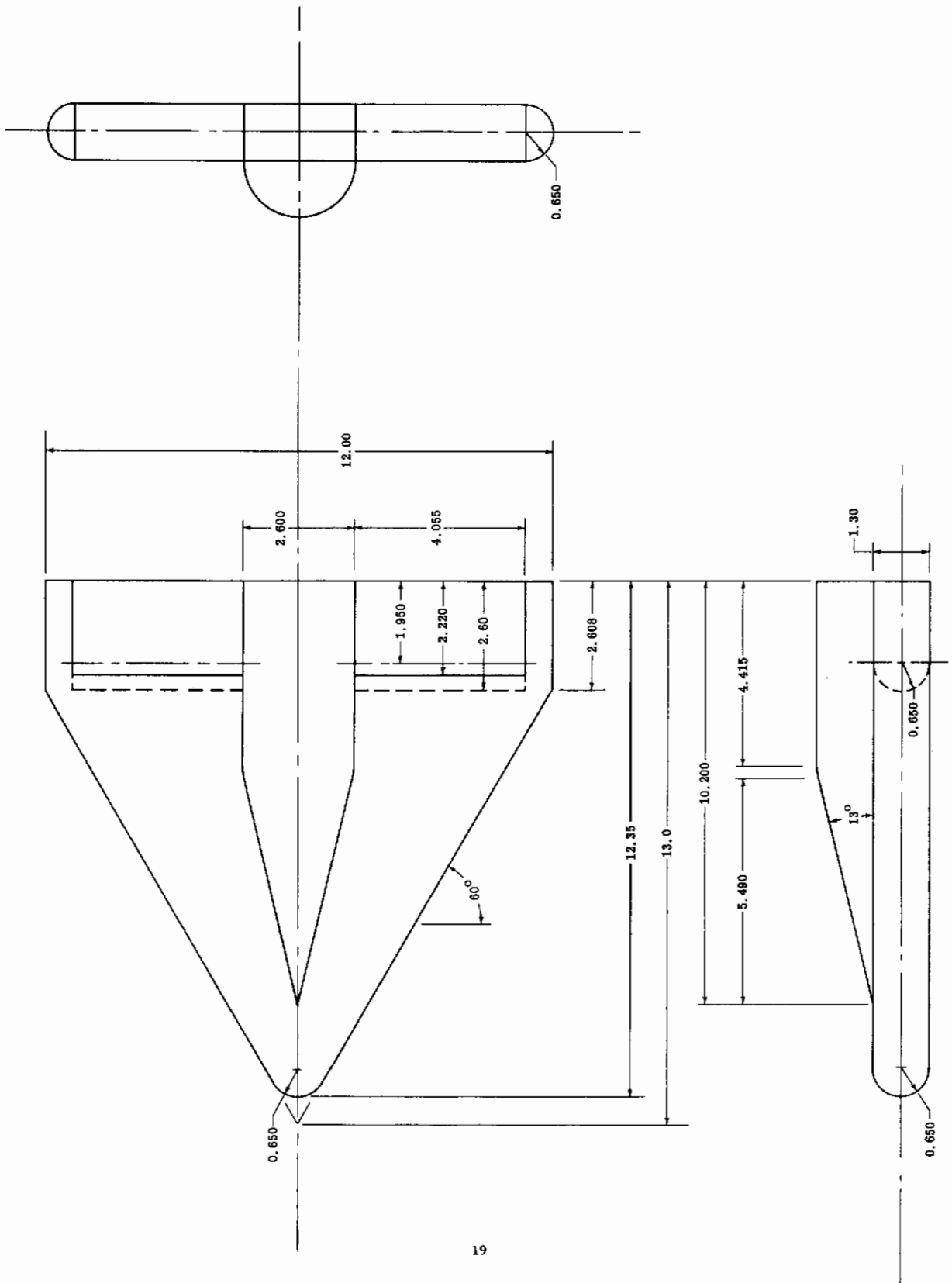


Fig. 1b Configuration I - Basic Wing-Body

Contrails

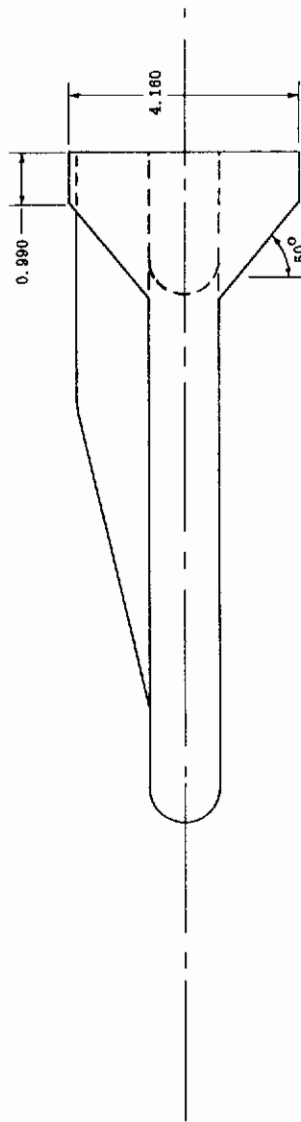
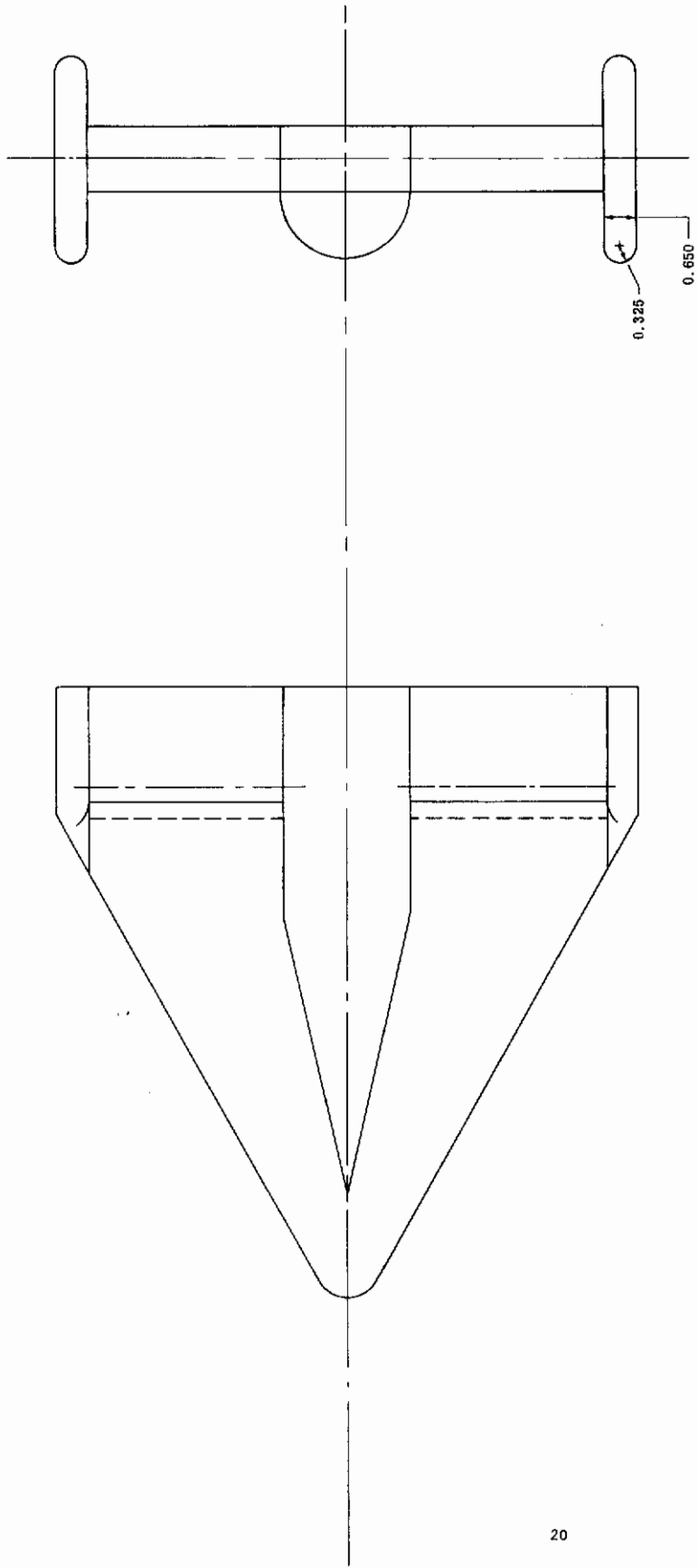


Fig. 1c Configuration IV - Basic Wing-Body + Tip Fins
(for dimensions see Fig. 1b)

Contrails

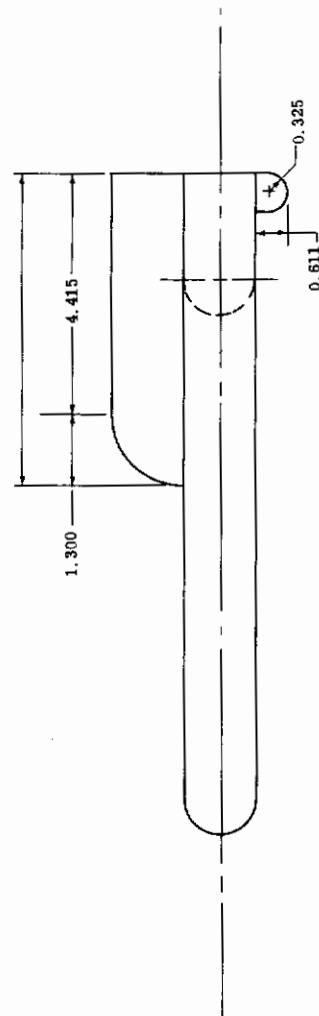
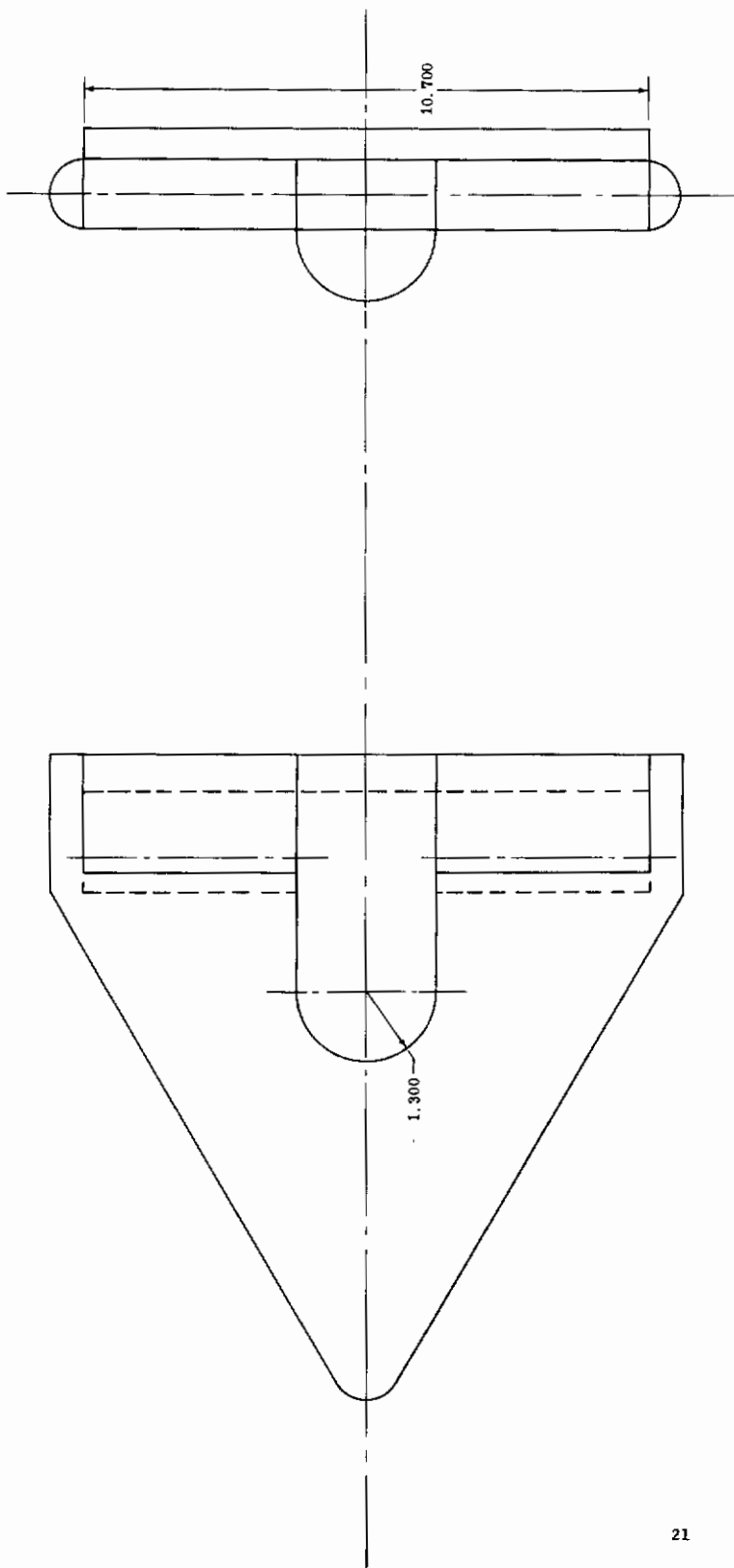


Fig. 1d Configuration VII - Wing-Blunt Body + Full Span Plug Spoiler (for dimensions see Fig. 1b)

Contrails

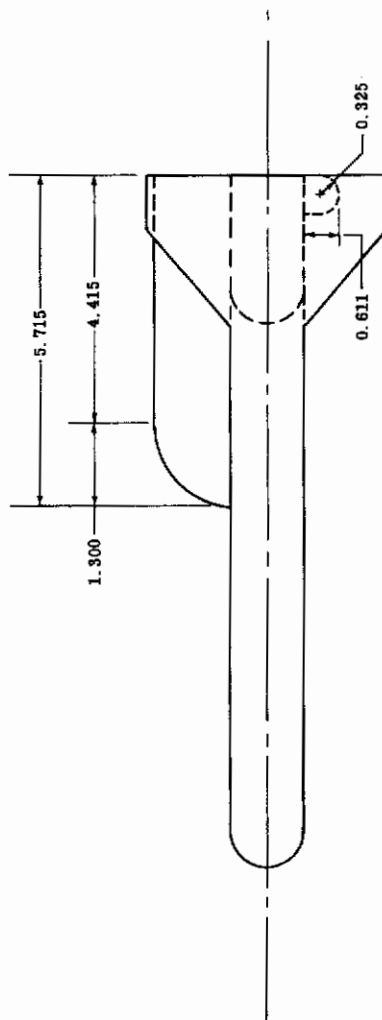
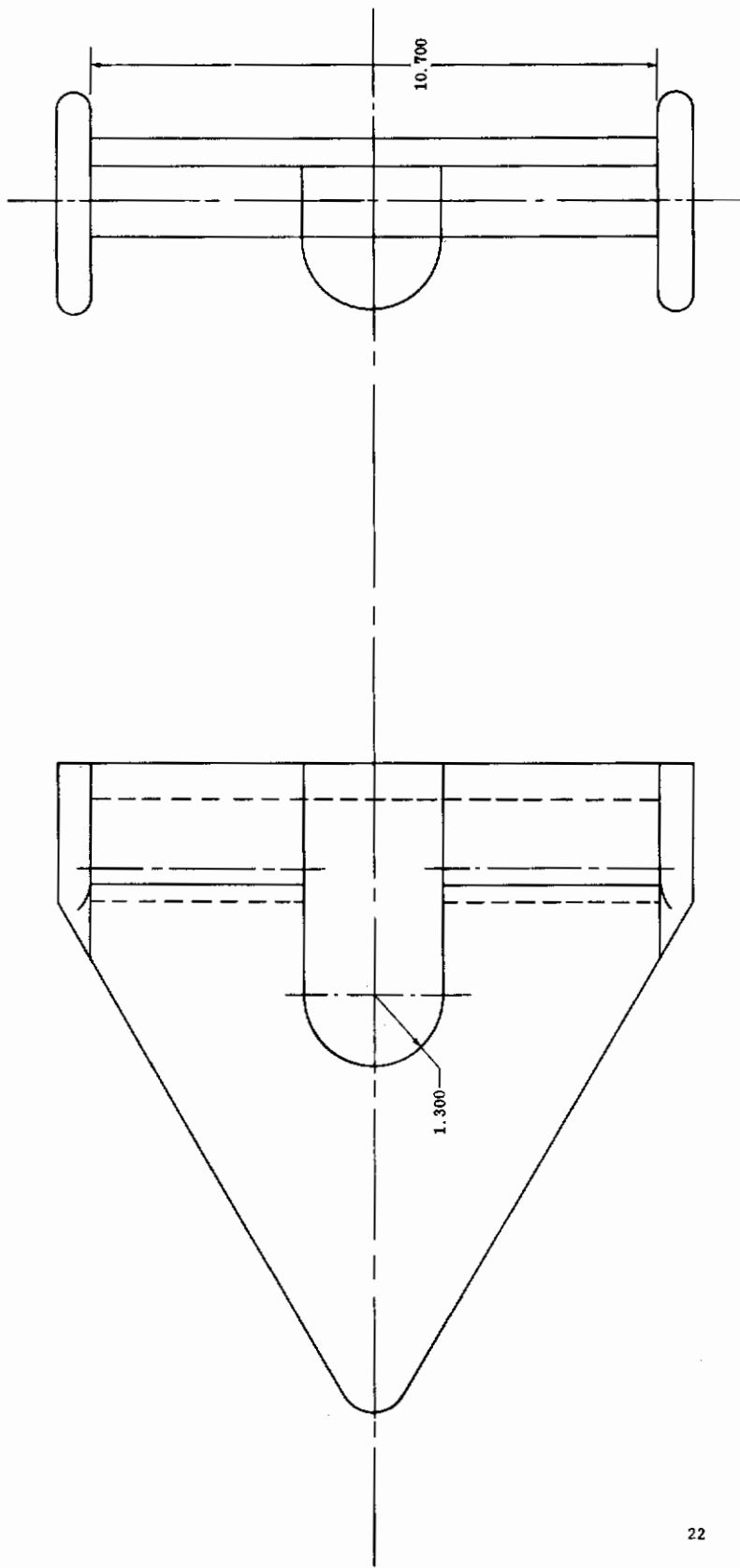


Fig. 1e Configuration VIII - Wing-Blunt Body + Full Span
Plug Spoiler + Tip Fins (for dimensions see Figs.
1b, 1c, 1d)

Contrails

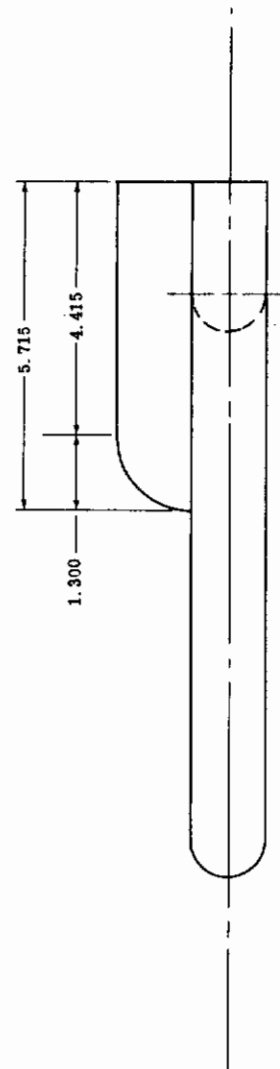
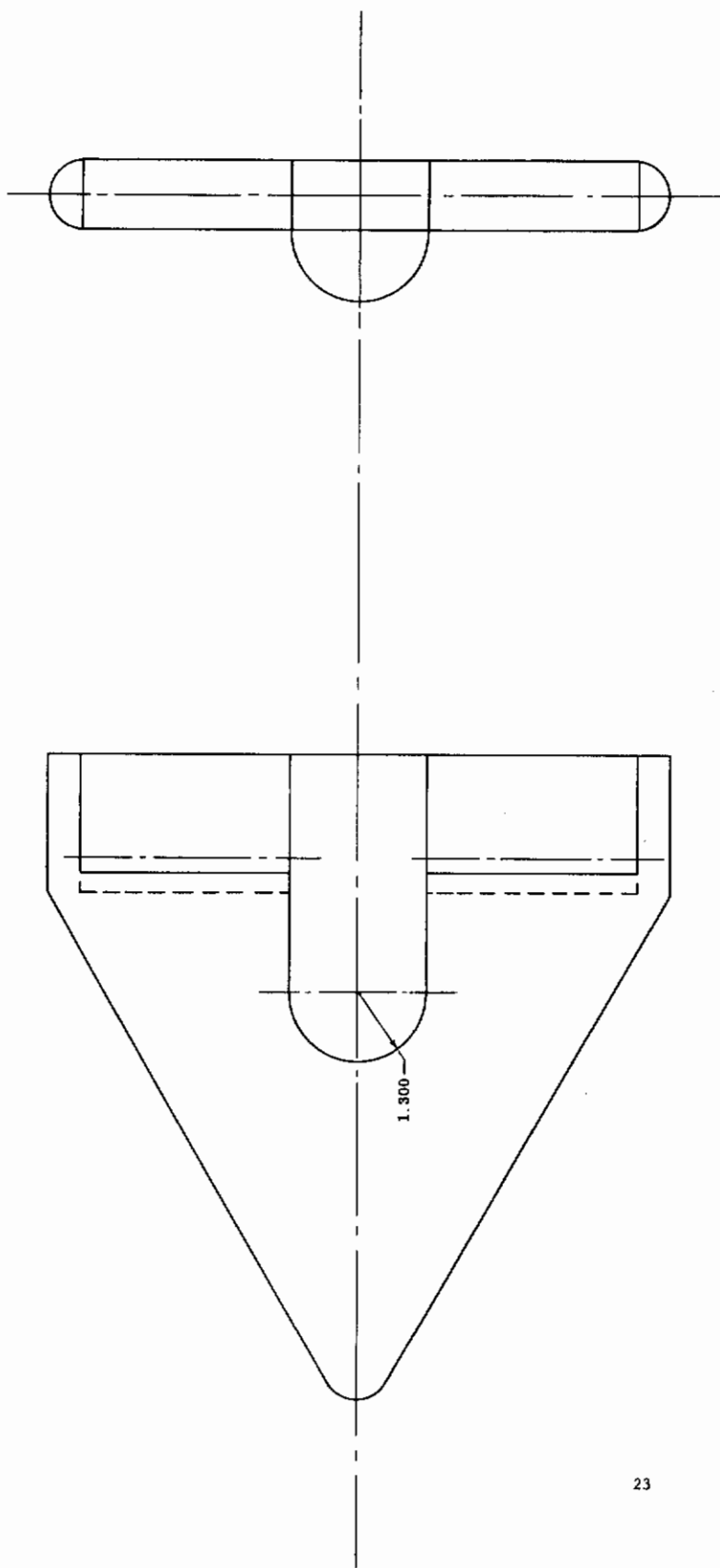


Fig. 1f Configuration IX - Wing-Blunt Body
(for dimensions see Figs. 1b, 1d)

Contrails

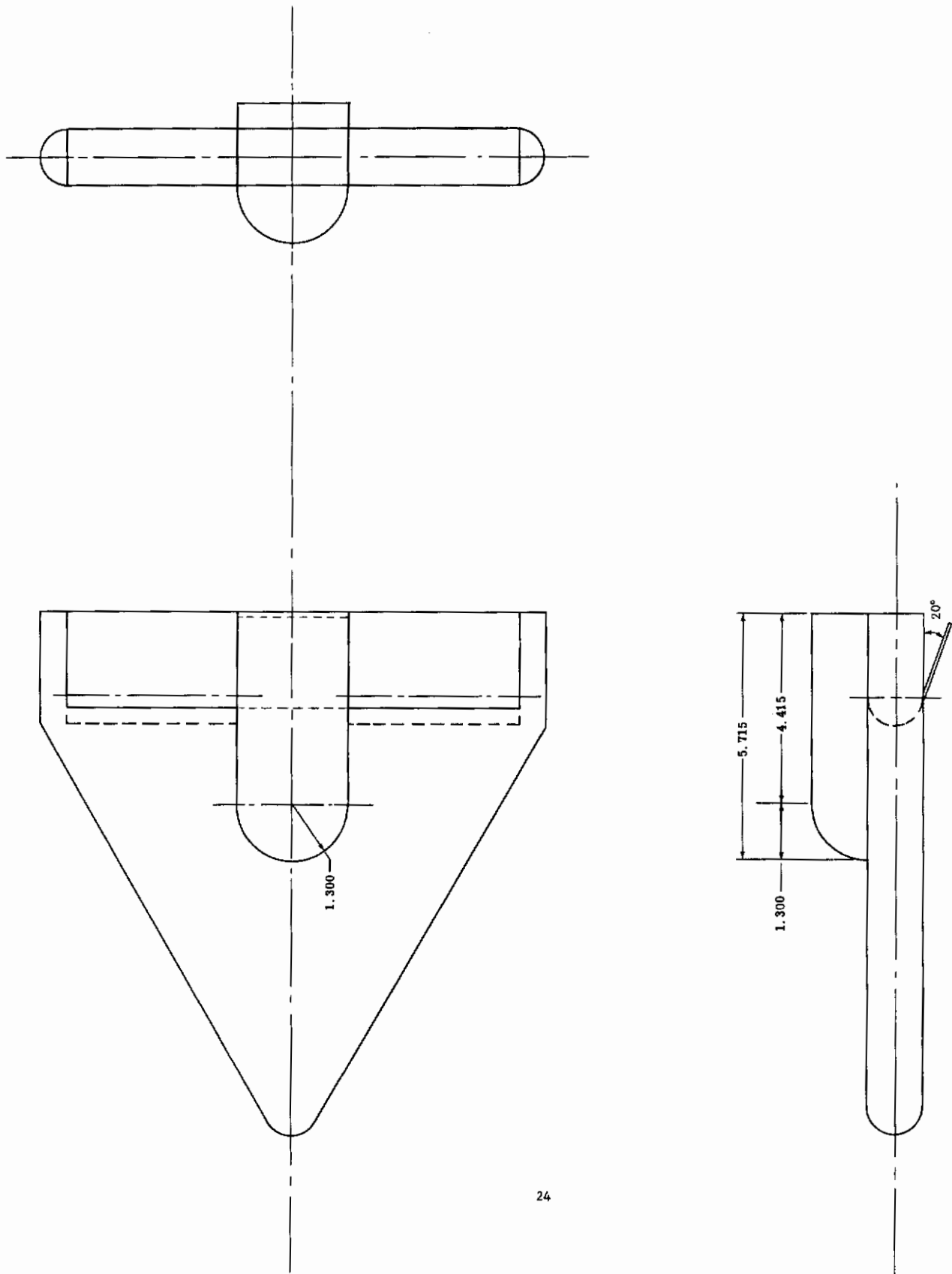


Fig. 1g Configuration X - Wing-Blunt Body + Full Span Flap (showing center flap deflected +20°)
(for dimensions see Figs. 1b, 1d)

Controls

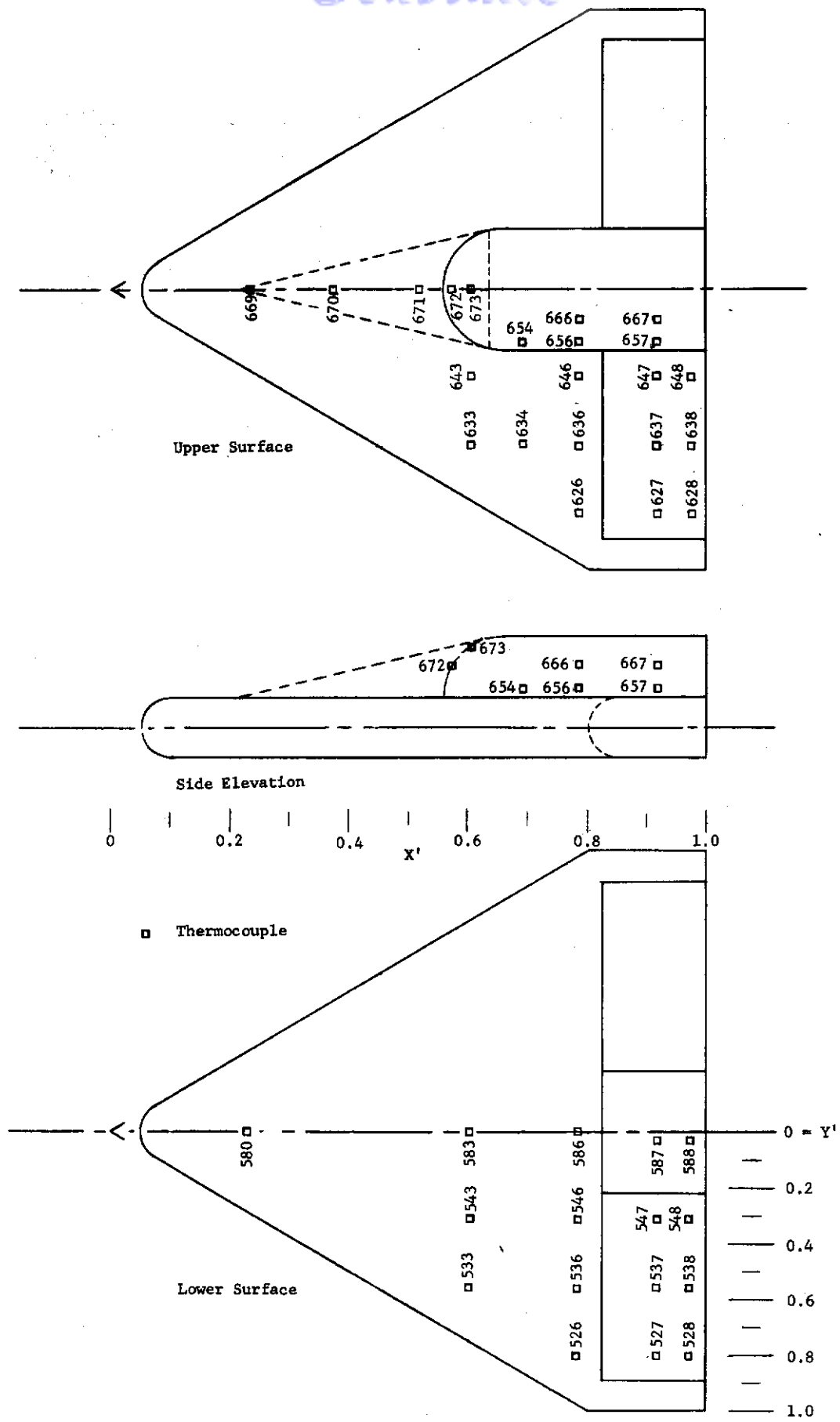


Fig. 1h Thermocouple Location and Model Coordinate System

Contrails



Fig. 11 Top View Photograph - Configuration I

Contrails

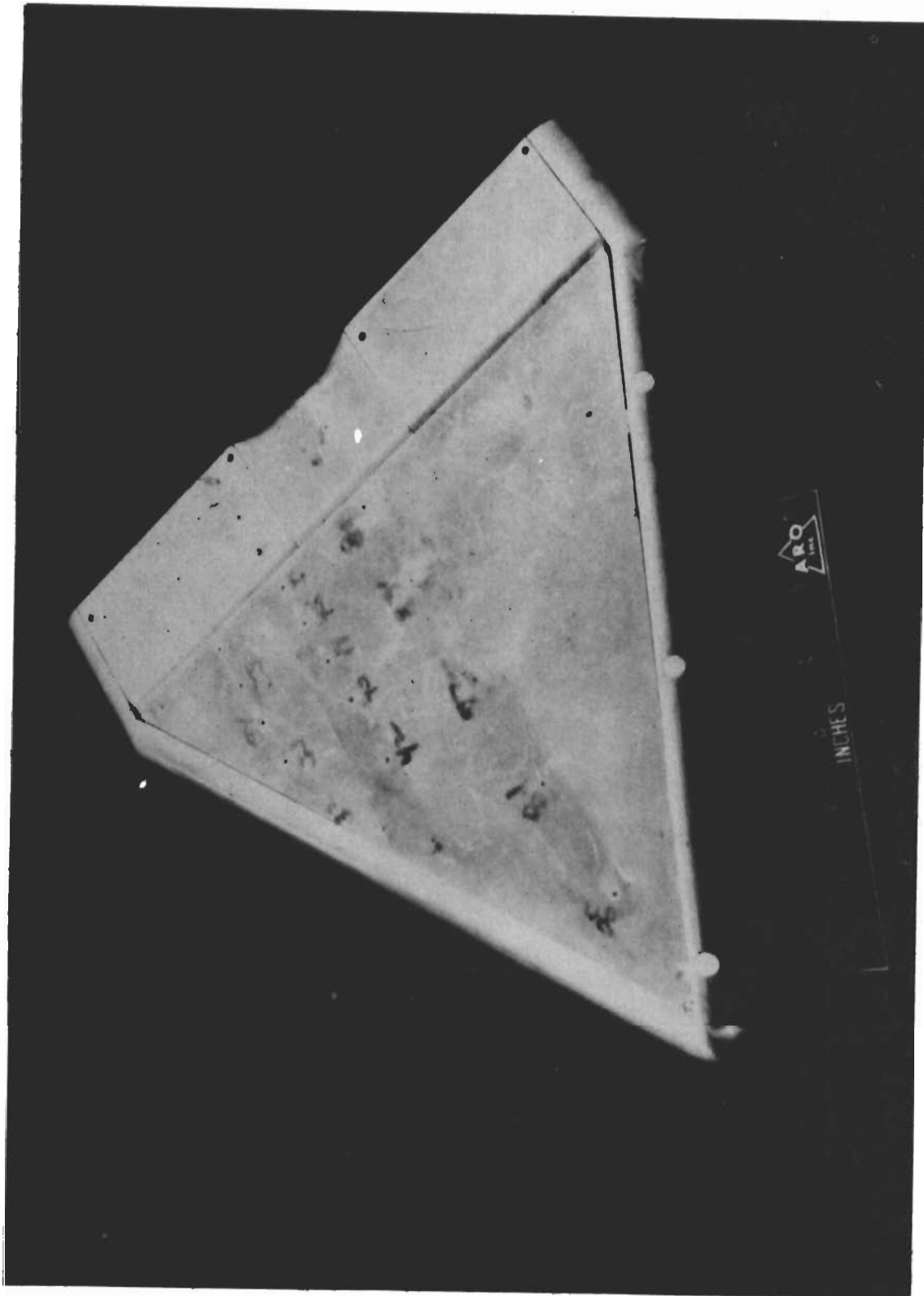


Fig. 1j Bottom View Photograph - Configuration I

Contrails

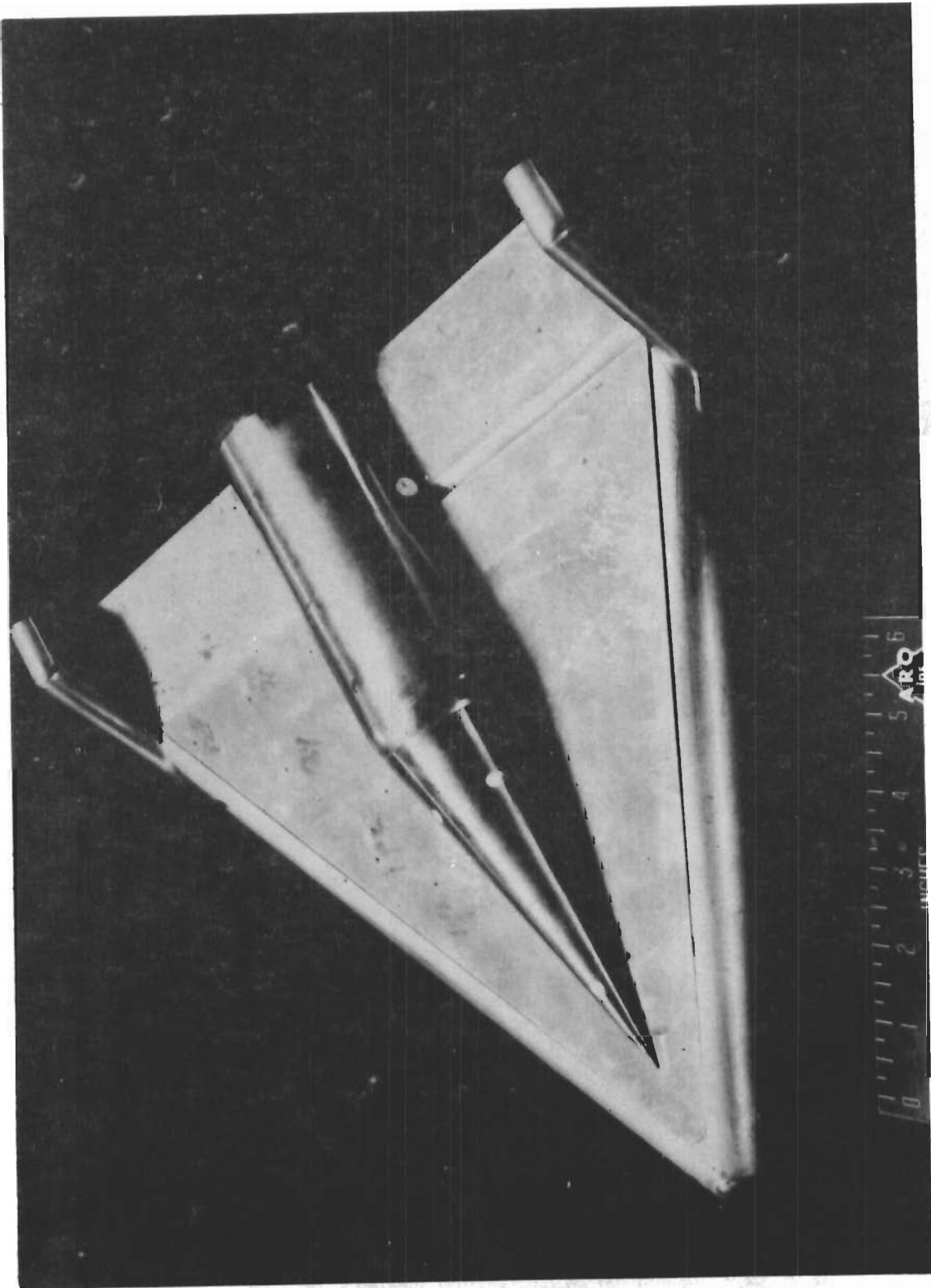


Fig. 1k Top View Photograph - Configuration IV

Contrails

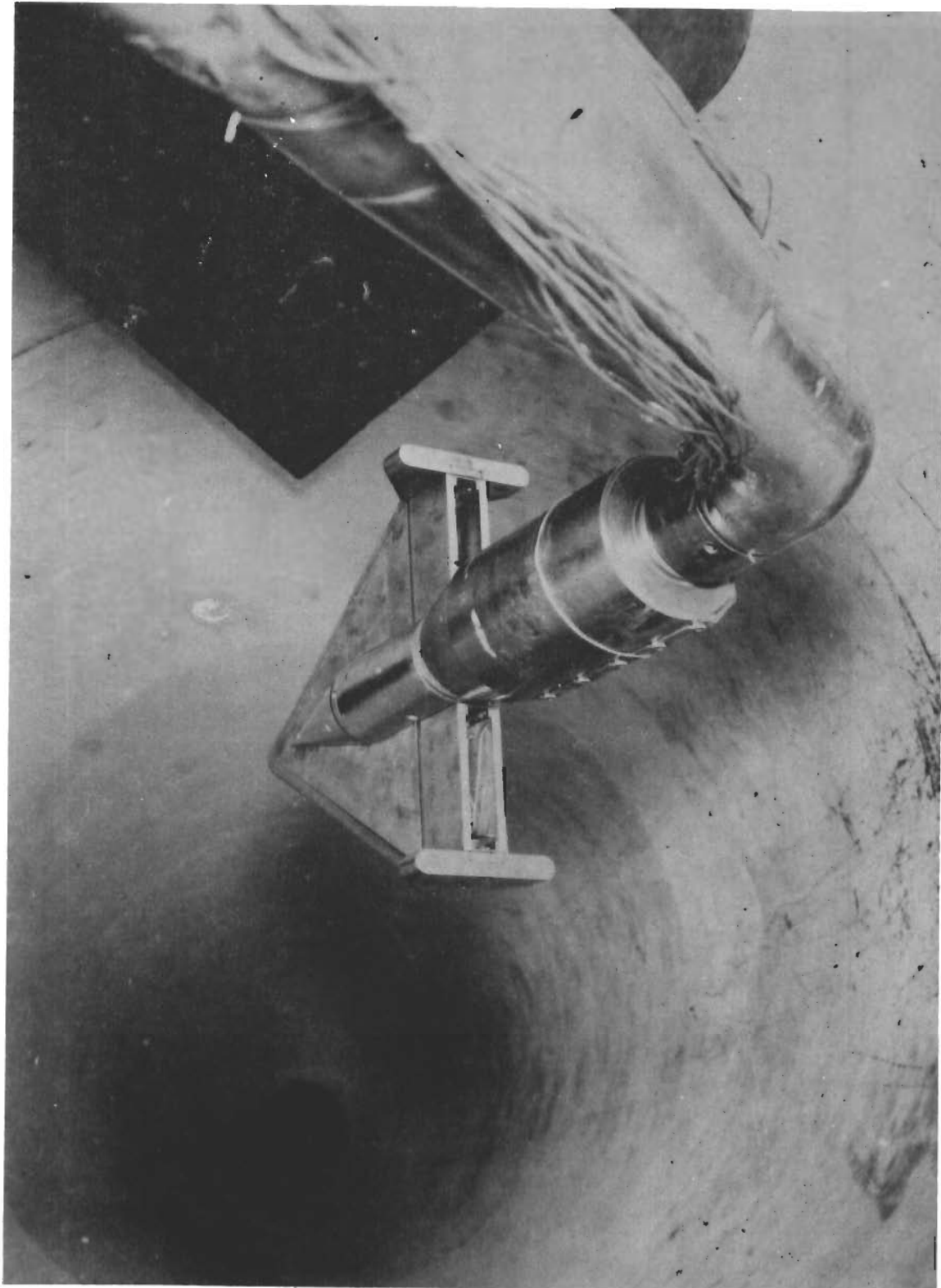


Fig. 1*f* Rear View Photograph - Configuration IV,
Mounted on Actuator Housing in the 50"
Hyperersonic Mach 8 Wind Tunnel

Contrails

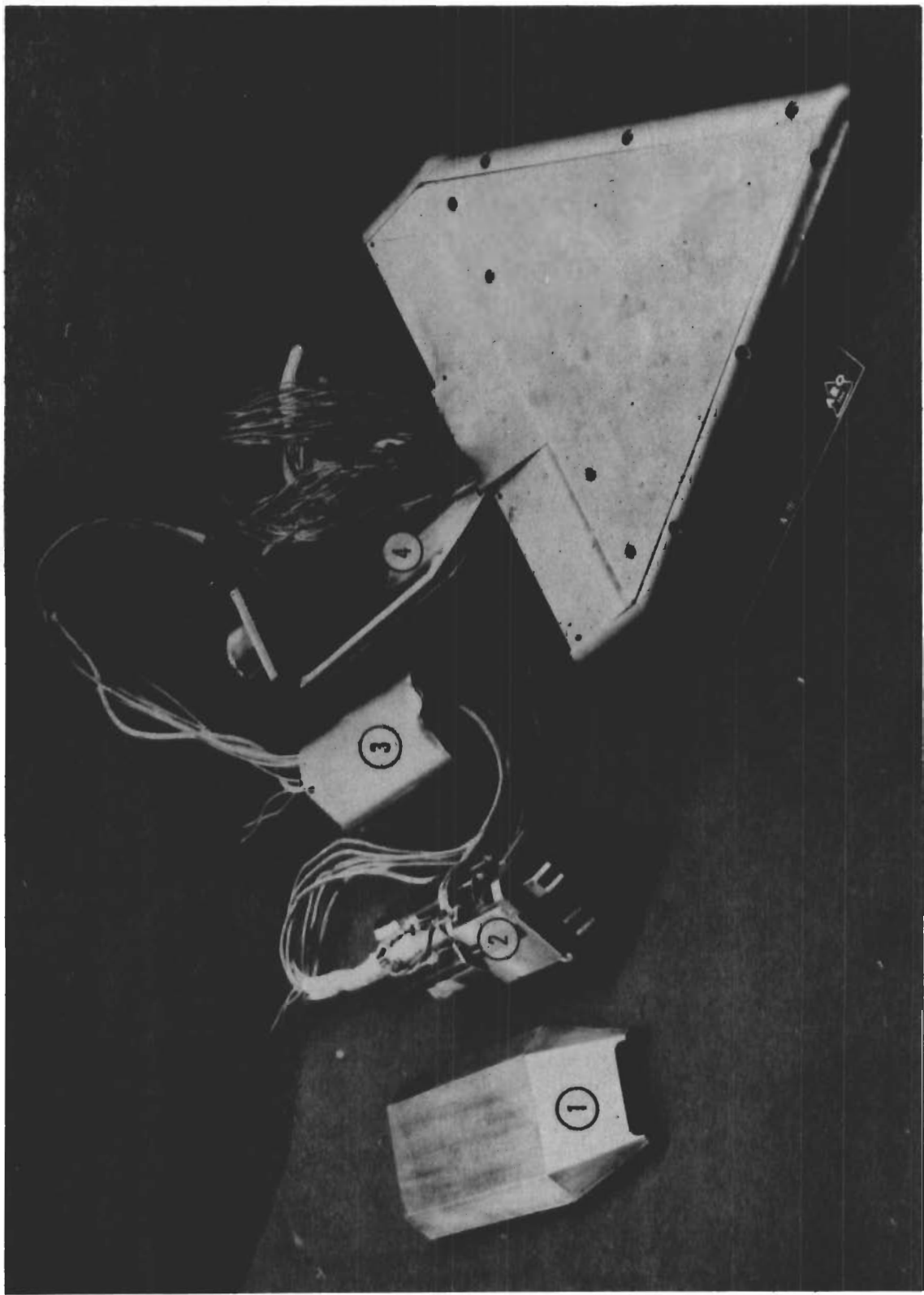


Fig. 1m Photograph - Actuator Housing Components
(1) Actuator Housing Cover, (2) Actuator Assembly,
(3) Water Jacket, (4) Actuator Housing

Controls

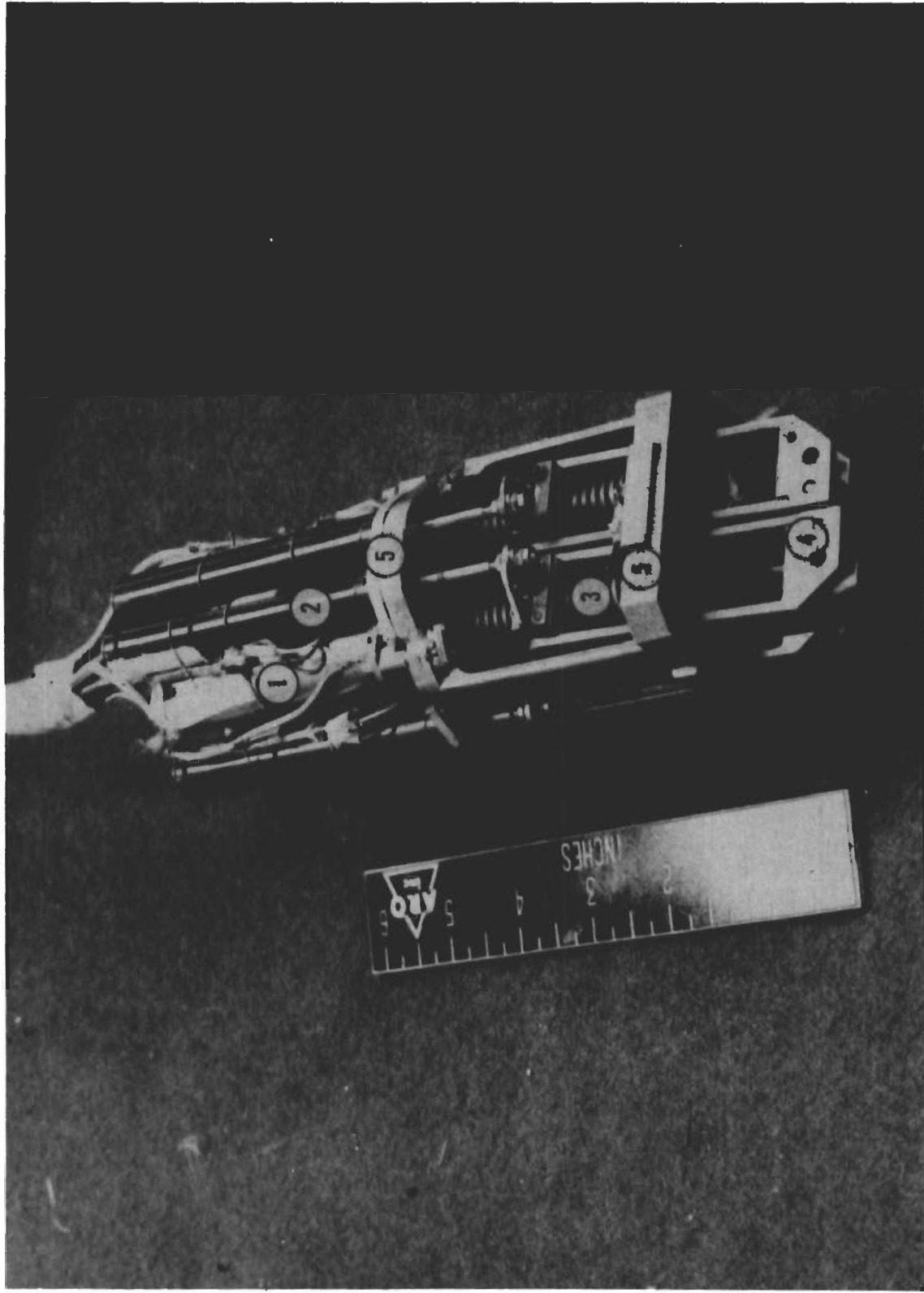


Fig. In Photograph - Actuator Assembly
(1) Electric Motors, (2) Potentiometers,
(3) Lead Screws, (4) Control Rods,
(5) Water Cooled Bulkheads

Controls

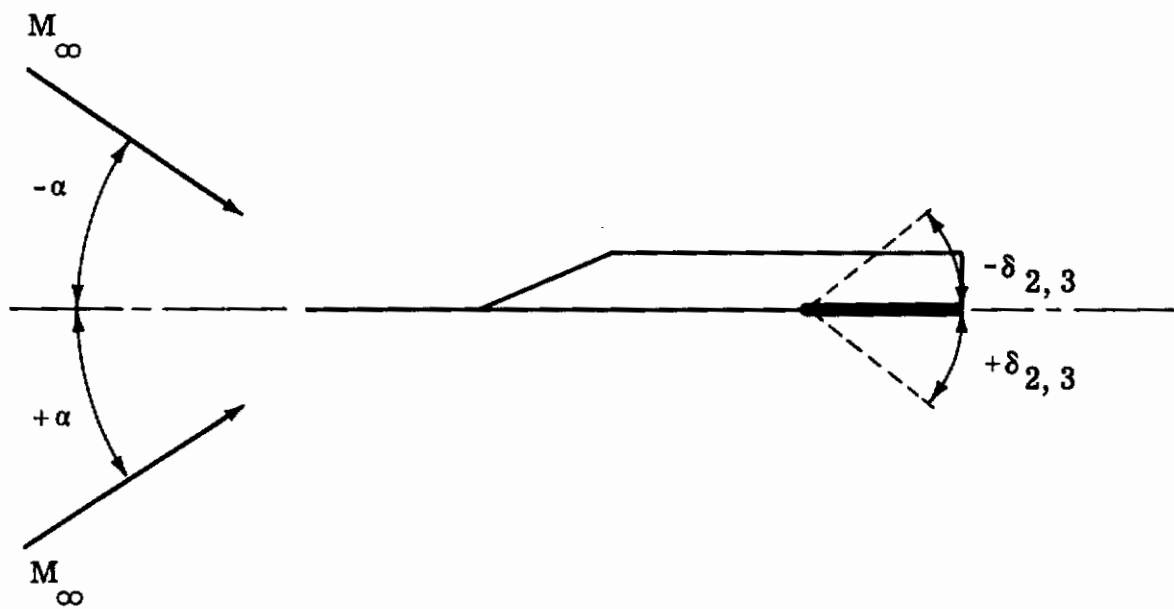


Fig. 2 Sign Convention for Model Angles
and Control Deflection Angles

Contrails

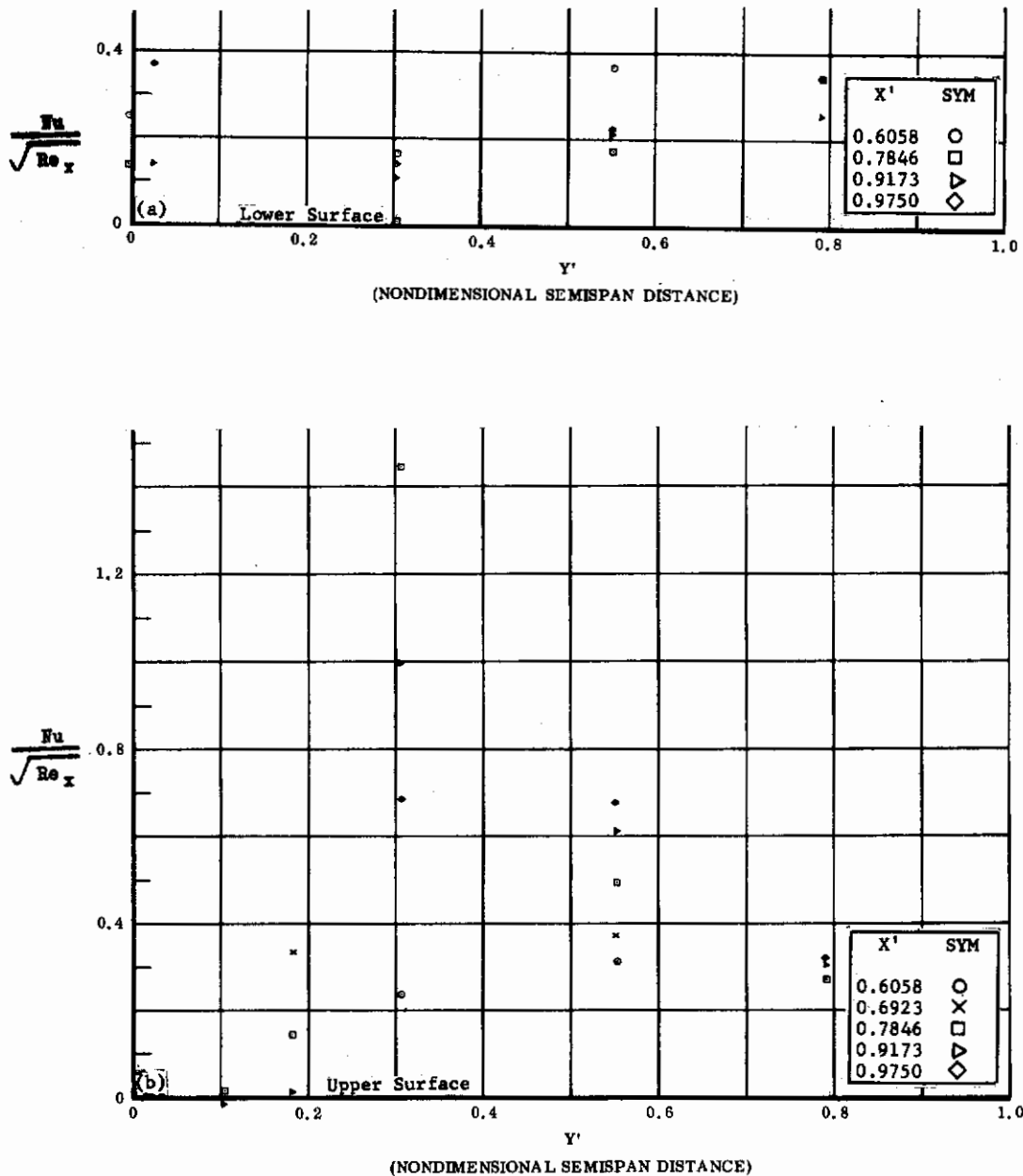


Fig. 3 Configuration I, $\alpha = 0$, $s_2 = s_3 = 0$

- a) $Nu/\sqrt{Re_x}$ vs. Y' lower surface.
- b) $Nu/\sqrt{Re_x}$ vs. Y' upper surface

Contrails

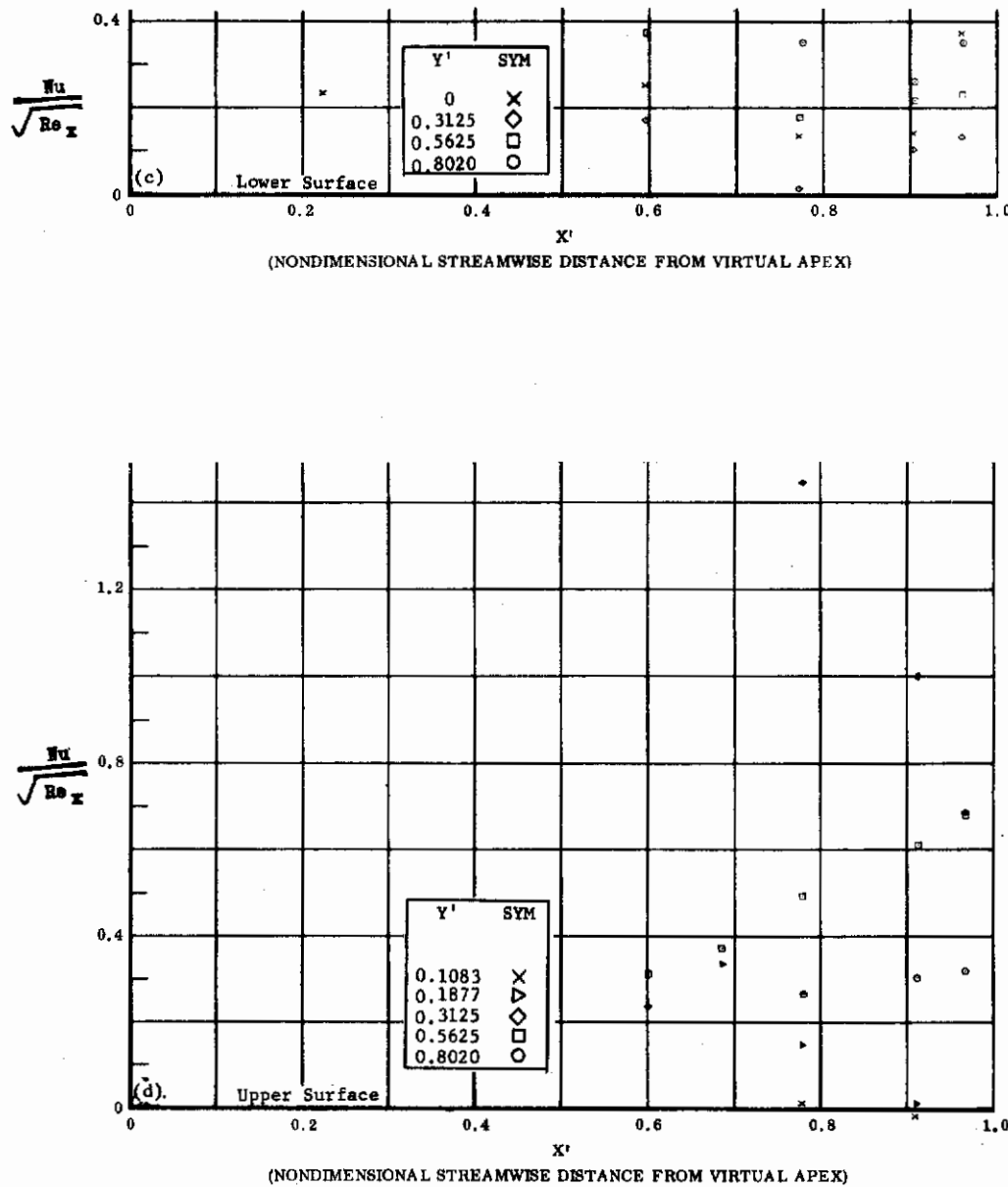


Fig. 3 Configuration I, $\alpha = 0$, $b_2 = b_3 = 0$

c) $Nu/\sqrt{Re_x}$ vs. X' lower surface

d) $Nu/\sqrt{Re_x}$ vs. X' upper surface

Contrails

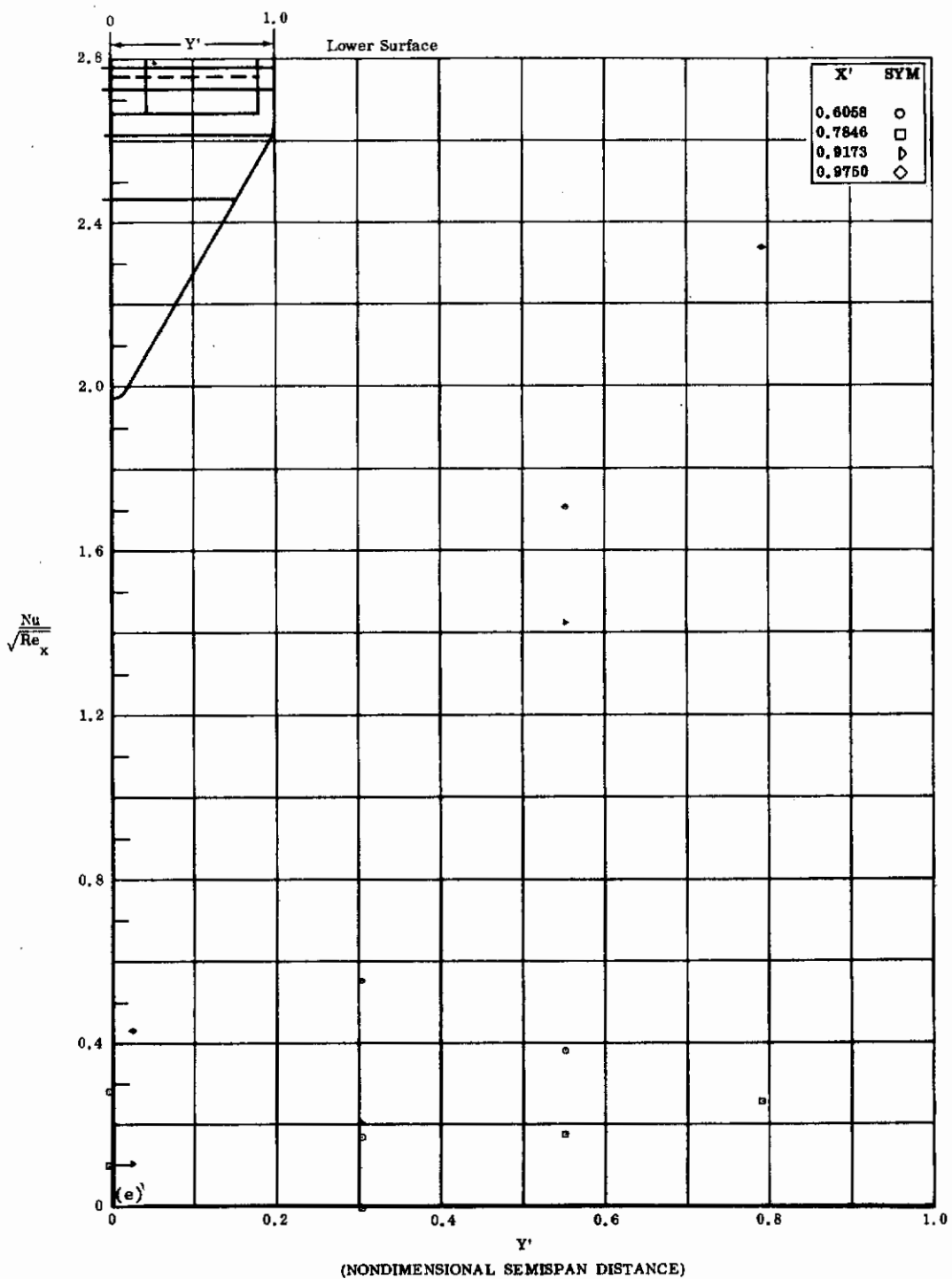


Fig. 3e Configuration I, $\alpha = 0$, $\delta_2 = \delta_3 = +10$
 $Nu/\sqrt{Re_x}$ vs. Y' lower surface

Contrails

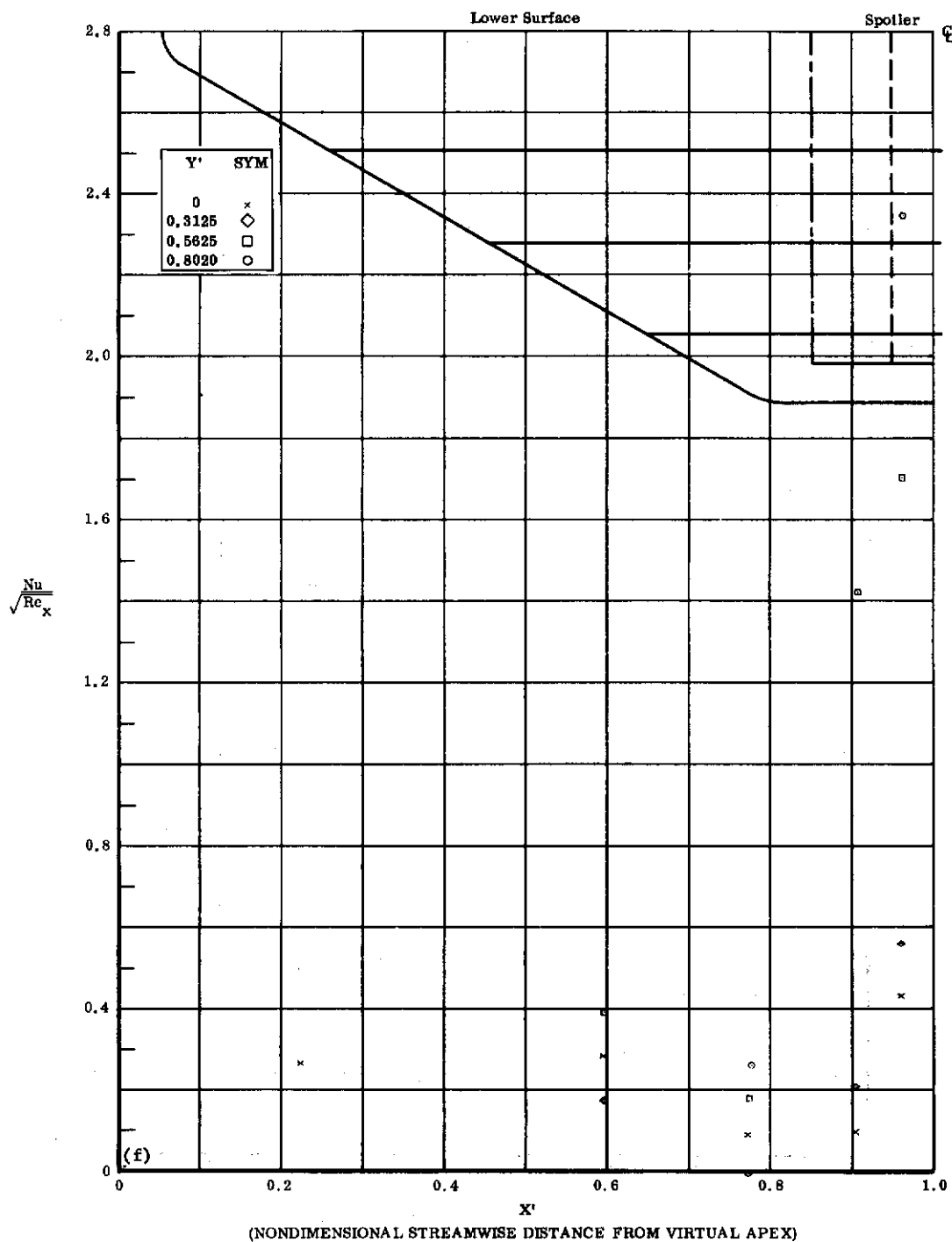


Fig. 3f Configuration I, $\alpha = 0$, $b_2 = b_3 = +10$
 $\text{Nu}/\sqrt{\text{Re}_x}$ vs. X' lower surface

Contrails

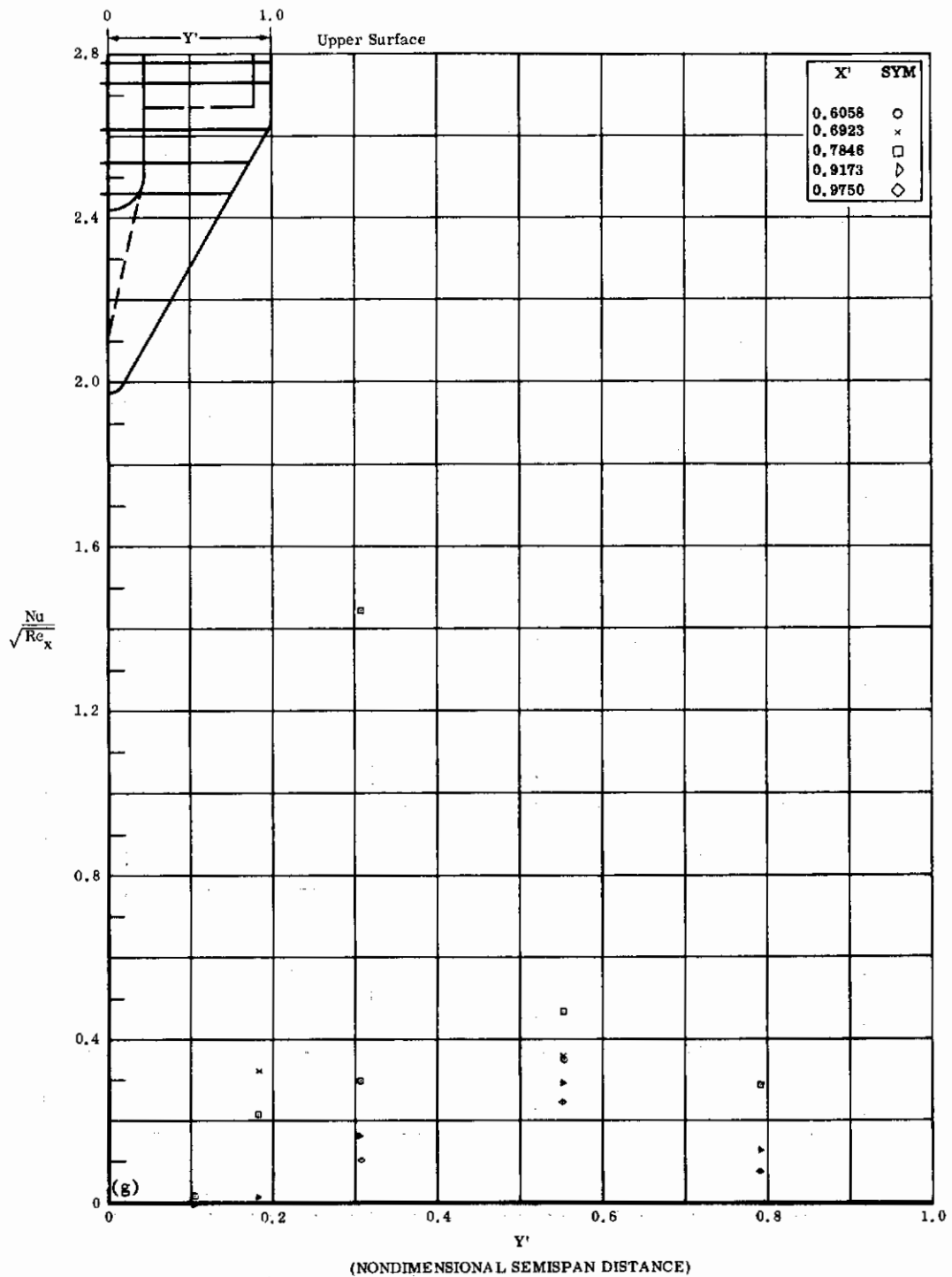


Fig. 3g Configuration I, $\alpha = 0$, $\delta_2 = \delta_3 = +10$
 $Nu/\sqrt{Re_x}$ vs. Y' upper surface

Contrails

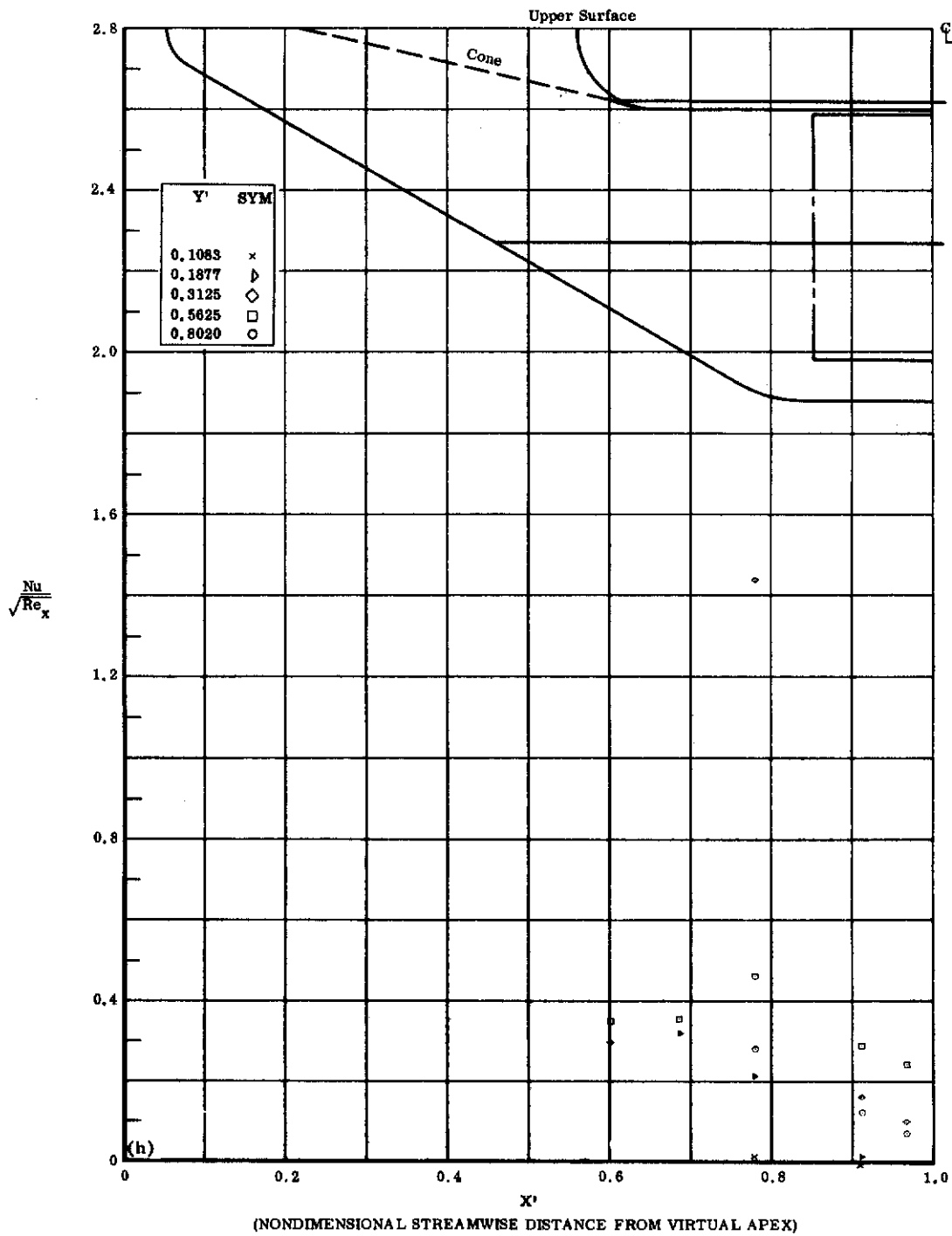


Fig. 3b Configuration I, $\alpha = 0$, $b_2 = b_3 = +10$

$\frac{Nu}{\sqrt{Re_x}}$ vs. X' upper surface

Contrails

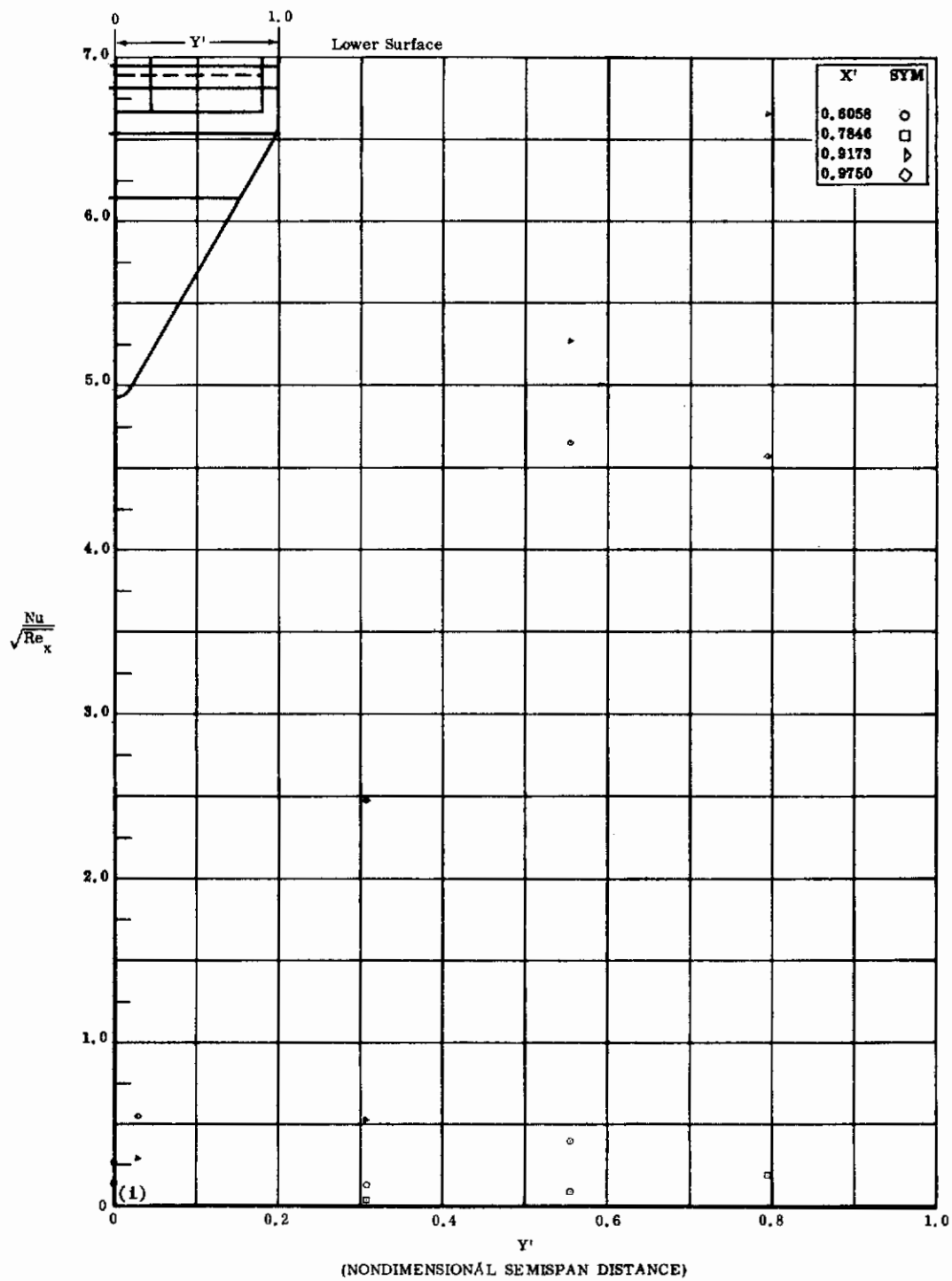


Fig. 31 Configuration I, $\alpha = 0$, $\delta_2 = \delta_3 = +20$
 $Nu/\sqrt{Re_x}$ vs. Y' lower surface

Contrails

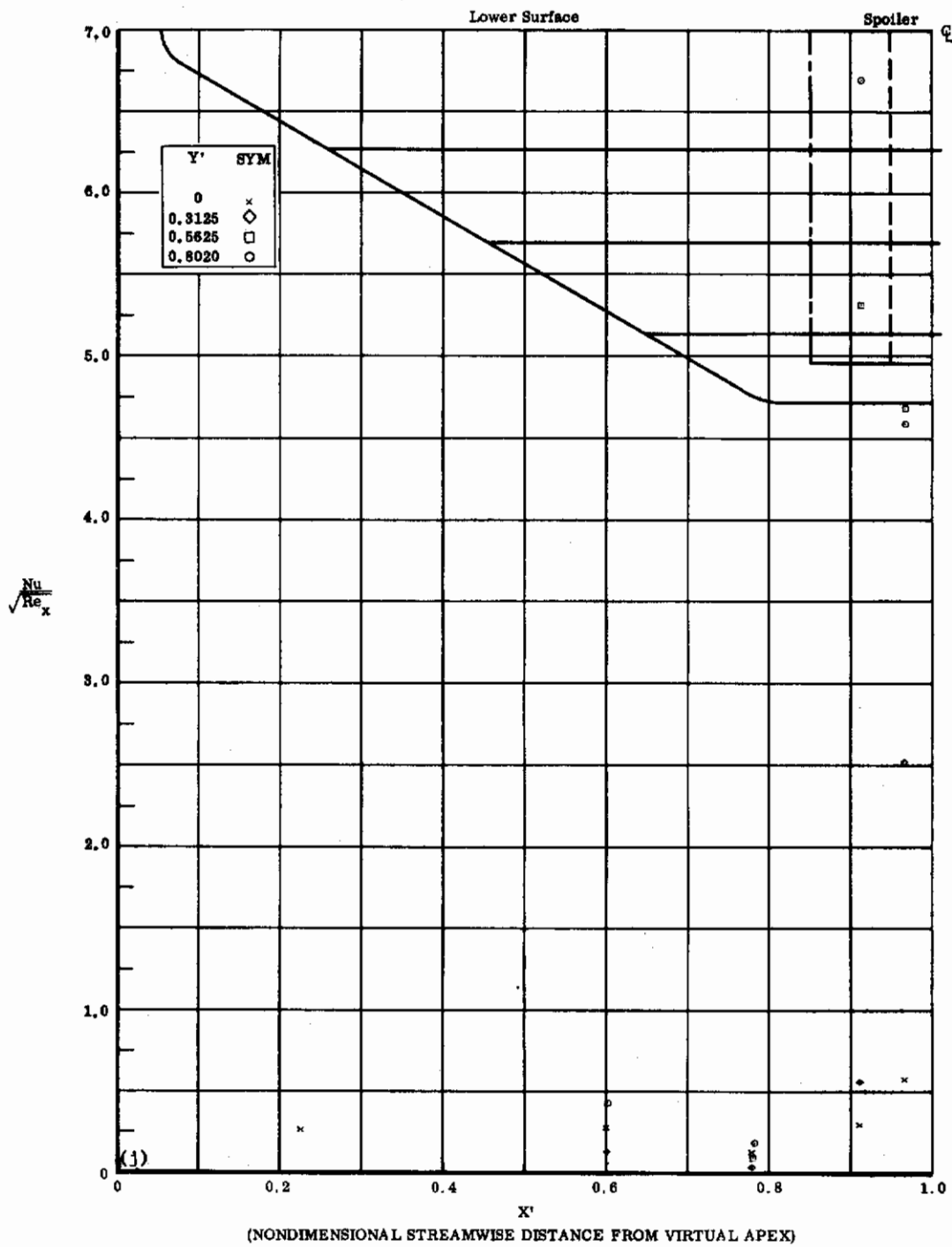


Fig. 3j Configuration I, $\alpha = 0$, $\delta_2 = \delta_3 = +20$

$\text{Nu}/\sqrt{\text{Re}_x}$ vs. X' lower surface

Contrails

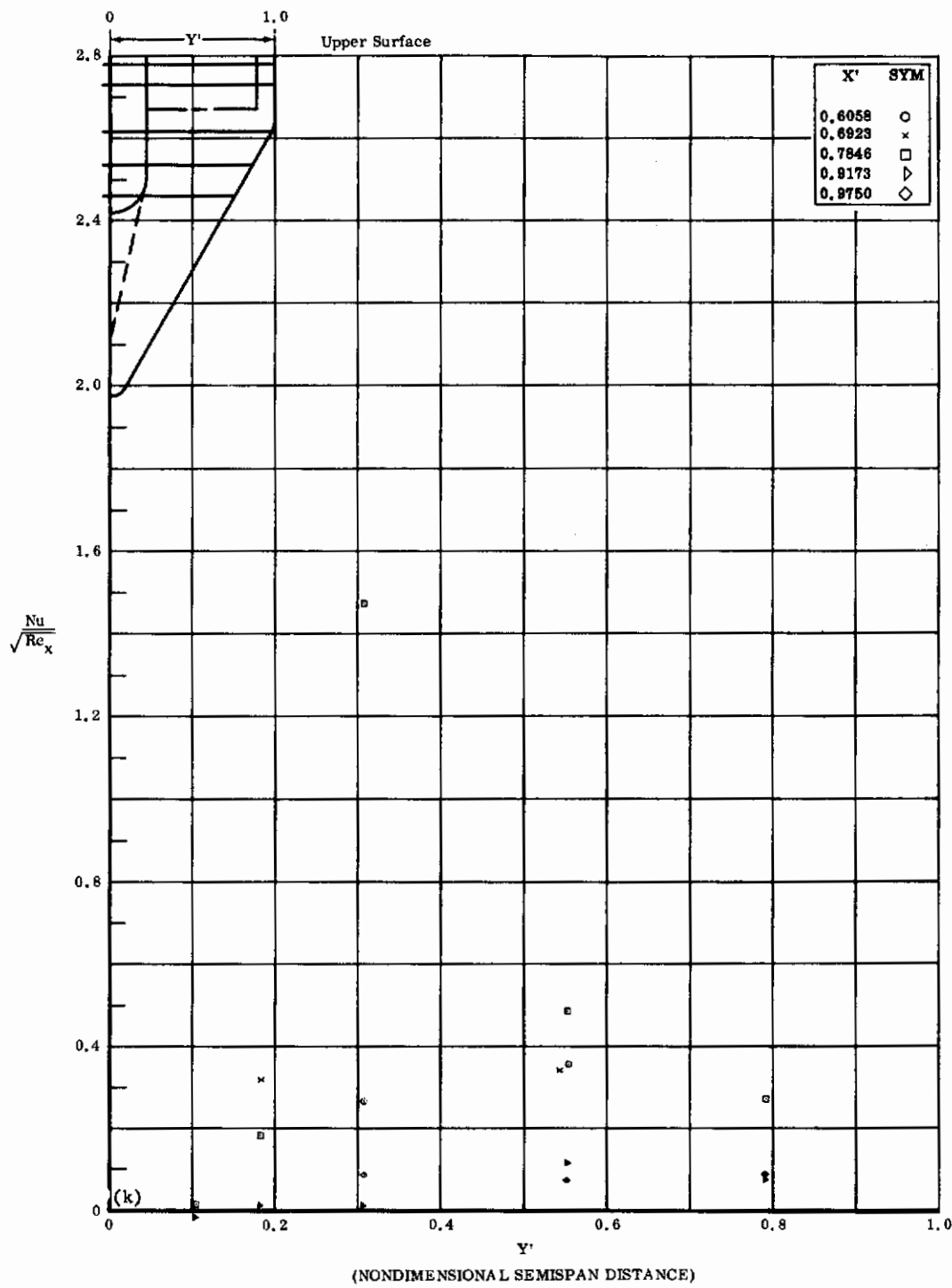


Fig. 3k Configuration I, $\alpha = 0$, $\delta_2 = \delta_3 = +20$
 $Nu/\sqrt{Re_x}$ vs. Y' upper surface

Contrails

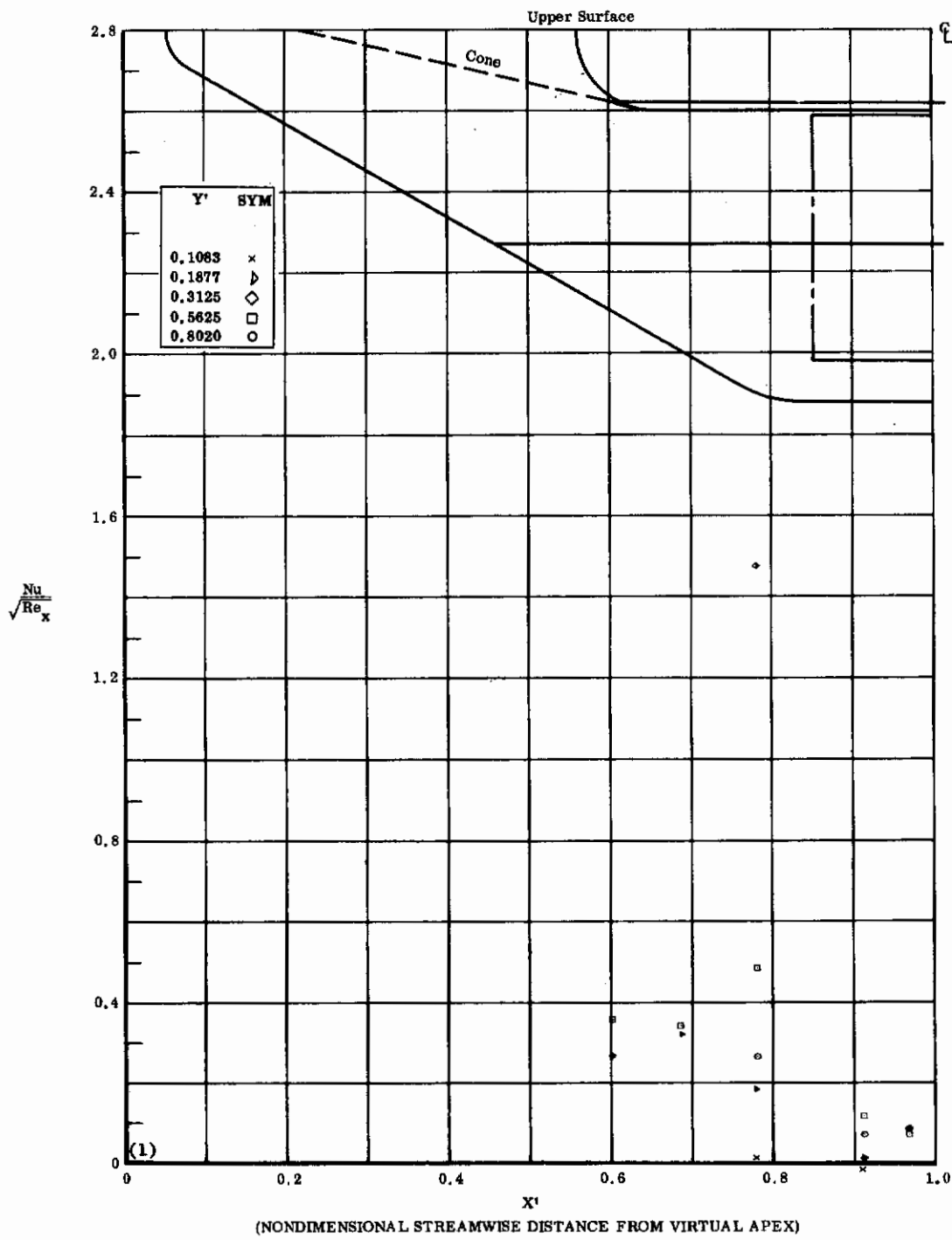


Fig. 32 Configuration I, $\alpha = 0$, $\delta_2 = \delta_3 = +20$

$Nu/\sqrt{Re_x}$ vs. X' upper surface

Contrails

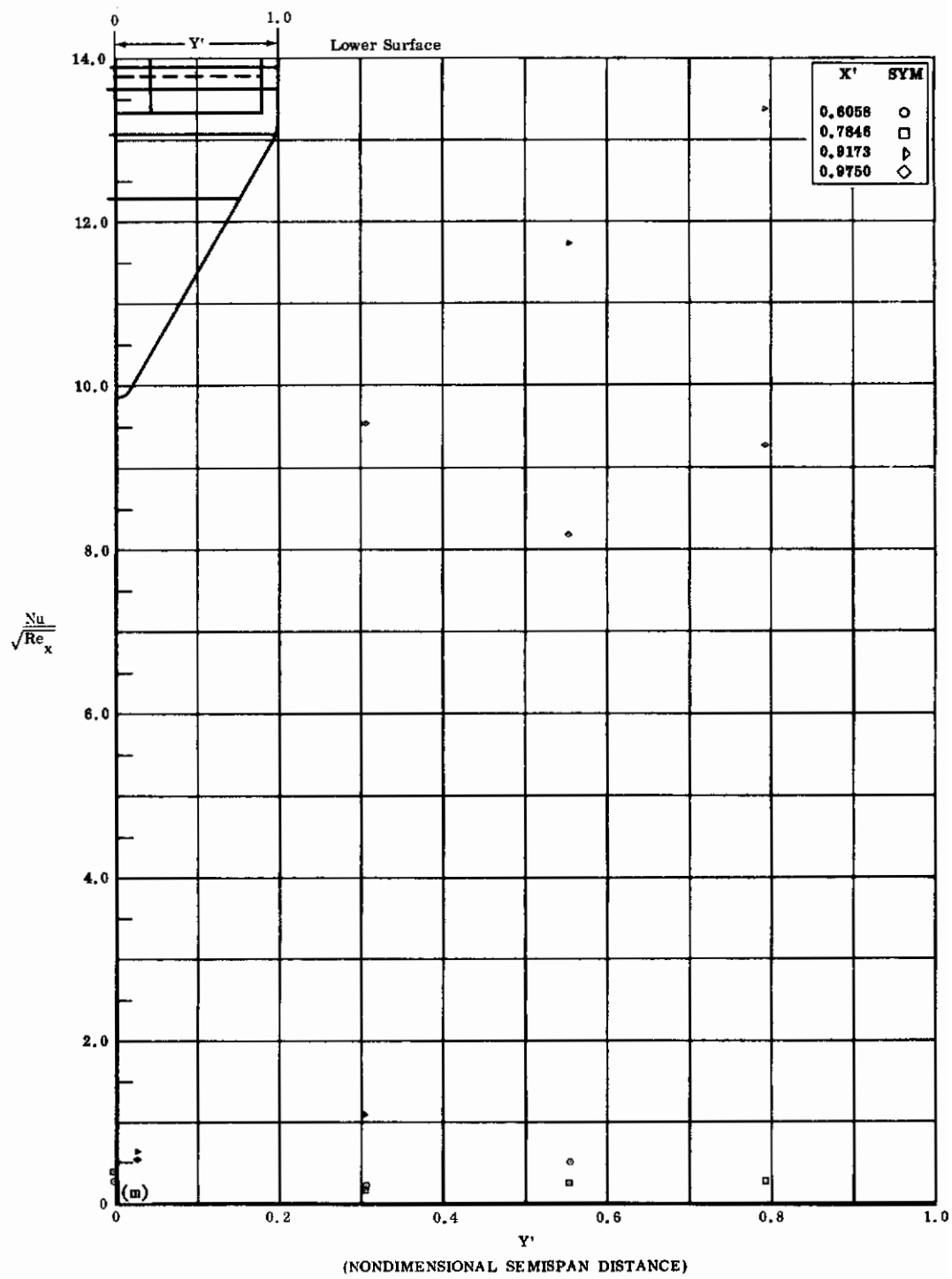


Fig. 3m Configuration I, $\alpha = 0$, $\delta_2 = \delta_3 = +30$
 $Nu/\sqrt{Re_x}$ vs. Y' lower surface

Contrails

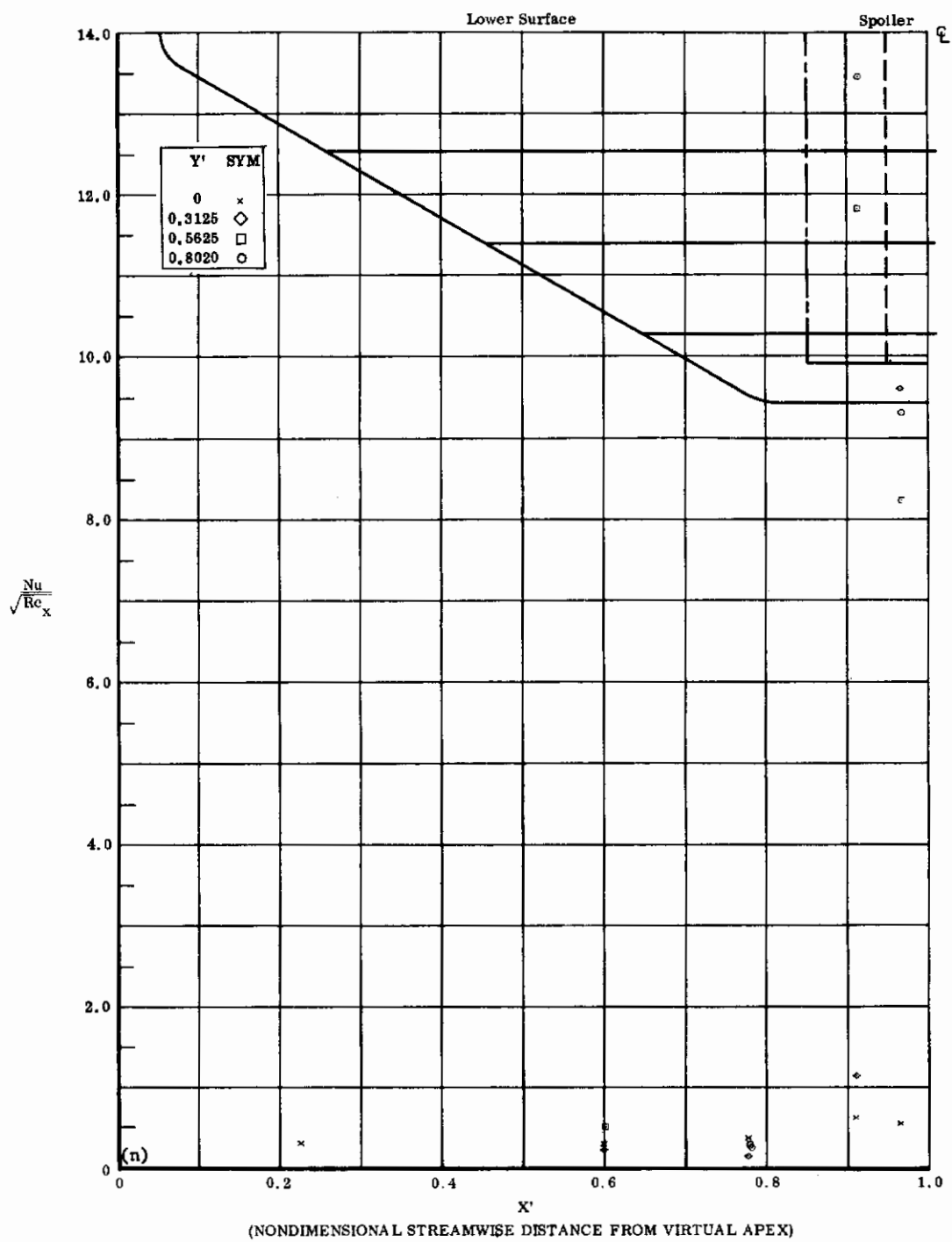


Fig. 3n Configuration I, $\alpha = 0$, $\delta_2 = \delta_3 = +30$
 $\text{Nu}/\sqrt{\text{Re}_x}$ vs. X' lower surface

Contrails

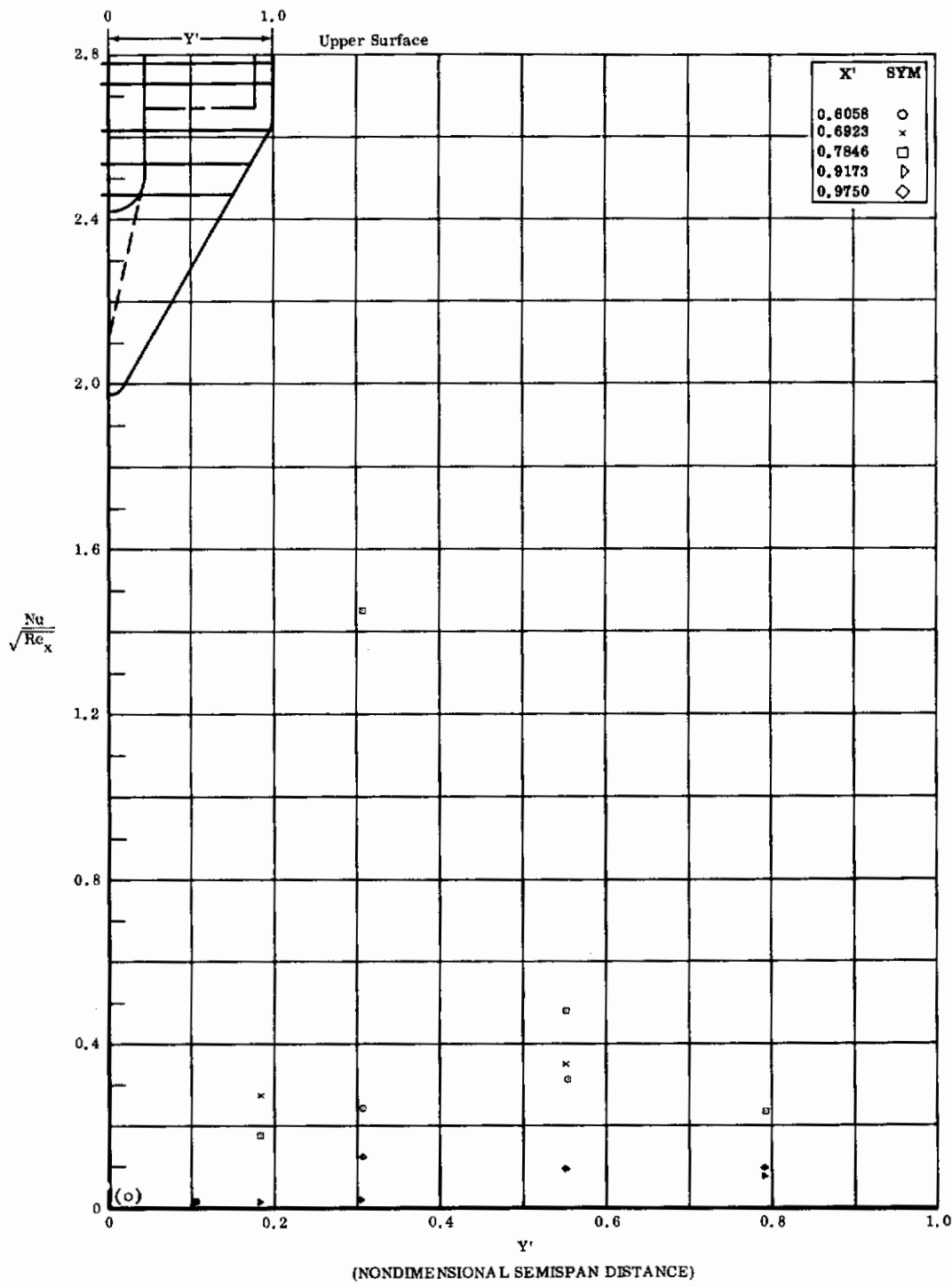


Fig. 3o Configuration I, $\alpha = 0$, $\delta_2 = \delta_3 = +30$
 $\frac{Nu}{\sqrt{Re_x}}$ vs. Y' upper surface

Contrails

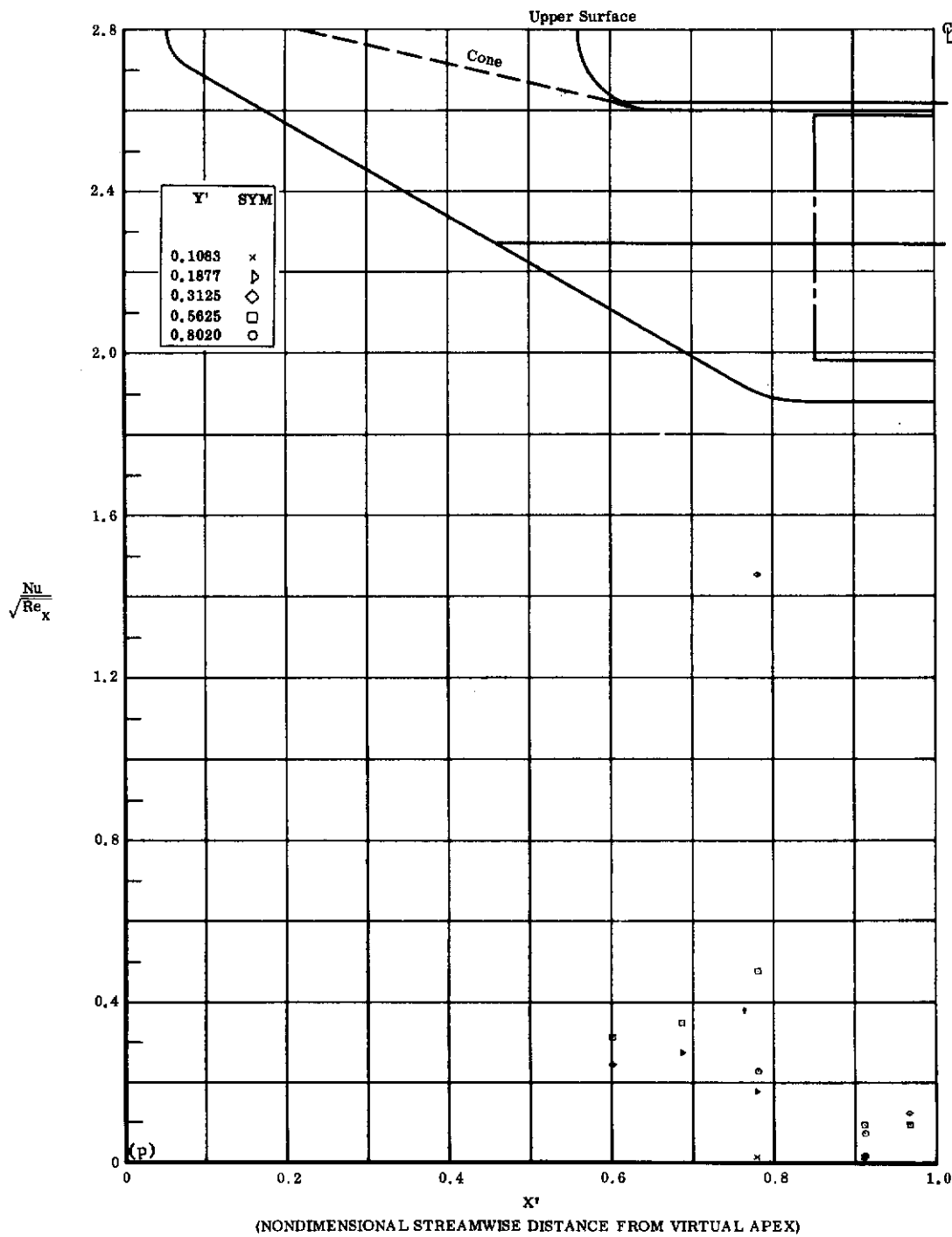


Fig. 3p Configuration I, $\alpha = 0$, $\delta_2 = \delta_3 = +30$
 $Nu/\sqrt{Re_x}$ vs. X' upper surface

Contrails

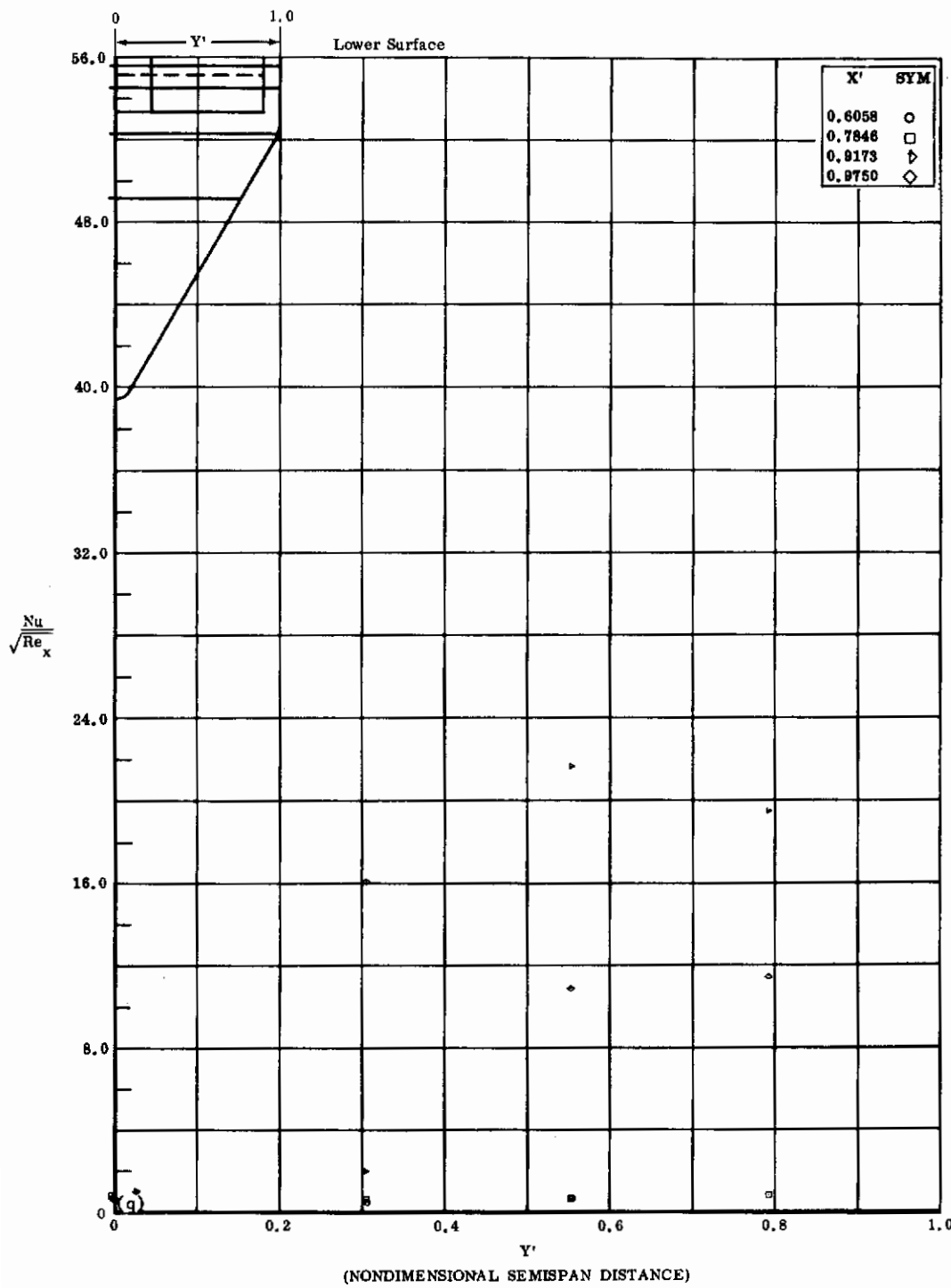


Fig. 3q Configuration I, $\alpha = 0$, $b_2 = b_3 = +39$
 $Nu/\sqrt{Re_x}$ vs. Y' lower surface

Contrails

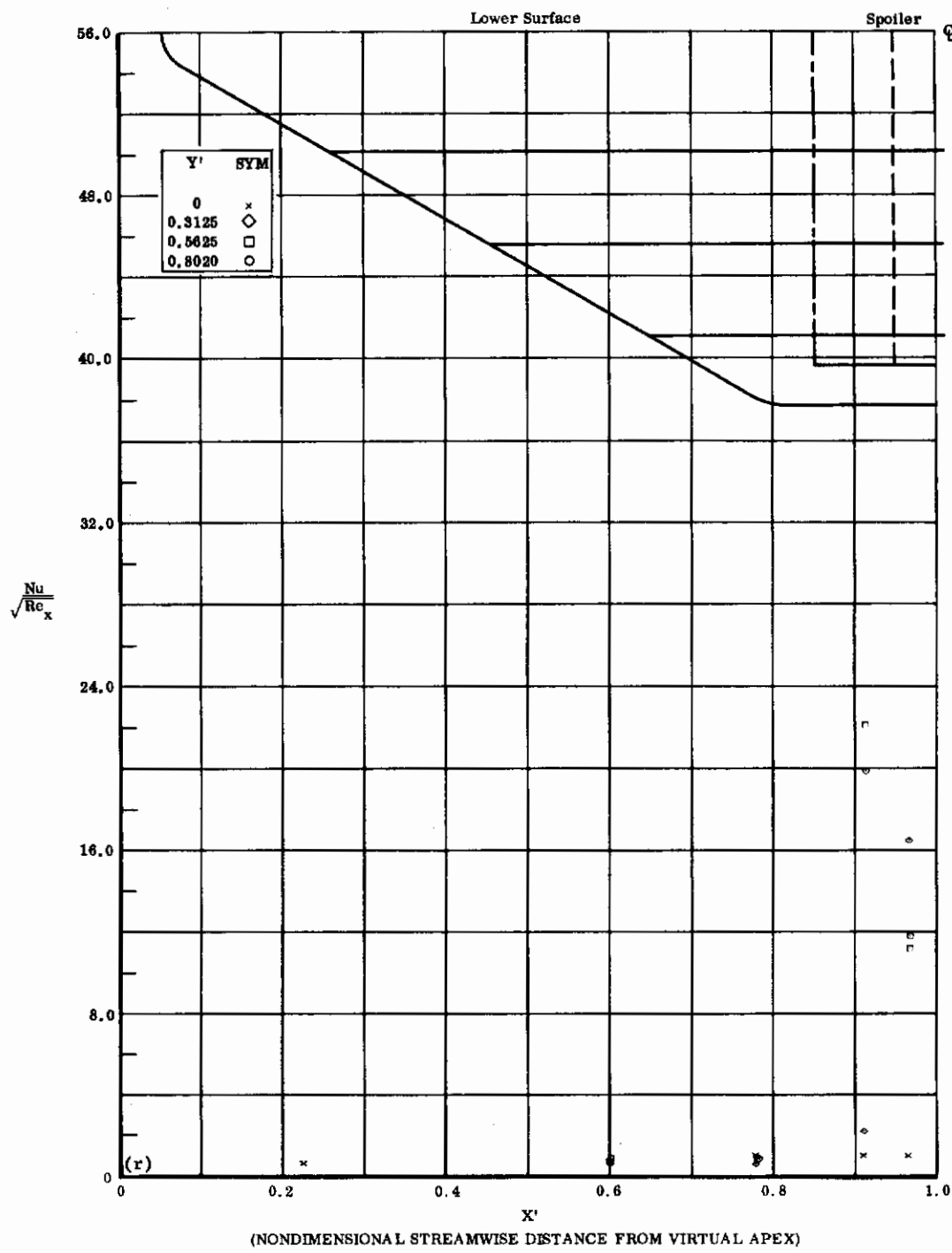


Fig. 3r Configuration I, $\alpha = 0$, $\delta_2 = \delta_3 = +39$

$Nu/\sqrt{Re_x}$ vs. X' lower surface

Contrails

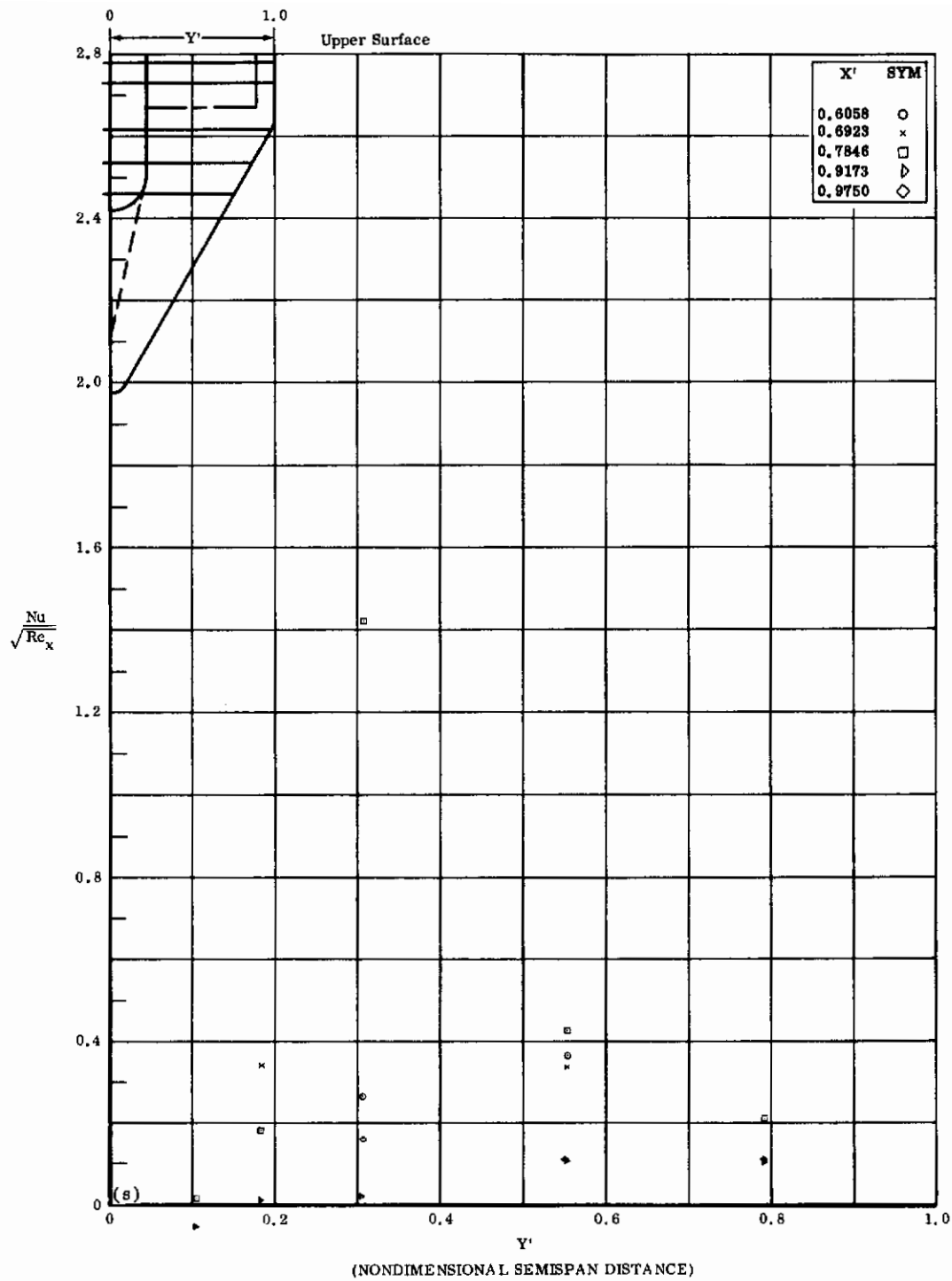


Fig. 3s Configuration I, $\alpha = 0$, $\delta_2 = \delta_3 = +39$
 $Nu/\sqrt{Re_x}$ vs. Y' upper surface

Contrails

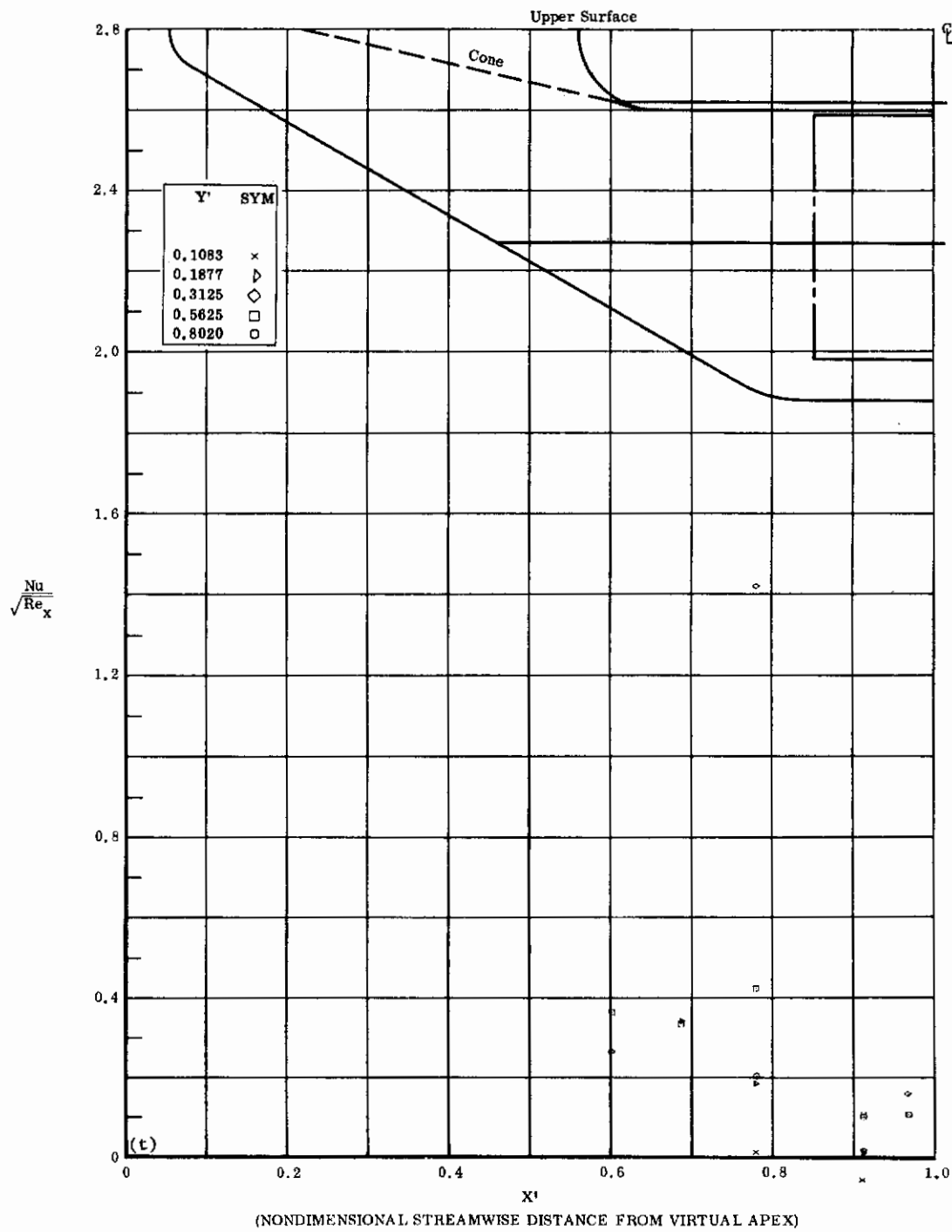


Fig. 3t Configuration I, $\alpha = 0$, $\delta_2 = \delta_3 = +39$

$Nu/\sqrt{Re_x}$ vs. X' upper surface

Contrails

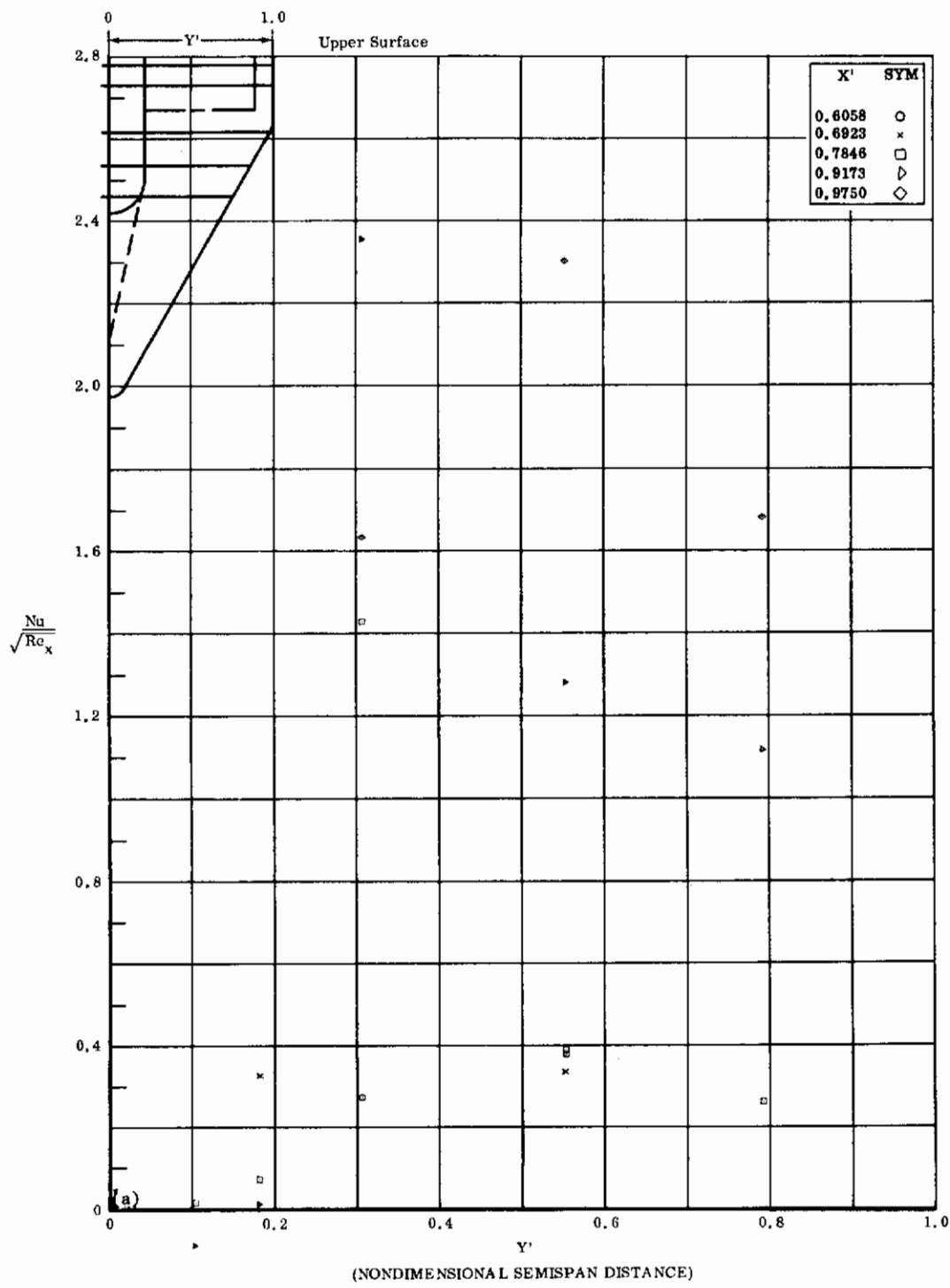


Fig. 4a Configuration I, $\alpha = 0$, $\delta_2 = \delta_3 = -10$

$\text{Nu}/\sqrt{\text{Re}_x}$ vs. Y' upper surface

Contrails

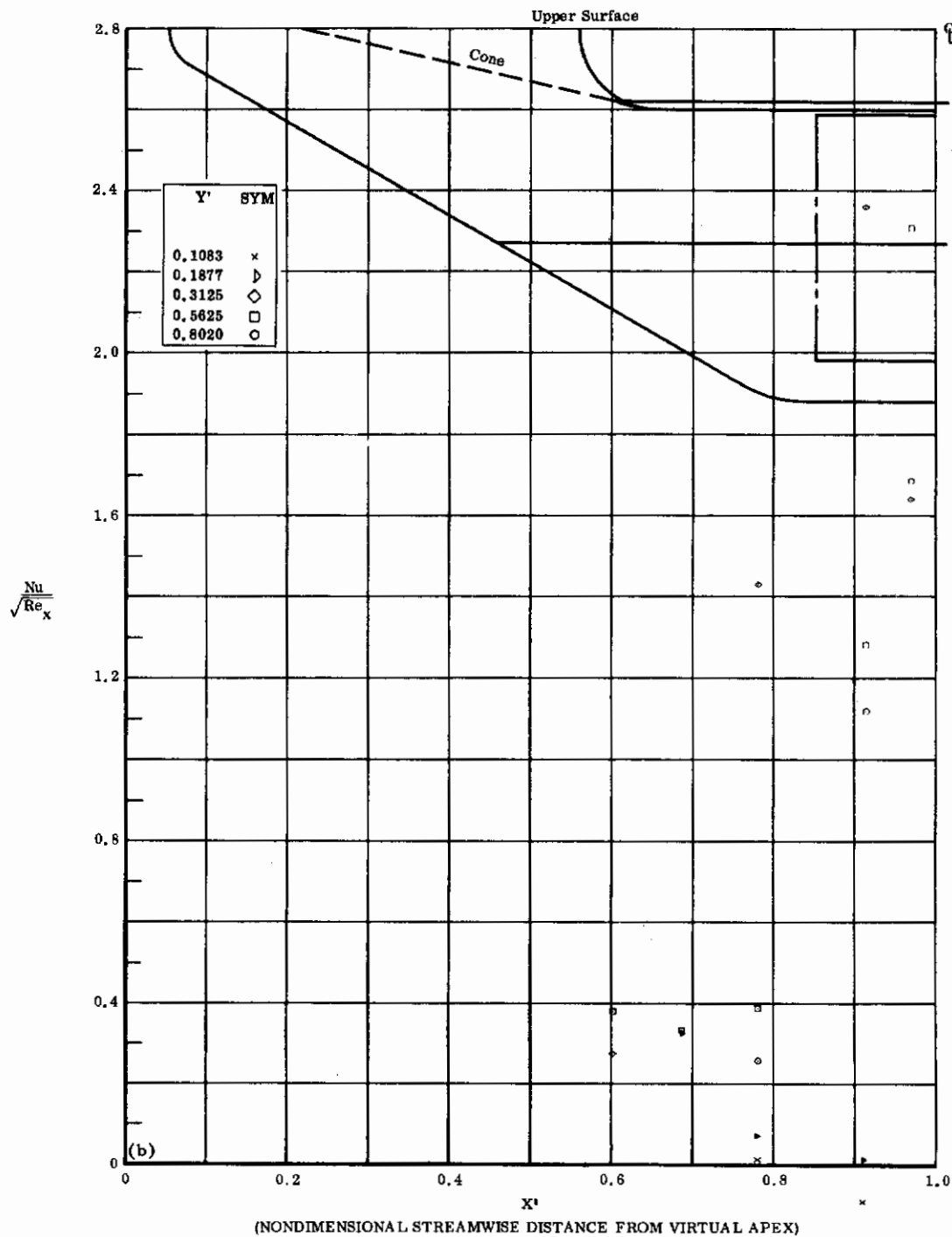


Fig. 4b Configuration I, $\alpha = 0$, $\delta_2 = \delta_3 = -10$

$Nu/\sqrt{Re_x}$ vs. X' upper surface

Contrails

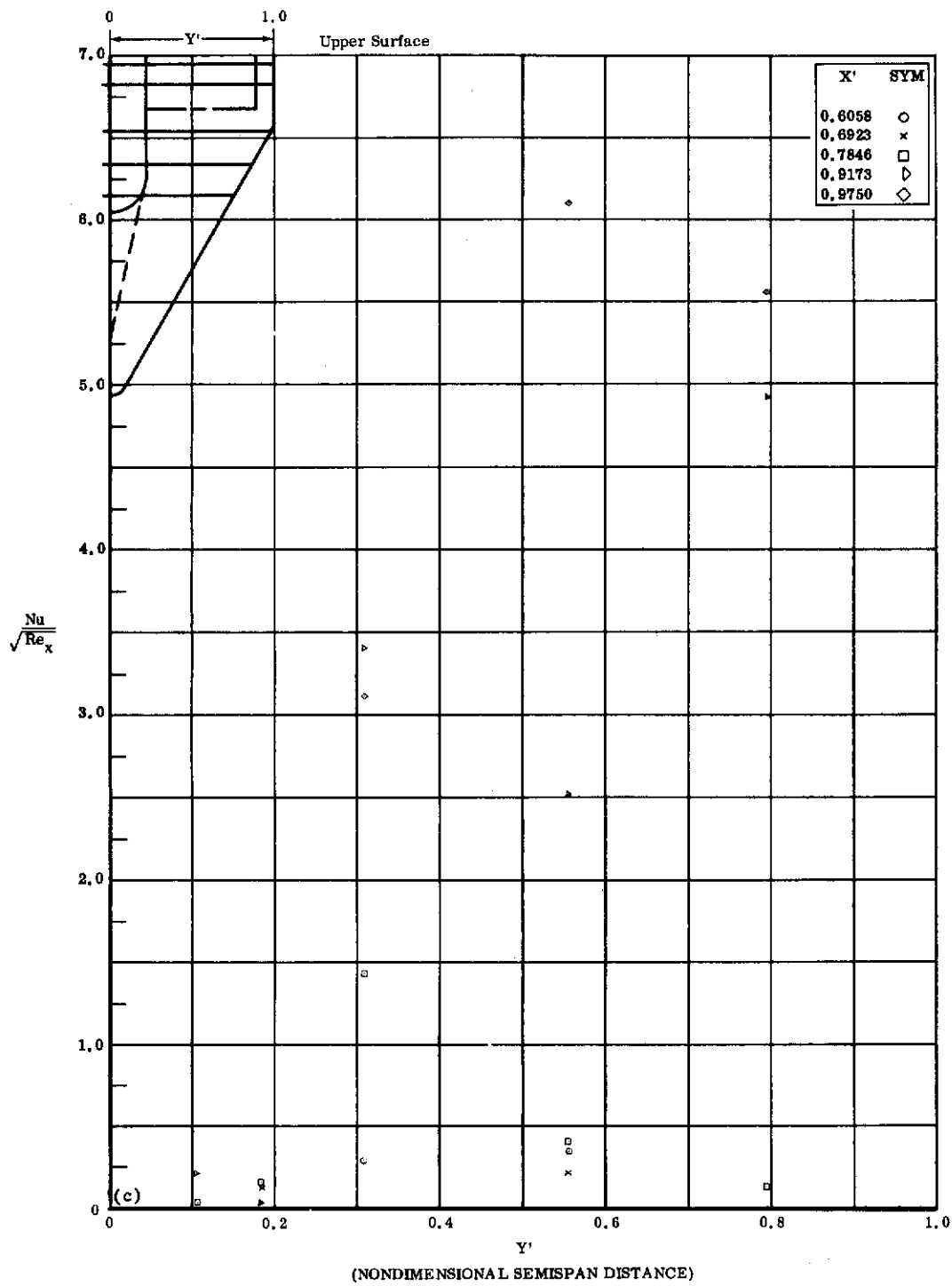


Fig. 4c Configuration I, $\alpha = 0$, $\delta_2 = \delta_3 = -20$

$\text{Nu}/\sqrt{\text{Re}_x}$ vs. Y' upper surface

Contrails

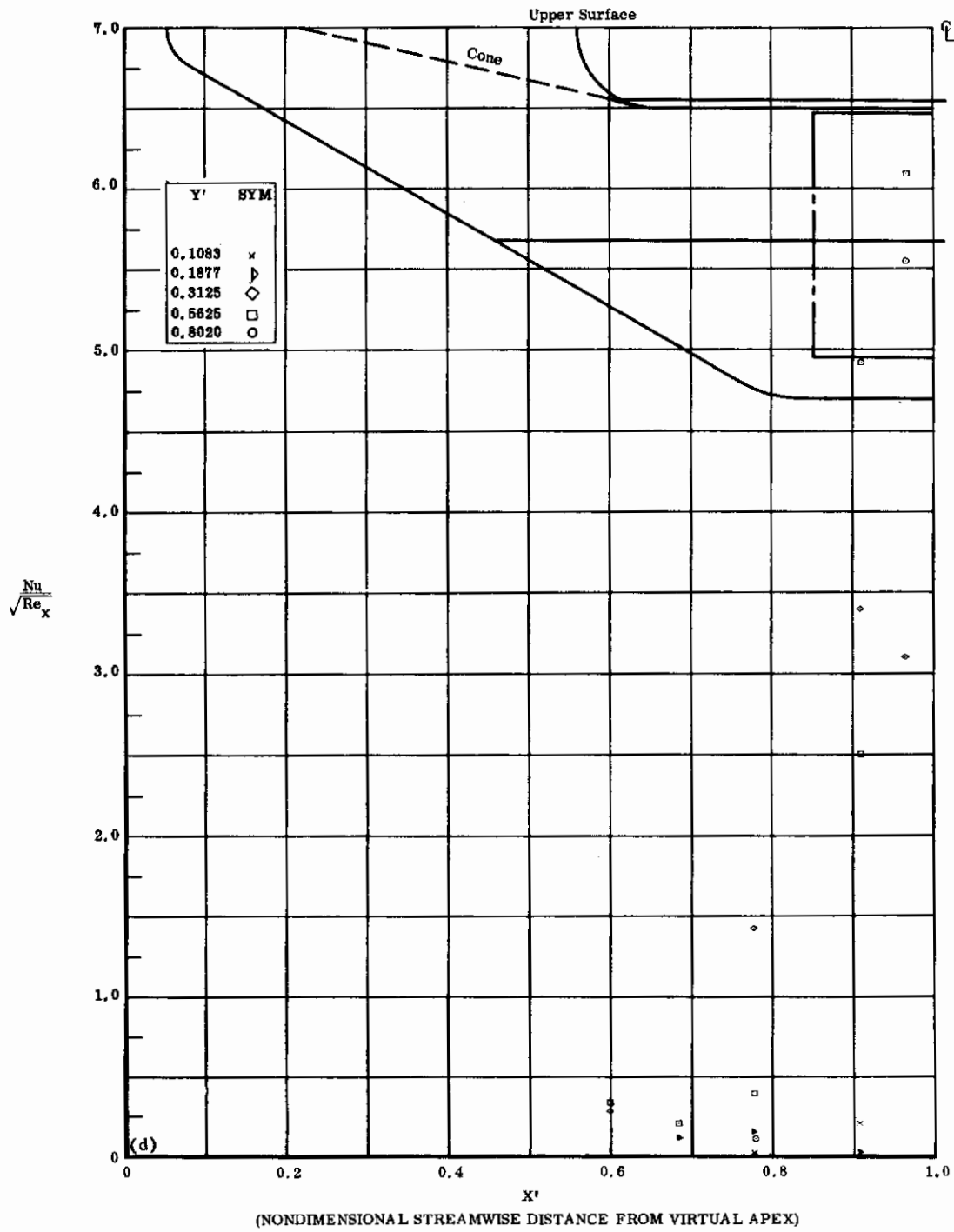


Fig. 4d Configuration I, $\alpha = 0$, $\delta_2 = \delta_3 = -20$

$\text{Nu}/\sqrt{\text{Re}_x}$ vs. X' upper surface

Contrails

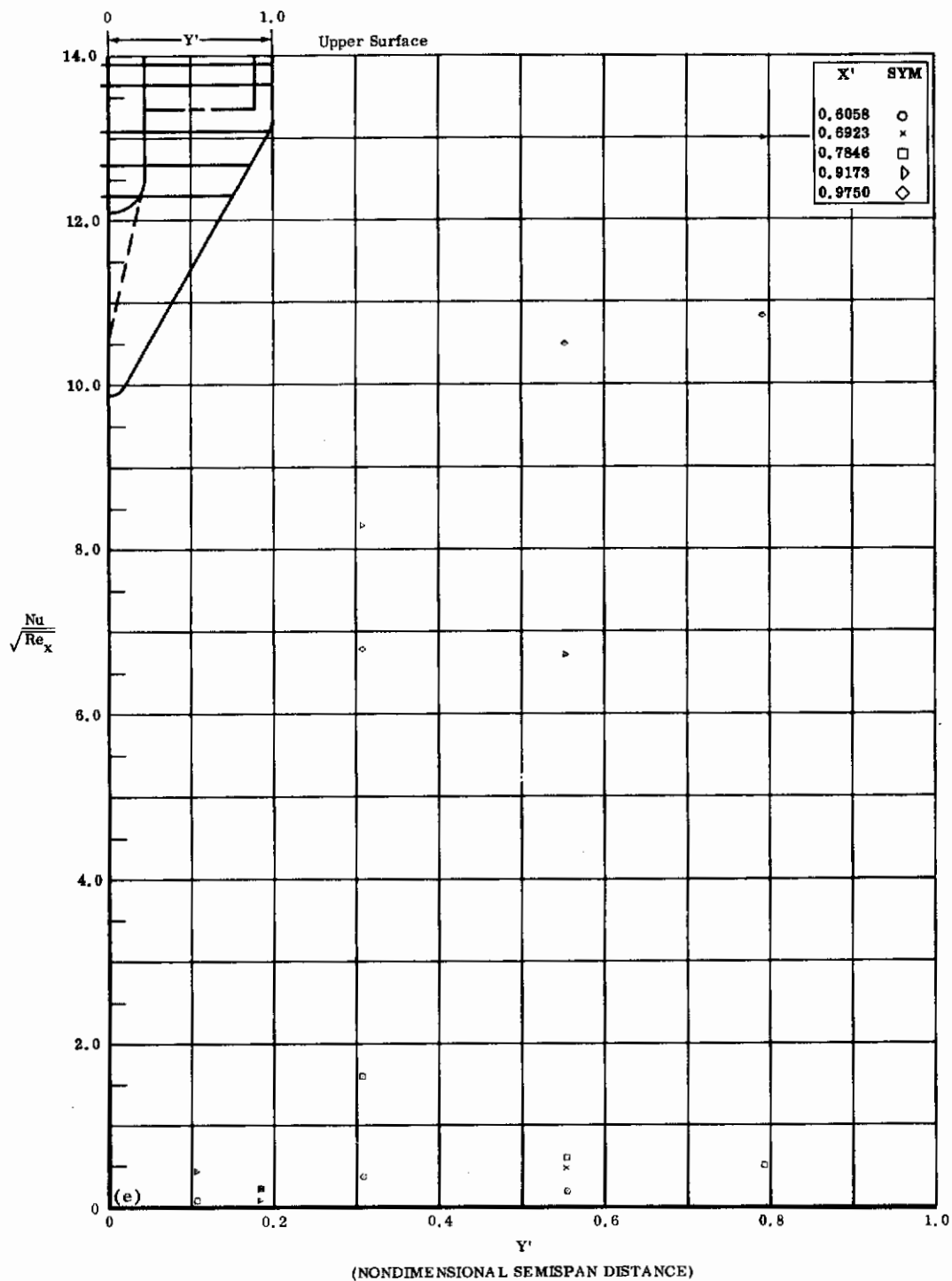


Fig. 4e Configuration I, $\alpha = 0$, $\delta_2 = \delta_3 = -30$
 $Nu/\sqrt{Re_x}$ vs. Y' upper surface

Contrails

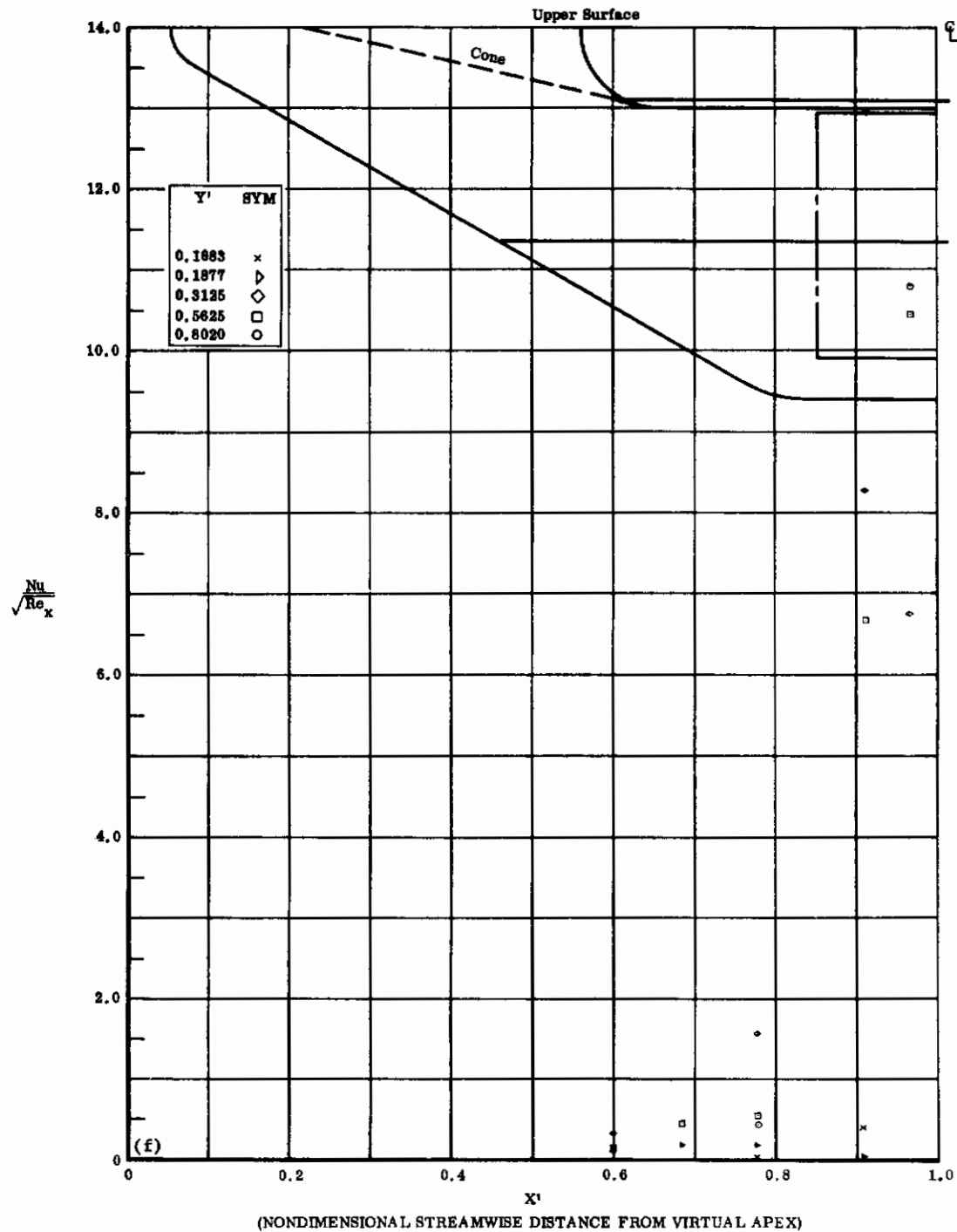


Fig. 4f Configuration I, $\alpha = 0$, $\delta_2 = \delta_3 = -30$

$Nu/\sqrt{Re_x}$ vs. X' upper surface

Contrails

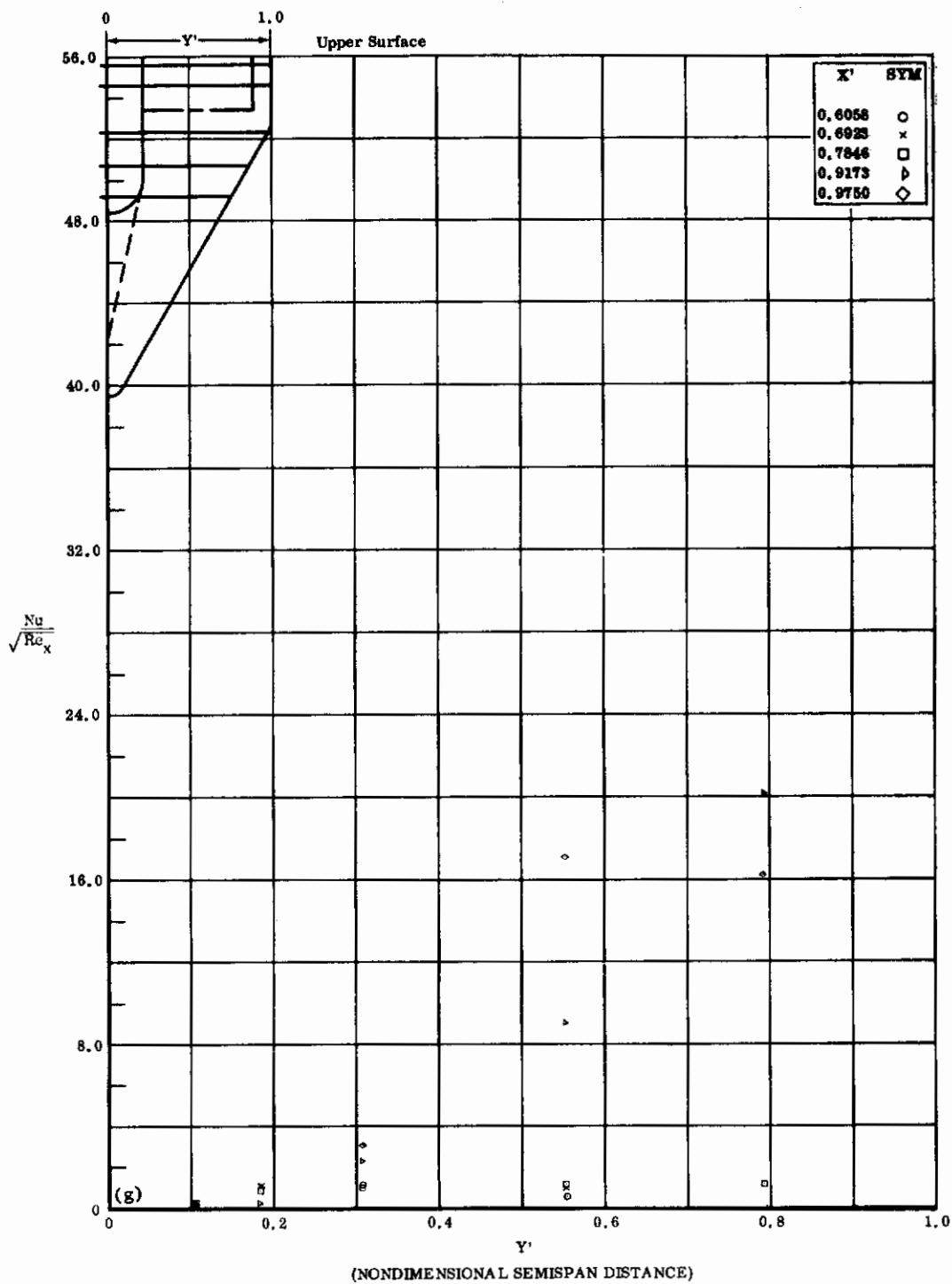


Fig. 4g Configuration I, $\alpha = 0$, $\delta_2 = \delta_3 = -39$
 $Nu/\sqrt{Re_x}$ vs. Y' upper surface

Contrails

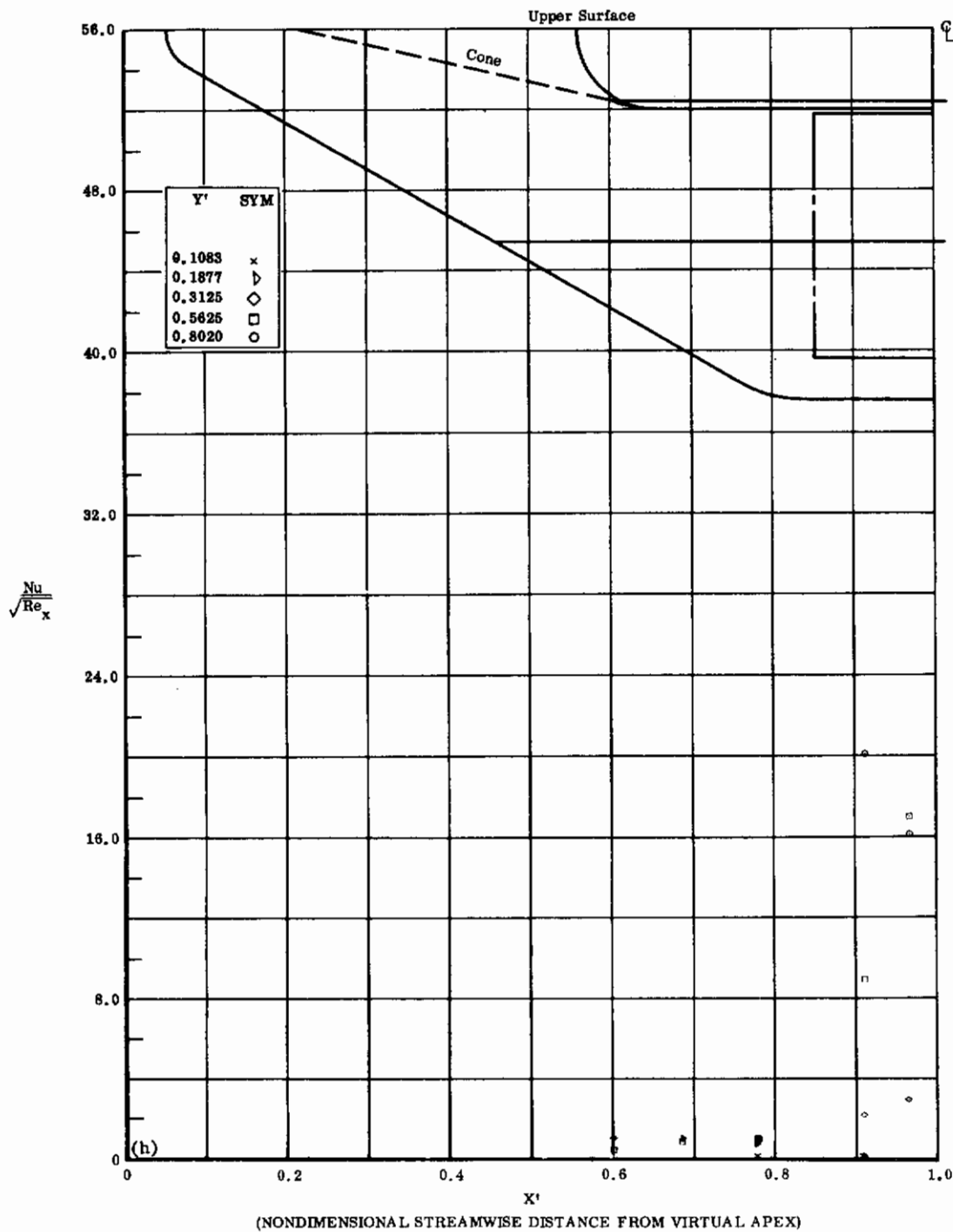


Fig. 4h Configuration I, $\alpha = 0$, $\delta_2 = \delta_3 = -39$
 $\frac{Nu}{\sqrt{Re_x}}$ vs. X' upper surface

Contrails

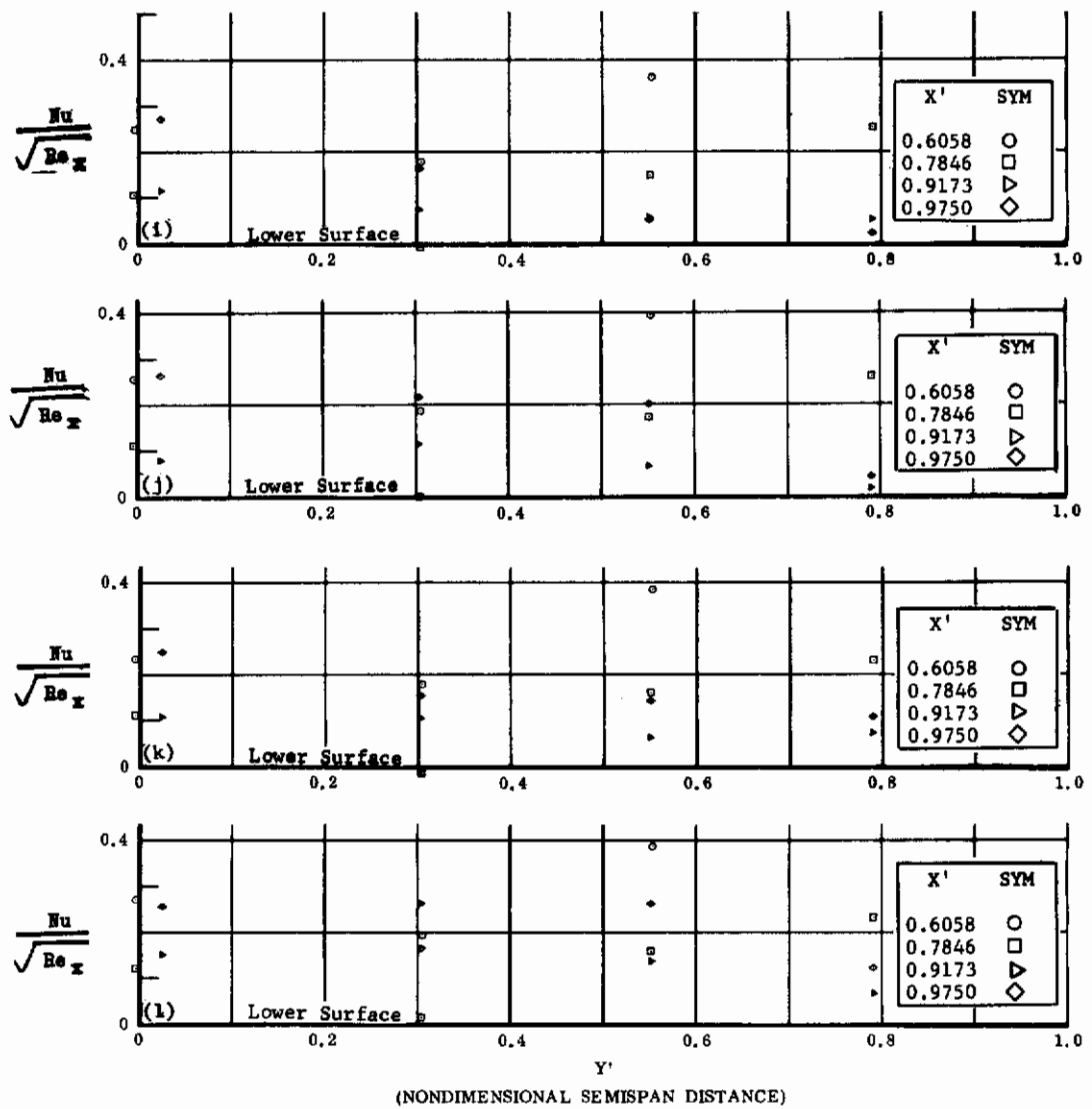


Fig. 4 Configuration I, $\alpha = 0$, $Nu/\sqrt{Re_x}$ vs. Y' , lower surface

i) $\delta_2 = \delta_3 = -10$

j) $\delta_2 = \delta_3 = -20$

k) $\delta_2 = \delta_3 = -30$

l) $\delta_2 = \delta_3 = -39$

Contrails

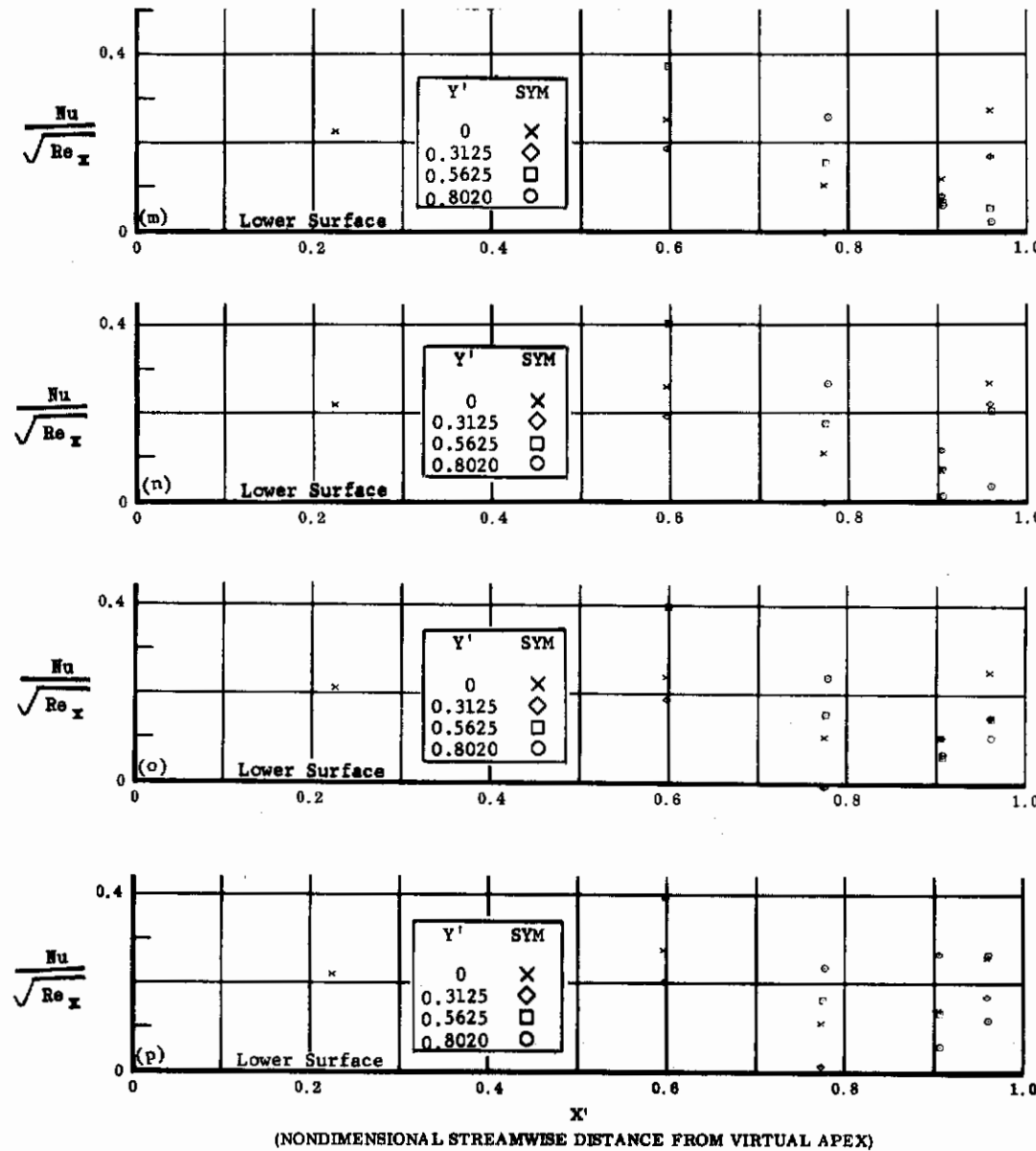


Fig. 4 Configuration I, $\alpha = 0$, $Nu/\sqrt{Re_x}$ vs. X' , lower surface

m) $\delta_2 = \delta_3 = -10$

n) $\delta_2 = \delta_3 = -20$

o) $\delta_2 = \delta_3 = -30$

p) $\delta_2 = \delta_3 = -39$

Contrails

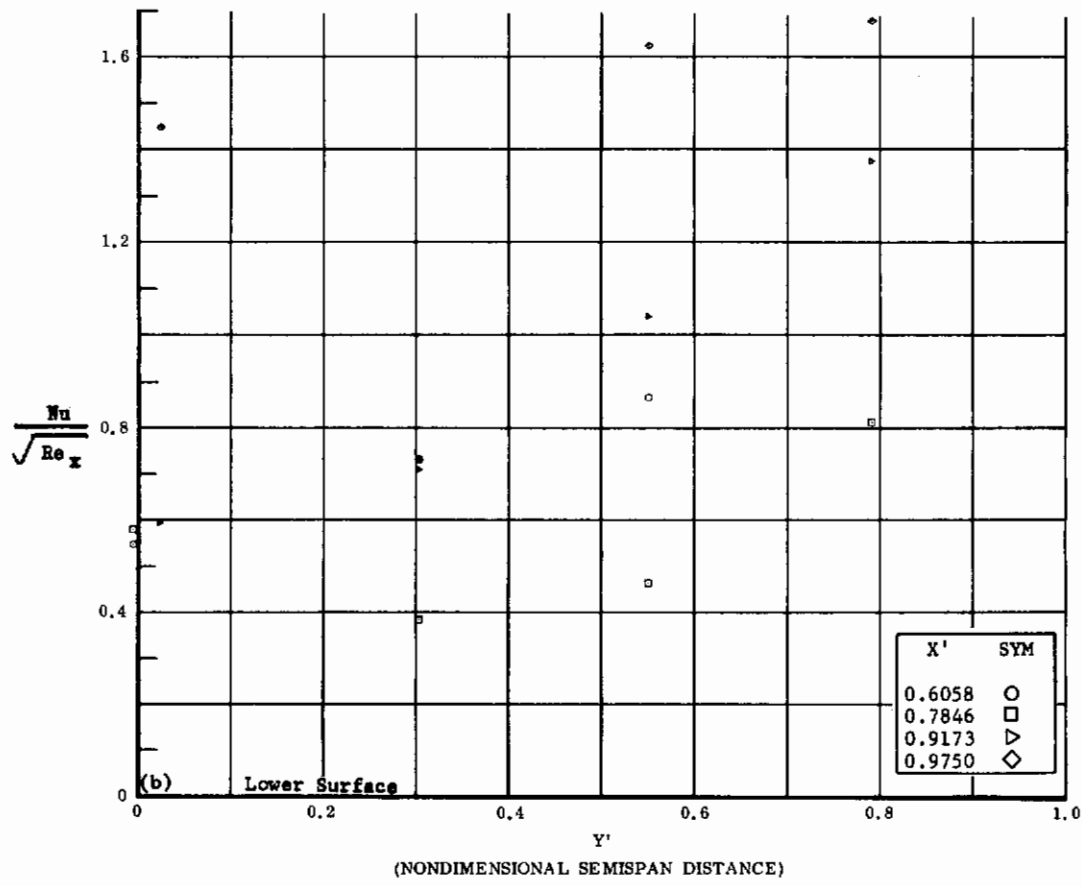
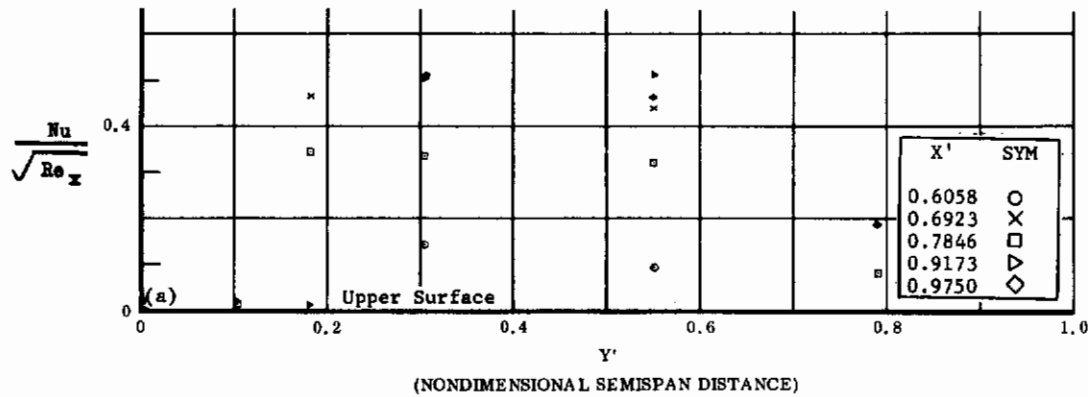


Fig. 5 Configuration I, $\alpha = +10$, $\delta_2 = \delta_3 = 0$
 a) $Nu/\sqrt{Re_x}$ vs. Y' upper surface
 b) $Nu/\sqrt{Re_x}$ vs. Y' lower surface

Contrails

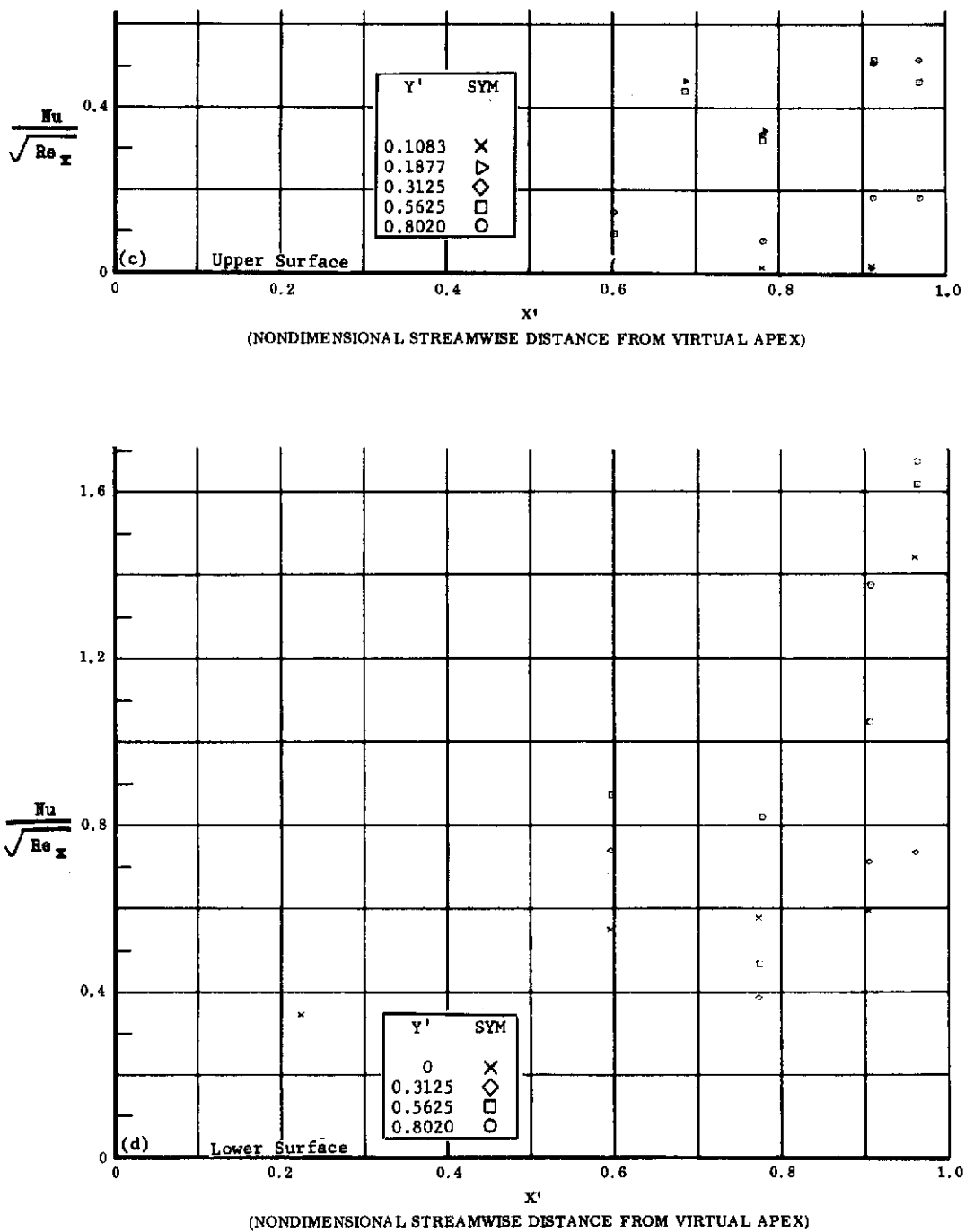


Fig. 5 Configuration I, $\alpha = +10$, $\delta_2 = \delta_3 = 0$

c) $Nu/\sqrt{Re_x}$ vs. X' upper surface

d) $Nu/\sqrt{Re_x}$ vs. X' lower surface

Contrails

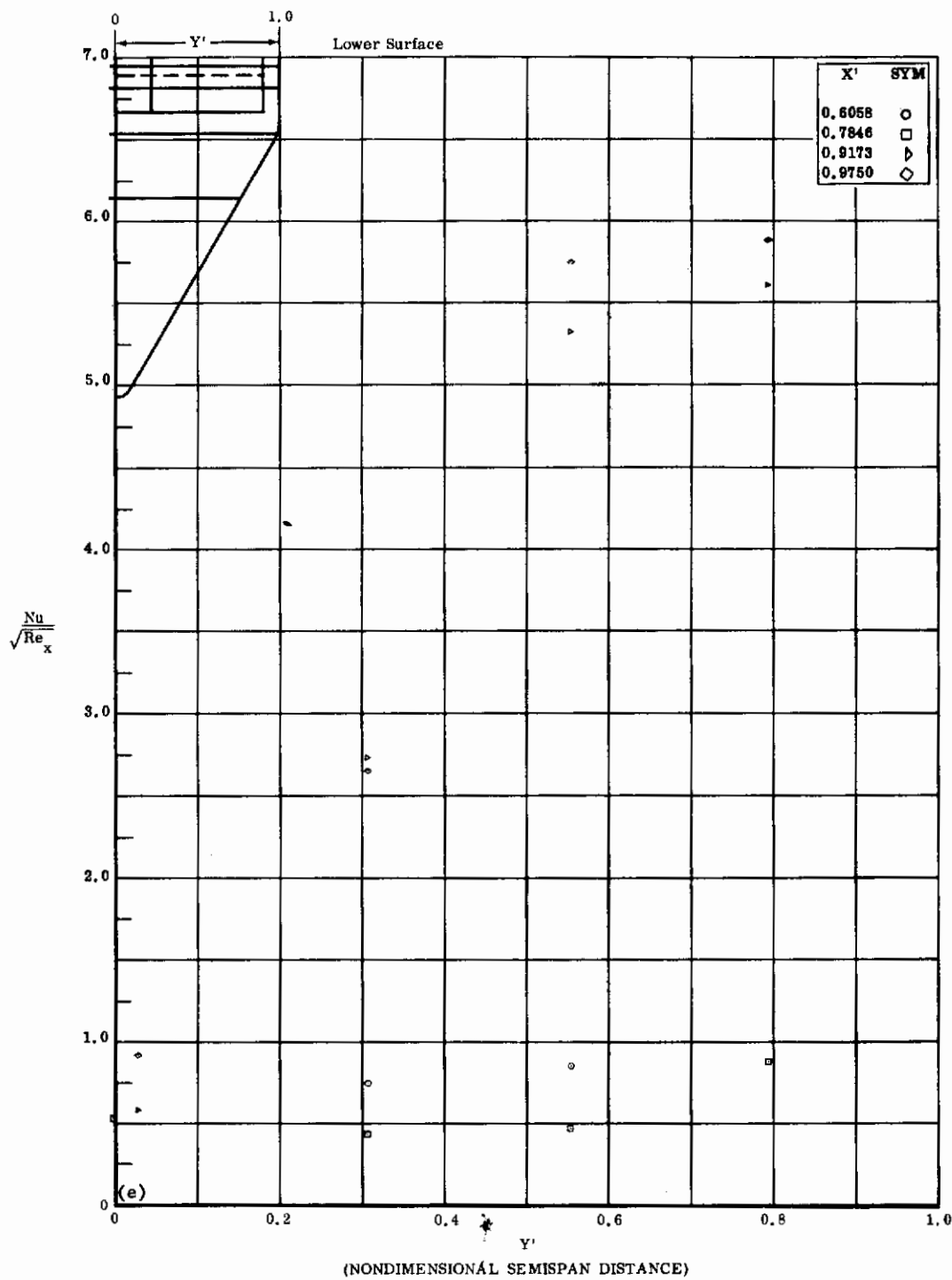


Fig. 5e Configuration I, $\alpha = +10$, $b_2 = b_3 = +10$

$Nu/\sqrt{Re_x}$ vs. Y' lower surface

Contrails

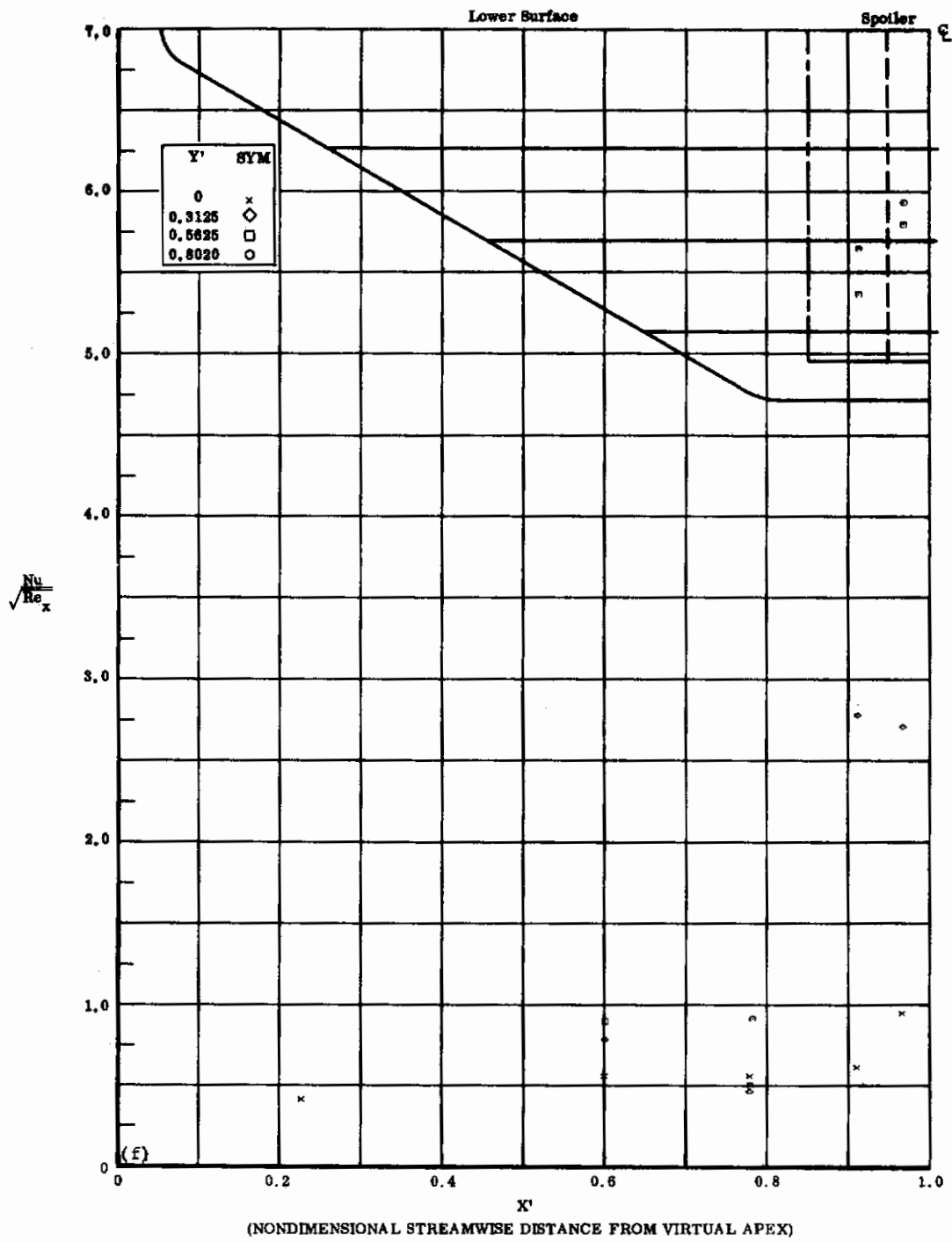


Fig. 5f Configuration I, $\alpha = +10$, $\delta_2 = \delta_3 = +10$

$Nu/\sqrt{Re_x}$ vs. X^i lower surface

Contrails

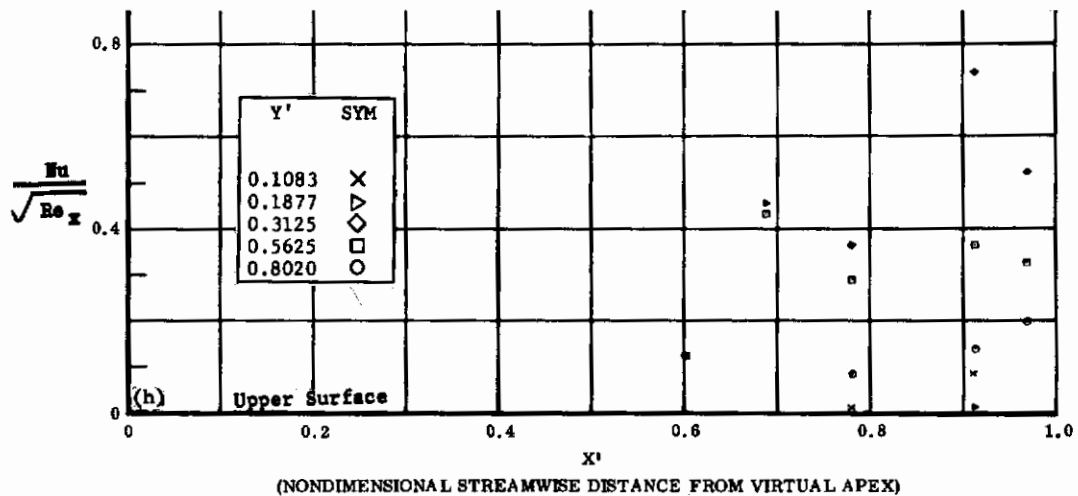
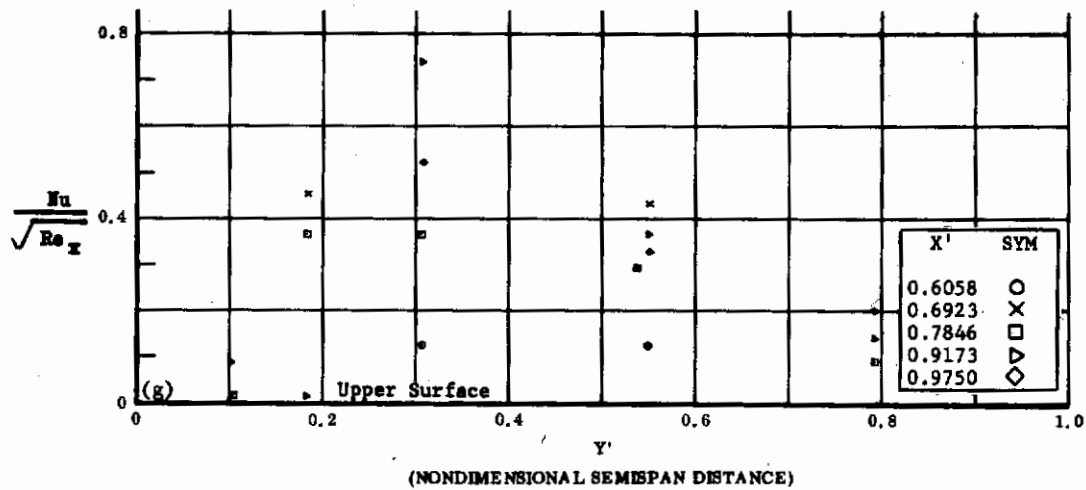


Fig. 5 Configuration I, $\alpha = +10$, $\delta_2 = \delta_3 = +10$

g) $Nu/\sqrt{Re_x}$ vs. Y' upper surface

h) $Nu/\sqrt{Re_x}$ vs. X' upper surface

Contrails

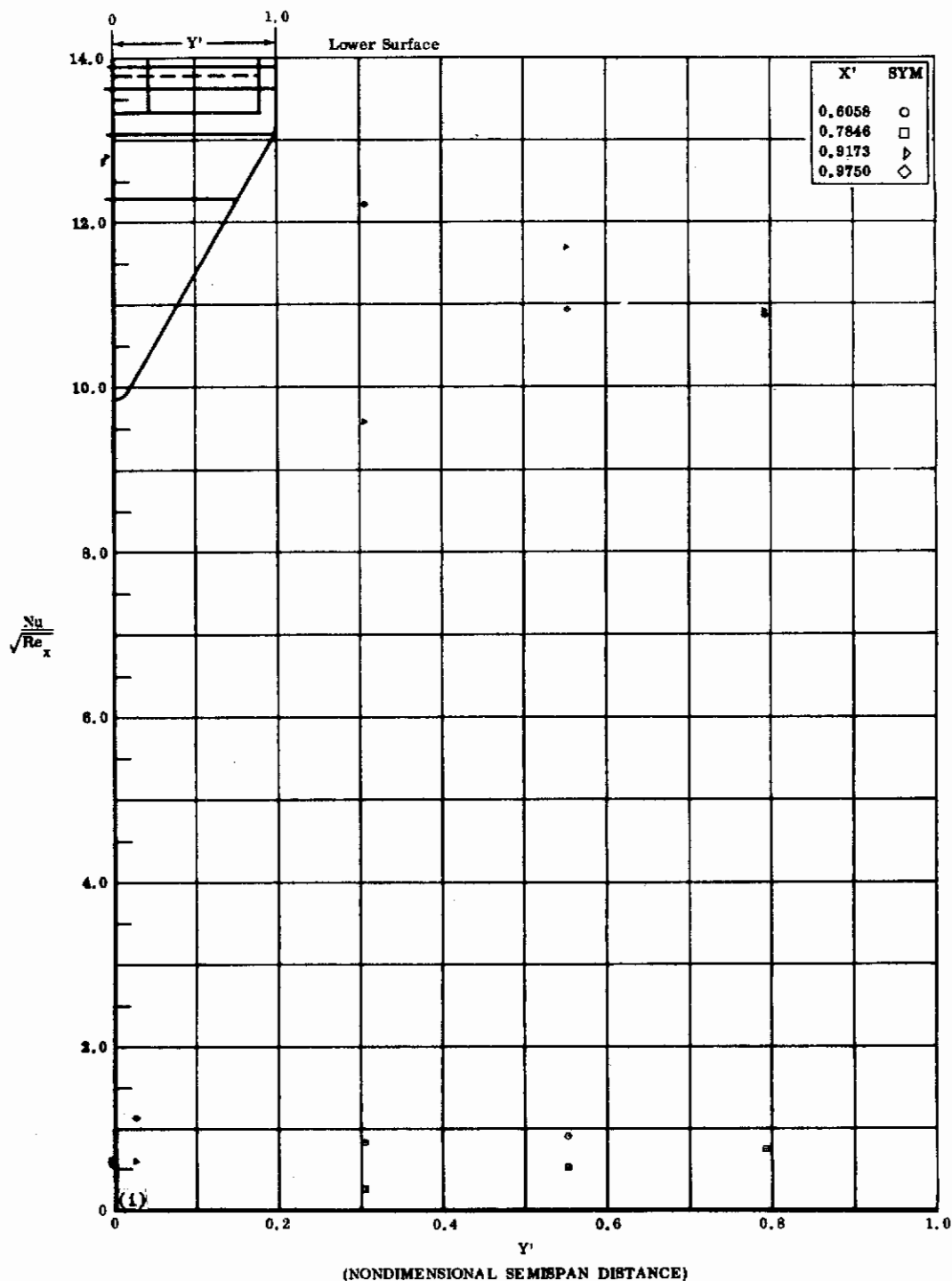


Fig. 5i Configuration I, $\alpha = +10$, $\delta_2 = \delta_3 = +20$
 $Nu/\sqrt{Re_x}$ vs. Y' lower surface

Contrails

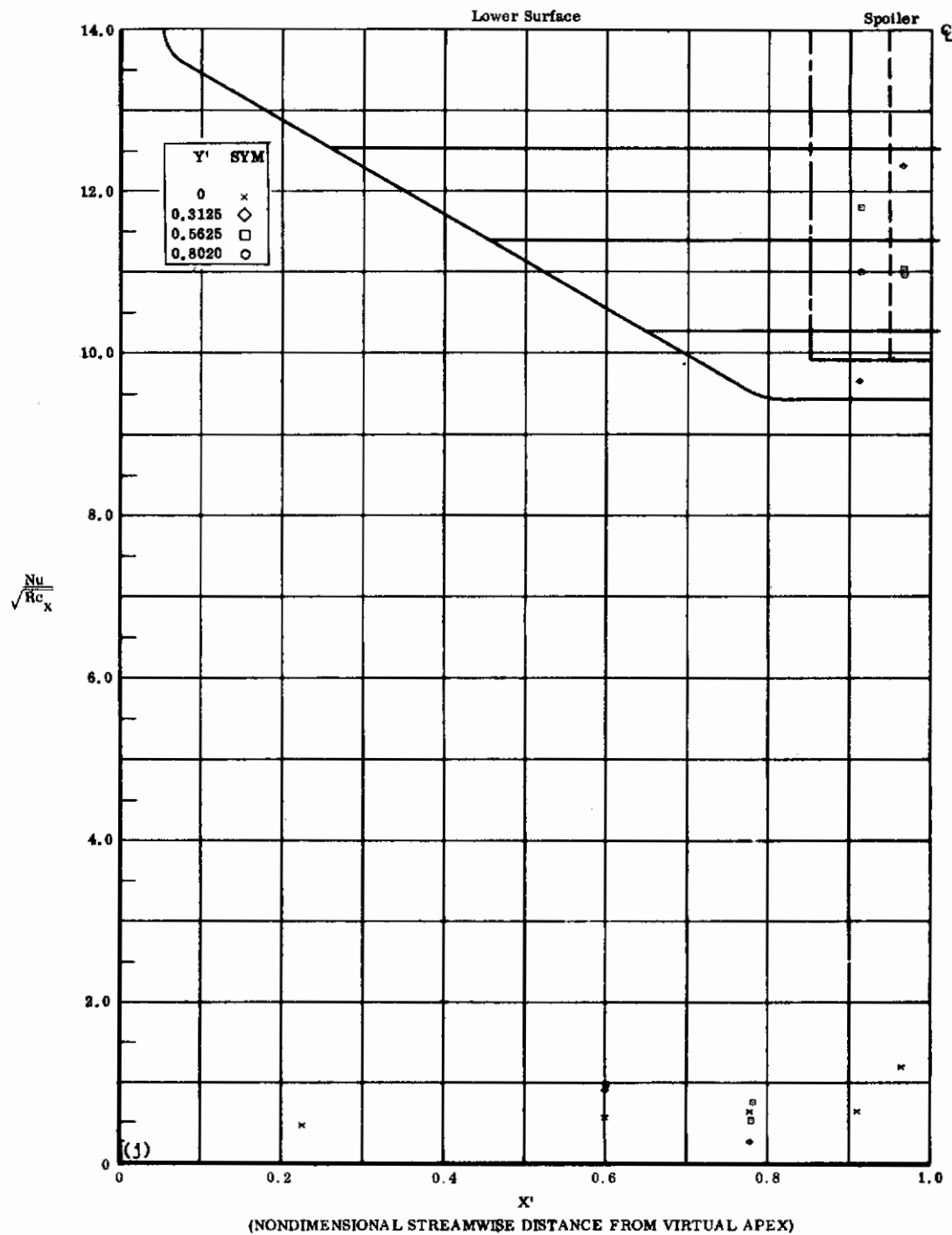


Fig. 5j Configuration I, $\alpha = +10$, $\delta_2 = \delta_3 = +20$

$\frac{\text{Nu}}{\sqrt{\text{Re}_x}}$ vs. X' lower surface

Contrails

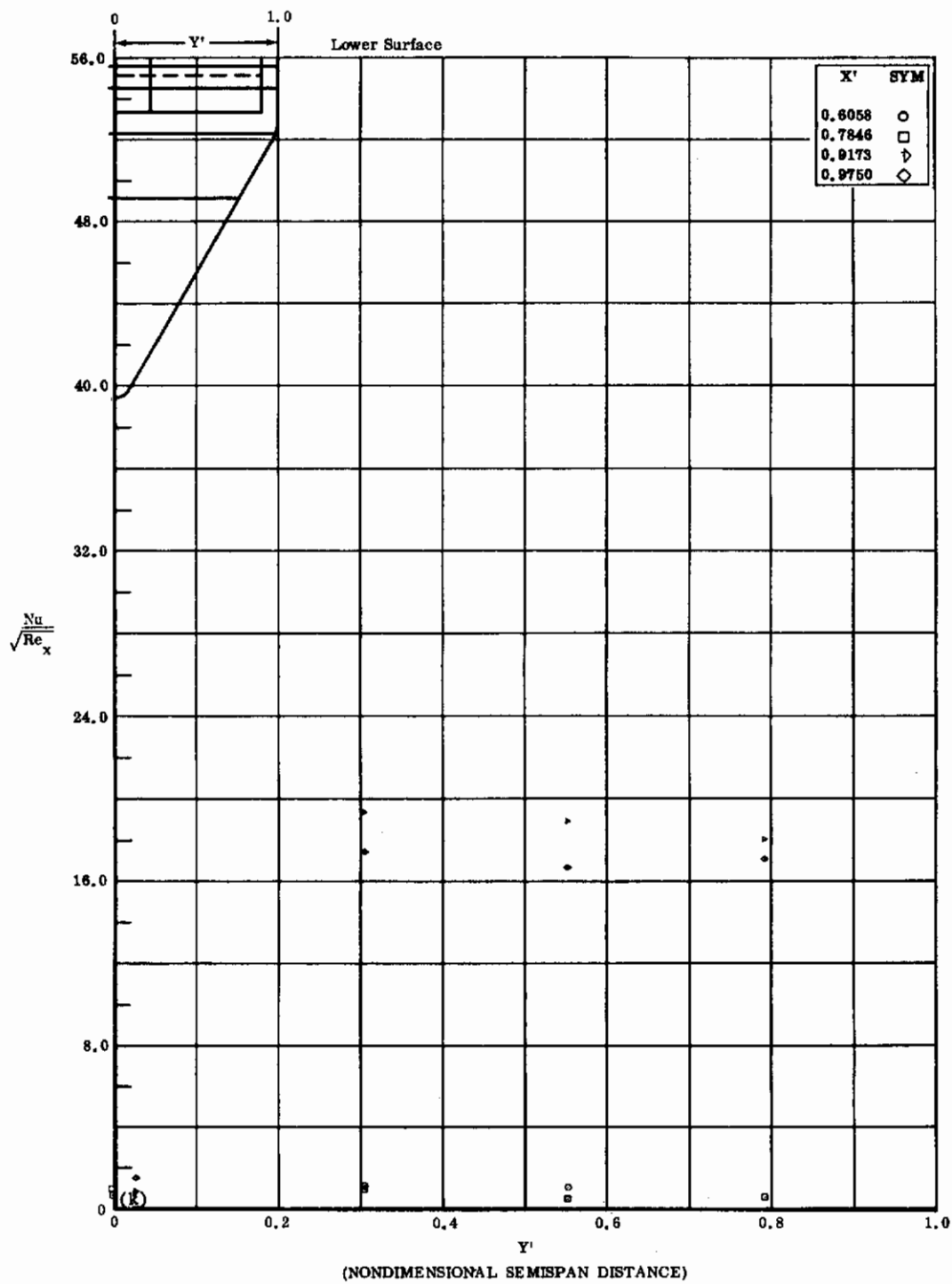


Fig. 5k Configuration I, $\alpha = +10$, $\delta_2 = \delta_3 = +30$
 $\frac{Nu}{\sqrt{Re_x}}$ vs. Y' lower surface

Contrails

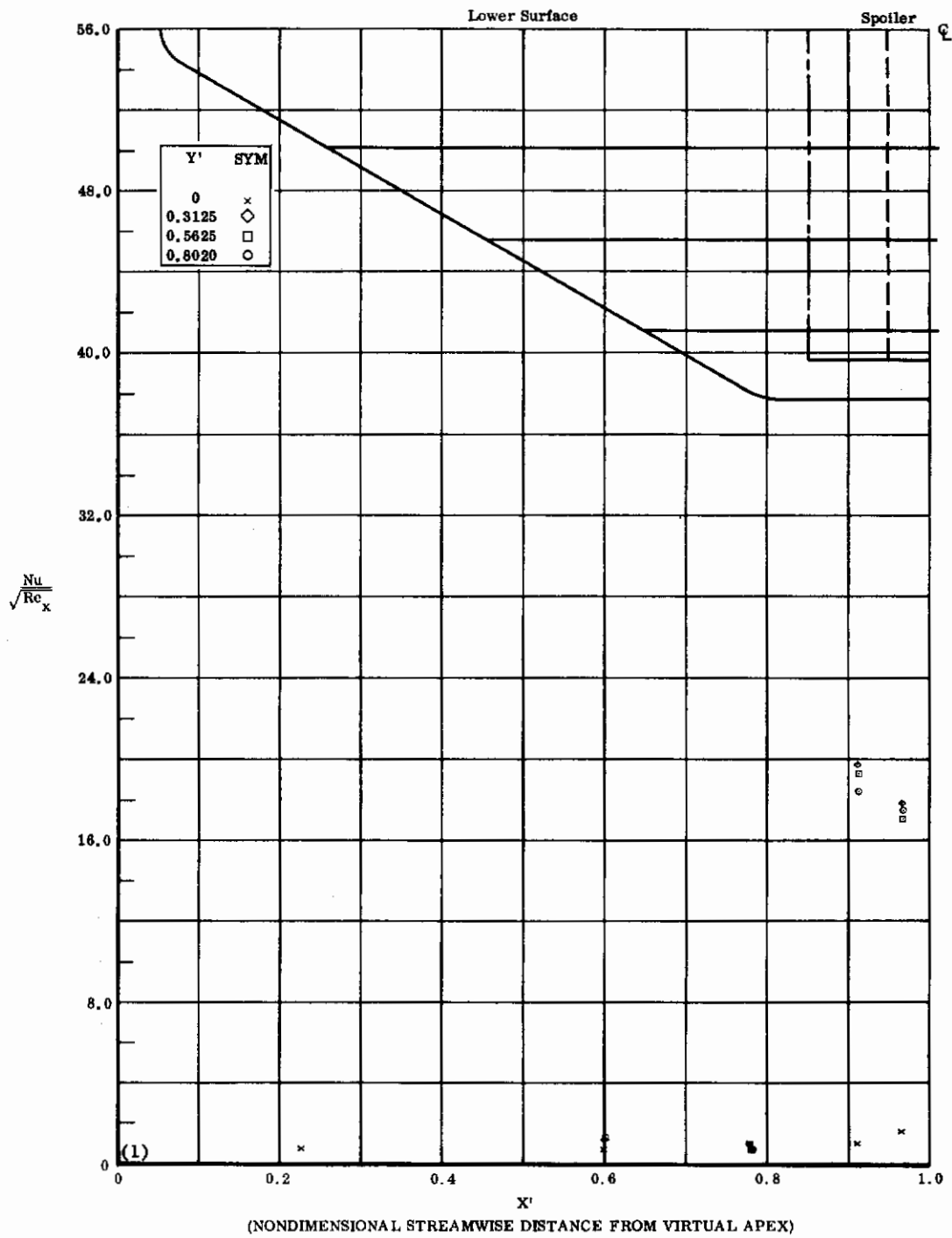


Fig. 5f Configuration I, $\alpha = +10$, $\delta_2 = \delta_3 = +30$

$Nu/\sqrt{Re_x}$ vs. X' lower surface

Contrails

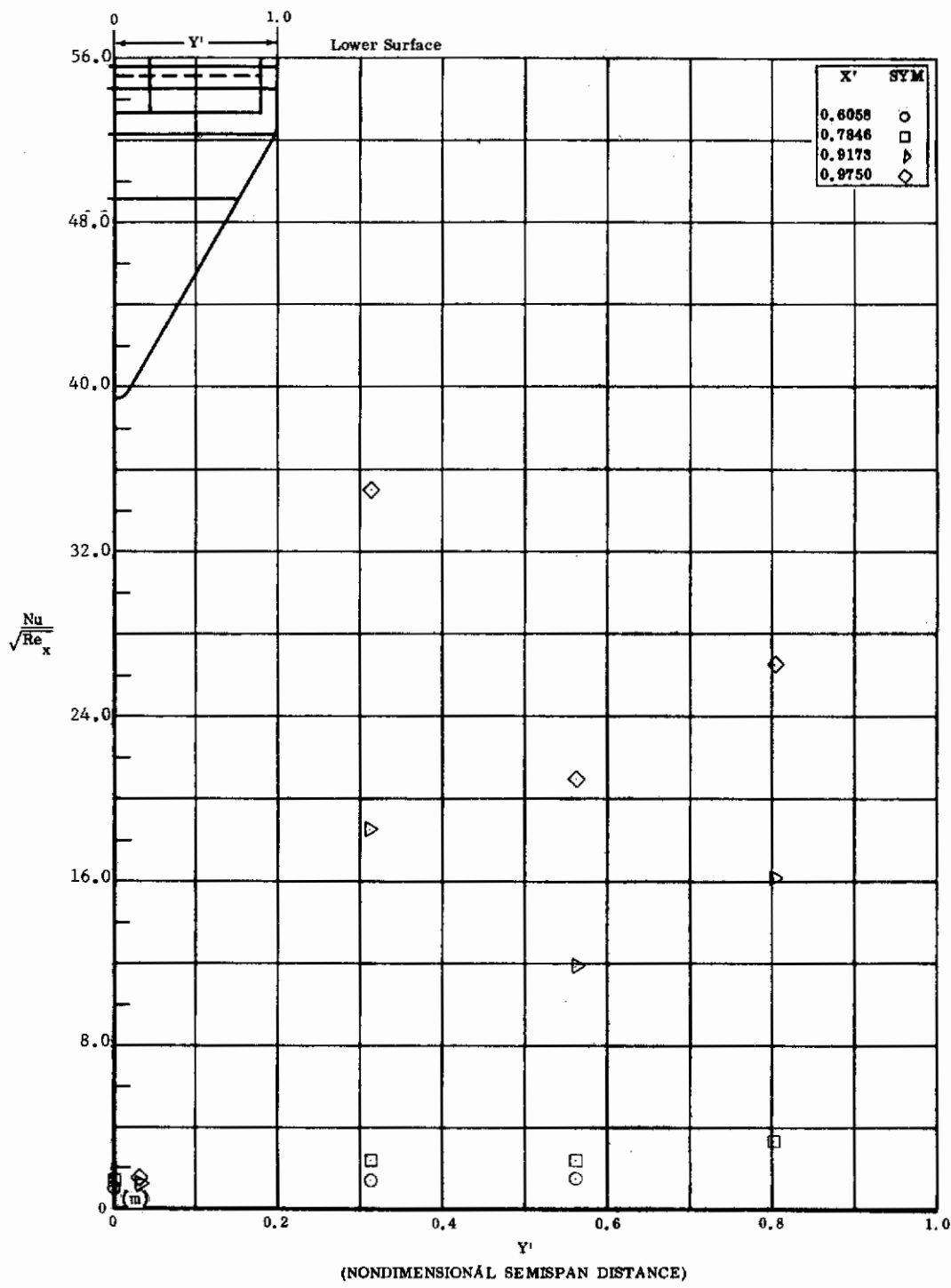


Fig. 5m Configuration I, $\alpha = +10$, $\delta_2 = \delta_3 = +39$
 $Nu/\sqrt{Re_x}$ vs. Y^i lower surface

Contrails

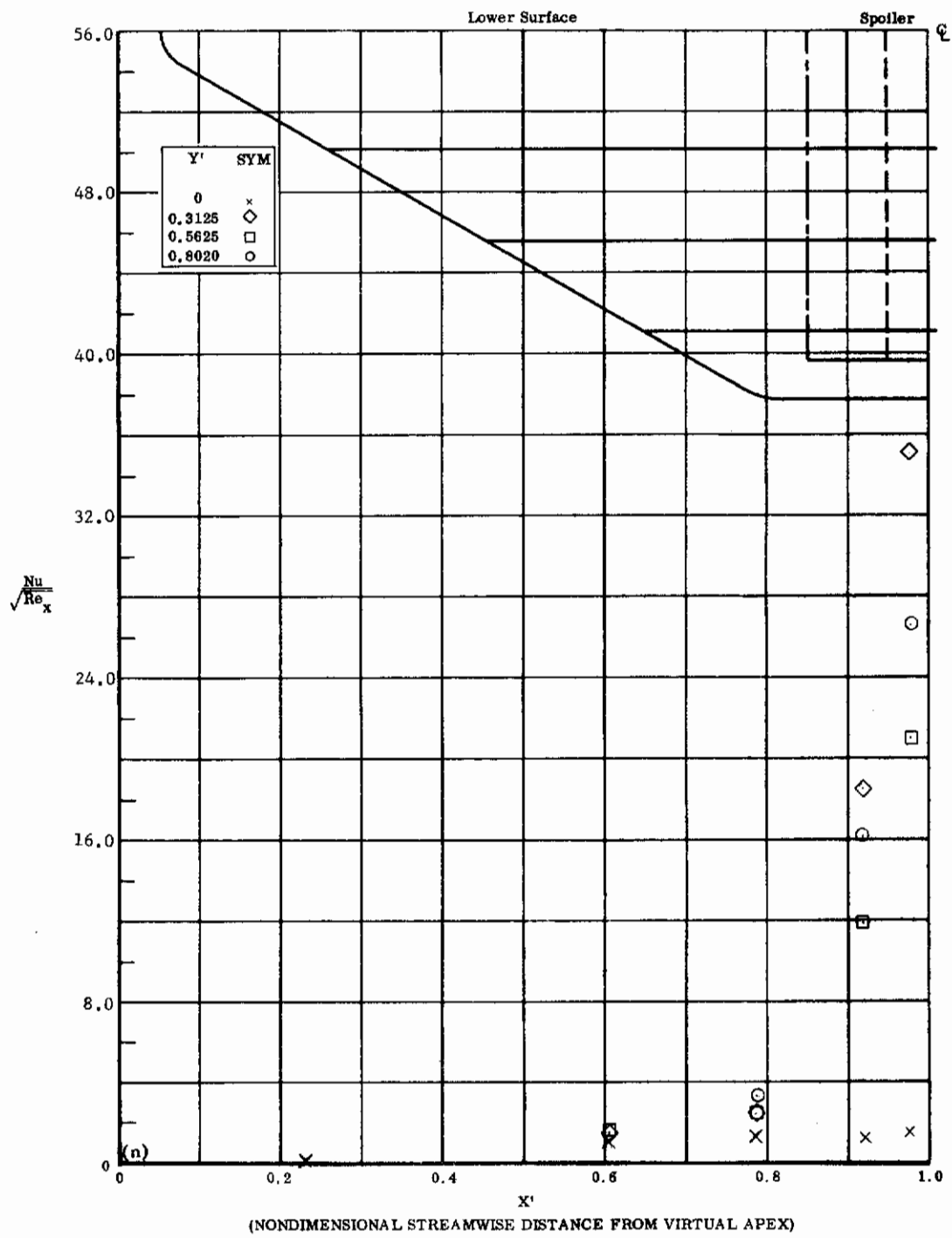


Fig. 5n Configuration I, $\alpha = +10$, $\delta_2 = \delta_3 = +39$
 $Nu/\sqrt{Re_x}$ vs. X' lower surface

Contrails

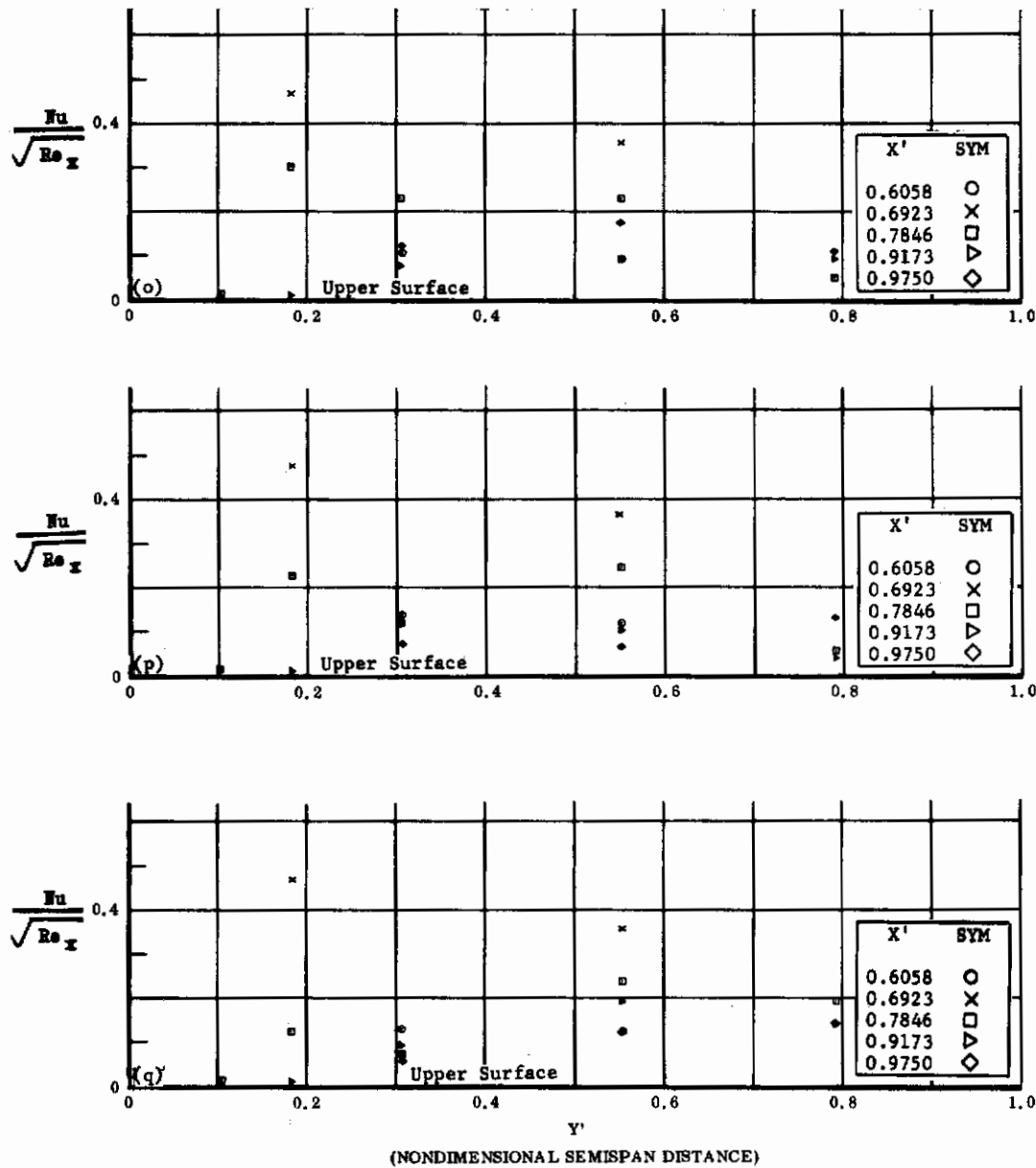


Fig. 5 Configuration I, $\alpha = +10$, $Nu/\sqrt{Re_x}$ vs. Y' , upper surface

- o) $\delta_2 = \delta_3 = +20$
- p) $\delta_2 = \delta_3 = +30$
- q) $\delta_2 = \delta_3 = +39$

Contrails

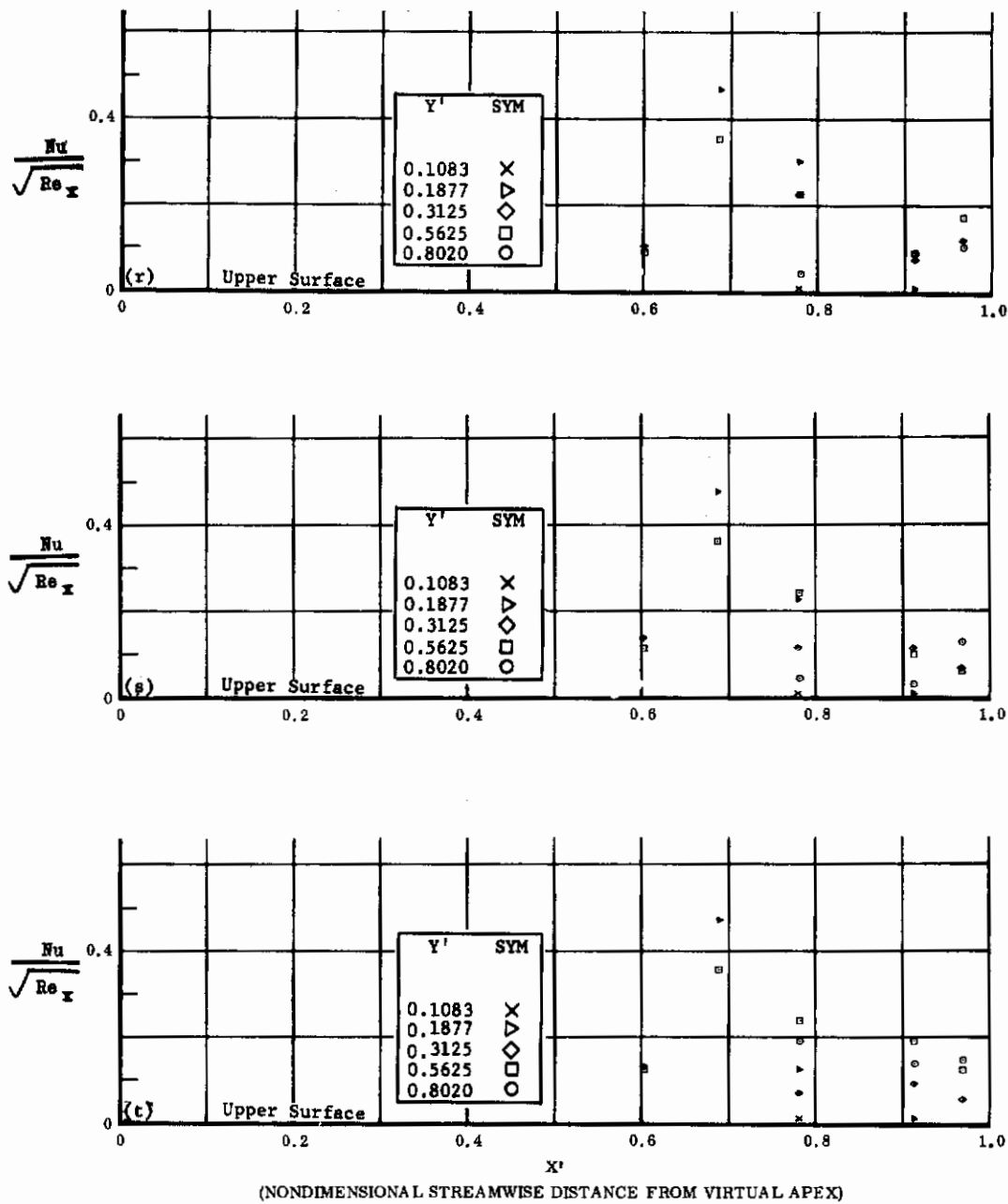


Fig. 5 Configuration I, $\alpha = +10$, $\text{Nu}/\sqrt{\text{Re}_x}$ vs. X' , upper surface

r) $\delta_2 = \delta_3 = +20$

s) $\delta_2 = \delta_3 = +30$

t) $\delta_2 = \delta_3 = +39$

Contrails

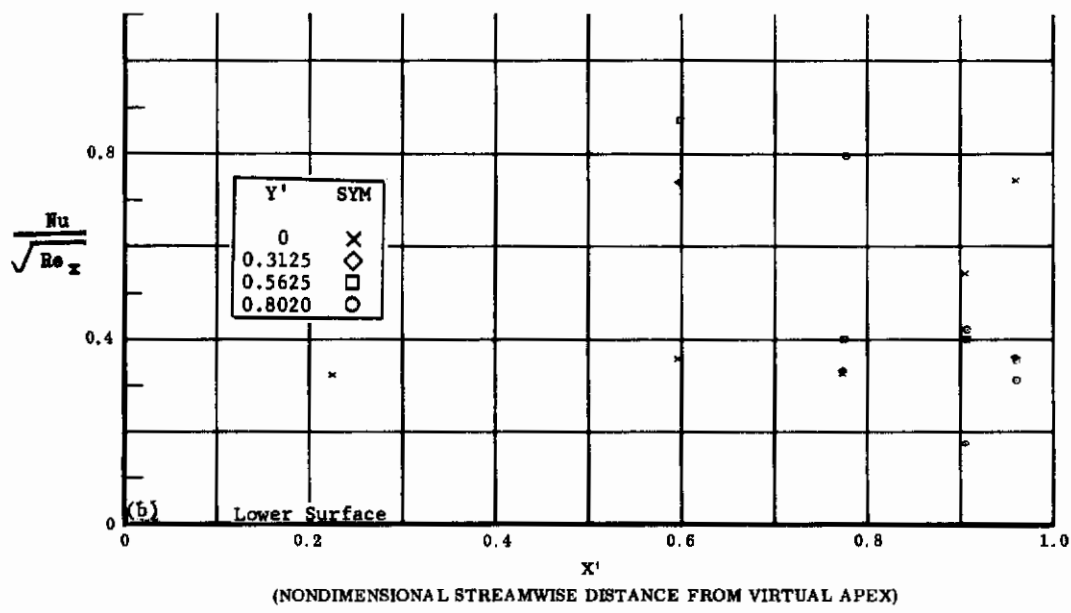
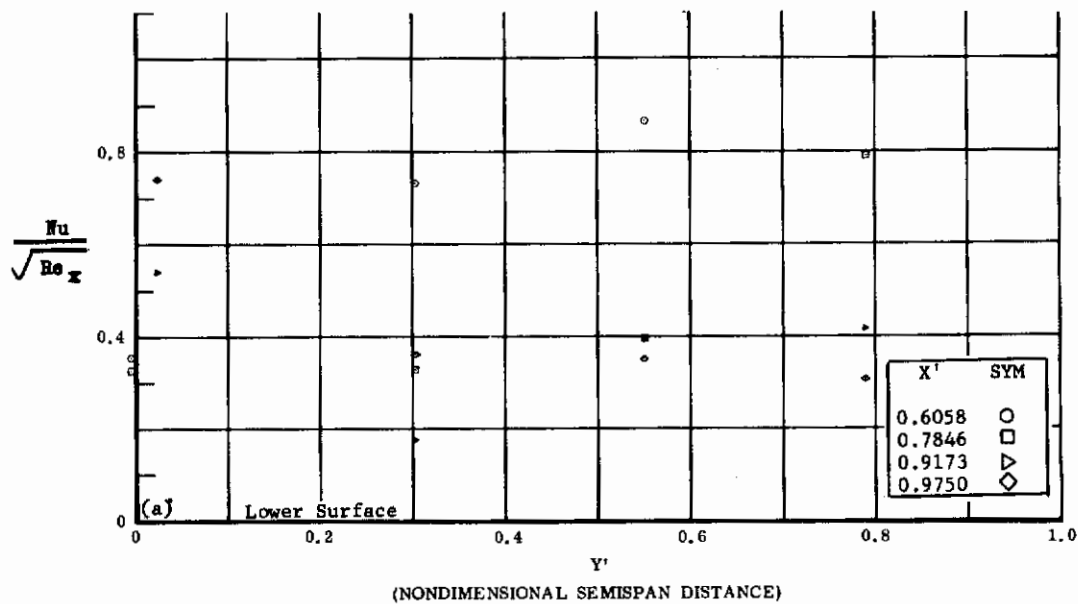


Fig. 6 Configuration I, $\alpha = +10$, $\delta_2 = \delta_3 = -10$

a) $Nu/\sqrt{Re_x}$ vs. Y' lower surface

b) $Nu/\sqrt{Re_x}$ vs. X' lower surface

Contrails

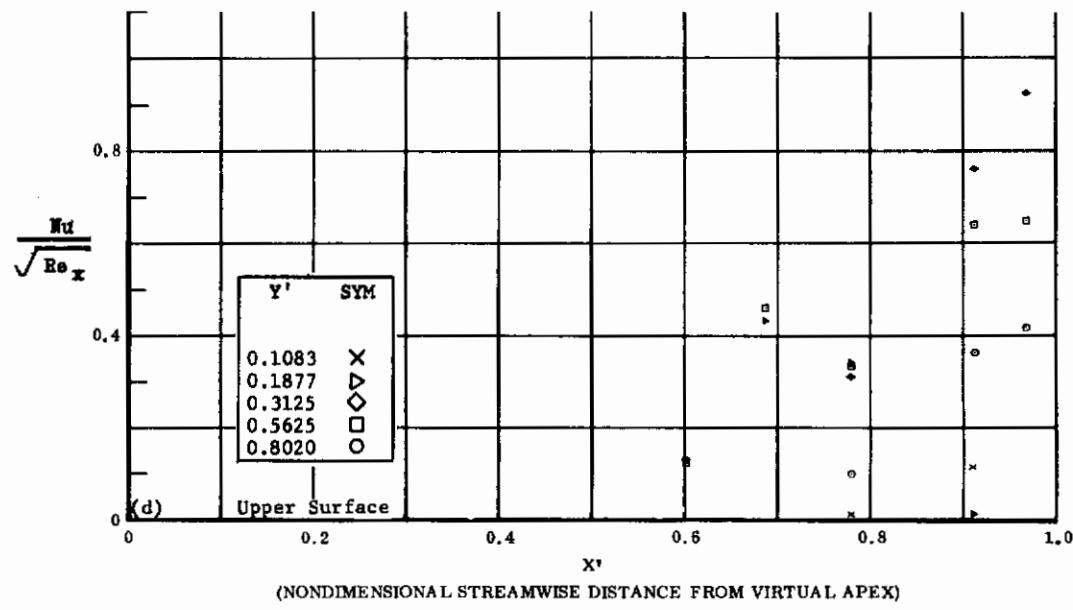
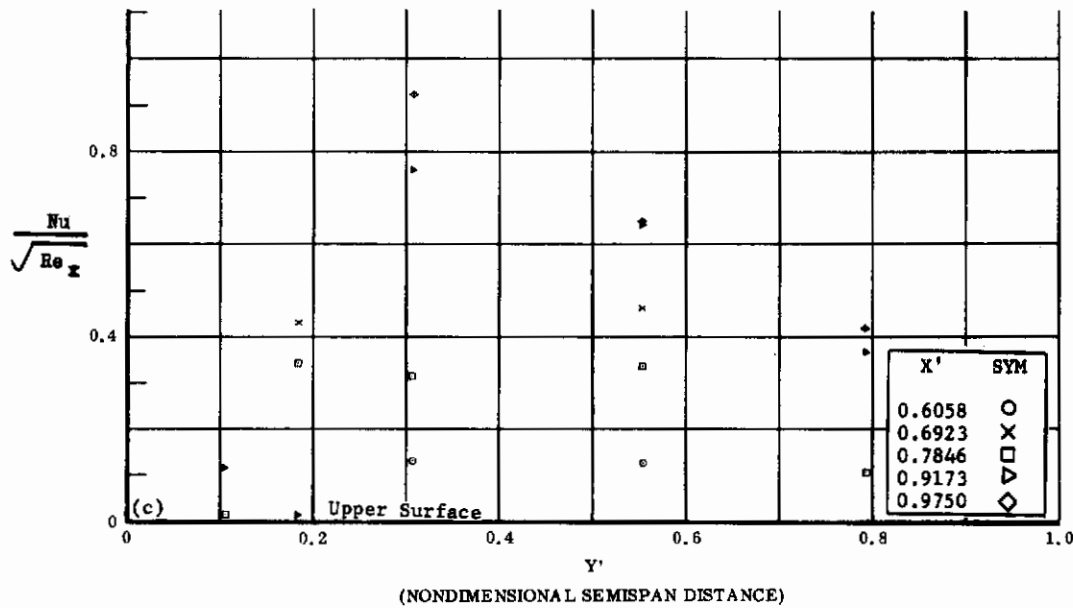


Fig. 6 Configuration I, $\alpha = +10$, $s_2 = s_3 = -10$

c) $Nu/\sqrt{Re_x}$ vs. Y' upper surface

d) $Nu/\sqrt{Re_x}$ vs. X' upper surface

Contrails

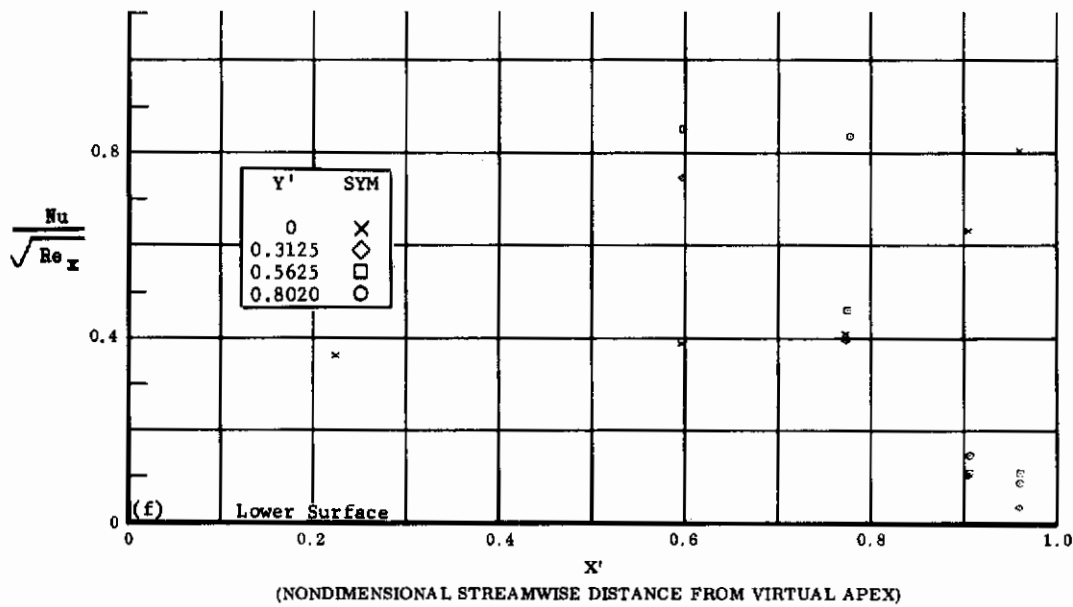
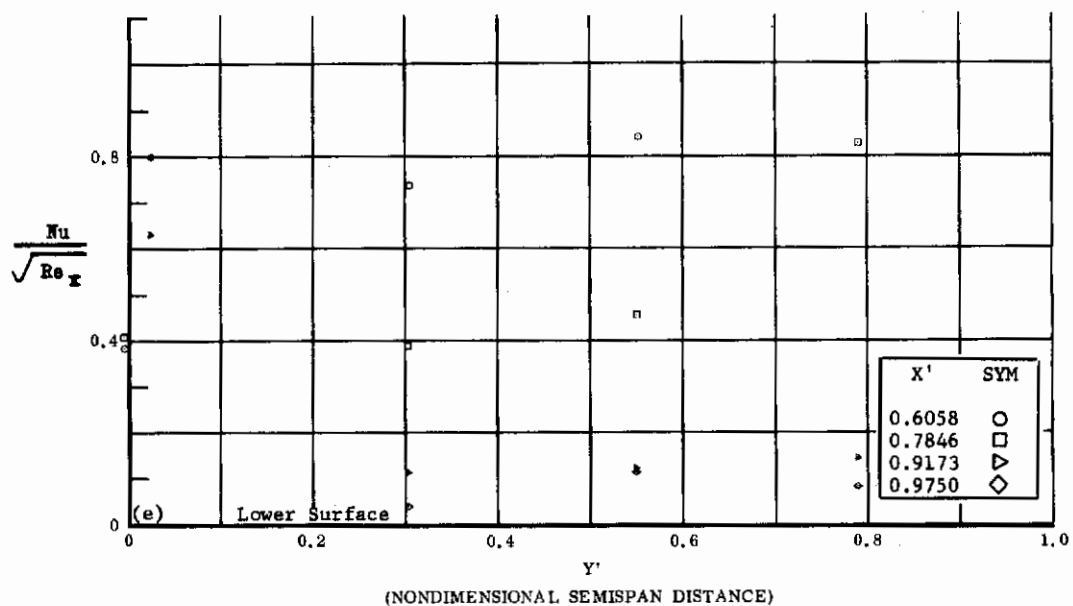


Fig. 6 Configuration I, $\alpha = +10$, $\delta_2 = \delta_3 = -20$

e) $Nu/\sqrt{Re_x}$ vs. Y' lower surface

f) $Nu/\sqrt{Re_x}$ vs. X' lower surface

Contrails

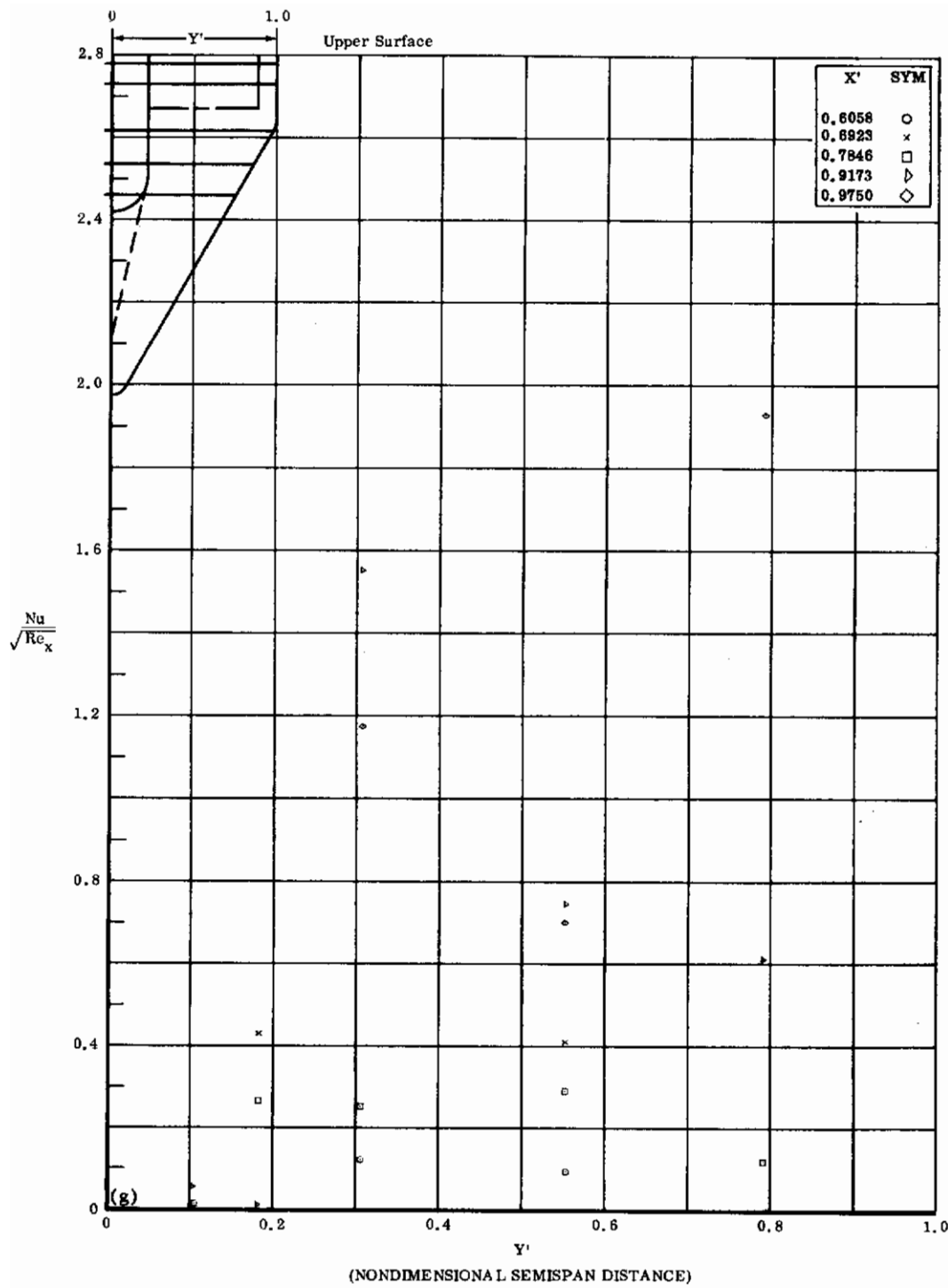


Fig. 6g Configuration I, $\alpha = +10$, $b_2 = b_3 = -20$
 $Nu/\sqrt{Re_x}$ vs. Y' upper surface

Contrails

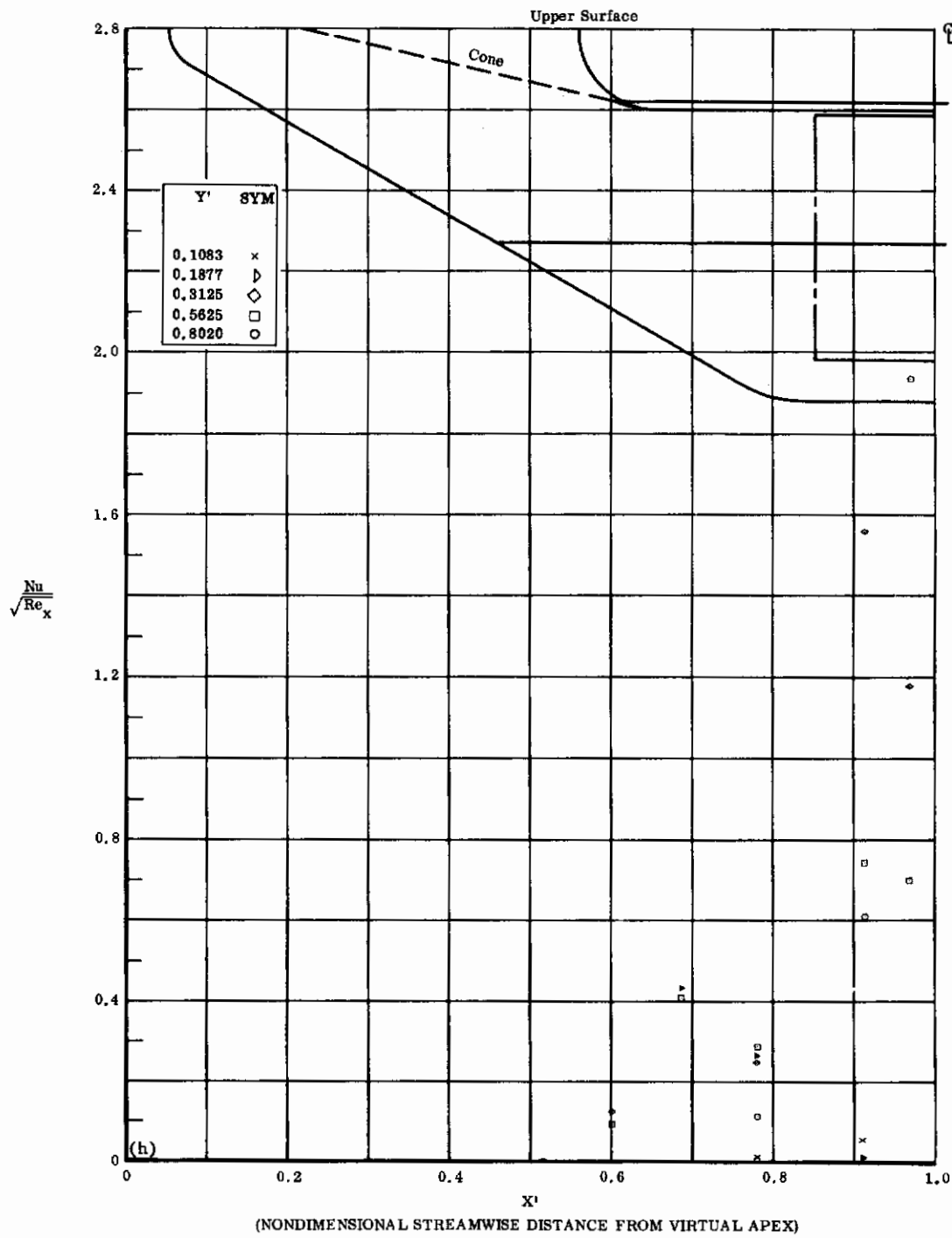


Fig. 6h Configuration I, $\alpha = +10$, $\delta_2 = \delta_3 = -20$

$Nu/\sqrt{Re_x}$ vs. X' upper surface

Contrails

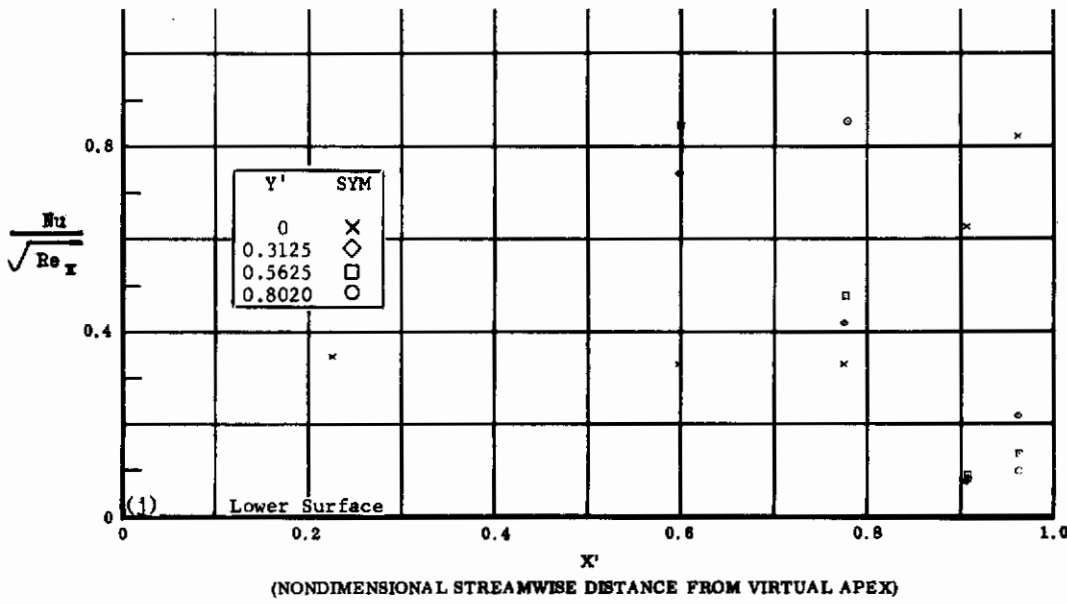
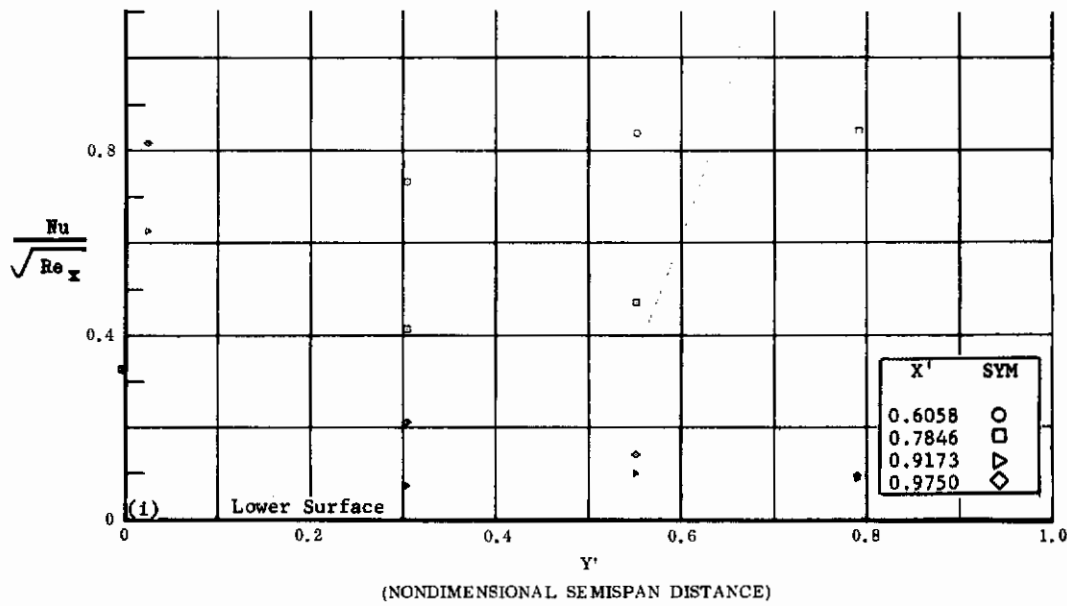


Fig. 6 Configuration I, $\alpha = +10$, $\delta_2 = \delta_3 = -30$

i) $Nu/\sqrt{Re_x}$ vs. Y' lower surface

j) $Nu/\sqrt{Re_x}$ vs. X' lower surface

Contrails

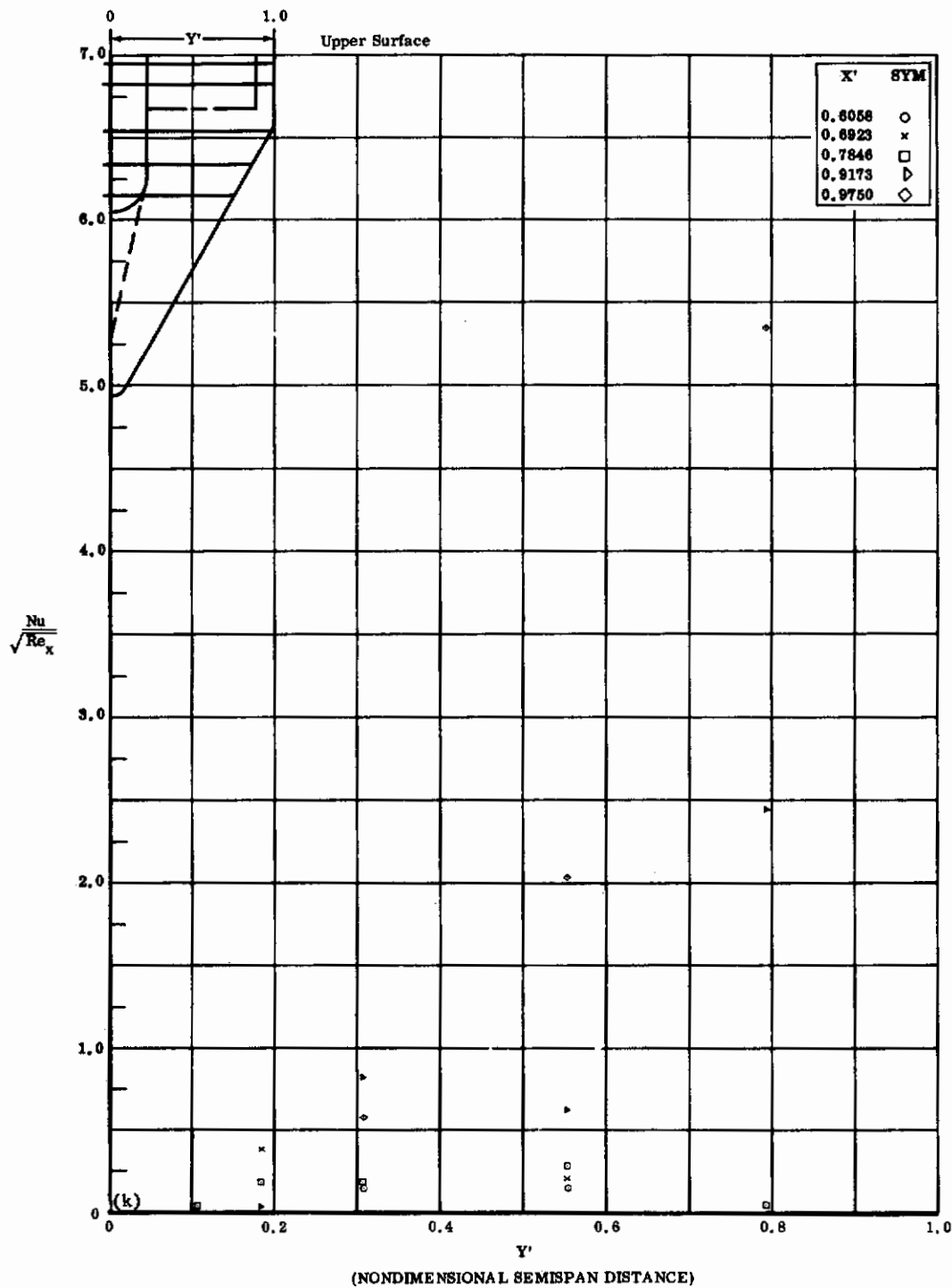


Fig. 6k Configuration I, $\alpha = +10$, $\delta_2 = \delta_3 = -30$
 $\frac{Nu}{\sqrt{Re_x}}$ vs. Y' upper surface

Contrails

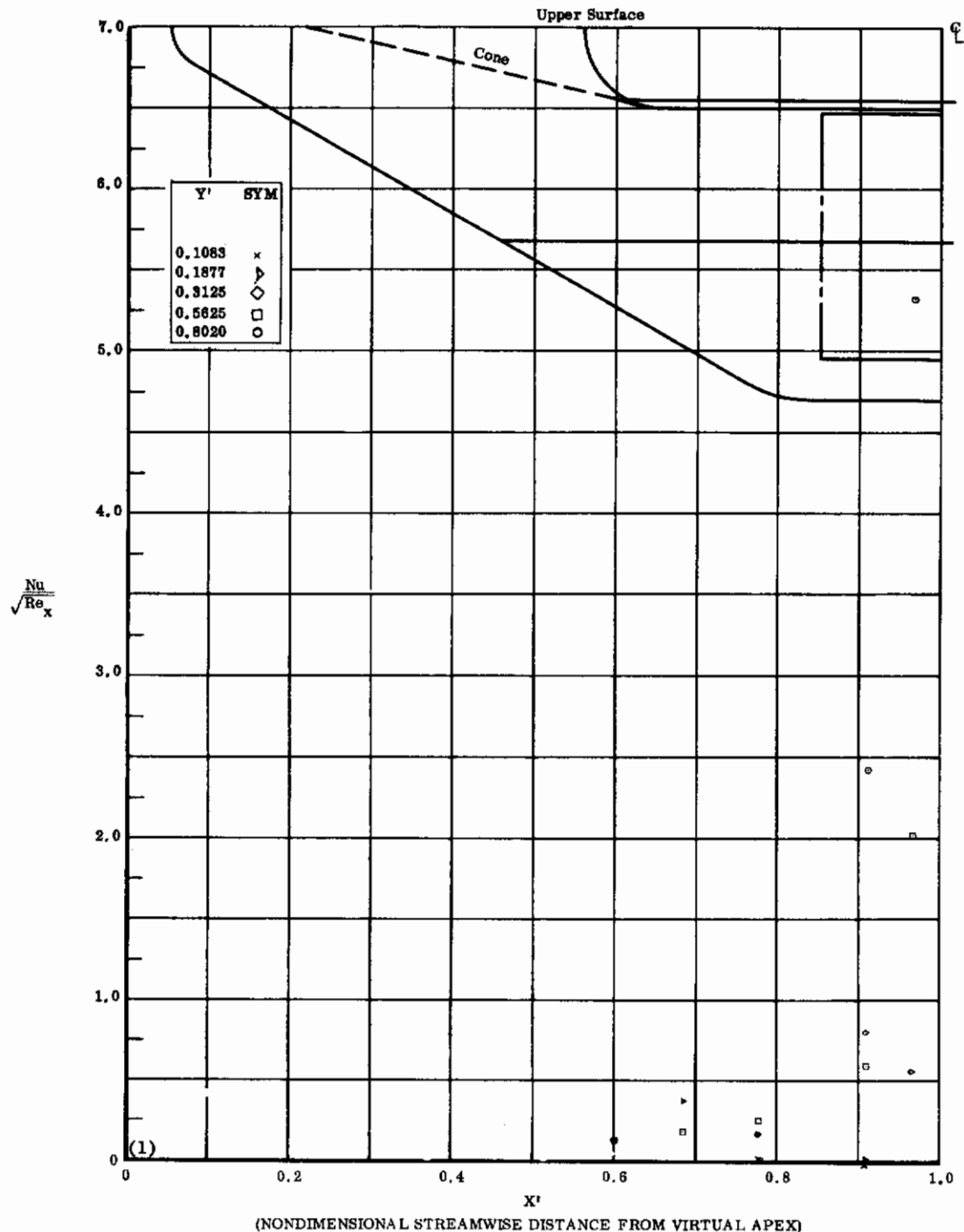


Fig. 62 Configuration I, $\alpha = +10^\circ$, $\delta_2 = \delta_3 = -30^\circ$

$Nu/\sqrt{Re_x}$ vs. X' upper surface

Contrails

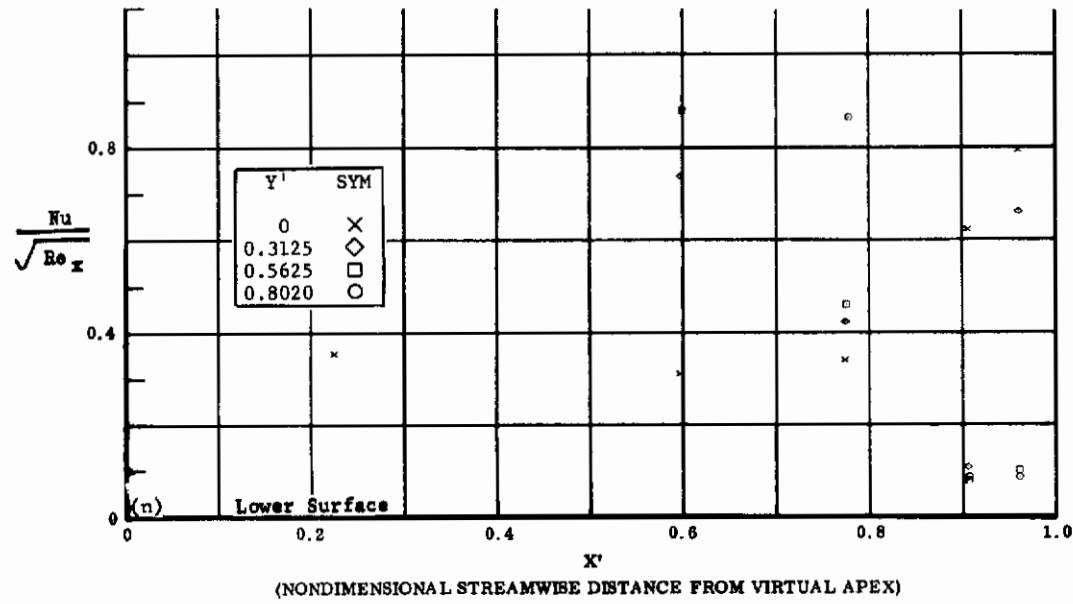
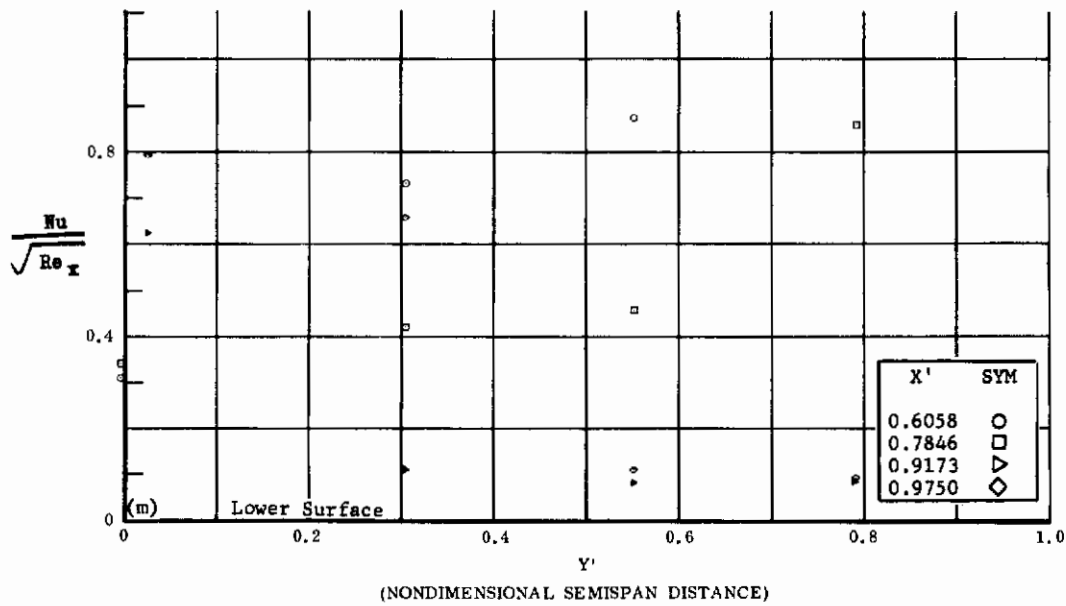


Fig. 6 Configuration I, $\alpha = +10$, $\delta_2 = \delta_3 = -39$

m) $Nu/\sqrt{Re_x}$ vs. Y' lower surface

n) $Nu/\sqrt{Re_x}$ vs. X' lower surface

Contrails

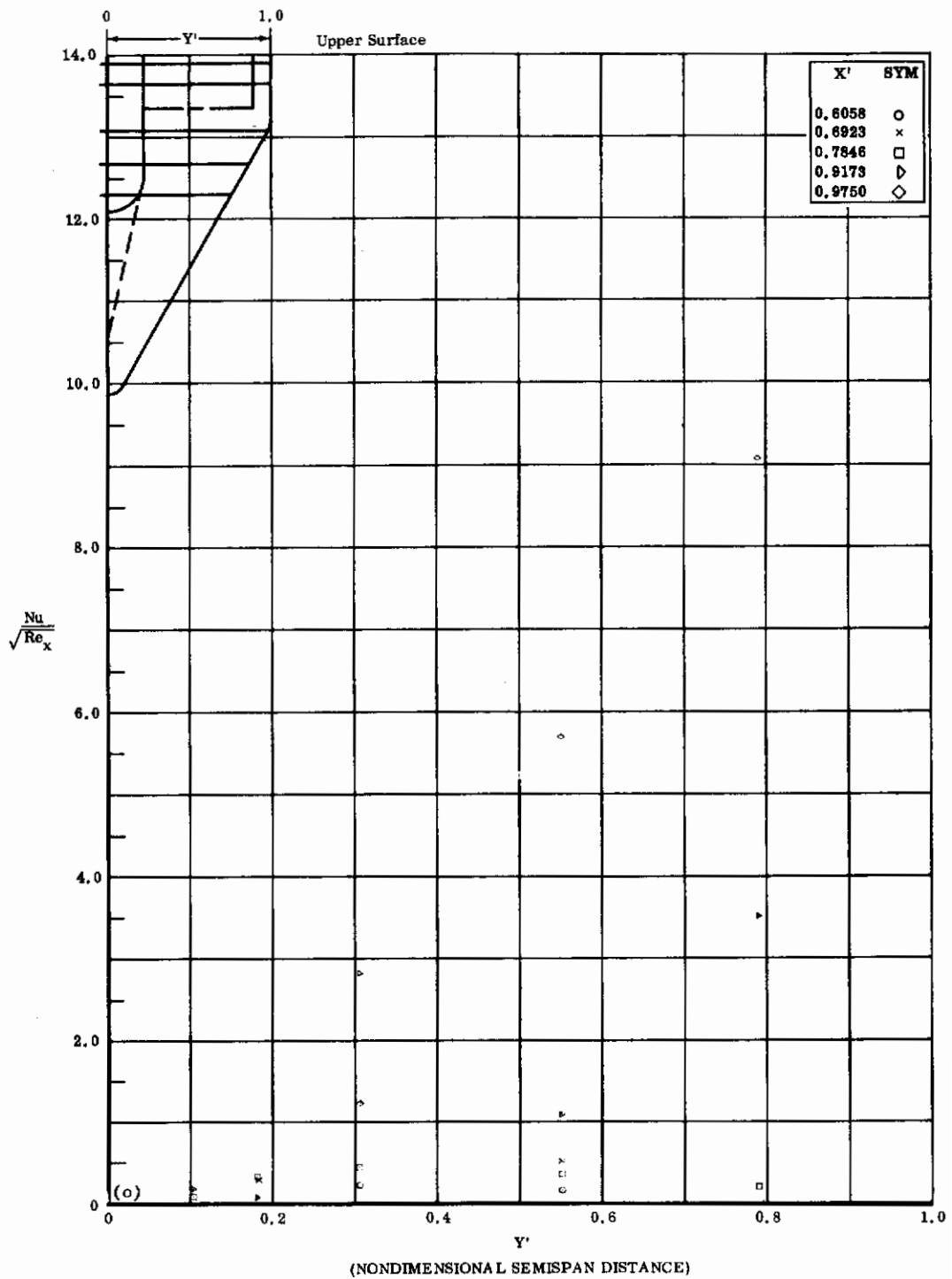


Fig. 6o Configuration I, $\alpha = +10$, $\delta_2 = \delta_3 = -39$
 $\text{Nu}/\sqrt{\text{Re}_x}$ vs. Y' upper surface

Contrails

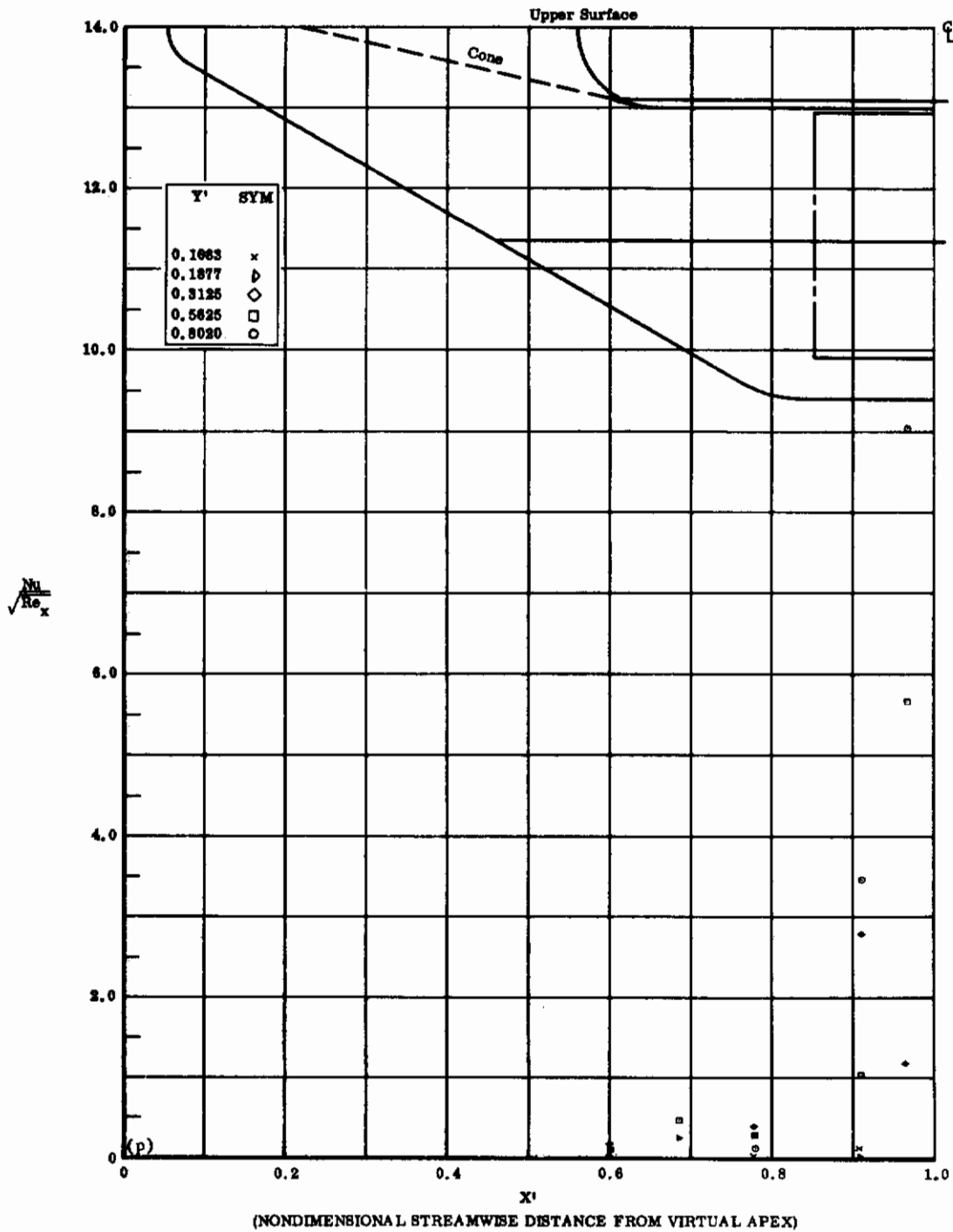


Fig. 6p Configuration I, $\alpha = +10$, $\delta_2 = \delta_3 = -39$
 $Nu/\sqrt{Re_x}$ vs. X' upper surface

Contrails

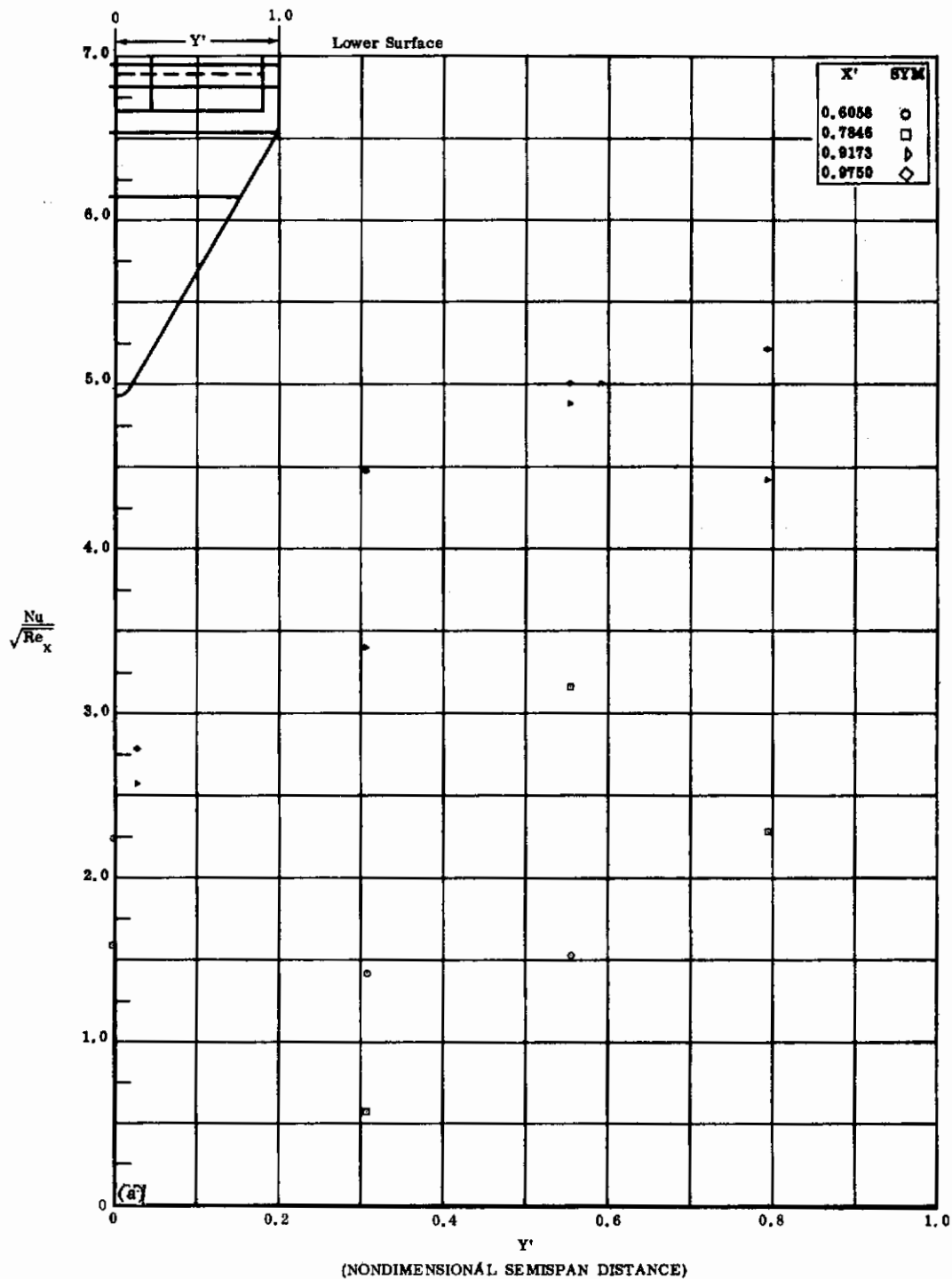


Fig. 7a Configuration I, $\alpha = +20$, $\delta_2 = \delta_3 = 0$
 $Nu/\sqrt{Re_x}$ vs. Y' lower surface

Contrails

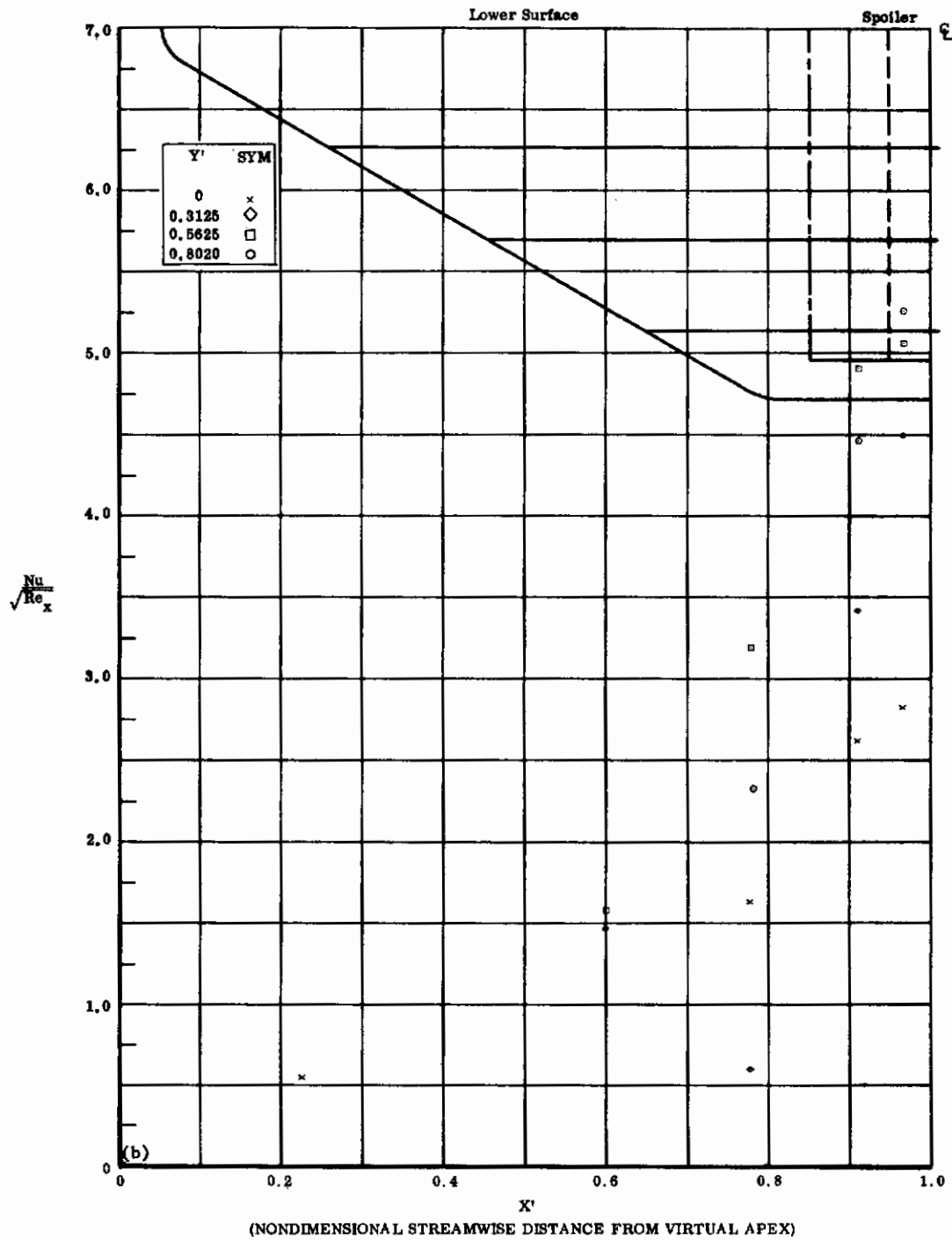


Fig. 7b Configuration I, $\alpha = +20^\circ$, $\delta_2 = \delta_3 = 0$

$Nu/\sqrt{Re_x}$ vs. X' lower surface

Contrails

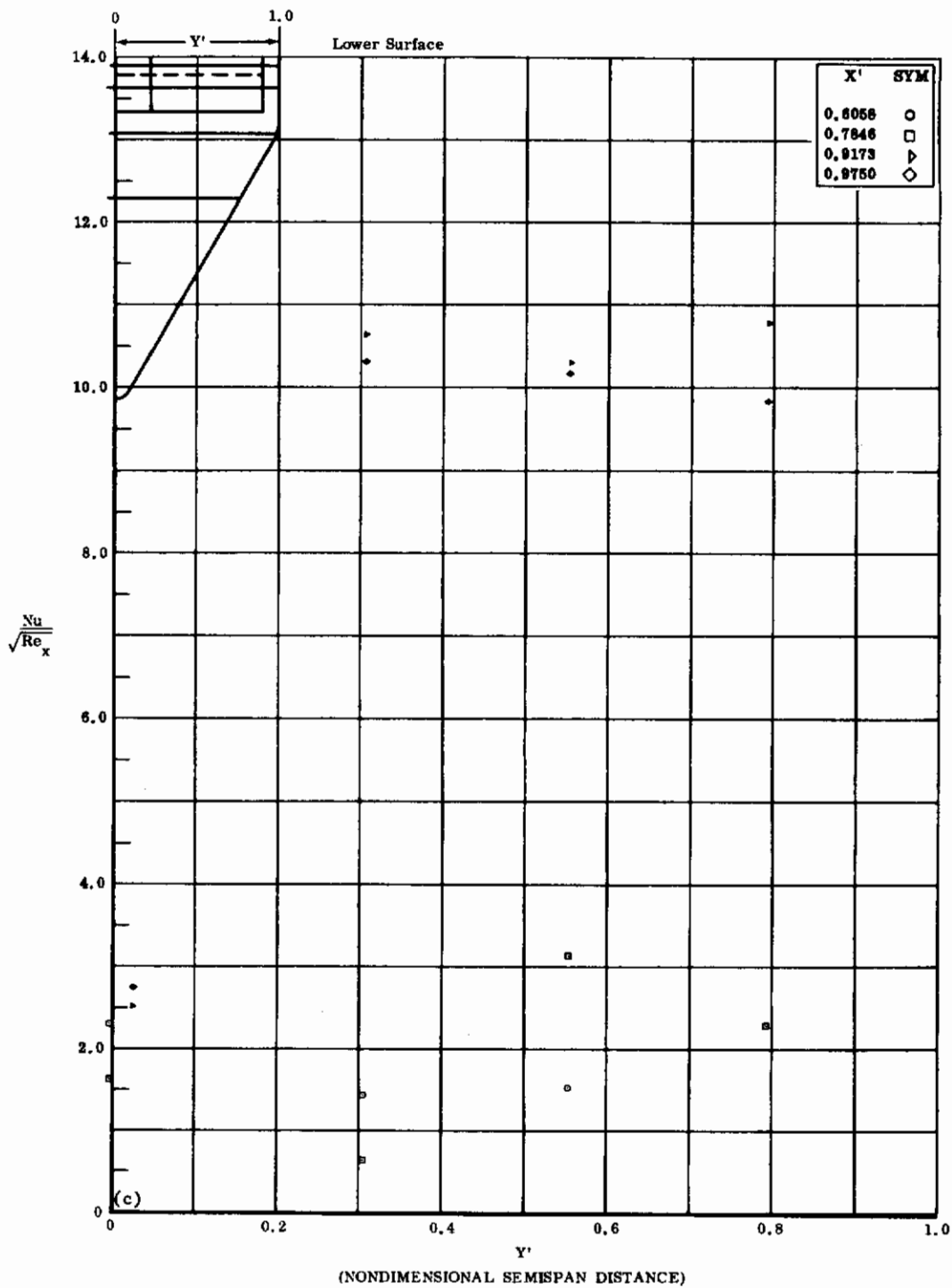


Fig. 7c Configuration I, $\alpha = +20^\circ$, $\delta_2 = \delta_3 = +10^\circ$
 $\frac{Nu}{\sqrt{Re_x}}$ vs. Y' lower surface

Contrails

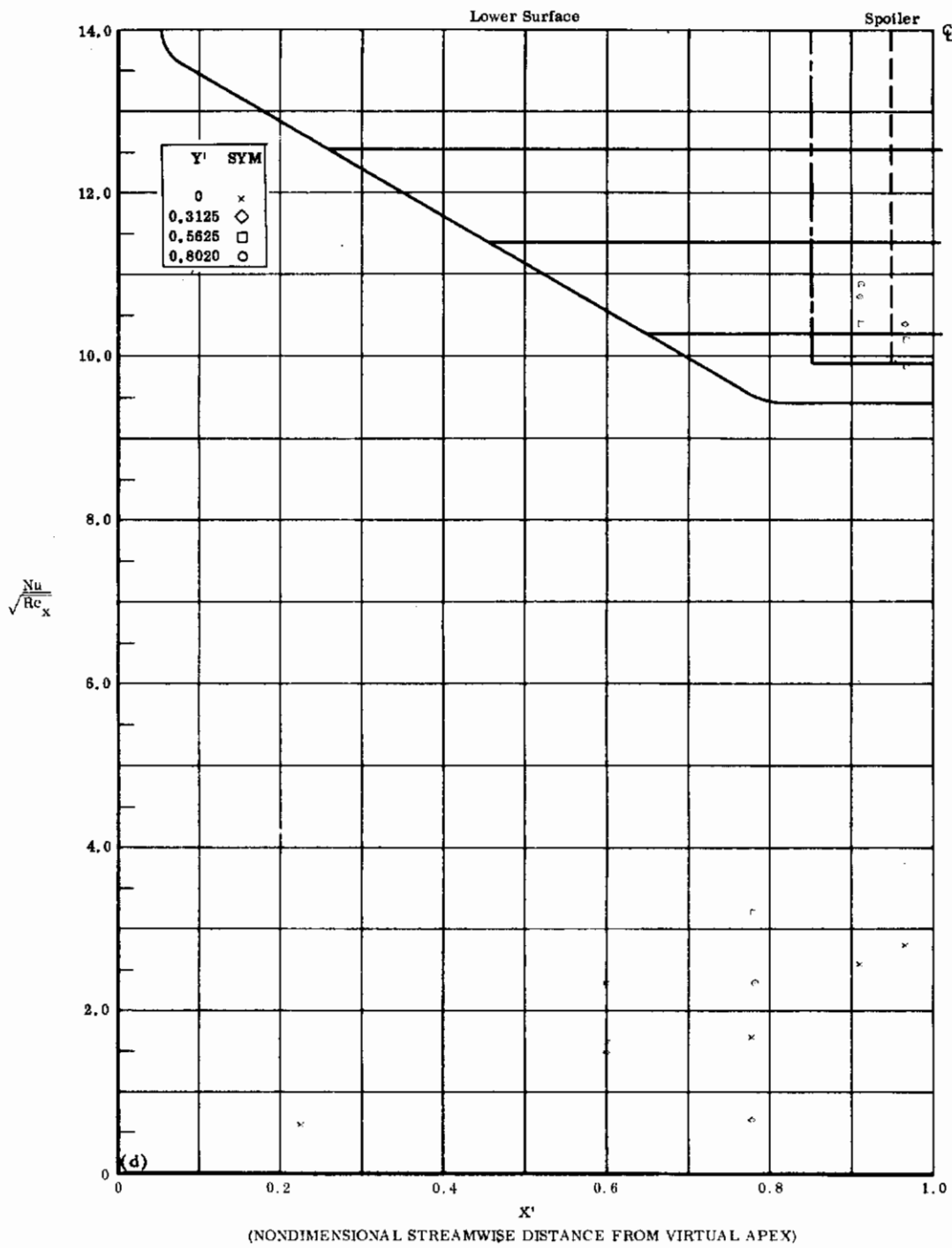


Fig. 7d Configuration I, $\alpha = +20^\circ$, $\delta_2 = \delta_3 = +10^\circ$

$\text{Nu}/\sqrt{\text{Re}_x}$ vs. X' lower surface

Contrails

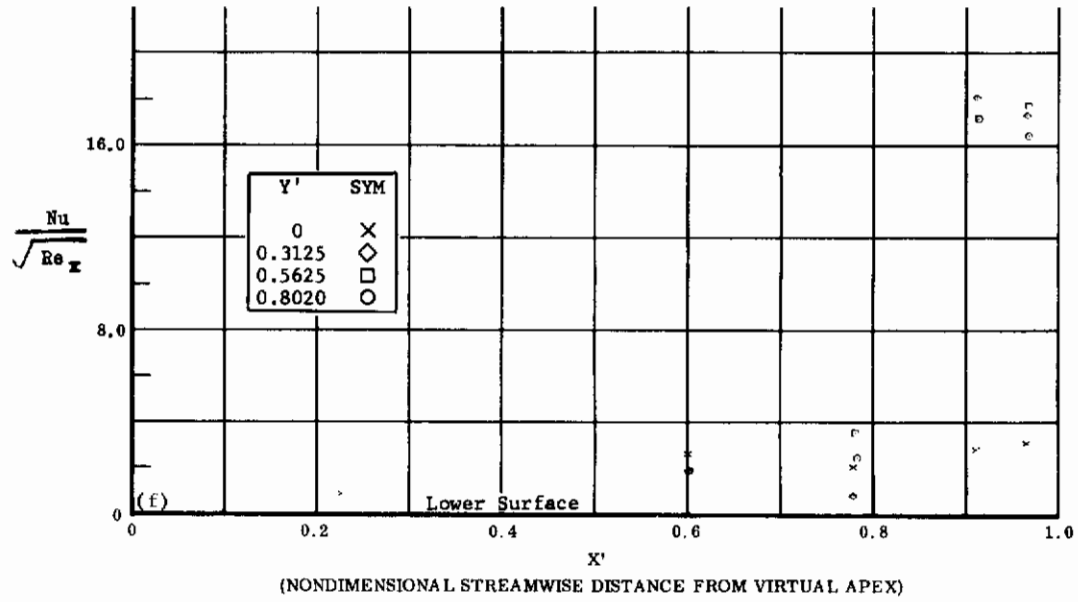
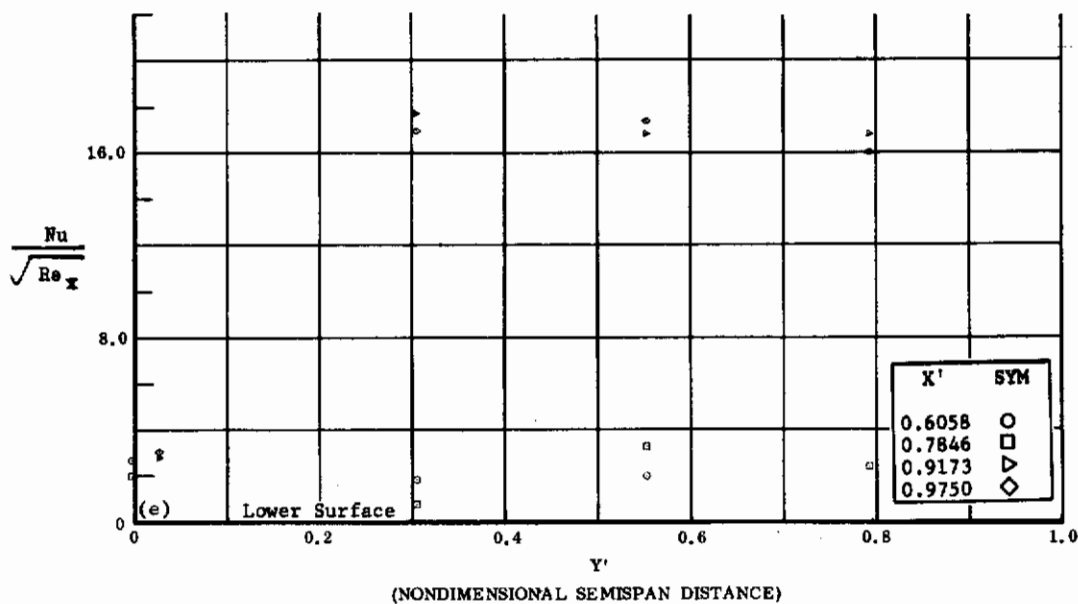


Fig. 7 Configuration I, $\alpha = +20^\circ$, $\delta_2 = \delta_3 = +20^\circ$

e) $Nu/\sqrt{Re_x}$ vs. Y' lower surface

f) $Nu/\sqrt{Re_x}$ vs. X' lower surface

Contrails

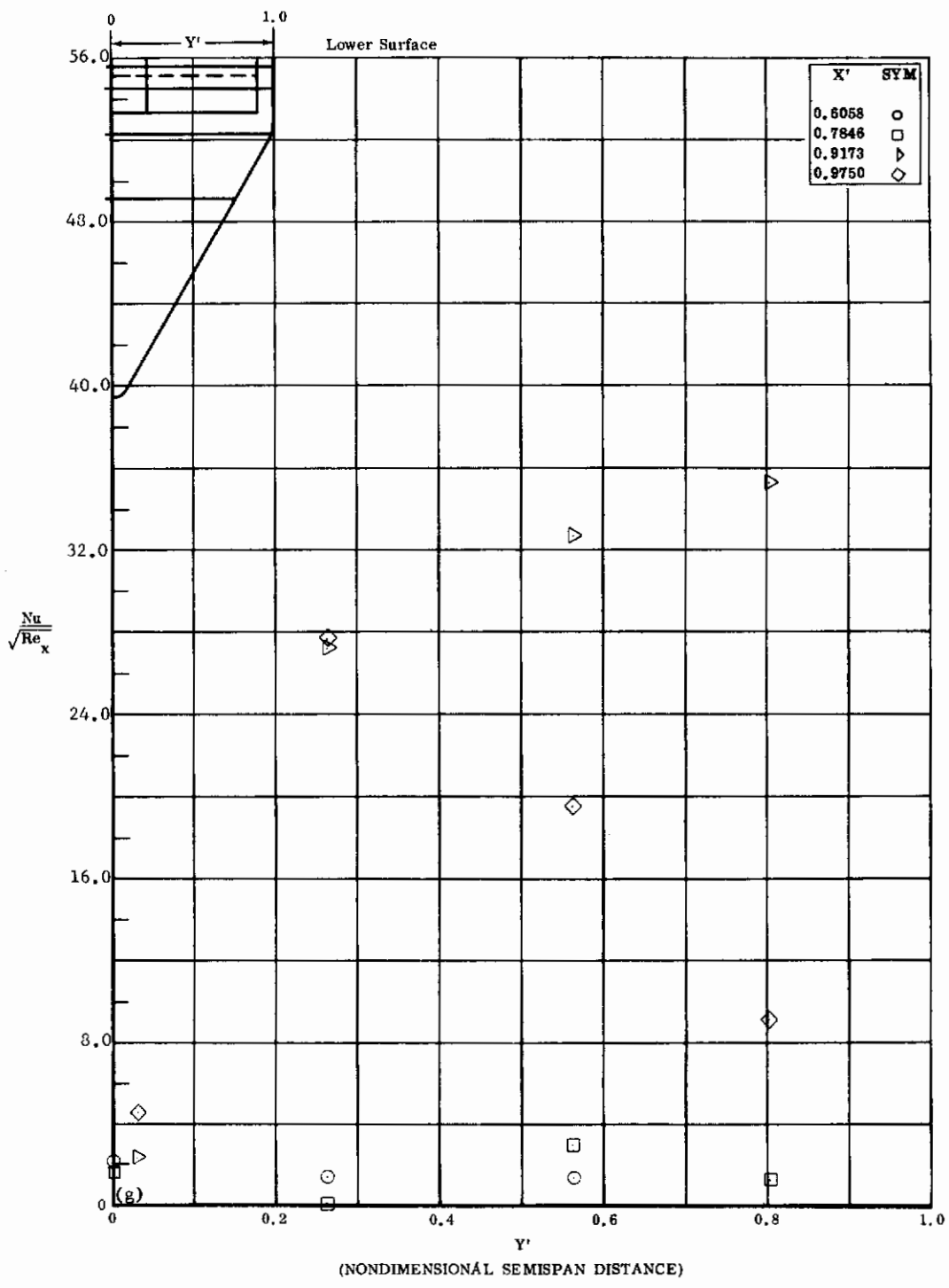


Fig. 7g Configuration I, $\alpha = +20$, $s_2 = s_3 = +30$

$Nu/\sqrt{Re_x}$ vs. Y' lower surface

Contrails

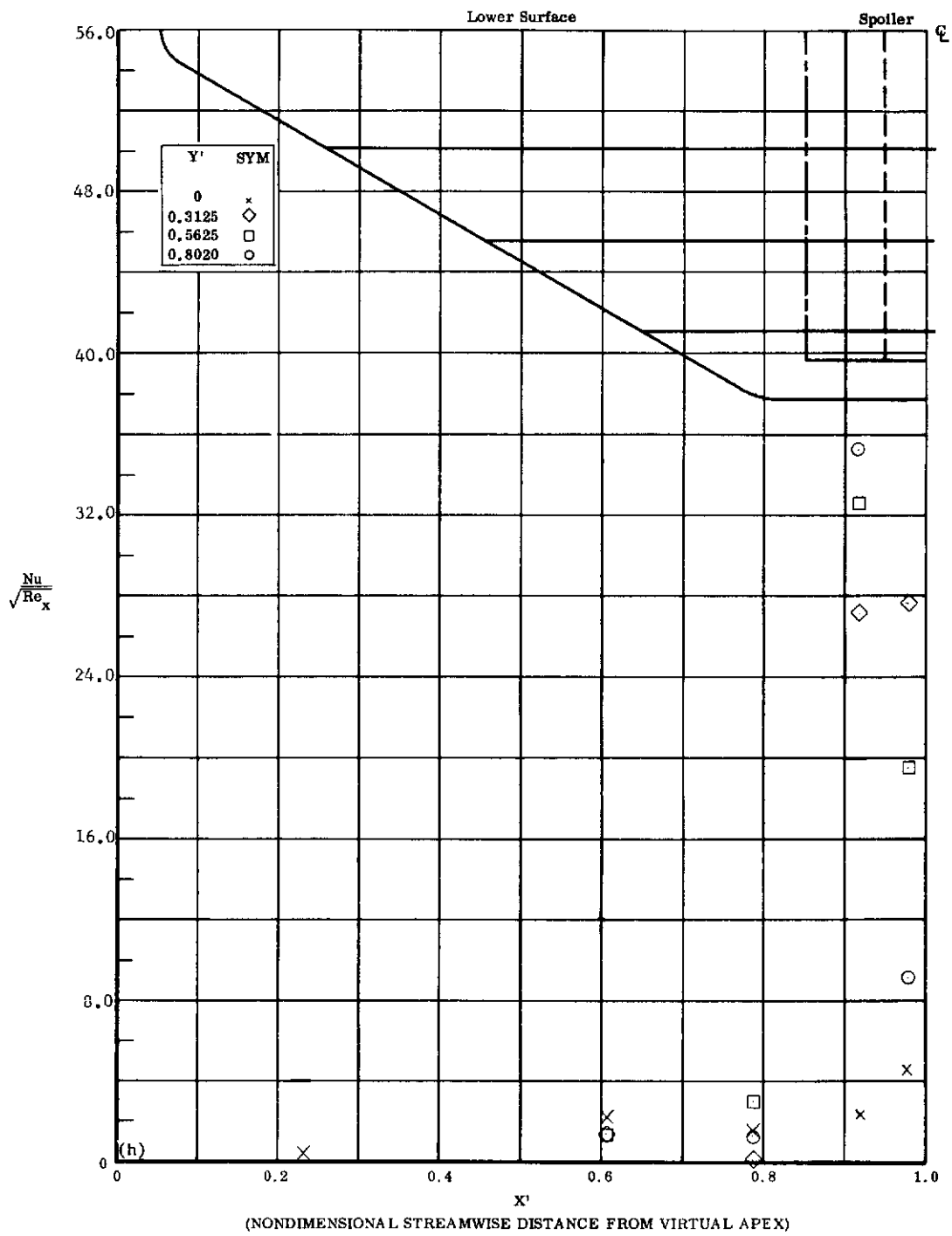


Fig. 7h Configuration I, $\alpha = +20$, $\delta_2 = \delta_3 = +30$
 $\frac{\text{Nu}}{\sqrt{\text{Re}_x}}$ vs. X' lower surface

Contrails

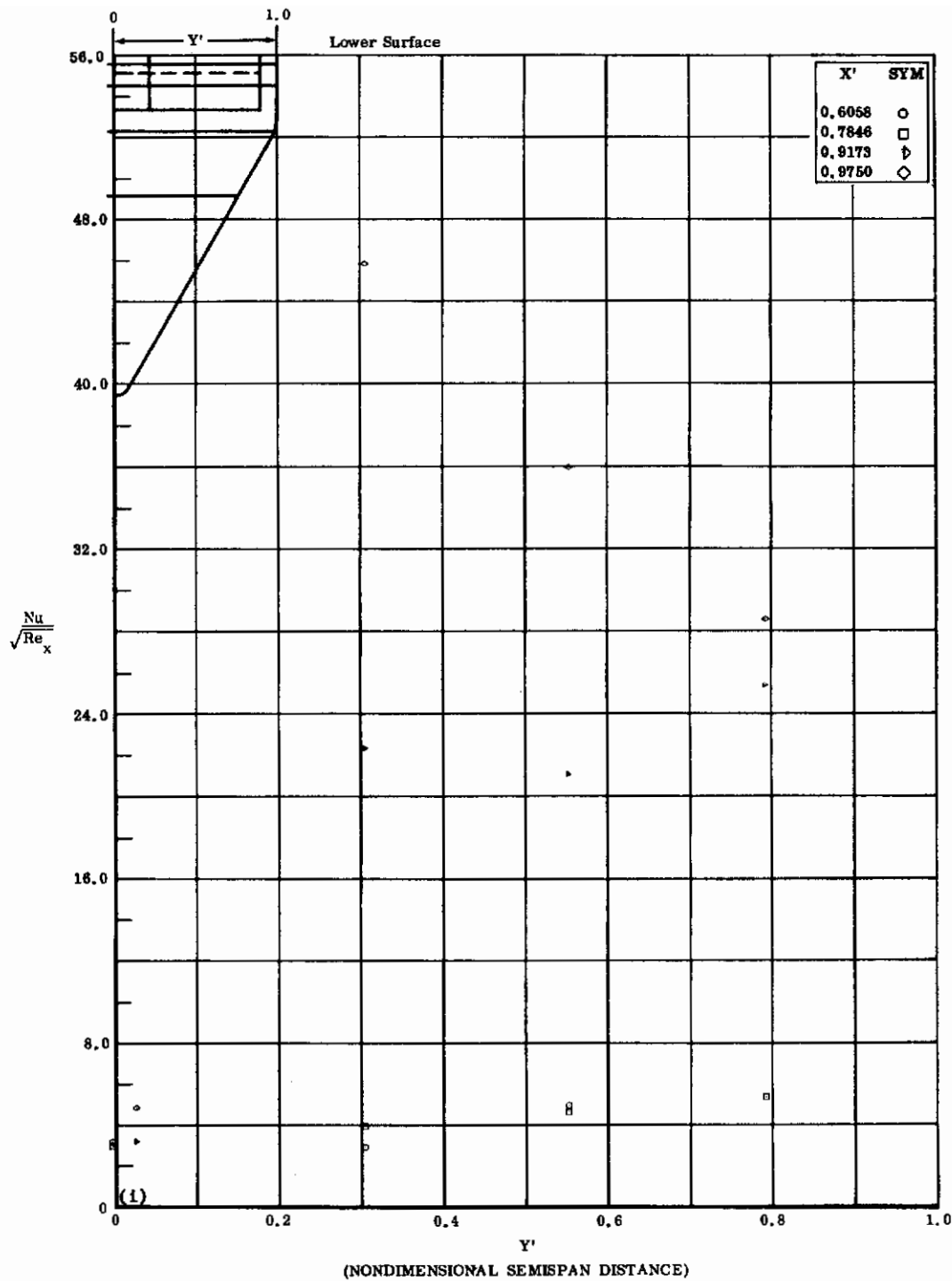


Fig. 71 Configuration I, $\alpha = +20$, $\delta_2 = \delta_3 = +39$
 $Nu/\sqrt{Re_x}$ vs. Y' lower surface

Contrails

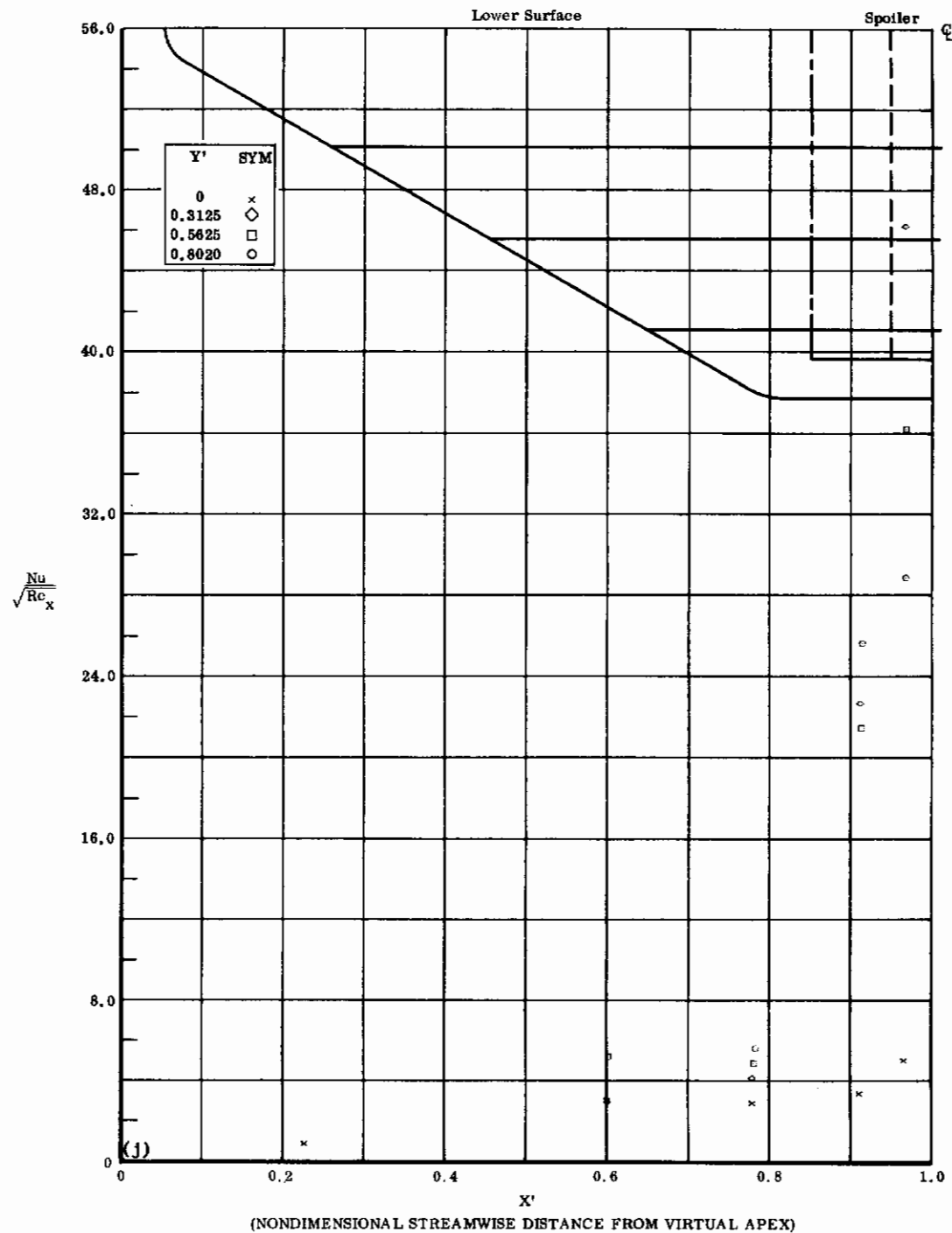


Fig. 7j Configuration I, $\alpha = +20^\circ$, $\delta_2 = \delta_3 = +39^\circ$

$Nu/\sqrt{Re_x}$ vs. X' lower surface

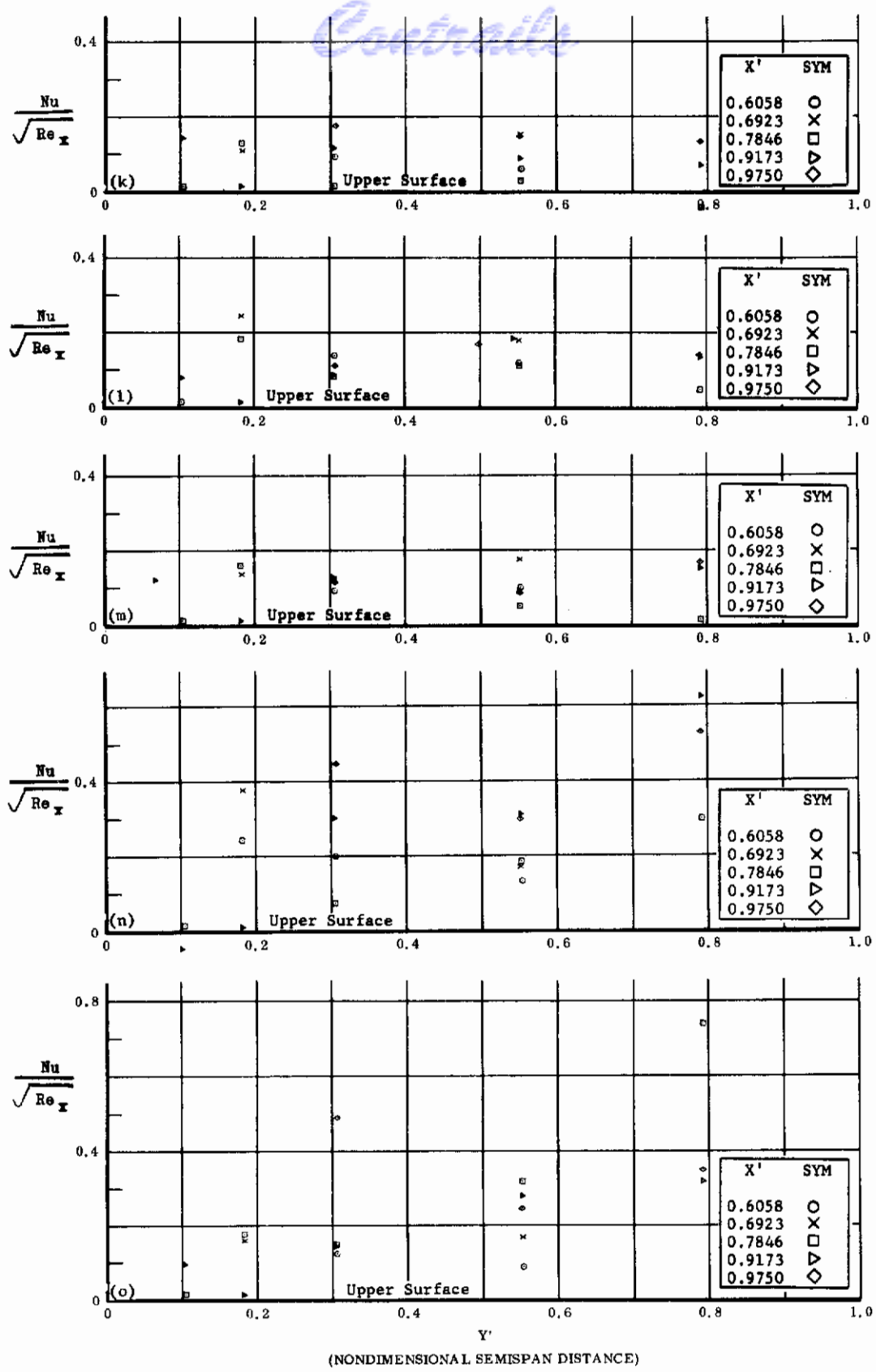


Fig. 7 Configuration I, $\alpha = +20$, $Nu/\sqrt{Re_x}$ vs. Y' , upper surface

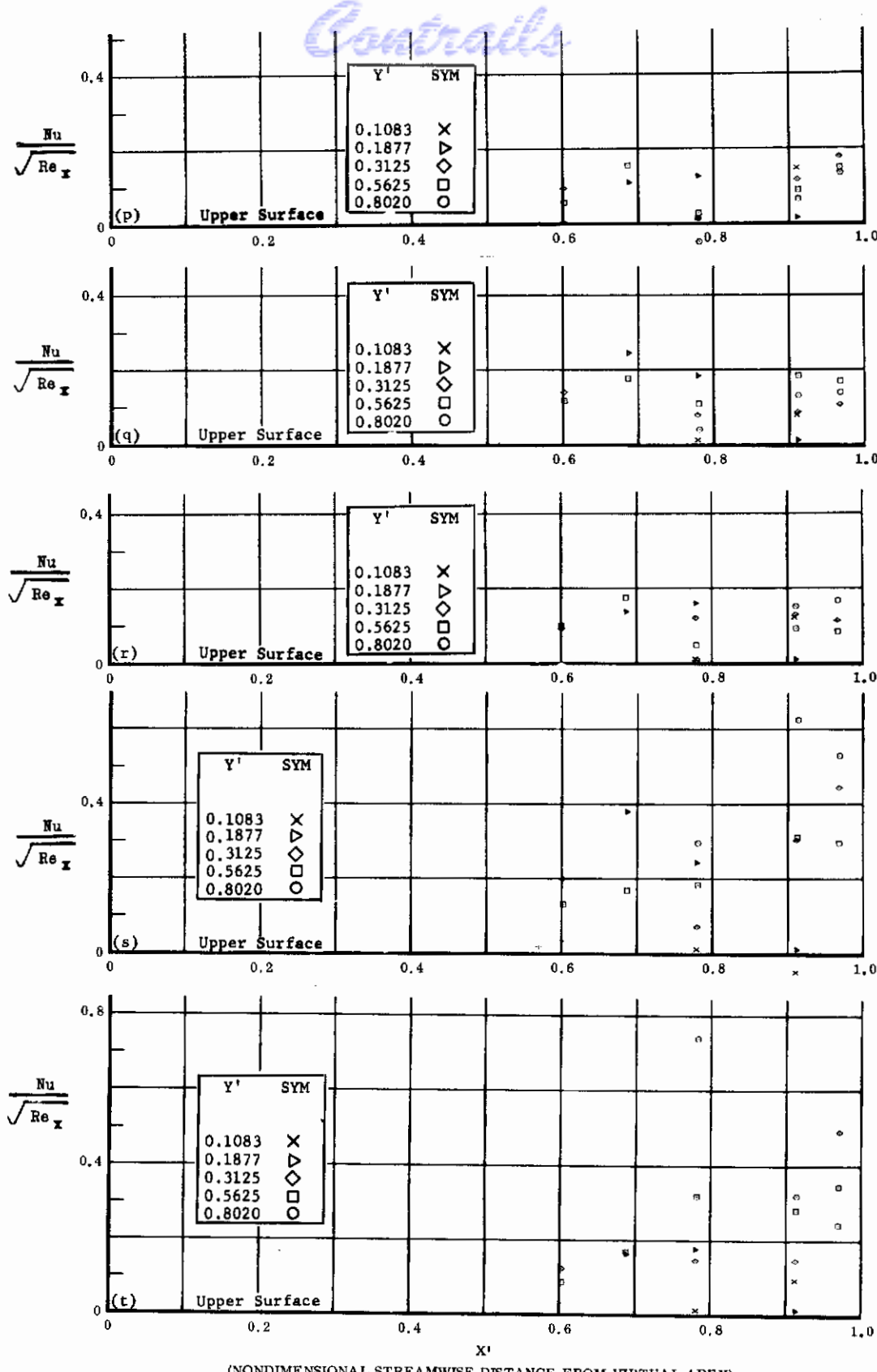
k) $\delta_2 = \delta_3 = 0$

l) $\delta_2 = \delta_3 = +10$

m) $\delta_2 = \delta_3 = +20$

n) $\delta_2 = \delta_3 = +30$

o) $\delta_2 = \delta_3 = +39$



(NONDIMENSIONAL STREAMWISE DISTANCE FROM VIRTUAL APEX)

Fig. 7 Configuration I, $\alpha = +20$, $Nu/\sqrt{Re_x}$ vs. X' , upper surface

p) $\delta_2 = \delta_3 = 0$

q) $\delta_2 = \delta_3 = +10$

r) $\delta_2 = \delta_3 = +20$

s) $\delta_2 = \delta_3 = +30$

t) $\delta_2 = \delta_3 = +39$

Contrails

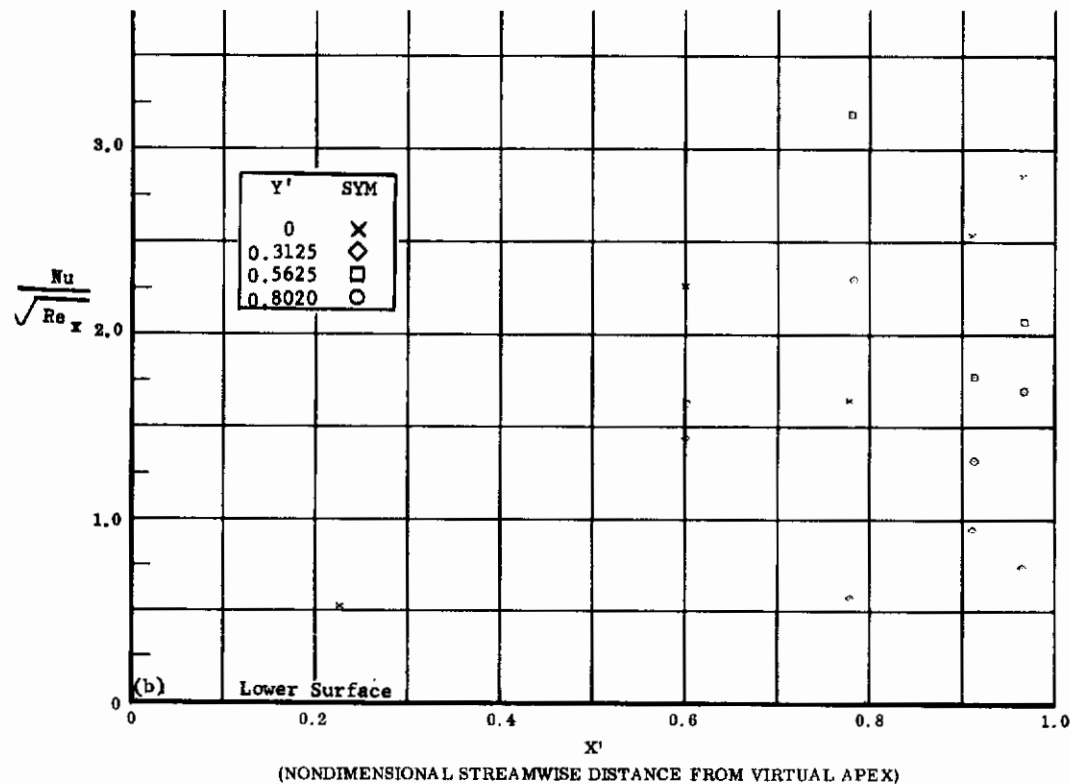
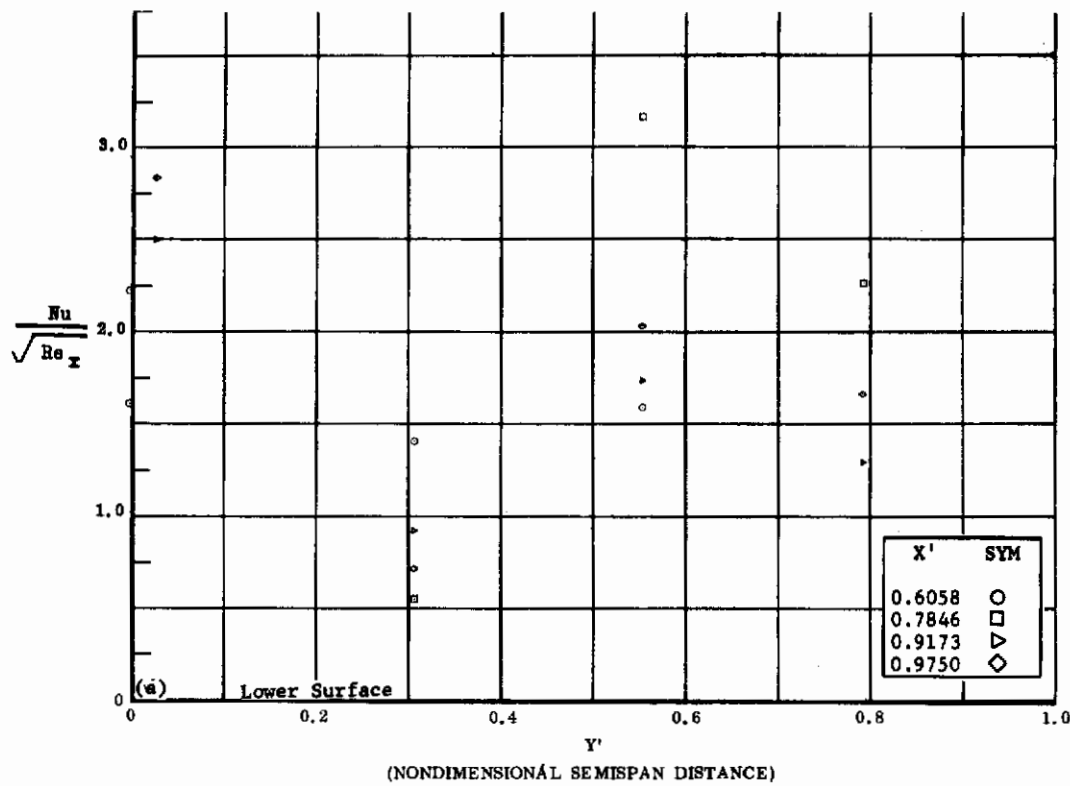


Fig. 8 Configuration I, $\alpha = +20$, $b_2 = b_3 = -10$

a) $Nu/\sqrt{Re_x}$ vs. Y' lower surface

b) $Nu/\sqrt{Re_x}$ vs. X' lower surface

Contrails

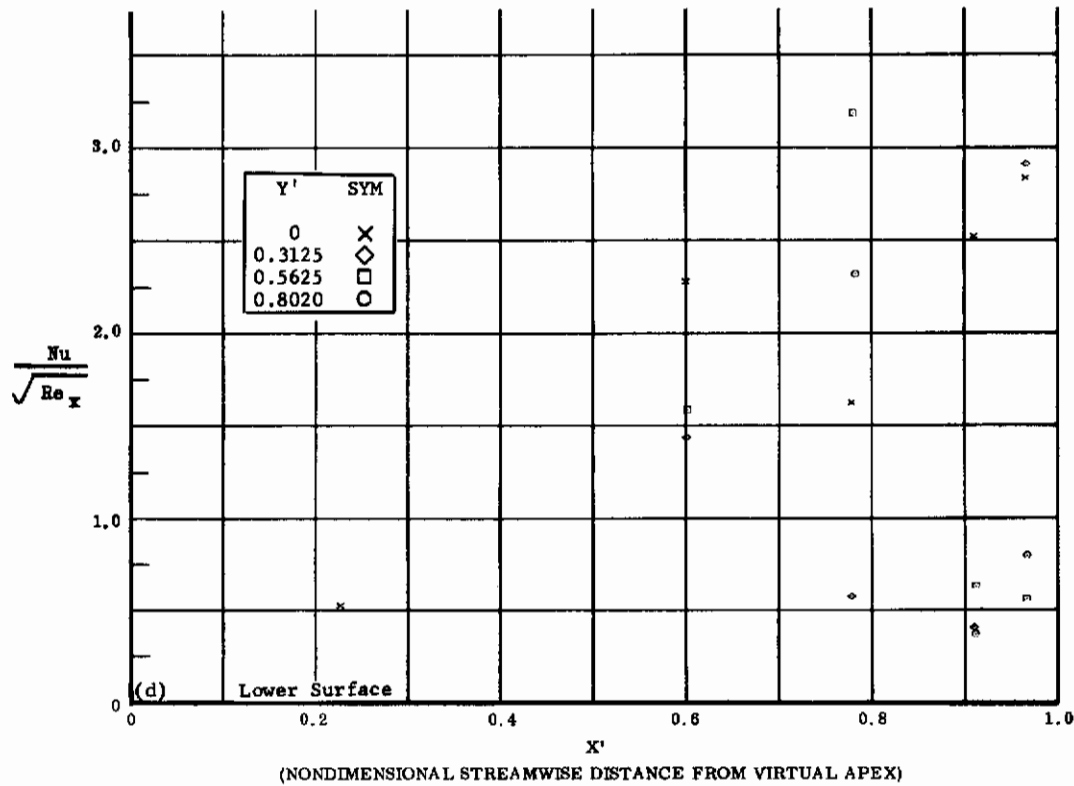
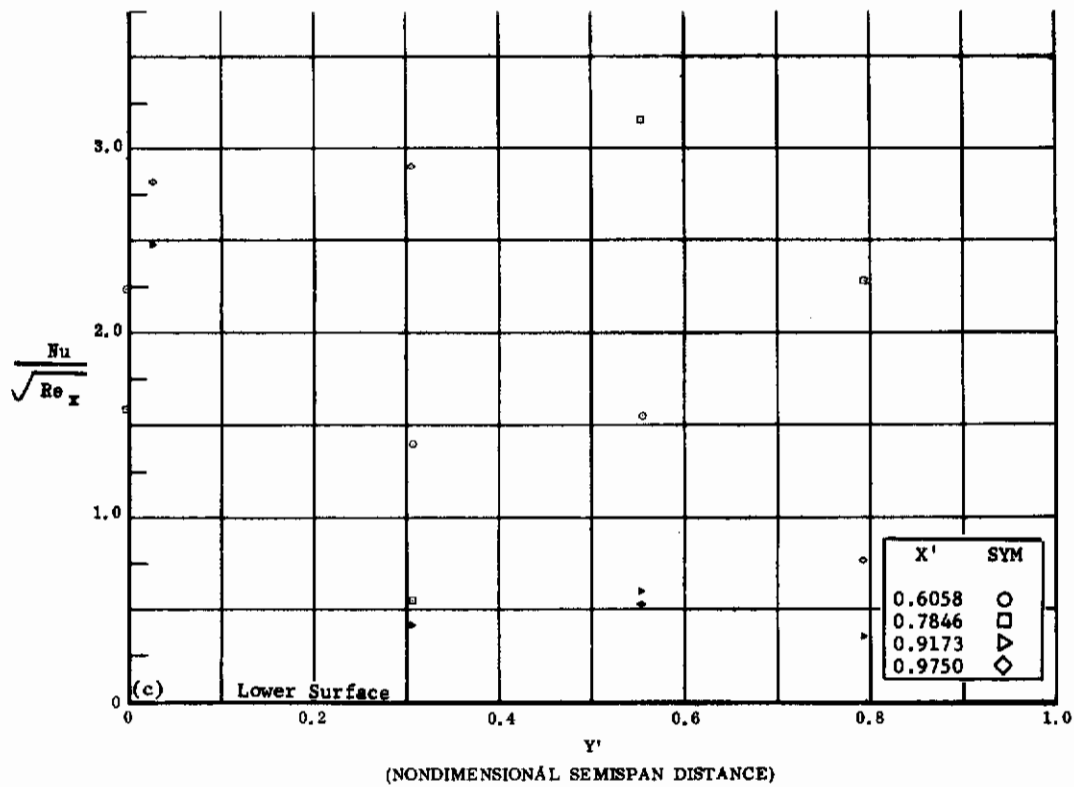


Fig. 8 Configuration I, $\alpha = +20^\circ$, $\delta_2 = \delta_3 = -20^\circ$

c) $\text{Nu}/\sqrt{\text{Re}_x}$ vs. Y' lower surface

d) $\text{Nu}/\sqrt{\text{Re}_x}$ vs. X' lower surface

Contrails

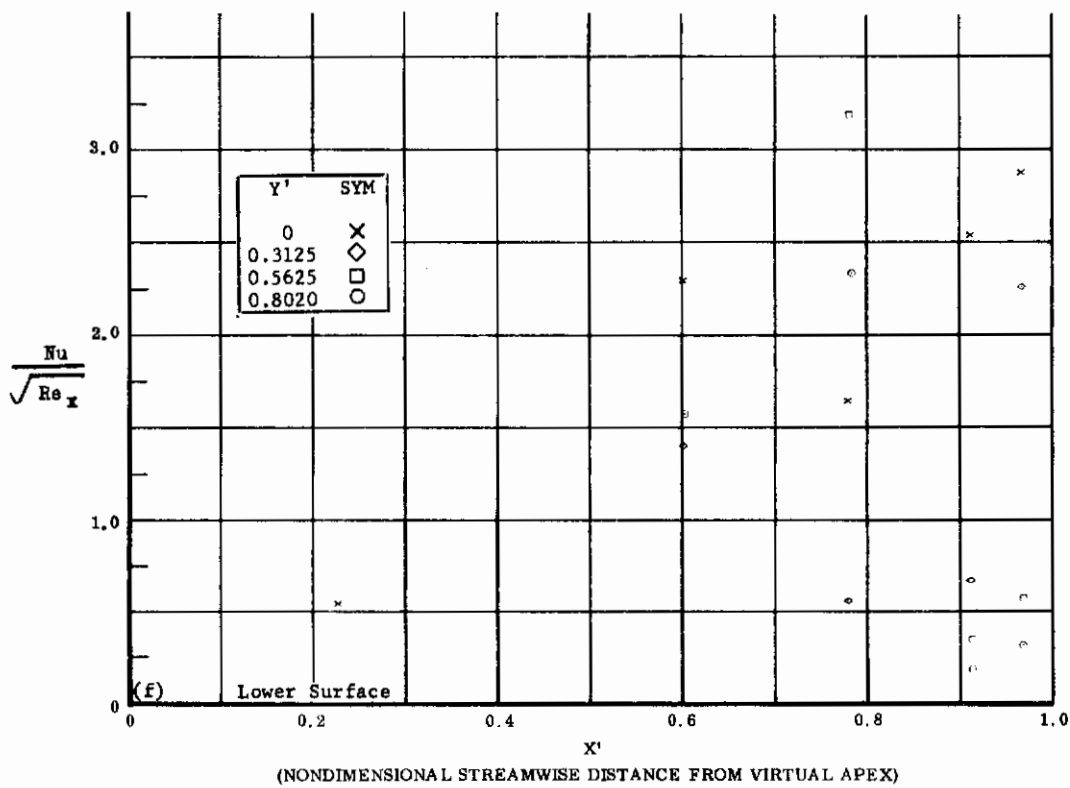
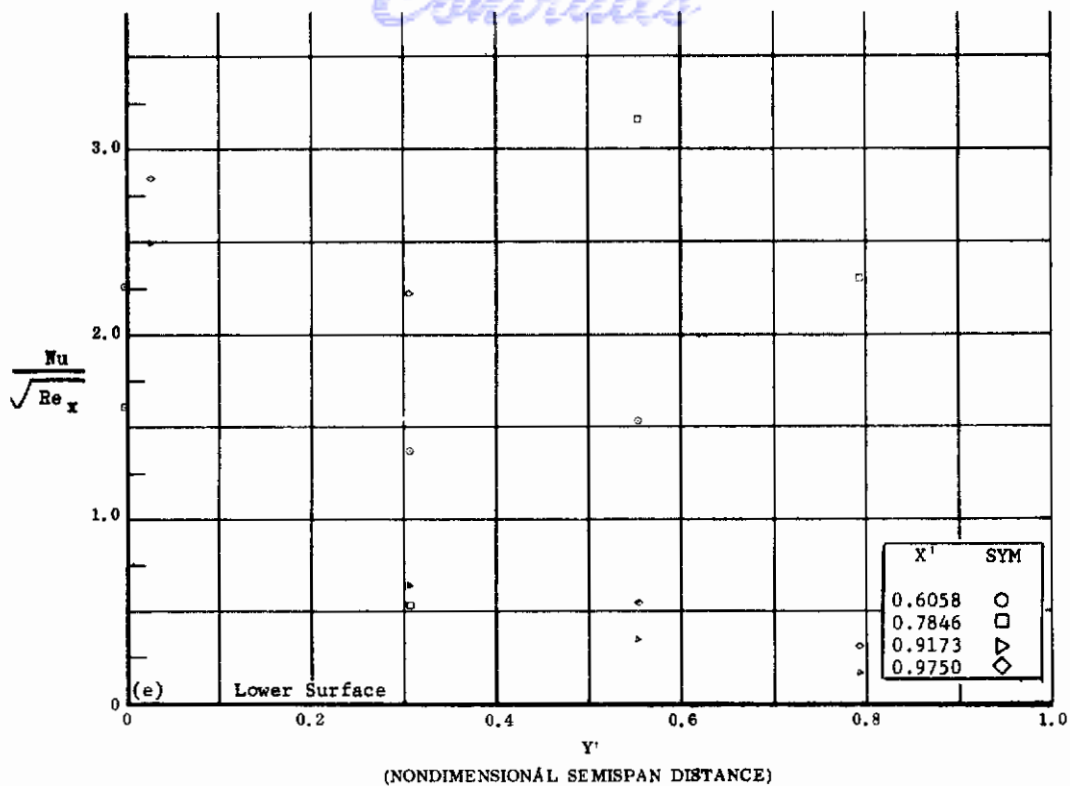


Fig. 8 Configuration I, $\alpha = +20$, $\delta_2 = \delta_3 = -30$

e) $Nu/\sqrt{Re_x}$ vs. Y' lower surface

f) $Nu/\sqrt{Re_x}$ vs. X' lower surface

Contrails

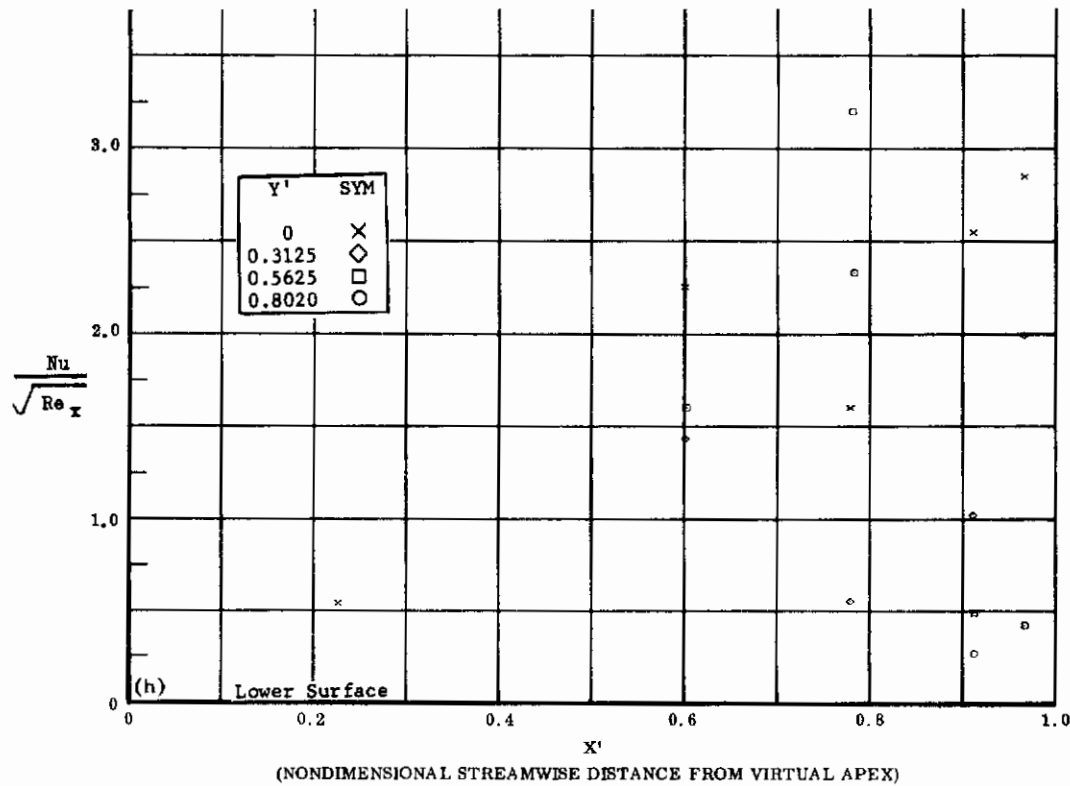
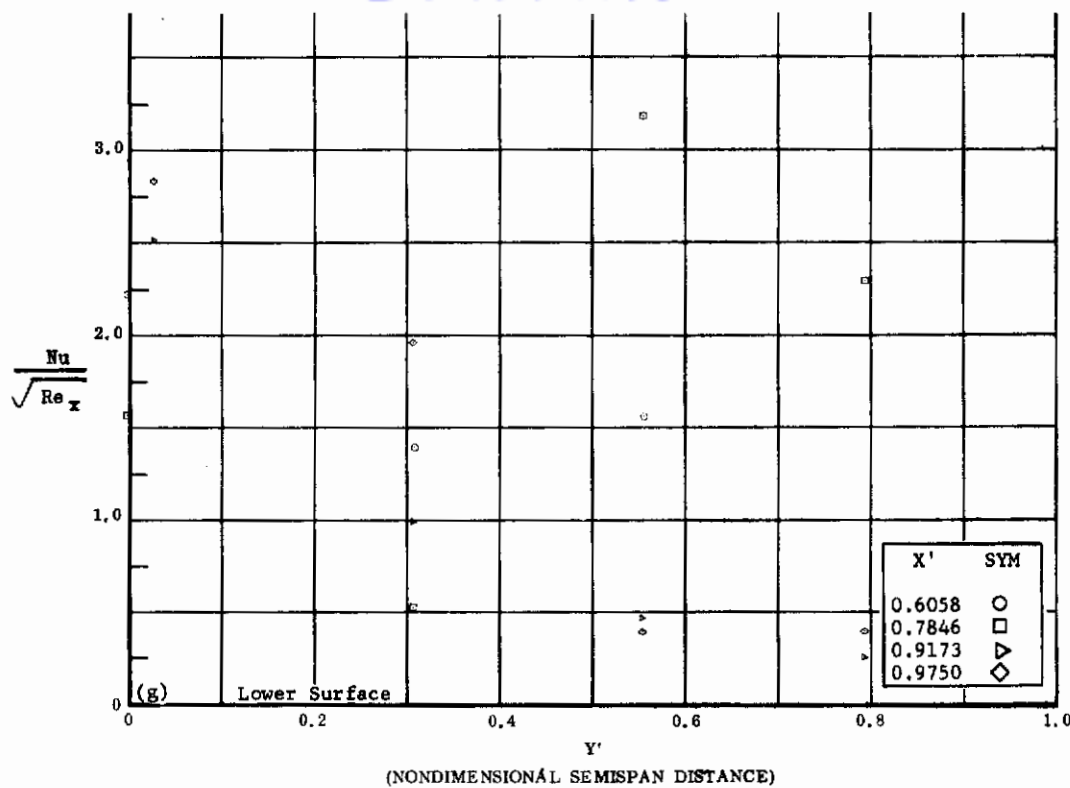


Fig. 8 Configuration I, $\alpha = +20$, $\delta_2 = \delta_3 = -39$

g) $\text{Nu}/\sqrt{\text{Re}_x}$ vs. Y' lower surface

h) $\text{Nu}/\sqrt{\text{Re}_x}$ vs. X' lower surface

Controls

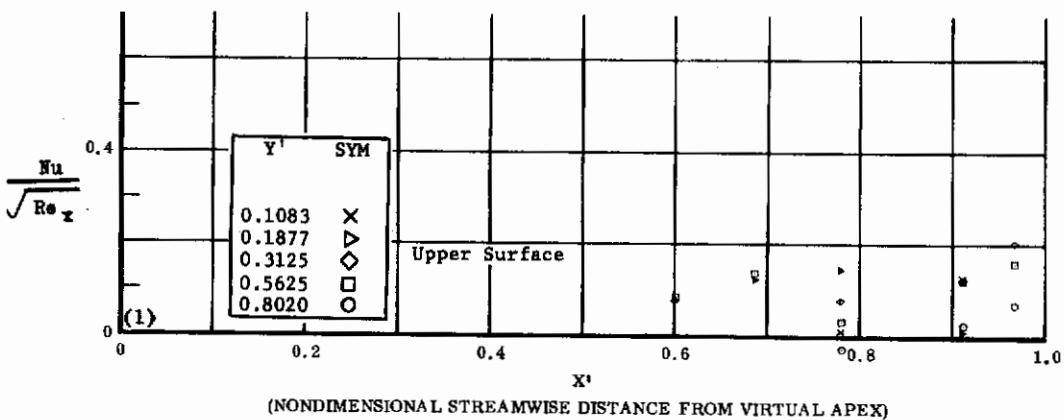
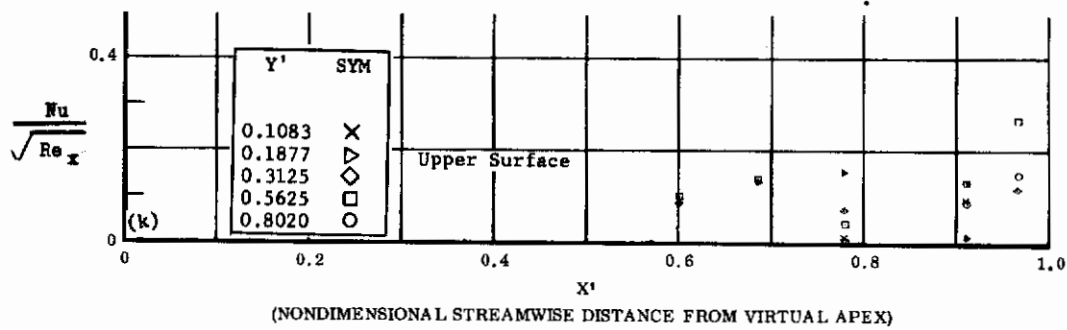
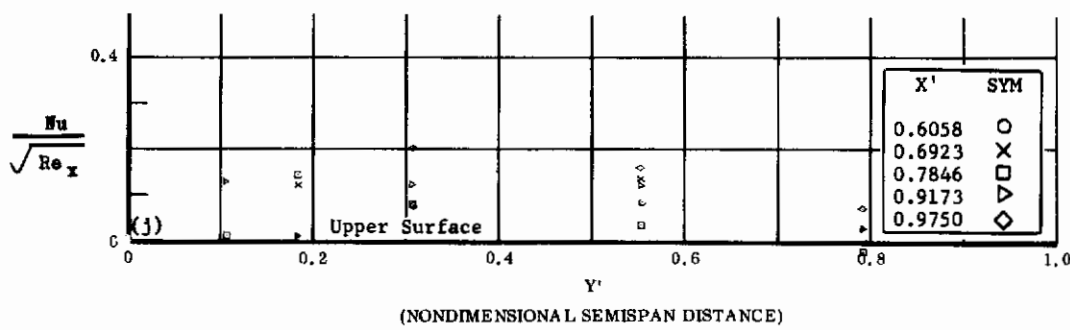
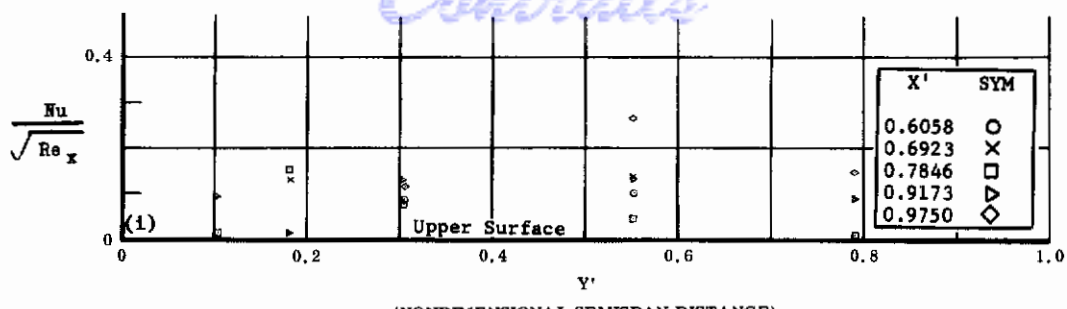


Fig. 8 Configuration I, $\alpha = +20$, upper surface

- 1) $Nu/\sqrt{Re_x}$ vs. Y' $\delta_2 = \delta_3 = -10$
- 2) $Nu/\sqrt{Re_x}$ vs. Y' $\delta_2 = \delta_3 = -20$
- 3) $Nu/\sqrt{Re_x}$ vs. X' $\delta_2 = \delta_3 = -10$
- 4) $Nu/\sqrt{Re_x}$ vs. X' $\delta_2 = \delta_3 = -20$

Contrails

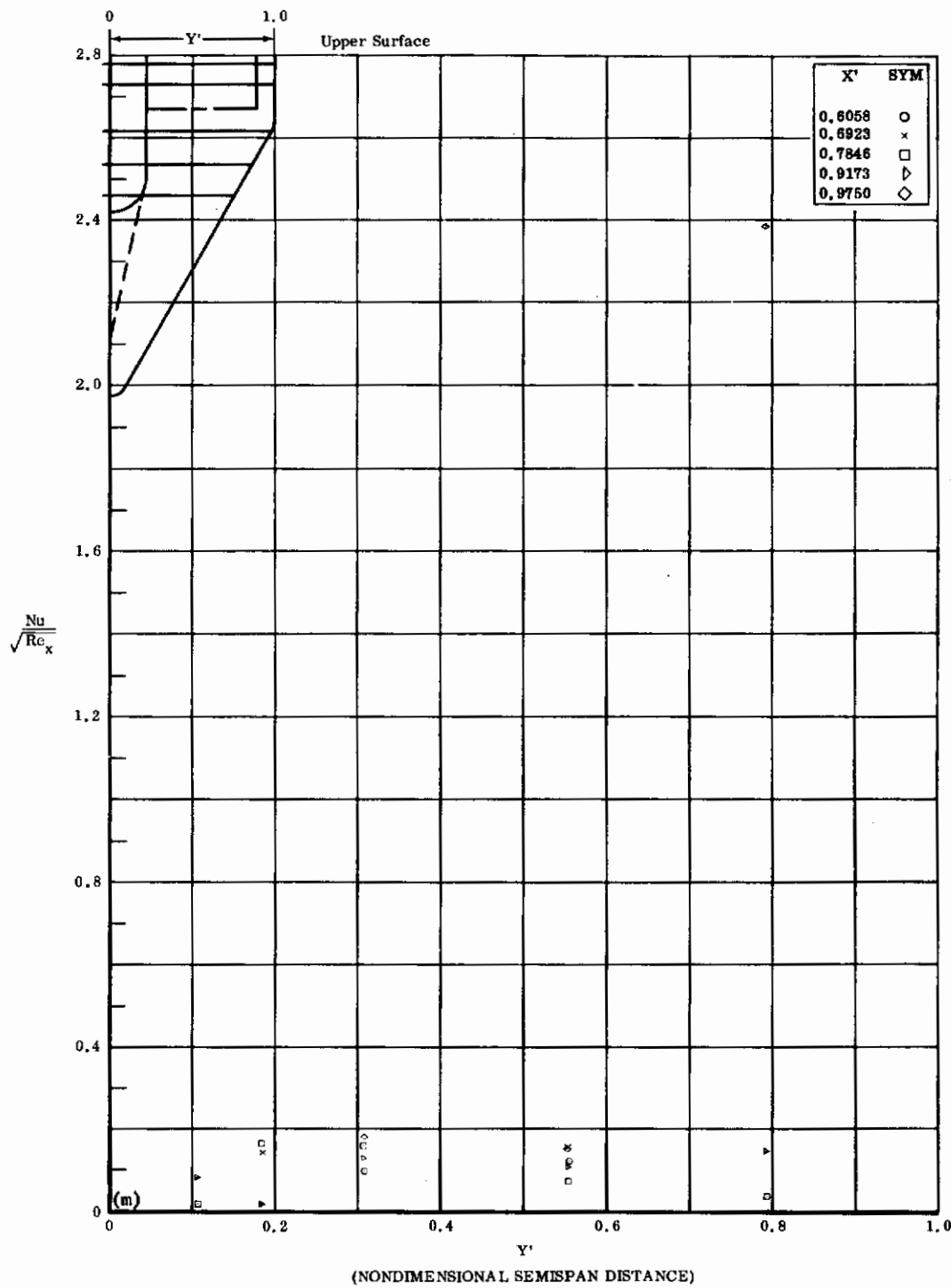


Fig. 8m Configuration I, $\alpha = +20$, $\delta_2 = \delta_3 = -30$
 $Nu/\sqrt{Re_x}$ vs. Y' upper surface

Contrails

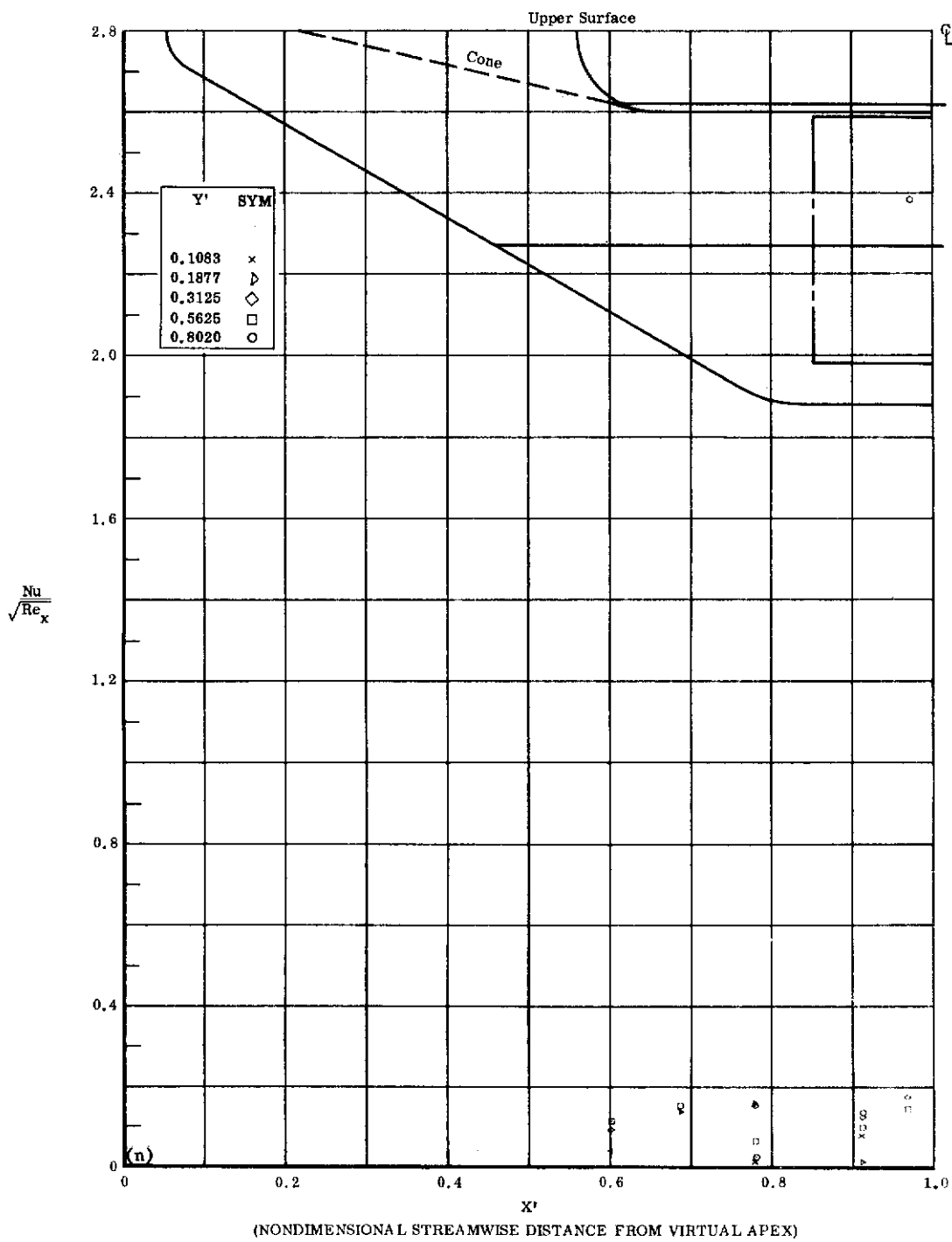


Fig. 8n Configuration I, $\alpha = +20^\circ$, $b_2 = b_3 = -30^\circ$

$\frac{Nu}{\sqrt{Re_x}}$ vs. X' upper surface

Contrails

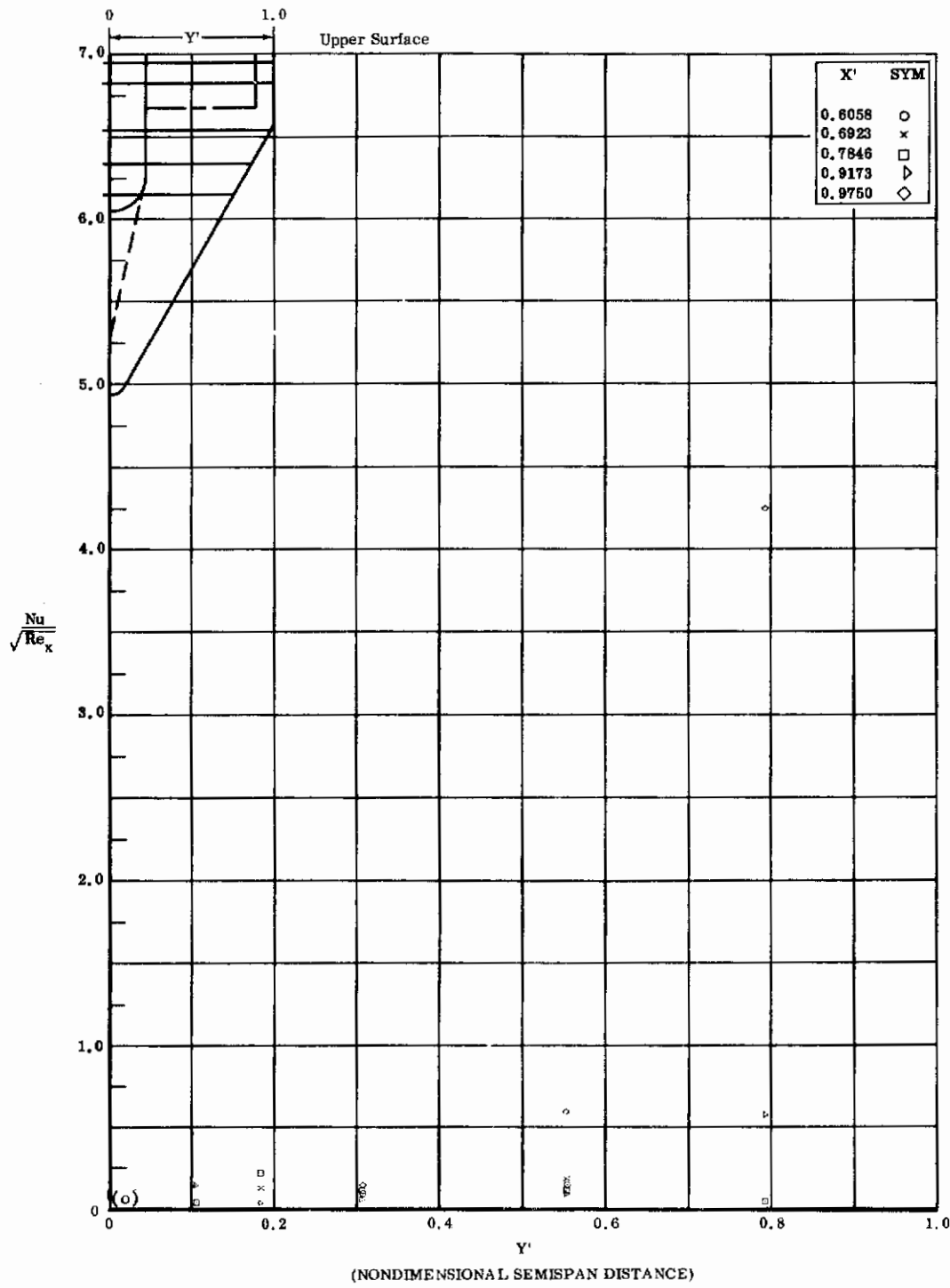


Fig. 8o Configuration I, $a = +20$, $\delta_2 = \delta_3 = -39$
 $Nu/\sqrt{Re_x}$ vs. Y' upper surface

Contrails

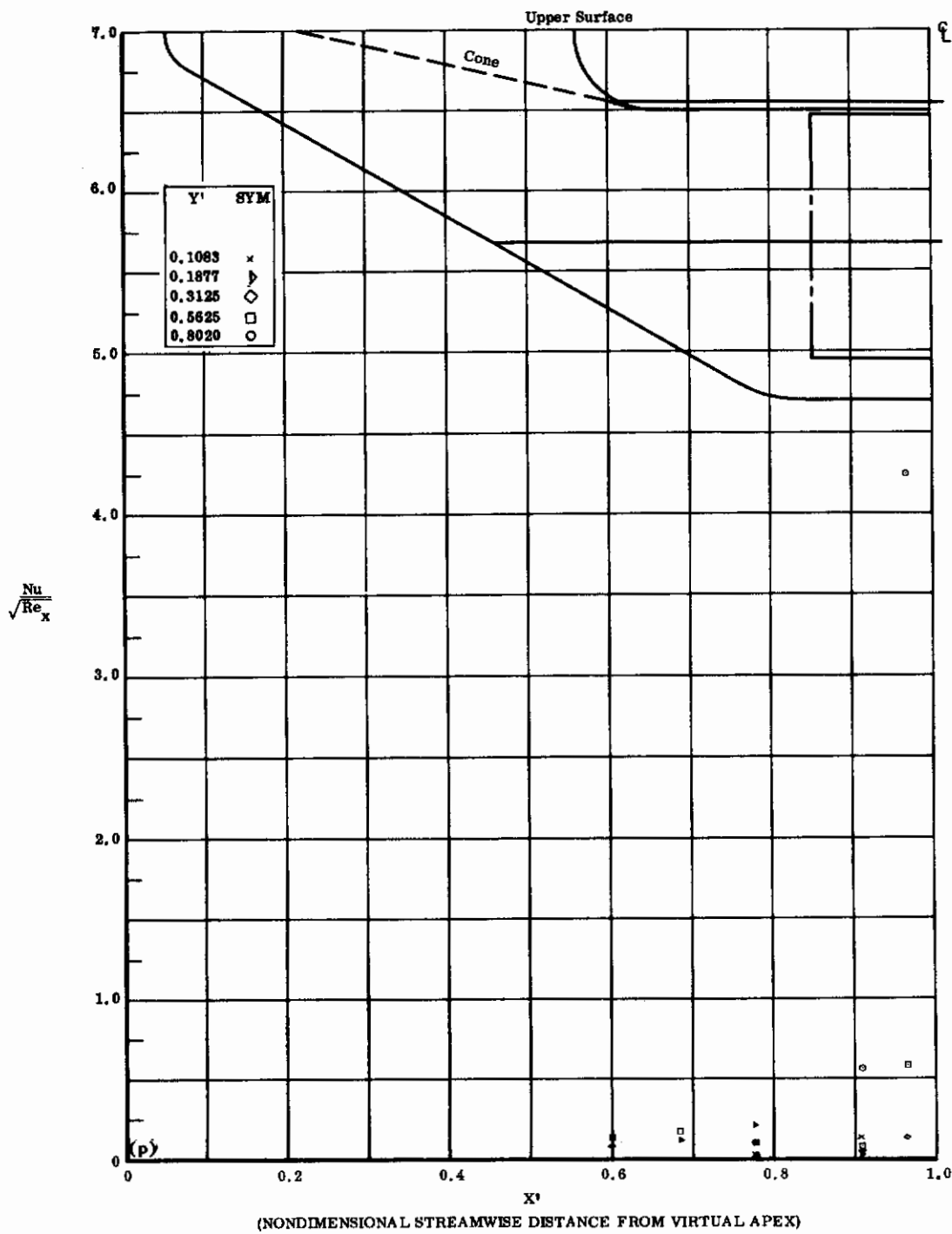


Fig. 8p Configuration I, $\alpha = +20^\circ$, $\delta_2 = \delta_3 = -39^\circ$

$Nu/\sqrt{Re_x}$ vs. X' upper surface

Contrails

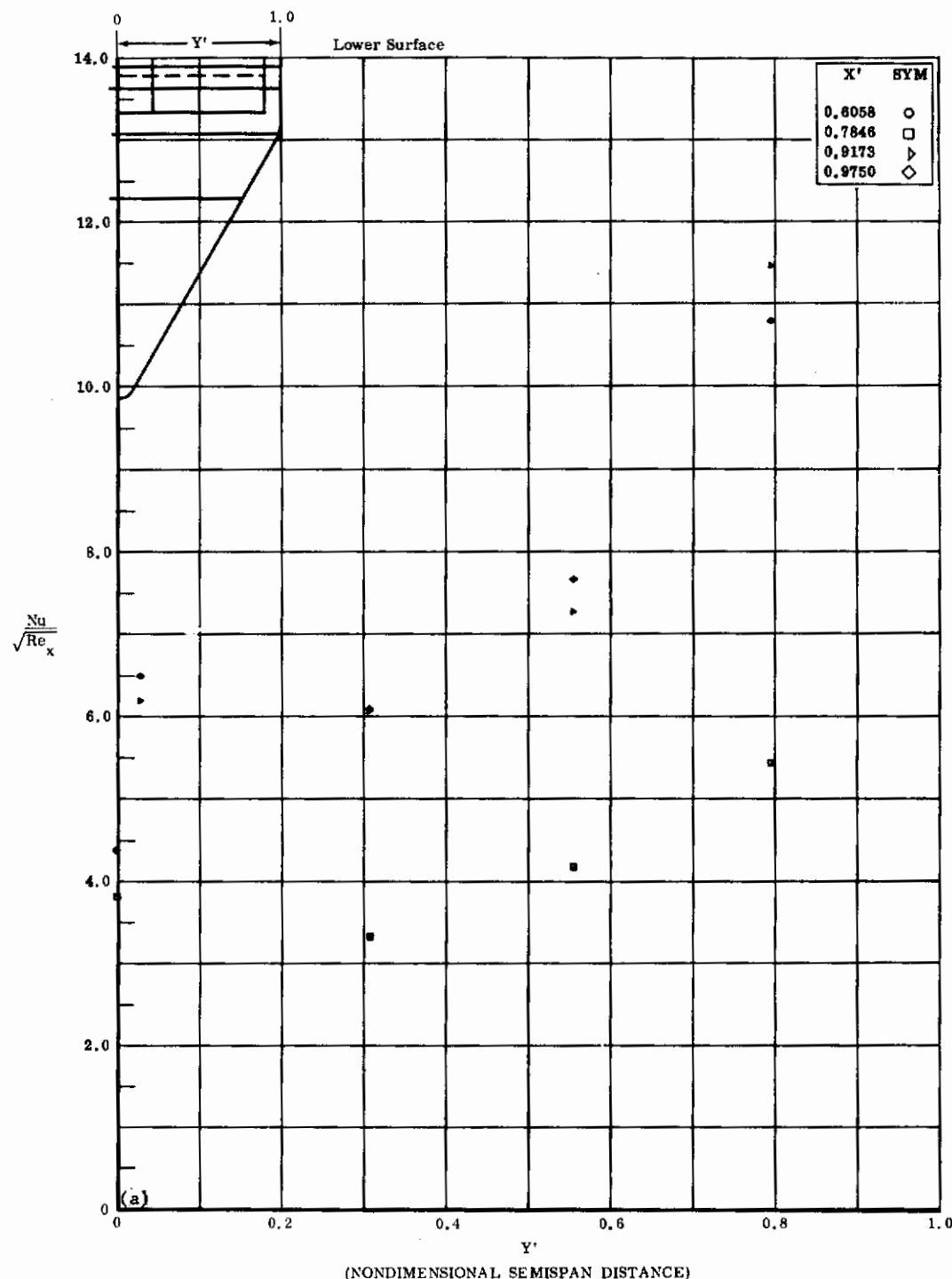


Fig. 9a Configuration I, $\alpha = +30^\circ$, $\delta_2 = \delta_3 = 0$
 $Nu/\sqrt{Re_x}$ vs. Y' lower surface

Contrails

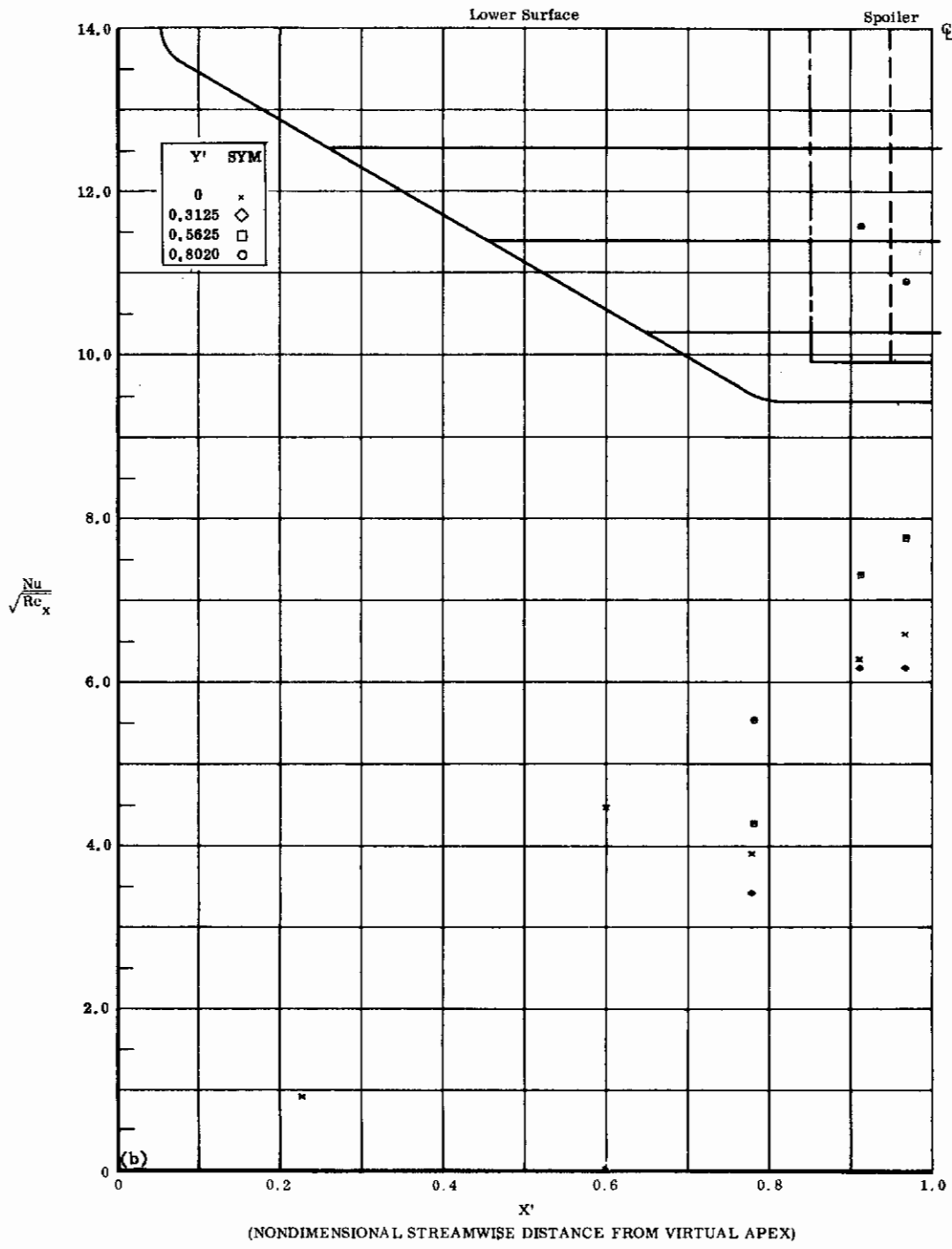


Fig. 9b Configuration I, $\alpha = +30^\circ$, $\delta_2 = \delta_3 = 0$
 $\text{Nu}/\sqrt{\text{Re}_x}$ vs. X' lower surface

Contrails

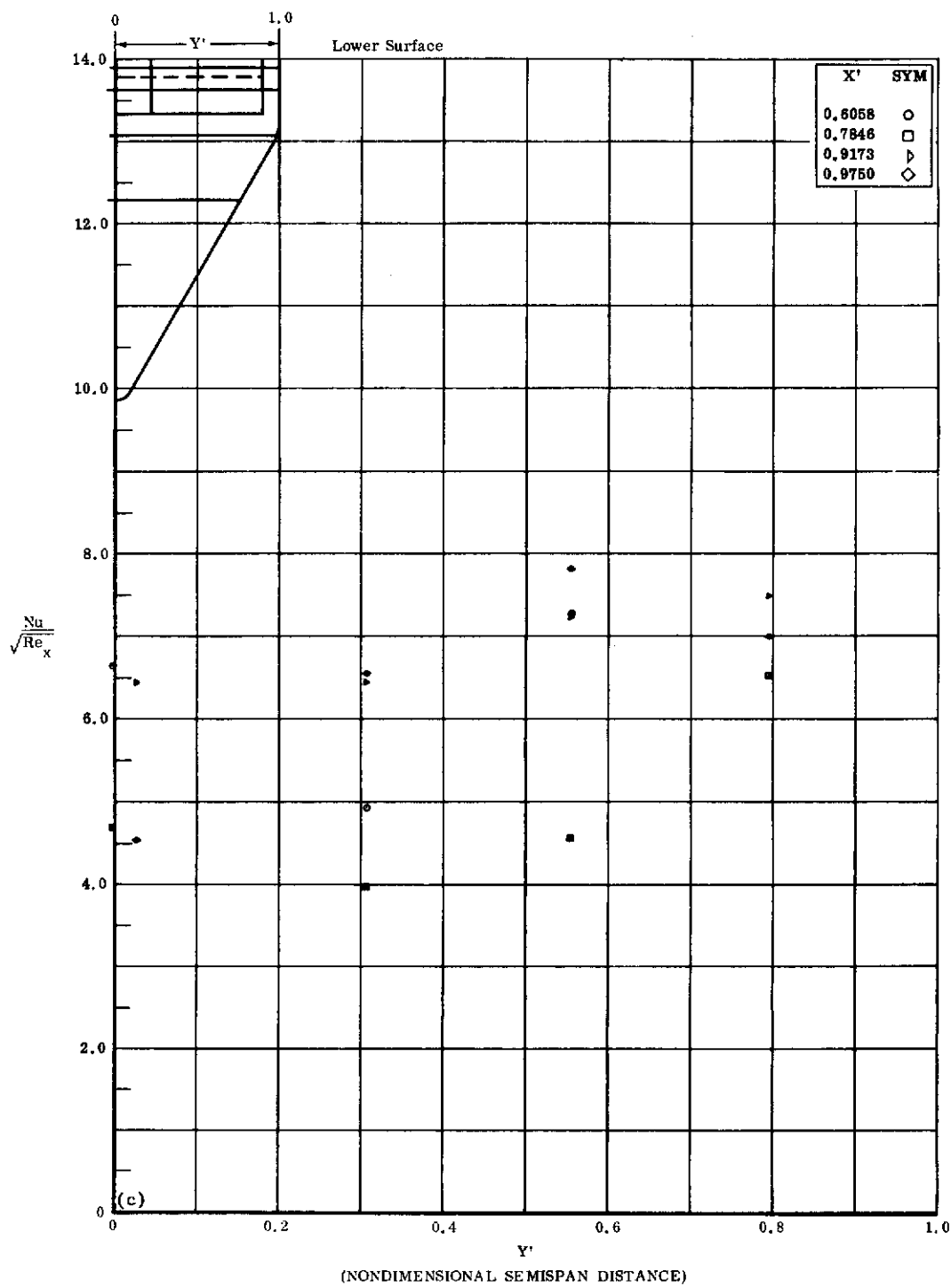


Fig. 9c Configuration I, $\alpha = +35^\circ$, $\delta_2 = \delta_3 = 0$
 $\frac{Nu}{\sqrt{Re_x}}$ vs. Y' lower surface

Contrails

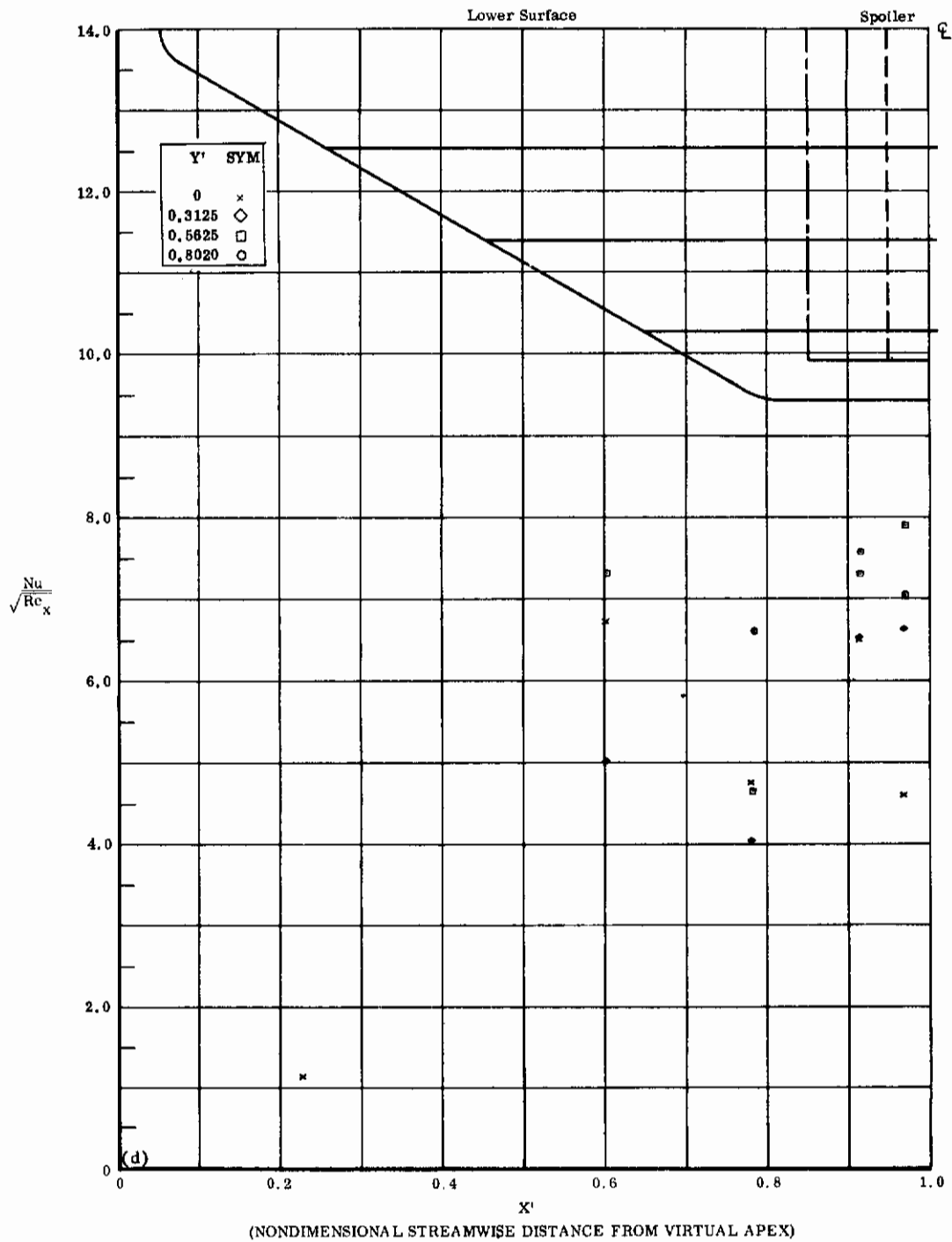


Fig. 9d Configuration I, $\alpha = +35$, $\delta_2 = \delta_3 = 0$

$Nu/\sqrt{Re_x}$ vs. X' lower surface

Contrails

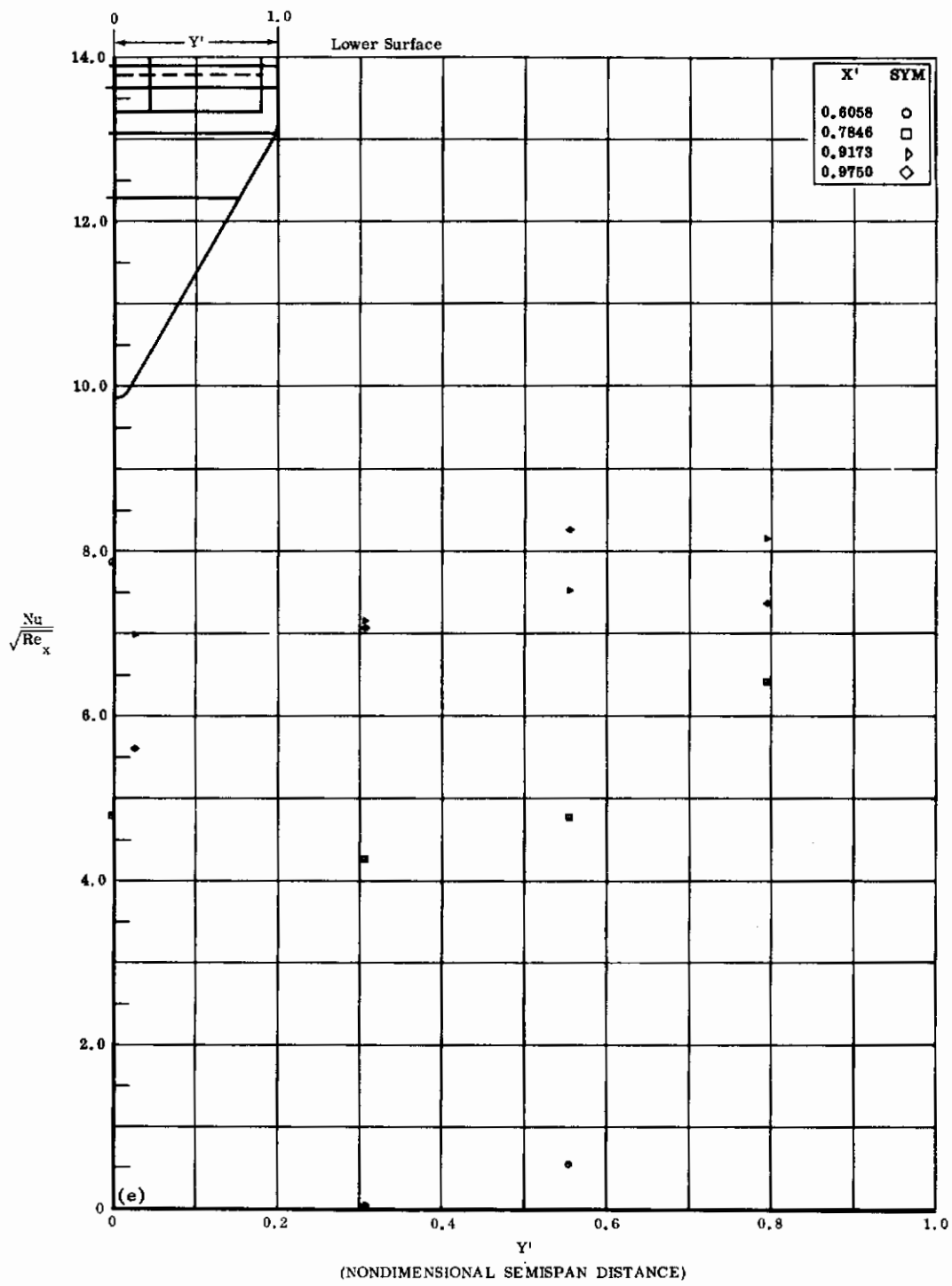


Fig. 9e Configuration I, $\alpha = +40^\circ$, $\delta_2 = \delta_3 = 0$
 $Nu/\sqrt{Re_x}$ vs. Y' lower surface

Contrails

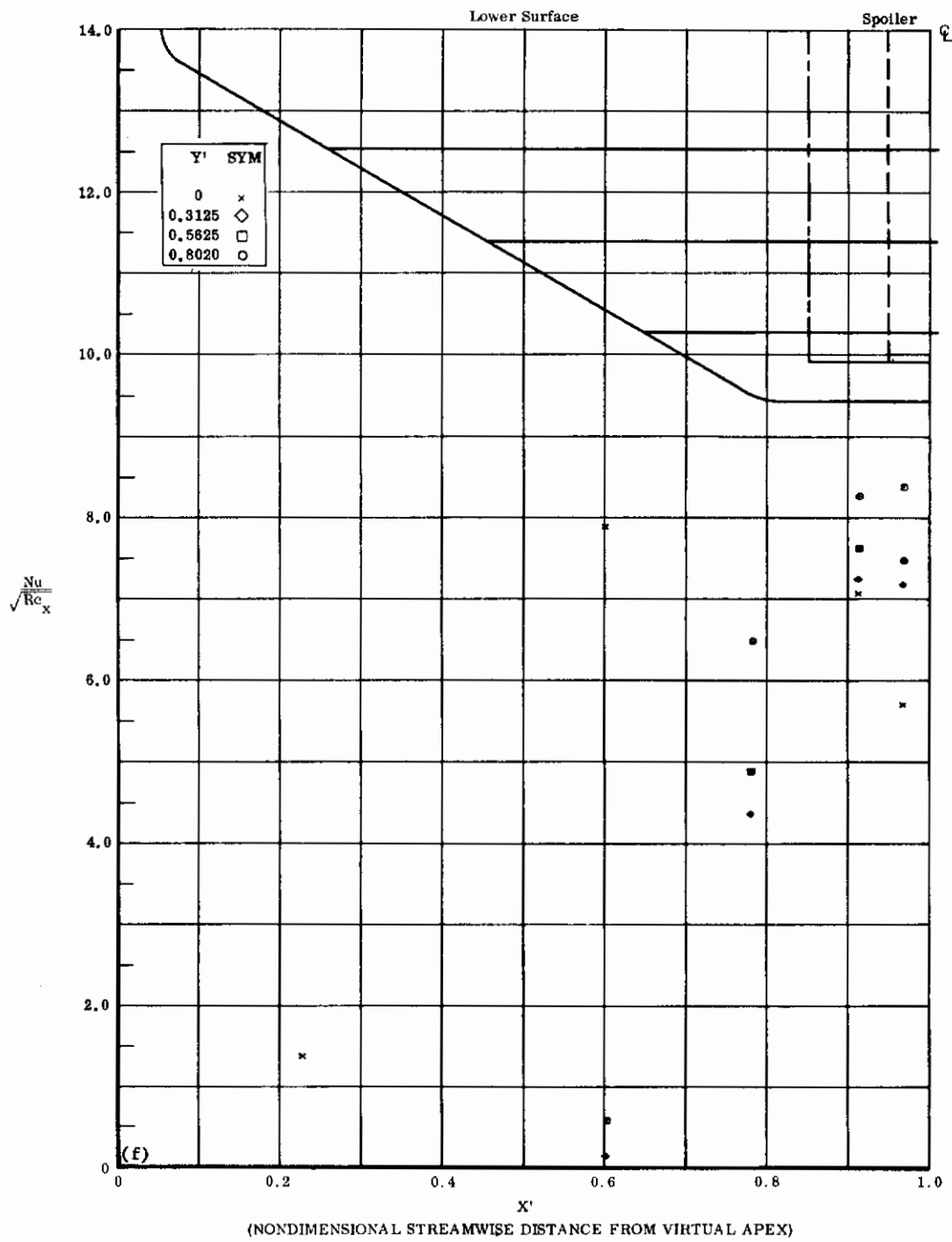


Fig. 9f Configuration I, $\alpha = +40$, $\delta_2 = \delta_3 = 0$
 $Nu/\sqrt{Re_x}$ vs. X' lower surface

Contrails

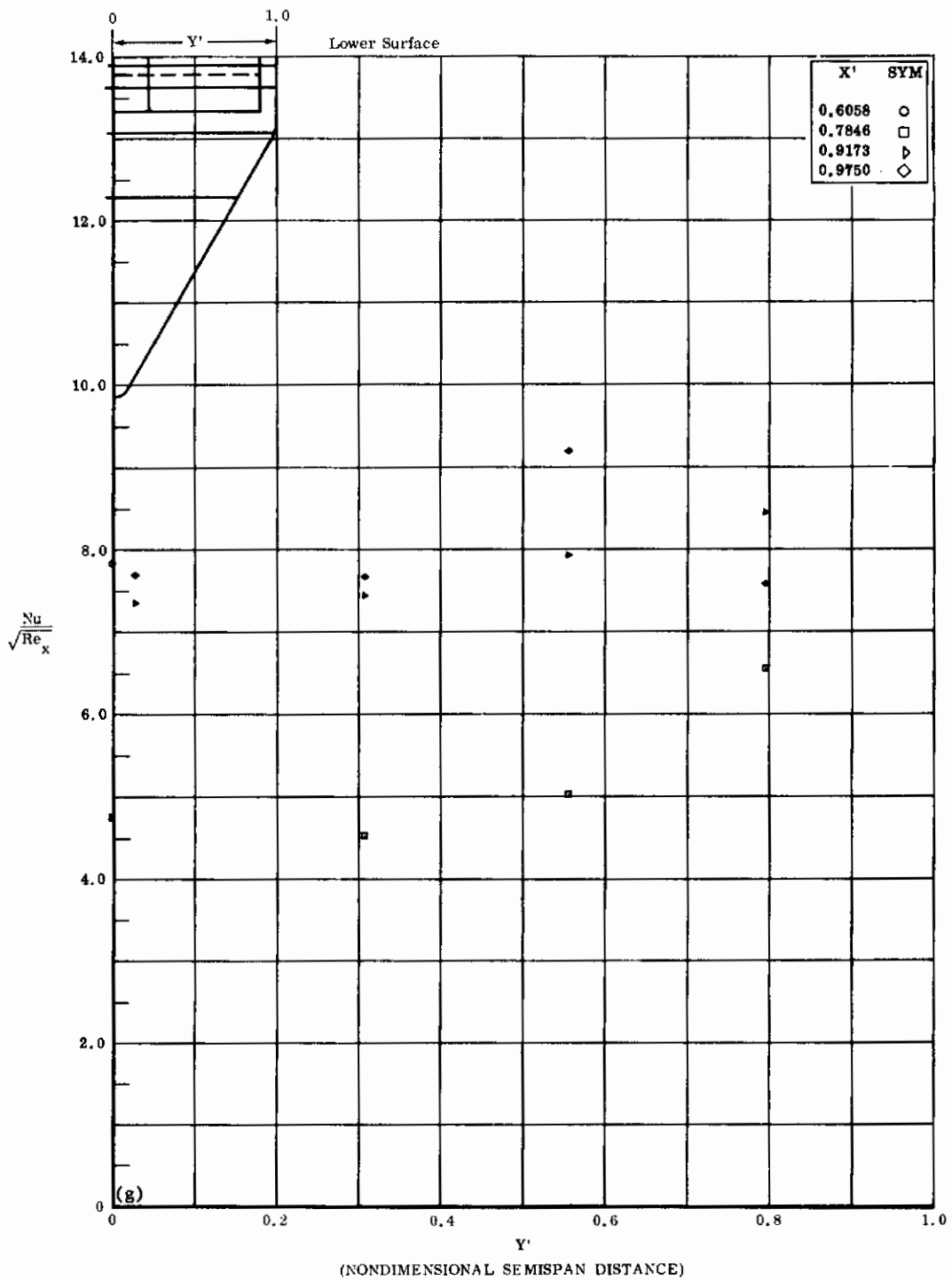


Fig. 9g Configuration I, $\alpha = +45^\circ$, $\delta_2 = \delta_3 = 0$

$\text{Nu}/\sqrt{\text{Re}_x}$ vs. Y' lower surface

Contrails

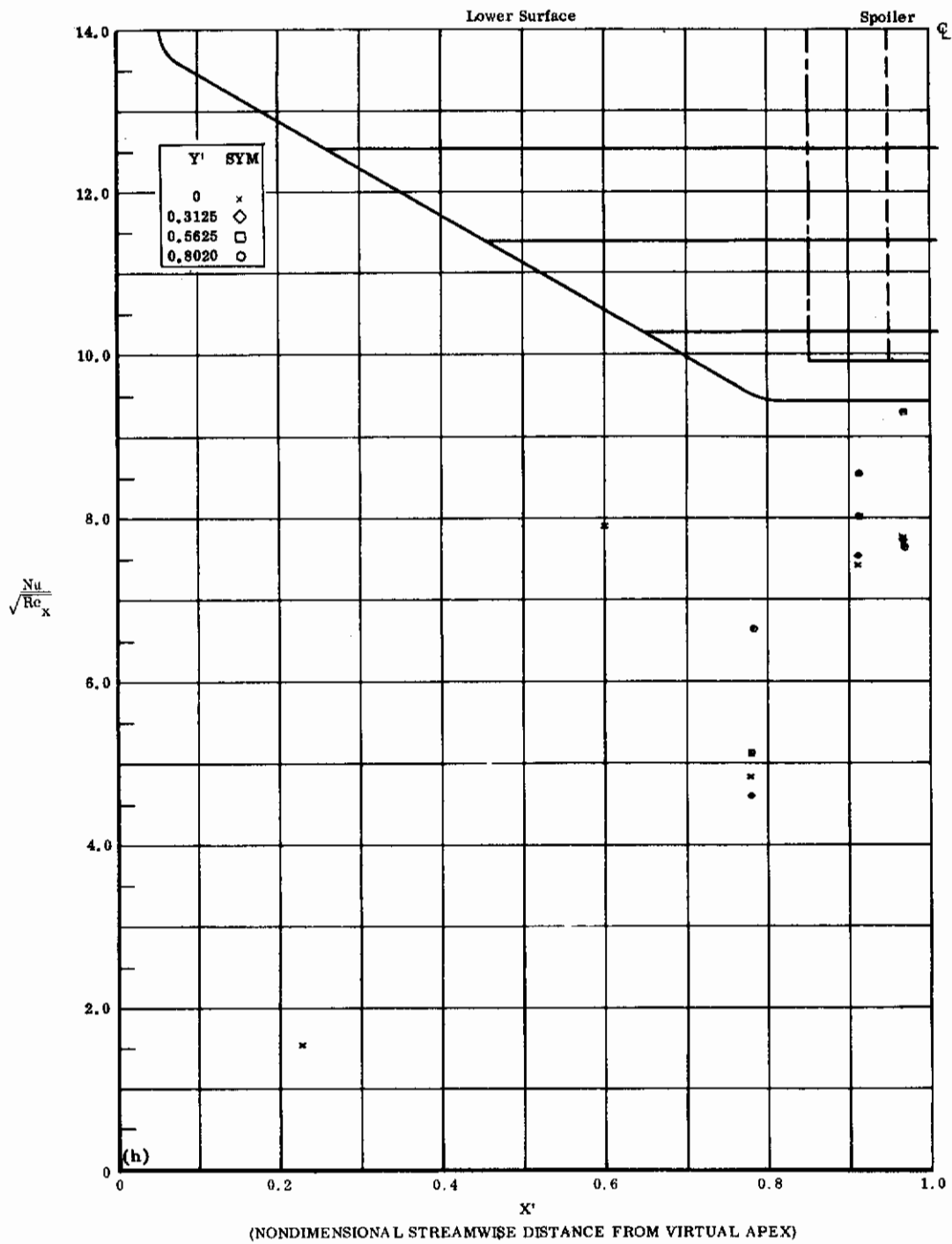


Fig. 9h Configuration I, $\alpha = +45^\circ$, $\delta_2 = \delta_3 = 0$

$Nu/\sqrt{Re_x}$ vs. X' lower surface

Contrails

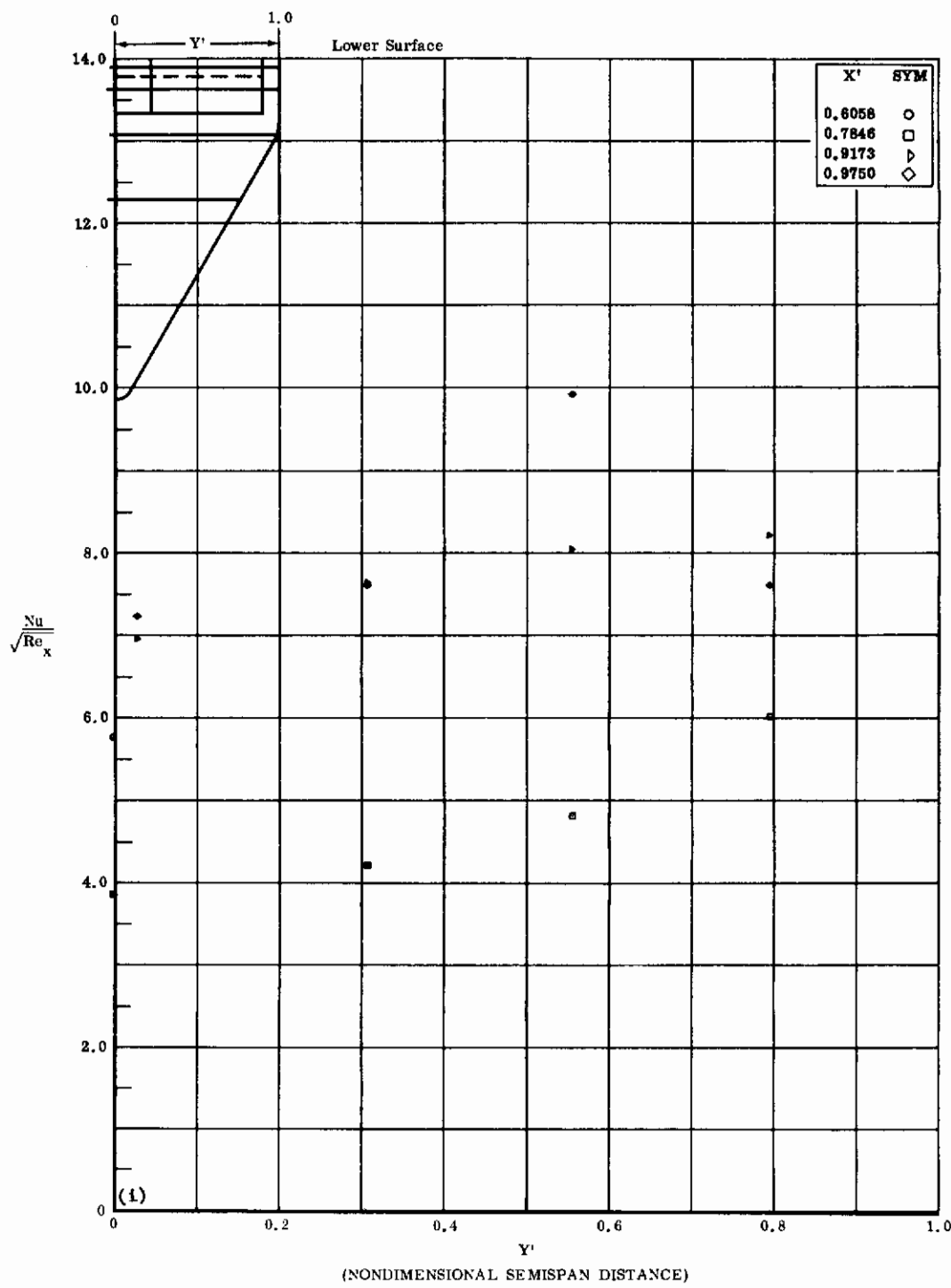


Fig. 9i Configuration I, $\alpha = +50$, $\delta_2 = \delta_3 = 0$
 $Nu/\sqrt{Re_x}$ vs. Y' lower surface

Contrails

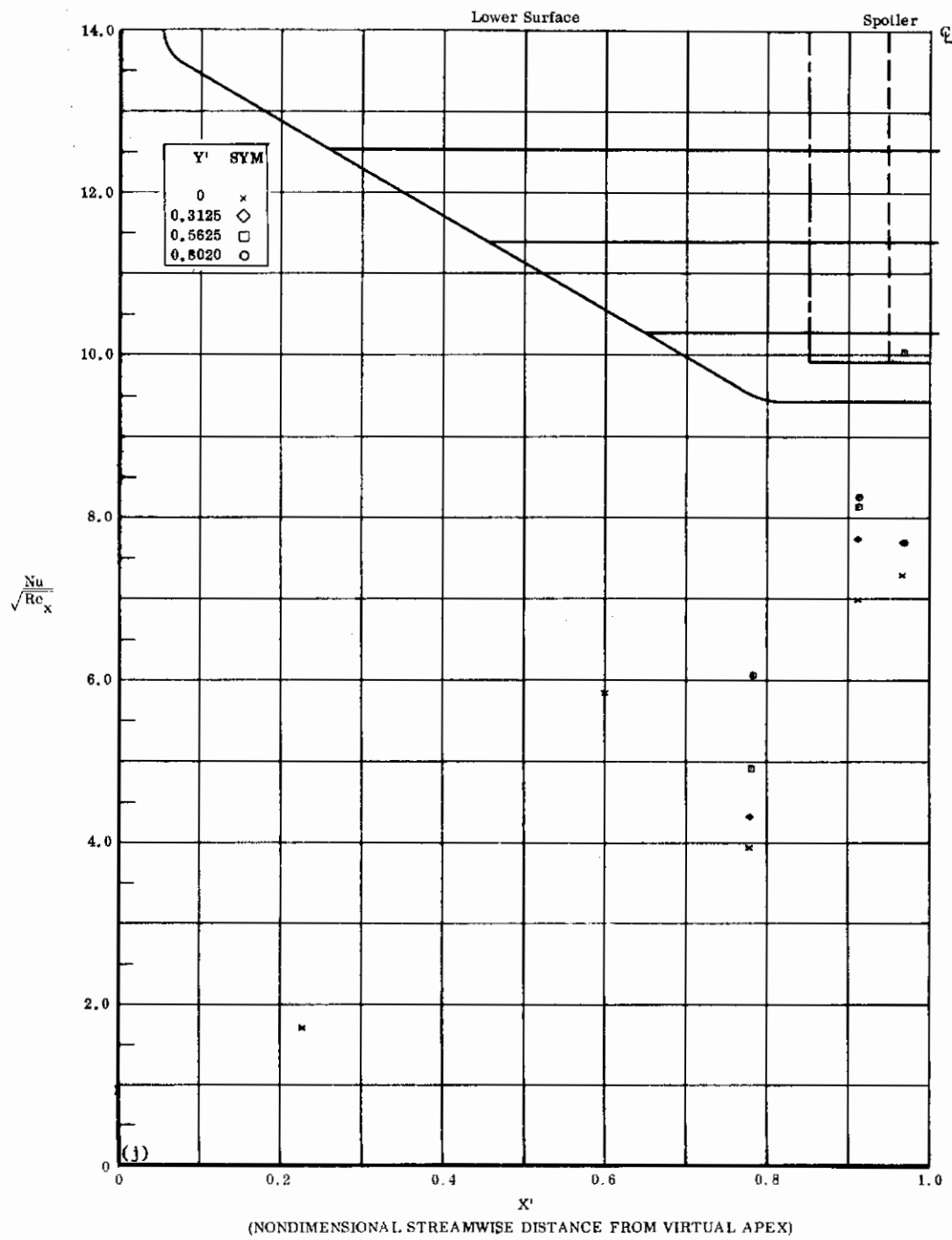
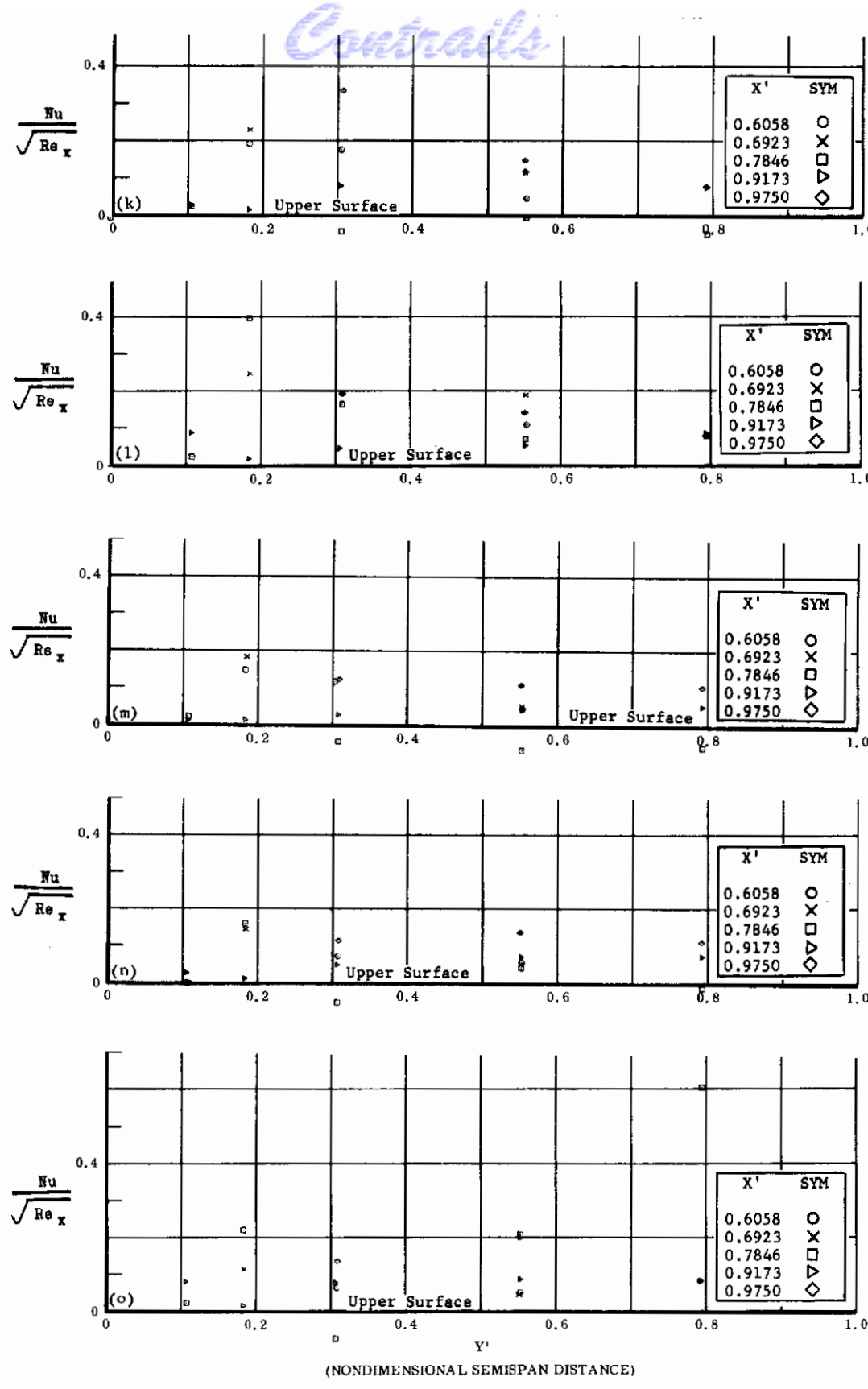


Fig. 9j Configuration I, $\alpha = +50^\circ$, $\delta_2 = \delta_3 = 0$
 $Nu/\sqrt{Re_x}$ vs. X' lower surface



(NONDIMENSIONAL SEMISPAN DISTANCE)

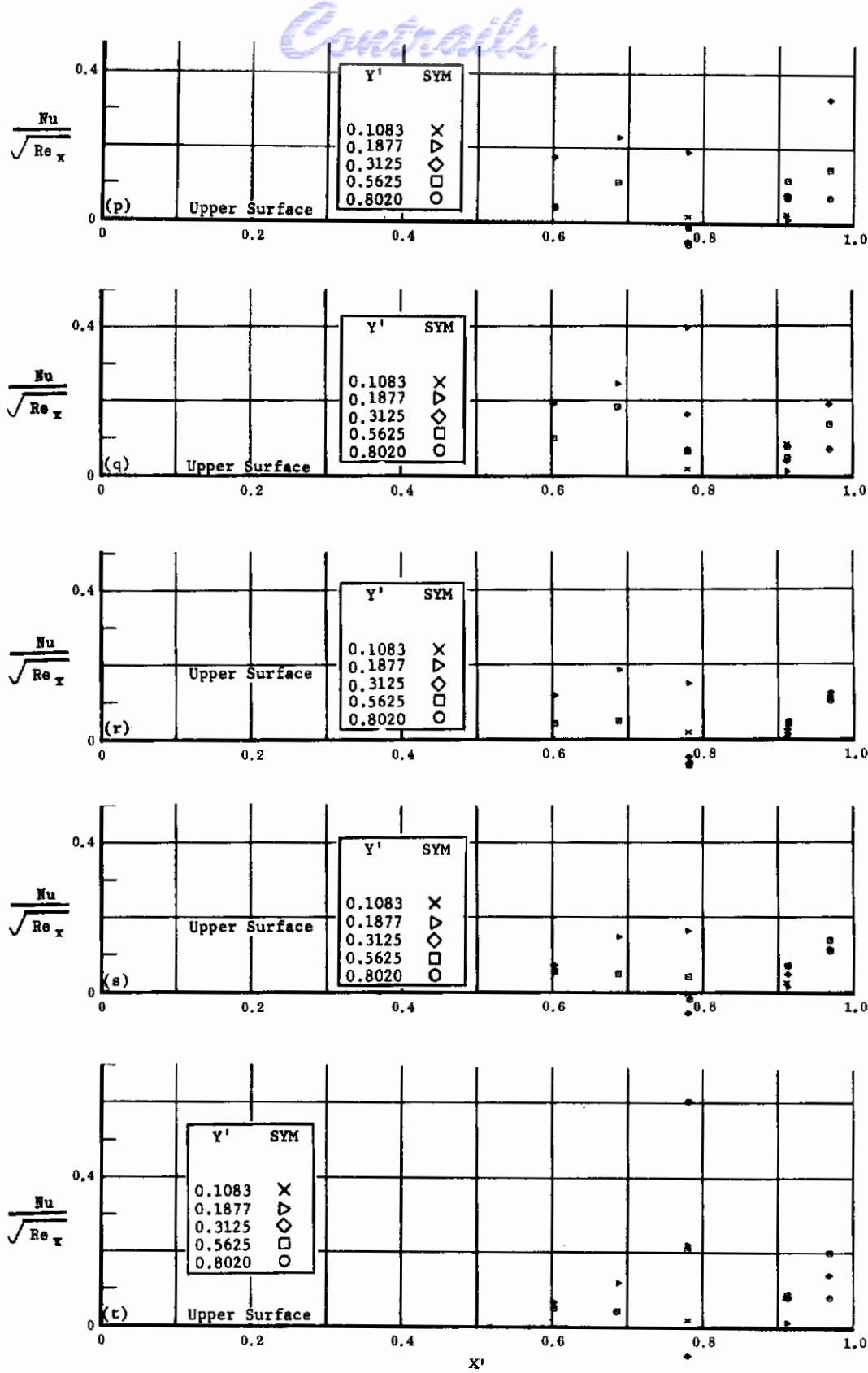
Fig. 9 Configuration I, $b_2 = b_3 = 0$, $Nu/\sqrt{Re_x}$ vs. Y' , upper surface
k) $\alpha = +30$

l) $\alpha = +35$

m) $\alpha = +40$

n) $\alpha = +45$

o) $\alpha = +50$



(NONDIMENSIONAL STREAMWISE DISTANCE FROM VIRTUAL APEX)

Fig. 9 Configuration I, $\delta_2 = \delta_3 = 0$, $Nu/\sqrt{Re_x}$ vs. X' , upper surface

p) $\alpha = +30$

q) $\alpha = +35$

r) $\alpha = +40$

s) $\alpha = +45$

t) $\alpha = +50$

Contrails

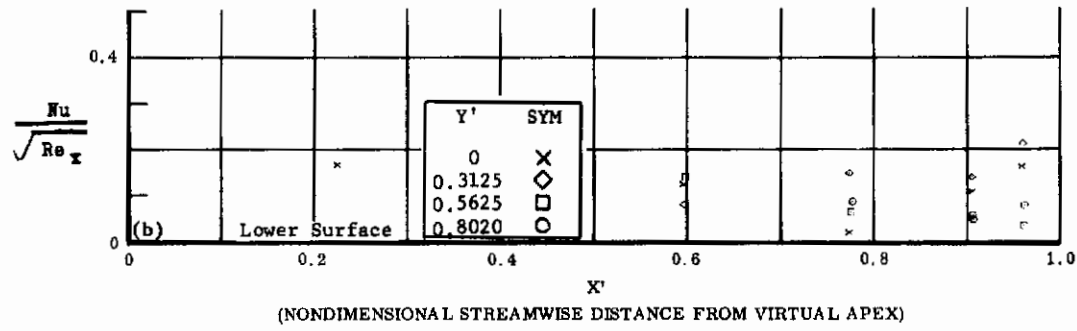
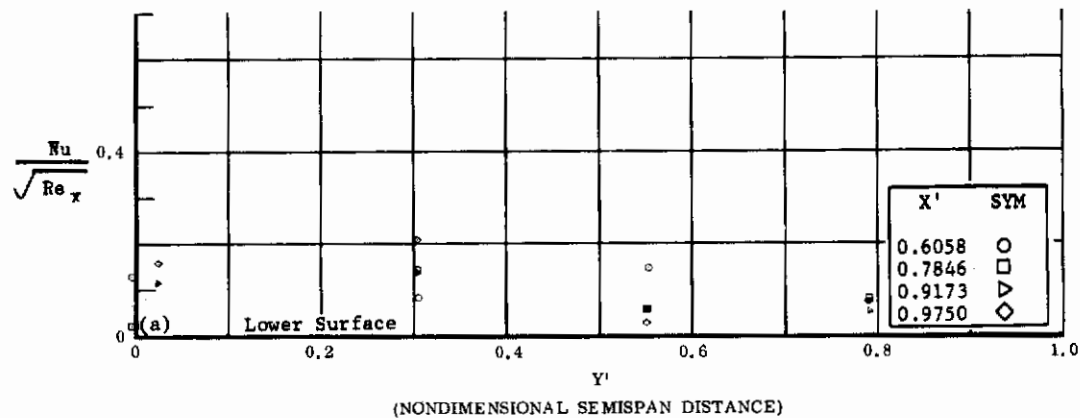


Fig. 10 Configuration I, $\alpha = -10$, $\delta_2 = \delta_3 = 0$

a) $Nu/\sqrt{Re_x}$ vs. Y' lower surface

b) $Nu/\sqrt{Re_x}$ vs. X' lower surface

Contrails

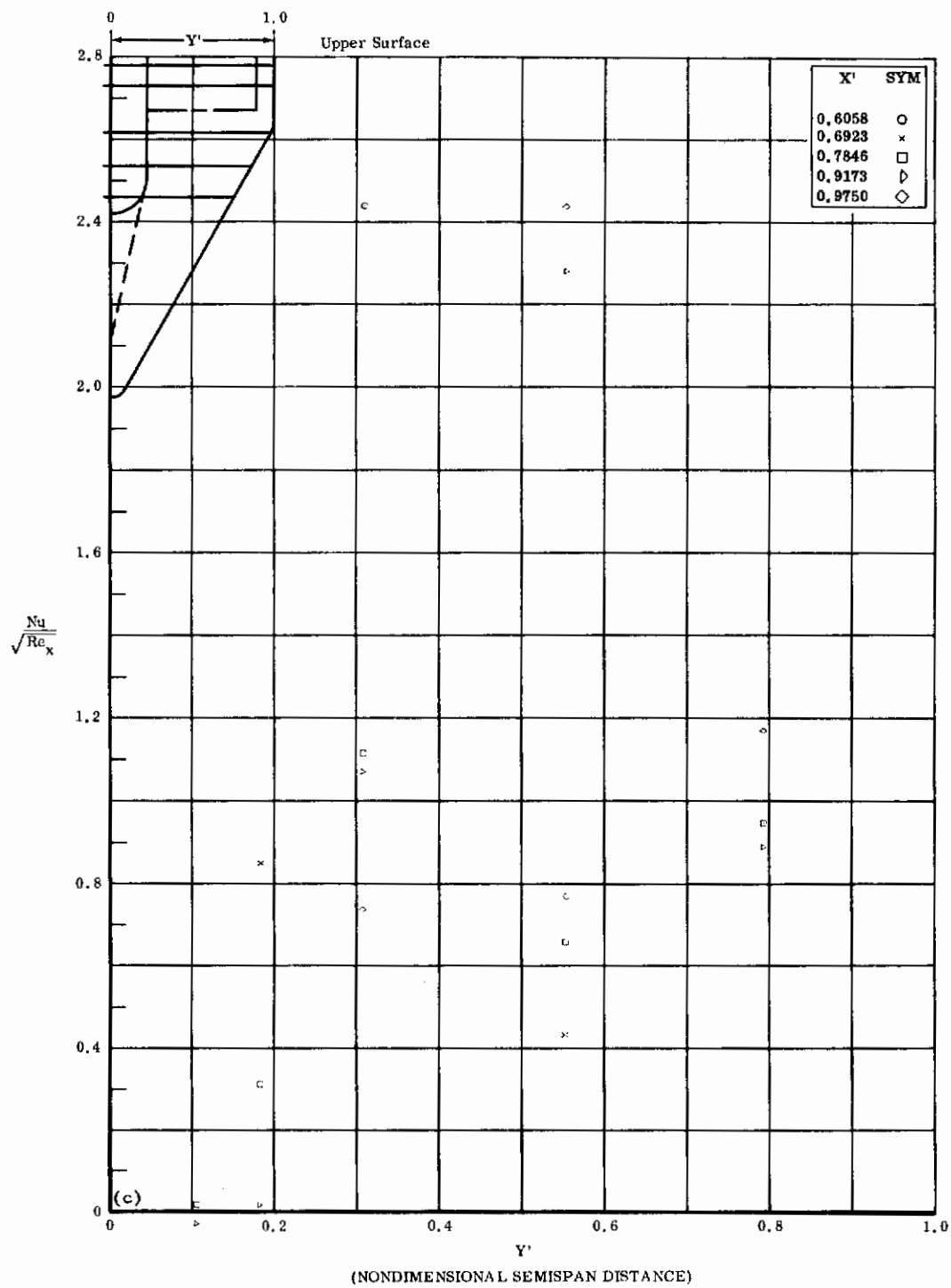


Fig. 10c Configuration I, $\alpha = -10$, $\delta_2 = \delta_3 = 0$
 $Nu/\sqrt{Re_x}$ vs. Y' upper surface

Contrails

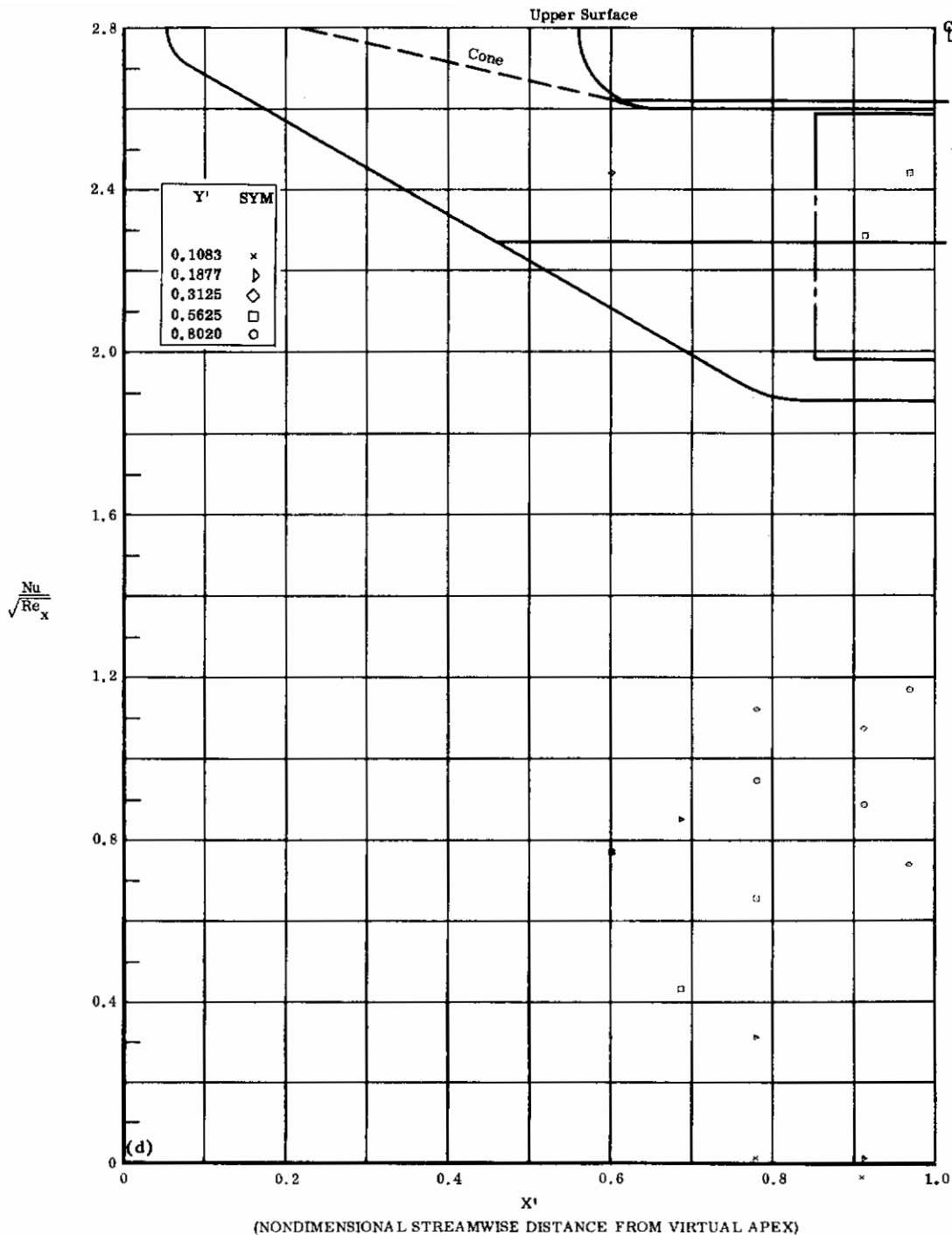


Fig. 10d Configuration I, $\alpha = -10$, $\delta_2 = \delta_3 = 0$

$Nu/\sqrt{Re_x}$ vs. X' upper surface

Contrails

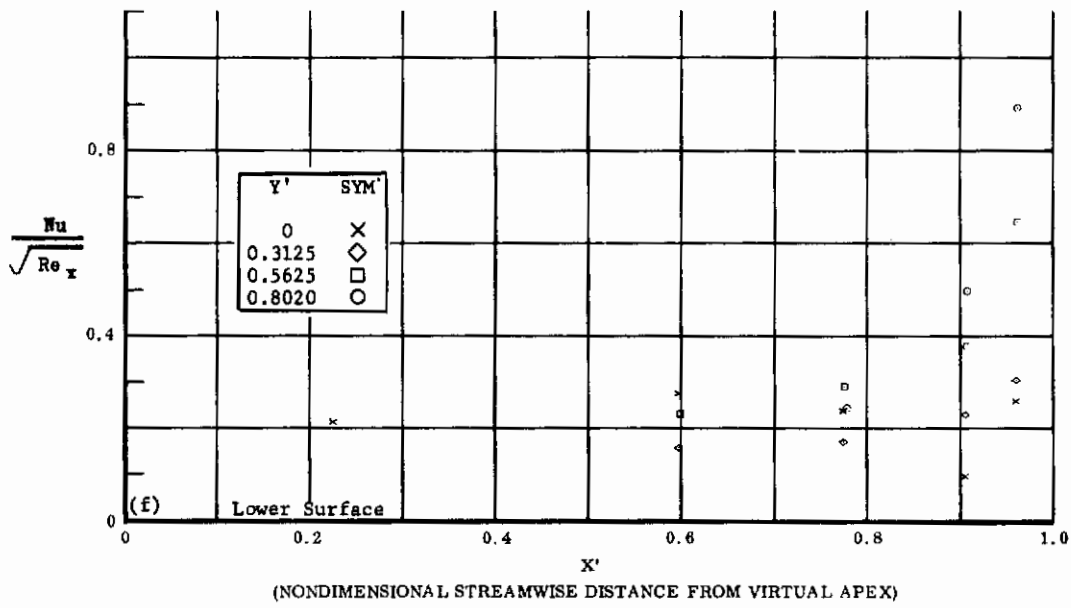
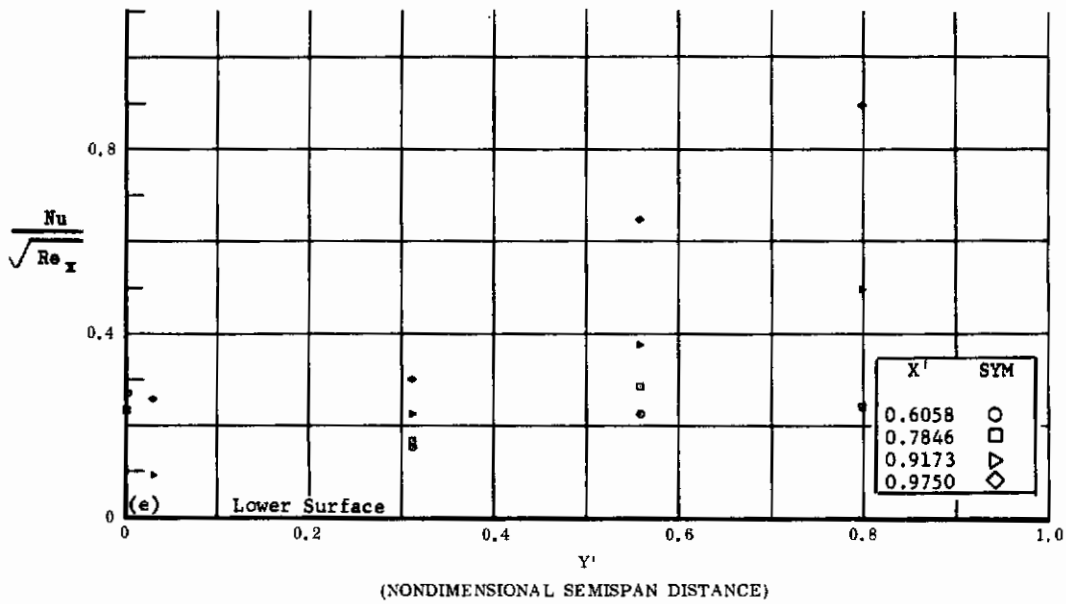


Fig. 10 Configuration I, $\alpha = -10$, $b_2 = b_3 = +10$

e) $Nu/\sqrt{Re_x}$ vs. Y' lower surface

f) $Nu/\sqrt{Re_x}$ vs. X' lower surface

Contrails

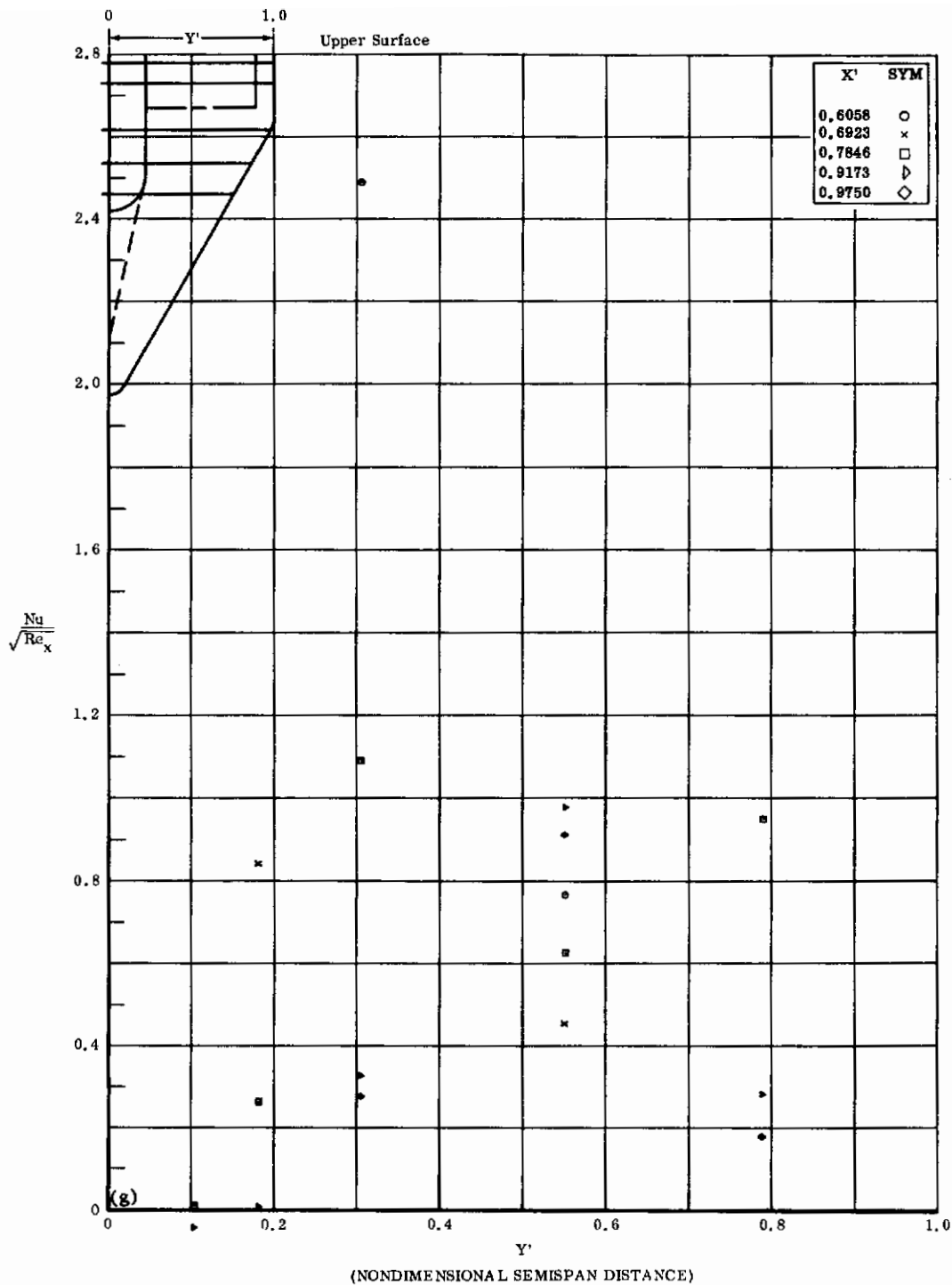


Fig. 10g Configuration I, $\alpha = -10$, $\delta_2 = \delta_3 = +10$
 $\text{Nu}/\sqrt{\text{Re}_x}$ vs. Y' upper surface

Contrails

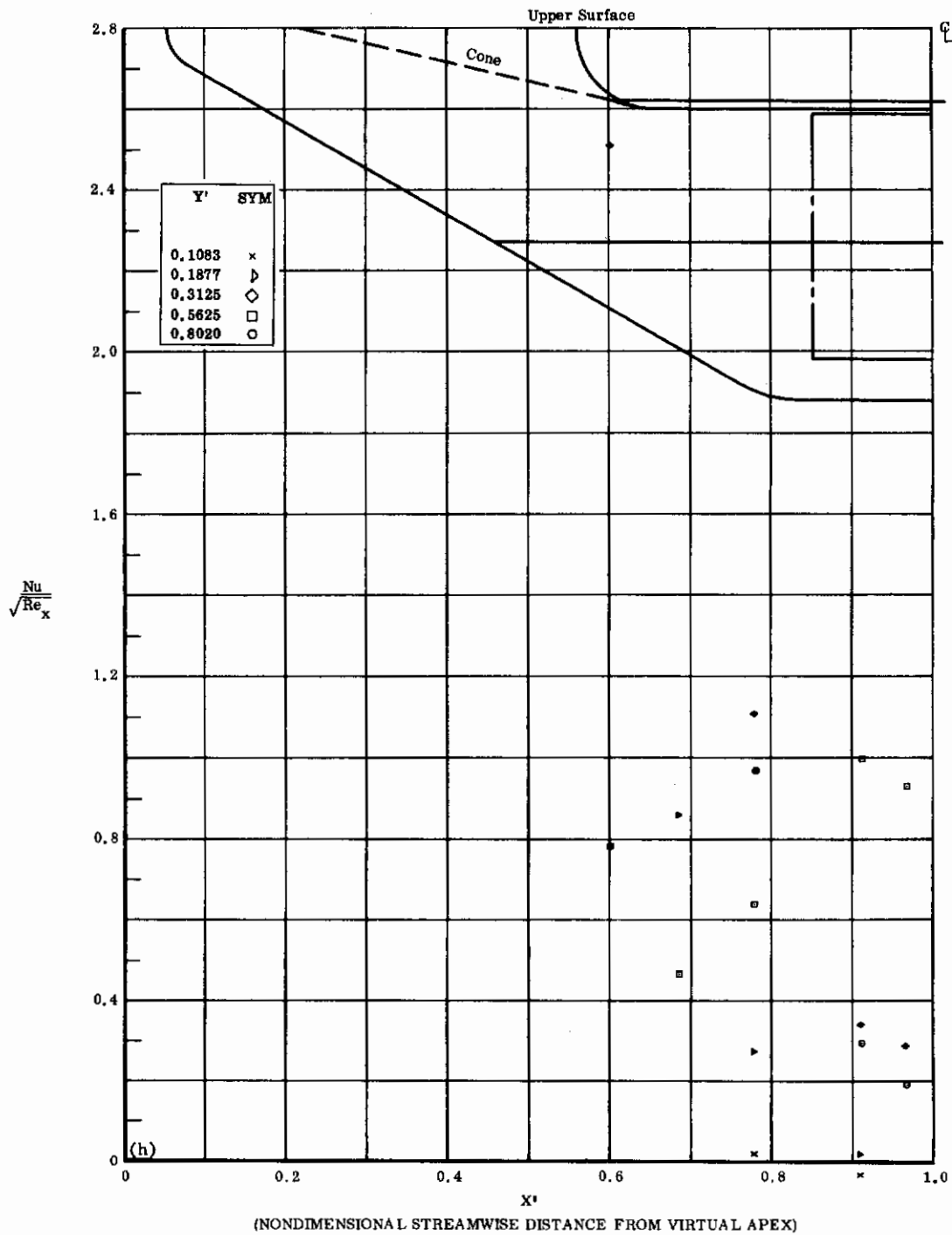


Fig. 10h Configuration I, $\alpha = -10$, $\delta_2 = \delta_3 = +10$

$Nu/\sqrt{Re_x}$ vs. X^1 upper surface

Contrails

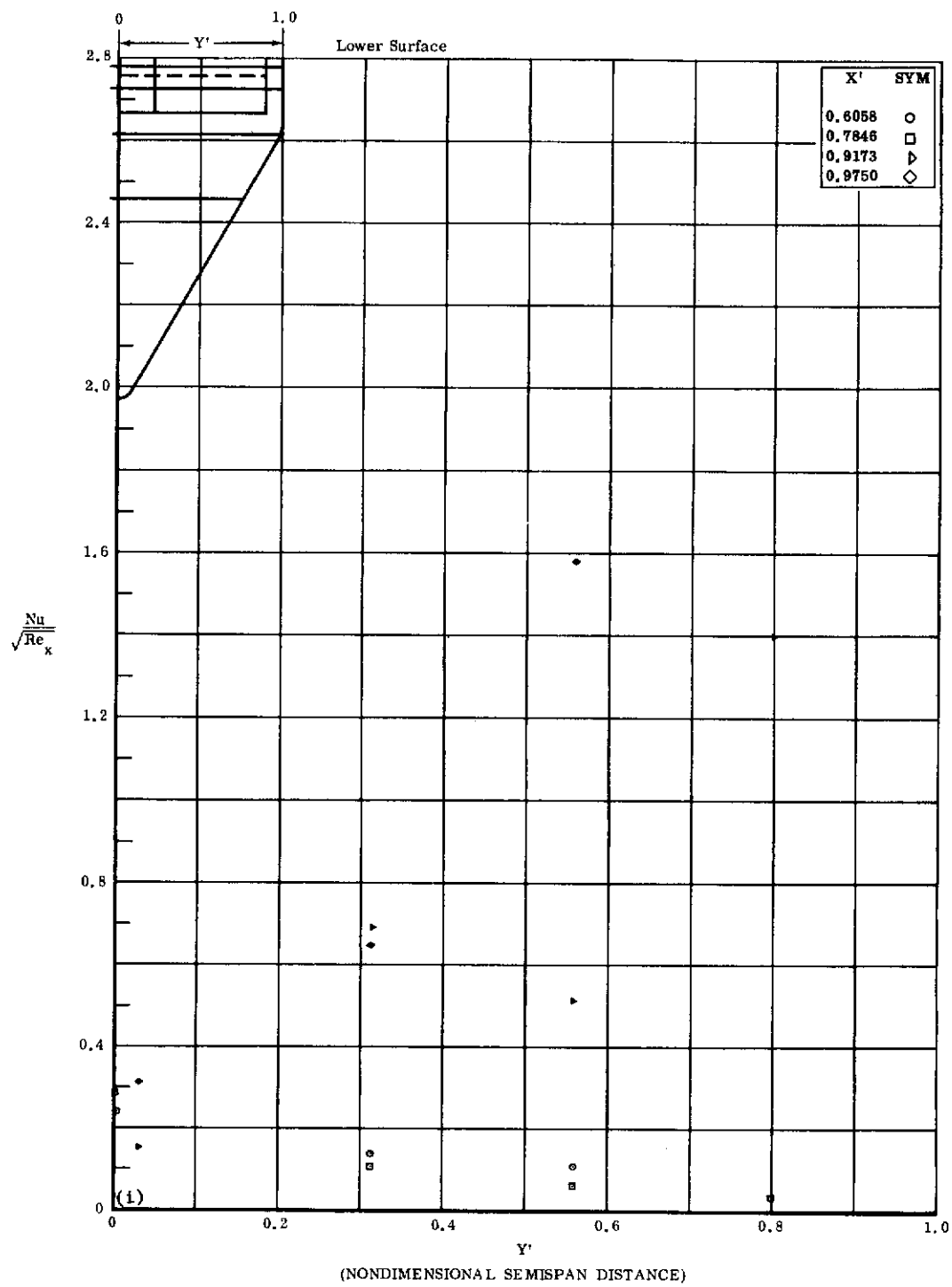


Fig. 10i Configuration I, $\alpha = -10$, $\delta_2 = \delta_3 = +20$
 $Nu/\sqrt{Re_x}$ vs. Y' lower surface

Contrails

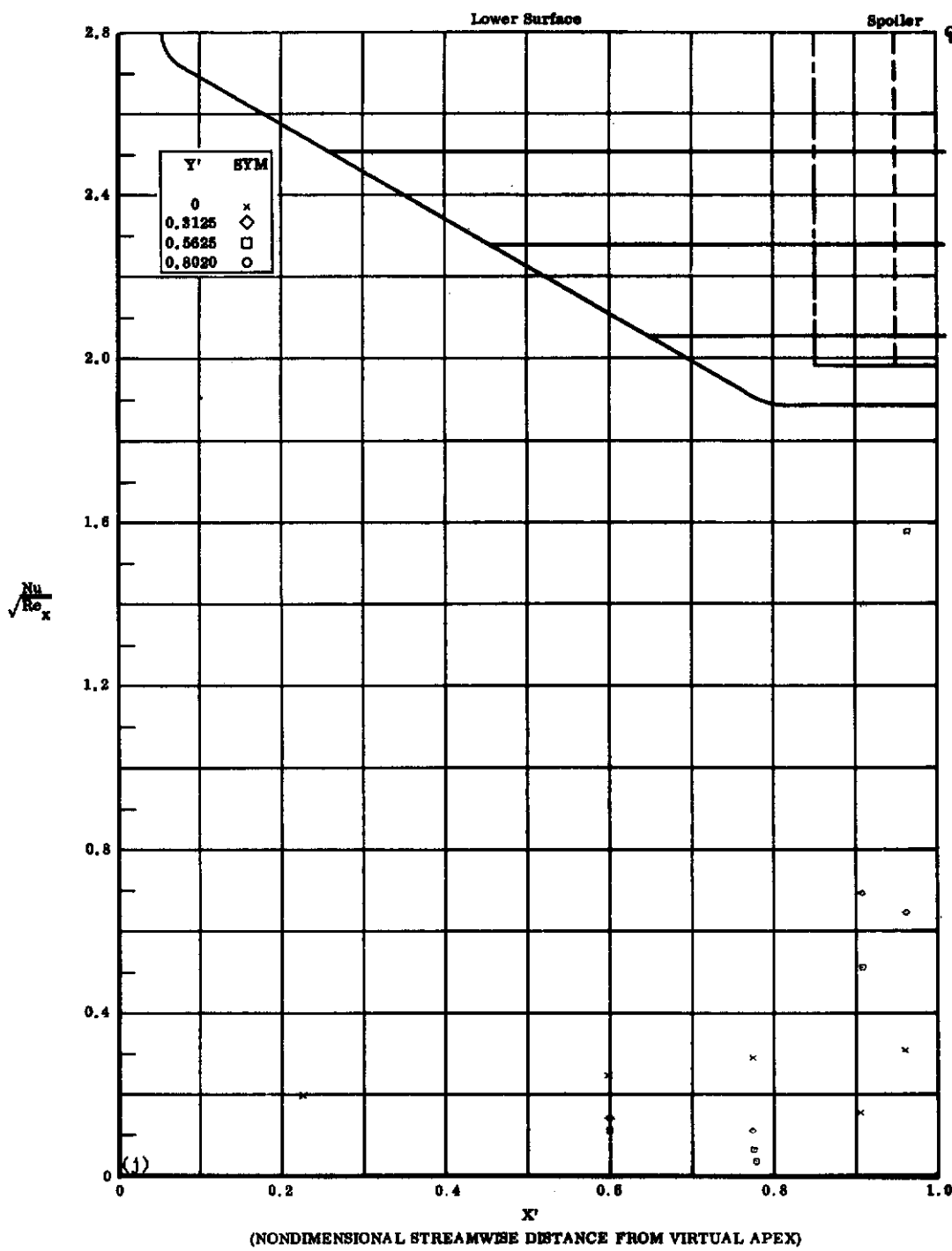


Fig. 10j Configuration I, $\alpha = -10$, $\delta_2 = \delta_3 = +20$

$Nu/\sqrt{Re_x}$ vs. X' lower surface

Contrails

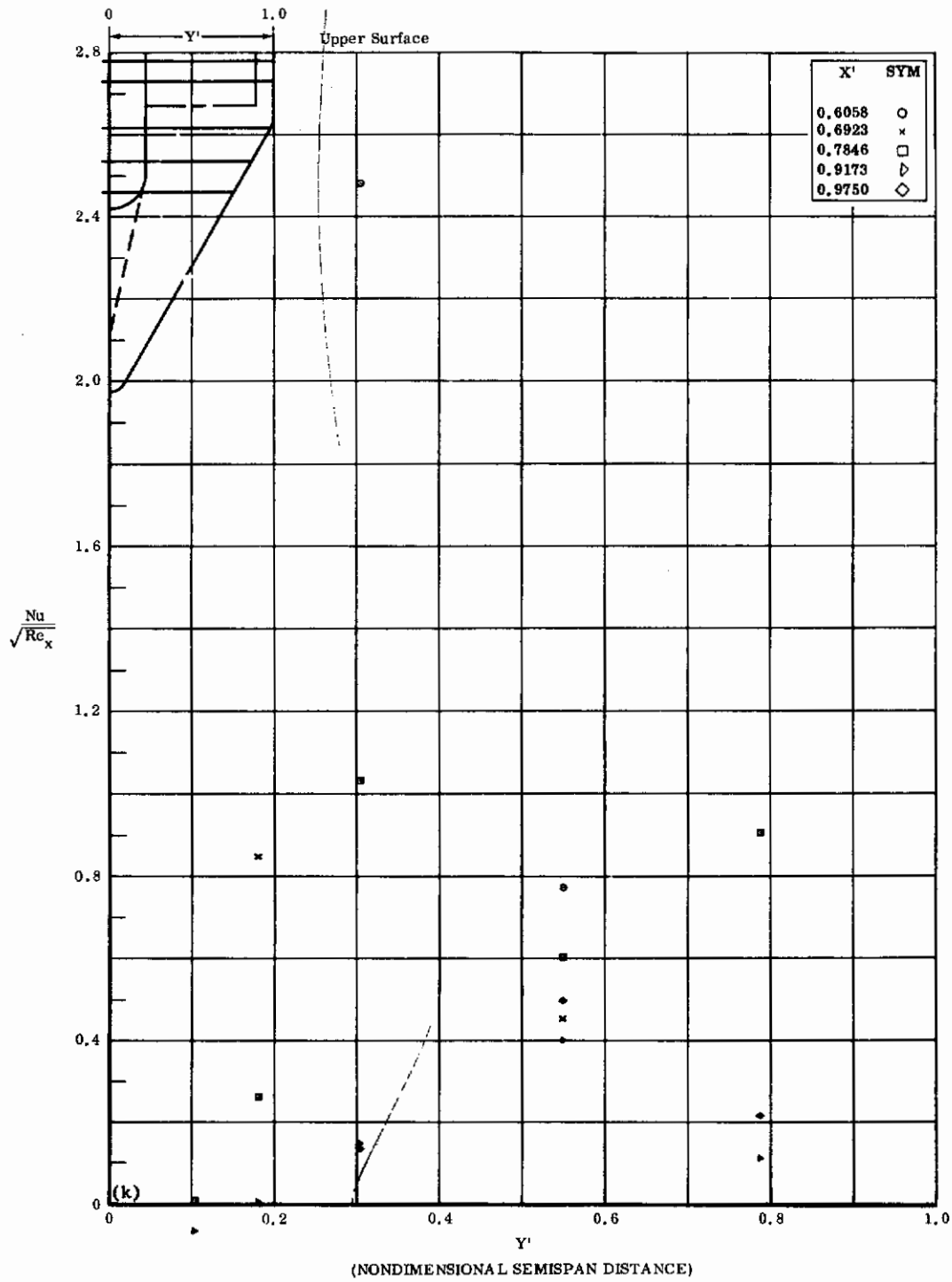


Fig. 10k Configuration I, $\alpha = -10$, $\delta_2 = \delta_3 = +20$
 $Nu/\sqrt{Re_x}$ vs. Y^* upper surface

Contrails

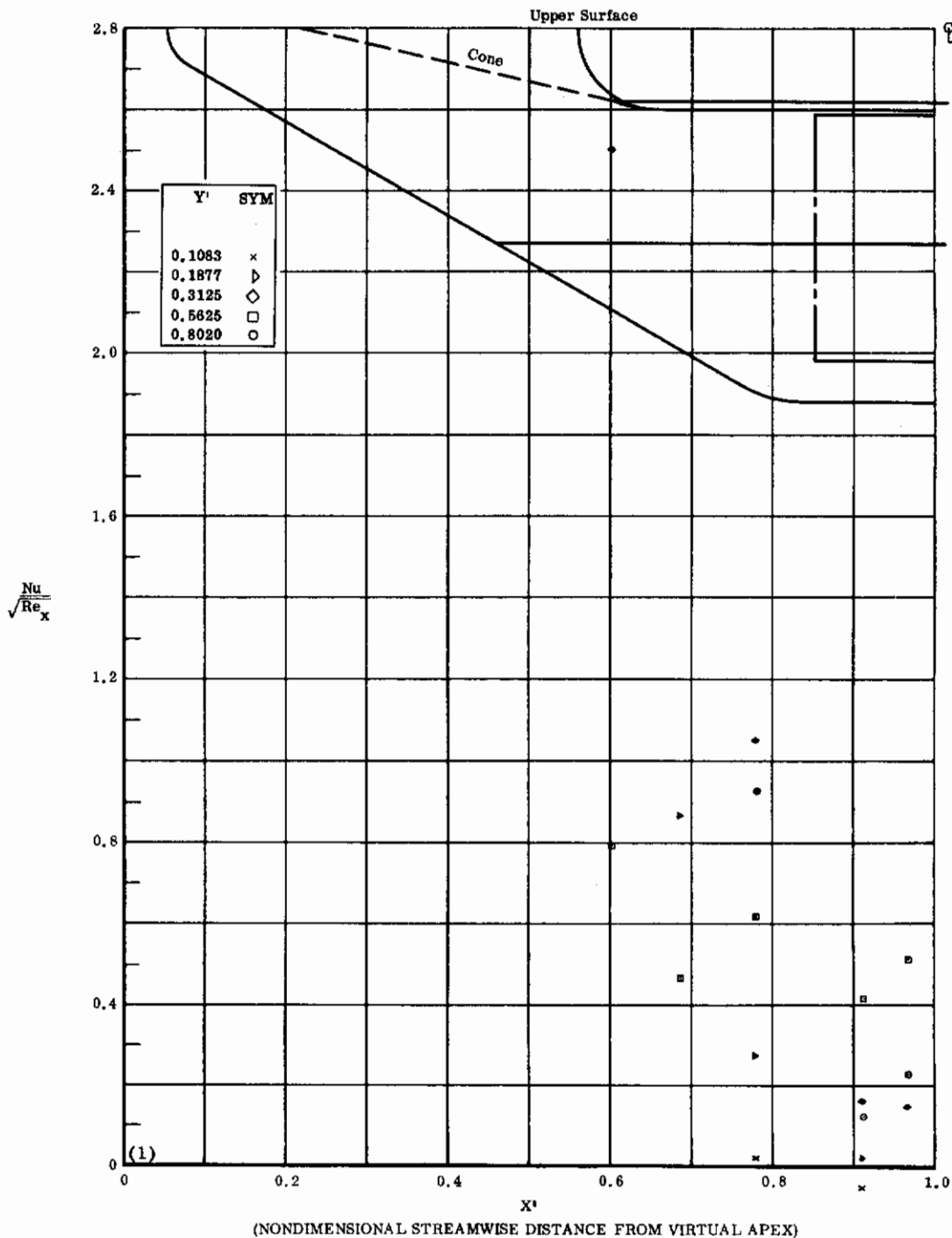


Fig. 102 Configuration I, $\alpha = -10$, $\delta_2 = \delta_3 = +20$
 $Nu/\sqrt{Re_x}$ vs. X^1 upper surface

Contrails

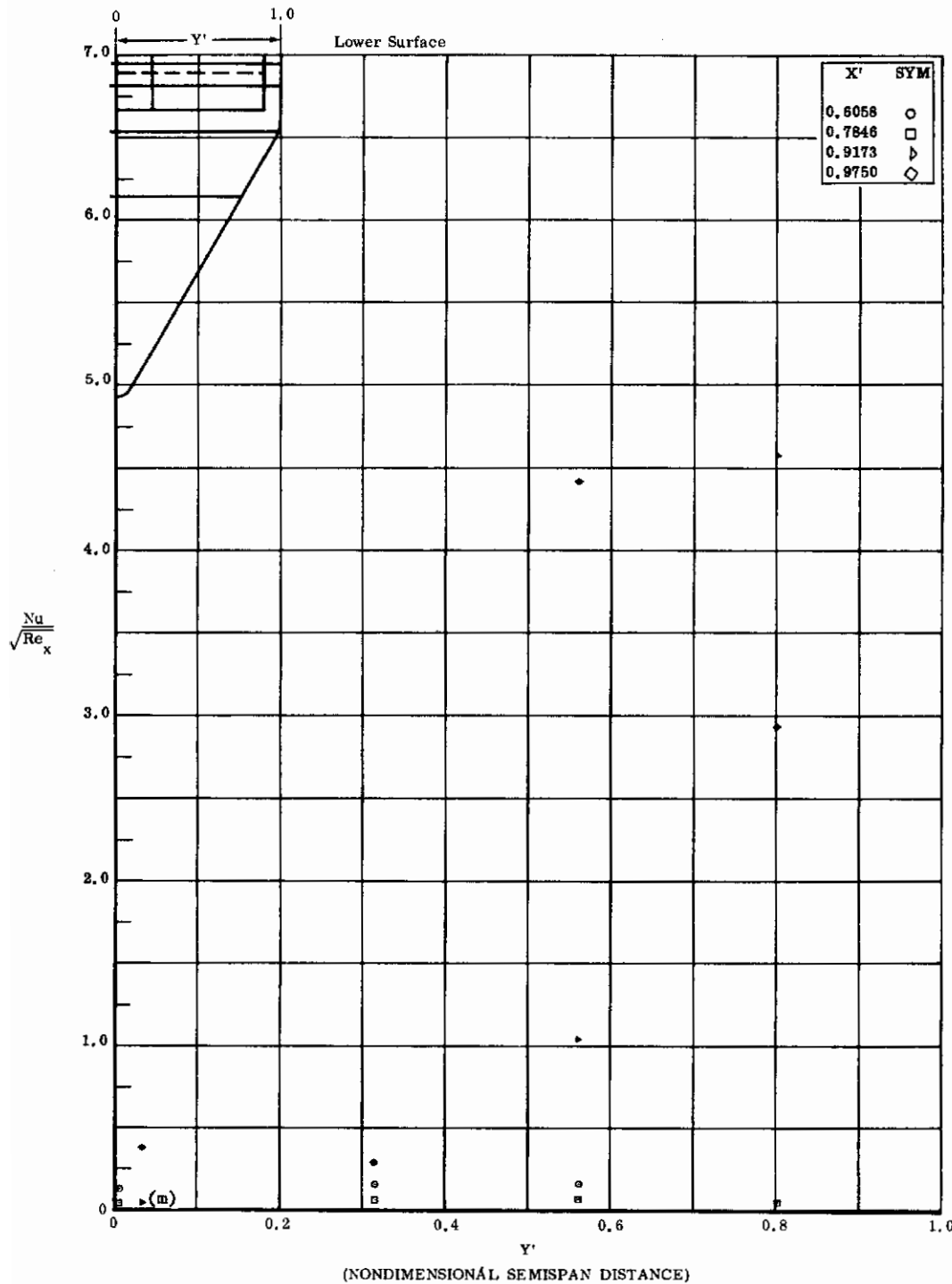


Fig. 10m Configuration I, $\alpha = -10$, $s_2 = s_3 = +30$
 $\frac{Nu}{\sqrt{Re_x}}$ vs. Y' lower surface

Contrails

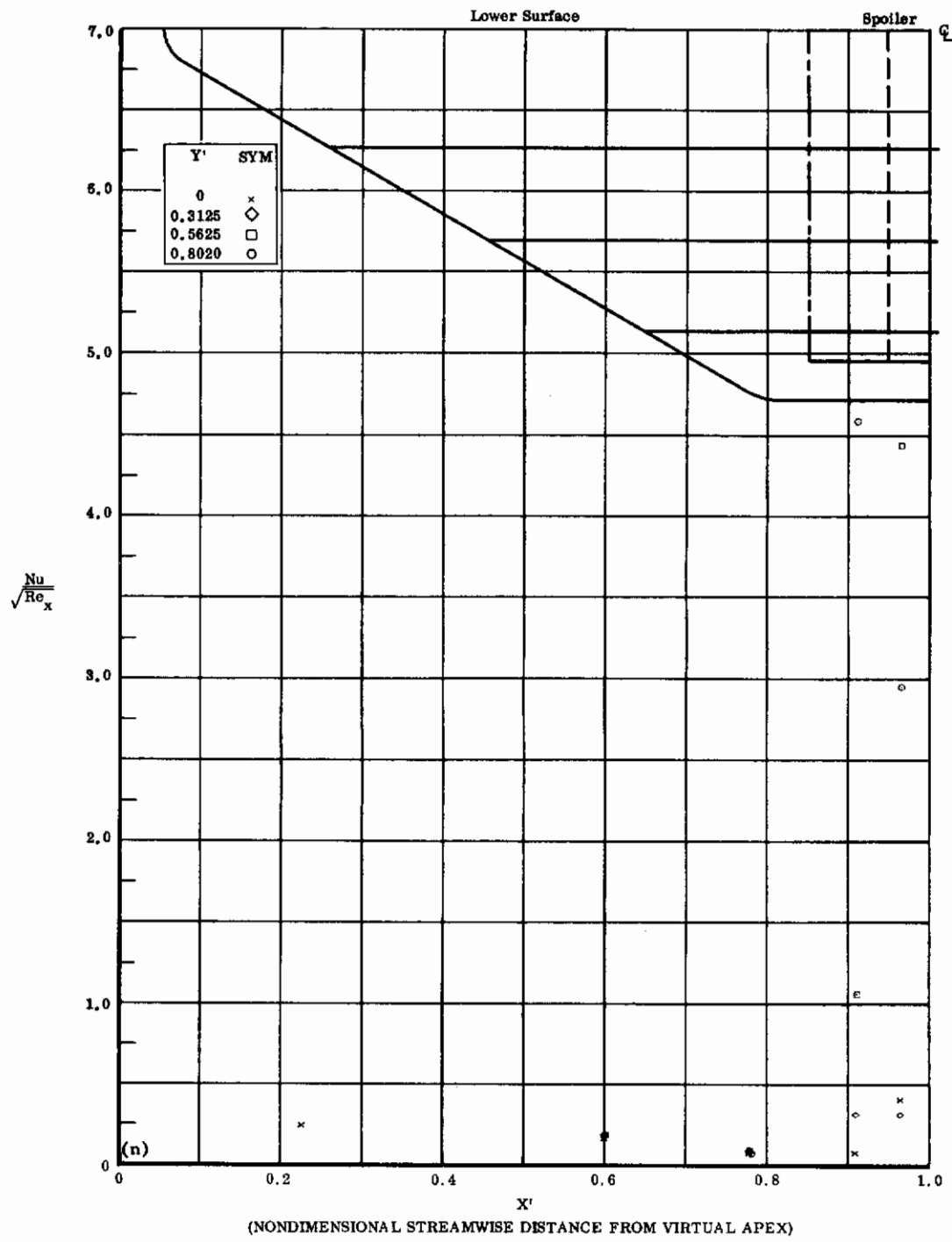


Fig. 10n Configuration I, $\alpha = -10$, $\delta_2 = \delta_3 = +30$

$Nu/\sqrt{Re_x}$ vs. X' lower surface

Contrails

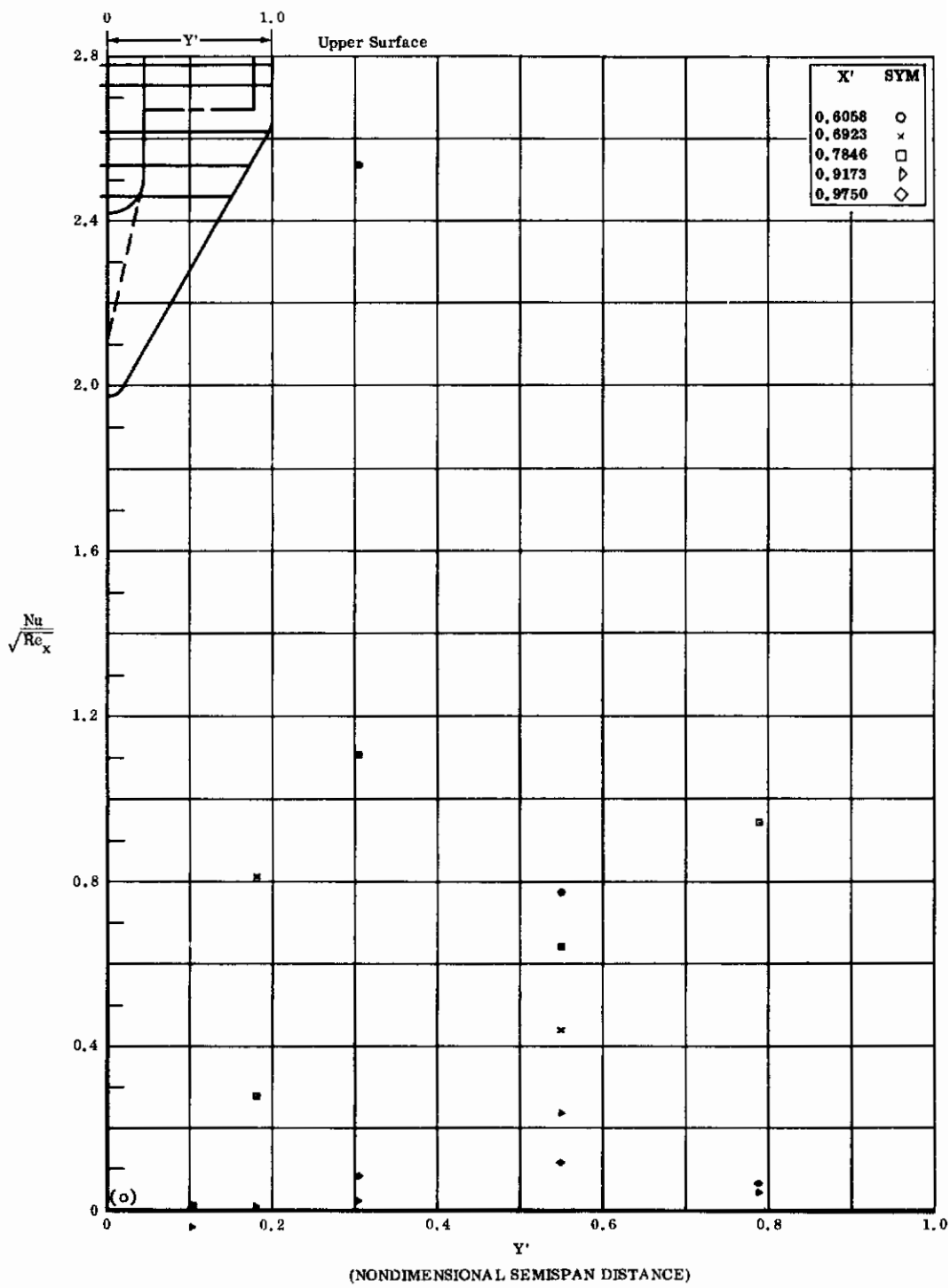


Fig. 10c Configuration I, $\alpha = -10$, $\delta_2 = \delta_3 = +30$

$Nu/\sqrt{Re_x}$ vs. Y' upper surface

Contrails

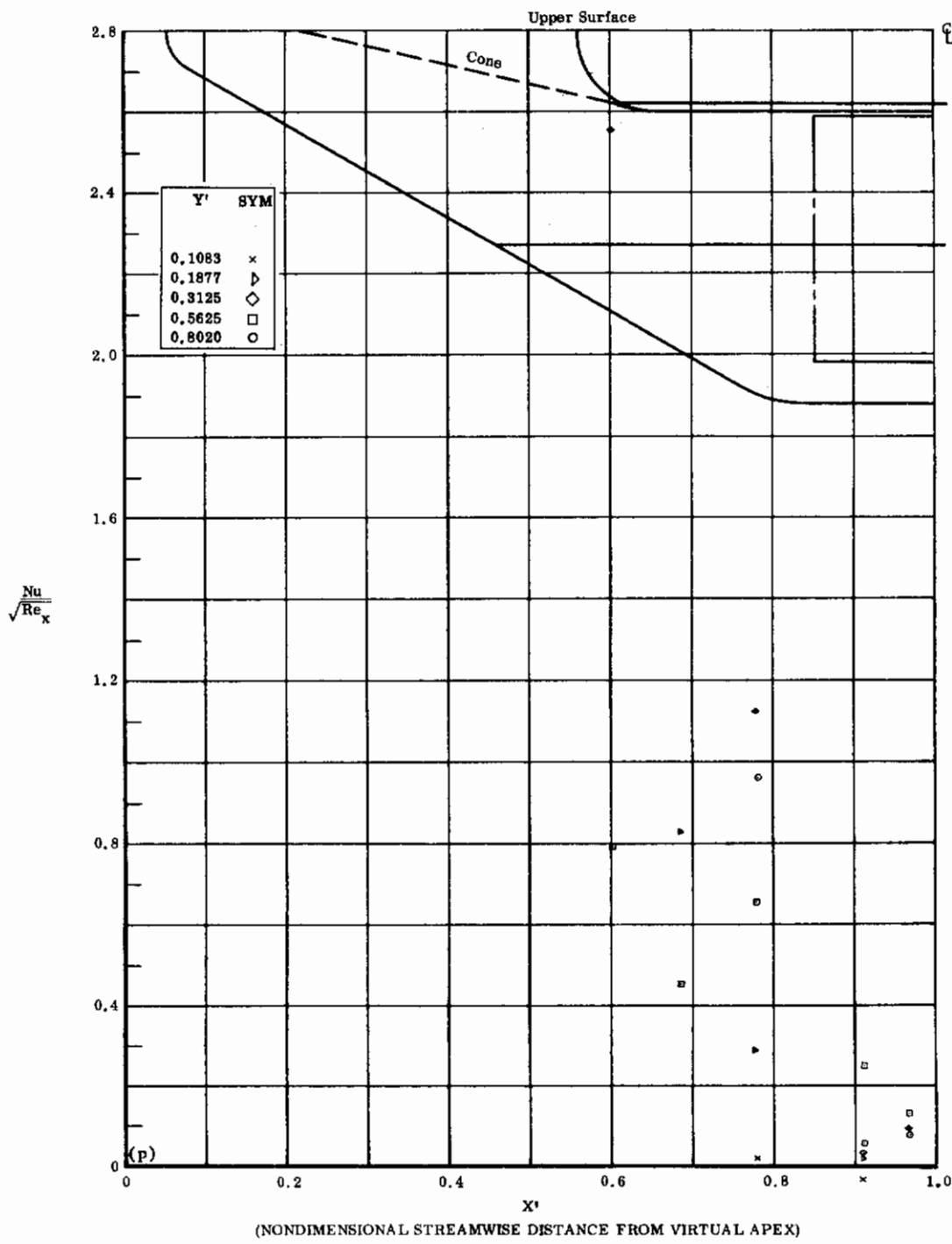


Fig. 10p Configuration I, $\alpha = -10$, $\delta_2 = \delta_3 = +30$

$\text{Nu}/\sqrt{\text{Re}_x}$ vs. X' upper surface

Contrails

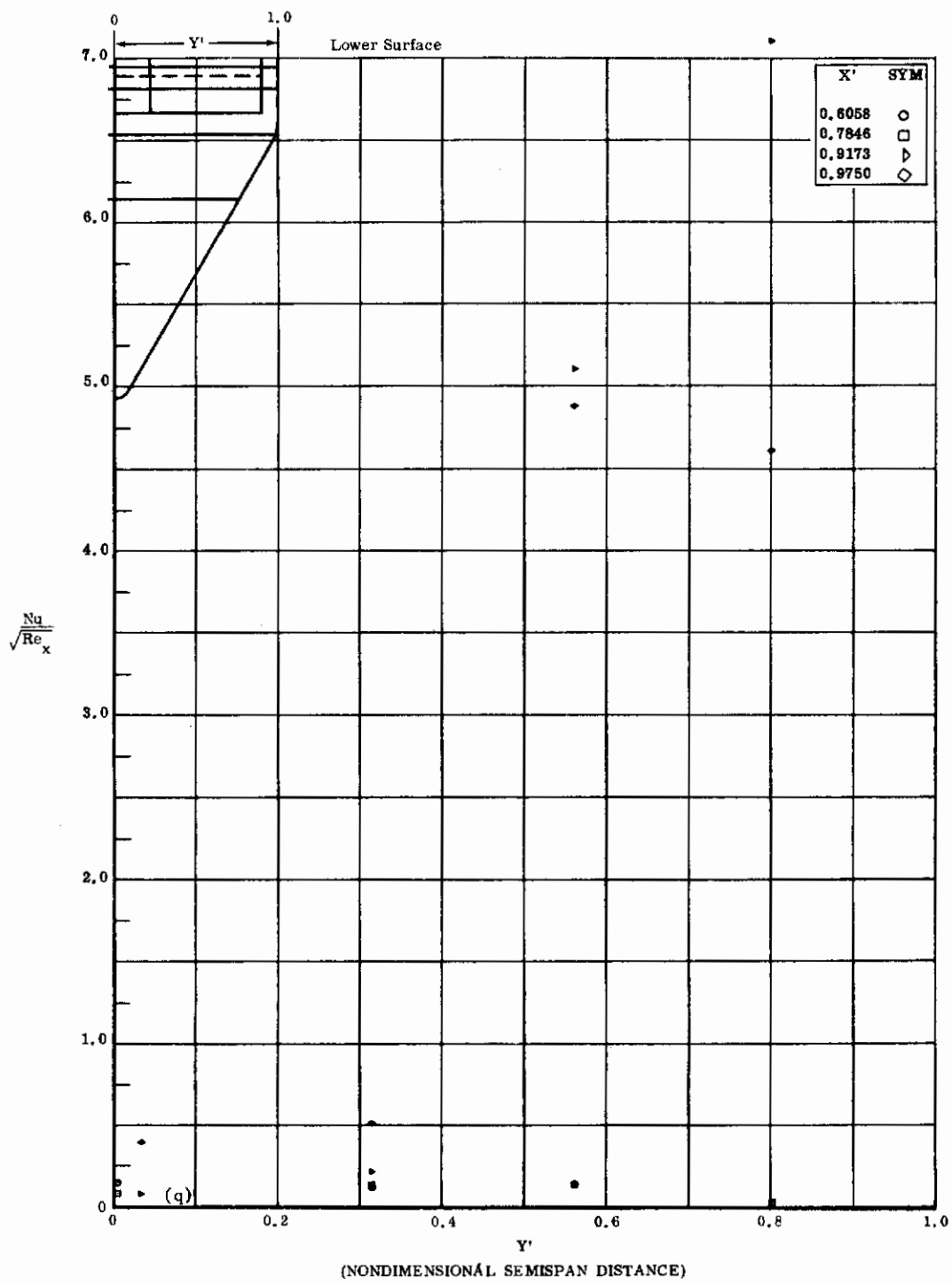


Fig. 10q Configuration I, $\alpha = -10$, $\delta_2 = \delta_3 = +39$
 $\frac{Nu}{\sqrt{Re_x}}$ vs. Y' lower surface

Contrails

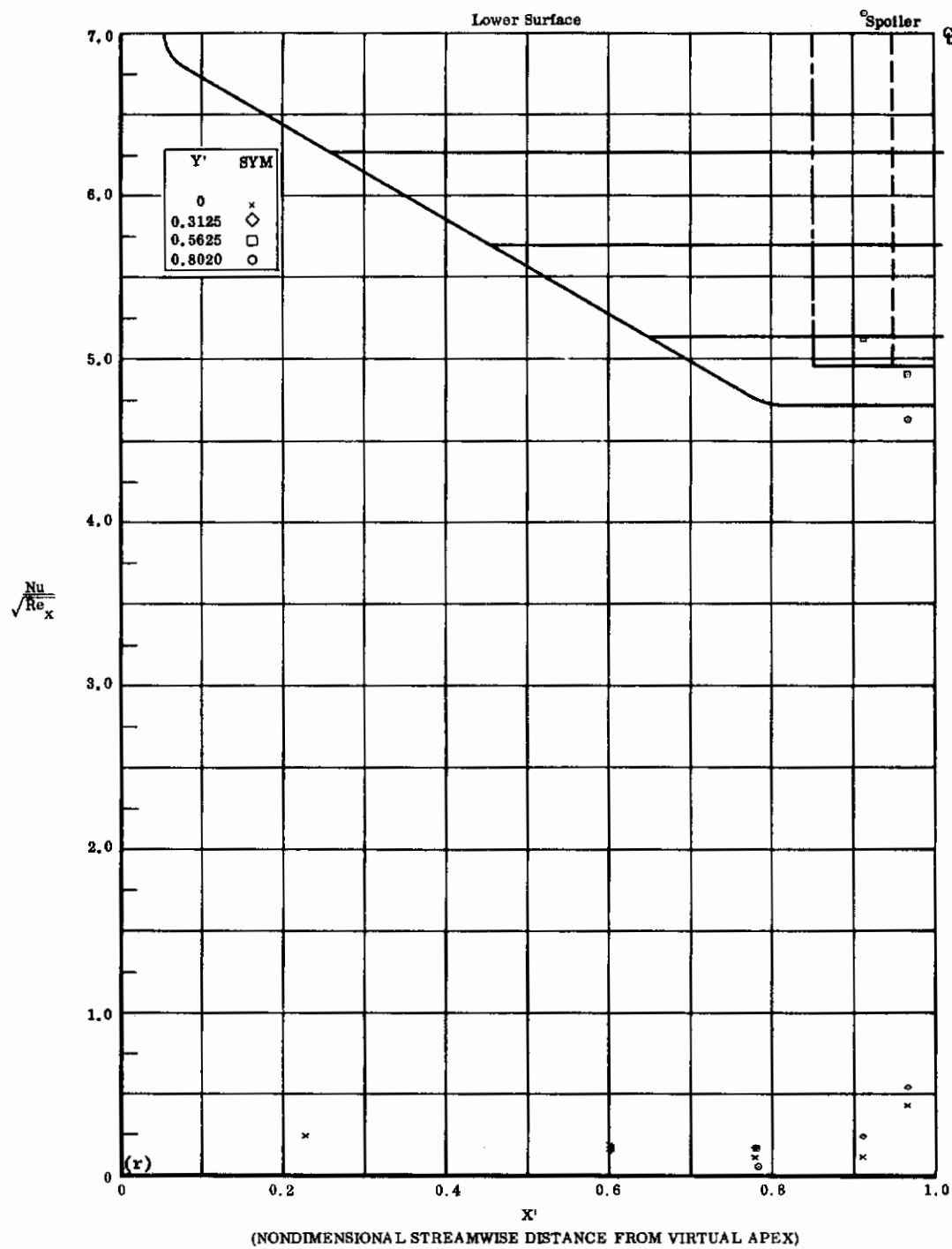


Fig. 10r Configuration I, $\alpha = -10$, $\delta_2 = \delta_3 = +39$

$\text{Nu}/\sqrt{\text{Re}_x}$ vs. X' lower surface

Contrails

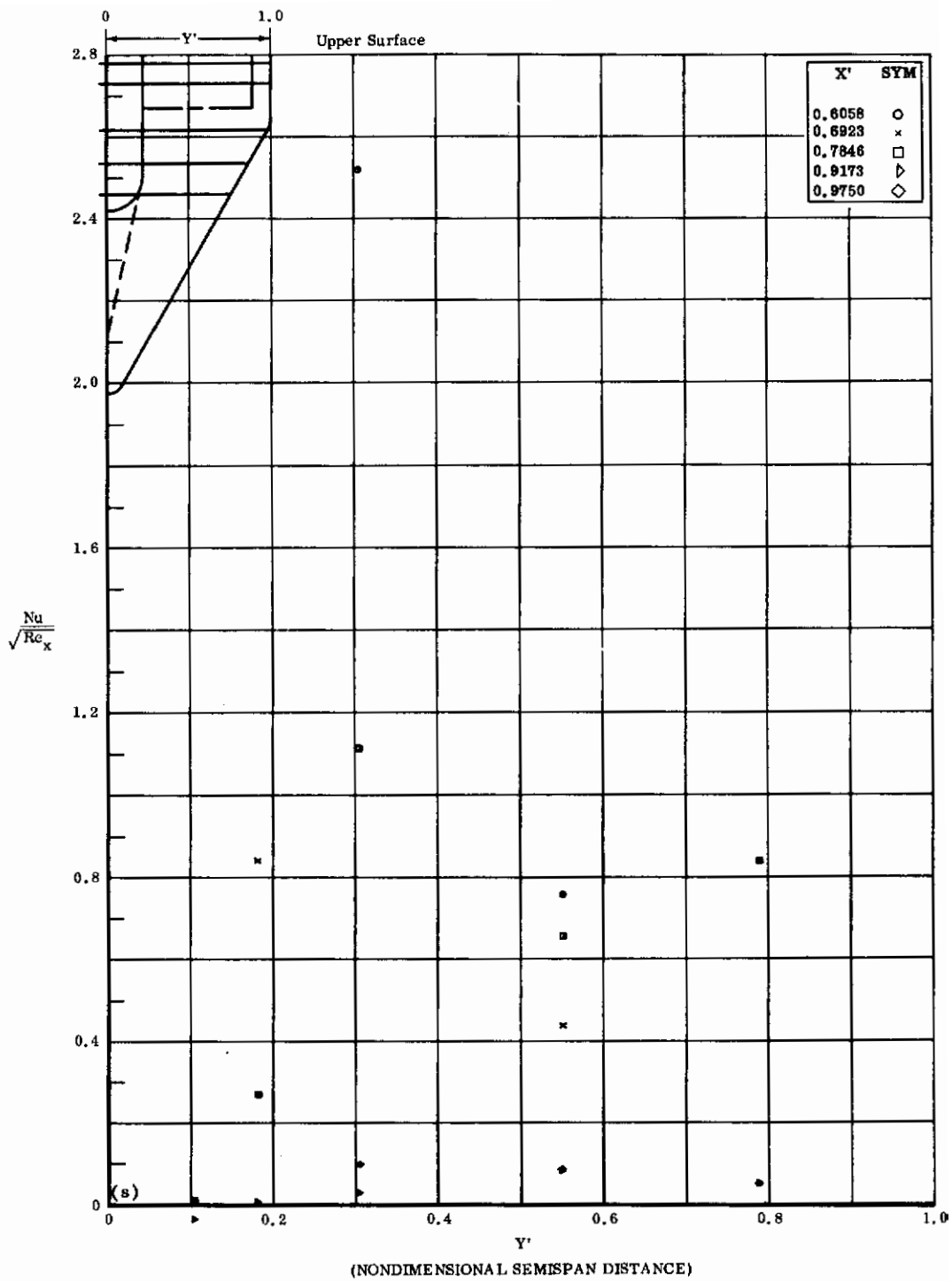


Fig. 10s Configuration I, $\alpha = -10$, $b_2 = b_3 = +39$
 $Nu/\sqrt{Re_x}$ vs. Y' upper surface

Contrails

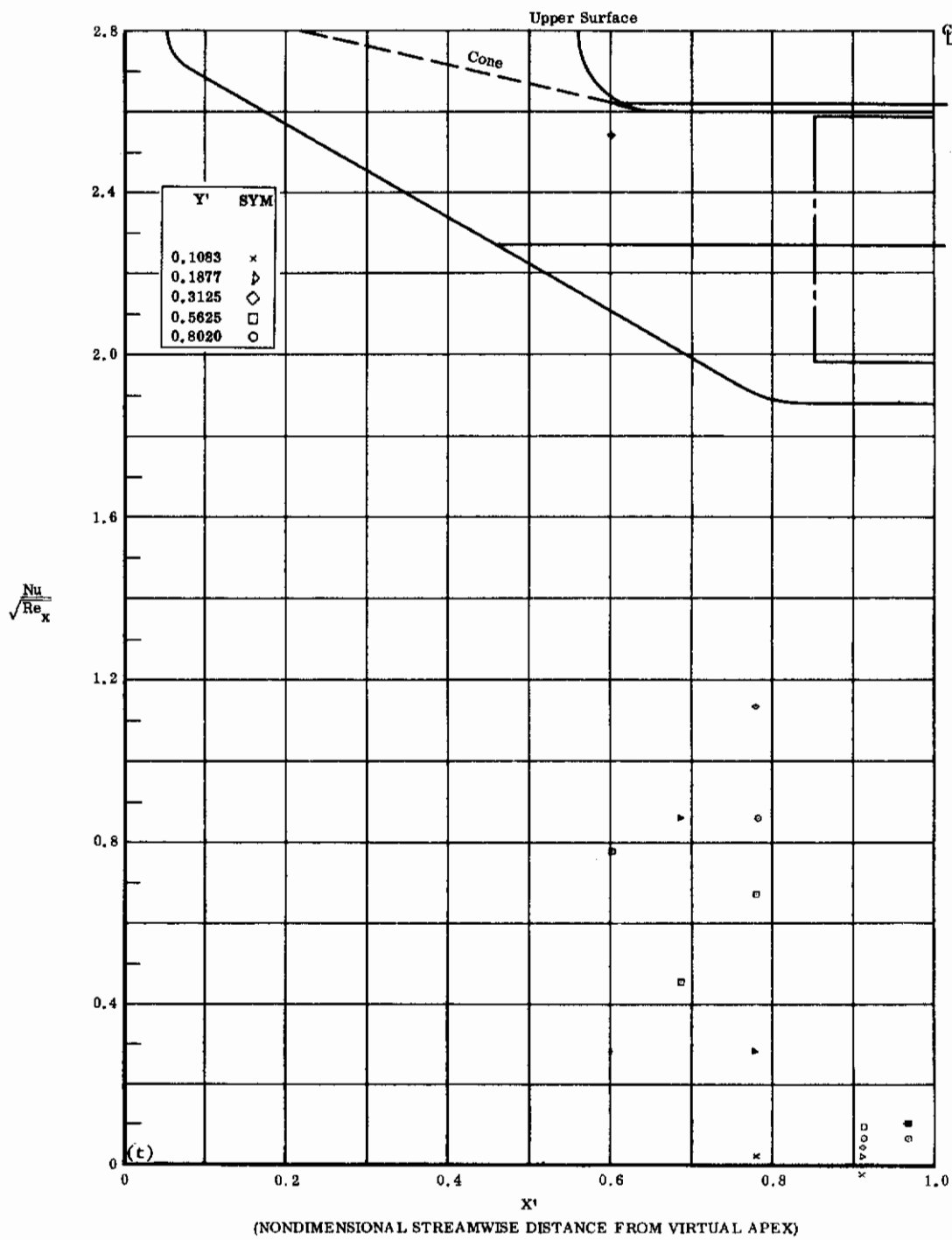


Fig. 10t Configuration I, $\alpha = -10$, $\delta_2 = \delta_3 = +39$
 $Nu/\sqrt{Re_x}$ vs. X' upper surface

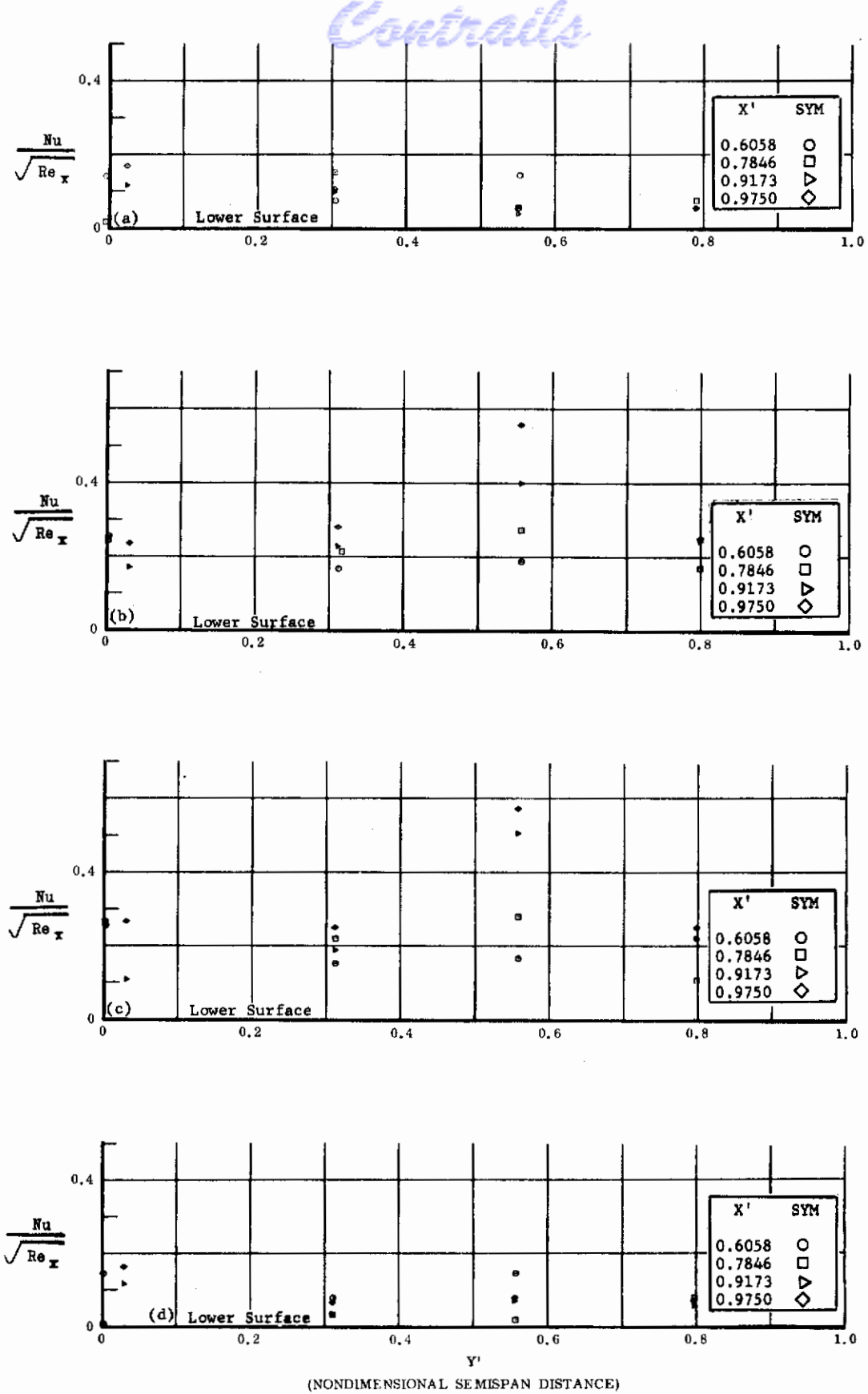


Fig. 11 Configuration I, $\alpha = -10$, $Nu/\sqrt{Re_x}$ vs. Y' , lower surface

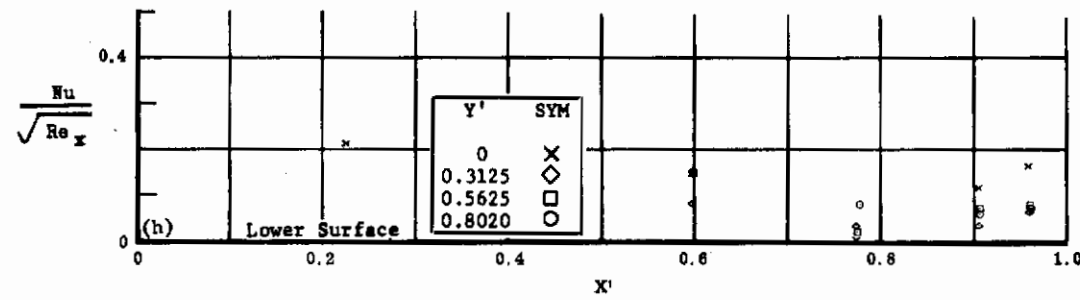
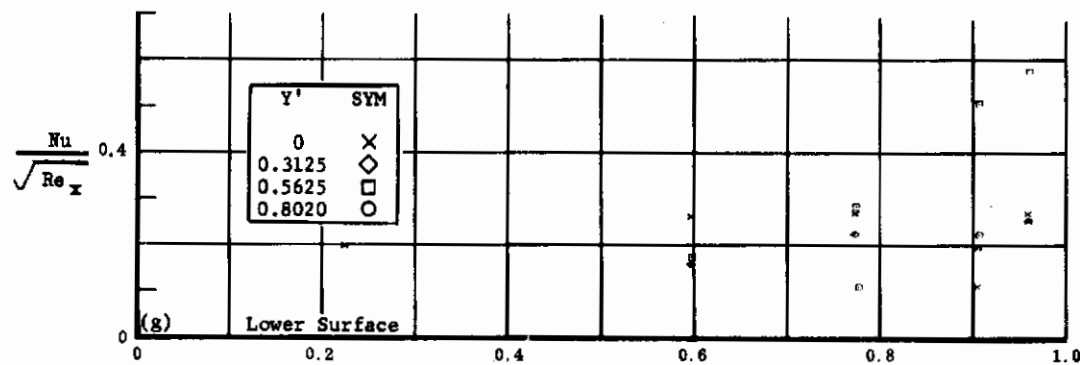
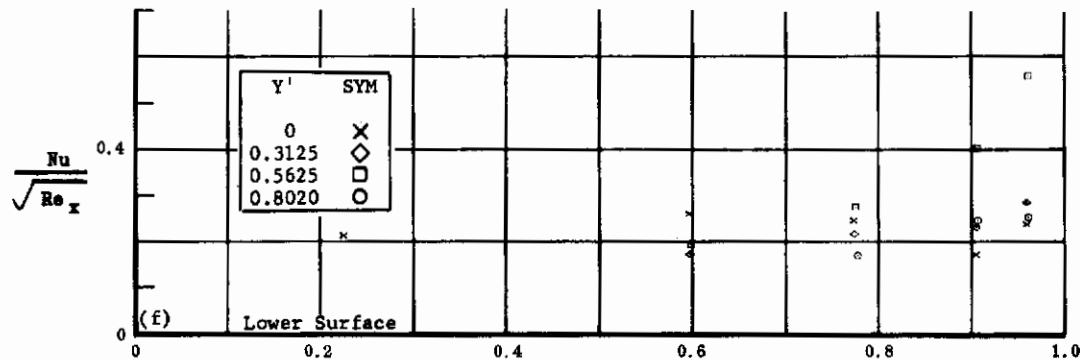
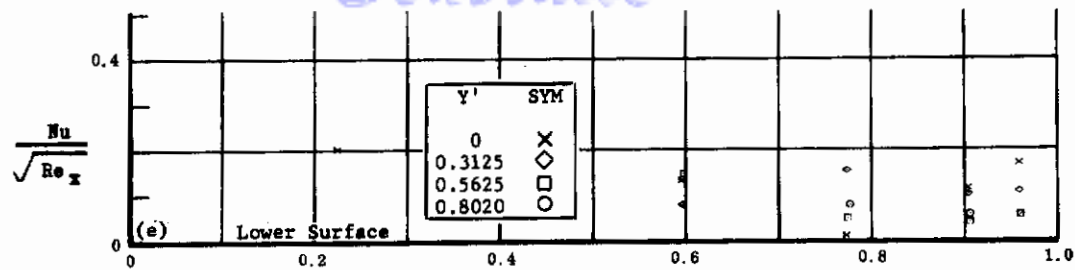
a) $b_2 = b_3 = -10$

b) $b_2 = b_3 = -20$

c) $b_2 = b_3 = -30$

d) $b_2 = b_3 = -39$

Controls



(NONDIMENSIONAL STREAMWISE DISTANCE FROM VIRTUAL APEX)

Fig. 11 Configuration I, $\alpha = -10$, $Nu/\sqrt{Re_x}$ vs. X' , lower surface

e) $\delta_2 = \delta_3 = -10$

f) $\delta_2 = \delta_3 = -20$

g) $\delta_2 = \delta_3 = -30$

h) $\delta_2 = \delta_3 = -39$

Contrails

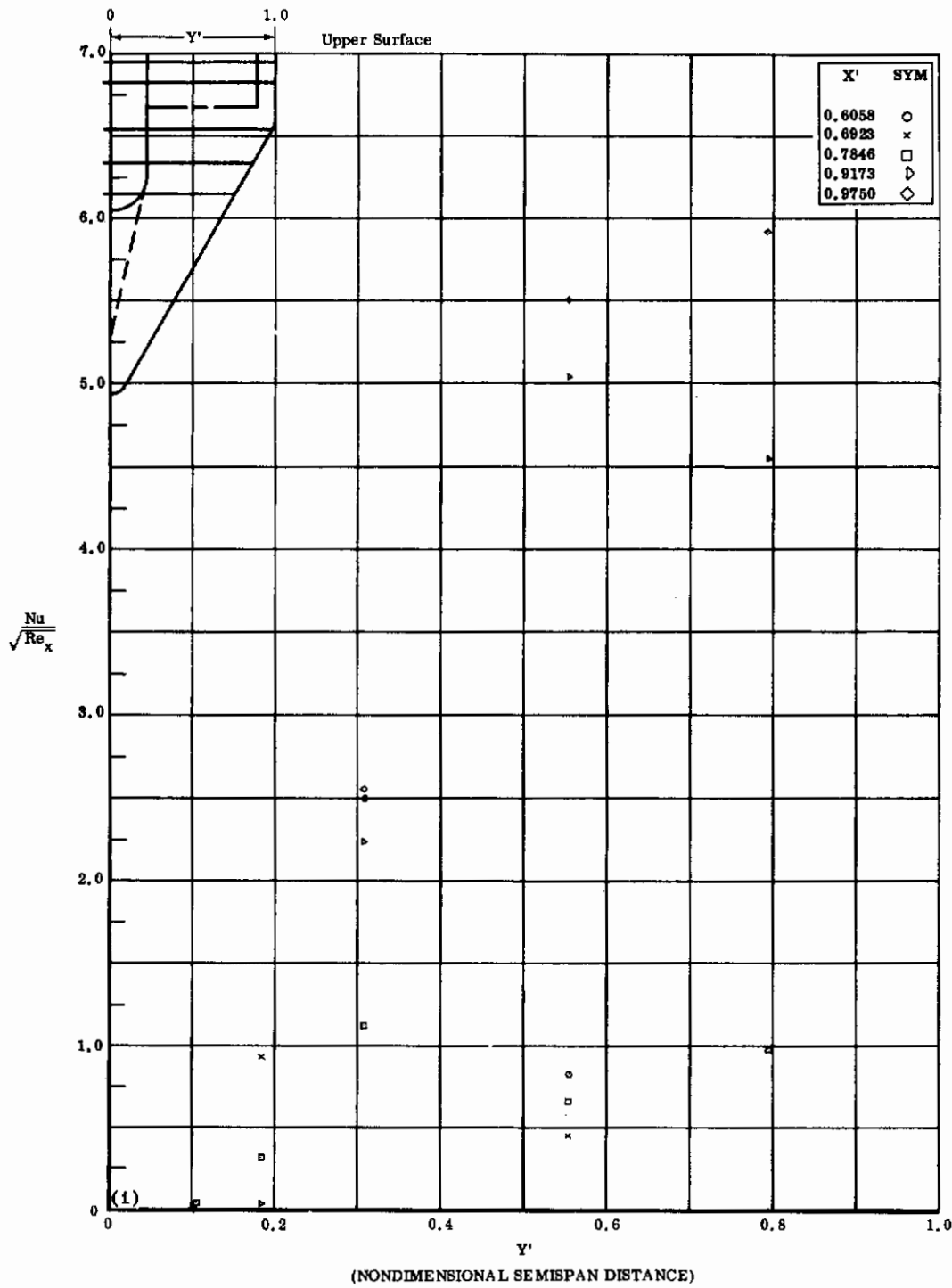


Fig. 11i Configuration I, $\alpha = -10$, $s_2 = s_3 = -10$
 $Nu/\sqrt{Re_x}$ vs. Y' upper surface

Contrails

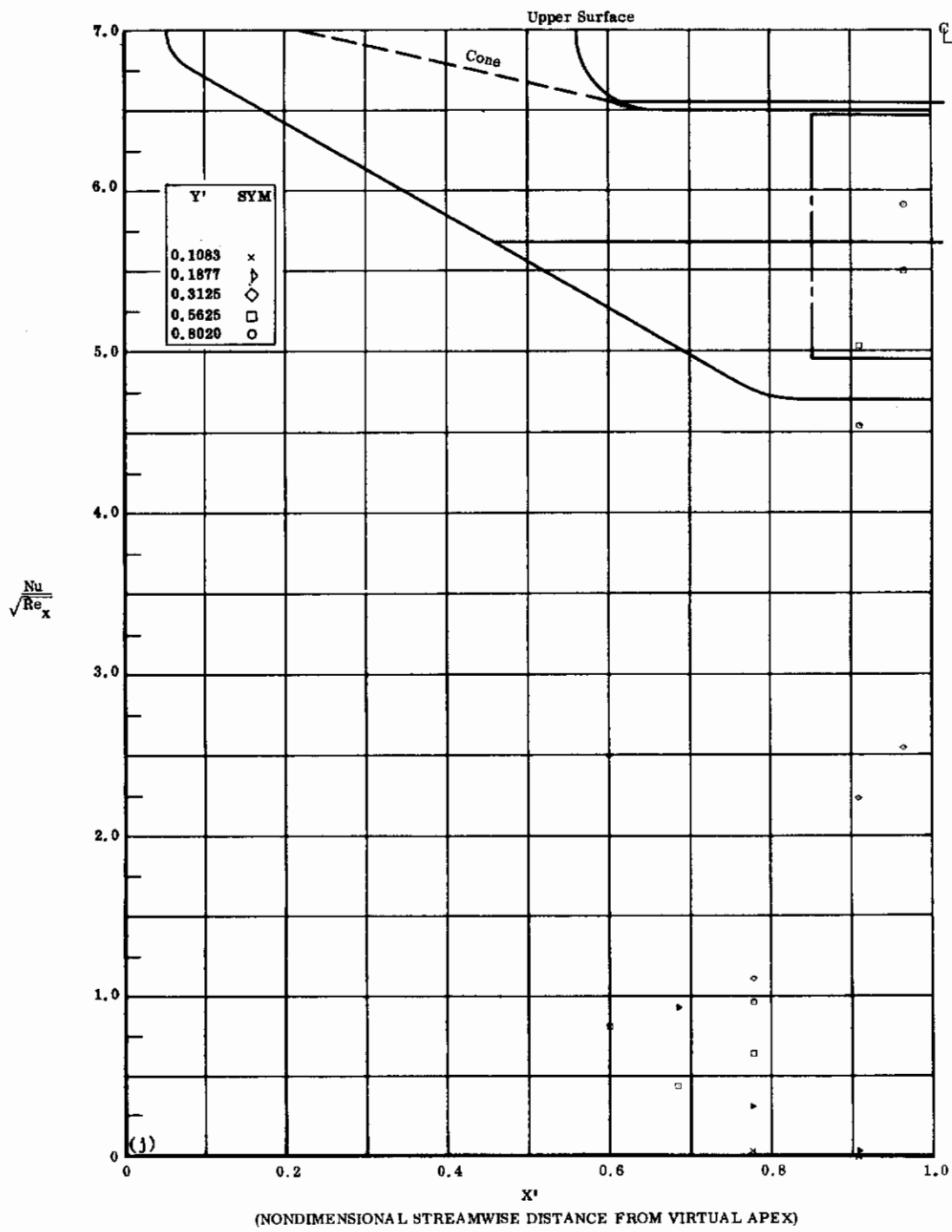


Fig. 11j Configuration I, $\alpha = -10$, $b_2 = b_3 = -10$
 $Nu/\sqrt{Re_x}$ vs. X' upper surface

Contrails

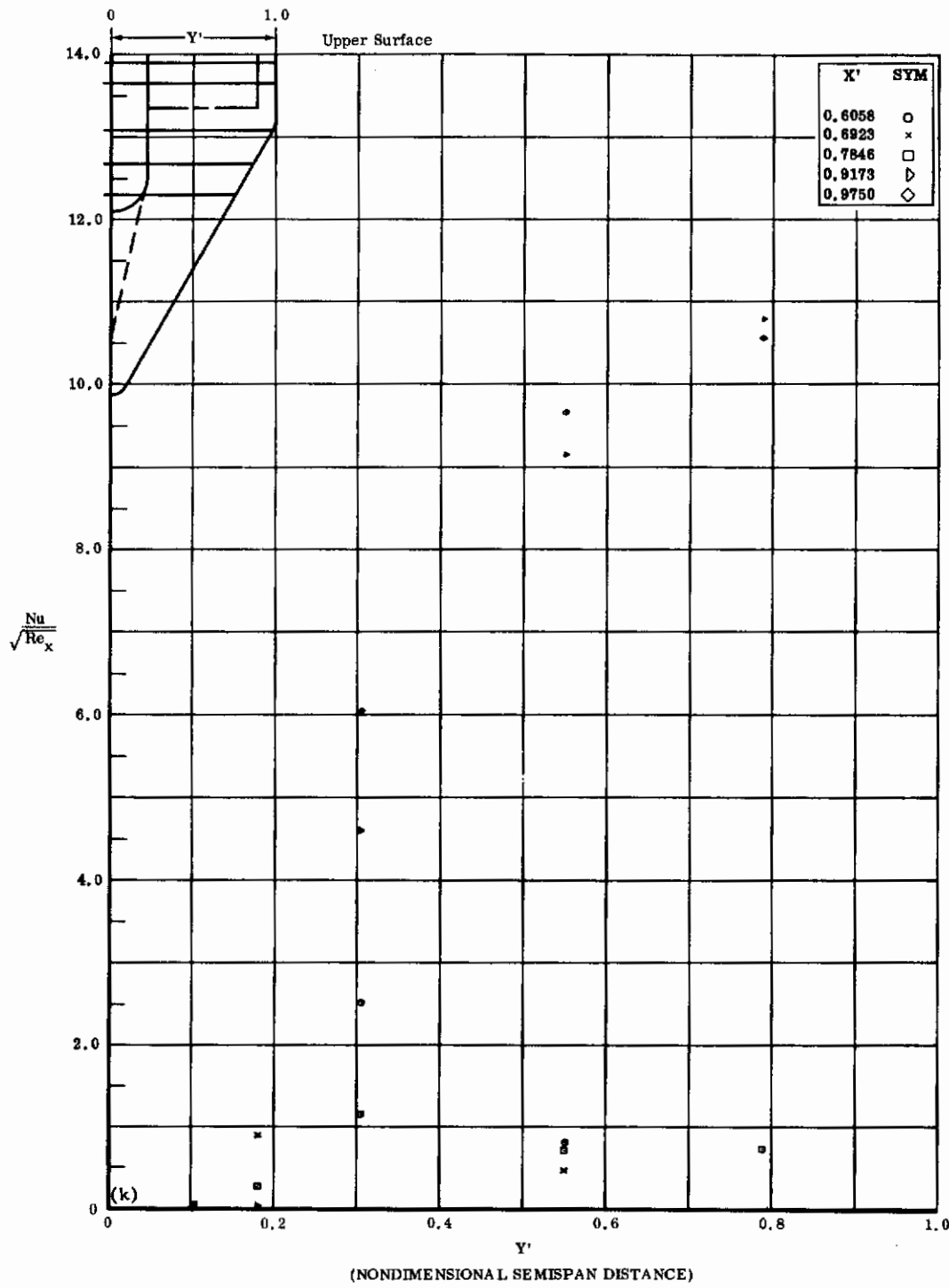


Fig. 11k Configuration I, $\alpha = -10$, $\delta_2 = \delta_3 = -20$
 $Nu/\sqrt{Re_x}$ vs. Y' upper surface

Contrails

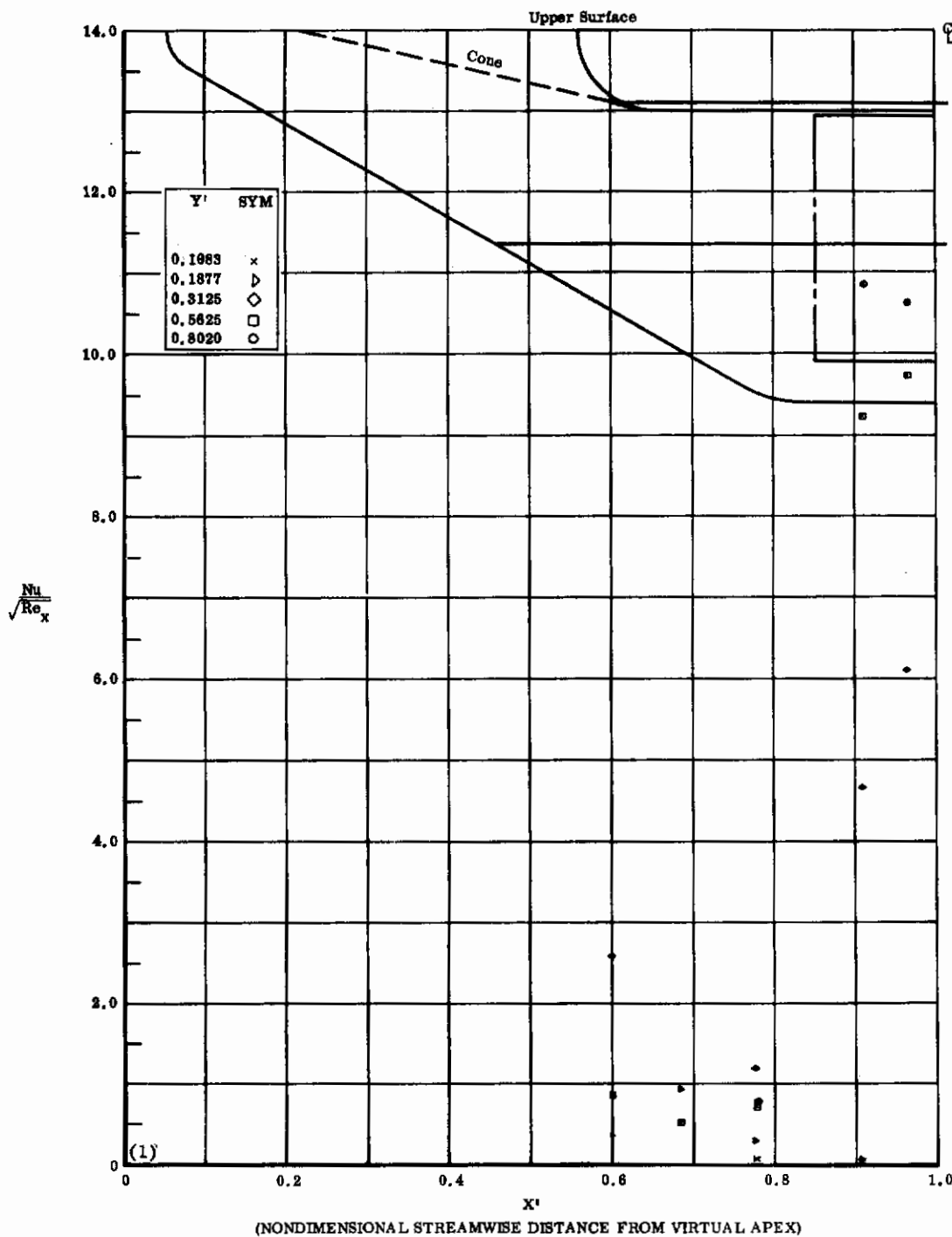


Fig. 11f Configuration I, $\alpha = -10$, $\delta_2 = \delta_3 = -20$
 $Nu/\sqrt{Re_x}$ vs. X' upper surface

Contrails

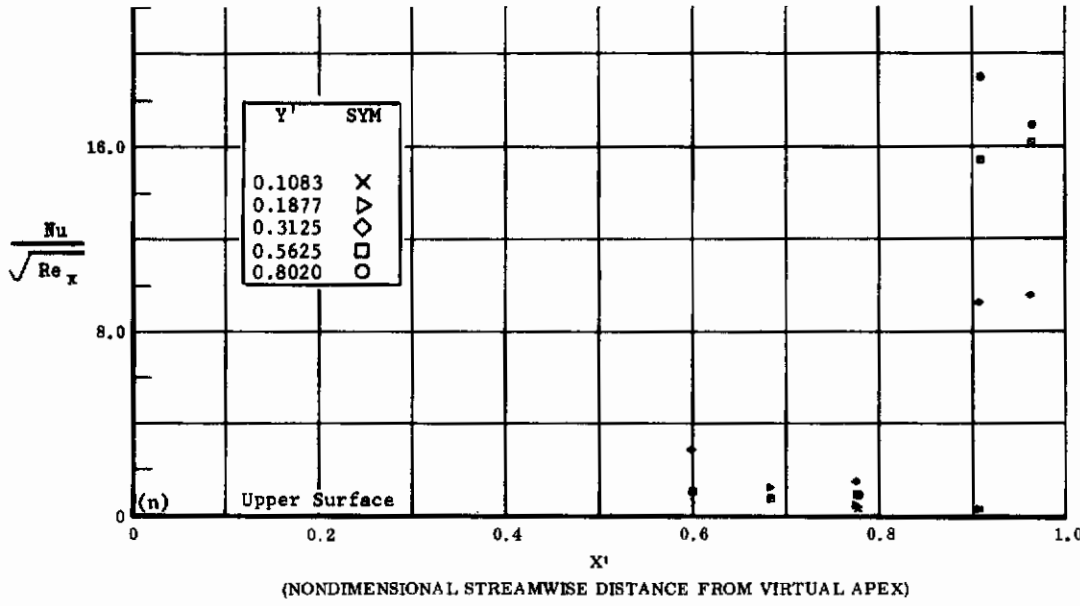
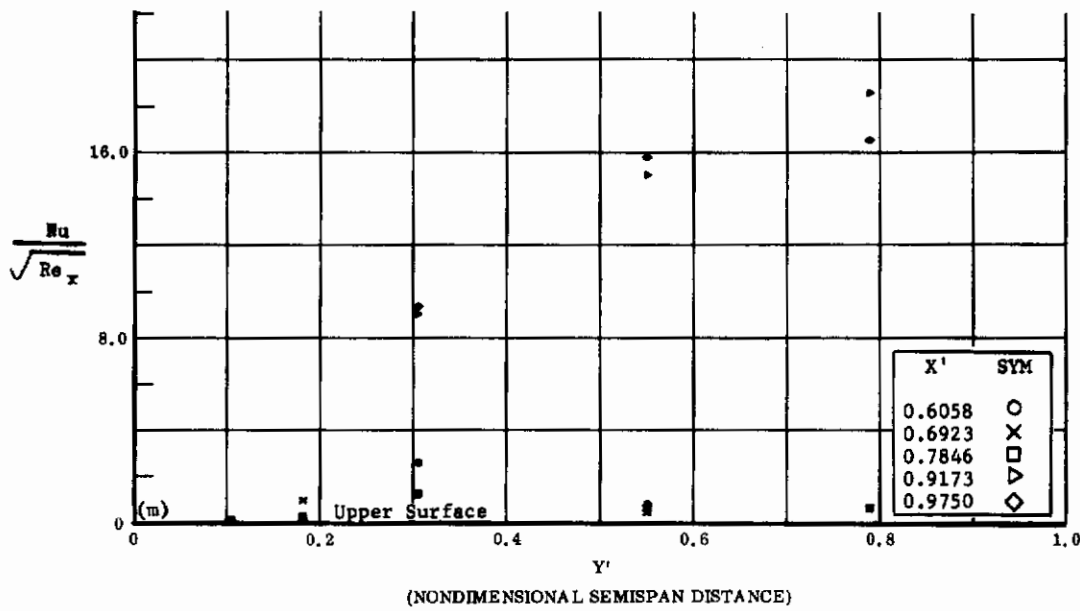


Fig. 11 Configuration I, $\alpha = -10$, $\delta_2 = \delta_3 = -30$

m) $Nu/\sqrt{Re_x}$ vs. Y' upper surface

n) $Nu/\sqrt{Re_x}$ vs. X' upper surface

Contrails

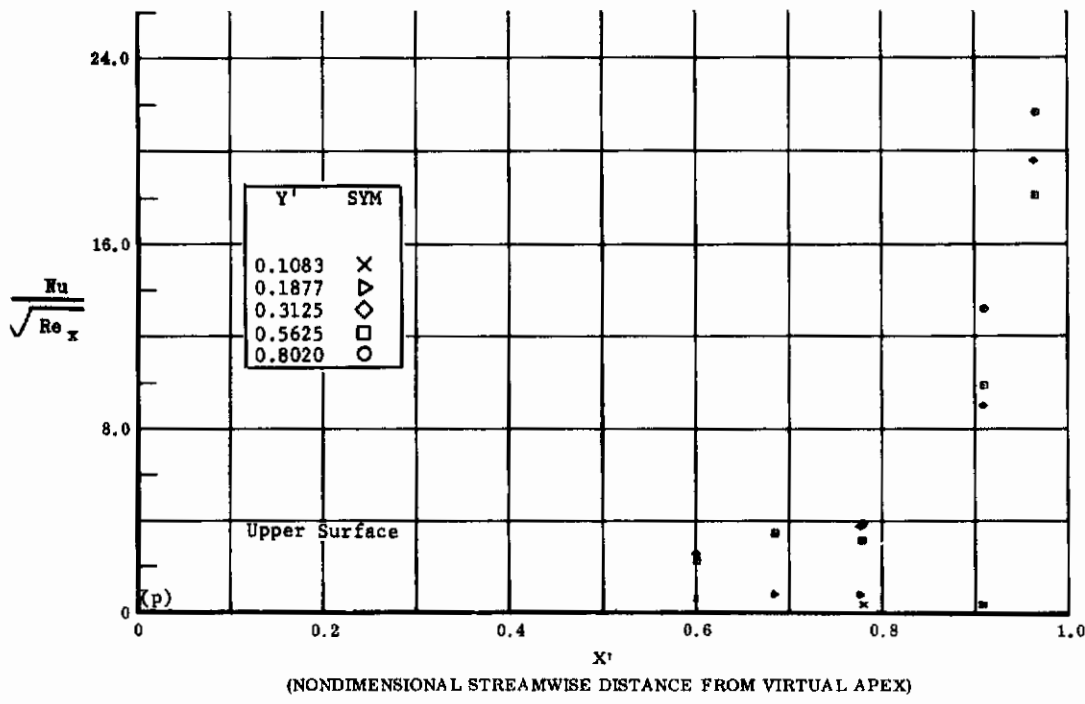
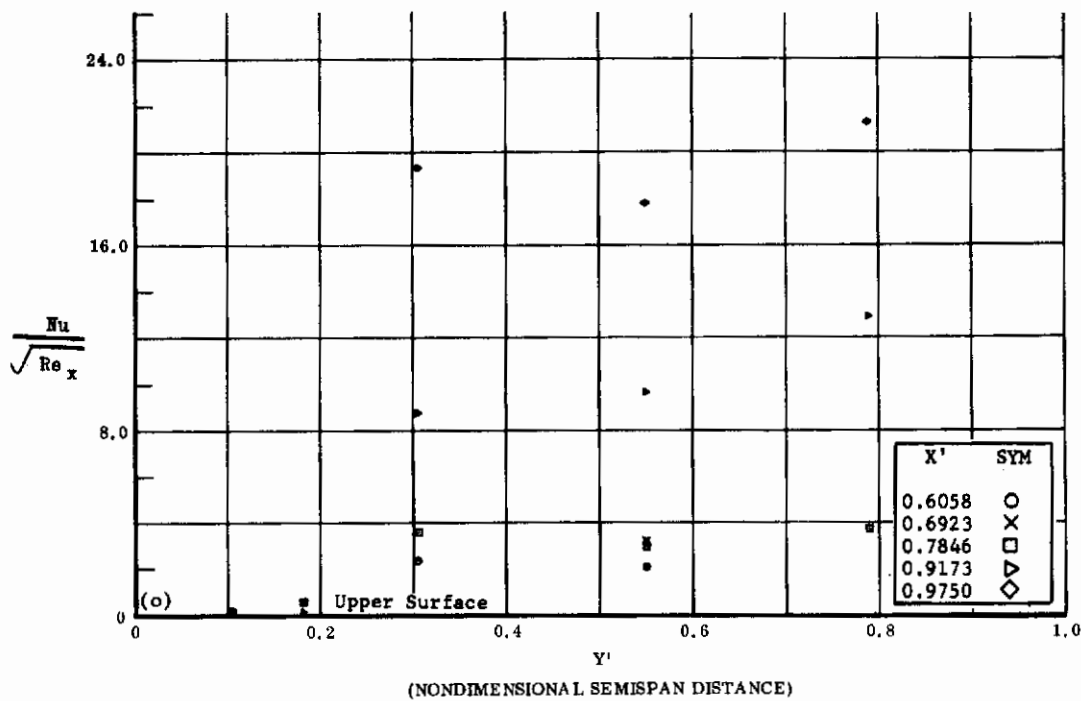


Fig. 11 Configuration I, $\alpha = -10$, $\delta_2 = \delta_3 = -39$

o) $Nu/\sqrt{Re_x}$ vs. Y' upper surface

p) $Nu/\sqrt{Re_x}$ vs. X' upper surface

Contrails

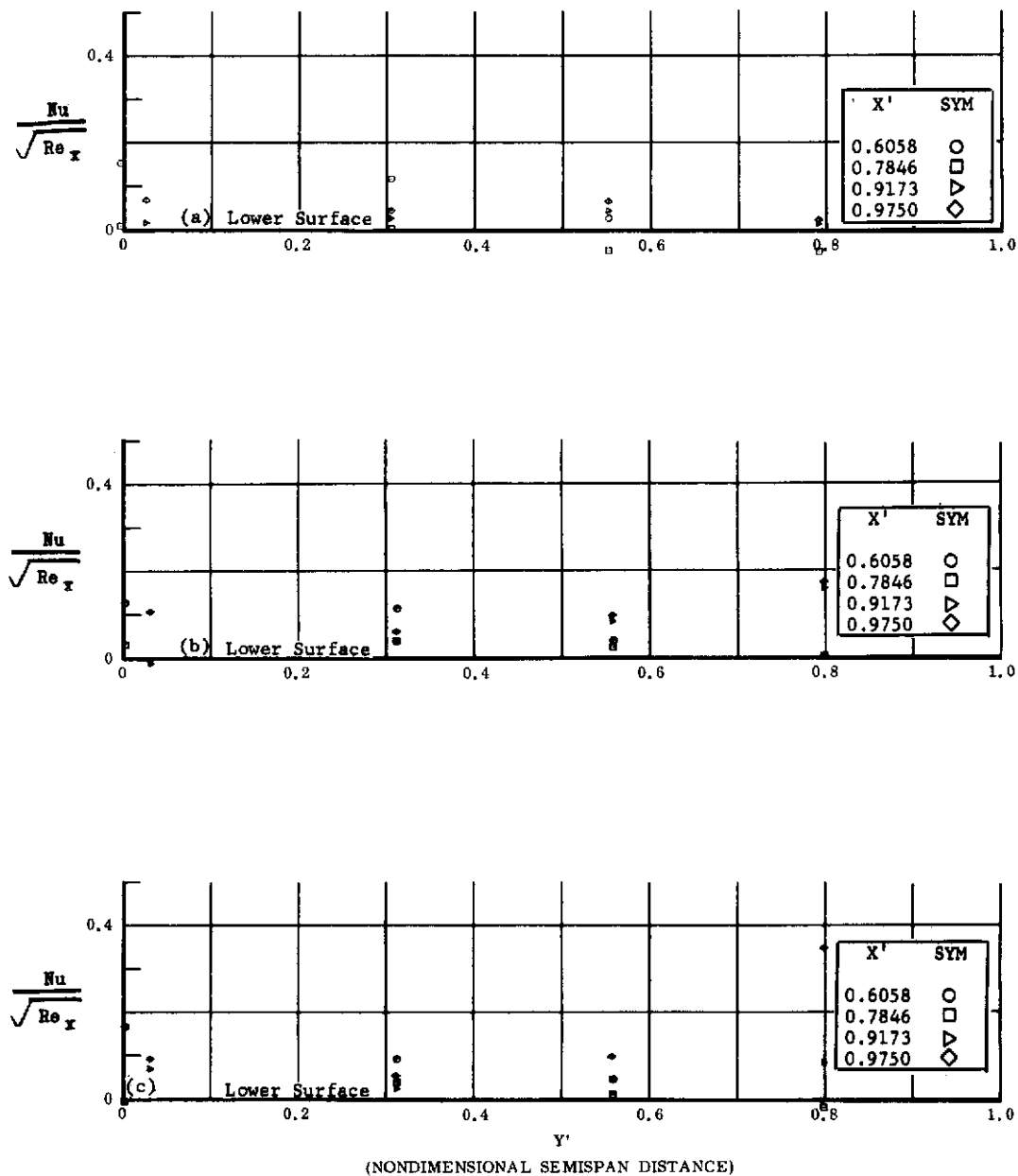


Fig. 12 Configuration I, $\alpha = -20$, $\text{Nu}/\sqrt{\text{Re}_x}$ vs. Y' , lower surface

a) $\delta_2 = \delta_3 = 0$

b) $\delta_2 = \delta_3 = +10$

c) $\delta_2 = \delta_3 = +20$

Contrails

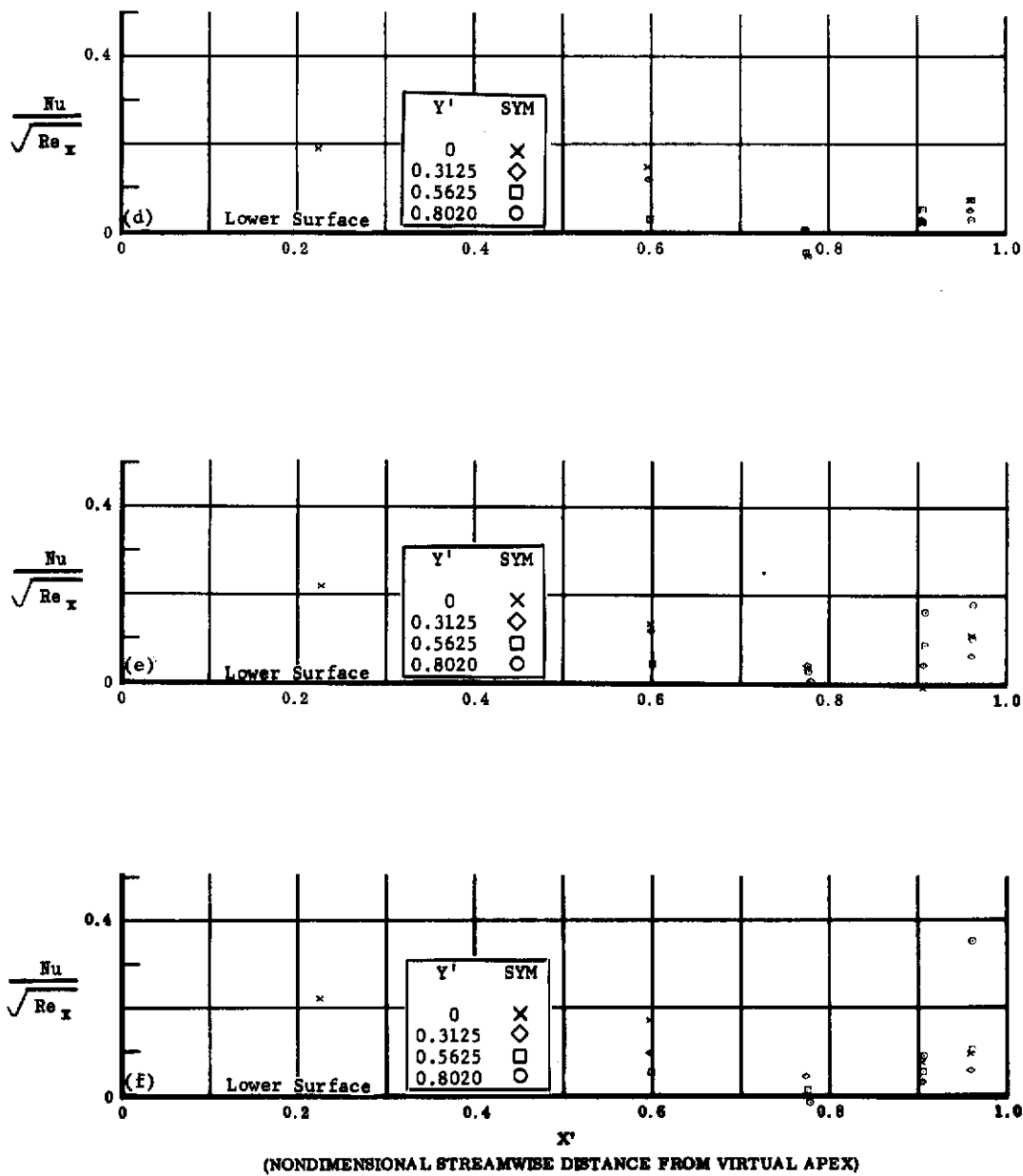


Fig. 12 Configuration I, $\alpha = -20$, $Nu/\sqrt{Re_x}$ vs. X' , lower surface

d) $\delta_2 = \delta_3 = 0$

e) $\delta_2 = \delta_3 = +10$

f) $\delta_2 = \delta_3 = +20$

Contrails

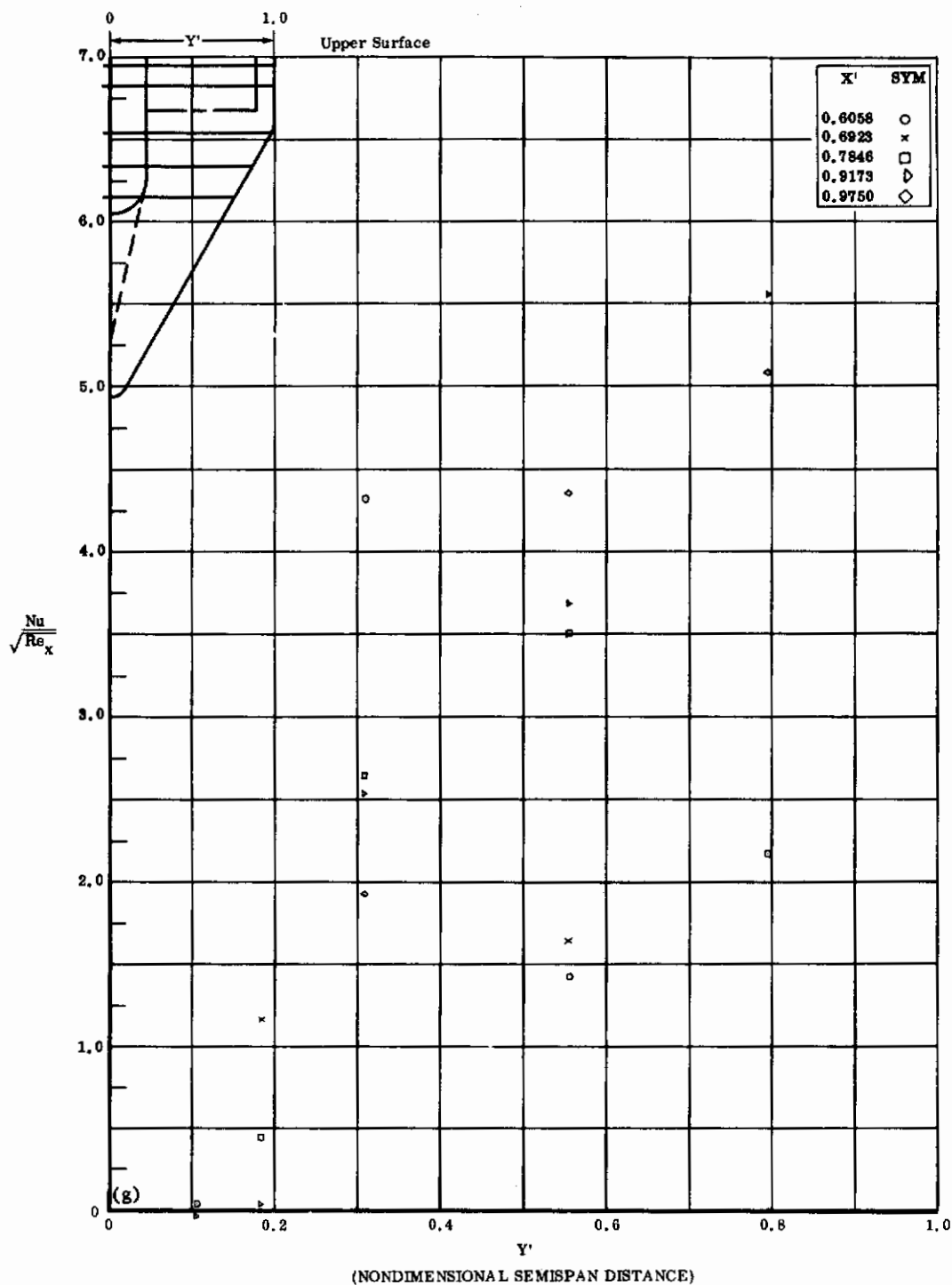


Fig. 12g Configuration I, $\alpha = -20$, $b_2 = b_3 = 0$

$\text{Nu}/\sqrt{\text{Re}_x}$ vs. Y' upper surface

Contrails

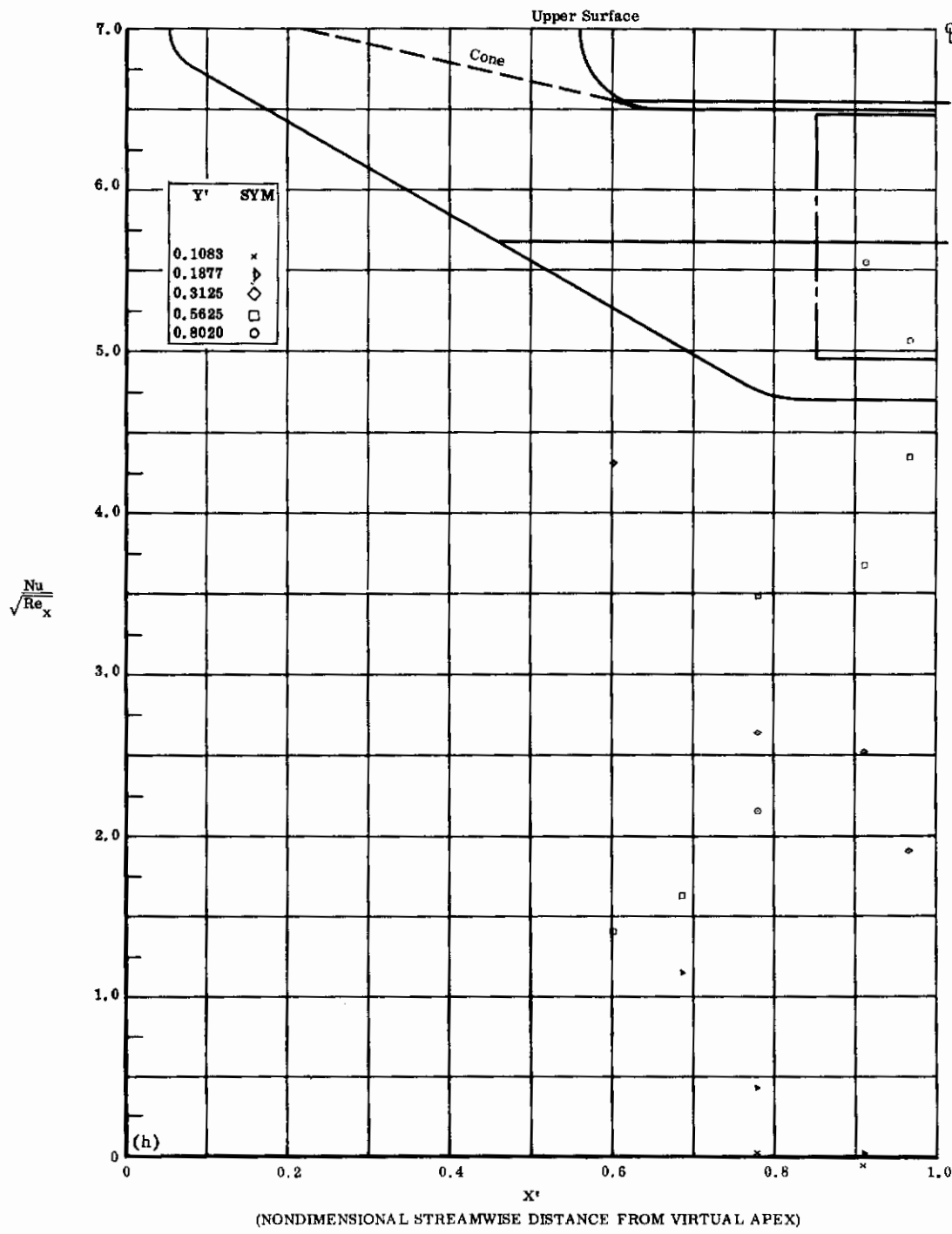


Fig. 12h Configuration I, $\alpha = -20$, $\delta_2 = \delta_3 = 0$

$Nu/\sqrt{Re_x}$ vs. X' upper surface

Contrails

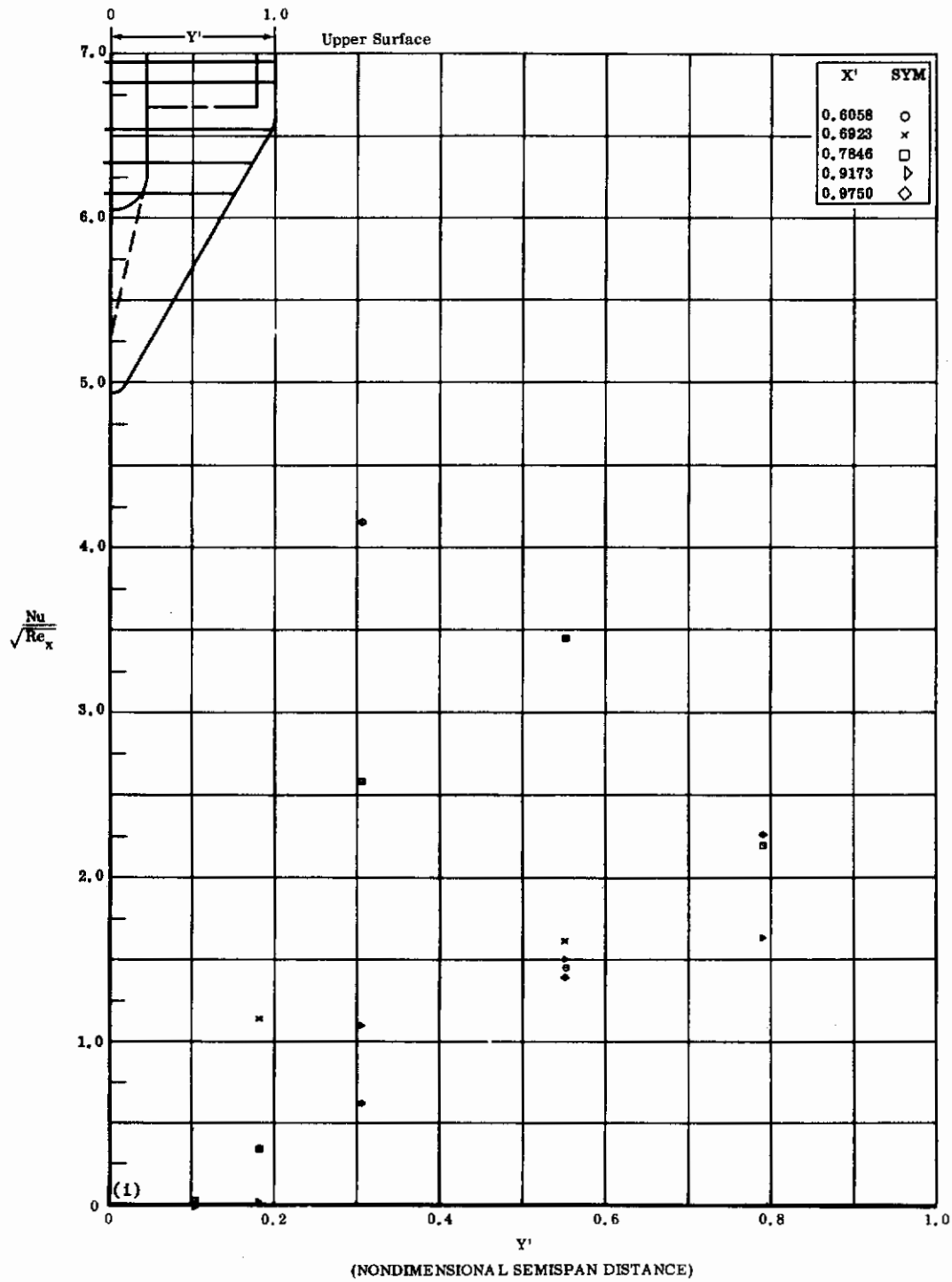


Fig. 12i Configuration I, $\alpha = -20$, $\delta_2 = \delta_3 = +10$
 $\text{Nu}/\sqrt{\text{Re}_x}$ vs. Y' upper surface

Contrails

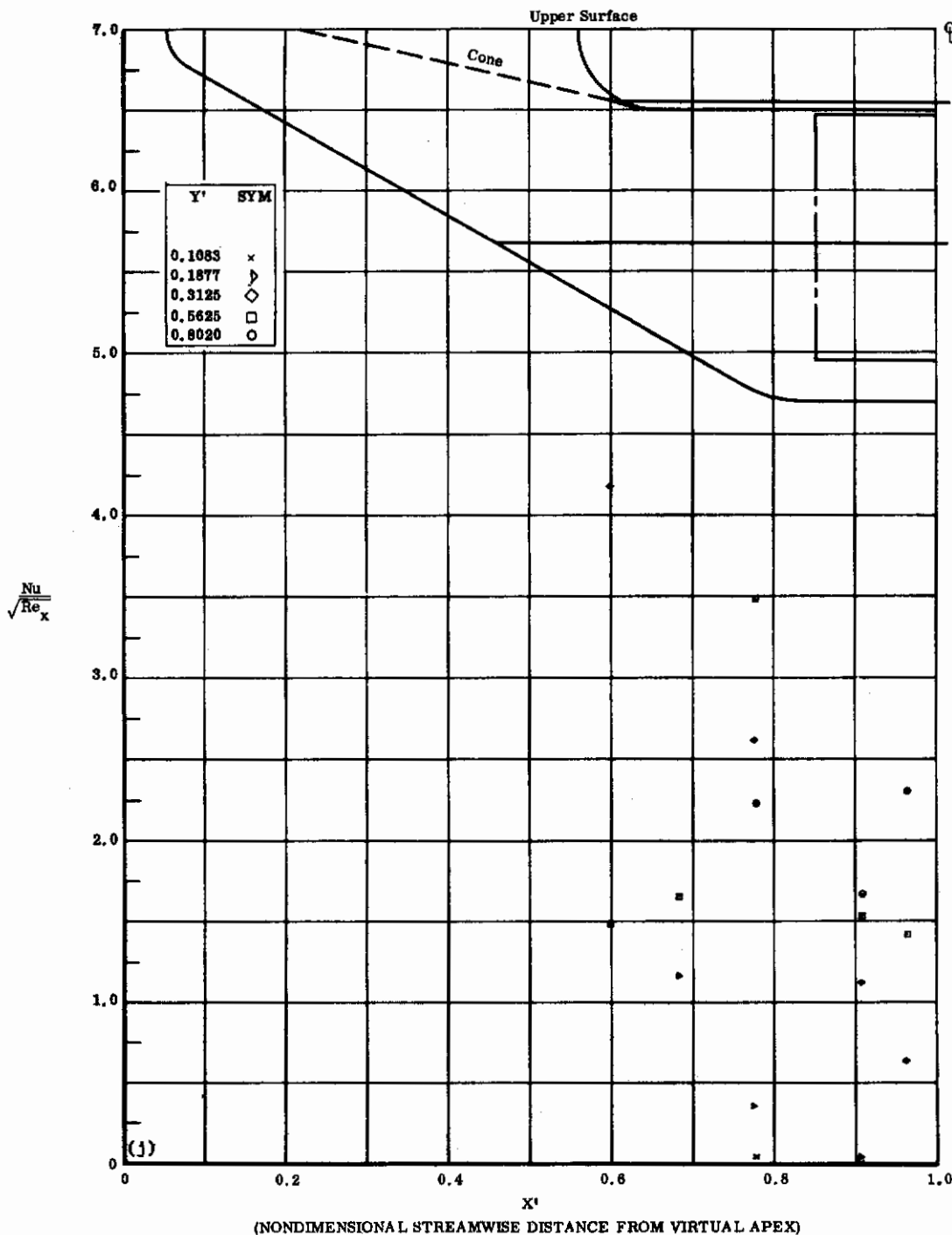


Fig. 12j Configuration I, $\alpha = -20$, $b_2 = b_3 = +10$
 $Nu/\sqrt{Re_x}$ vs. X' upper surface

Contrails

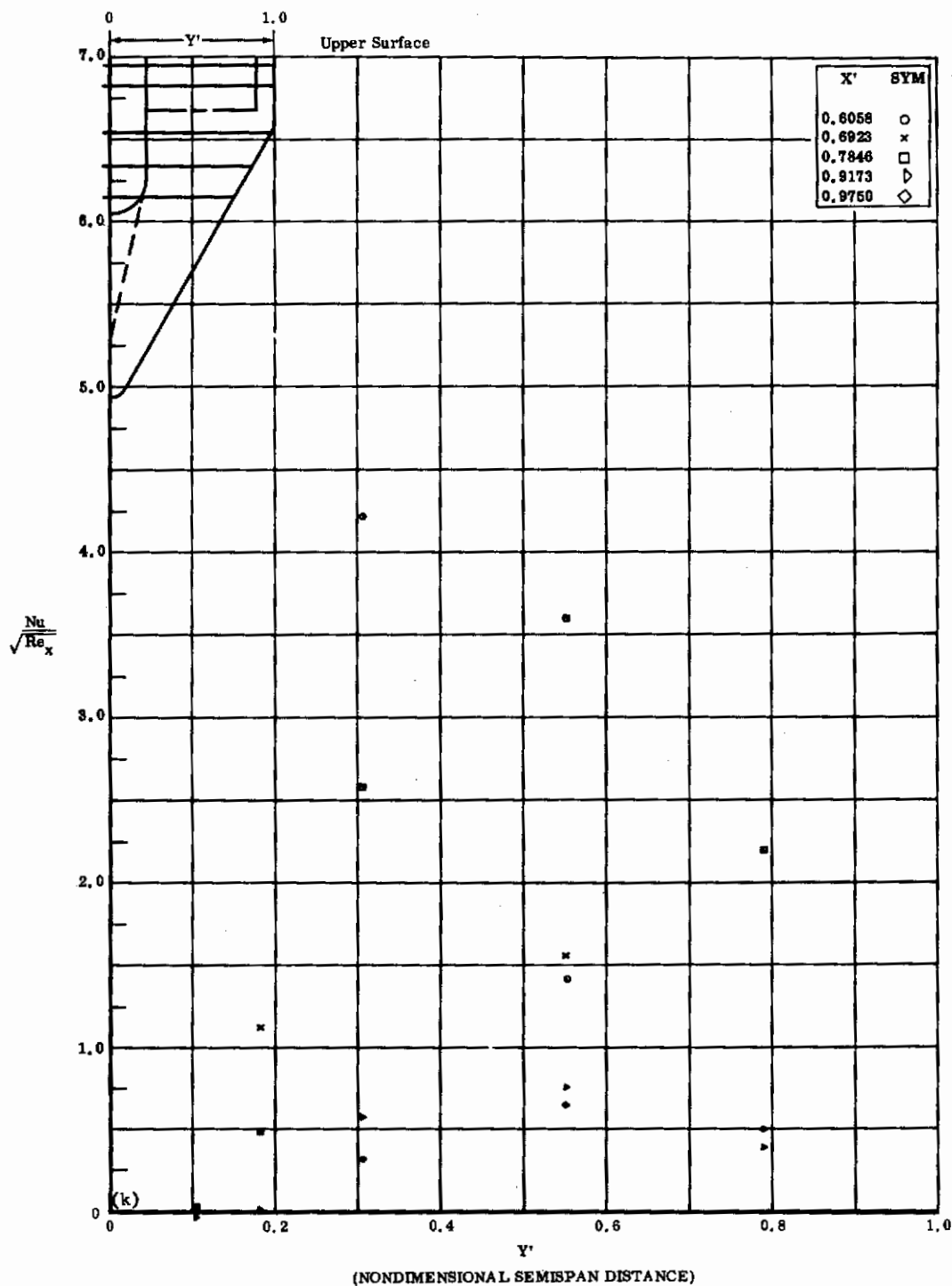


Fig. 12k Configuration I, $\alpha = -20$, $\delta_2 = \delta_3 = +20$

$\text{Nu}/\sqrt{\text{Re}_x}$ vs. Y' upper surface

Contrails

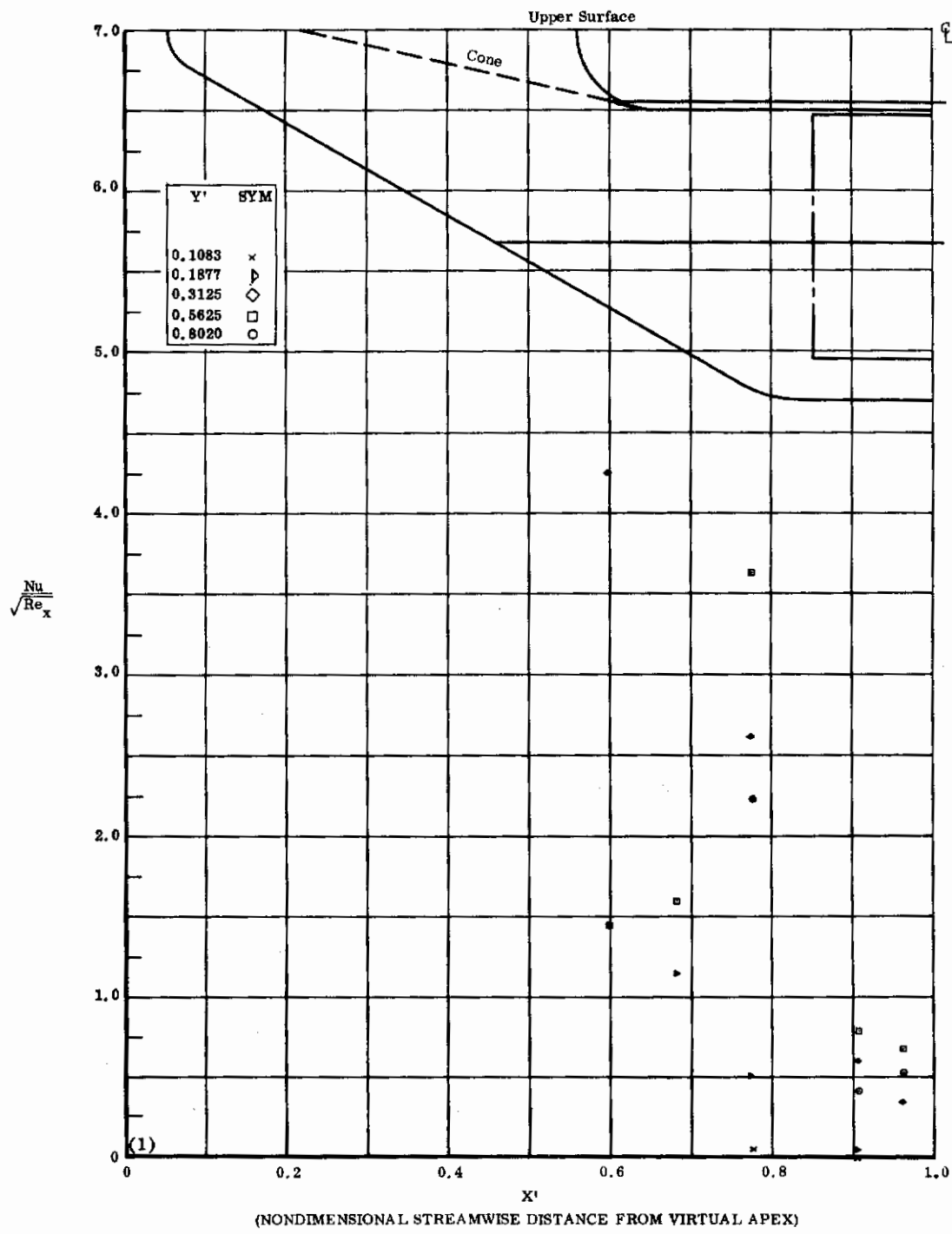


Fig. 12*f* Configuration I, $\alpha = -20$, $\delta_2 = \delta_3 = +20$
 $Nu/\sqrt{Re_x}$ vs. X' upper surface

Contrails

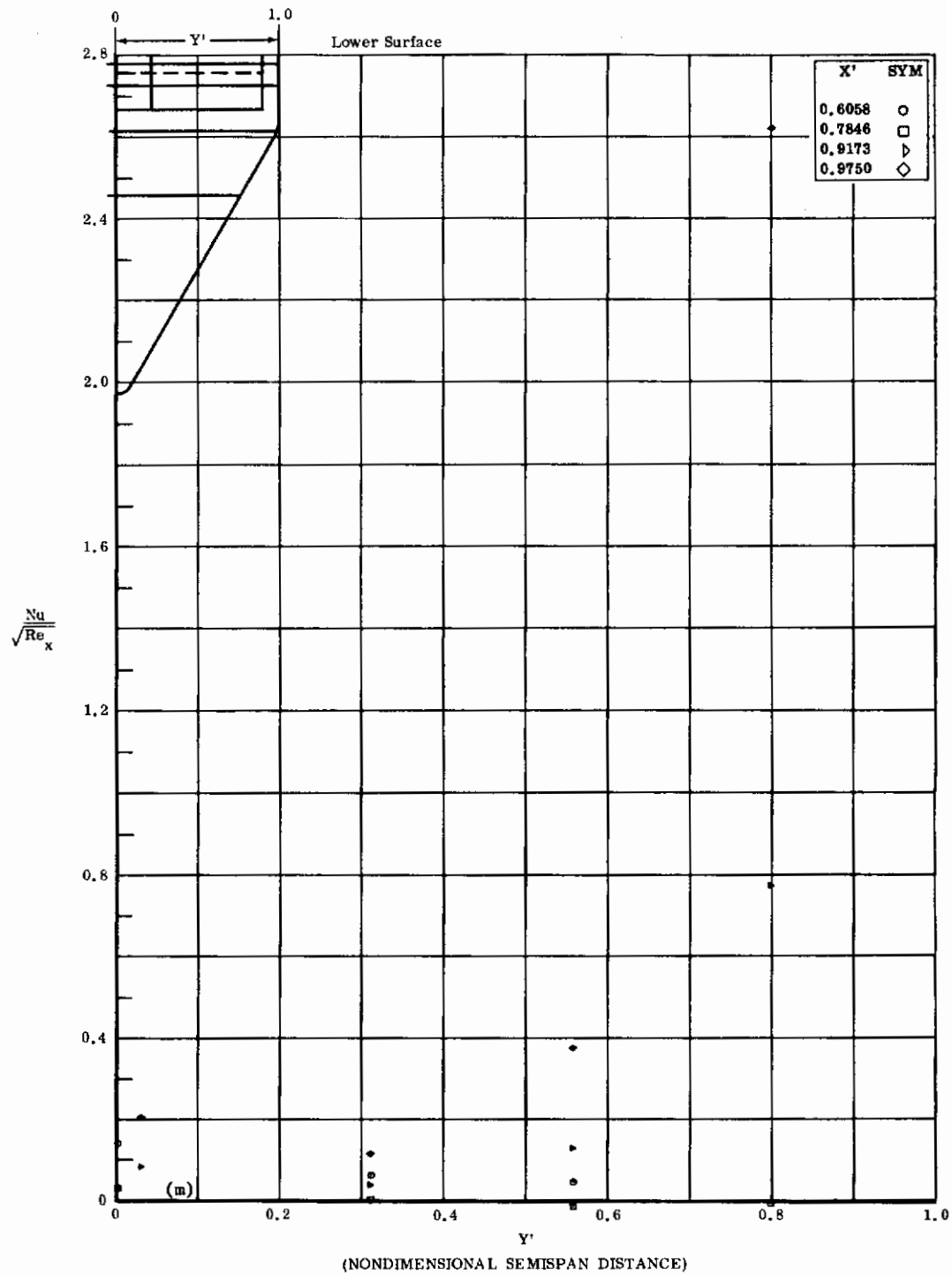


Fig. 12m Configuration I, $\alpha = -20$, $s_2 = s_3 = +30$

$Nu/\sqrt{Re_x}$ vs. Y' lower surface

Contrails

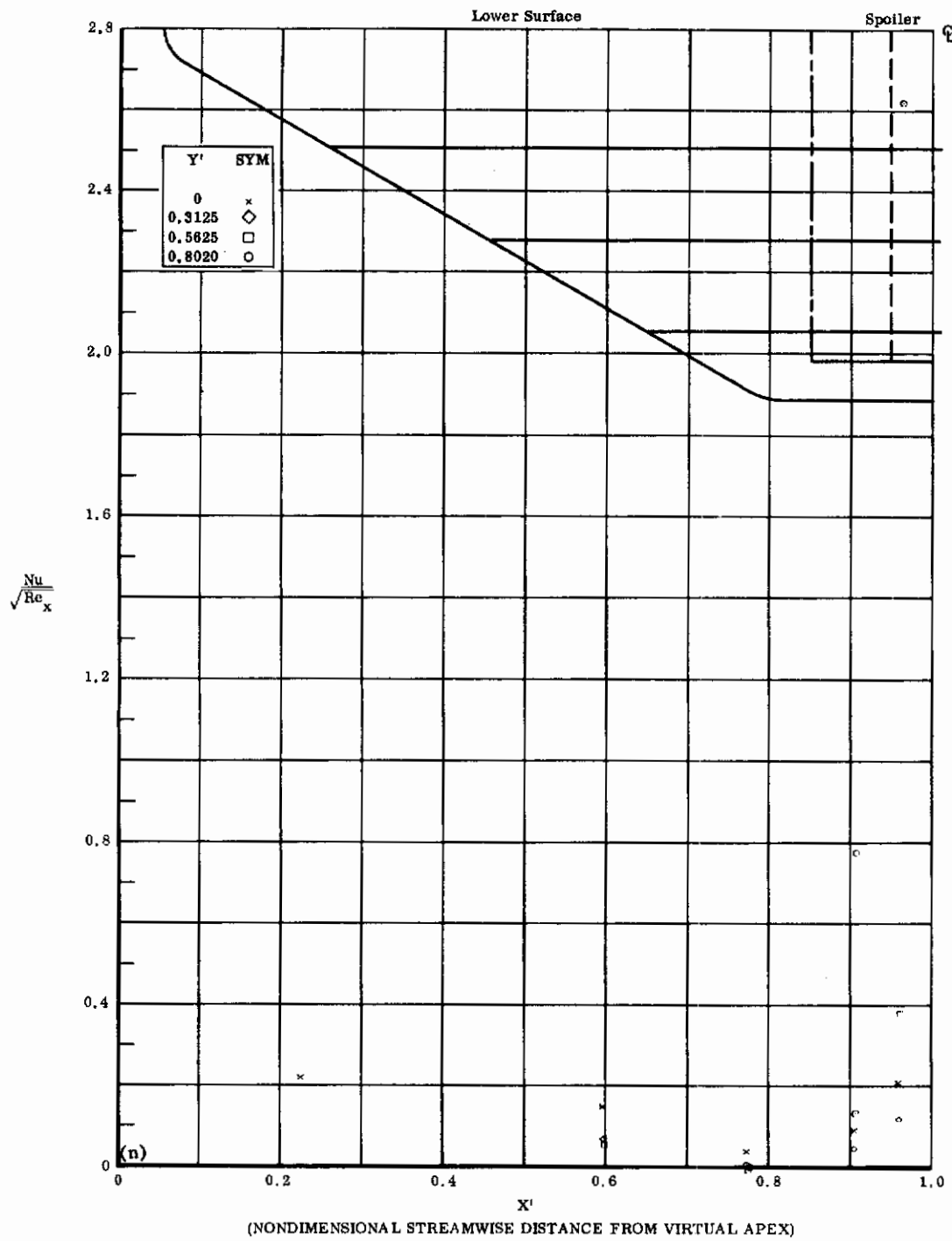


Fig. 12n Configuration I, $\alpha = -20$, $\delta_2 = \delta_3 = +30$
 $Nu/\sqrt{Re_x}$ vs. X' lower surface

Contrails

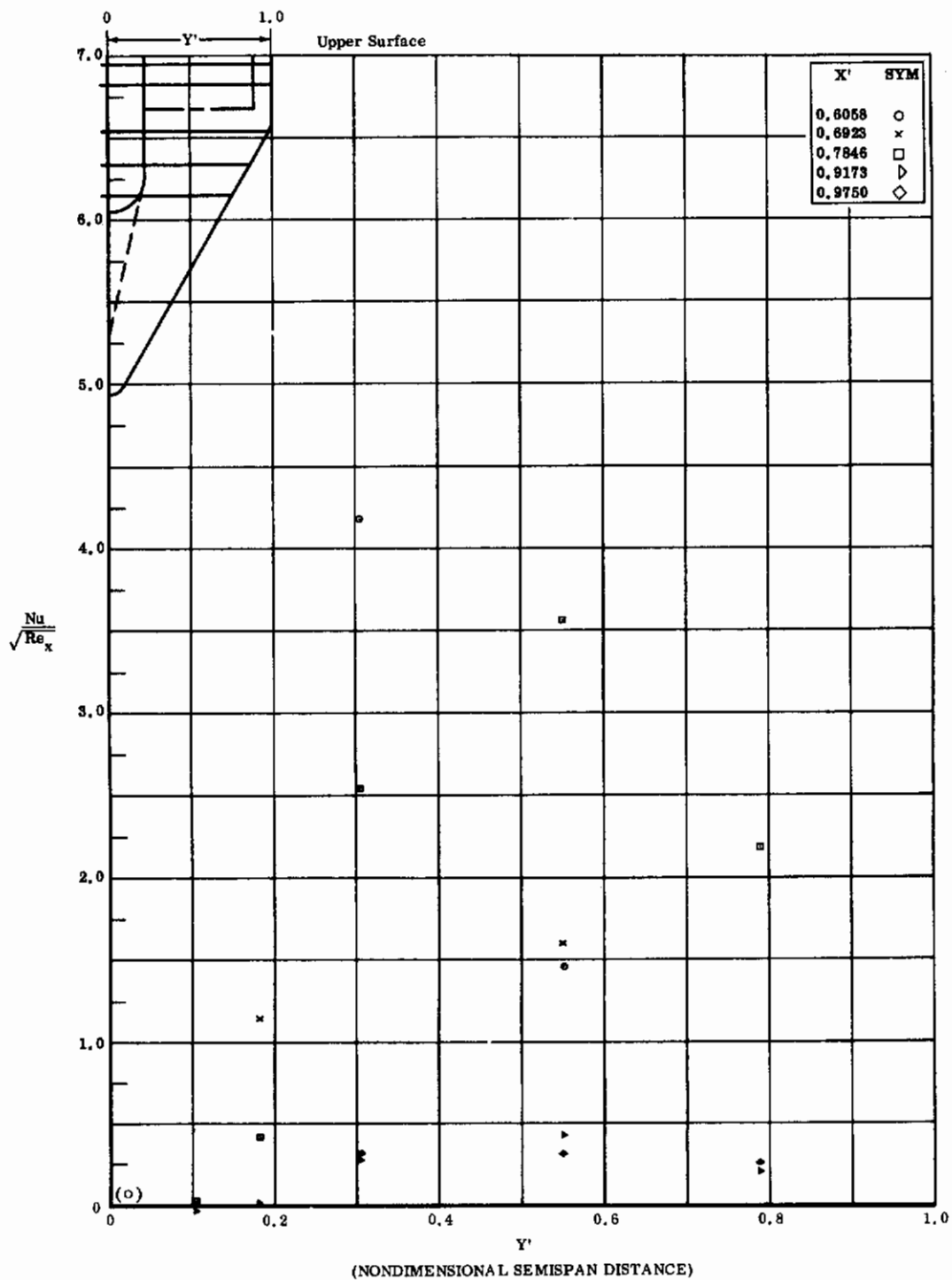


Fig. 12o Configuration I, $\alpha = -20$, $\delta_2 = \delta_3 = +30$
 $Nu/\sqrt{Re_x}$ vs. Y' upper surface

Contrails

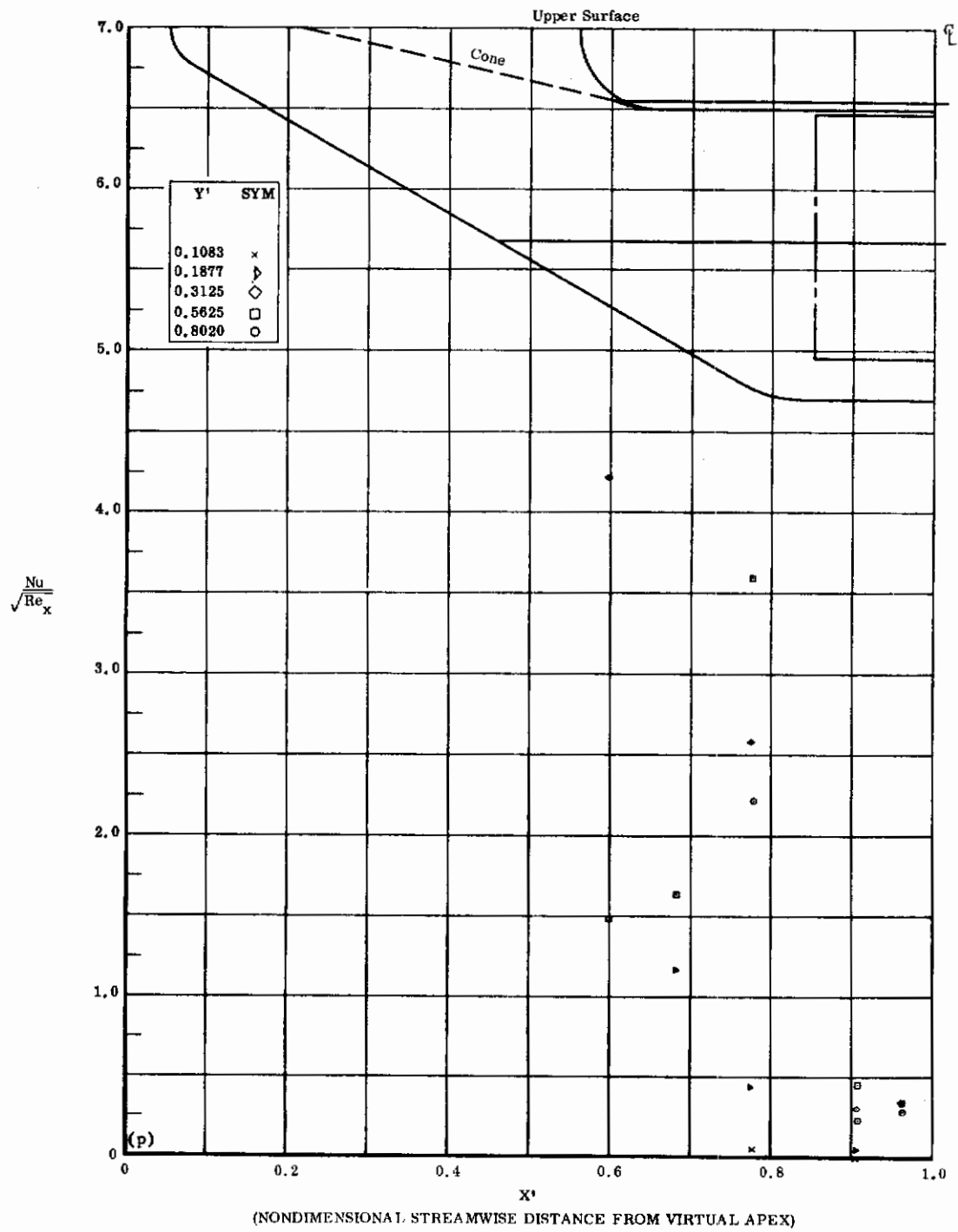


Fig. 12p Configuration I, $\alpha = -20$, $\delta_2 = \delta_3 = +30$

$\text{Nu}/\sqrt{\text{Re}_x}$ vs. X' upper surface

Contrails

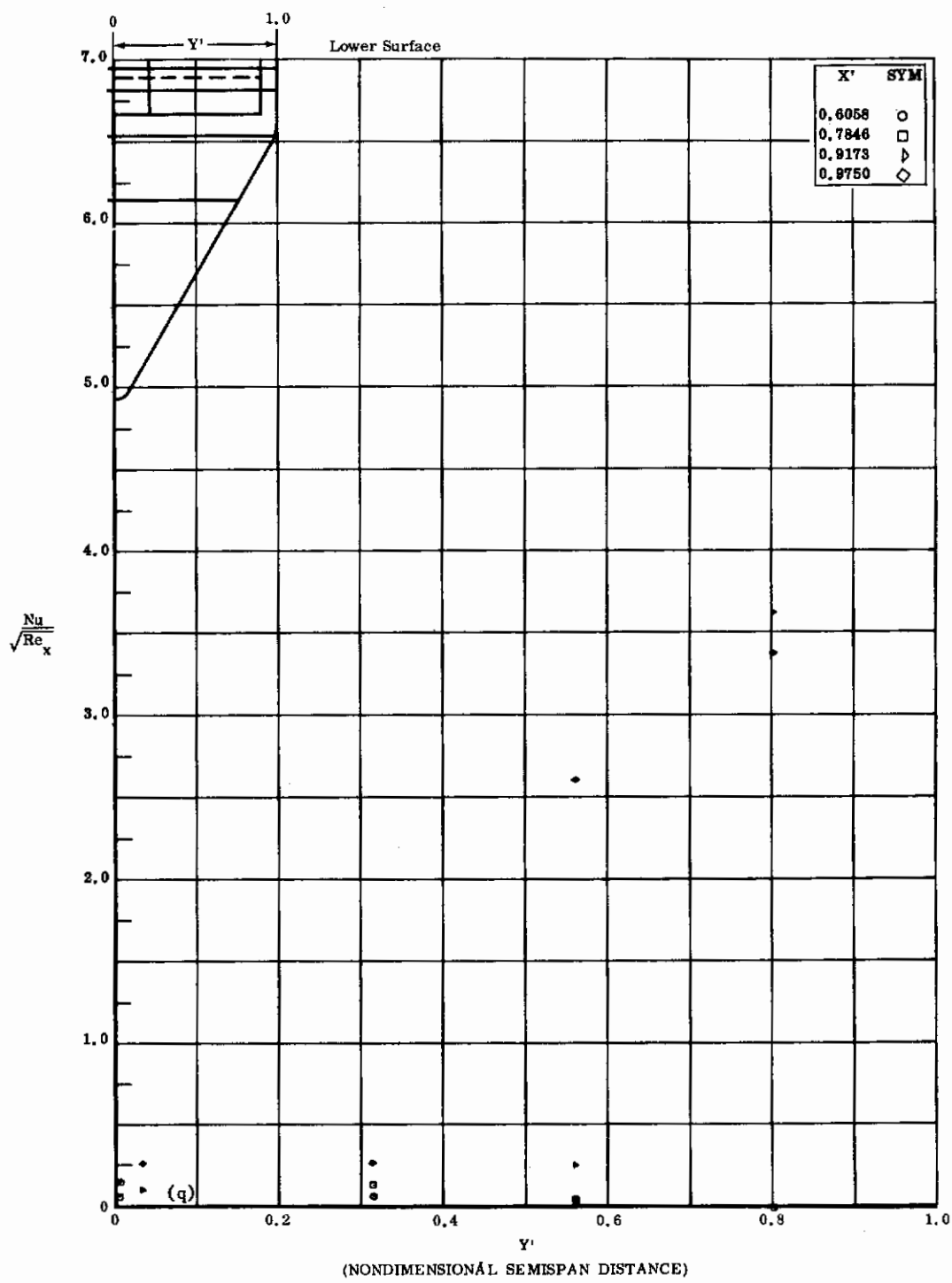


Fig. 12q Configuration I, $\alpha = -20$, $\delta_2 = \delta_3 = +39$
 $Nu/\sqrt{Re_x}$ vs. Y' lower surface

Contrails

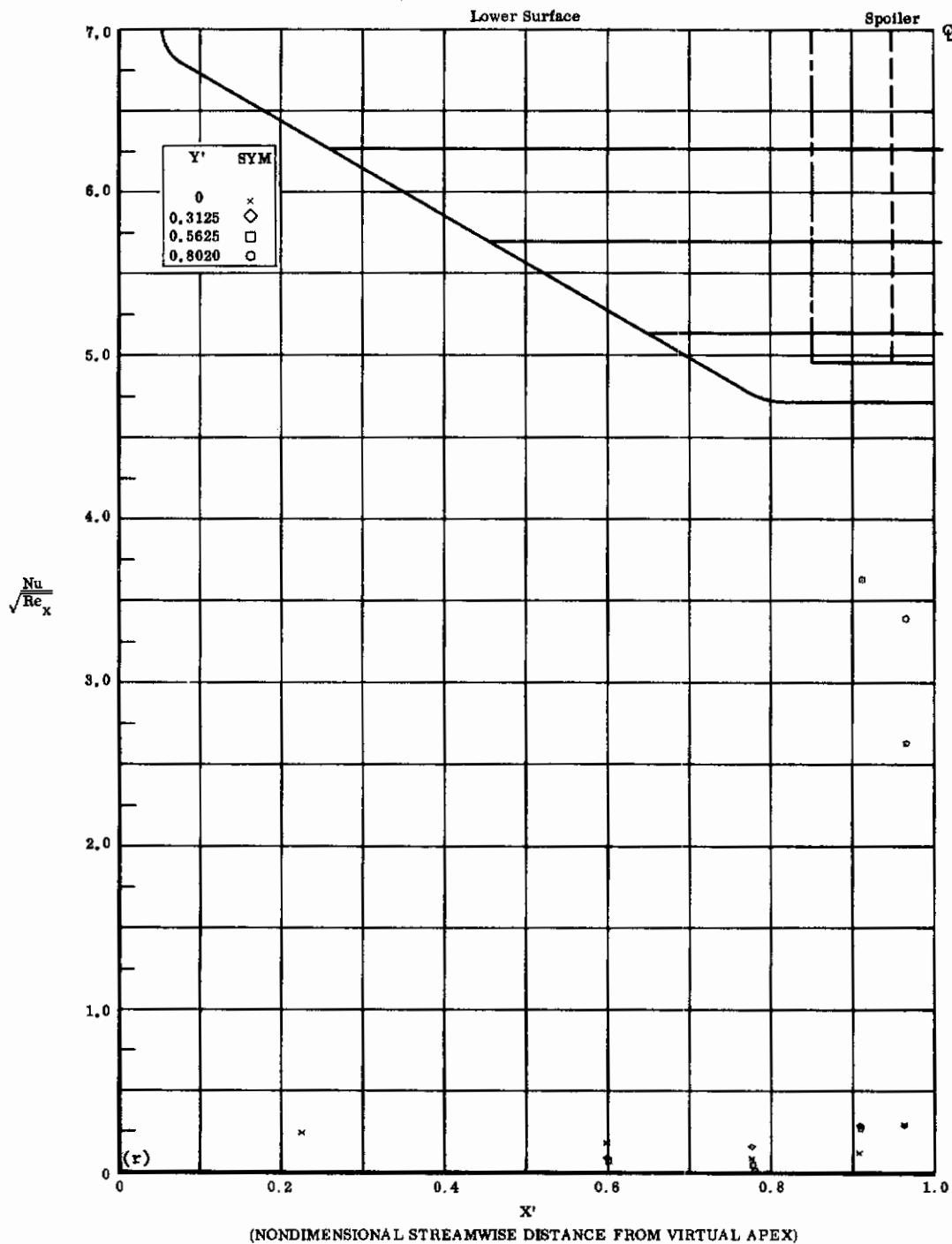


Fig. 12r Configuration I, $\alpha = -20$, $\delta_2 = \delta_3 = +39$
 $Nu/\sqrt{Re_x}$ vs. X' lower surface

Contrails

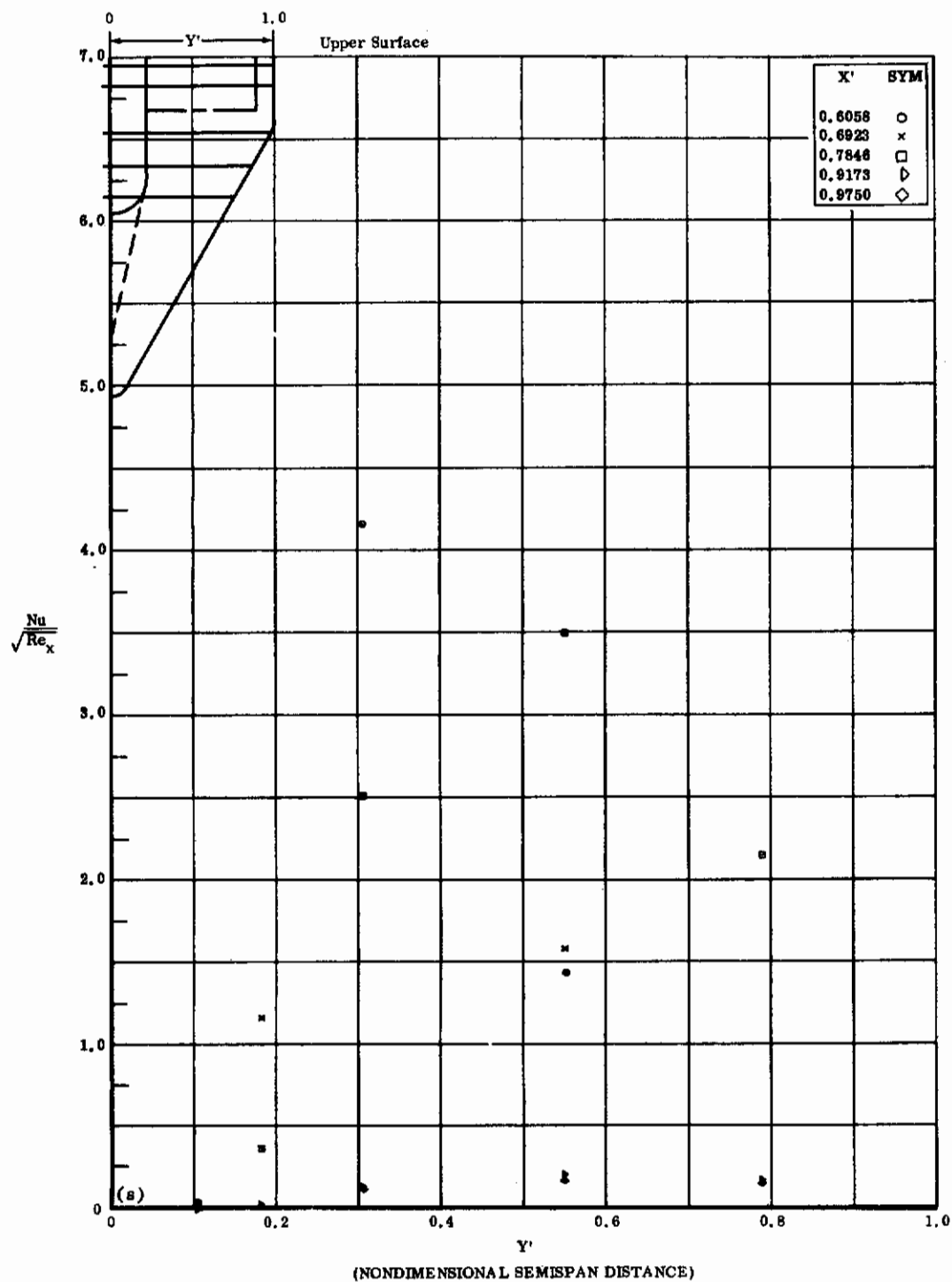


Fig. 12s Configuration I, $\alpha = -20$, $\delta_2 = \delta_3 = +39$
 $\frac{Nu}{\sqrt{Re_x}}$ vs. Y' upper surface

Contrails

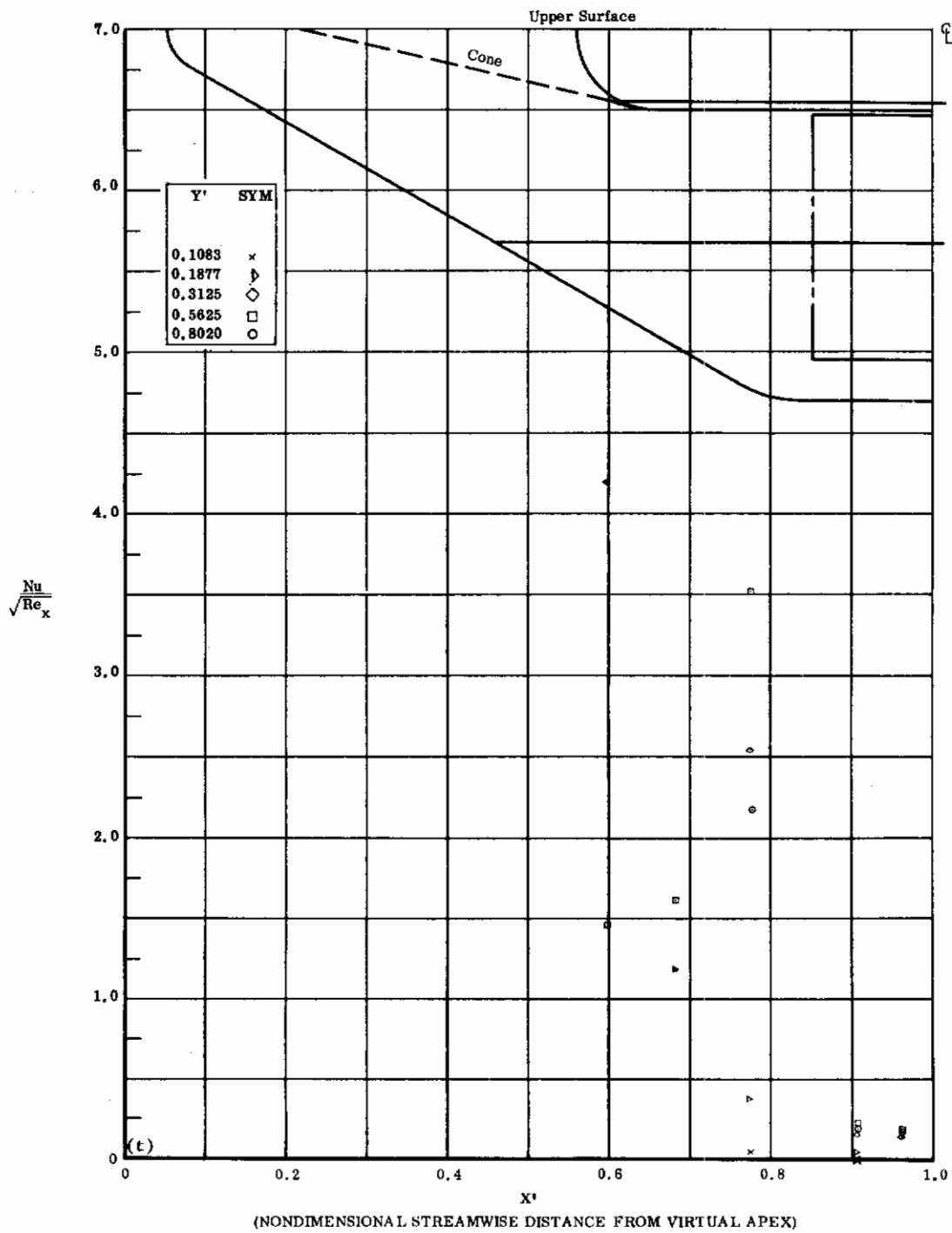
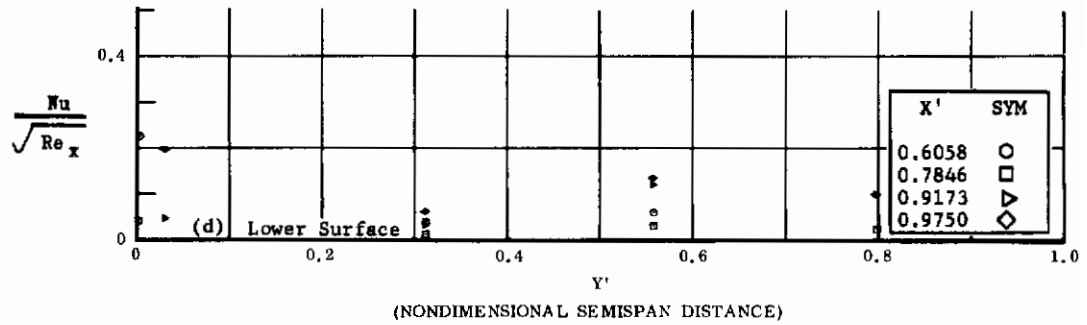
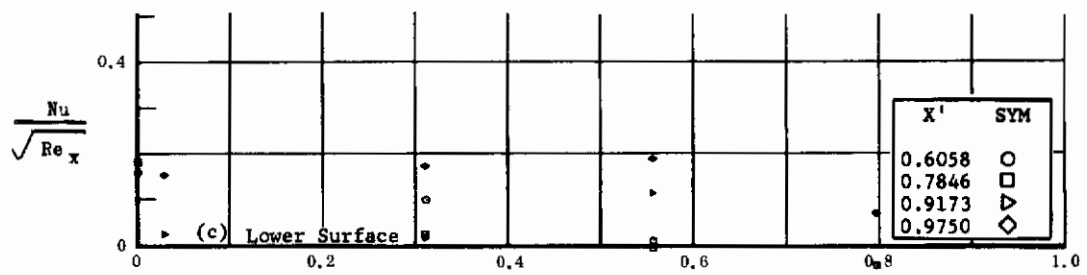
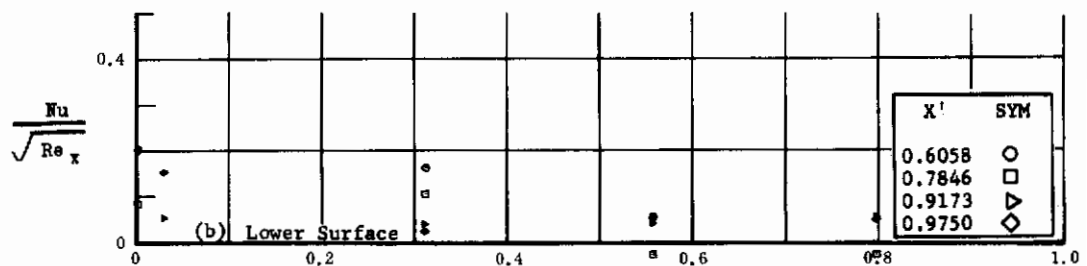
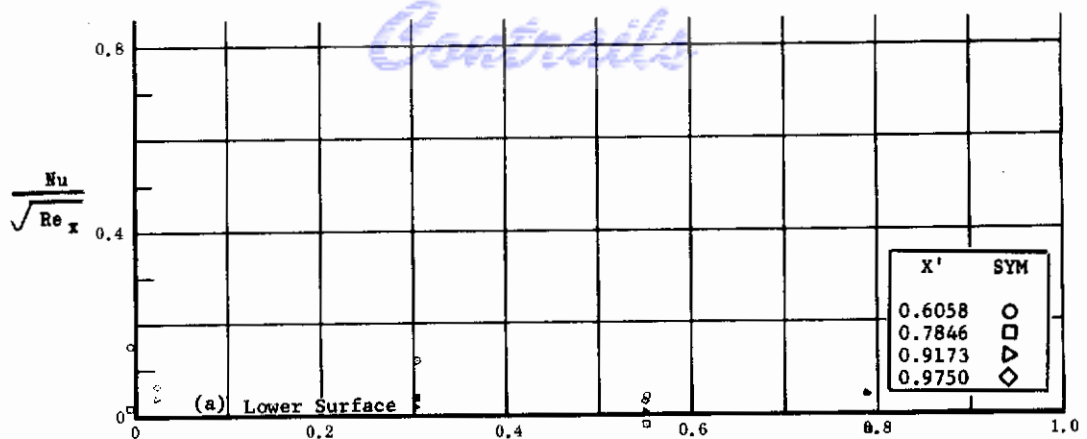


Fig. 12t Configuration I, $\alpha = -20$, $\delta_2 = \delta_3 = +39$

$Nu/\sqrt{Re_x}$ vs. X' upper surface



(NONDIMENSIONAL SEMISPAN DISTANCE)

Fig. 13 Configuration I, $\alpha = -20$, $Nu/\sqrt{Re_x}$ vs. Y' , lower surface

a) $\delta_2 = \delta_3 = -10$

b) $\delta_2 = \delta_3 = -20$

c) $\delta_2 = \delta_3 = -30$

d) $\delta_2 = \delta_3 = -39$

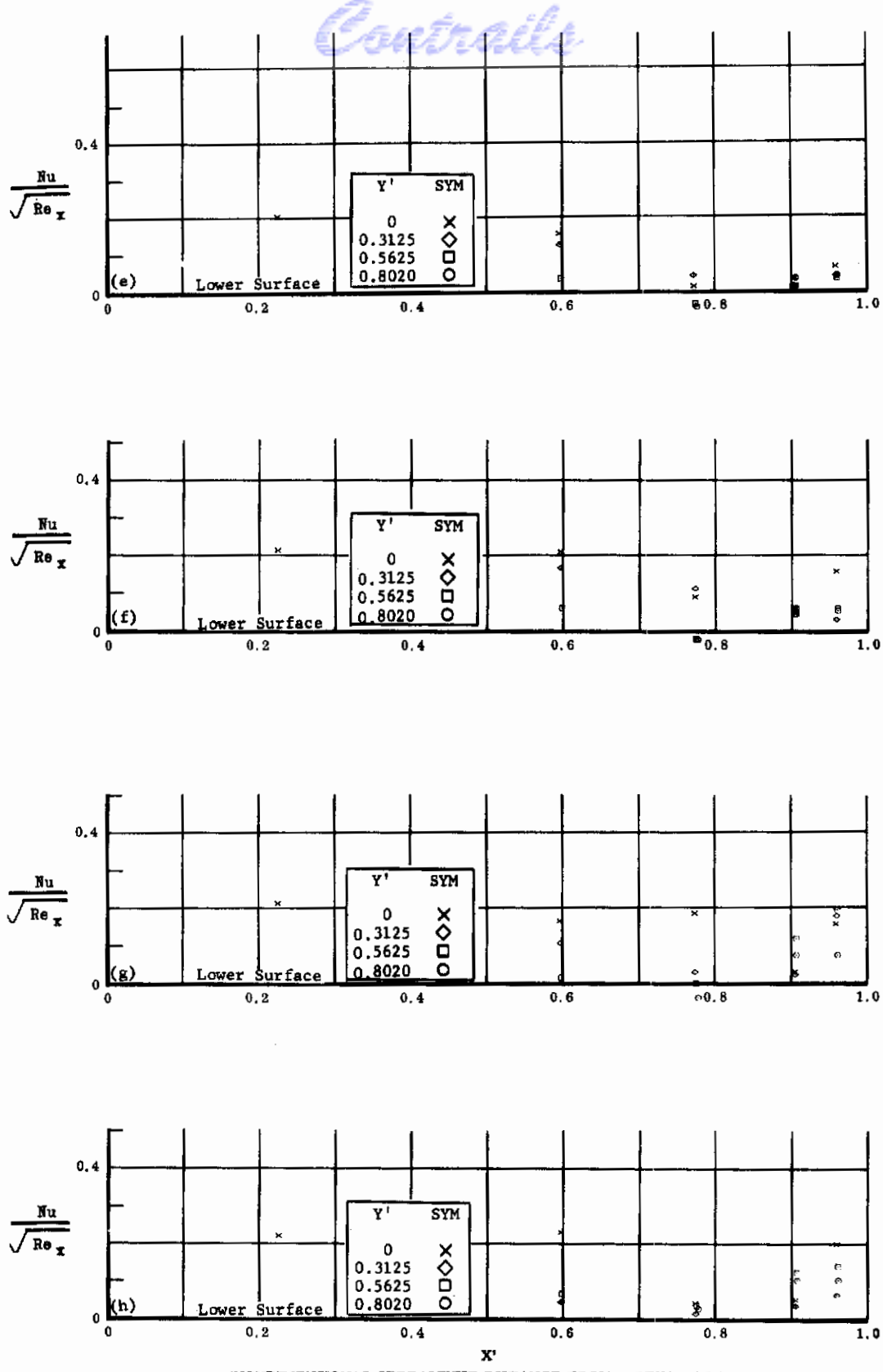


Fig. 13 Configuration I, $\alpha = -20$, $Nu/\sqrt{Re_x}$ vs. X' , lower surface

e) $\delta_2 = \delta_3 = -10$

f) $\delta_2 = \delta_3 = -20$

g) $\delta_2 = \delta_3 = -30$

h) $\delta_2 = \delta_3 = -39$

Contrails

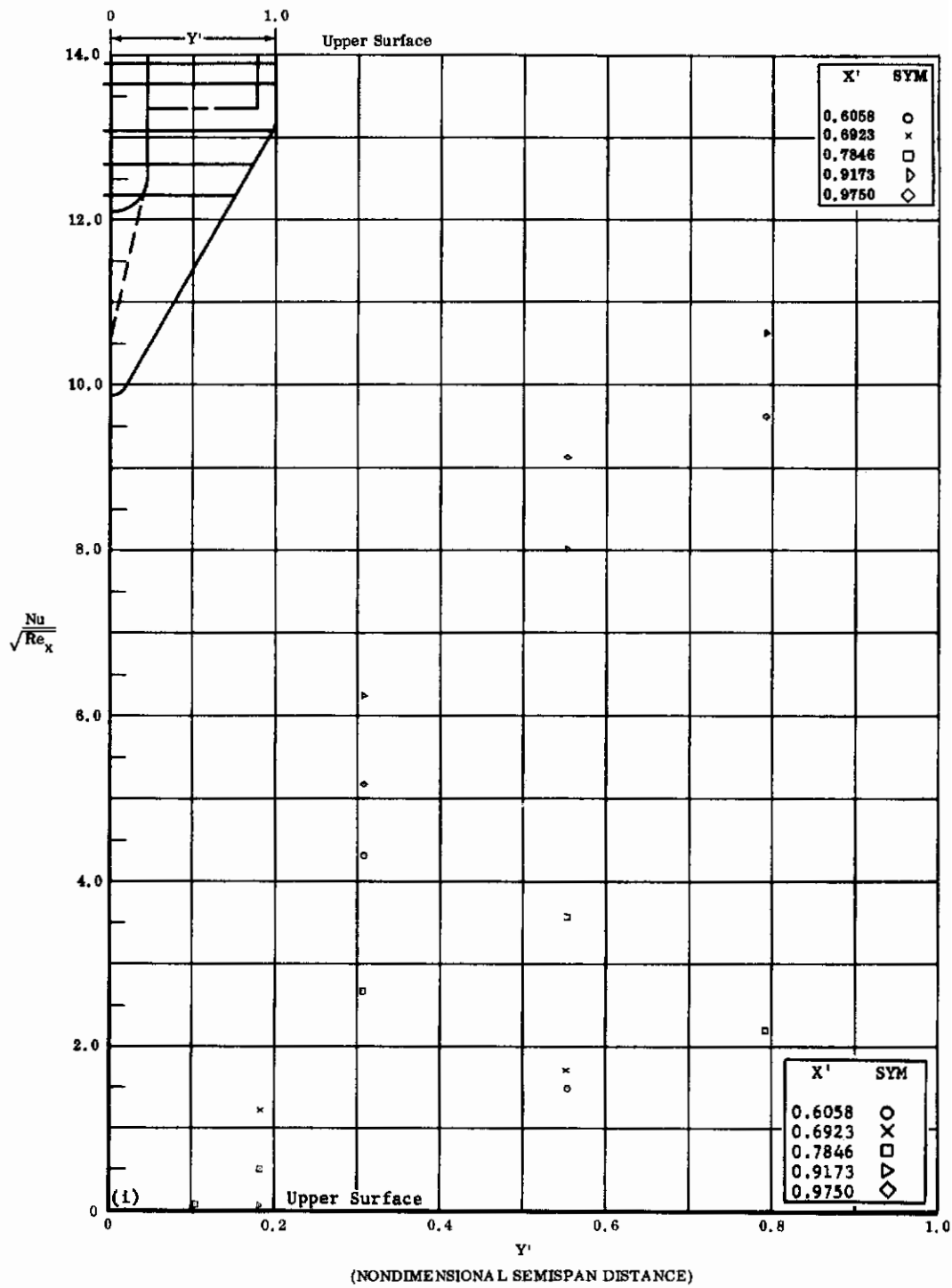


Fig. 131 Configuration I, $\alpha = -20$, $\delta_2 = \delta_3 = -10$
 $Nu/\sqrt{Re_x}$ vs. Y' upper surface

Contrails

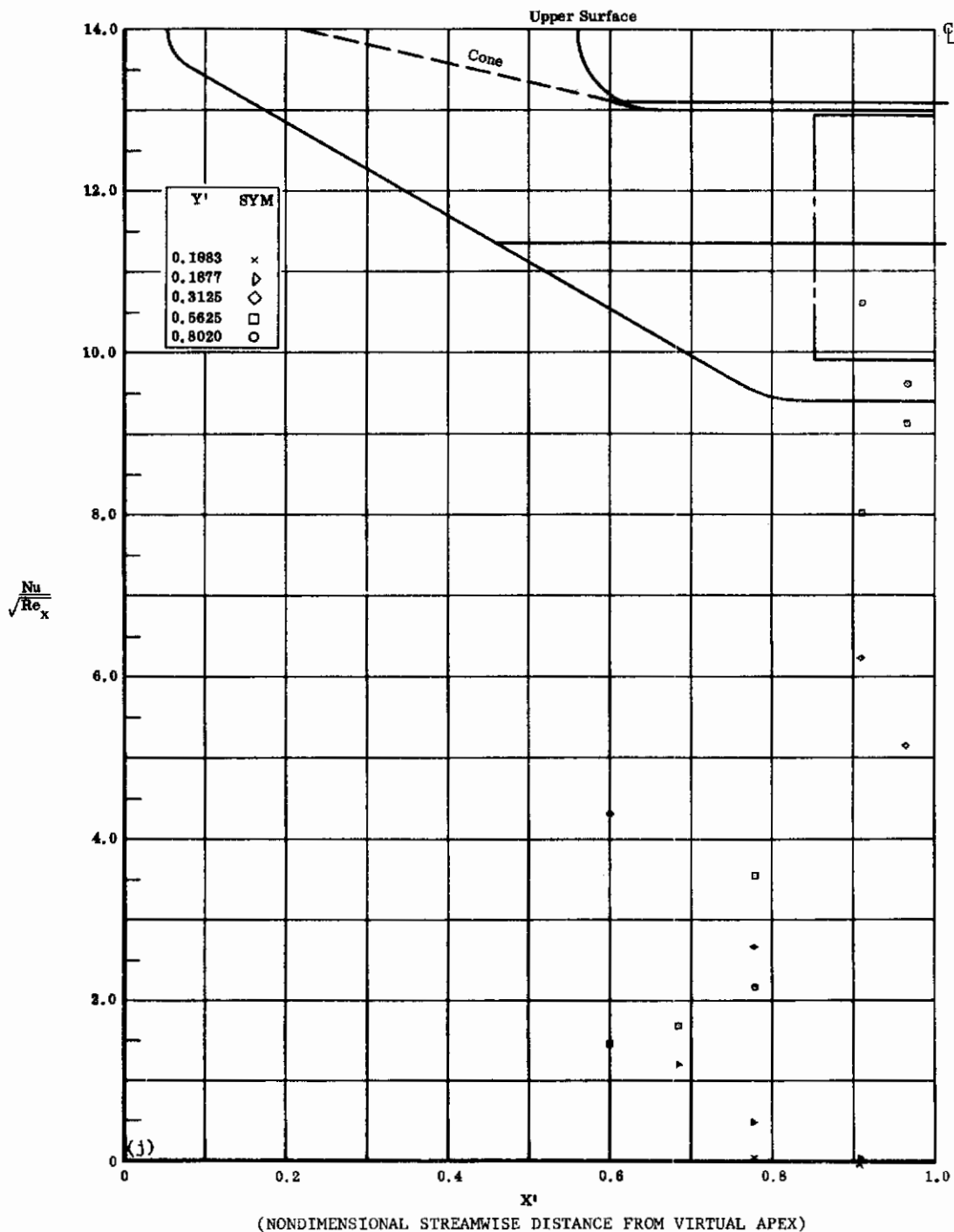


Fig. 13j Configuration I, $\alpha = -20$, $\delta_2 = \delta_3 = -10$

$Nu/\sqrt{Re_x}$ vs. X' upper surface

Contrails

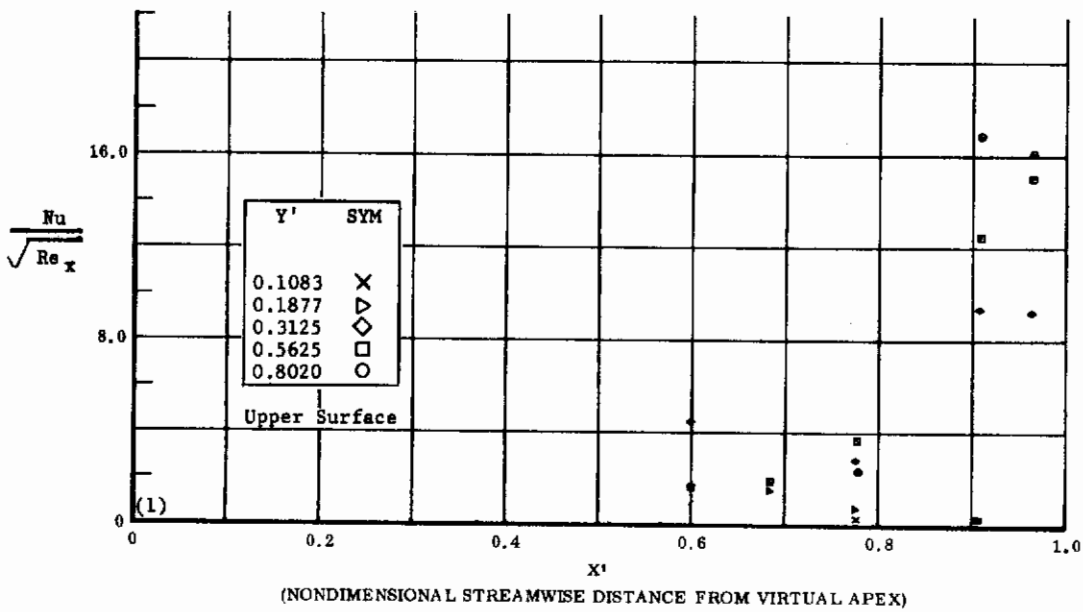
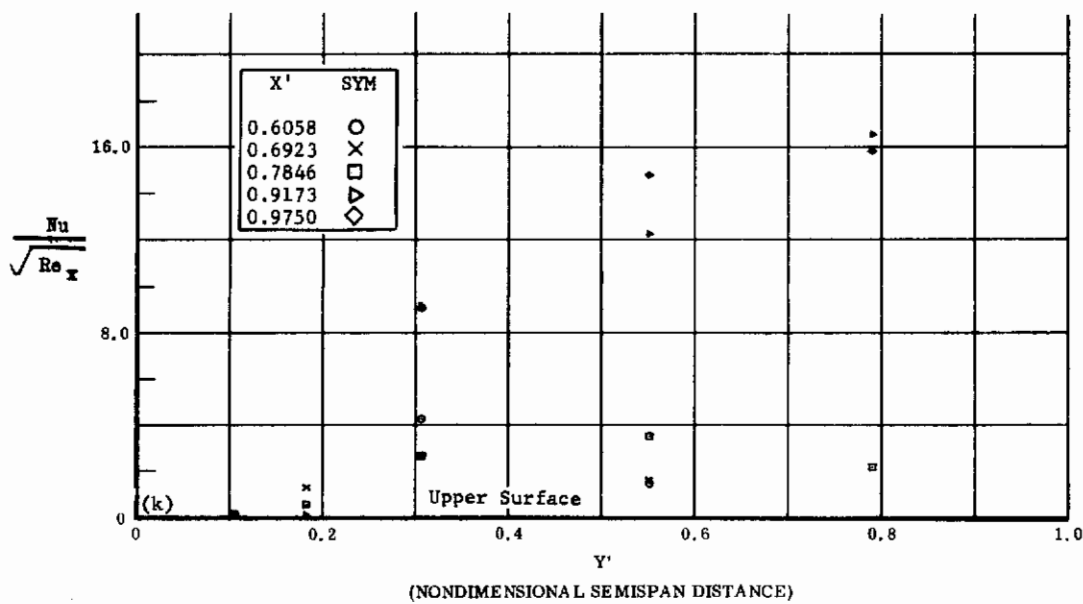


Fig. 13 Configuration I, $\alpha = -20$, $\delta_2 = \delta_3 = -20$

k) $Nu/\sqrt{Re_x}$ vs. Y' upper surface

l) $Nu/\sqrt{Re_x}$ vs. X' upper surface

Contrails

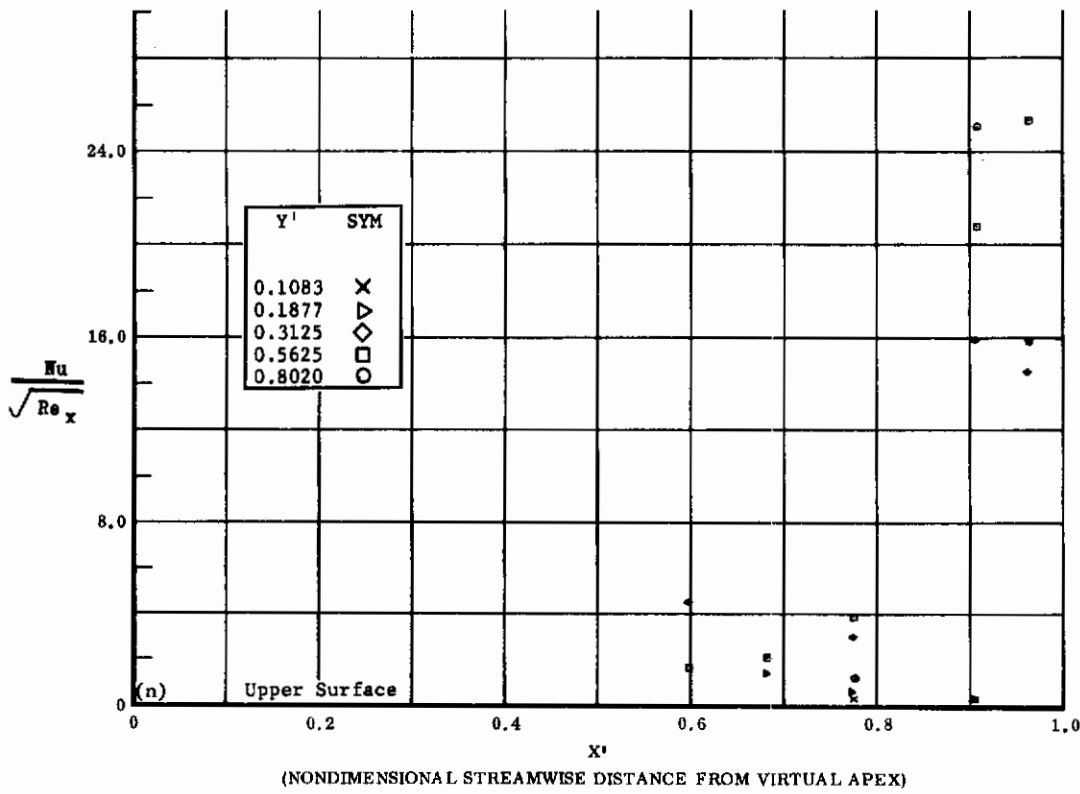
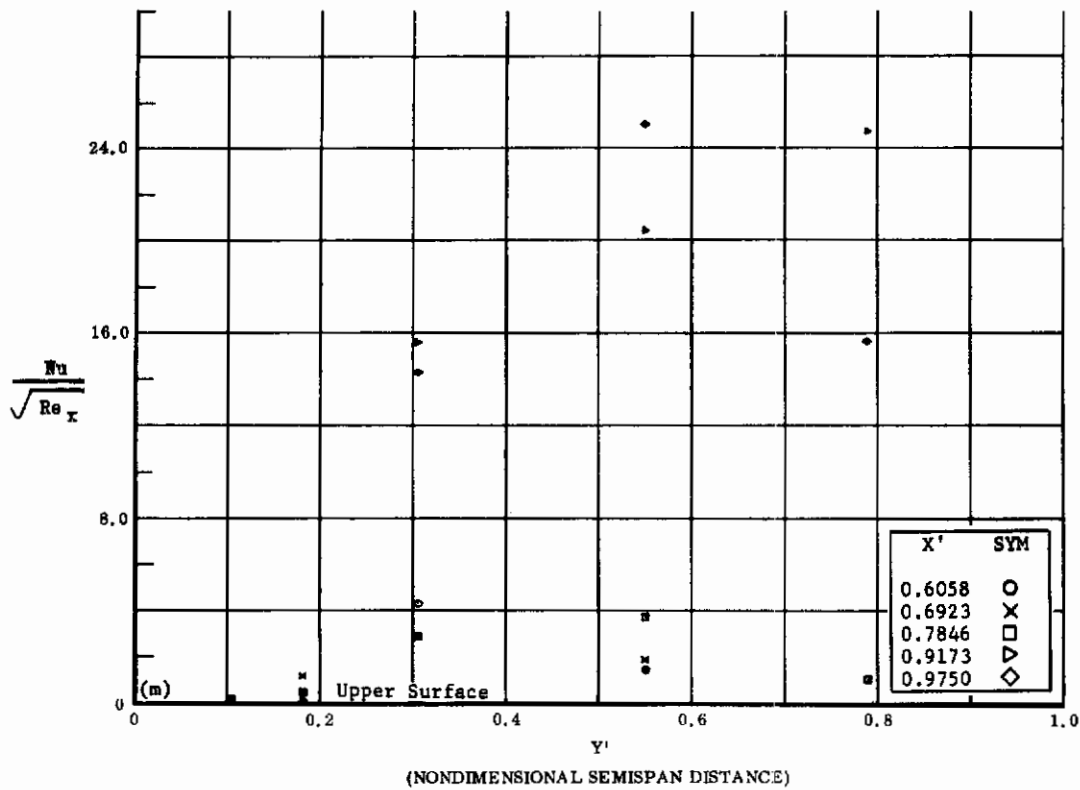


Fig. 13 Configuration I, $\alpha = -20$, $\delta_2 = \delta_3 = -30$

m) $Nu/\sqrt{Re_x}$ vs. Y' upper surface

n) $Nu/\sqrt{Re_x}$ vs. X' upper surface

Contrails

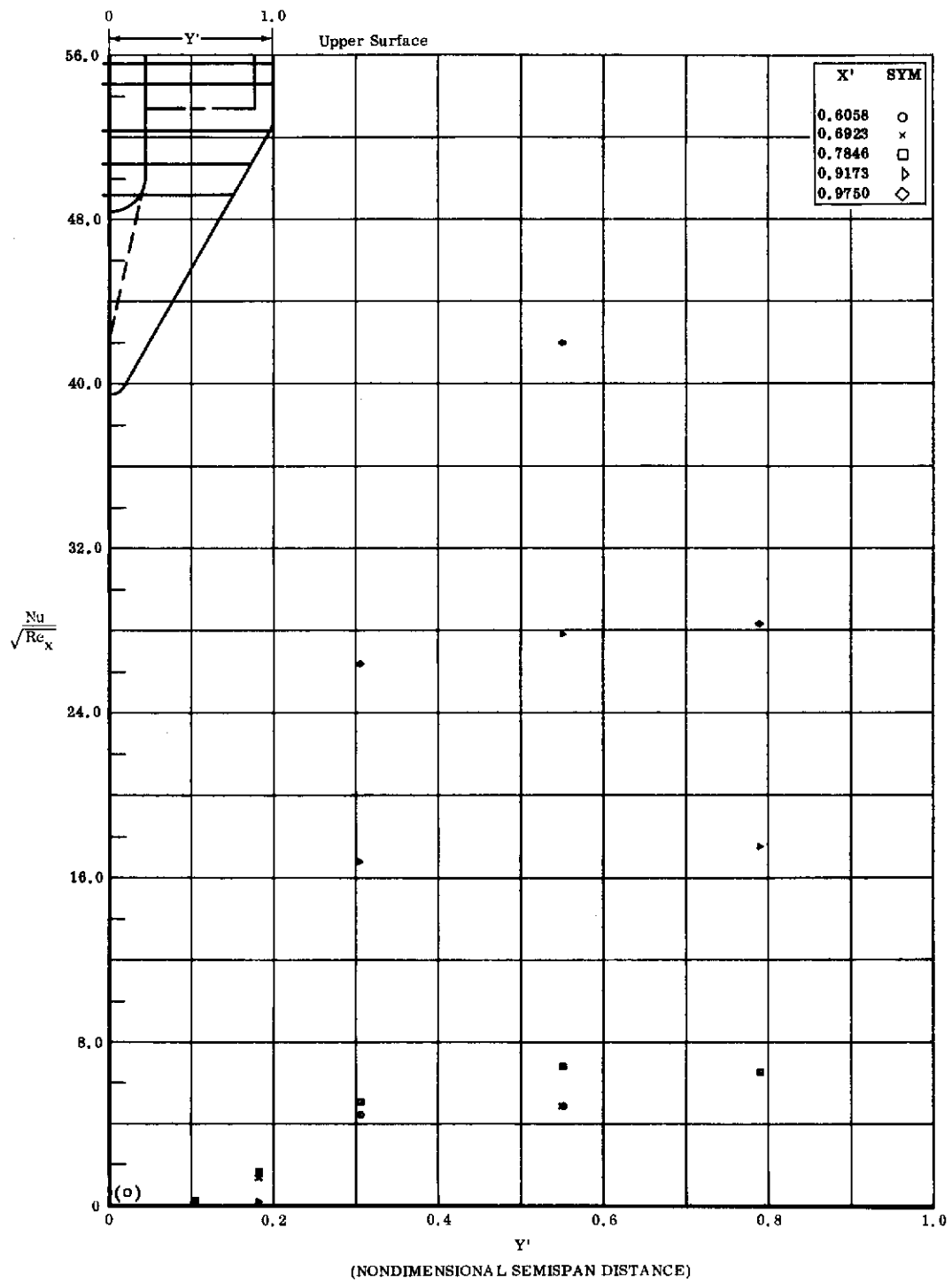


Fig. 13o Configuration I, $\alpha = -20$, $\delta_2 = \delta_3 = -39$
 $Nu/\sqrt{Re_x}$ vs. Y' upper surface

Contrails

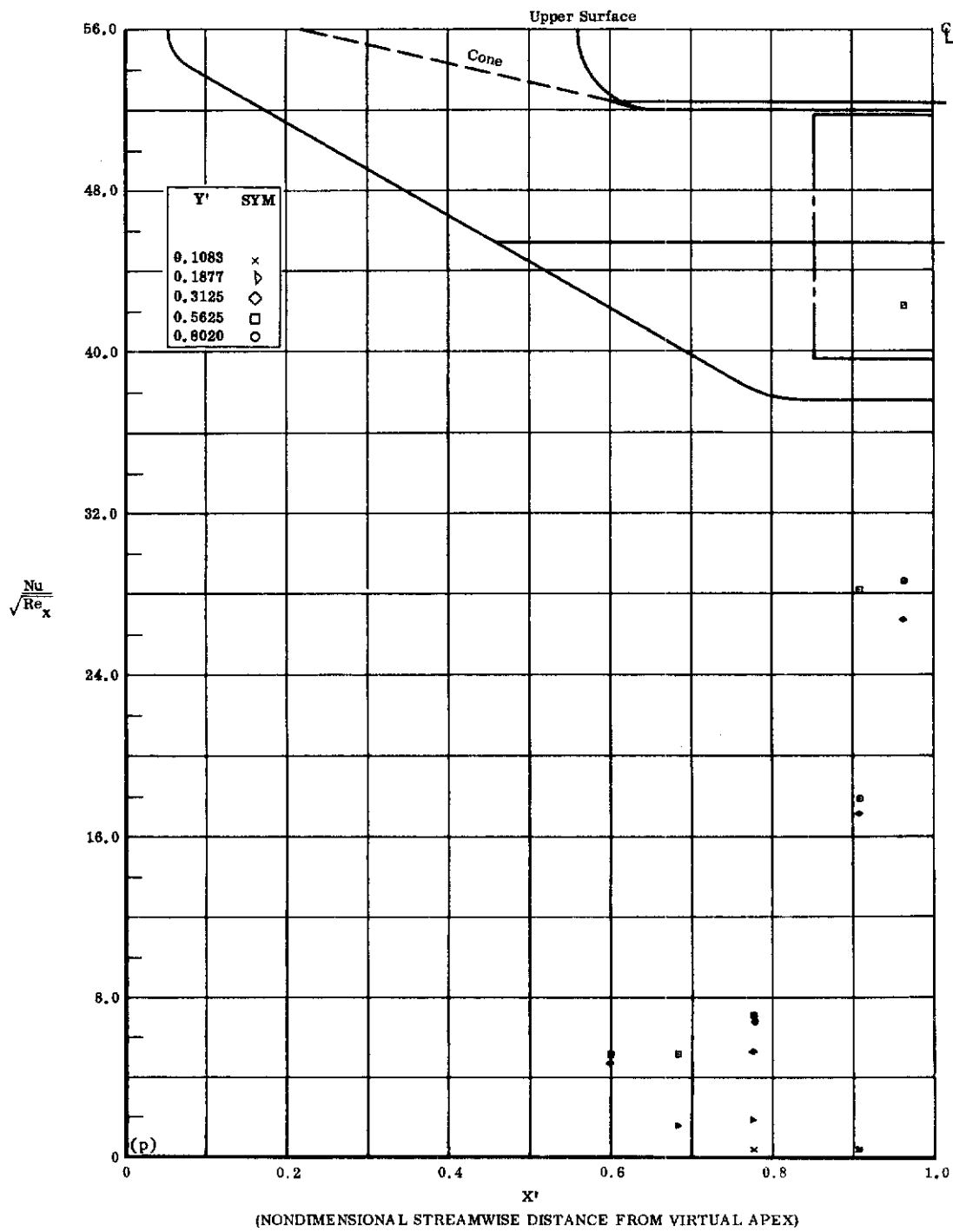


Fig. 13p Configuration I, $\alpha = -20$, $\delta_2 = \delta_3 = -39$

$\text{Nu}/\sqrt{\text{Re}_x}$ vs. X' upper surface

Contrails

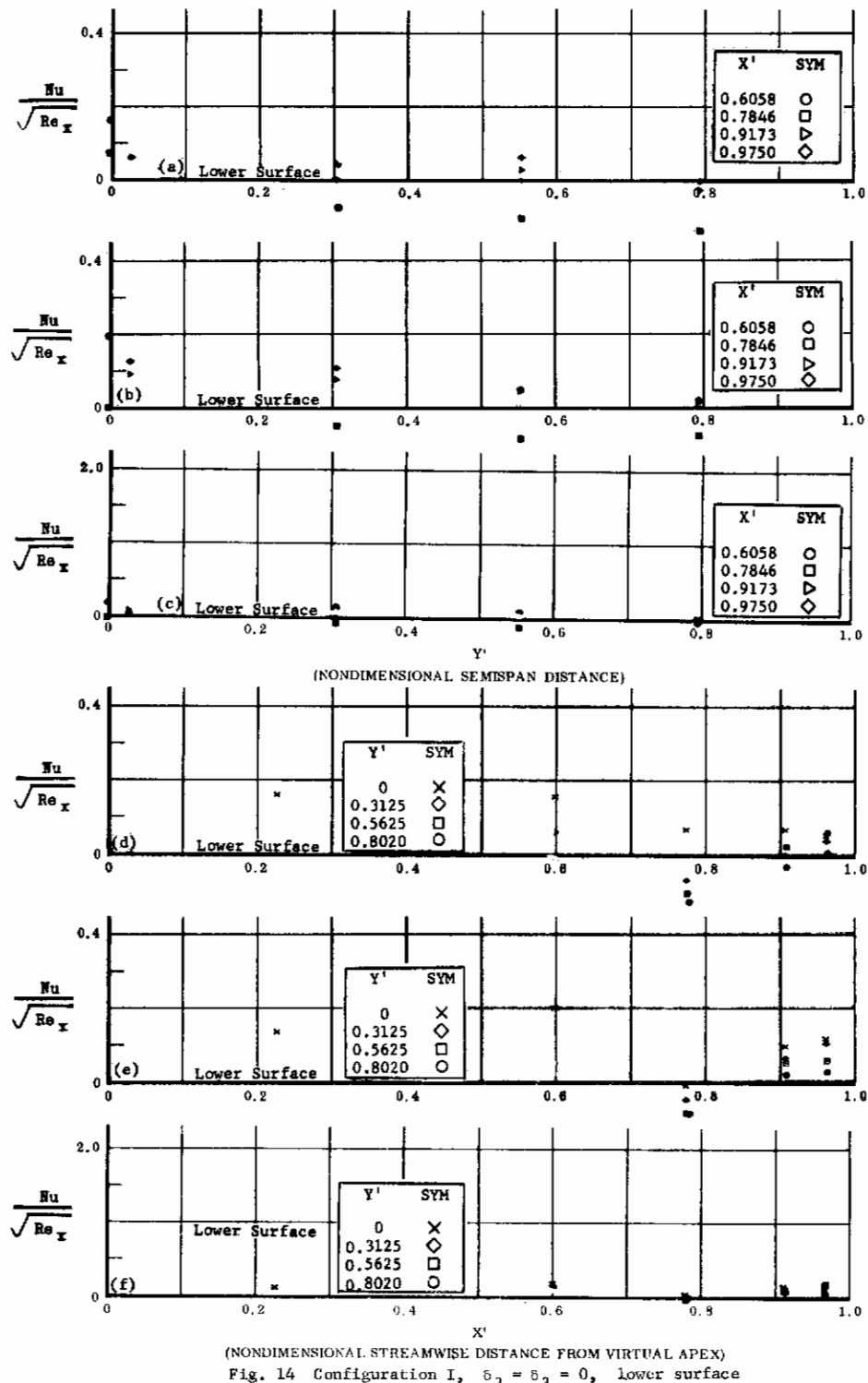


Fig. 14 Configuration I, $\delta_2 = \delta_3 = 0$, lower surface

a) $Nu/\sqrt{Re_x}$ vs. Y^1 $\alpha = -30$

b) $Nu/\sqrt{Re_x}$ vs. Y^1 $\alpha = -40$

c) $Nu/\sqrt{Re_x}$ vs. Y^1 $\alpha = -50$

d) $Nu/\sqrt{Re_x}$ vs. X^1 $\alpha = -30$

e) $Nu/\sqrt{Re_x}$ vs. X^1 $\alpha = -40$

f) $Nu/\sqrt{Re_x}$ vs. X^1 $\alpha = -50$

Contrails

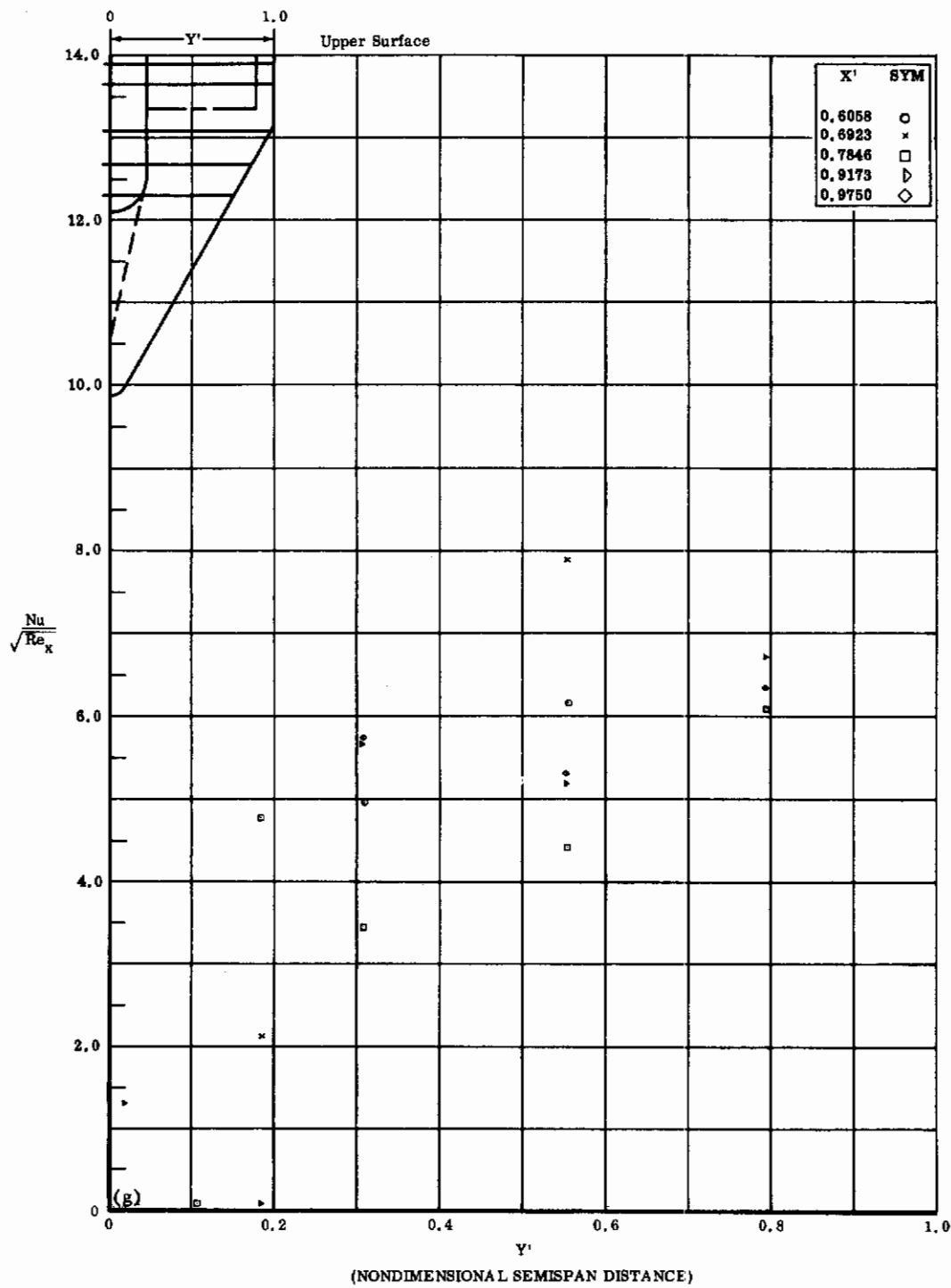


Fig. 14g Configuration I, $\alpha = -30^\circ$, $\delta_2 = \delta_3 = 0$
 $Nu/\sqrt{Re_x}$ vs. Y' upper surface

Contrails

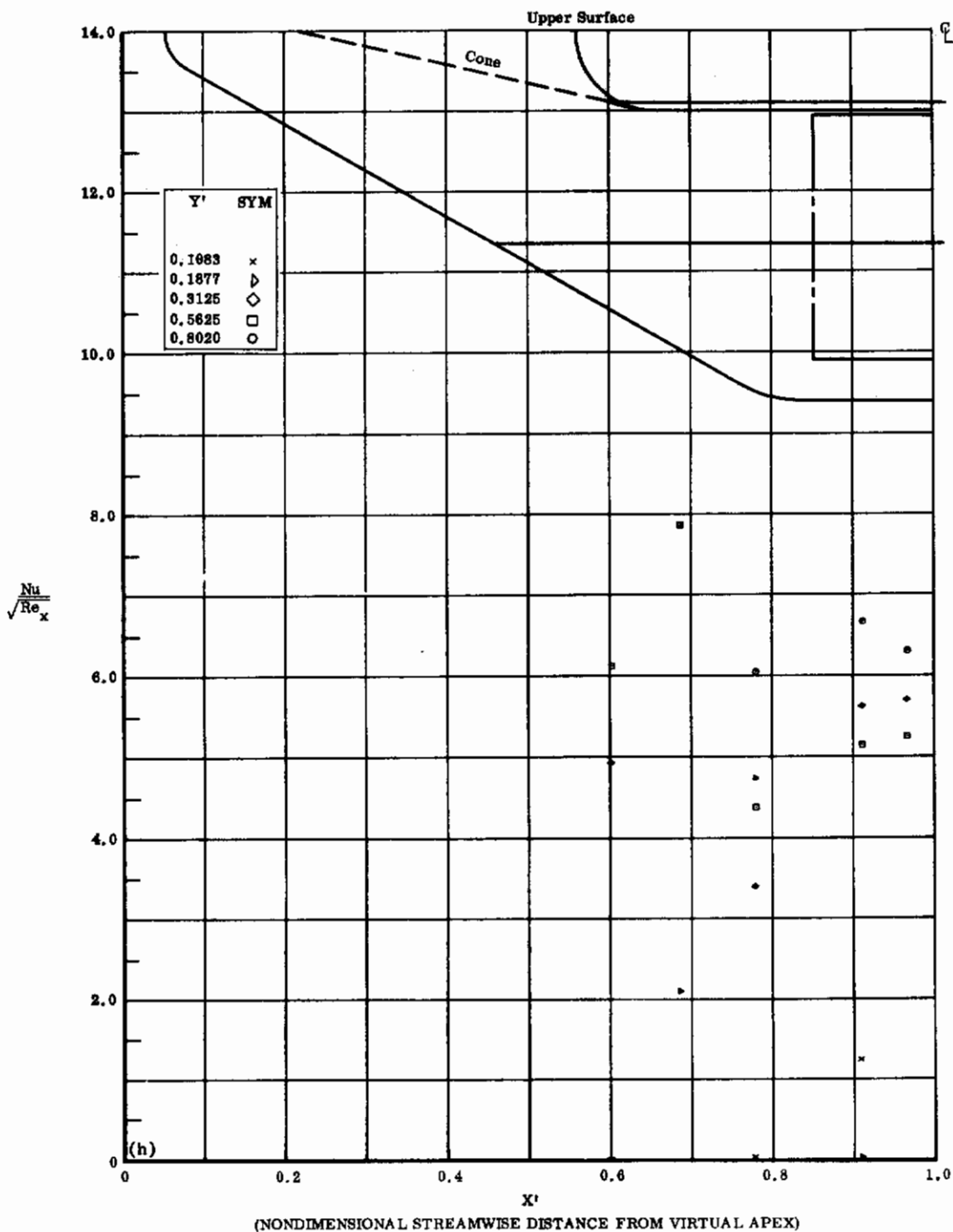


Fig. 14h Configuration I, $\alpha = -30^\circ$, $\delta_2 = \delta_3 = 0$

$\text{Nu}/\sqrt{\text{Re}_x}$ vs. X' upper surface

Contrails

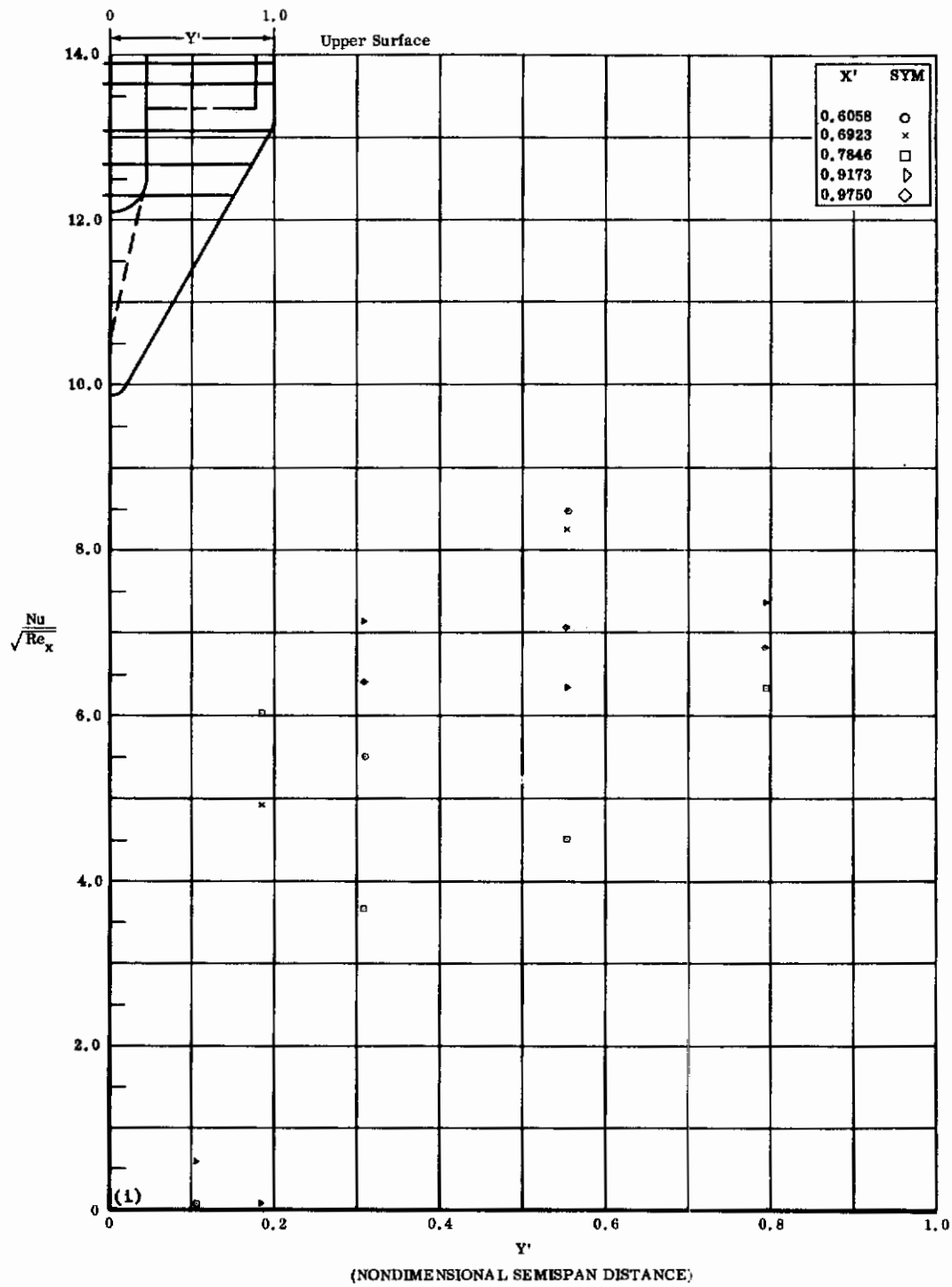


Fig. 14i Configuration I, $\alpha = -40$, $\beta_2 = \beta_3 = 0$
 $\text{Nu}/\sqrt{\text{Re}_x}$ vs. Y' upper surface

Contrails

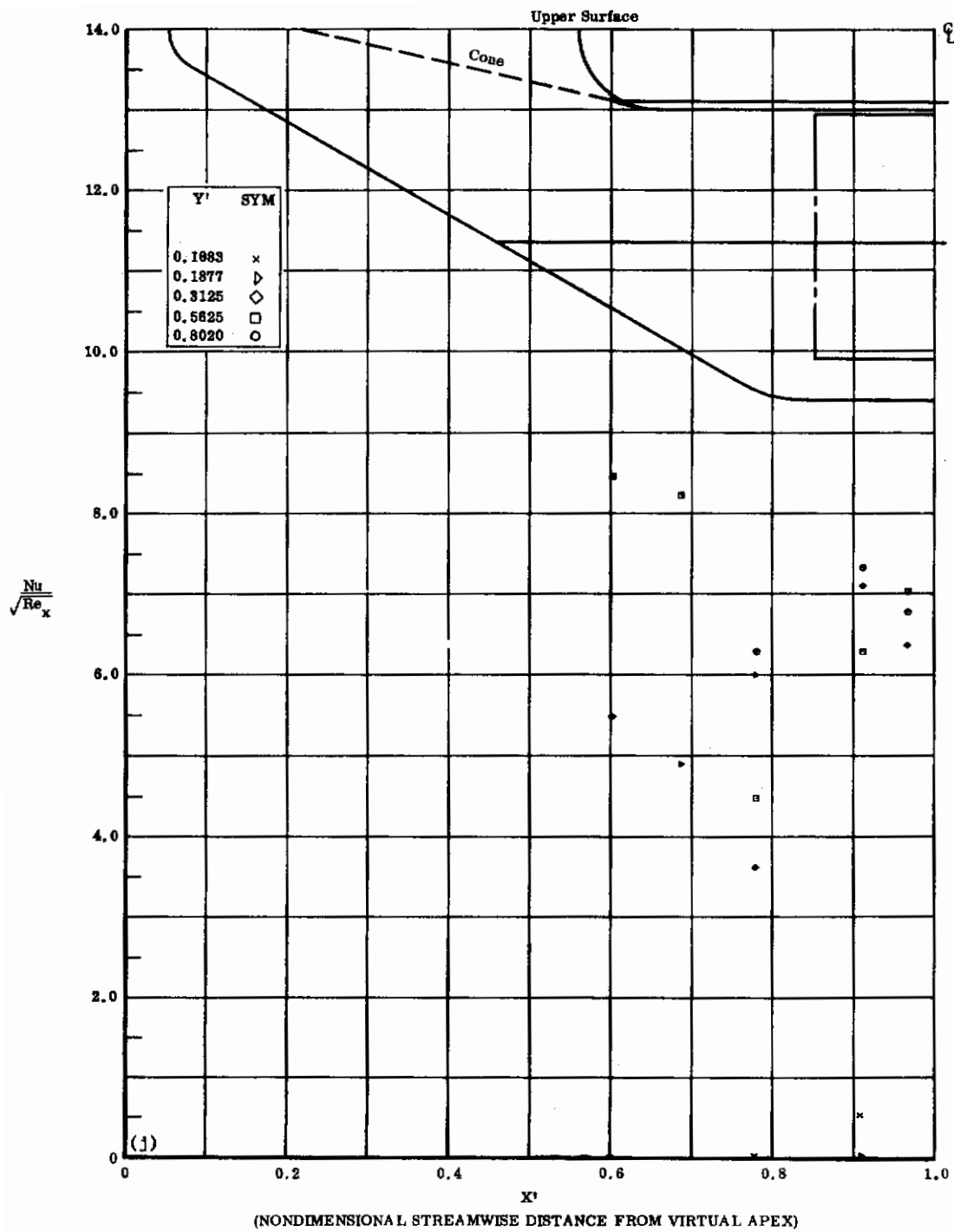


Fig. 14j Configuration I, $\alpha = -40$, $\delta_2 = \delta_3 = 0$
 $\frac{\text{Nu}}{\sqrt{\text{Re}_x}}$ vs. X^1 upper surface

Contrails

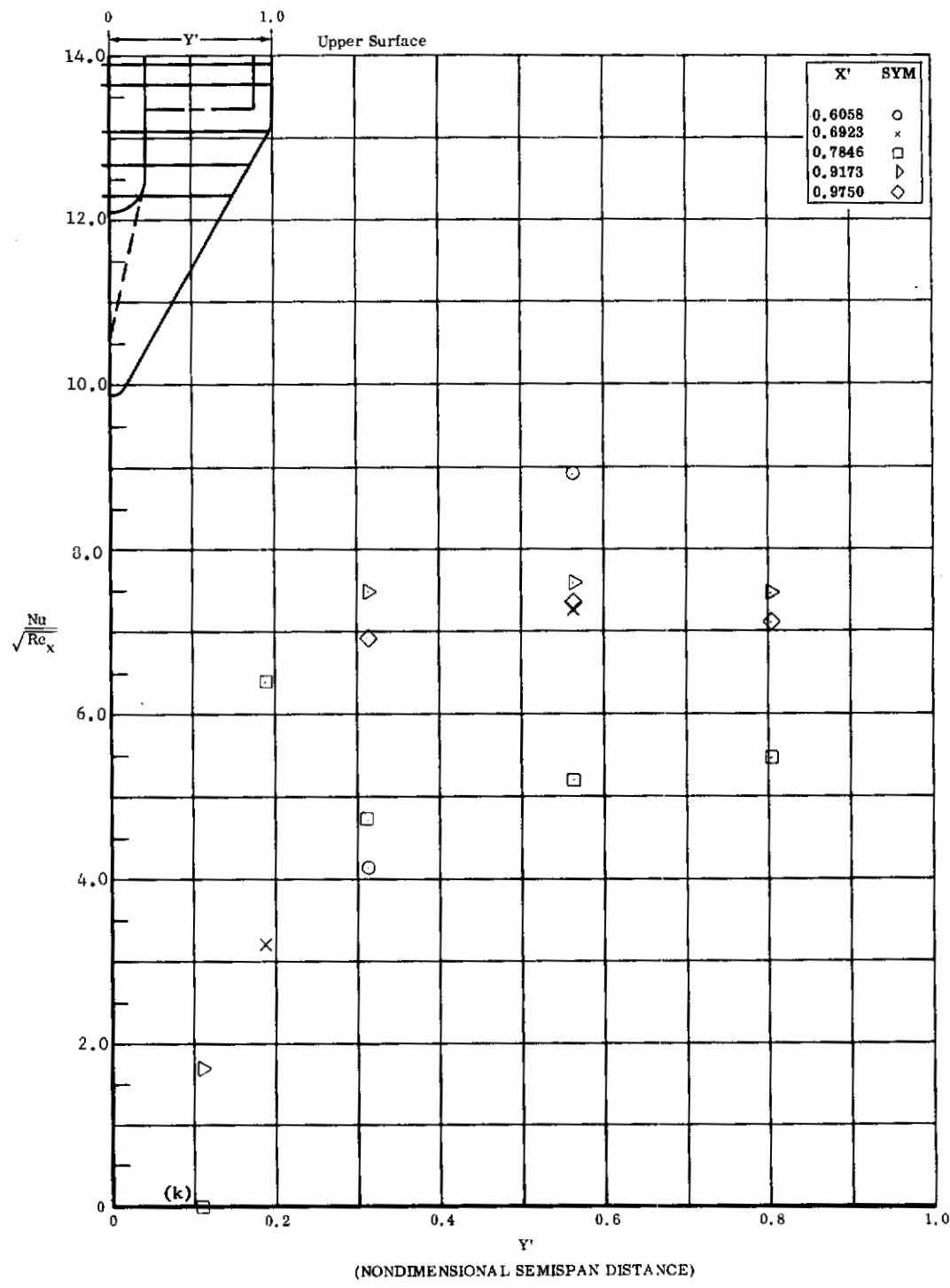


Fig. 14k Configuration I, $\alpha = -50$, $\delta_2 = \delta_3 = 0$
 $Nu/\sqrt{Re_x}$ vs. Y' upper surface

Contrails

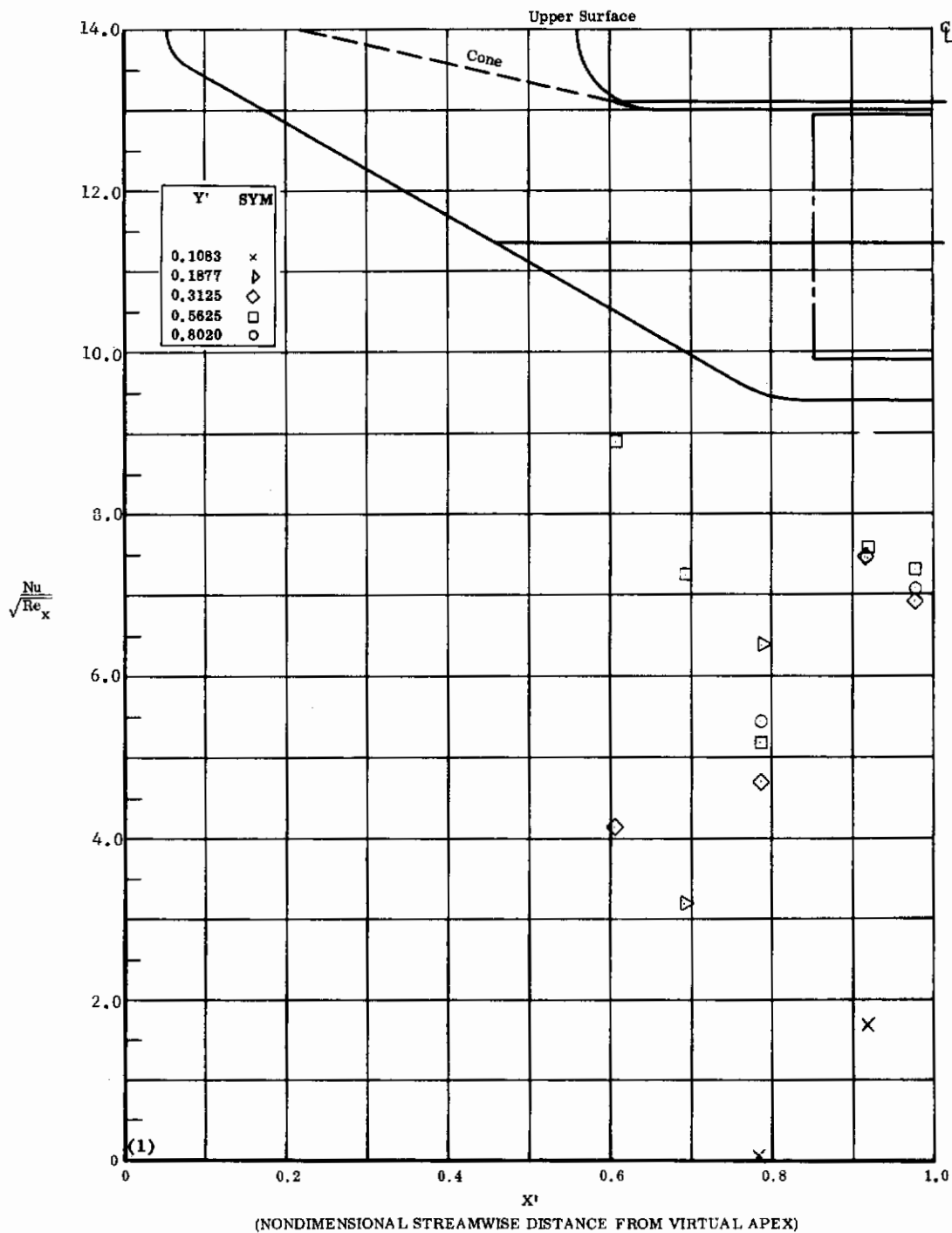


Fig. 14 ℓ Configuration I, $\alpha = -50^\circ$, $\delta_2 = \delta_3 = 0$

$Nu/\sqrt{Re_x}$ vs. X' upper surface

Contrails

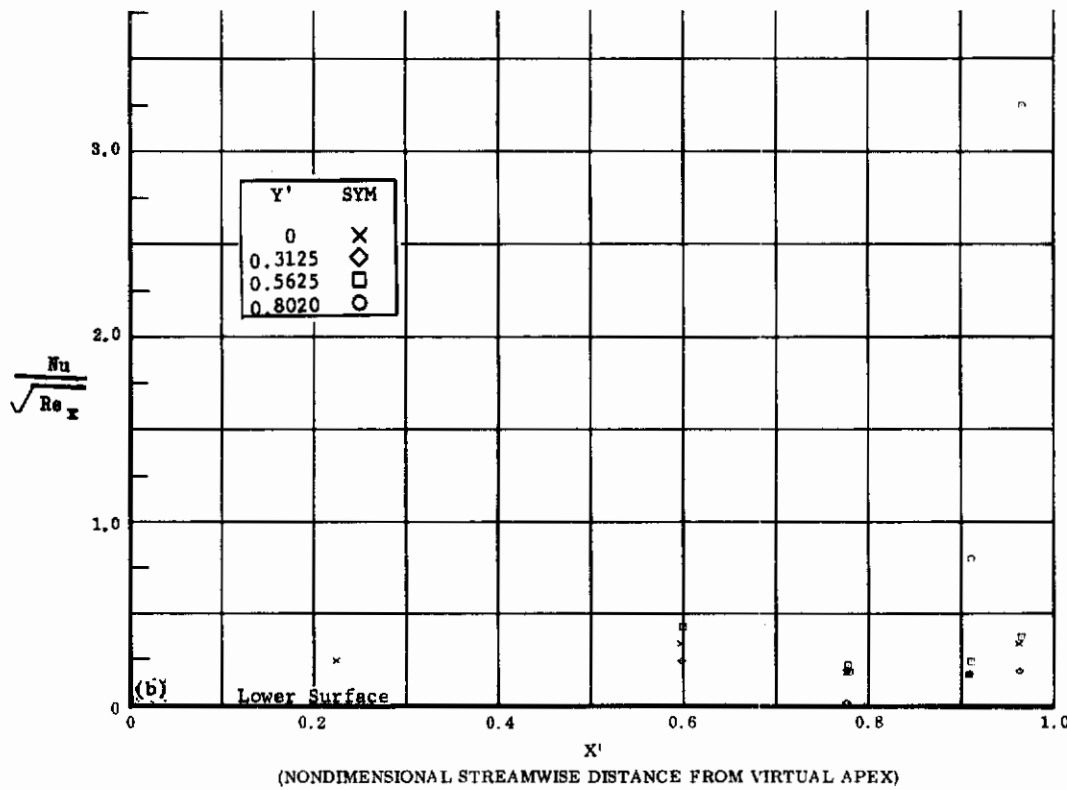
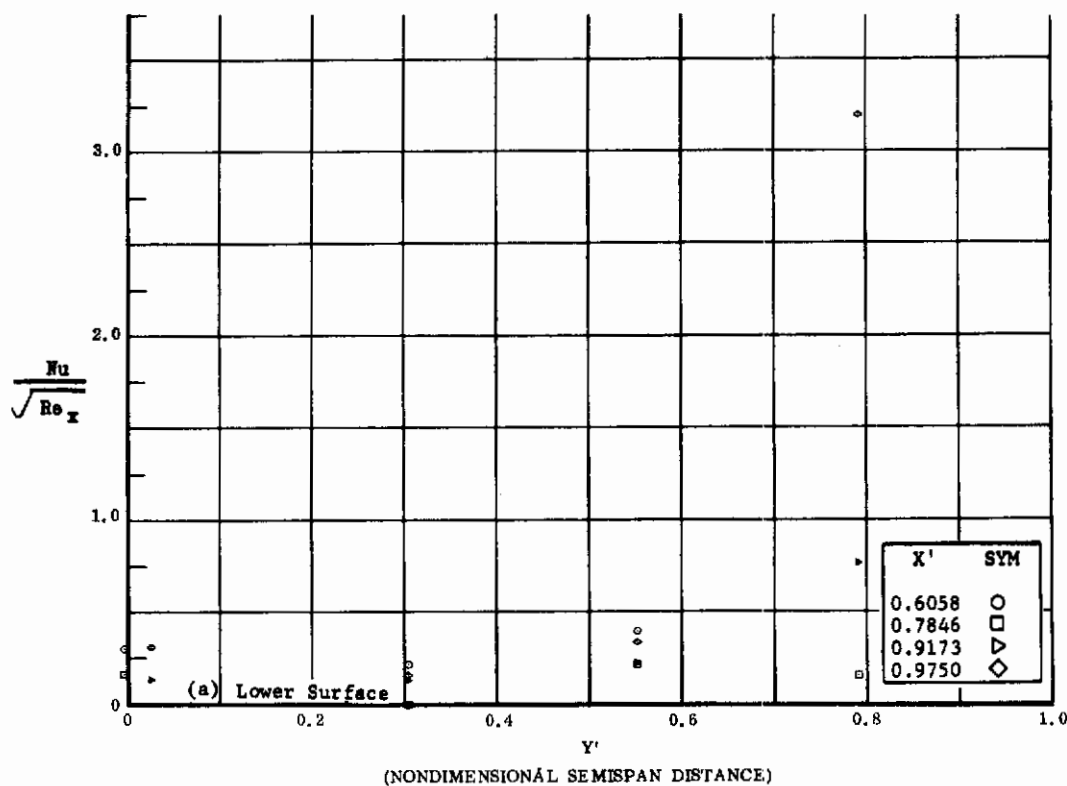


Fig. 15 Configuration IV, $\alpha = 0$, $b_2 = b_3 = 0$

a) $Nu/\sqrt{Re_x}$ vs. Y' lower surface

b) $Nu/\sqrt{Re_x}$ vs. X' lower surface

Contrails

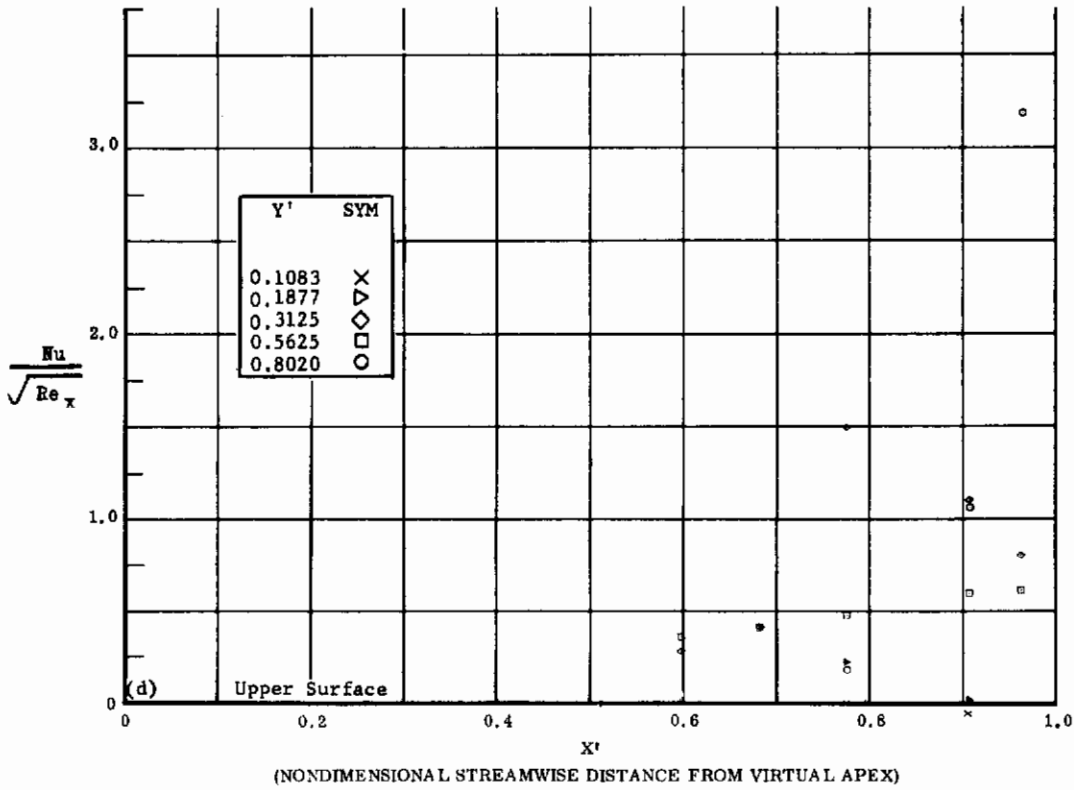
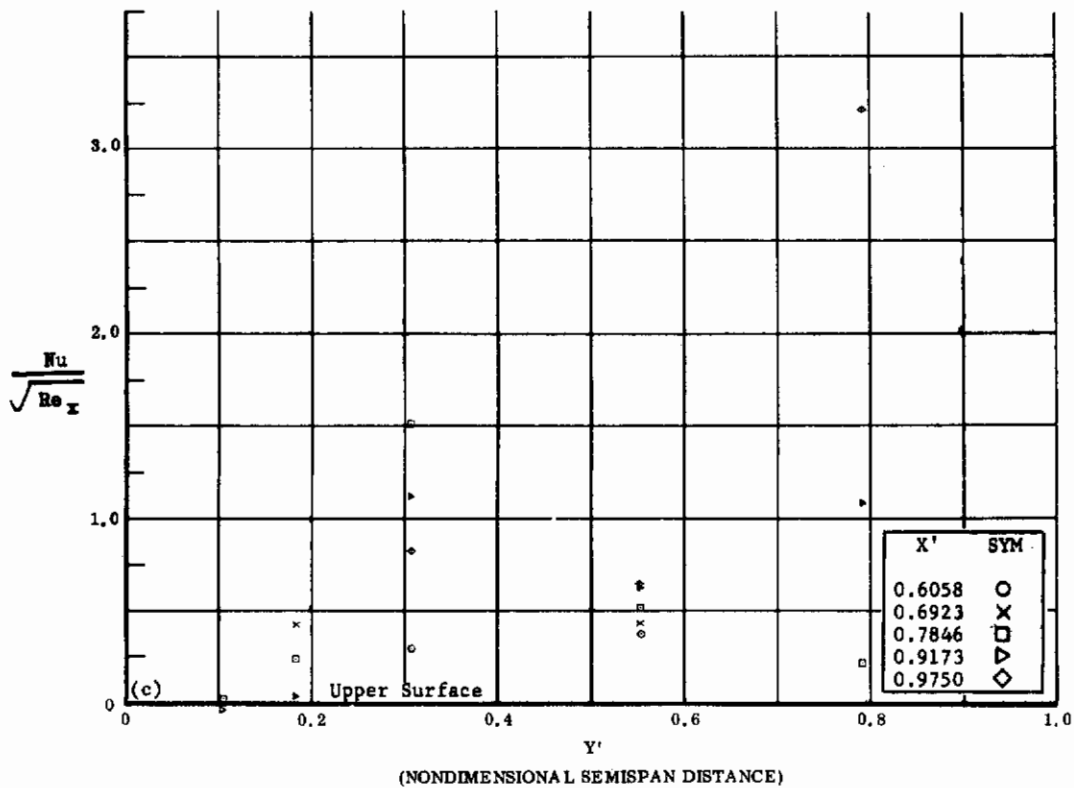


Fig. 15 Configuration IV, $\alpha = 0$, $\delta_2 = \delta_3 = 0$

c) $Nu/\sqrt{Re_x}$ vs. Y' upper surface

d) $Nu/\sqrt{Re_x}$ vs. X' upper surface

Contrails

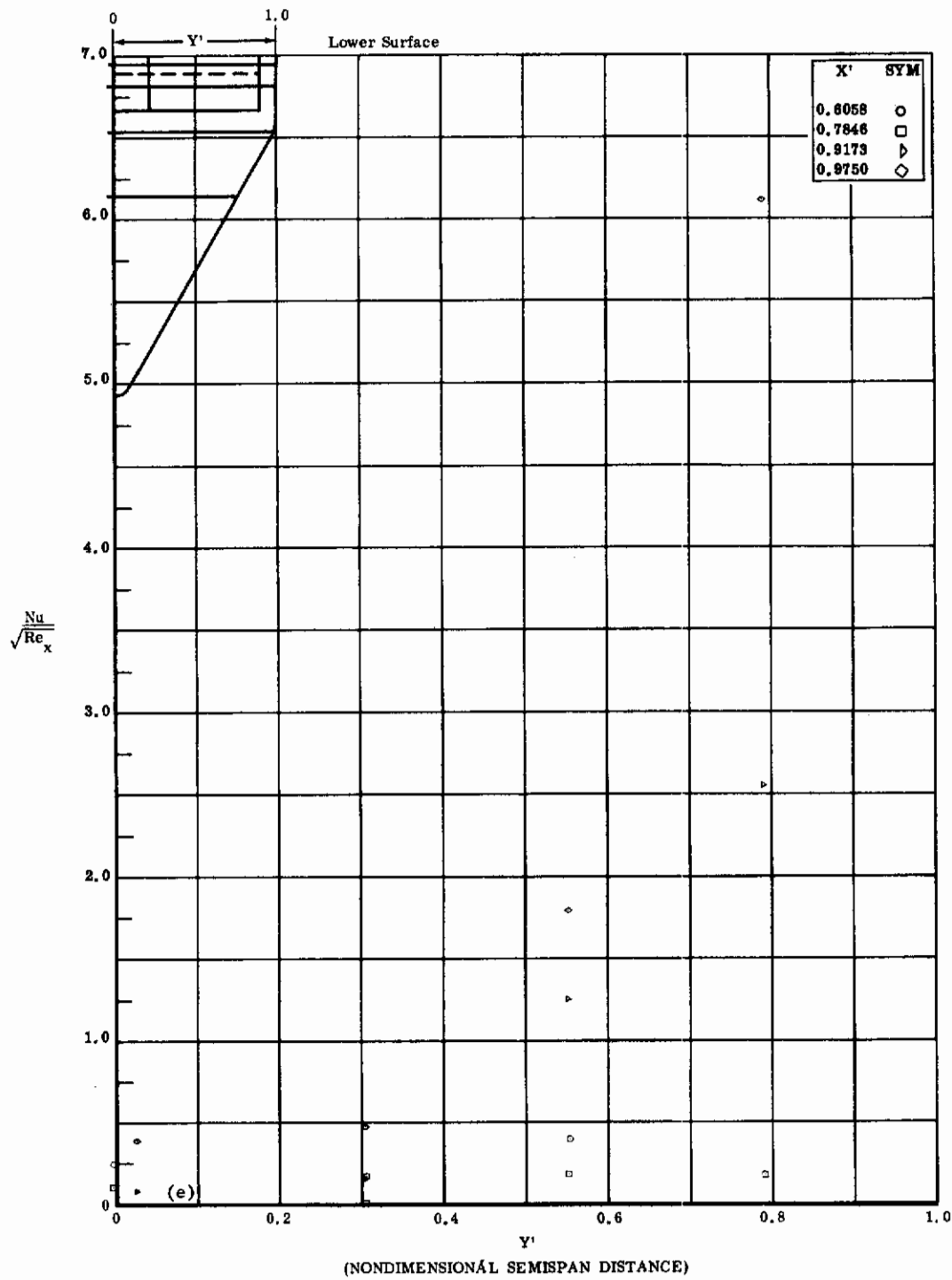


Fig. 15e Configuration IV, $\alpha = 0$, $b_2 = b_3 = +10$

$\text{Nu}/\sqrt{\text{Re}_x}$ vs. Y' lower surface

Contrails

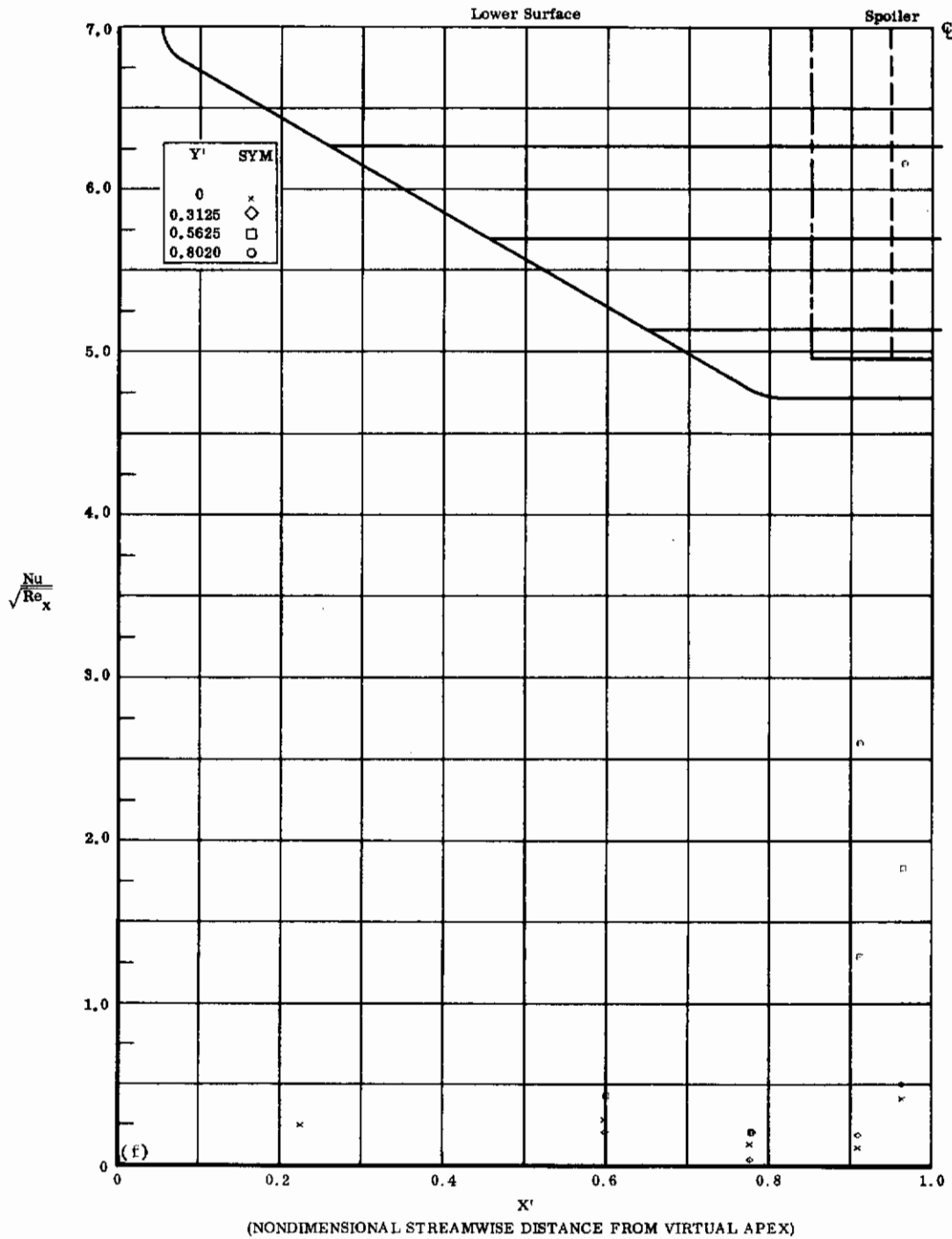


Fig. 15f Configuration IV, $\alpha = 0$, $b_2 = b_3 = +10$
 $Nu/\sqrt{Re_x}$ vs. X' lower surface

Contrails

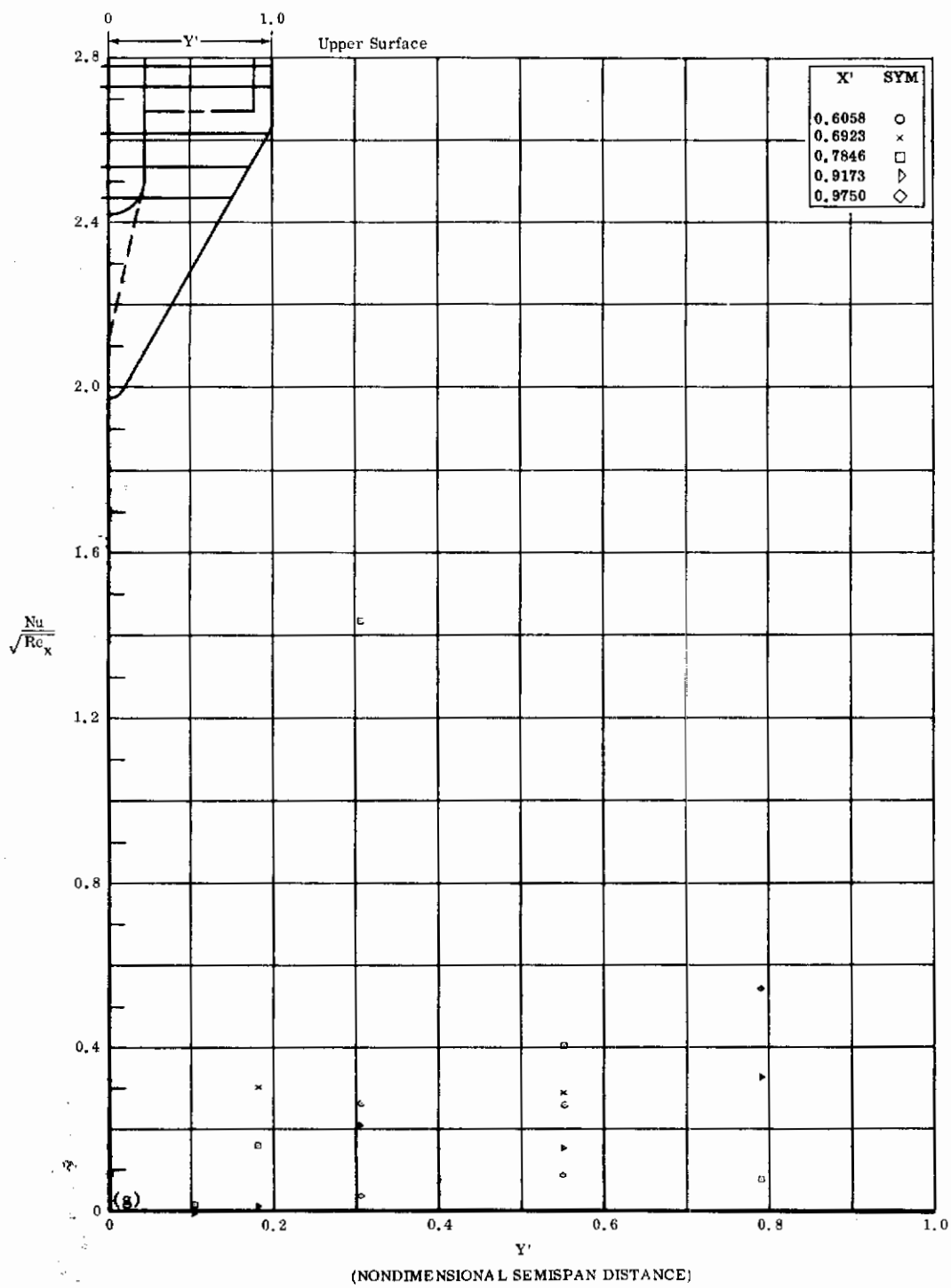


Fig. 15g Configuration IV, $\alpha = 0$, $\delta_2 = \delta_3 = +10$
 $Nu/\sqrt{Re_x}$ vs. Y' upper surface

Contrails

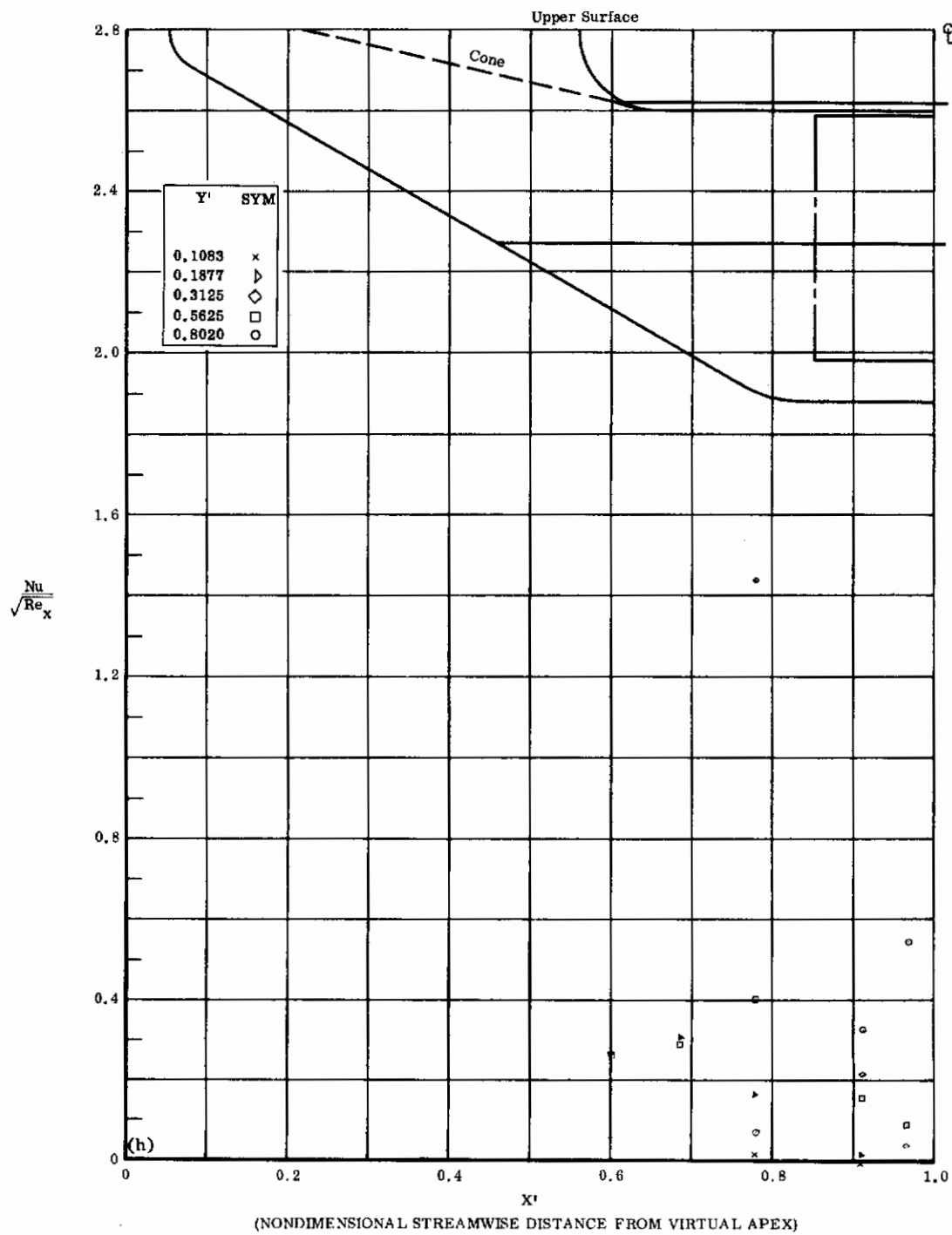


Fig. 15h Configuration IV, $\alpha = 0$, $\delta_2 = \delta_3 = +10$
 $\text{Nu}/\sqrt{\text{Re}_x}$ vs. X' upper surface

Contrails

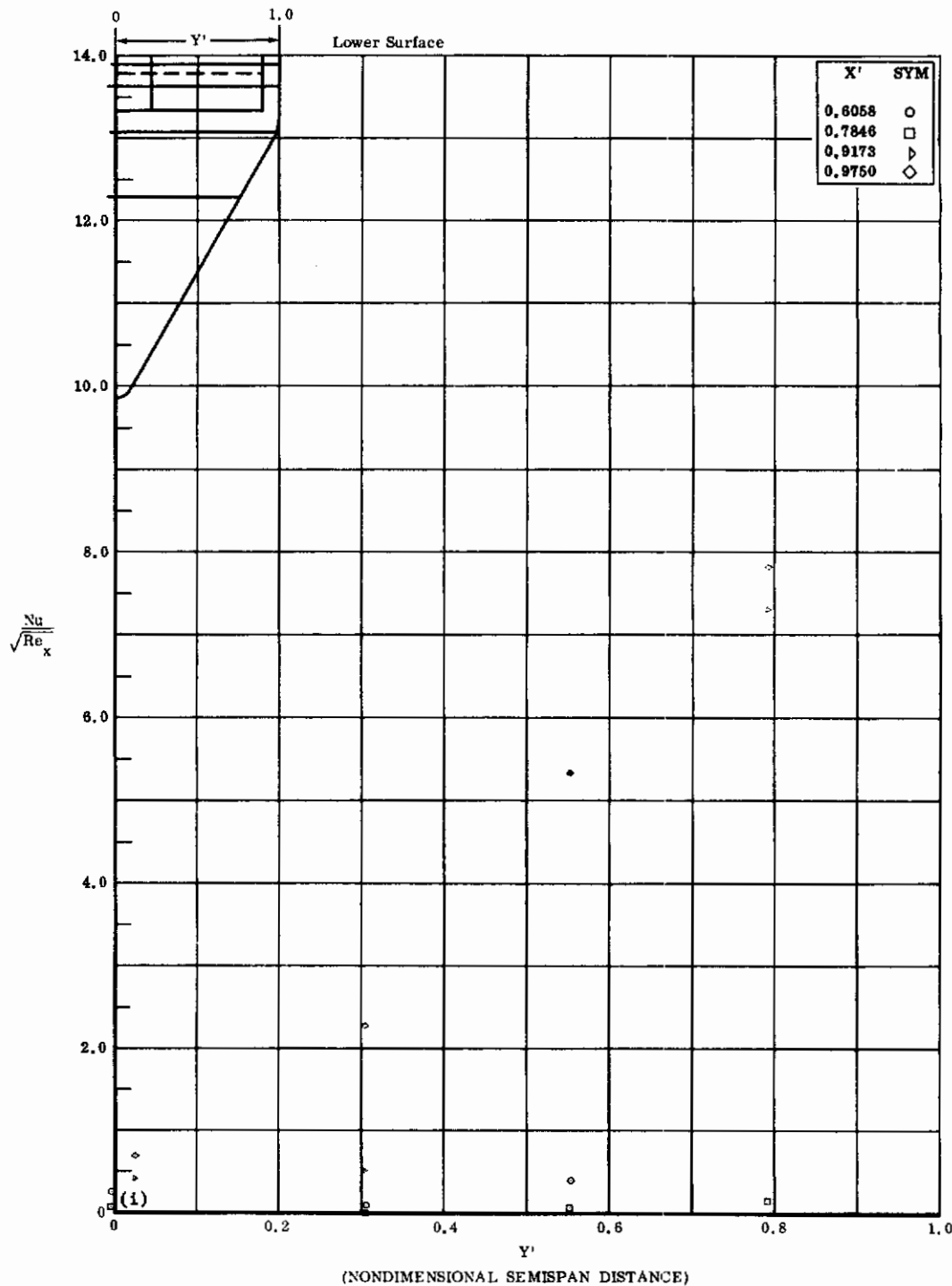


Fig. 15i Configuration IV, $\alpha = 0$, $\delta_2 = \delta_3 = +20$
 $Nu/\sqrt{Re_x}$ vs. Y' lower surface

Contrails

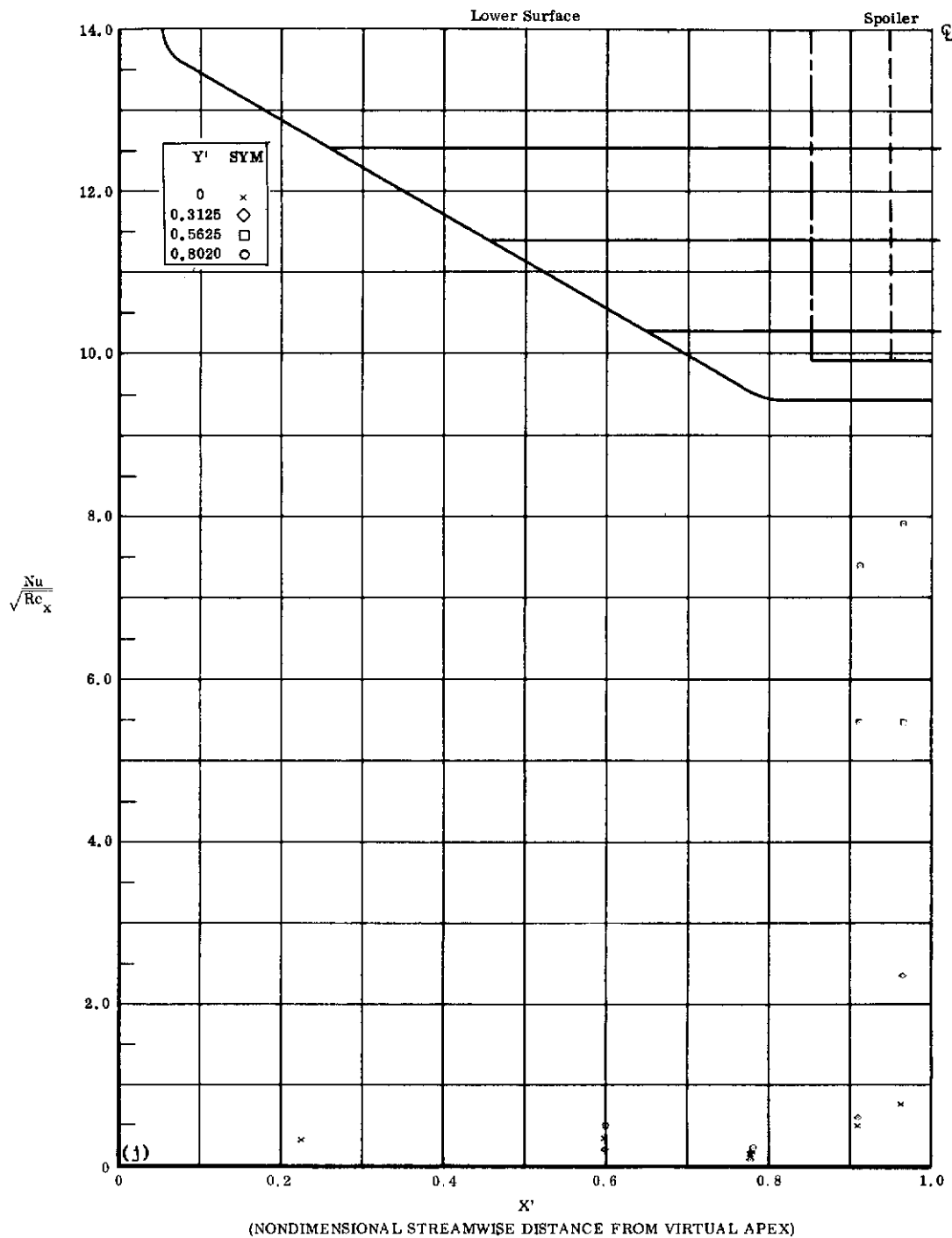


Fig. 15j Configuration IV, $\alpha = 0$, $\delta_2 = \delta_3 = +20$
 $\text{Nu}/\sqrt{\text{Re}_x}$ vs. X' lower surface

Contrails

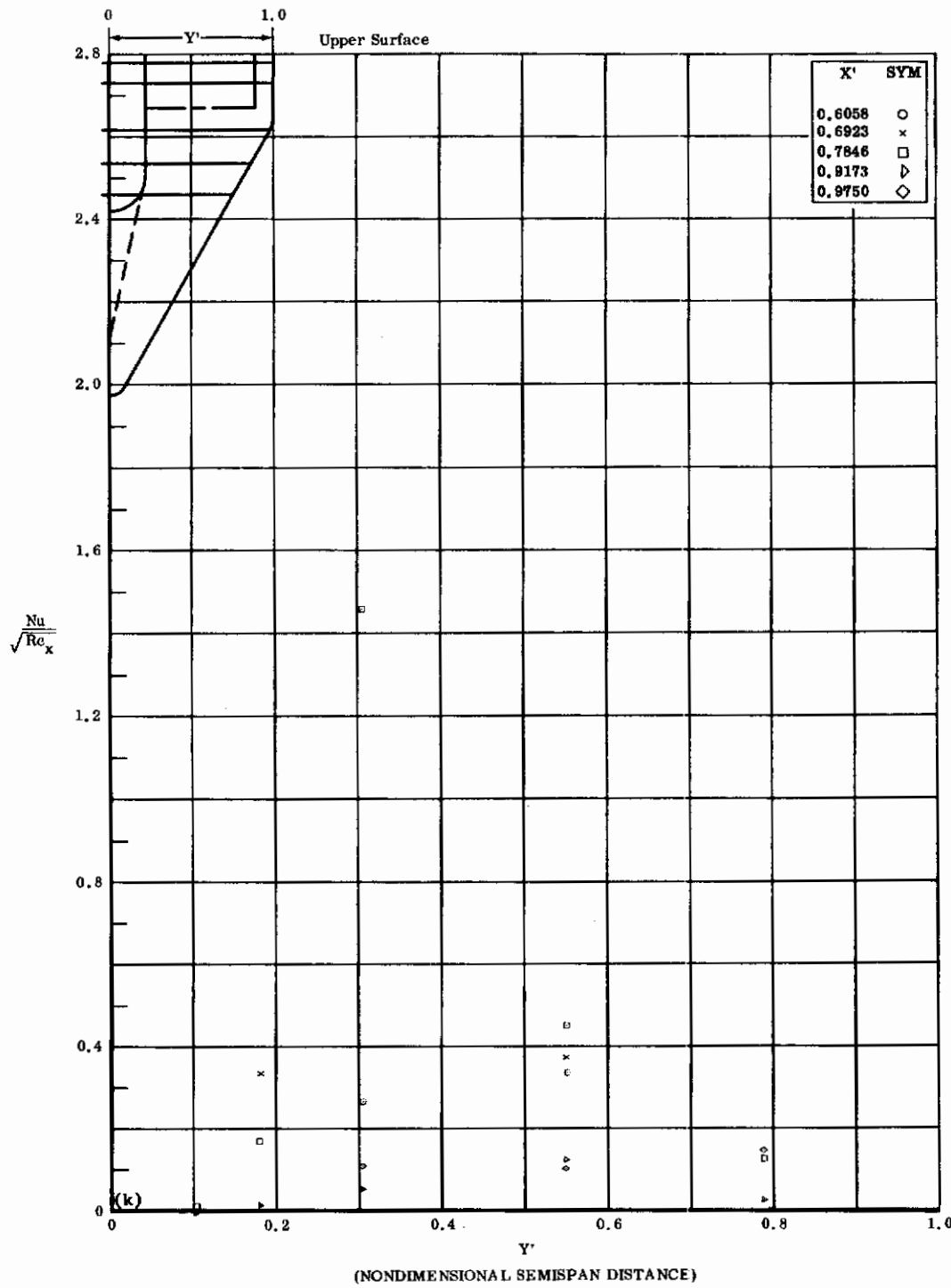


Fig. 15k Configuration IV, $\alpha = 0$, $\delta_2 = \delta_3 = +20$
 $\text{Nu}/\sqrt{\text{Re}_x}$ vs. Y' upper surface

Contrails

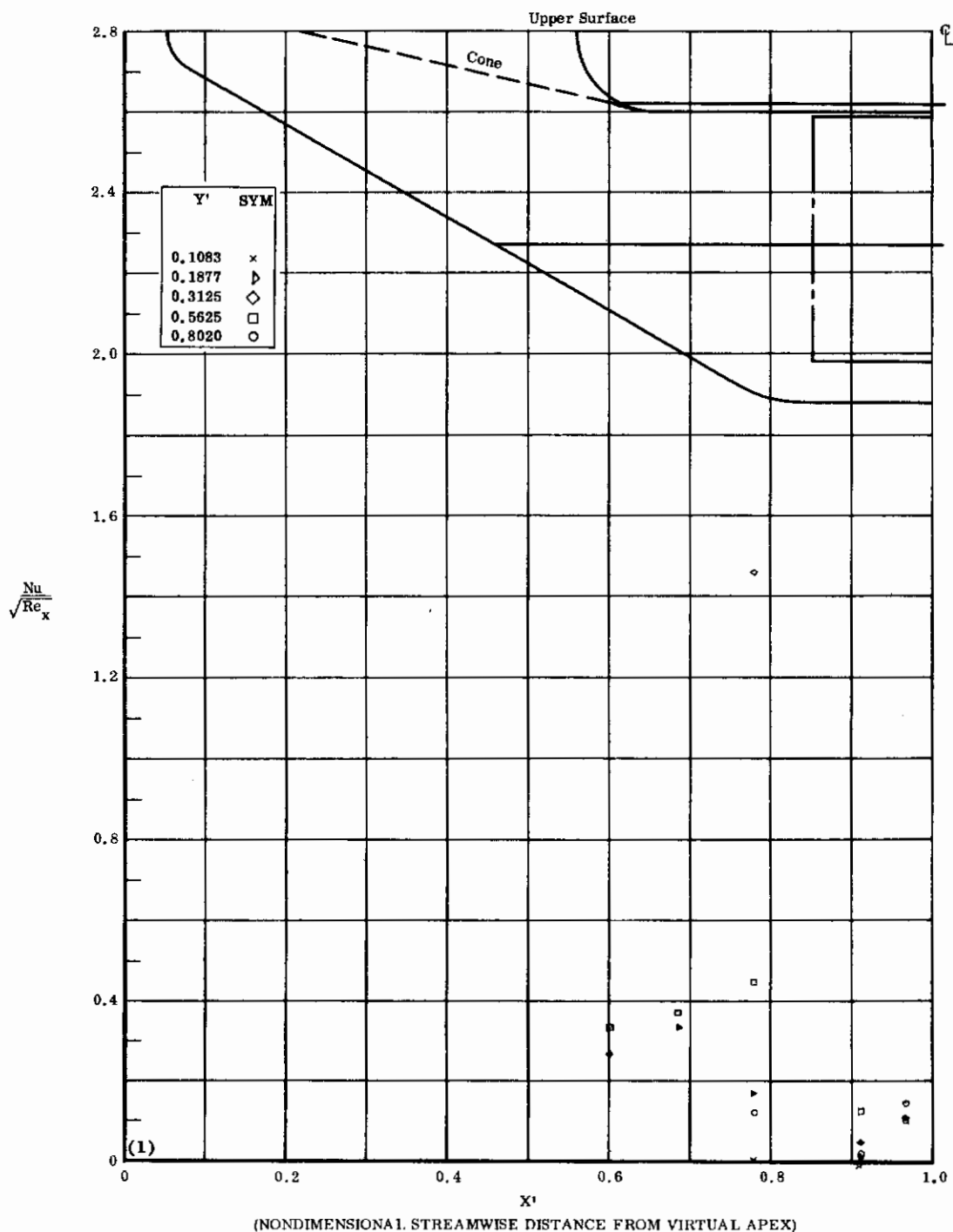


Fig. 15& Configuration IV, $\alpha = 0$, $\delta_2 = \delta_3 = +20$

$Nu/\sqrt{Re_x}$ vs. X' upper surface

Contrails

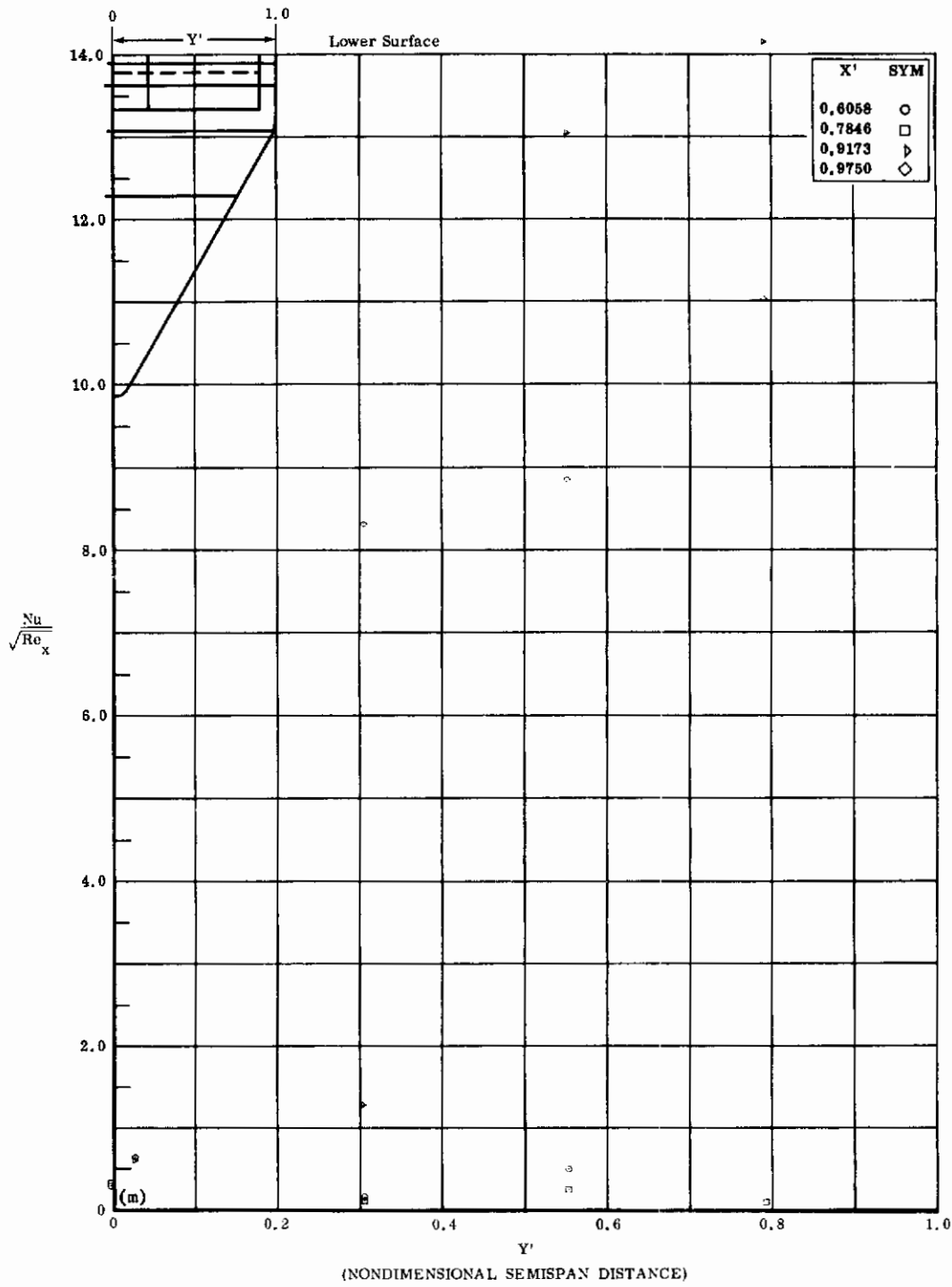


Fig. 15m Configuration IV, $\alpha = 0$, $\delta_2 = \delta_3 = +30$
 $Nu/\sqrt{Re_x}$ vs. Y' lower surface

Contrails

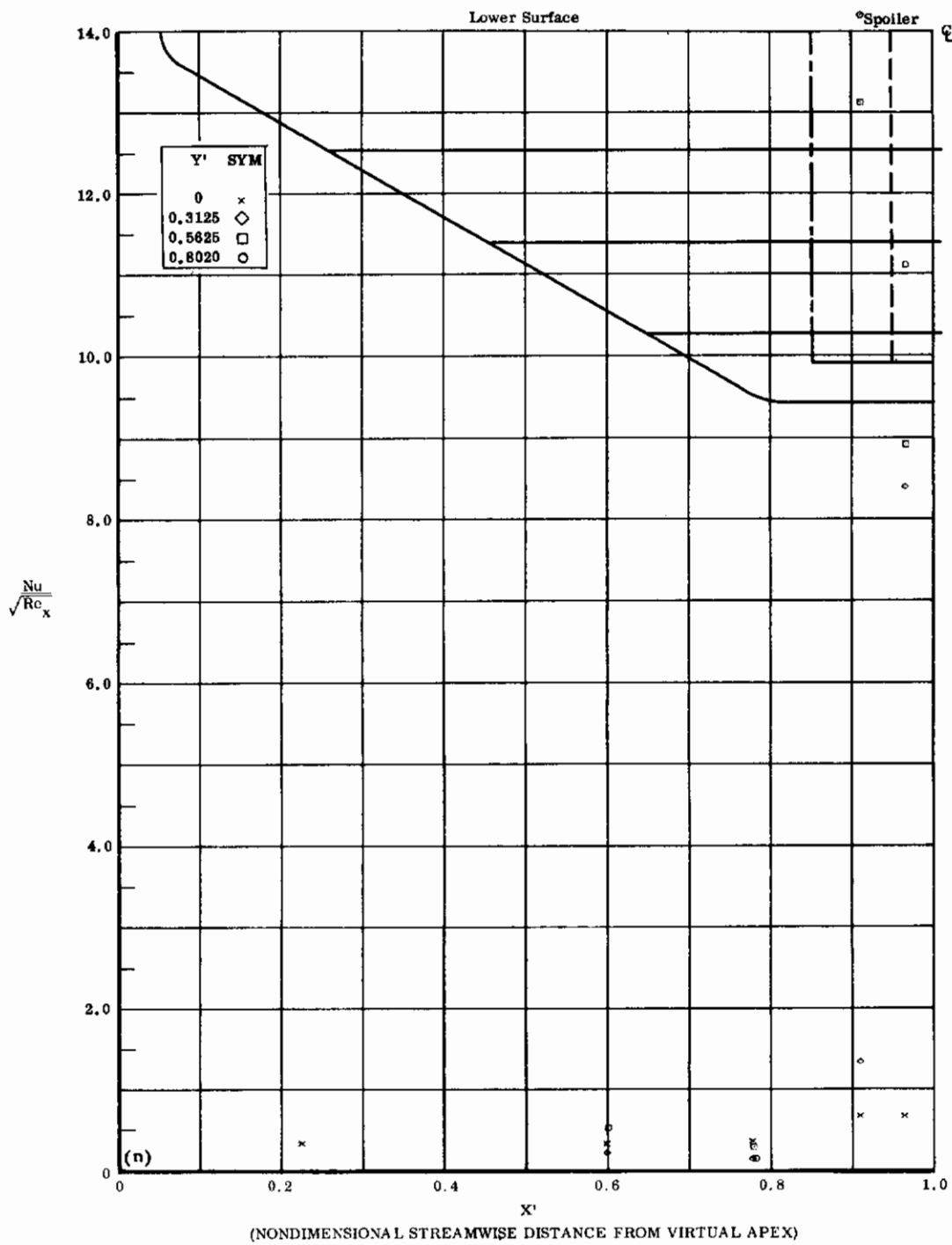


Fig. 15n Configuration IV, $\alpha = 0$, $\delta_2 = \delta_3 = +30$
 $Nu/\sqrt{Re_x}$ vs. X' lower surface

Contrails

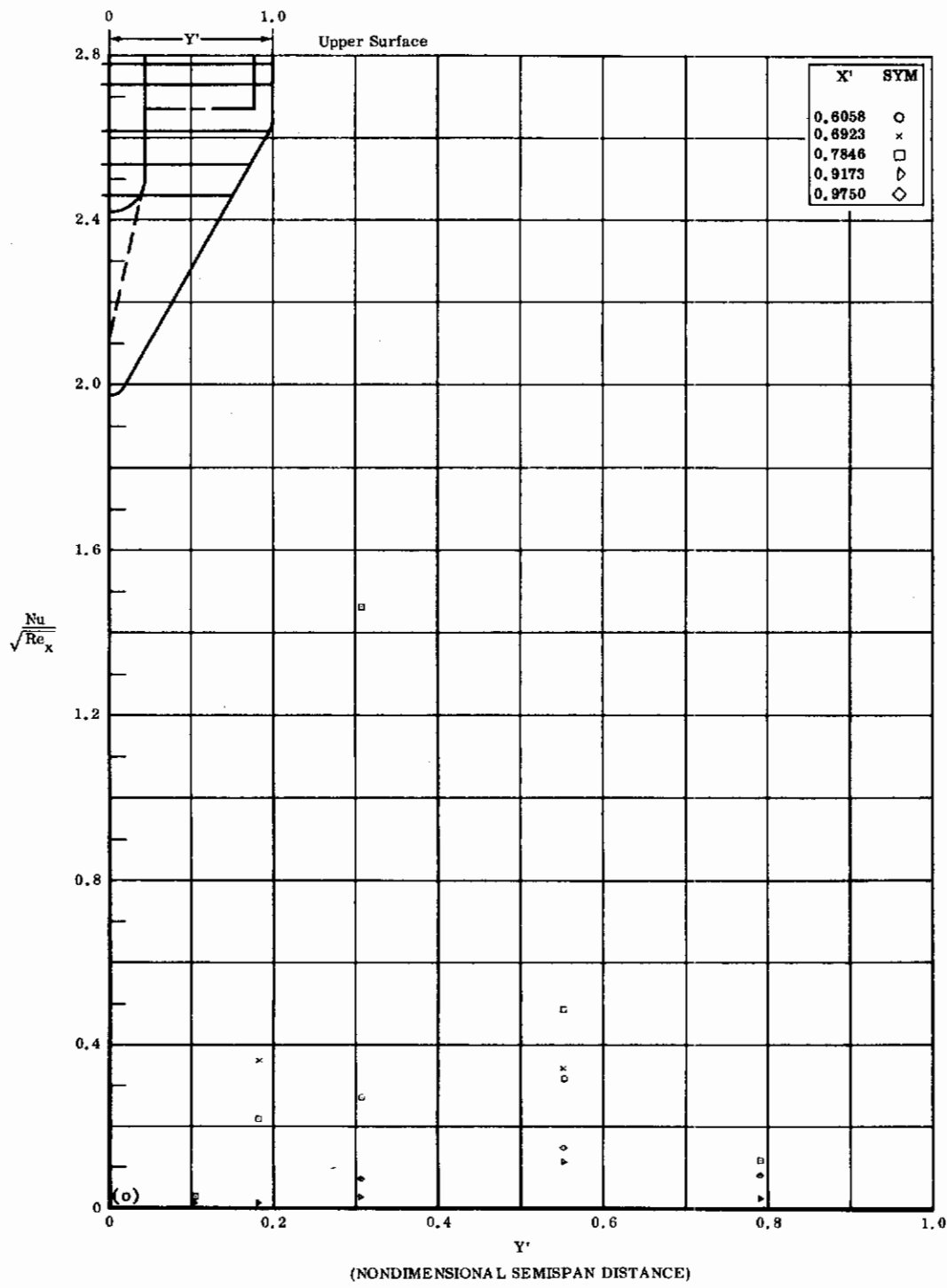


Fig. 15o Configuration IV, $\alpha = 0$, $b_2 = b_3 = +30$
 $Nu/\sqrt{Re_x}$ vs. Y' upper surface

Contrails

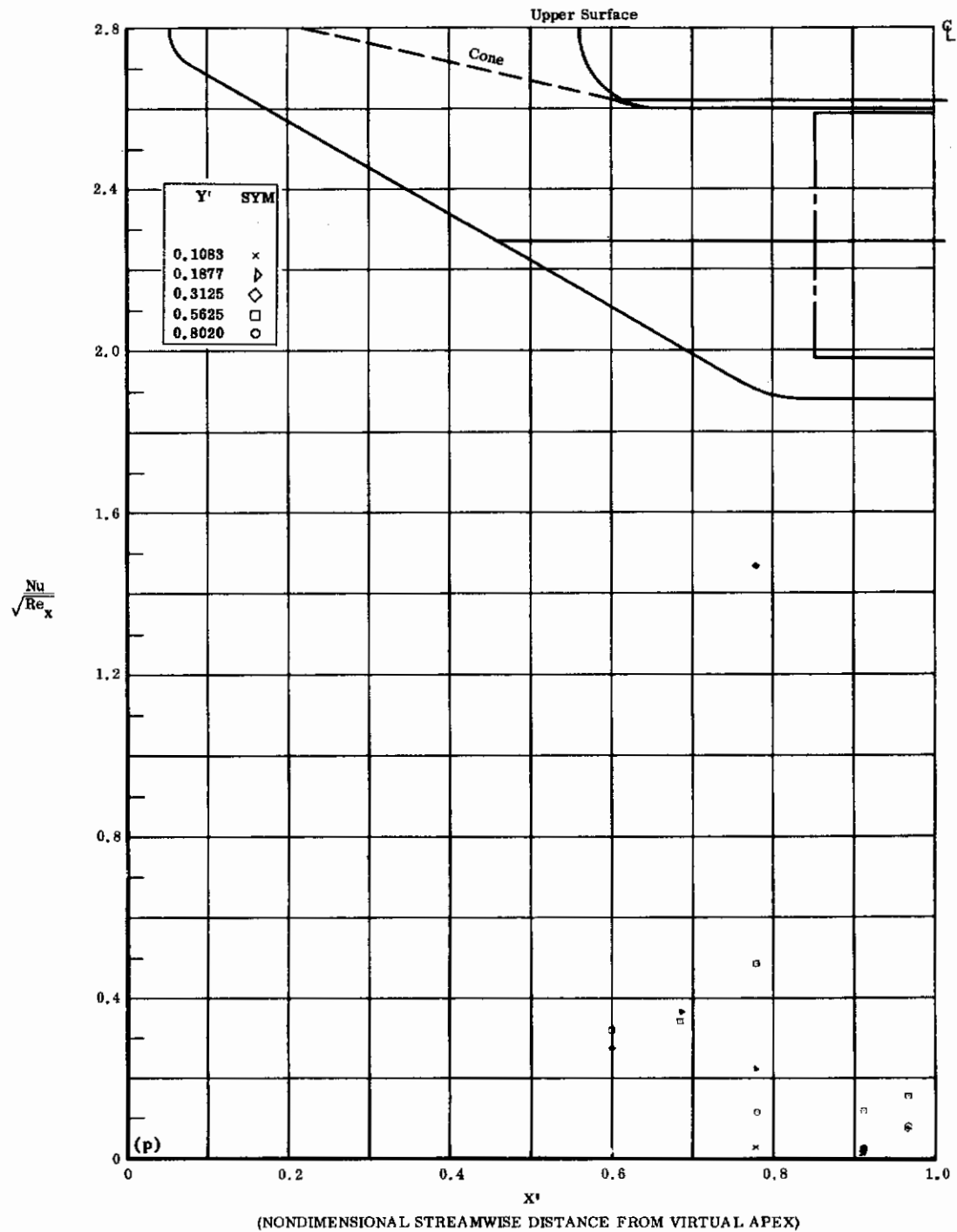


Fig. 15p Configuration IV, $\alpha = 0$, $\delta_2 = \delta_3 = +30$
 $\text{Nu}/\sqrt{\text{Re}_x}$ vs. X' upper surface

Contrails

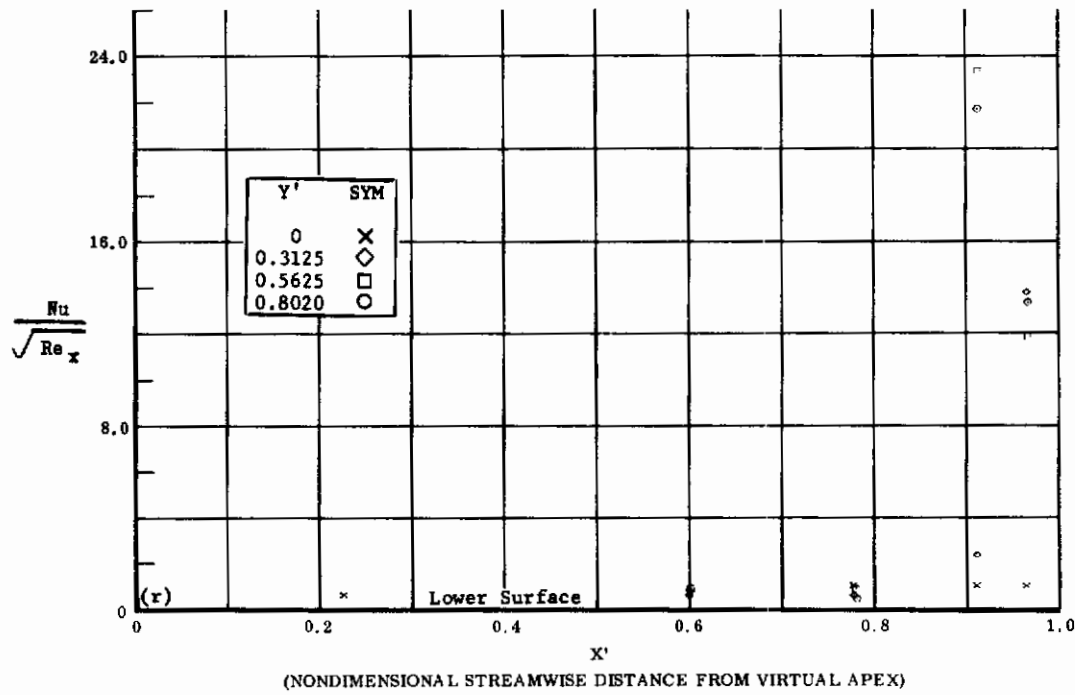
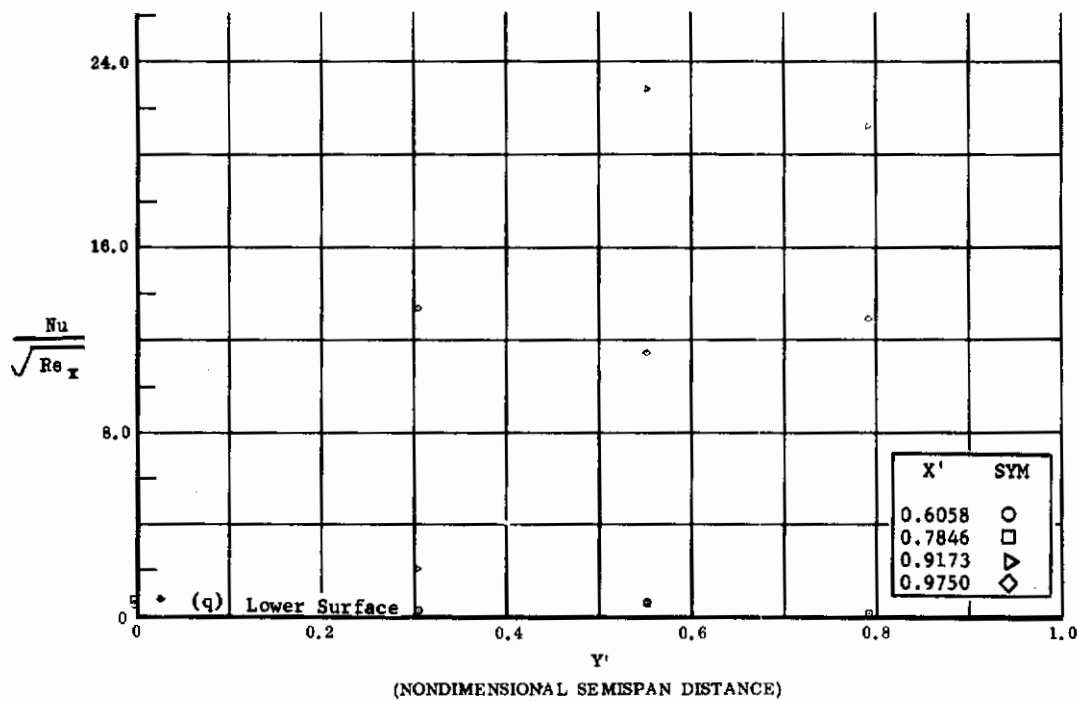


Fig. 15 Configuration IV, $\alpha = 0$, $\delta_2 = \delta_3 = +39$

q) $Nu/\sqrt{Re_x}$ vs. Y' lower surface

r) $Nu/\sqrt{Re_x}$ vs. X' lower surface

Contrails

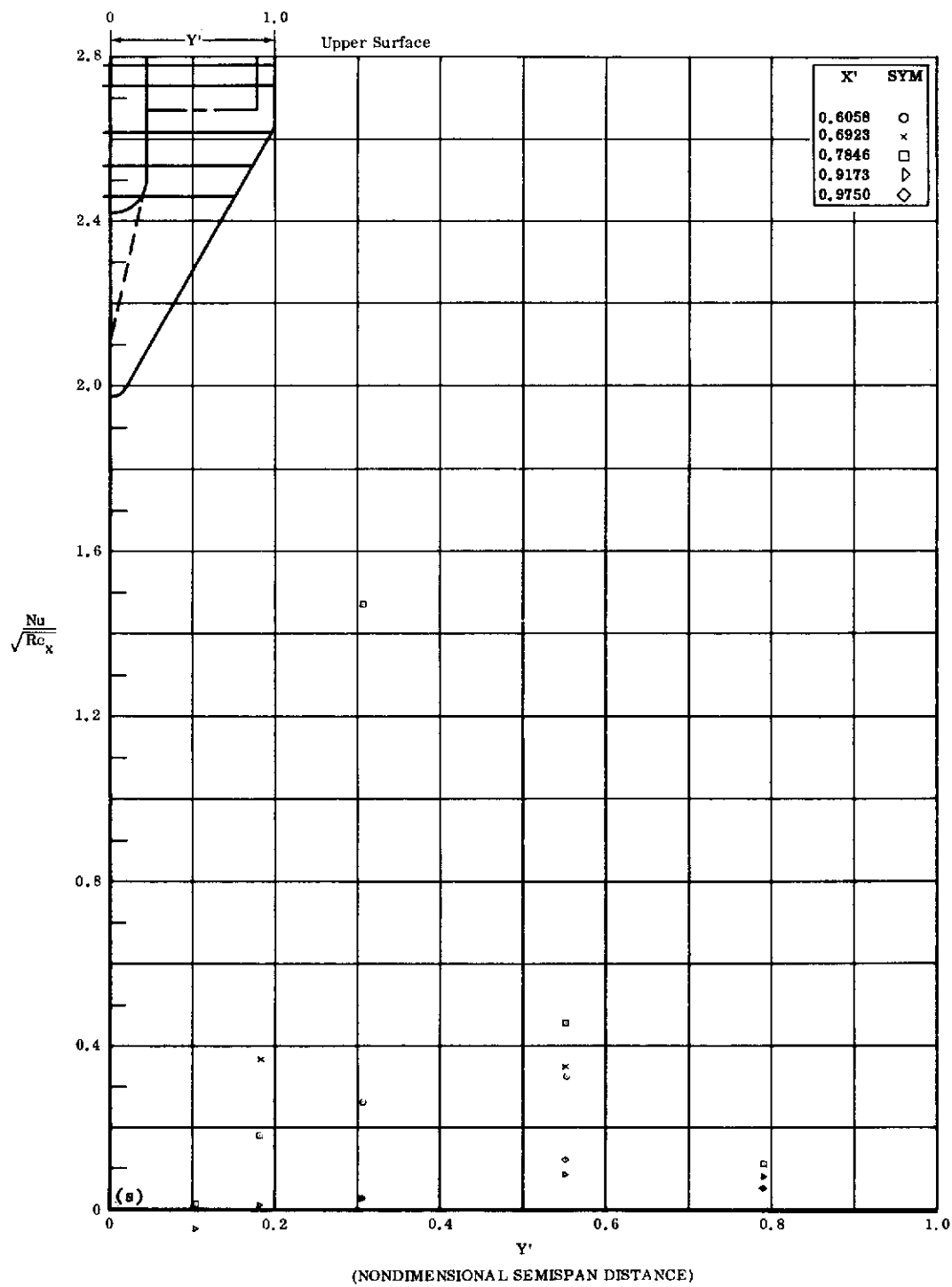


Fig. 15s Configuration IV, $\alpha = 0$, $\delta_2 = \delta_3 = +39$
 $Nu/\sqrt{Re_x}$ vs. Y' upper surface

Contrails

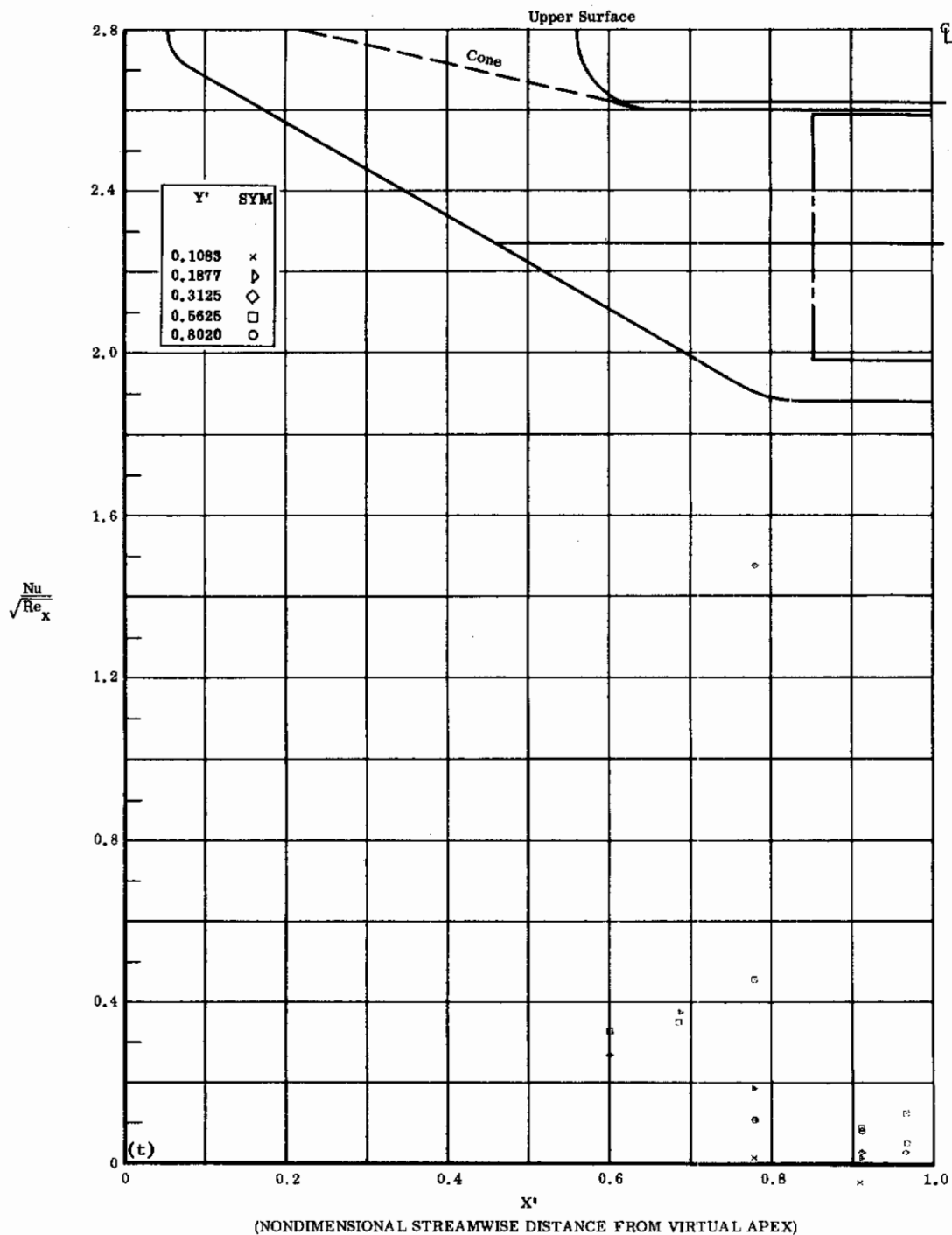


Fig. 15t Configuration IV, $\alpha = 0$, $\delta_2 = \delta_3 = +39$

$\text{Nu}/\sqrt{\text{Re}_x}$ vs. X^t upper surface

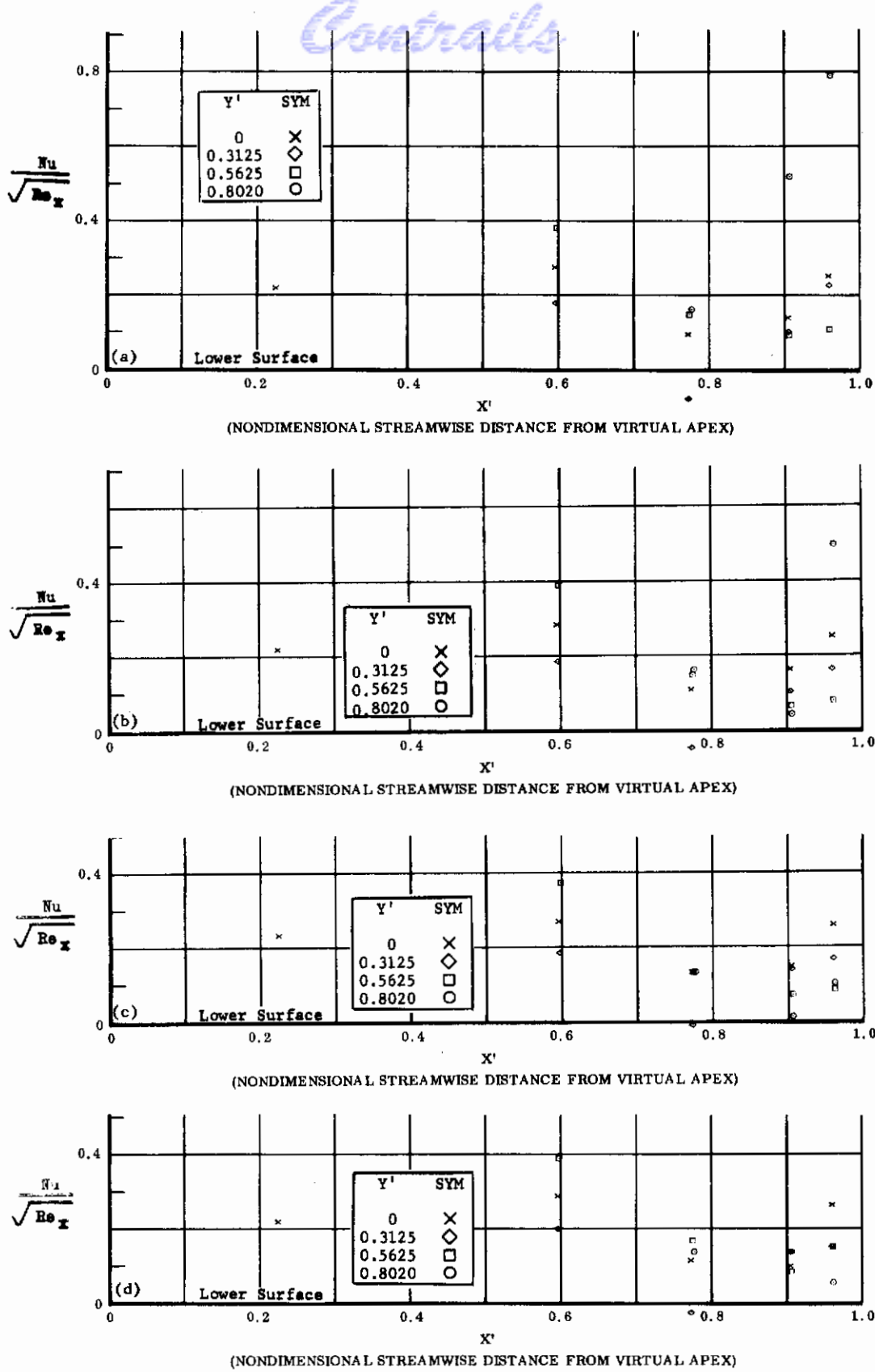
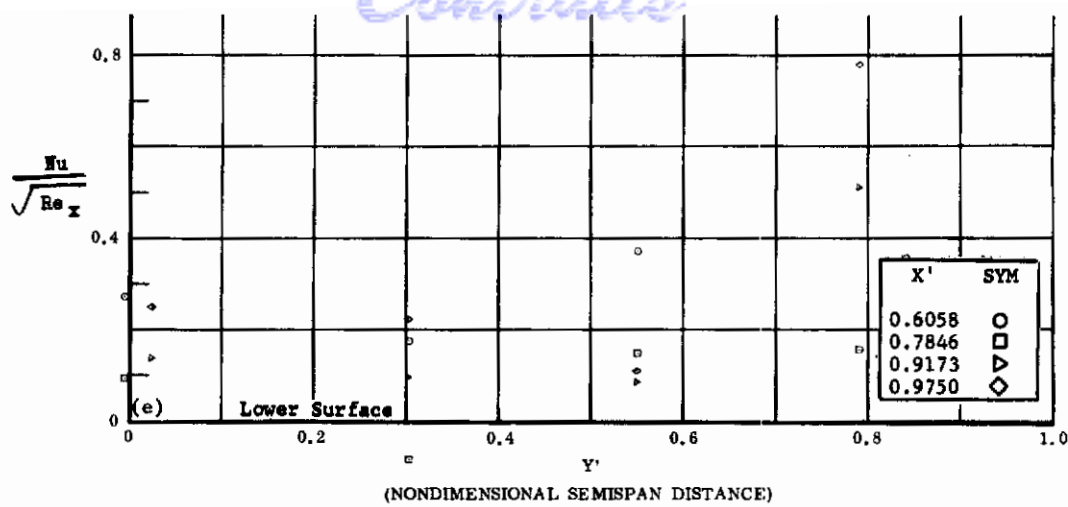


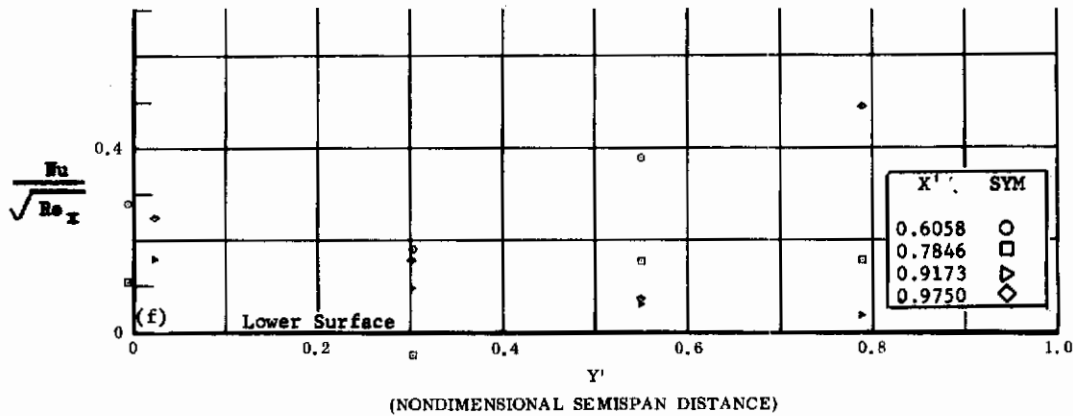
Fig. 16 Configuration IV, $\alpha = 0$, $Nu/\sqrt{Re_x}$ vs. Y' , lower surface

- a) $\delta_2 = \delta_3 = -10$
- b) $\delta_2 = \delta_3 = -20$
- c) $\delta_2 = \delta_3 = -30$
- d) $\delta_2 = \delta_3 = -39$

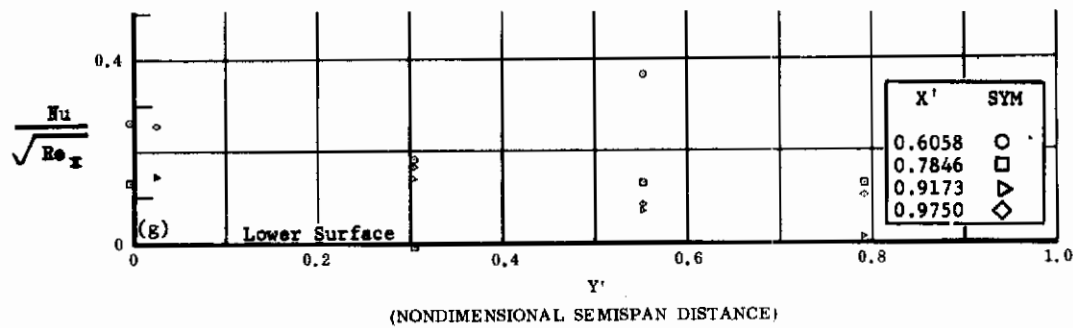
Controls



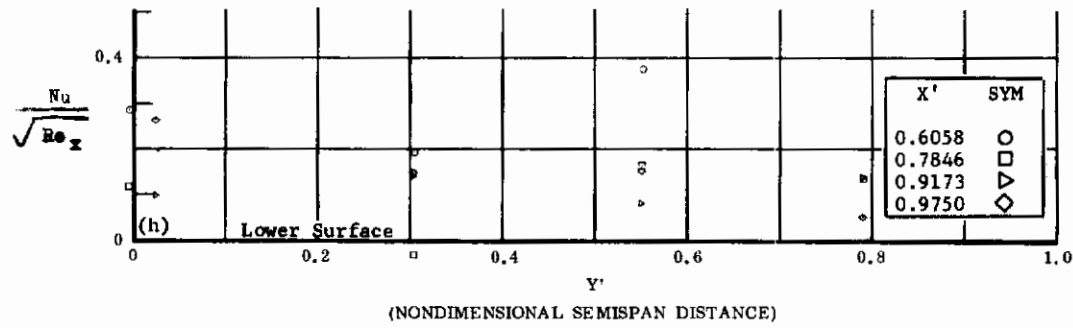
(NONDIMENSIONAL SEMISPAN DISTANCE)



(NONDIMENSIONAL SEMISPAN DISTANCE)



(NONDIMENSIONAL SEMISPAN DISTANCE)



(NONDIMENSIONAL SEMISPAN DISTANCE)

Fig. 16 Configuration IV, $\alpha = 0$, $Nu/\sqrt{Re_x}$ vs. X' , lower surface

e) $\delta_2 = \delta_3 = -10$

f) $\delta_2 = \delta_3 = -20$

g) $\delta_2 = \delta_3 = -30$

h) $\delta_2 = \delta_3 = -39$

Contrails

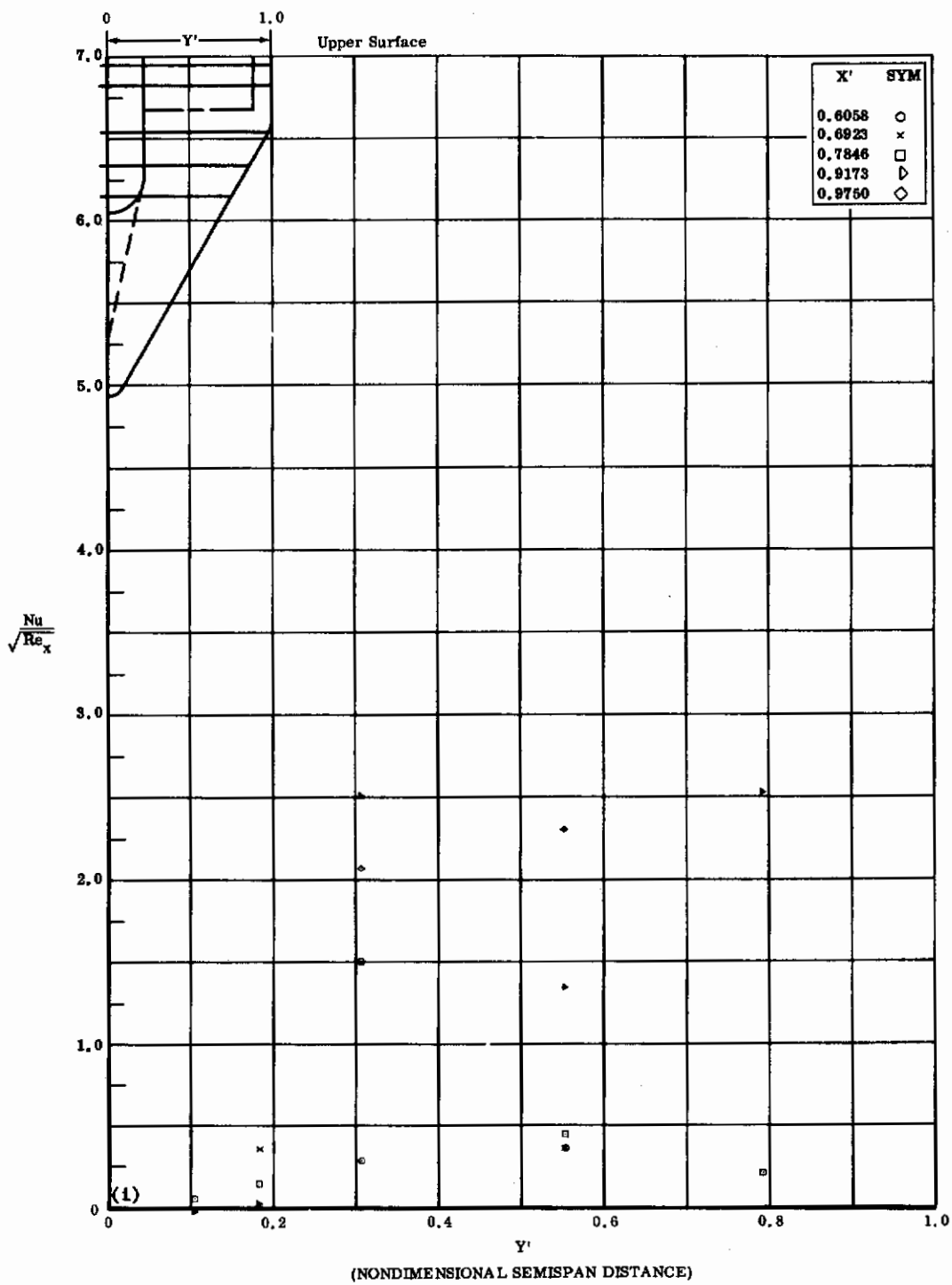


Fig. 16i Configuration IV, $\alpha = 0$, $\beta_2 = \beta_3 = -10$
 $\text{Nu}/\sqrt{\text{Re}_x}$ vs. Y' upper surface

Contrails

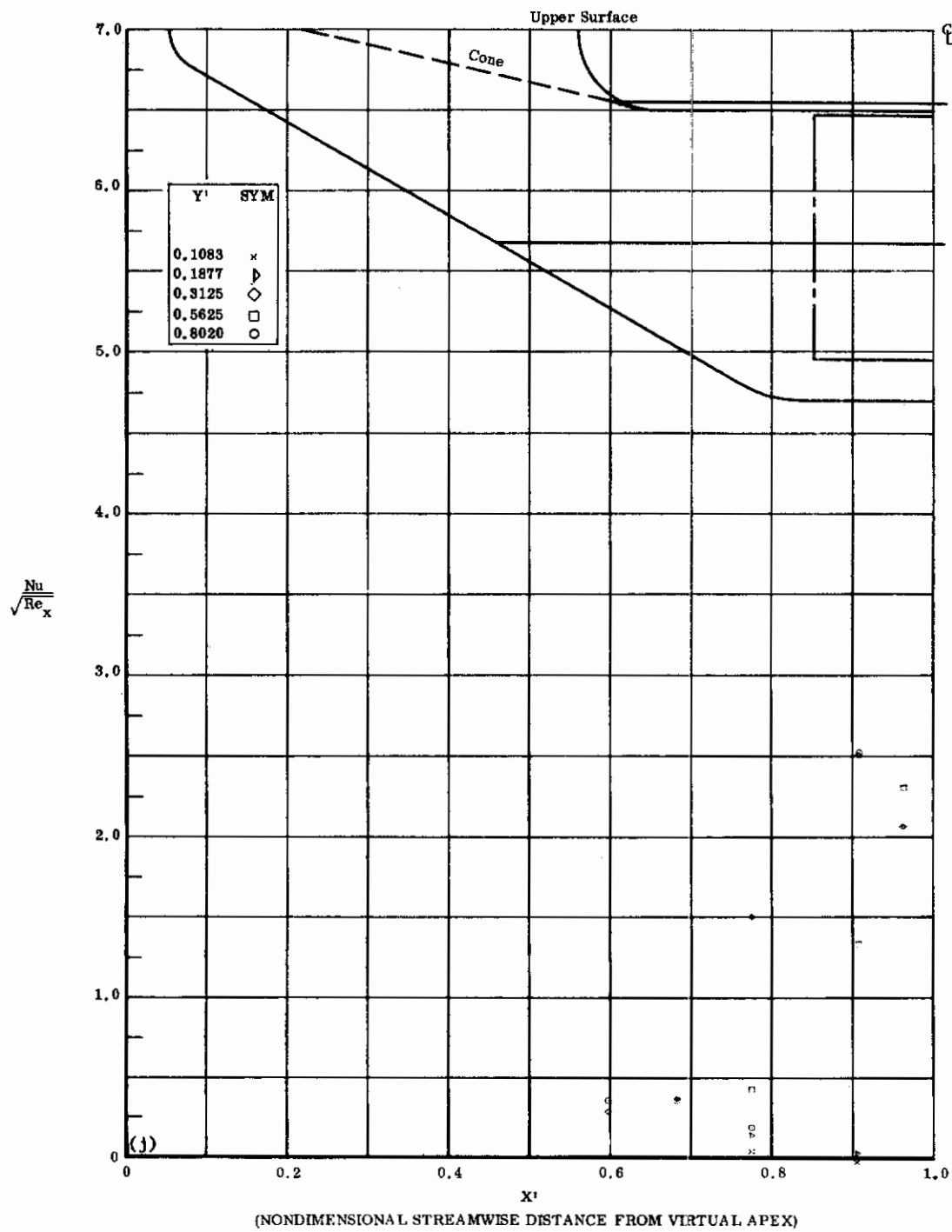


Fig. 16j Configuration IV, $\alpha = 0$, $\delta_2 = \delta_3 = -10$
 $Nu/\sqrt{Re_x}$ vs. X' upper surface

Contrails

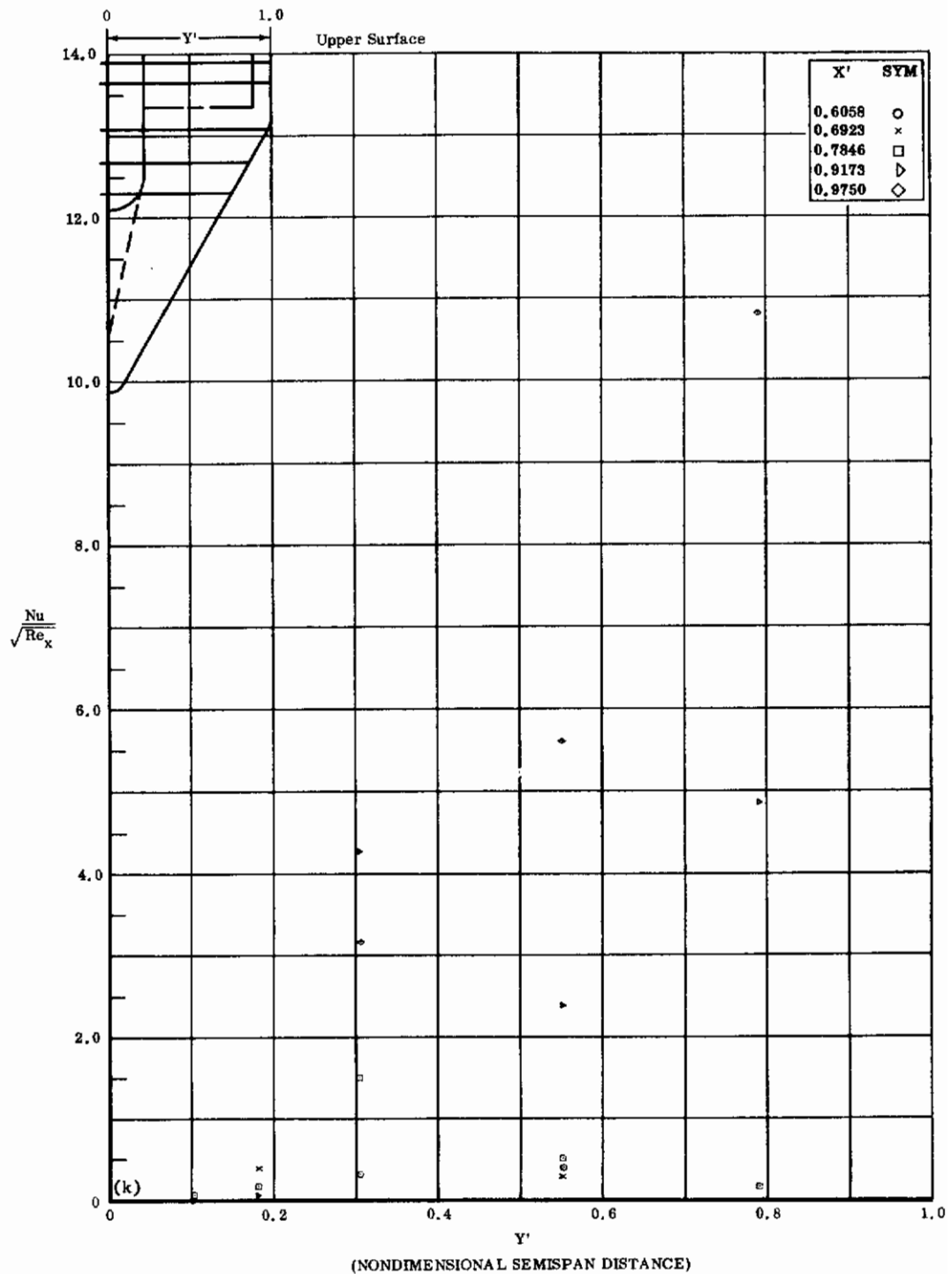


Fig. 16k Configuration IV, $\alpha = 0$, $\delta_2 = \delta_3 = -20$
 $\text{Nu}/\sqrt{\text{Re}_x}$ vs. Y' upper surface

Contrails

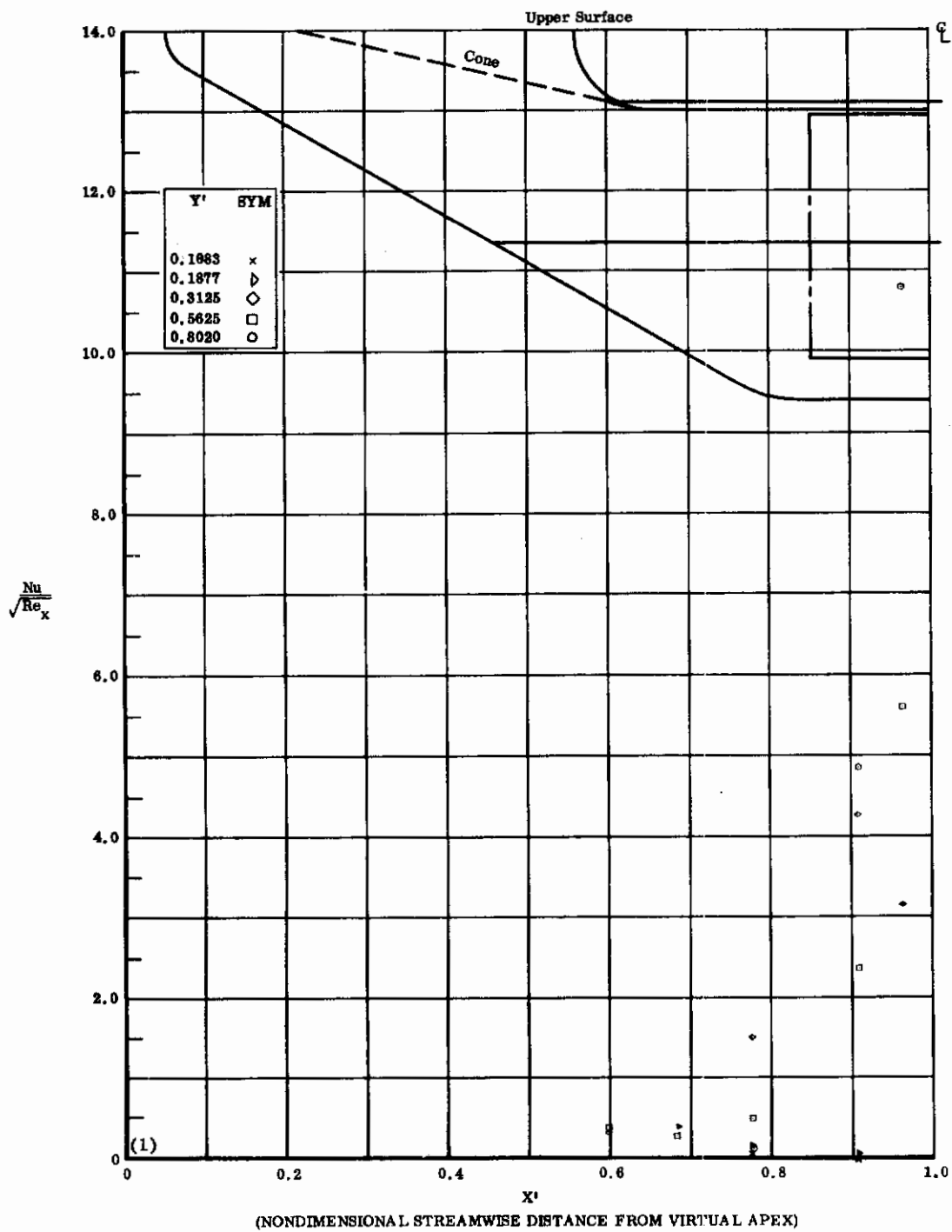


Fig. 16t Configuration IV, $\alpha = 0$, $\delta_2 = \delta_3 = -20$

$Nu/\sqrt{Re_x}$ vs. X' upper surface

Contrails

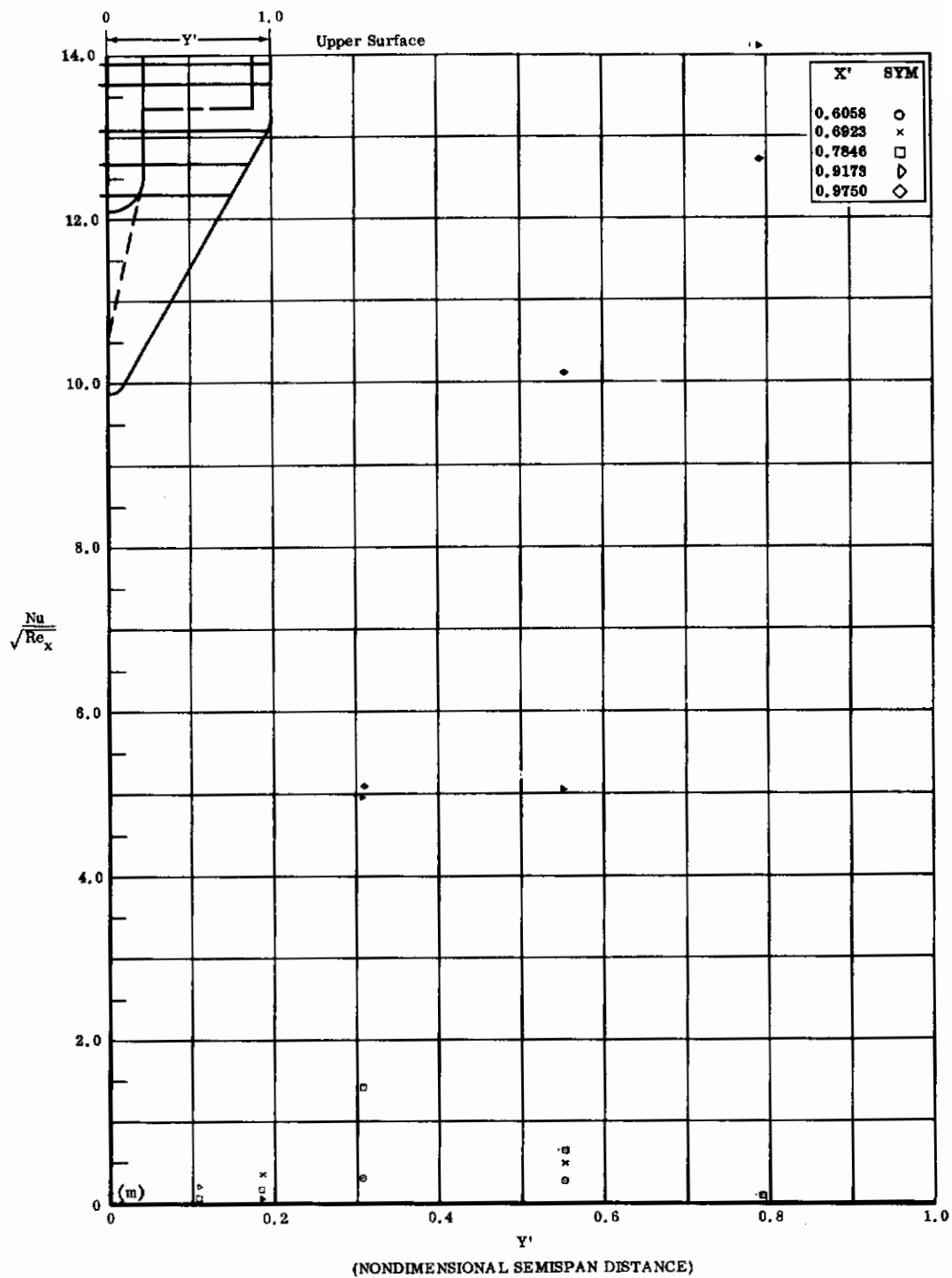


Fig. 16m Configuration IV, $\alpha = 0$, $\delta_2 = \delta_3 = -30$
 $Nu/\sqrt{Re_x}$ vs. Y' upper surface

Contrails

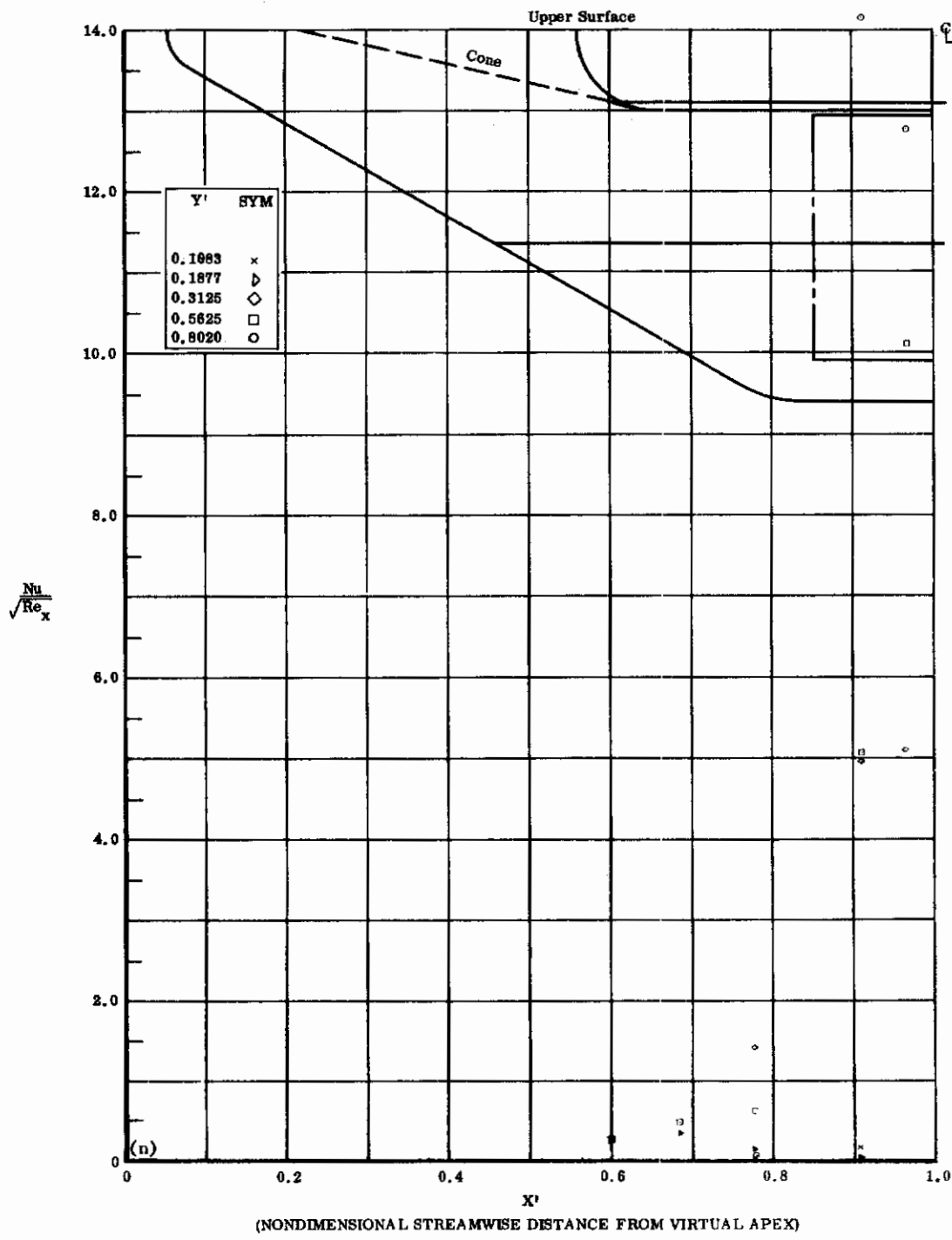


Fig. 16n Configuration IV, $\alpha = 0$, $\delta_2 = \delta_3 = -30$
 $Nu/\sqrt{Re_x}$ vs. X^i upper surface

Contrails

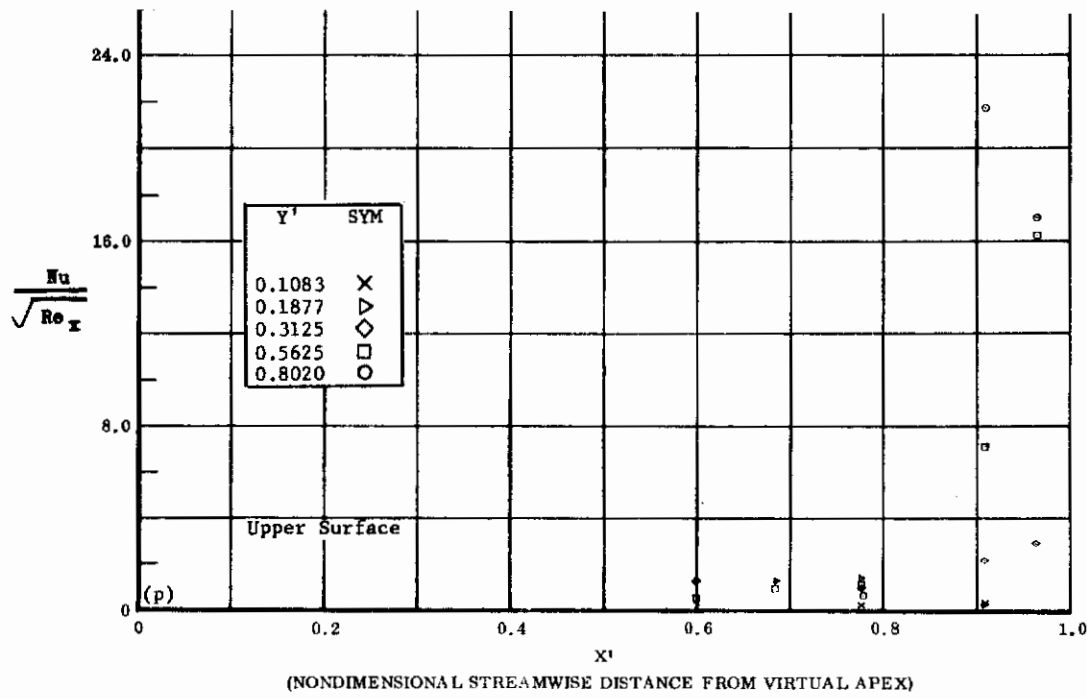
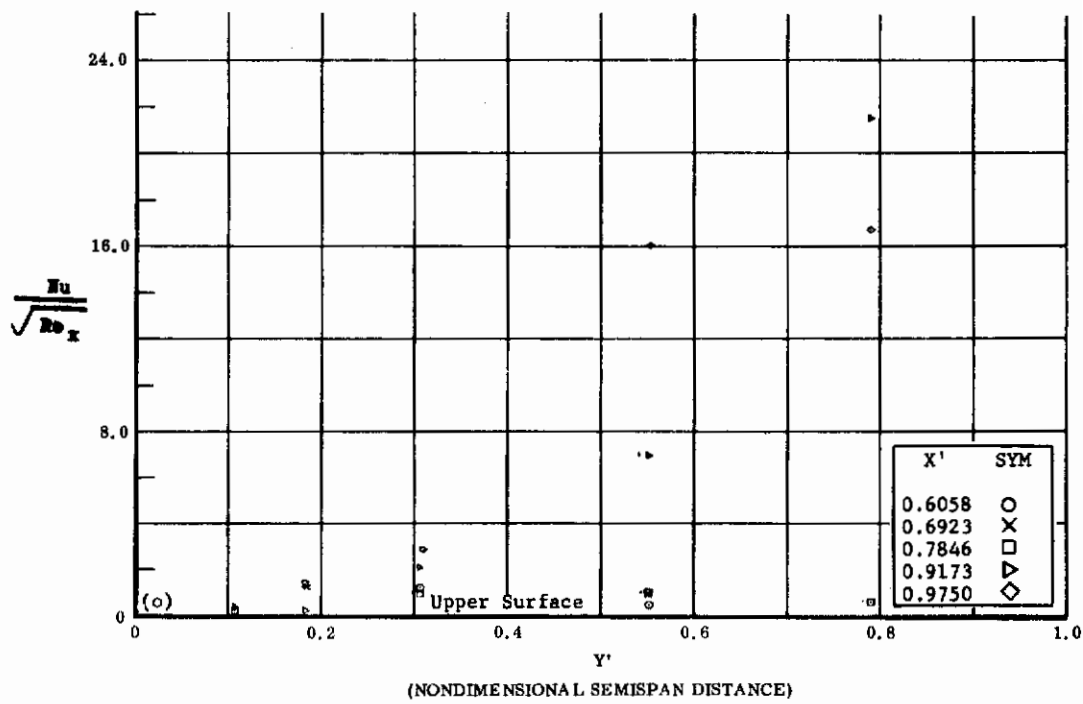


Fig. 16 Configuration IV, $\alpha = 0$, $\delta_2 = \delta_3 = -39$

- (a) $Nu/\sqrt{Re_x}$ vs. Y' upper surface
- (p) $Nu/\sqrt{Re_x}$ vs. X' upper surface

Contrails

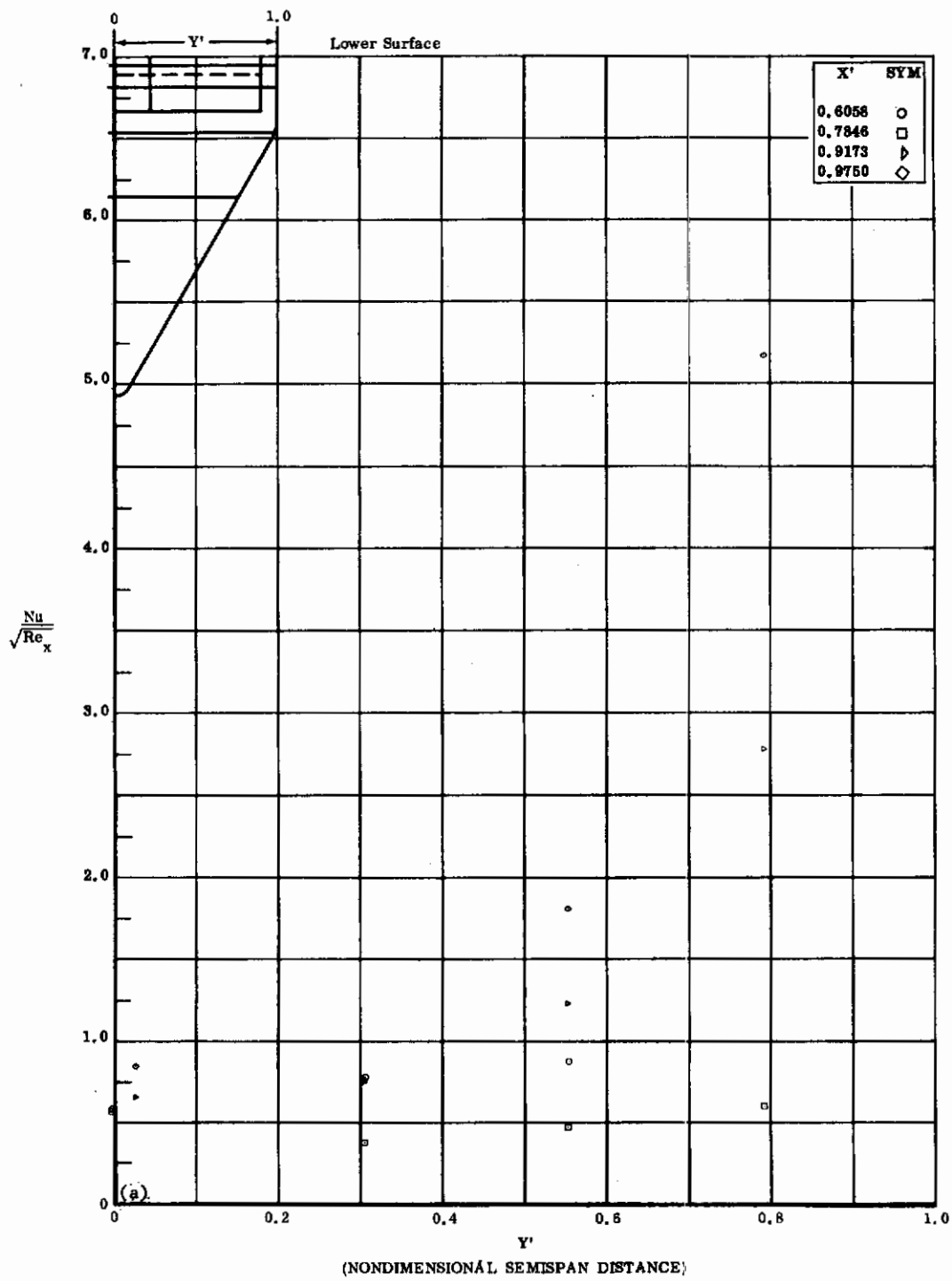


Fig. 17a Configuration IV, $\alpha = +10$, $\delta_2 = \delta_3 = 0$
 $Nu/\sqrt{Re_x}$ vs. Y' lower surface

Contrails

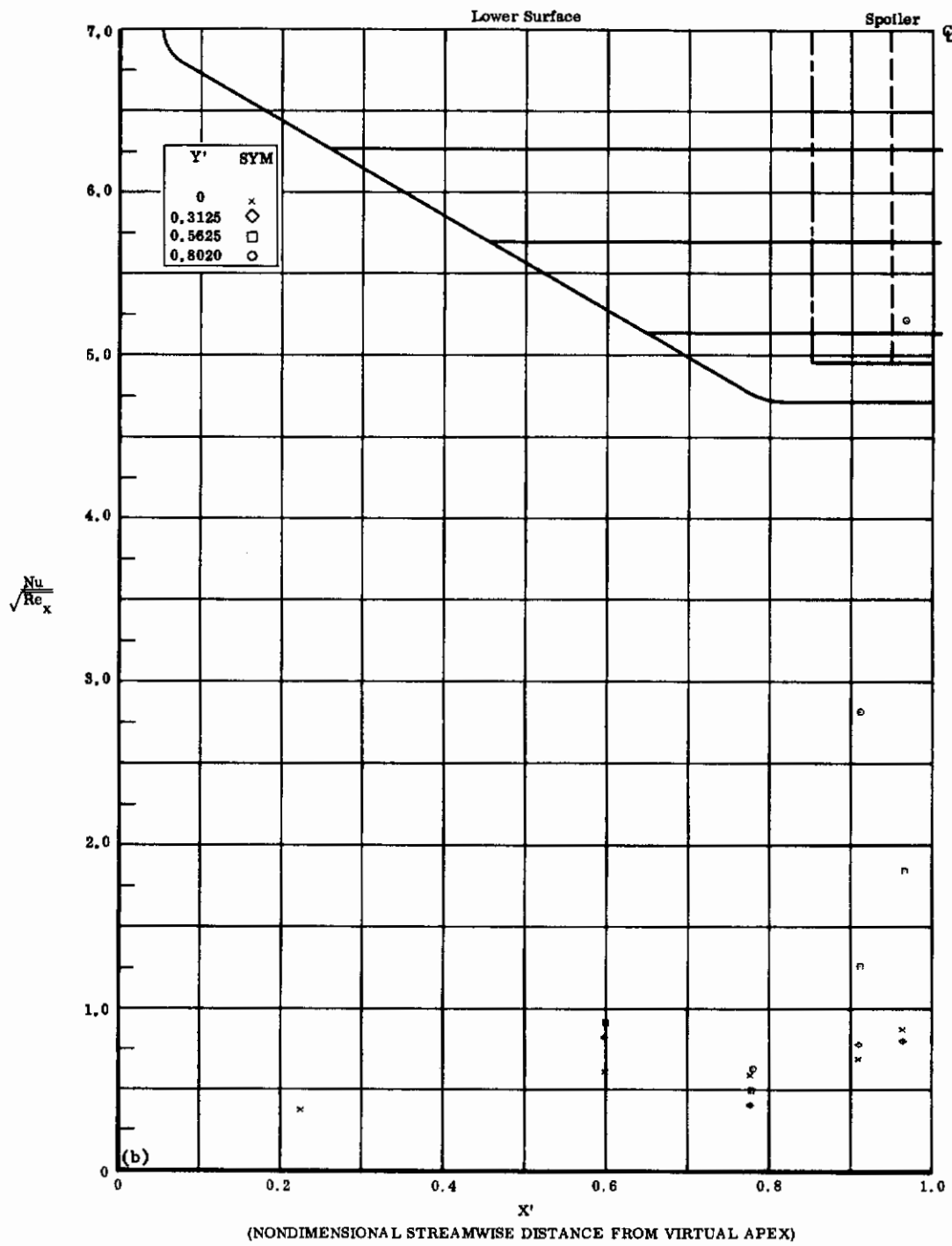


Fig. 17b Configuration IV, $\alpha = +10$, $\delta_2 = \delta_3 = 0$
 $Nu/\sqrt{Re_x}$ vs. X' lower surface

Contrails

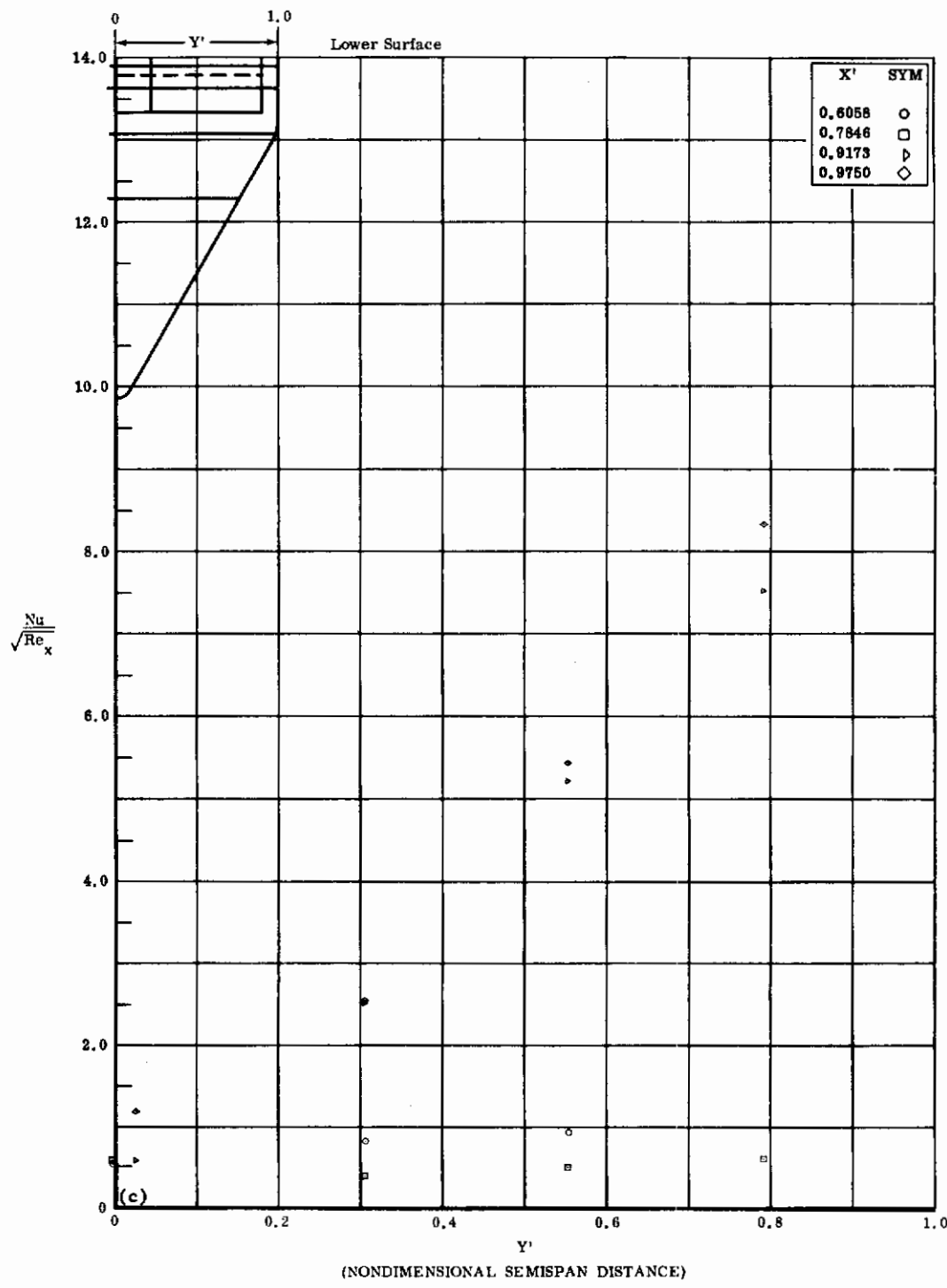


Fig. 17c Configuration IV, $\alpha = +10$, $\delta_2 = \delta_3 = +10$
 $\text{Nu}/\sqrt{\text{Re}_x}$ vs. Y' lower surface

Contrails

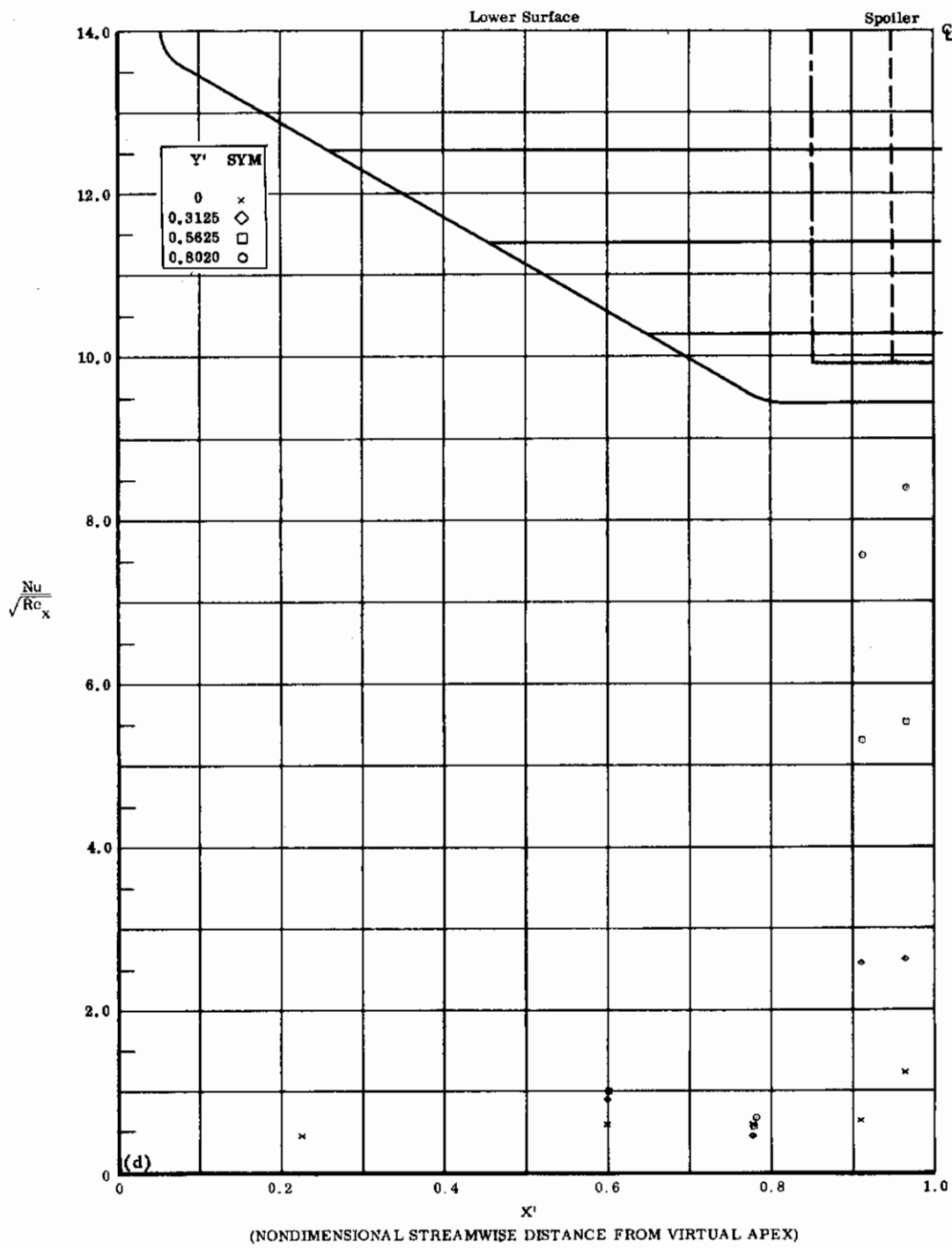


Fig. 17d Configuration IV, $\alpha = +10$, $\delta_2 = \delta_3 = +10$
 $\frac{Nu}{\sqrt{Re_x}}$ vs. X' lower surface

Contrails

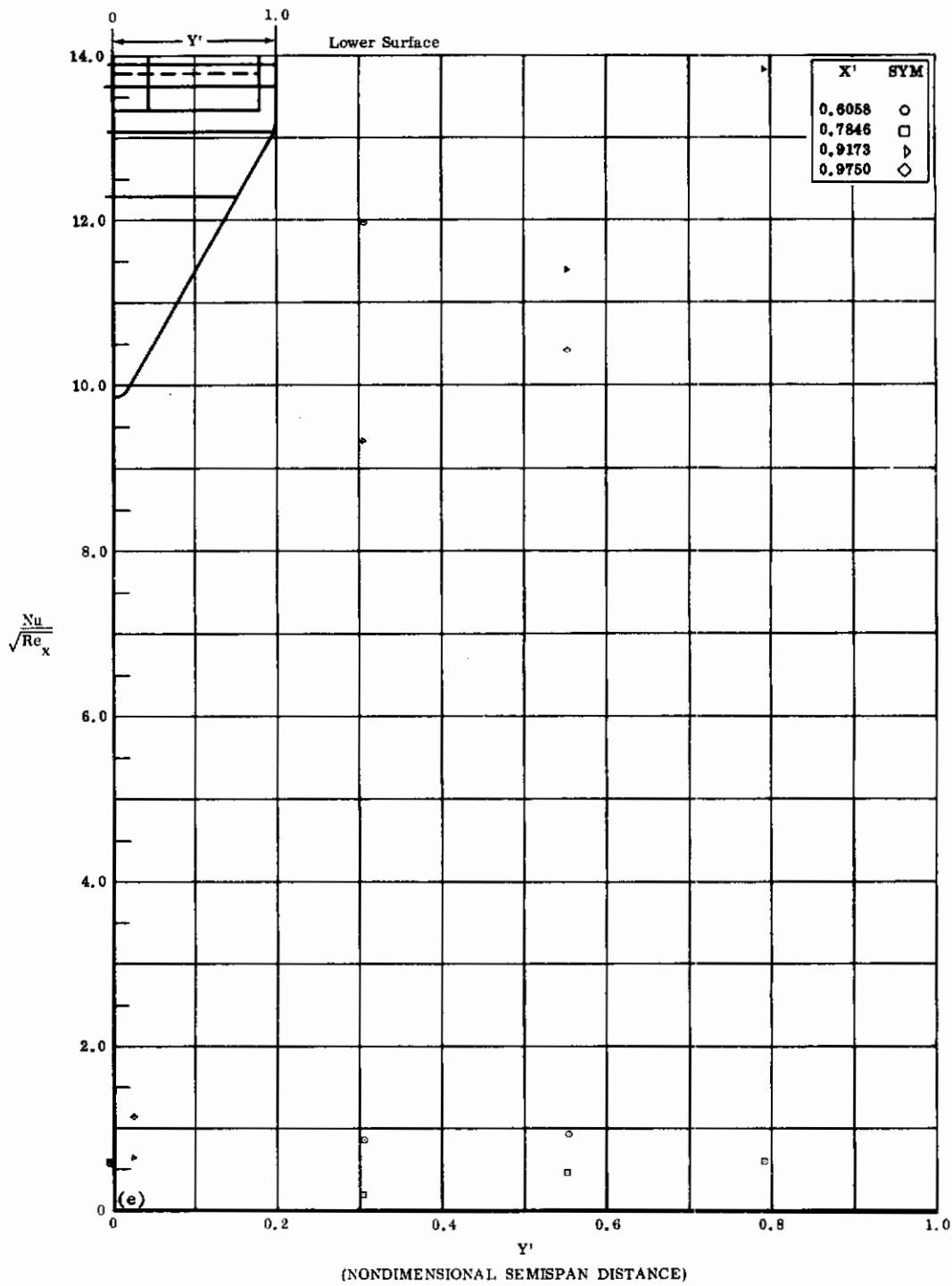


Fig. 17e Configuration IV, $\alpha = +10$, $s_2 = s_3 = +20$
 $Nu/\sqrt{Re_x}$ vs. Y' lower surface

Contrails

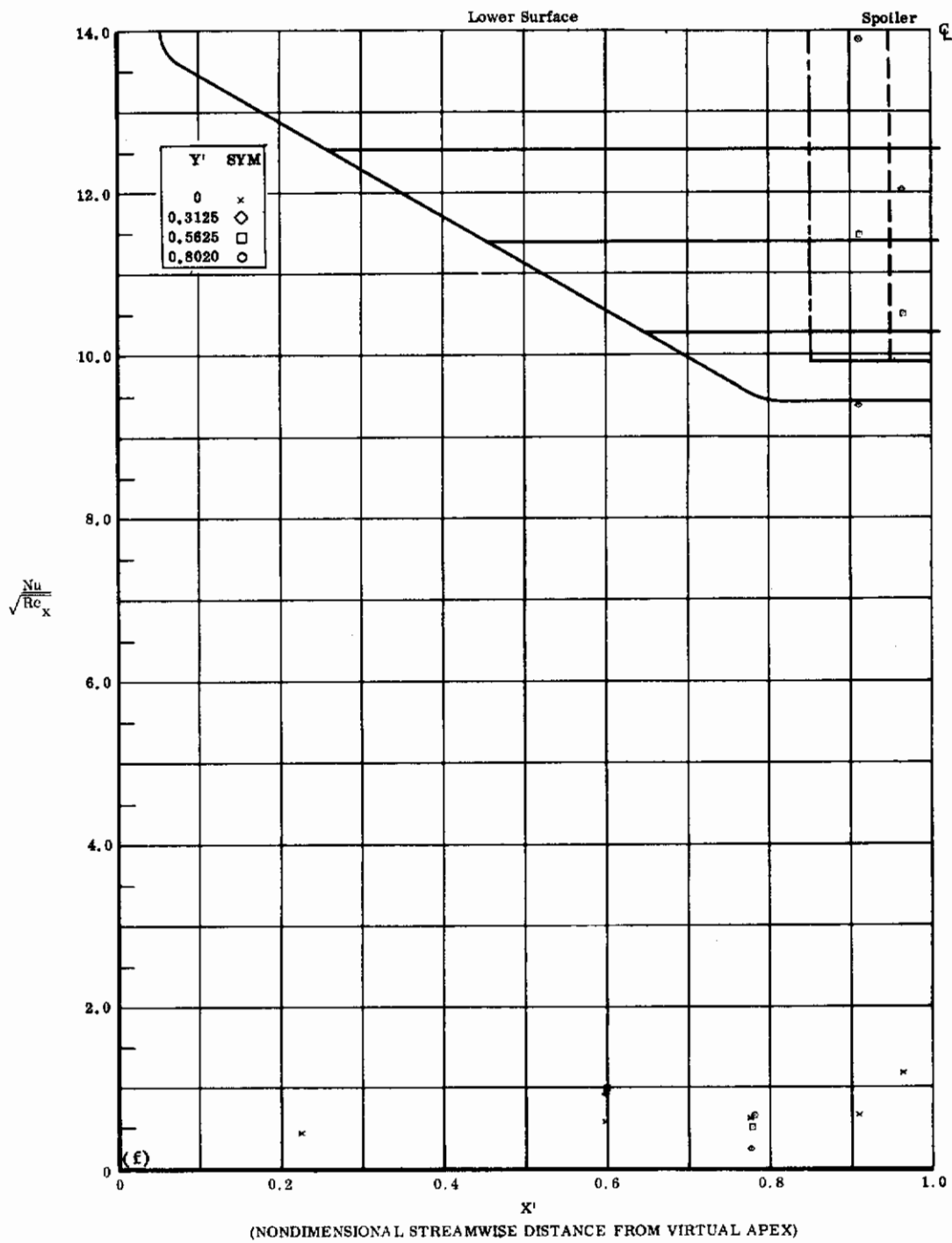


Fig. 17f Configuration IV, $\alpha = +10$, $b_2 = b_3 = +20$
 $\frac{Nu}{\sqrt{Re_x}}$ vs. X' lower surface

Contrails

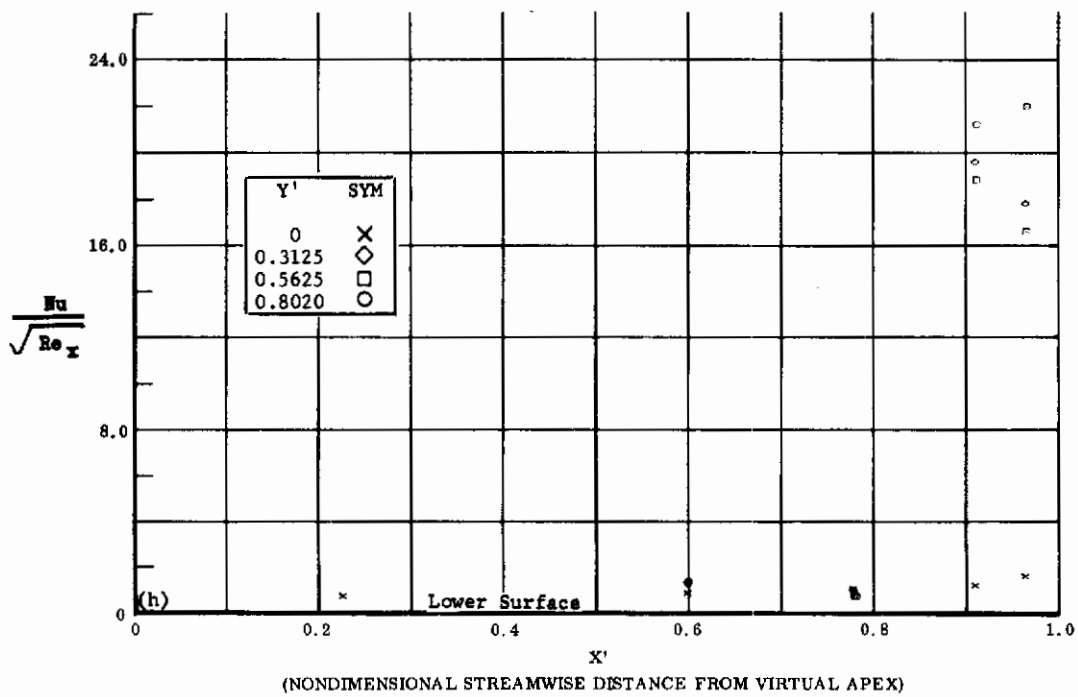
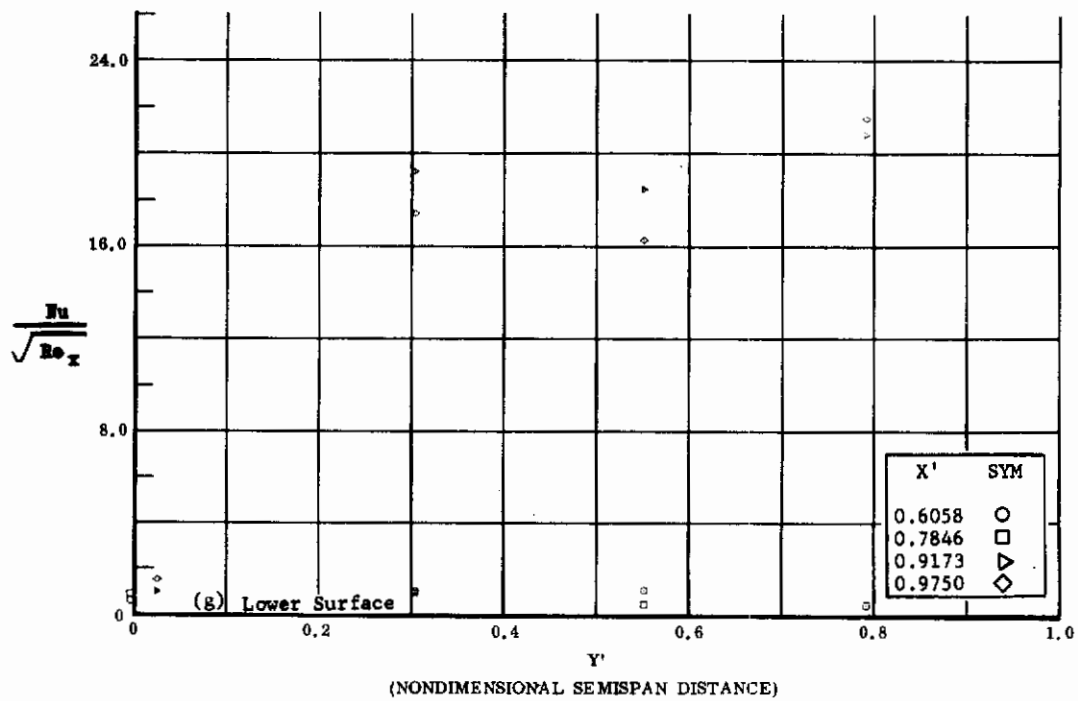


Fig. 17 Configuration IV, $\alpha = +10$, $\delta_2 = \delta_3 = +30$

g) $\text{Nu}/\sqrt{\text{Re}_x}$ vs. Y' lower surface

h) $\text{Nu}/\sqrt{\text{Re}_x}$ vs. X' lower surface

Contrails

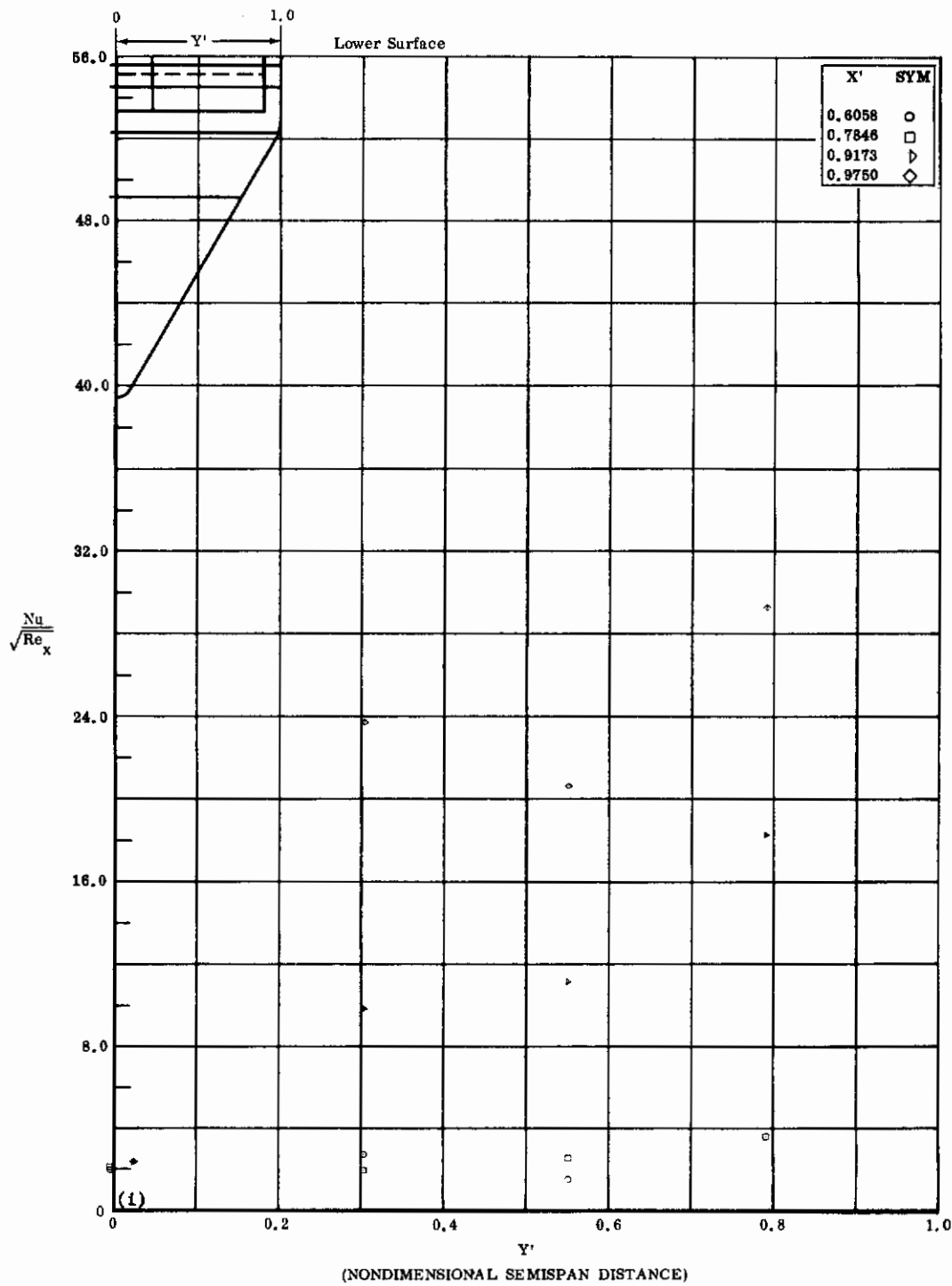


Fig. 17i Configuration IV, $\alpha = +10$, $\delta_2 = \delta_3 = +39$
 $Nu/\sqrt{Re_x}$ vs. Y' lower surface

Contrails

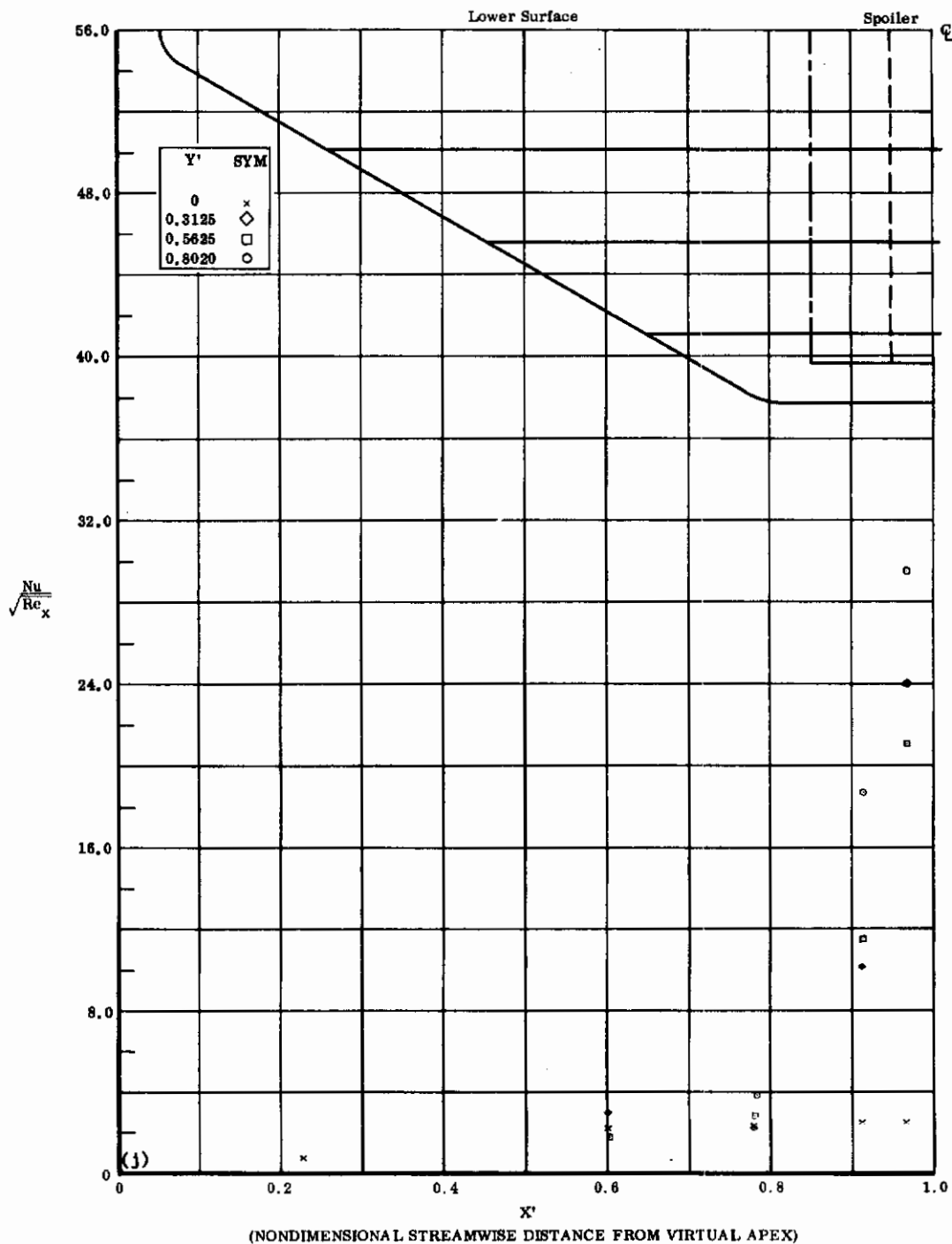


Fig. 17j Configuration IV, $\alpha = +10$, $b_2 = b_3 = +39$
 $\frac{Nu}{\sqrt{Re_x}}$ vs. X' lower surface

Contrails

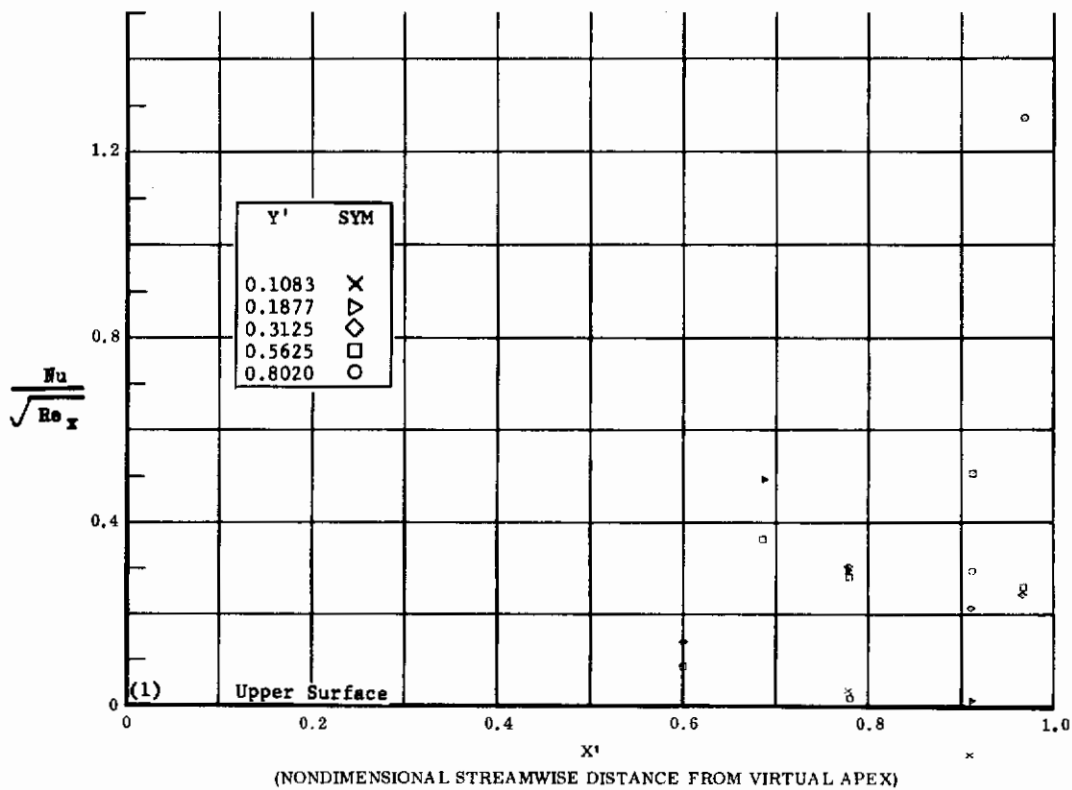
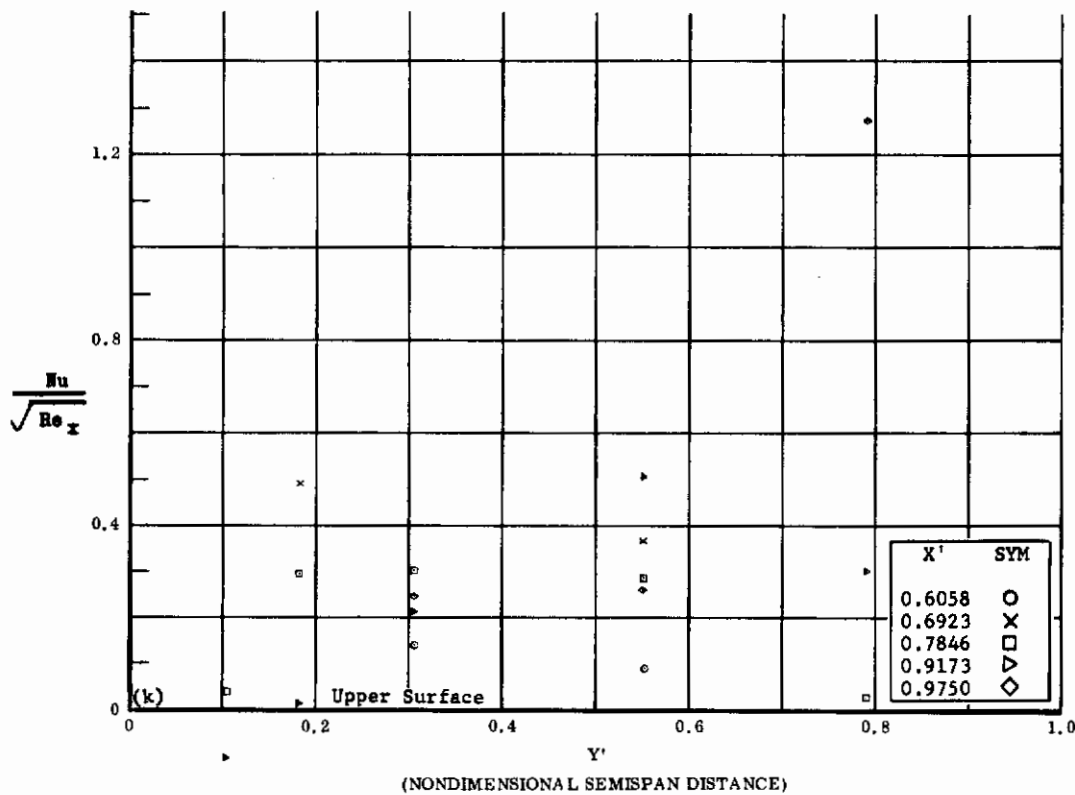
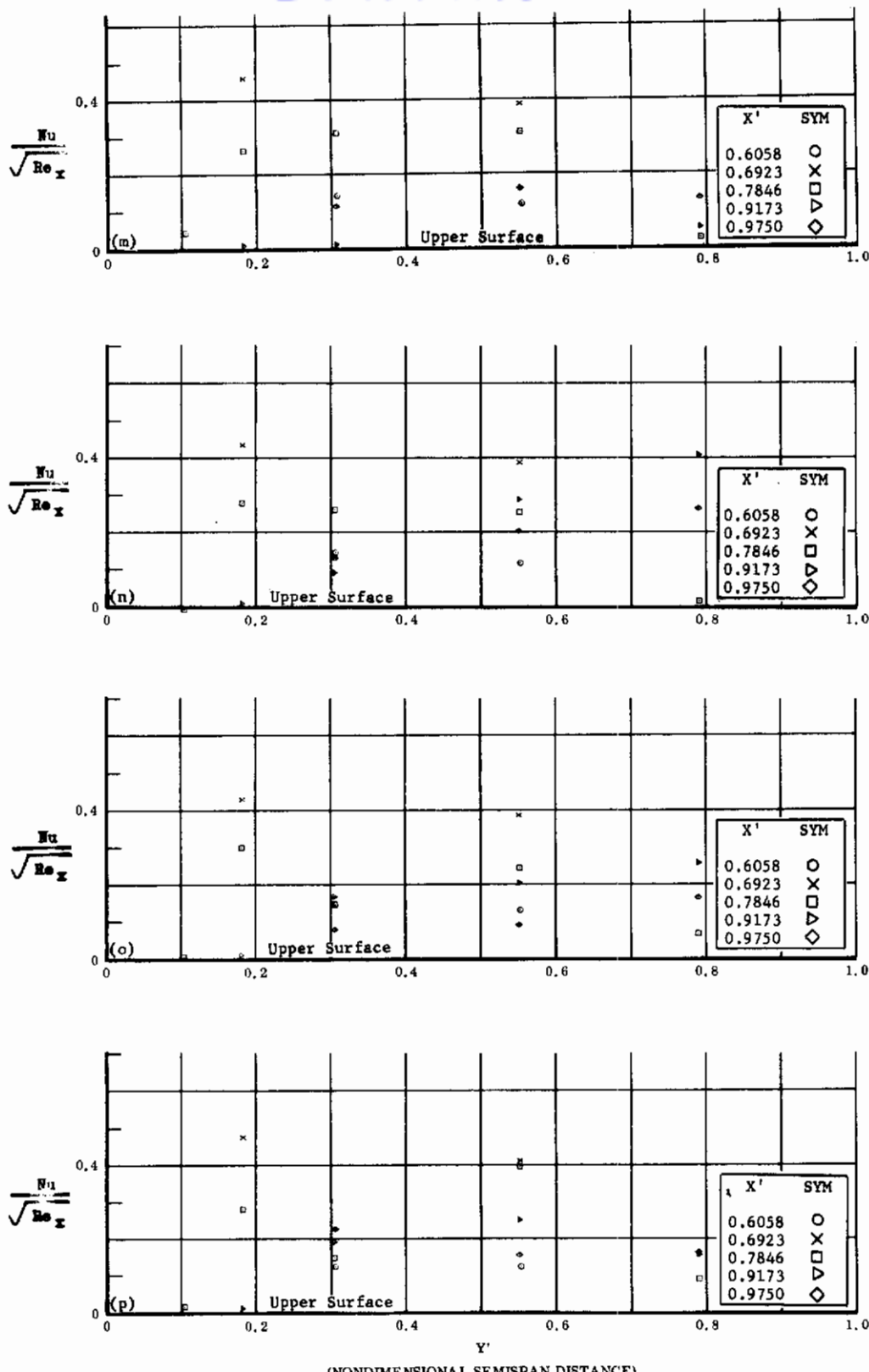


Fig. 17 Configuration IV, $\alpha = +10$, $\delta_2 = \delta_3 = 0$

k) $\text{Nu}/\sqrt{\text{Re}_x}$ vs. Y' upper surface

l) $\text{Nu}/\sqrt{\text{Re}_x}$ vs. X' upper surface

Contrails



(NONDIMENSIONAL SEMISPAN DISTANCE)

Fig. 17 Configuration IV, $\alpha = +10$, $Nu/\sqrt{Re_x}$ vs. Y' , upper surface

m) $\delta_2 = \delta_3 = +10$

n) $\delta_2 = \delta_3 = +20$

o) $\delta_2 = \delta_3 = +30$

p) $\delta_2 = \delta_3 = +39$

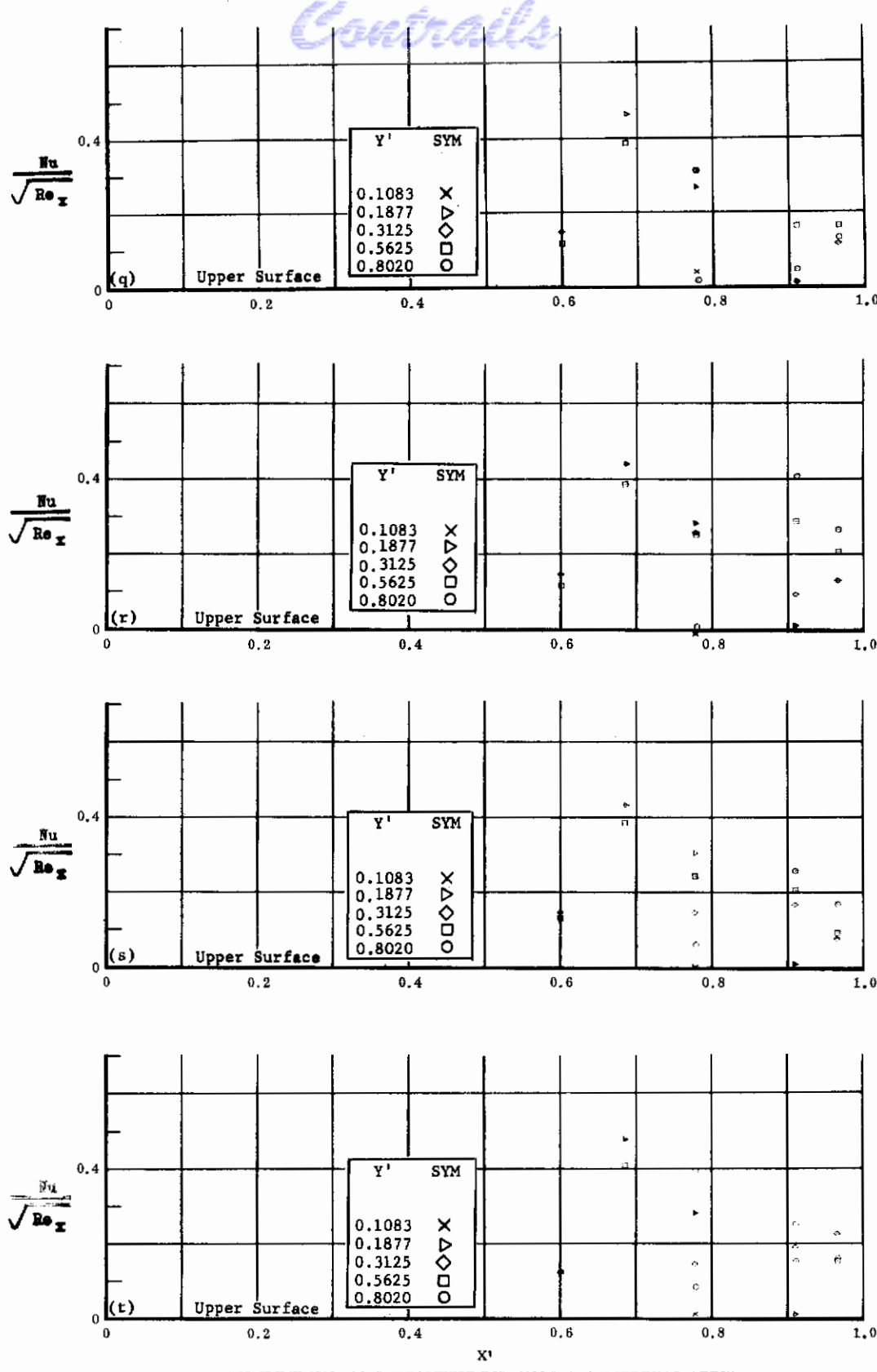


Fig. 17 Configuration IV, $\alpha = +10$, $Nu/\sqrt{Re_x}$ vs. X' , upper surface

q) $\delta_2 = \delta_3 = +10$

r) $\delta_2 = \delta_3 = +20$

s) $\delta_2 = \delta_3 = +30$

t) $\delta_2 = \delta_3 = +39$

Contrails

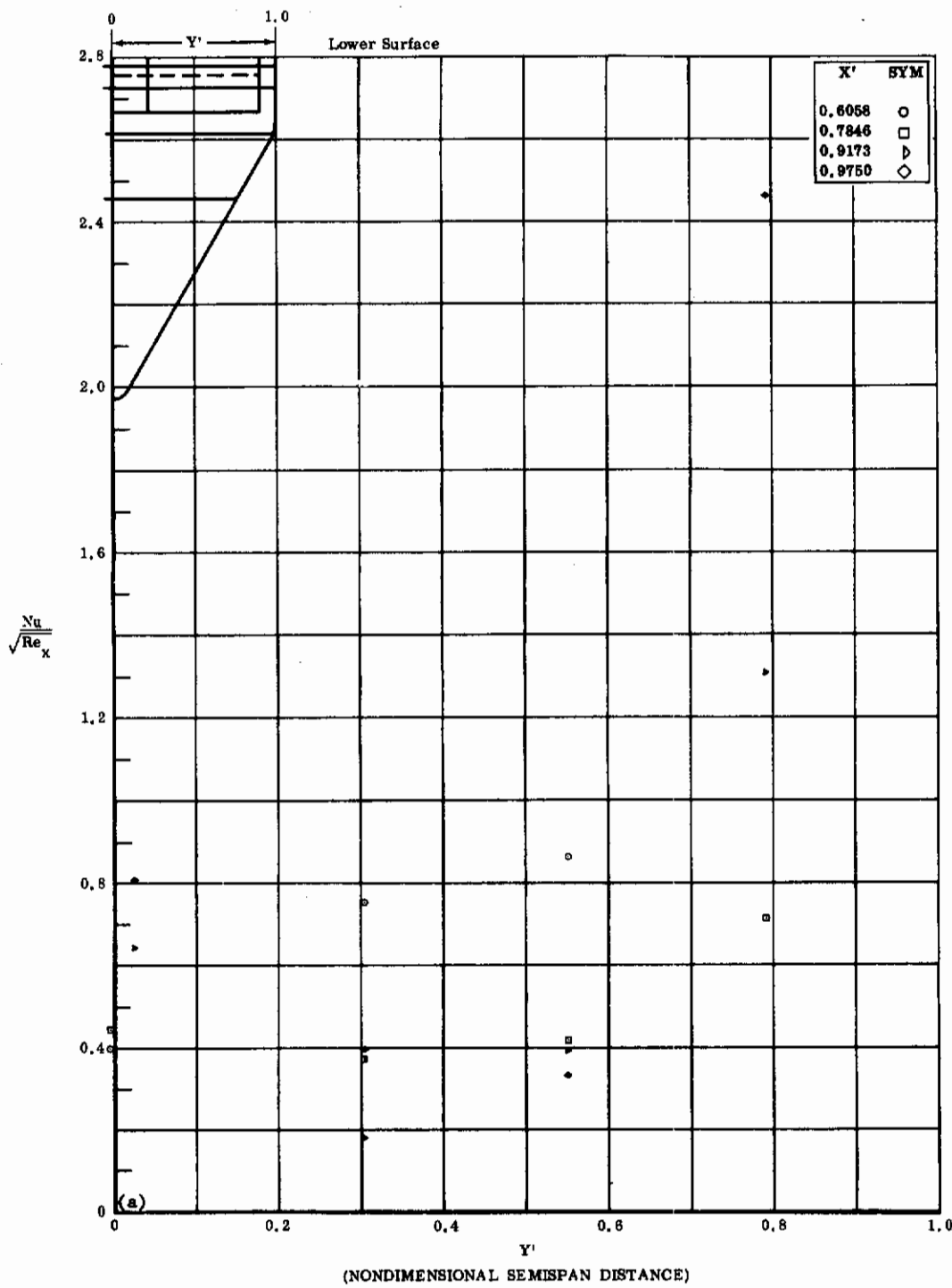


Fig. 18a Configuration IV, $\alpha = +10$, $\delta_2 = \delta_3 = -10$
 $Nu/\sqrt{Re_x}$ vs. Y' lower surface

Contrails

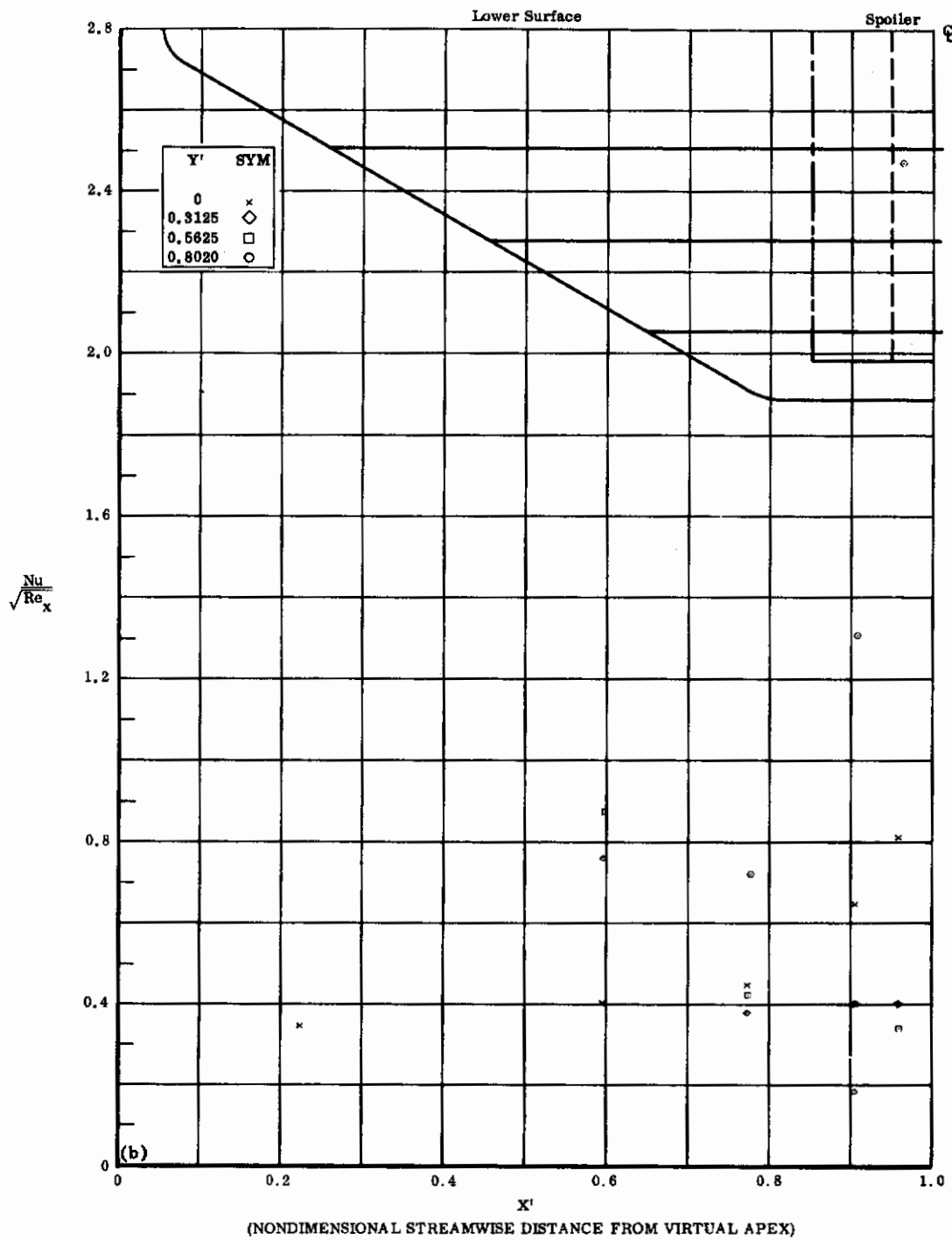


Fig. 18b Configuration IV, $\alpha = +10$, $\delta_2 = \delta_3 = -10$
 $Nu/\sqrt{Re_x}$ vs. X' lower surface

Contrails

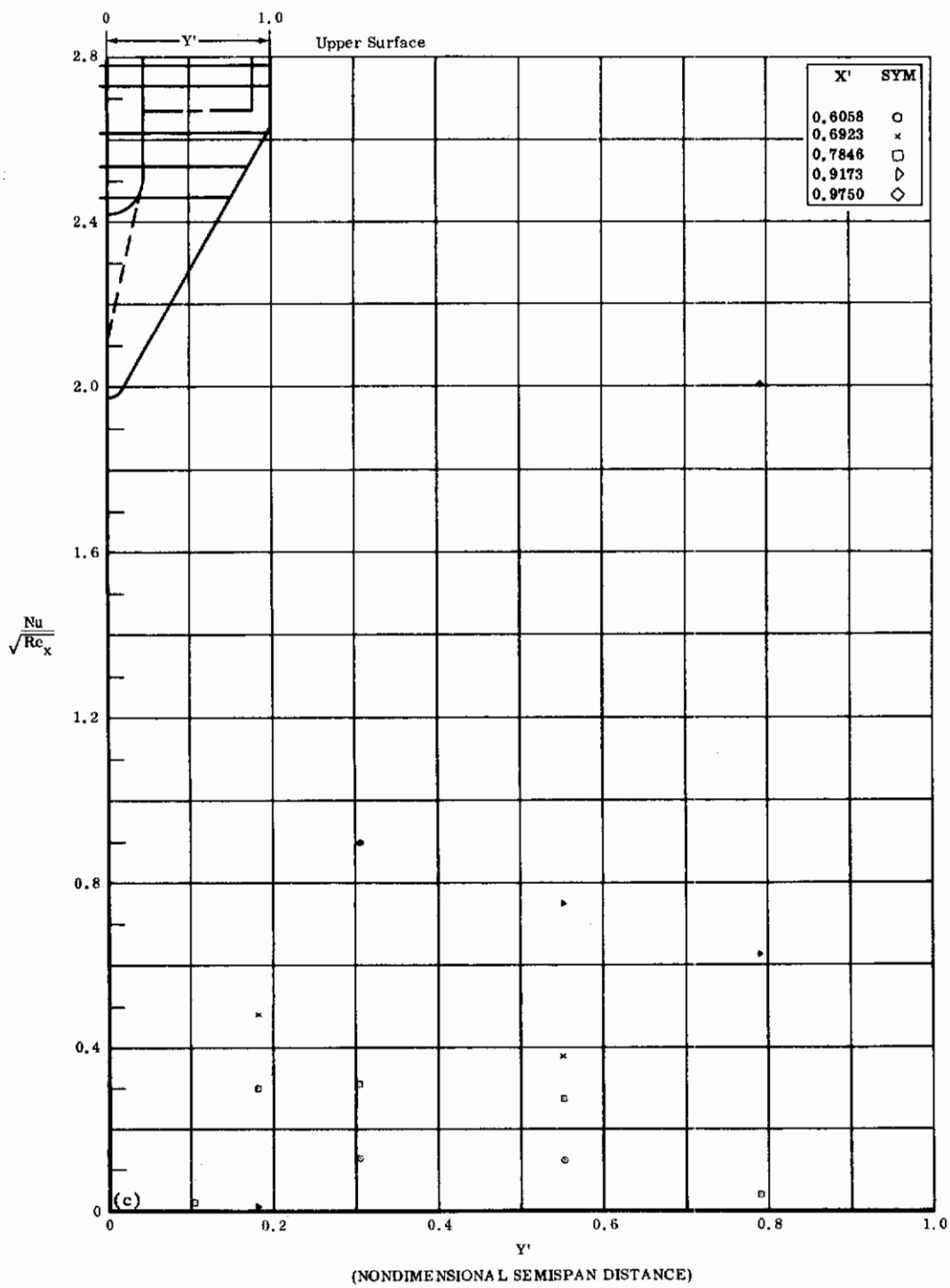


Fig. 18c Configuration IV, $\alpha = +10$, $\delta_2 = \delta_3 = -10$
 $Nu/\sqrt{Re_x}$ vs. Y' upper surface

Contrails

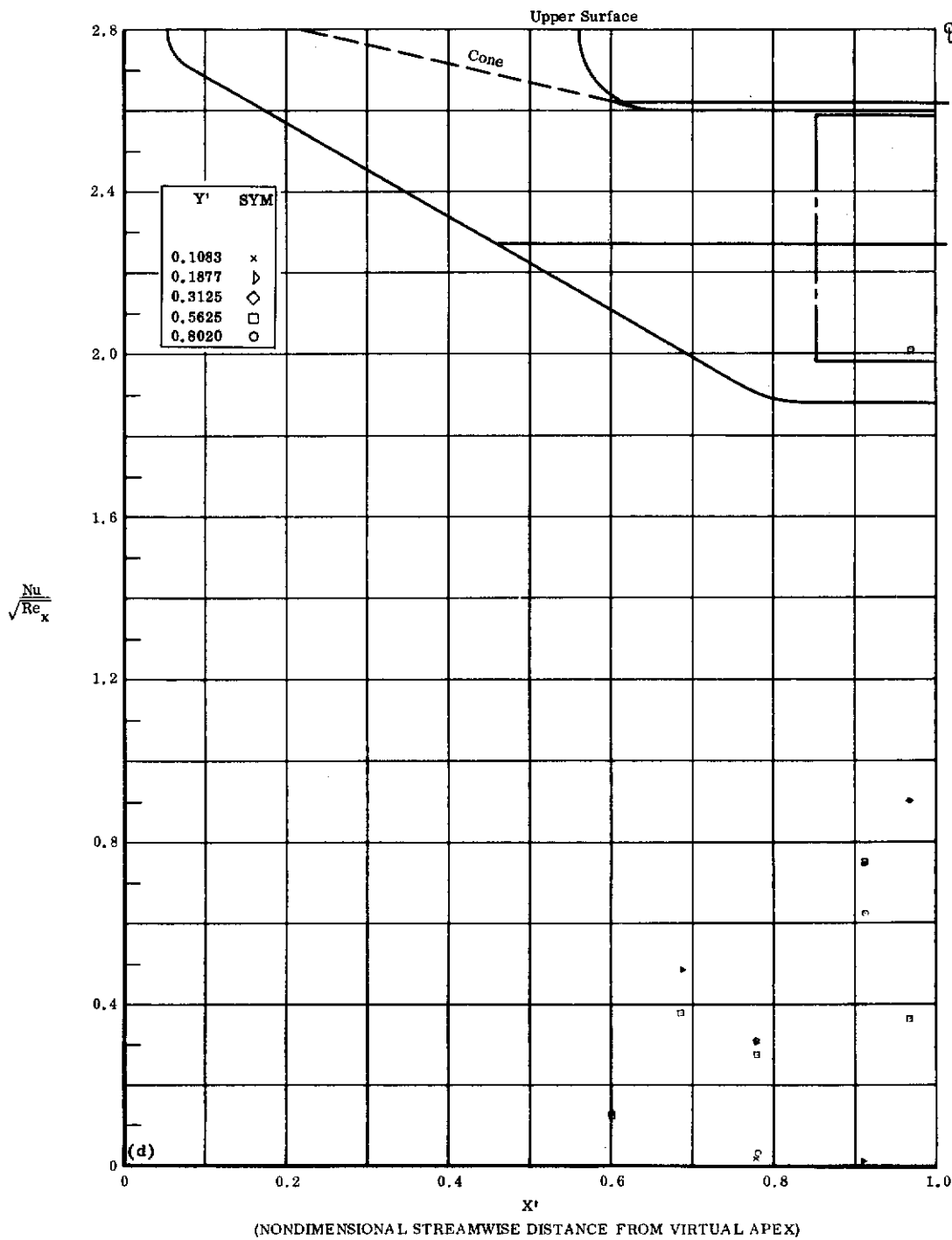


Fig. 18d Configuration IV, $\alpha = +10$, $\delta_2 = \delta_3 = -10$
 $Nu/\sqrt{Re_x}$ vs. X' upper surface

Contrails

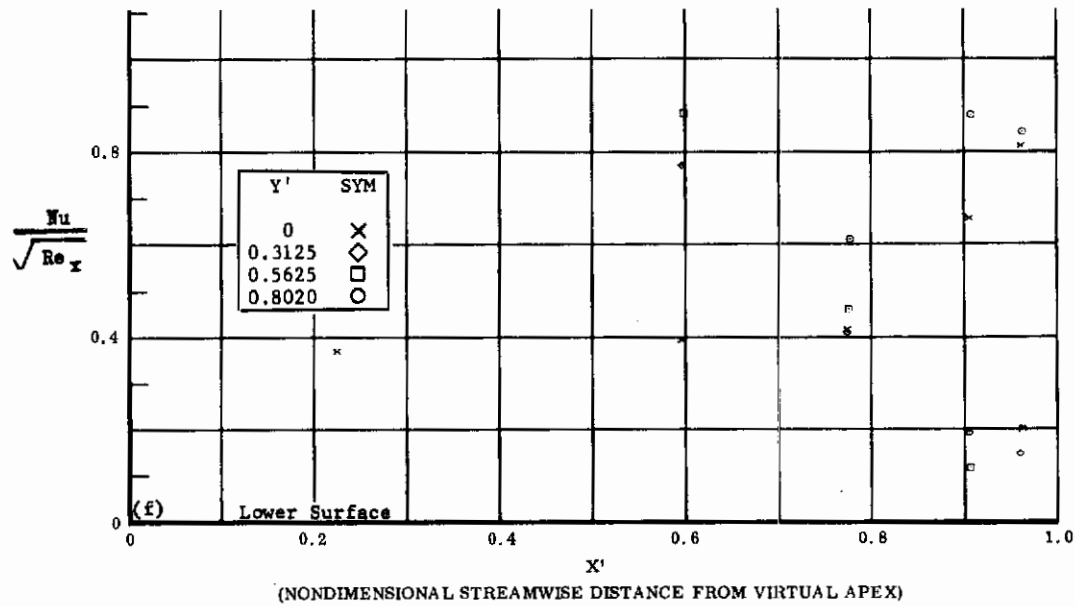
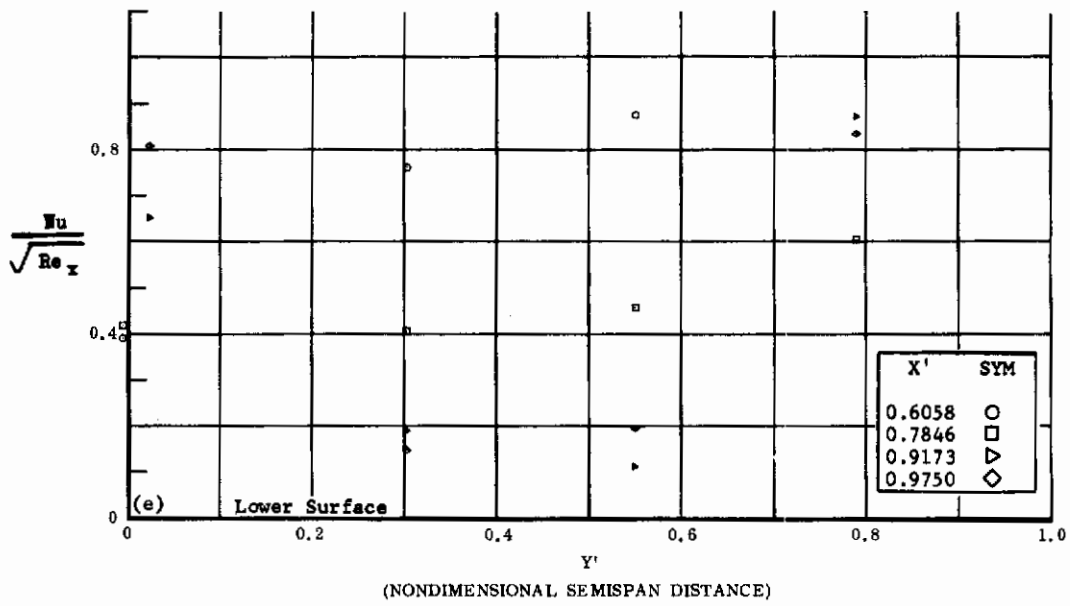


Fig. 18 Configuration IV, $\alpha = +10$, $\delta_2 = \delta_3 = -20$

e) $Nu/\sqrt{Re_x}$ vs. Y' lower surface

f) $Nu/\sqrt{Re_x}$ vs. X' lower surface

Contrails

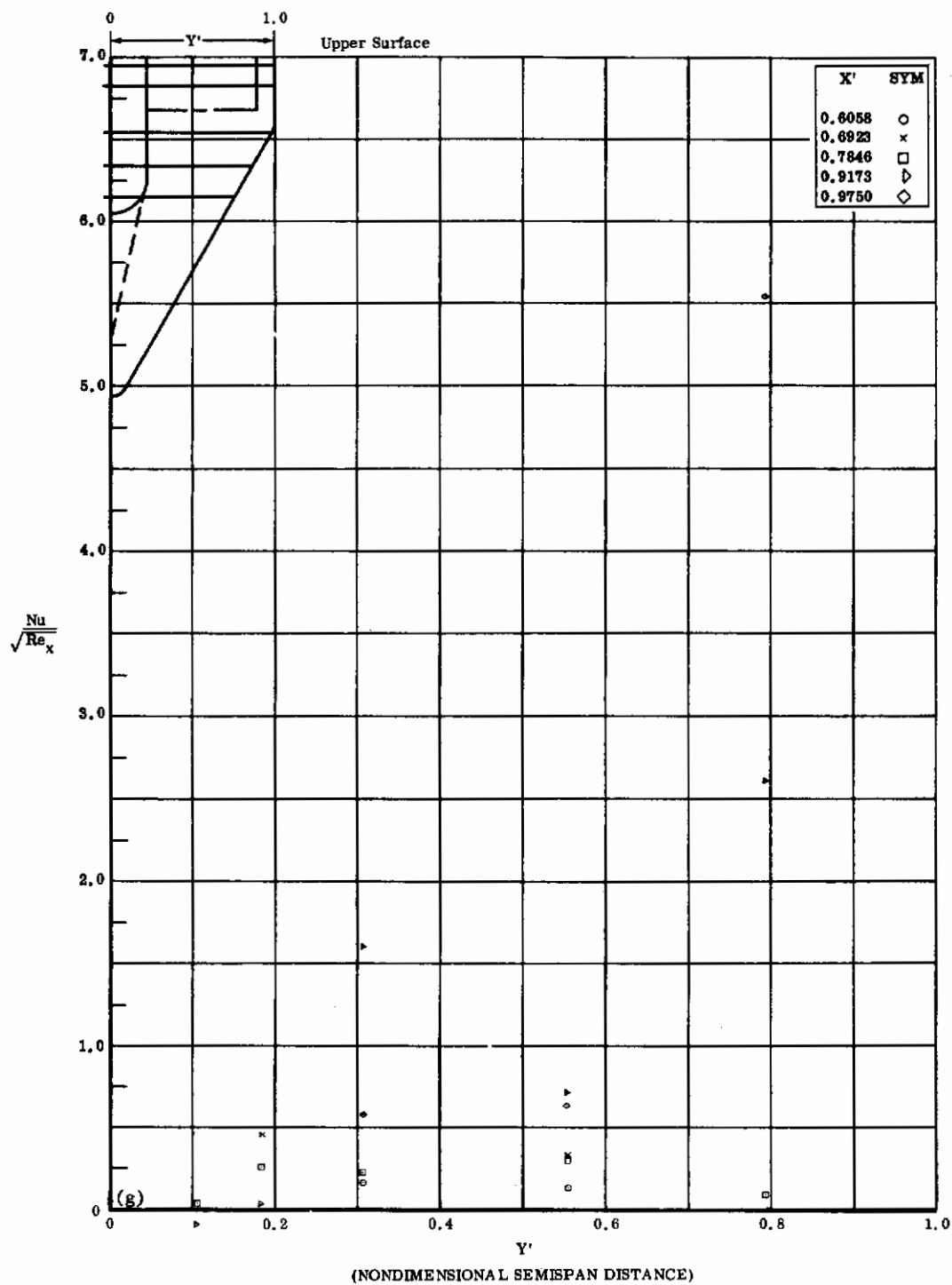


Fig. 18g Configuration IV, $\alpha = +10$, $\delta_2 = \delta_3 = -20$
 $\frac{Nu}{\sqrt{Re_x}}$ vs. Y' upper surface

Contrails

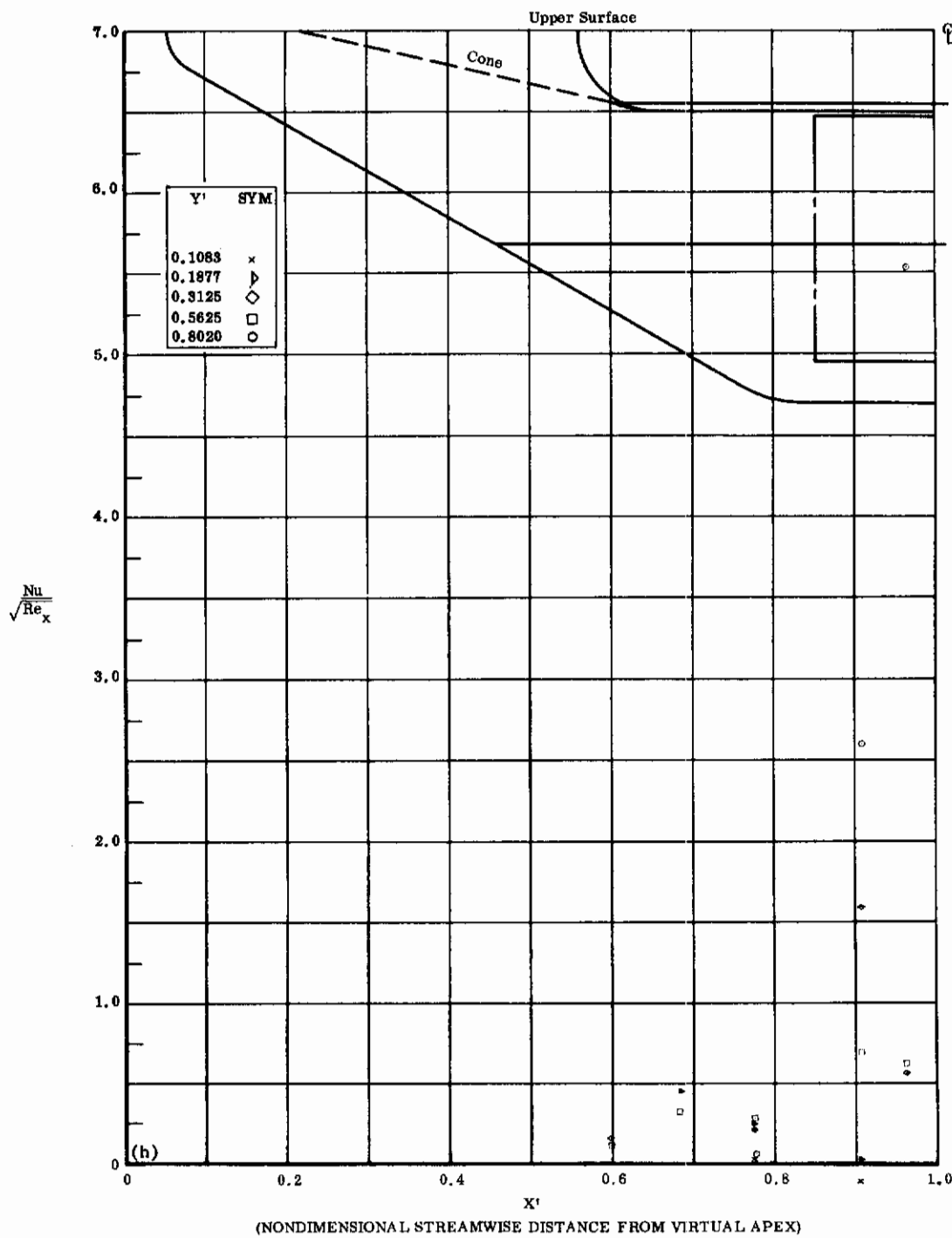


Fig. 18h Configuration IV, $\alpha = +10$, $\delta_2 = \delta_3 = -20$
 $\frac{Nu}{\sqrt{Re_x}}$ vs. X' upper surface

Contrails

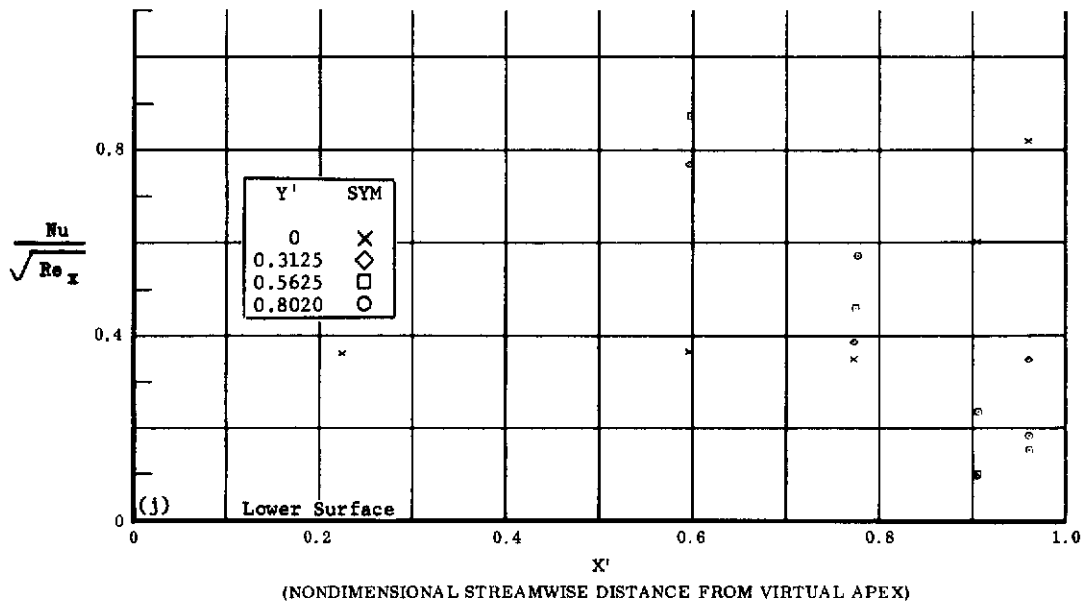
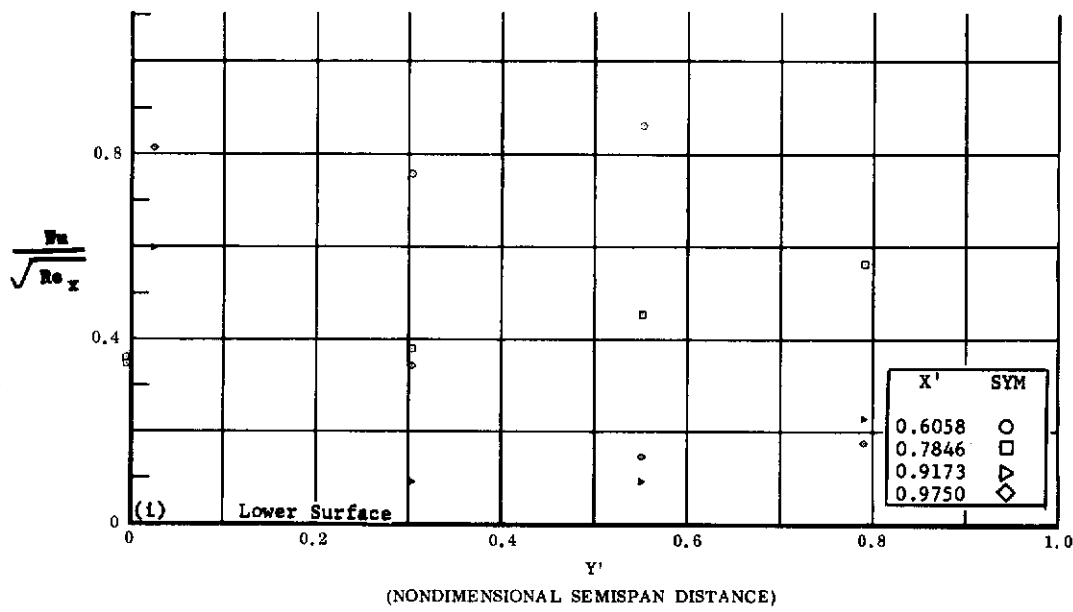


Fig. 18 Configuration IV, $\alpha = +10$, $\delta_2 = \delta_3 = -30$

i) $\text{Nu}/\sqrt{\text{Re}_x}$ vs. Y' lower surface

j) $\text{Nu}/\sqrt{\text{Re}_x}$ vs. X' lower surface

Contrails

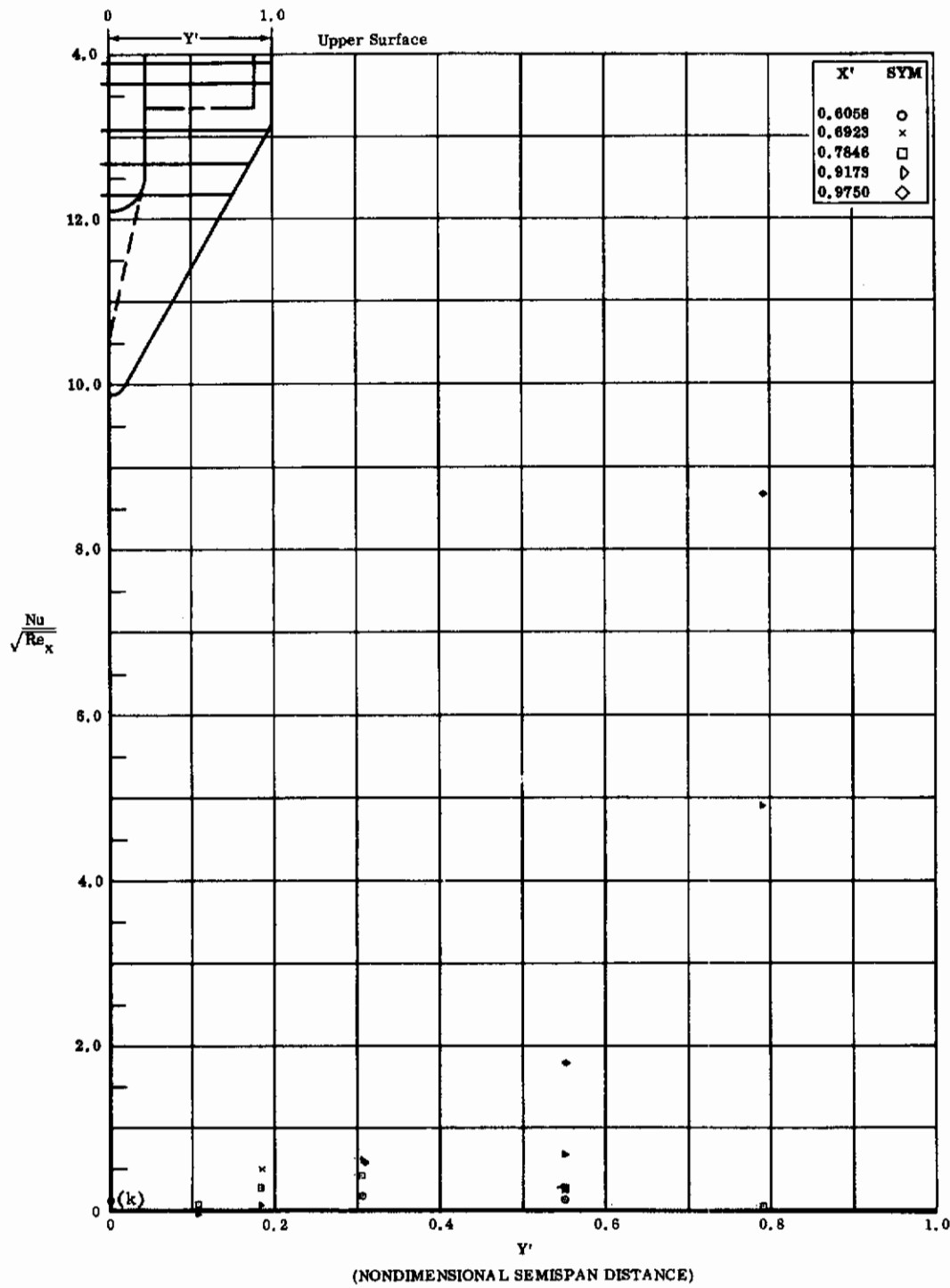


Fig. 18k Configuration IV, $\alpha = +10$, $\delta_2 = \delta_3 = -30$
 $Nu/\sqrt{Re_x}$ vs. Y' upper surface

Contrails

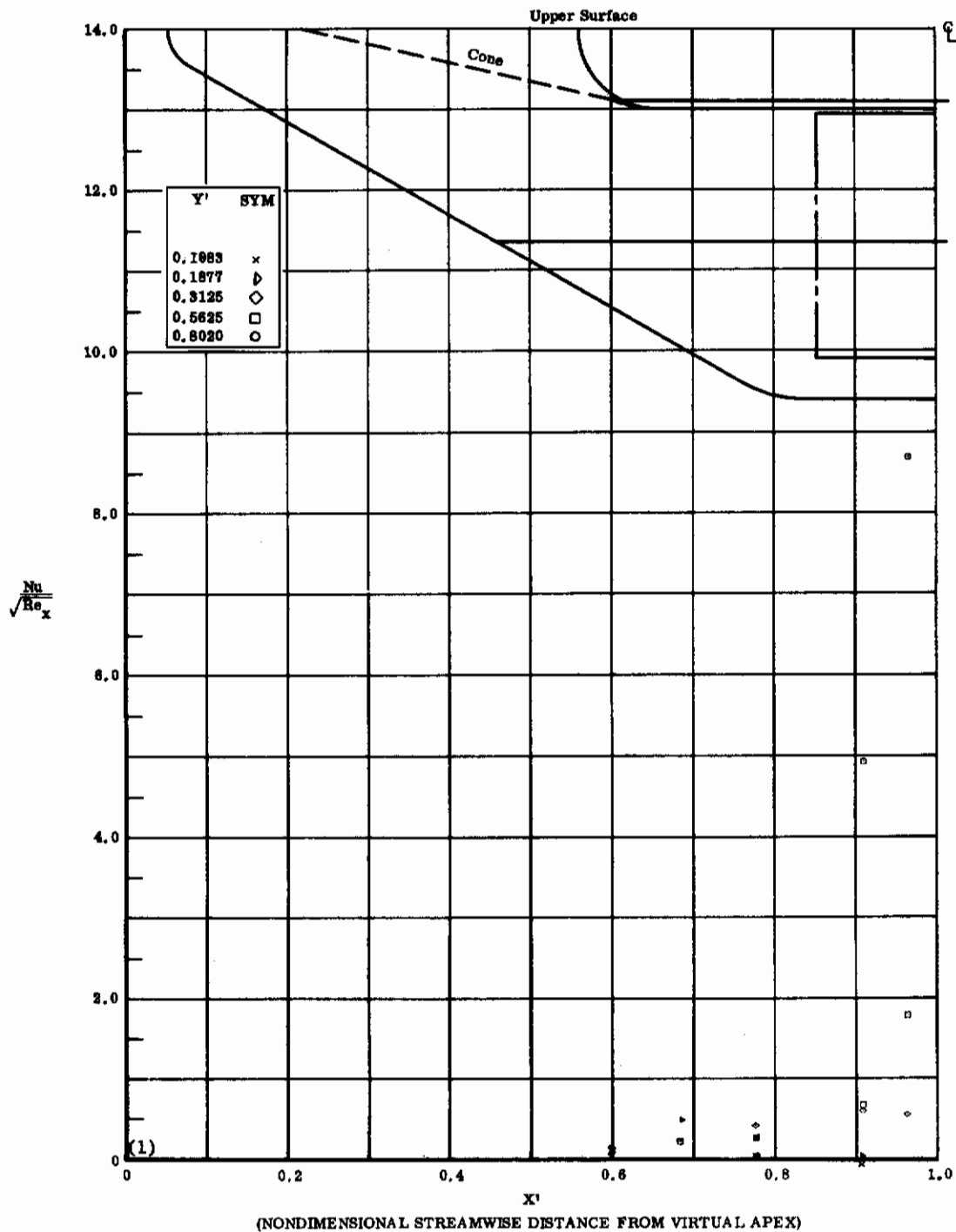


Fig. 18f Configuration IV, $\alpha = +10$, $\delta_2 = \delta_3 = -30$

$\text{Nu}/\sqrt{\text{Re}_x}$ vs. X' upper surface

Contrails

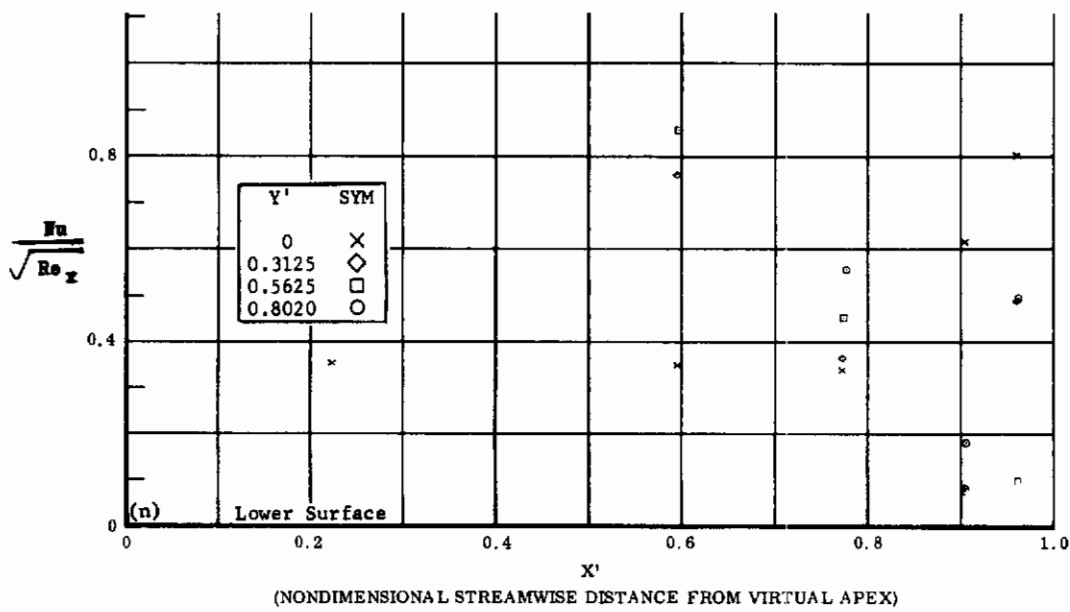
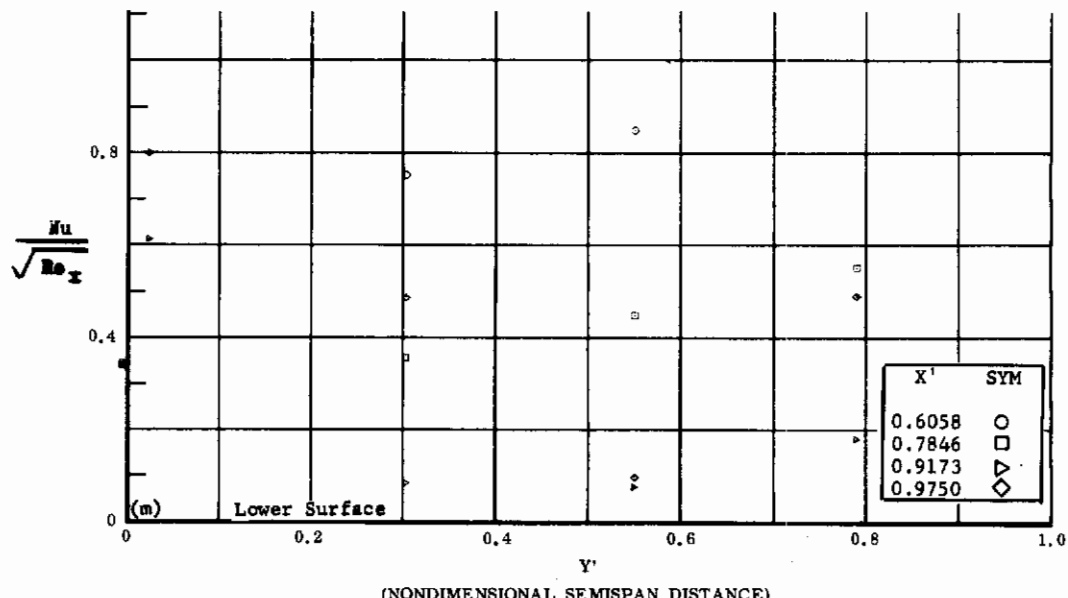


Fig. 18 Configuration IV, $\alpha = +10$, $\delta_2 = \delta_3 = -39$

m) $Nu/\sqrt{Re_x}$ vs. Y' lower surface

n) $Nu/\sqrt{Re_x}$ vs. X' lower surface

Contrails

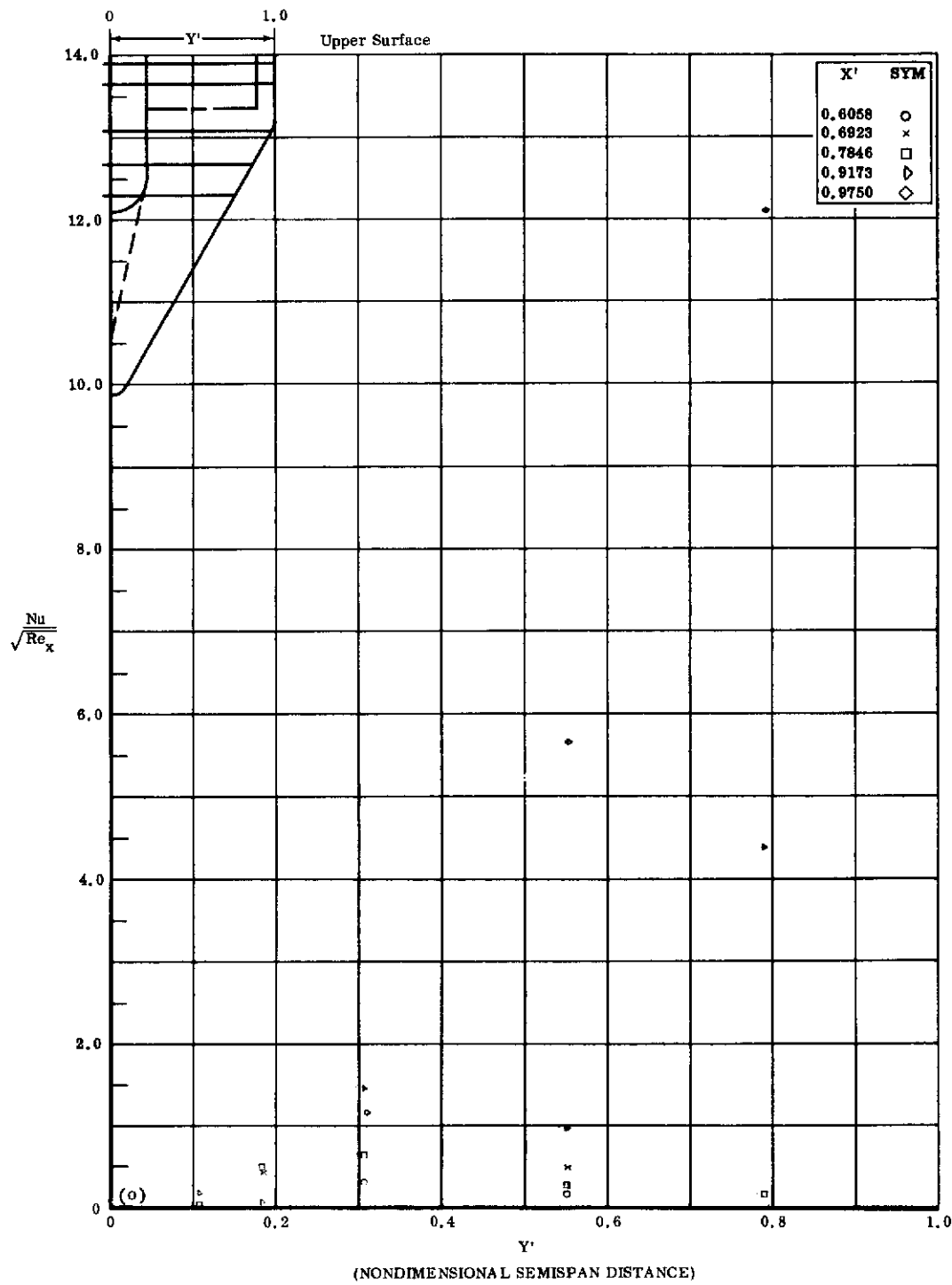


Fig. 18o Configuration IV, $\alpha = +10$, $\delta_2 = \delta_3 = -39$
 $\text{Nu}/\sqrt{\text{Re}_x}$ vs. Y' upper surface

Contrails

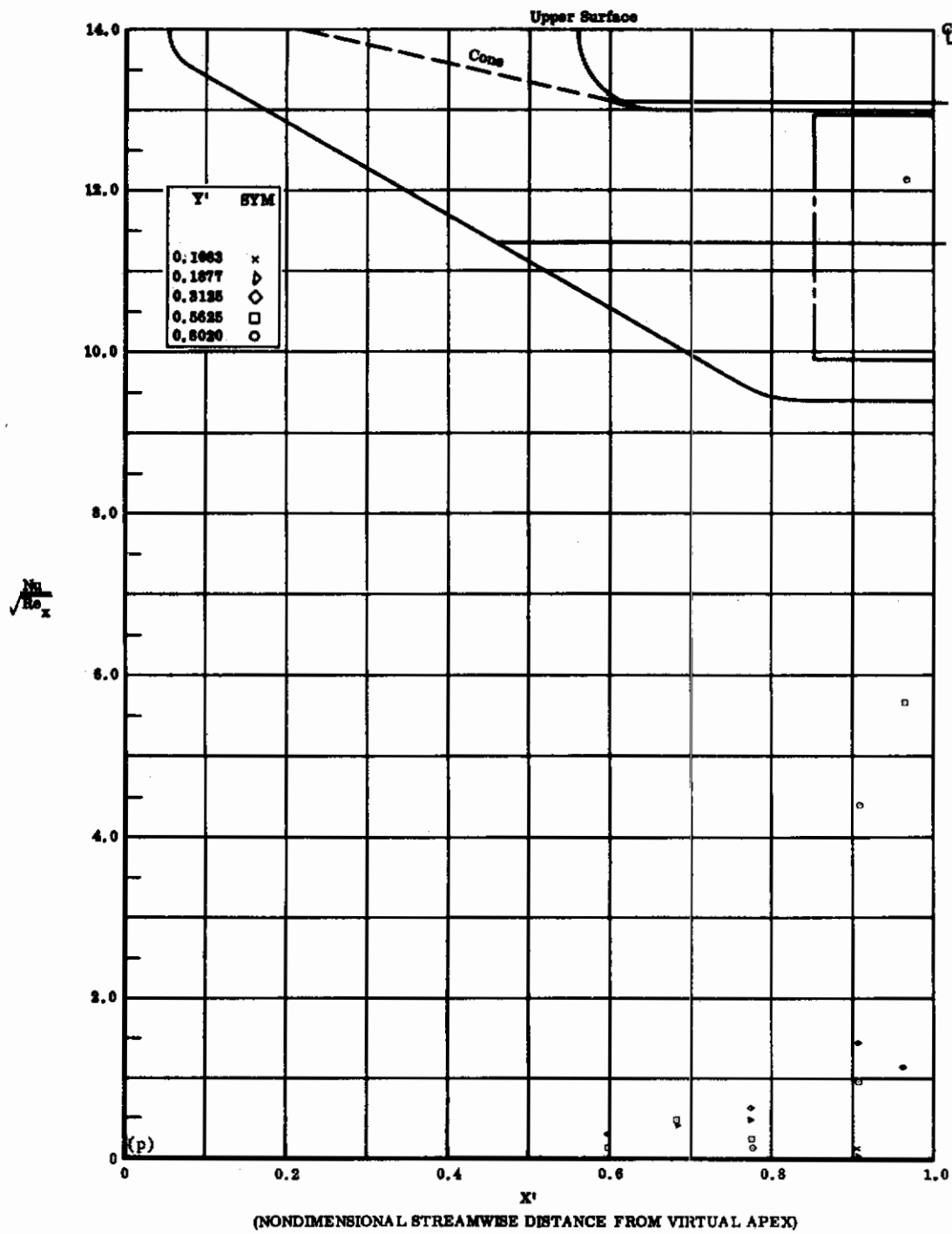


Fig. 18p Configuration IV, $\alpha = +10$, $\delta_2 = \delta_3 = -39$
 $Nu/\sqrt{Re_x}$ vs. X' upper surface

Contrails

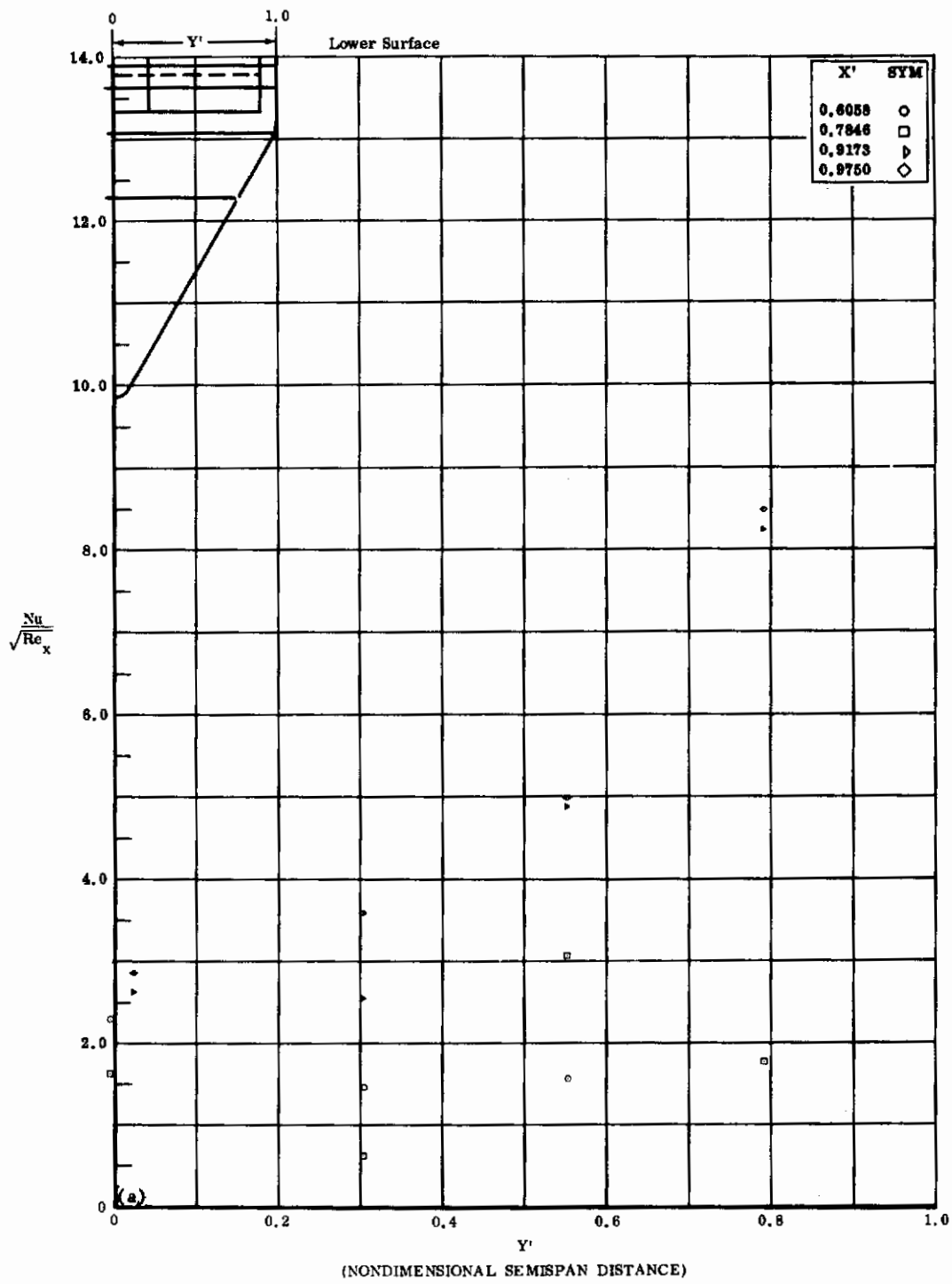


Fig. 19a Configuration IV, $\alpha = +20$, $\delta_2 = \delta_3 = 0$
 $Nu/\sqrt{Re_x}$ vs. Y' lower surface

Contrails

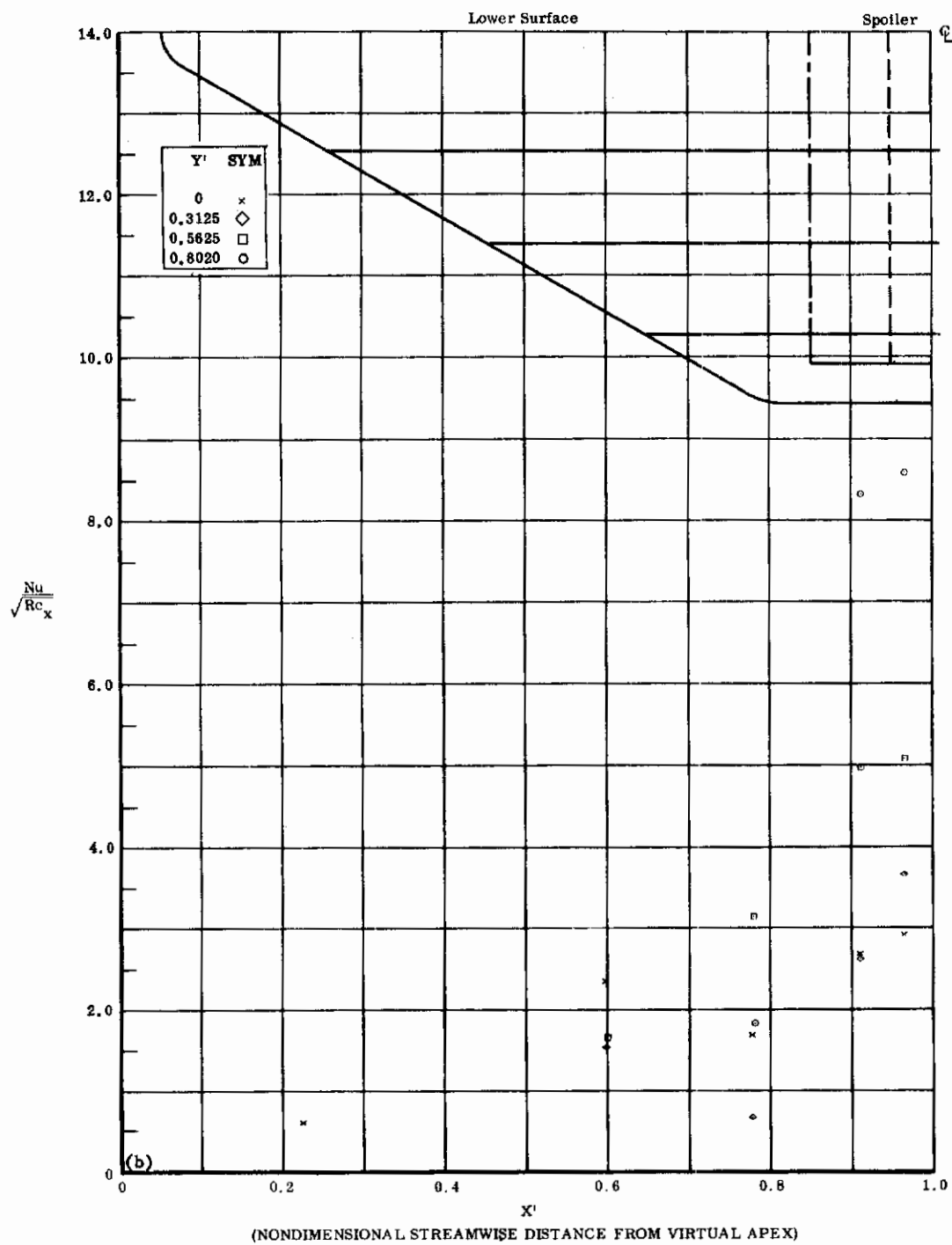


Fig. 19b Configuration IV, $\alpha = +20$, $\delta_2 = \delta_3 = 0$

$Nu/\sqrt{Re_x}$ vs. X' lower surface

Contrails

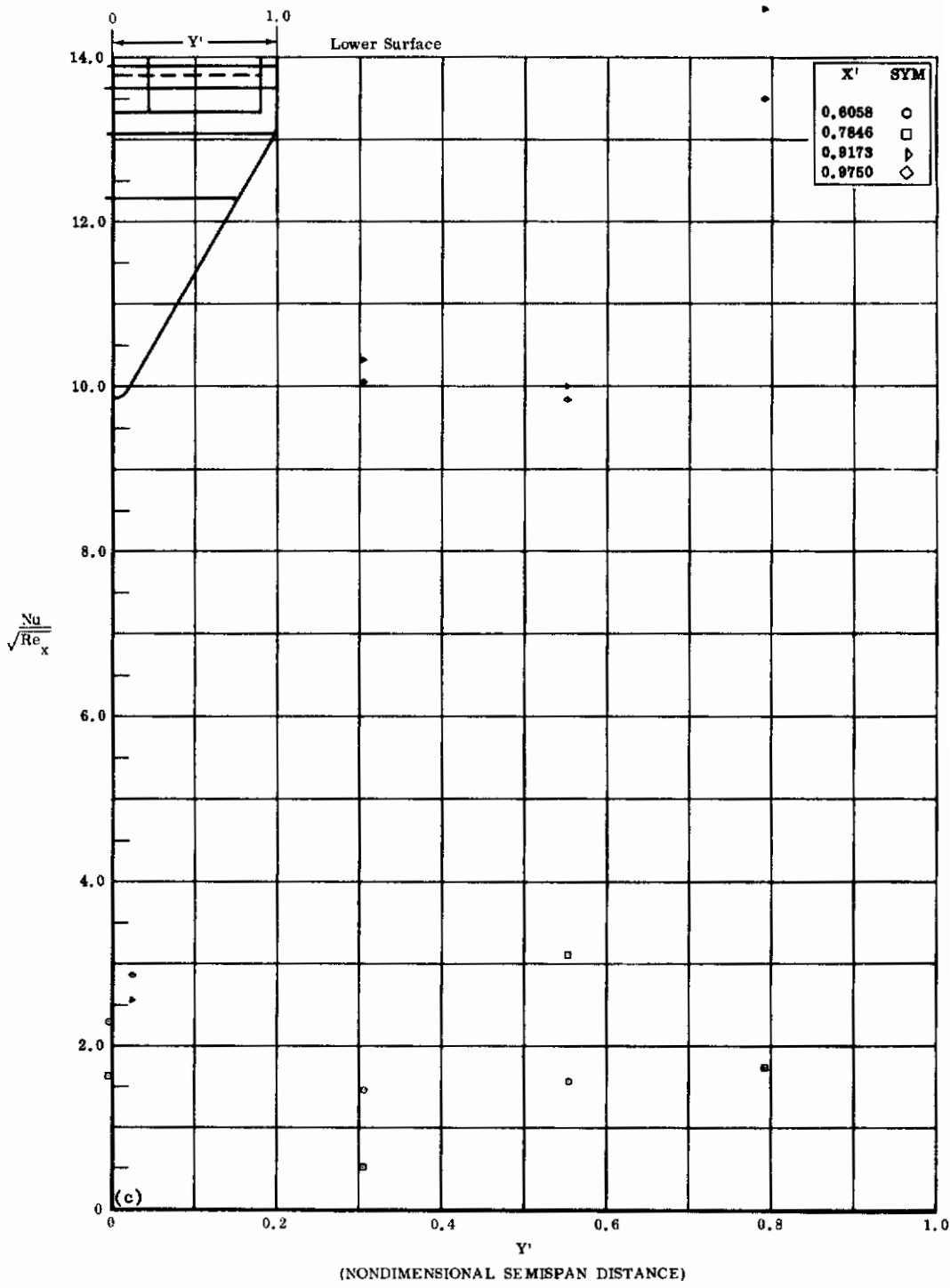


Fig. 19c Configuration IV, $\alpha = +20$, $\delta_2 = \delta_3 = +10$
 $\text{Nu}/\sqrt{\text{Re}_x}$ vs. Y' lower surface

Contrails

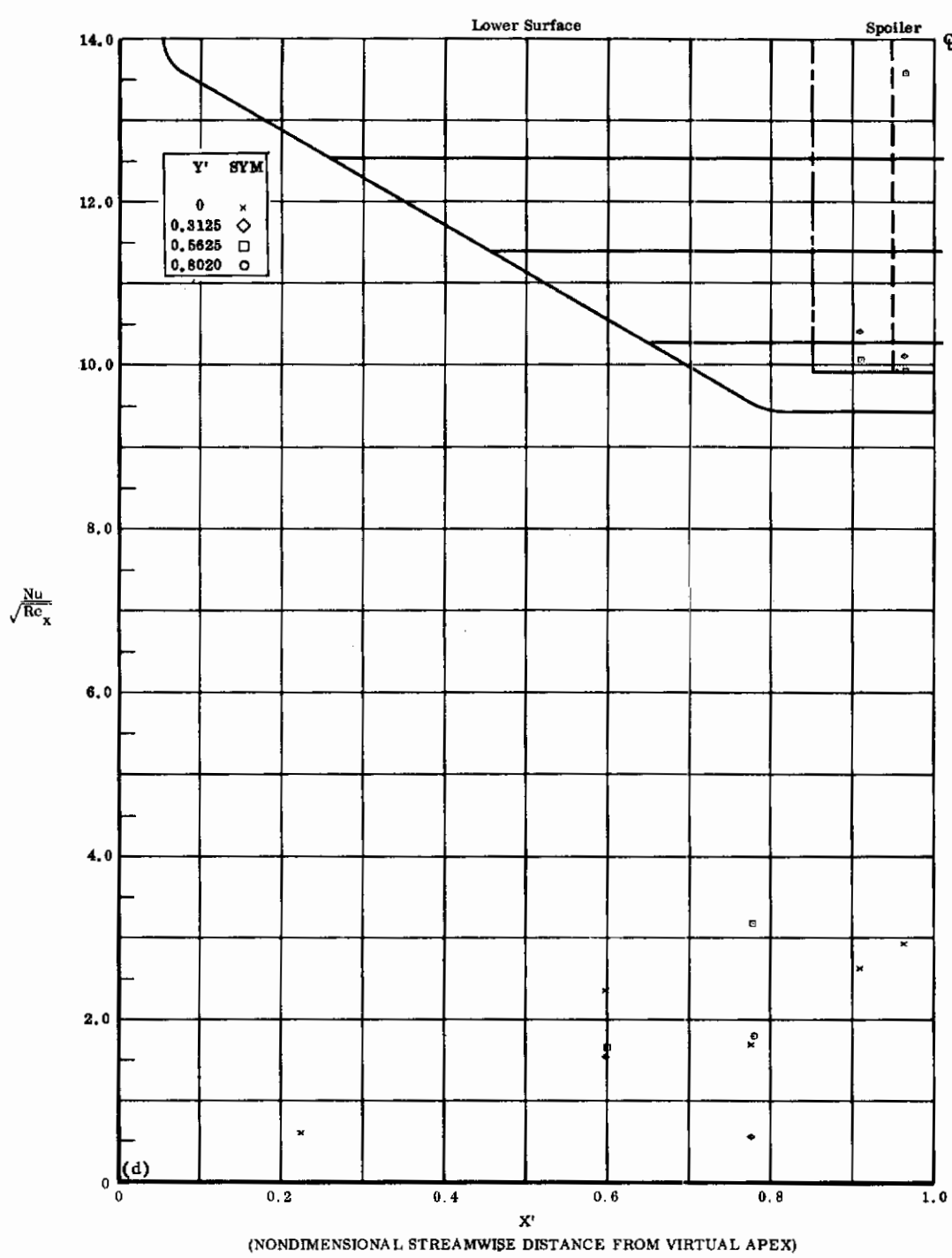


Fig. 19d Configuration IV, $\alpha = +20$, $\delta_2 = \delta_3 = +10$
 $Nu/\sqrt{Re_x}$ vs. X' lower surface

Contrails

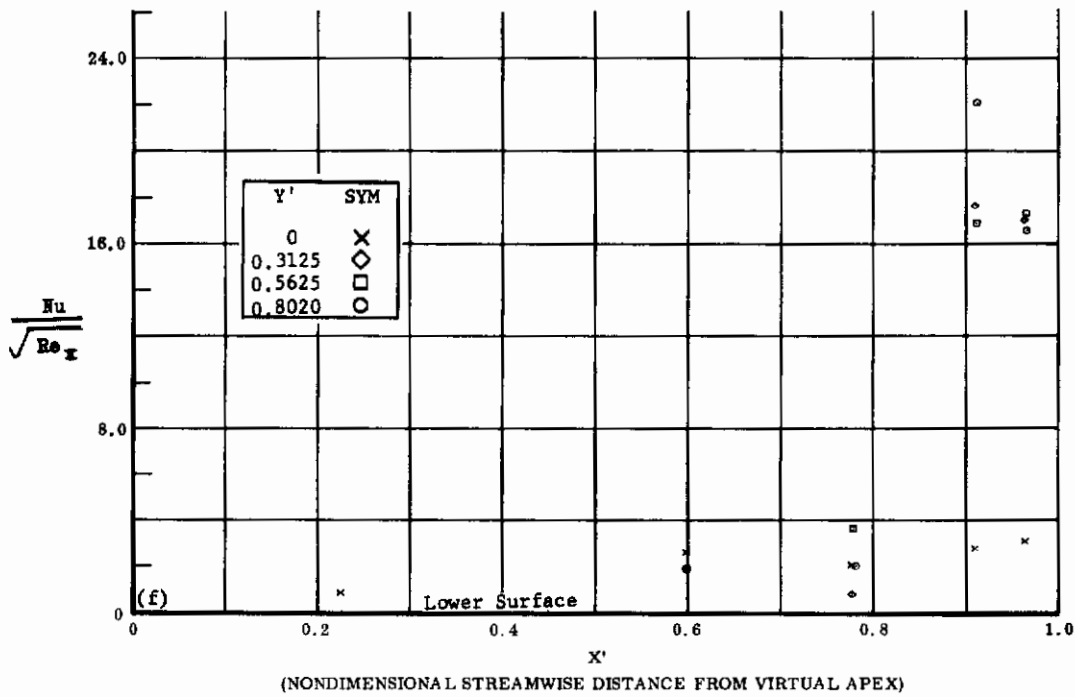
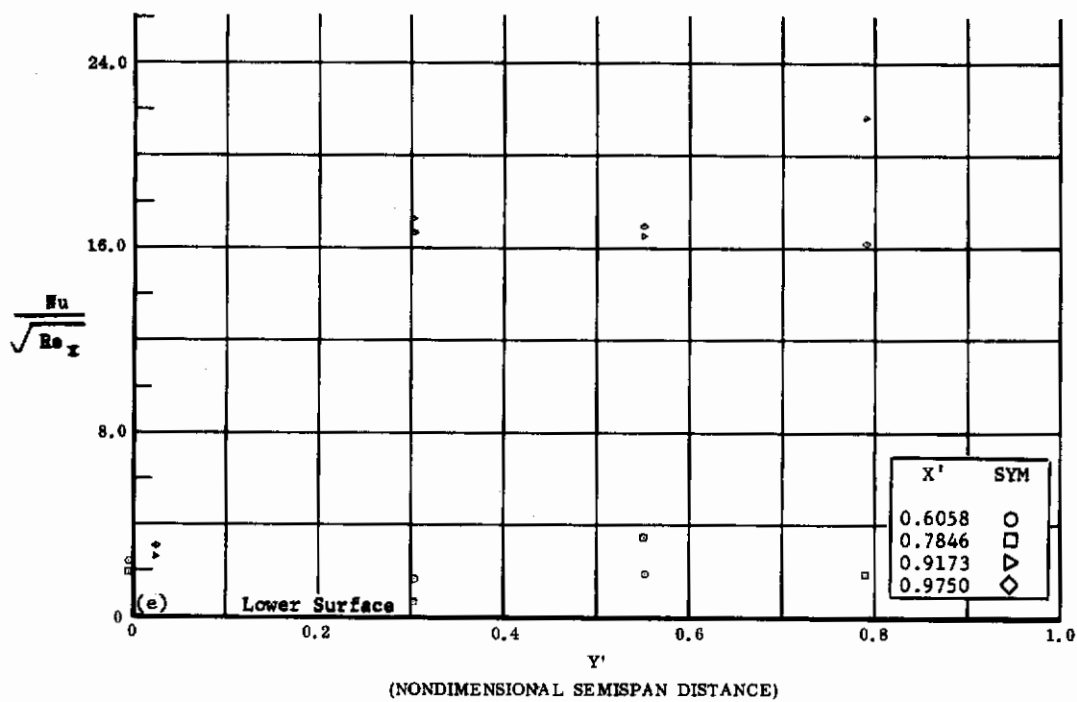


Fig. 19 Configuration IV, $\alpha = +20$, $\delta_2 = \delta_3 = +20$

e) $Nu/\sqrt{Re_x}$ vs. Y' lower surface

f) $Nu/\sqrt{Re_x}$ vs. X' lower surface

Contrails

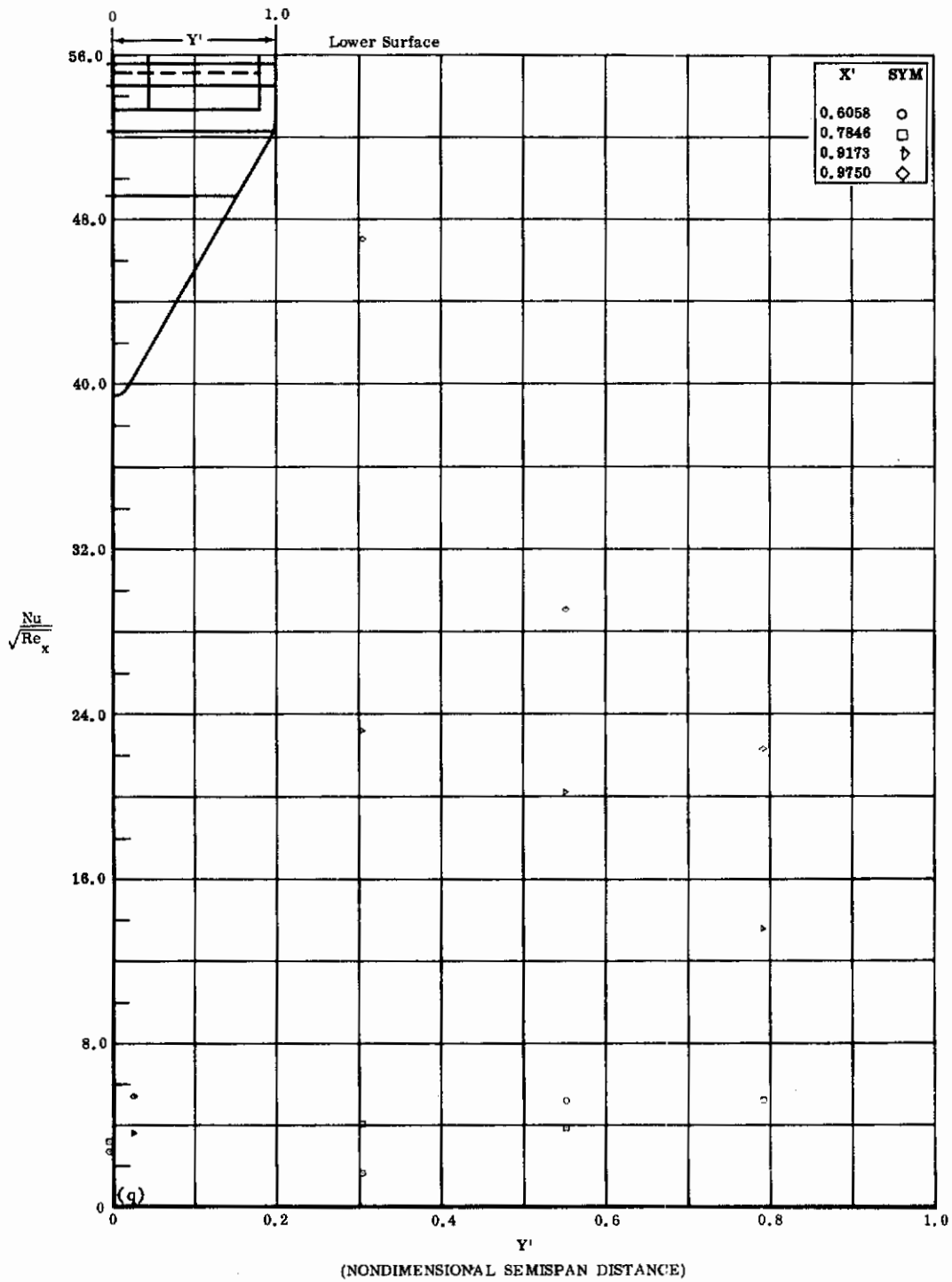


Fig. 19g Configuration IV, $\alpha = +20$, $\delta_2 = \delta_3 = +30$
 $Nu/\sqrt{Re_x}$ vs. Y^* lower surface

Contrails

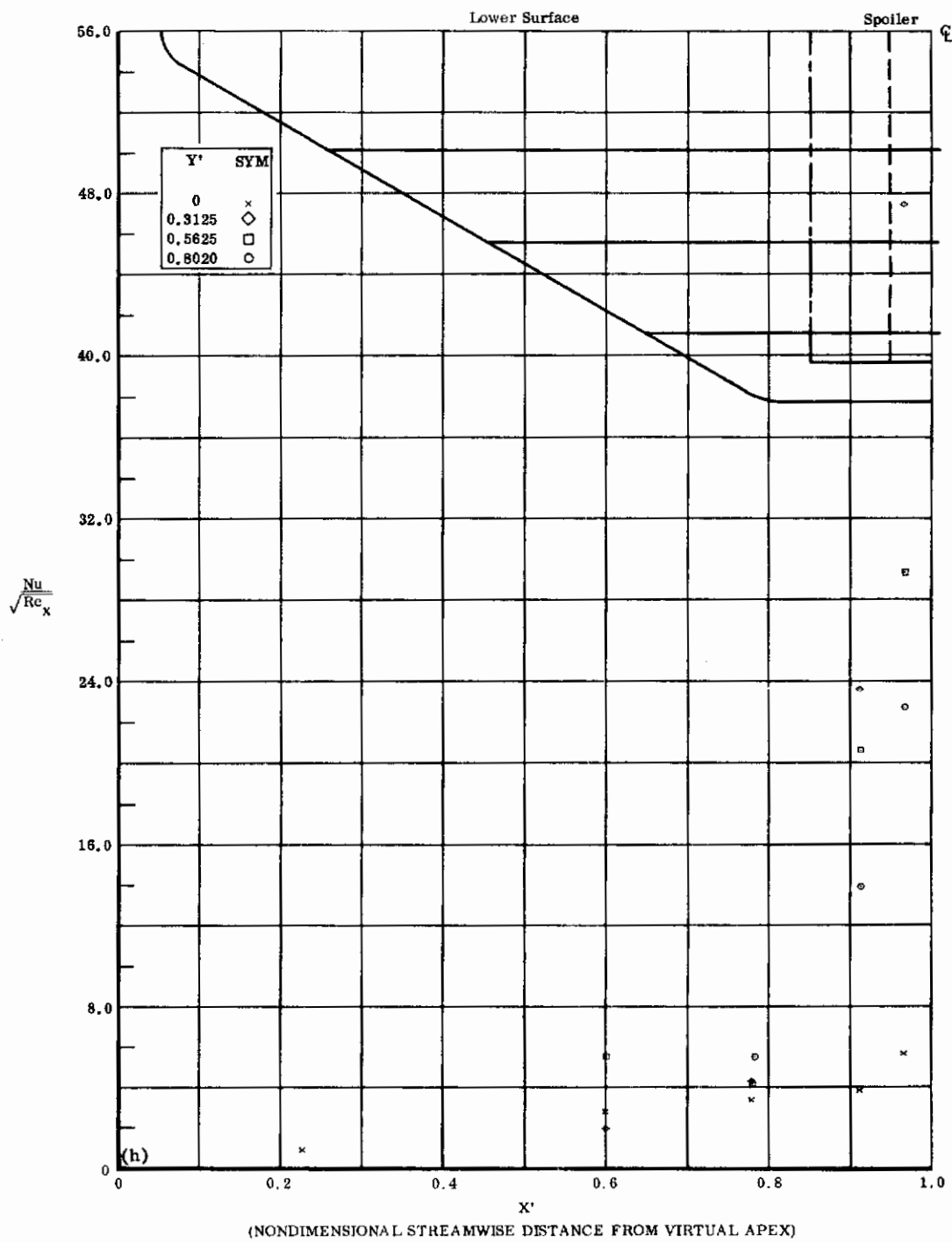


Fig. 19b Configuration IV, $\alpha = +20^\circ$, $\delta_2 = \delta_3 = +30^\circ$
 $\text{Nu}/\sqrt{\text{Re}_x}$ vs. X' lower surface

Contrails

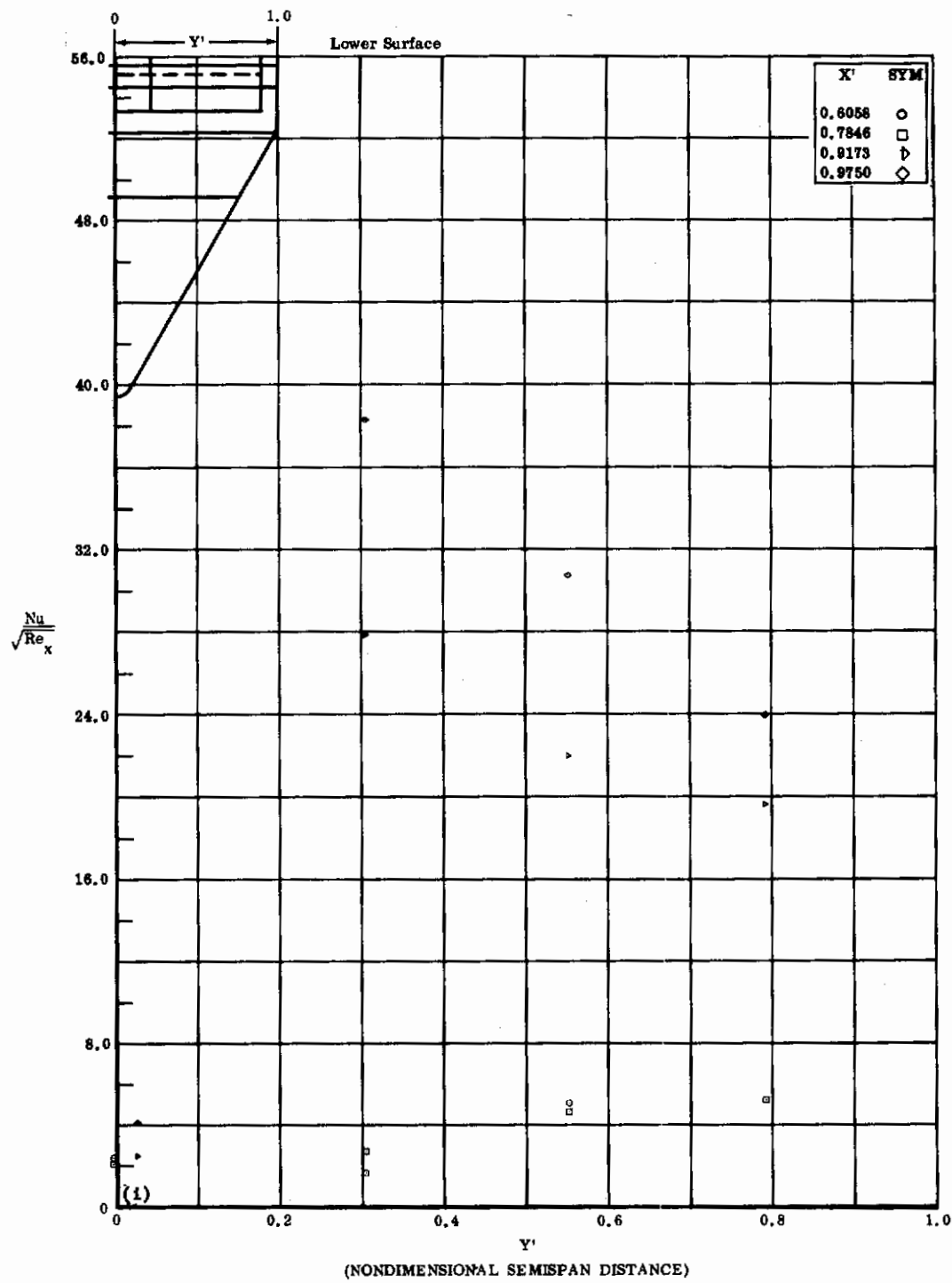


Fig. 191 Configuration IV, $\alpha = +20$, $b_2 = b_3 = +39$
 $Nu/\sqrt{Re_x}$ vs. Y' lower surface

Contrails

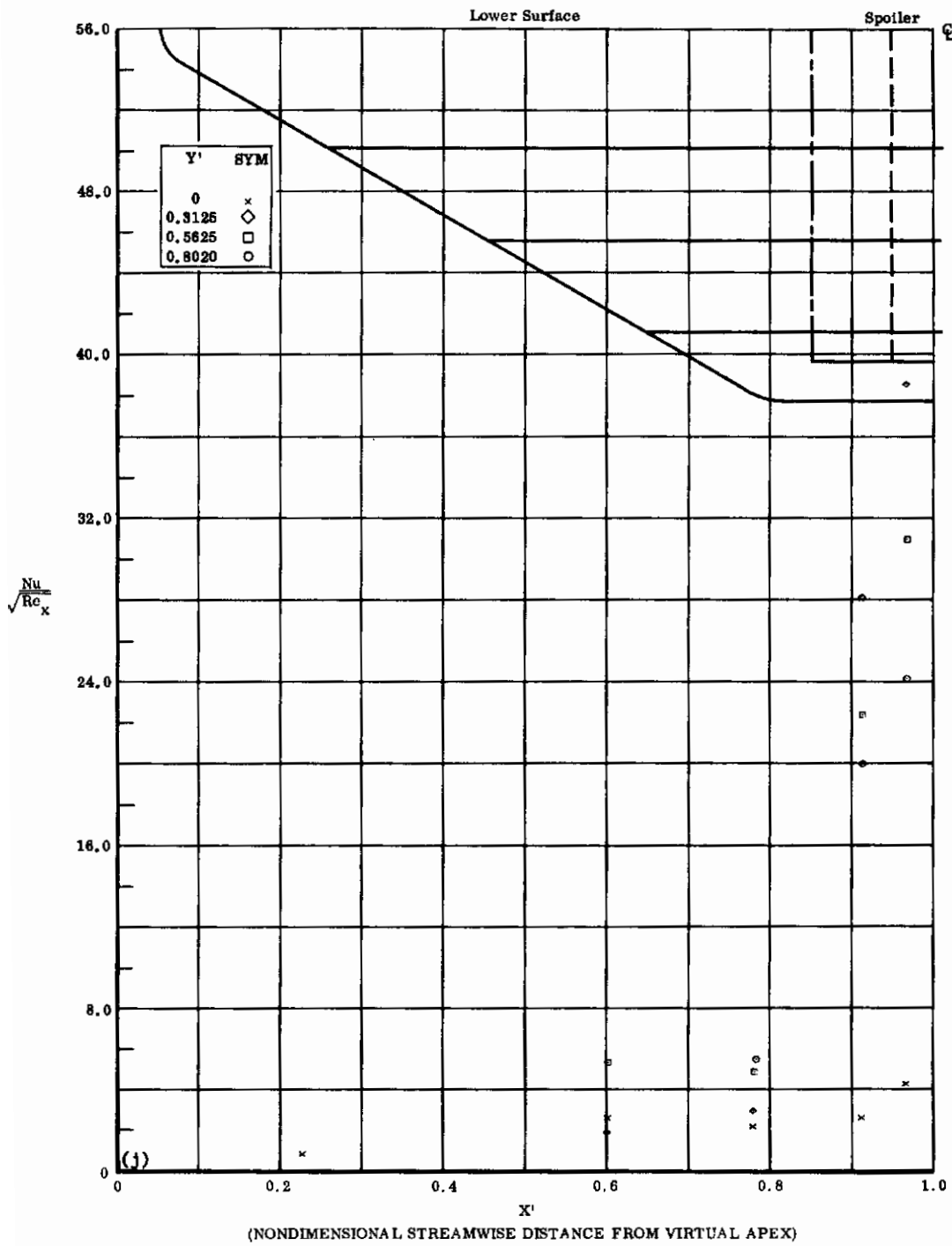


Fig. 19j Configuration IV, $\alpha = +20$, $\delta_2 = \delta_3 = +39$
 $Nu/\sqrt{Re_x}$ vs. X^1 lower surface

Contrails

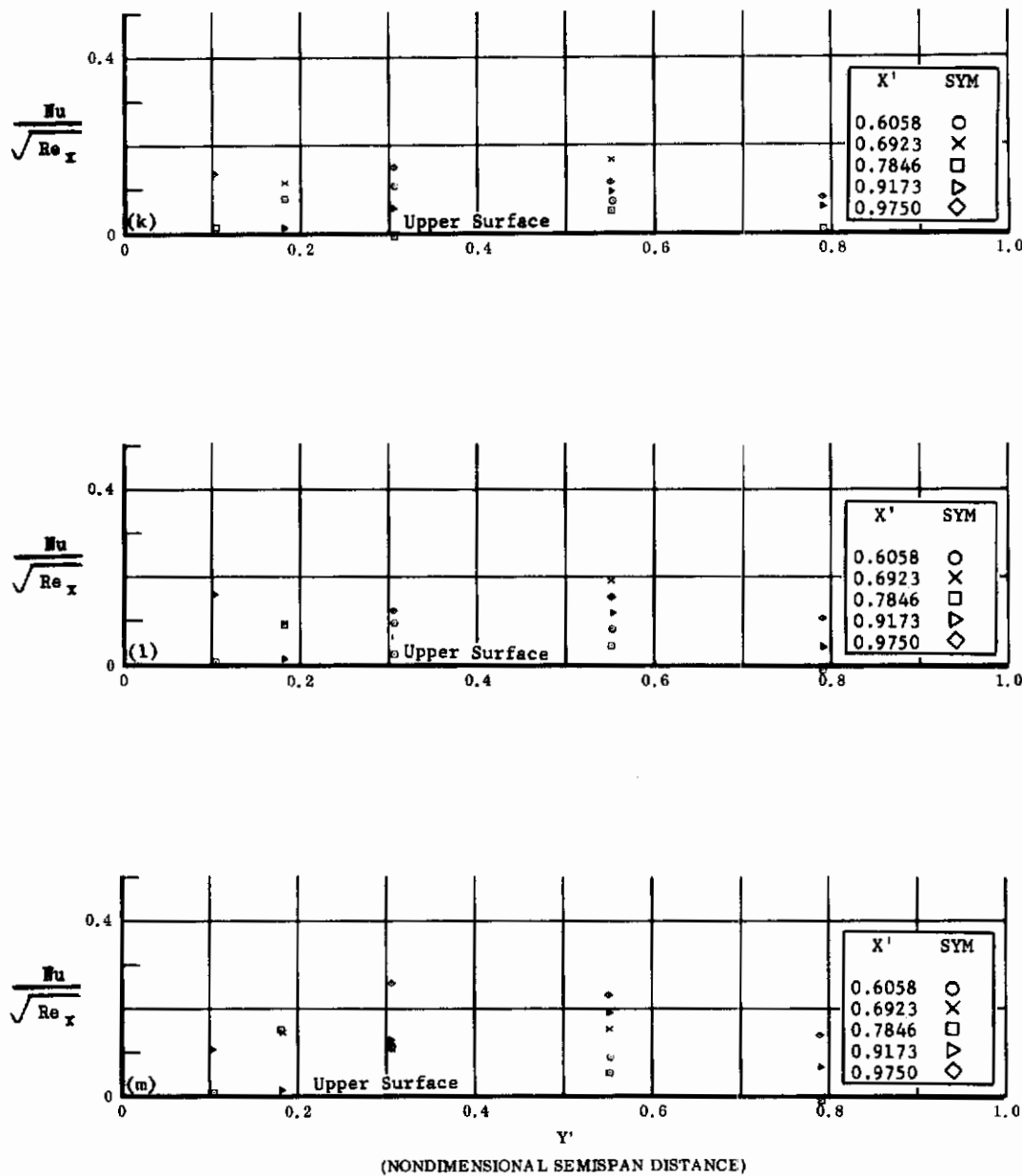


Fig. 19 Configuration IV, $\alpha = +20$, $Nu/\sqrt{Re_x}$ vs. Y' , upper surface

k) $\delta_2 = \delta_3 = 0$

l) $\delta_2 = \delta_3 = +10$

m) $\delta_2 = \delta_3 = +20$

Contrails

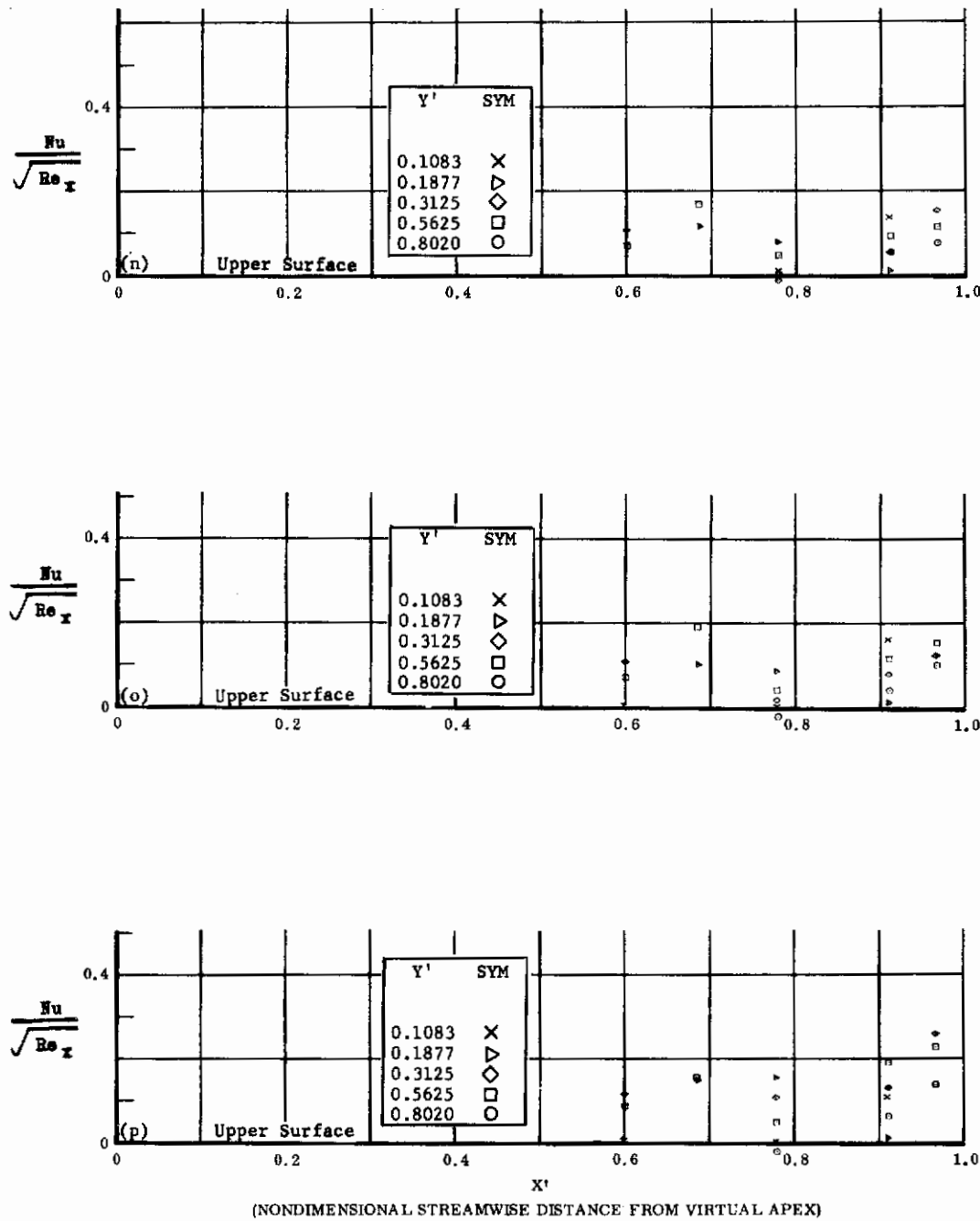


Fig. 19 Configuration IV, $\alpha = +20$, $Nu/\sqrt{Re_x}$ vs. X' , upper surface

n) $b_2 = b_3 = 0$

o) $b_2 = b_3 = +10$

p) $b_2 = b_3 = +20$

Contrails

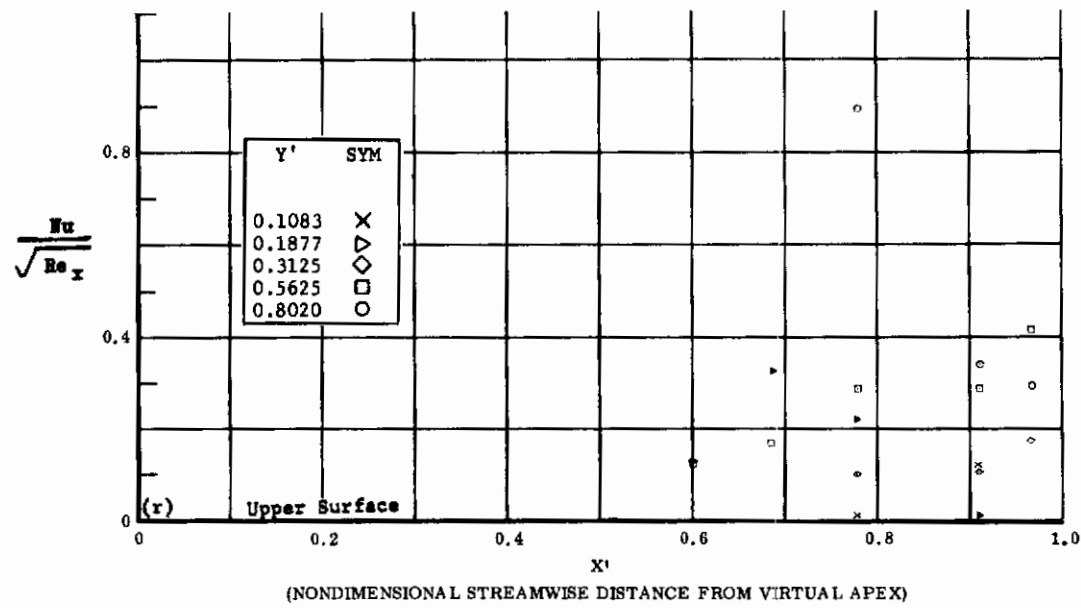
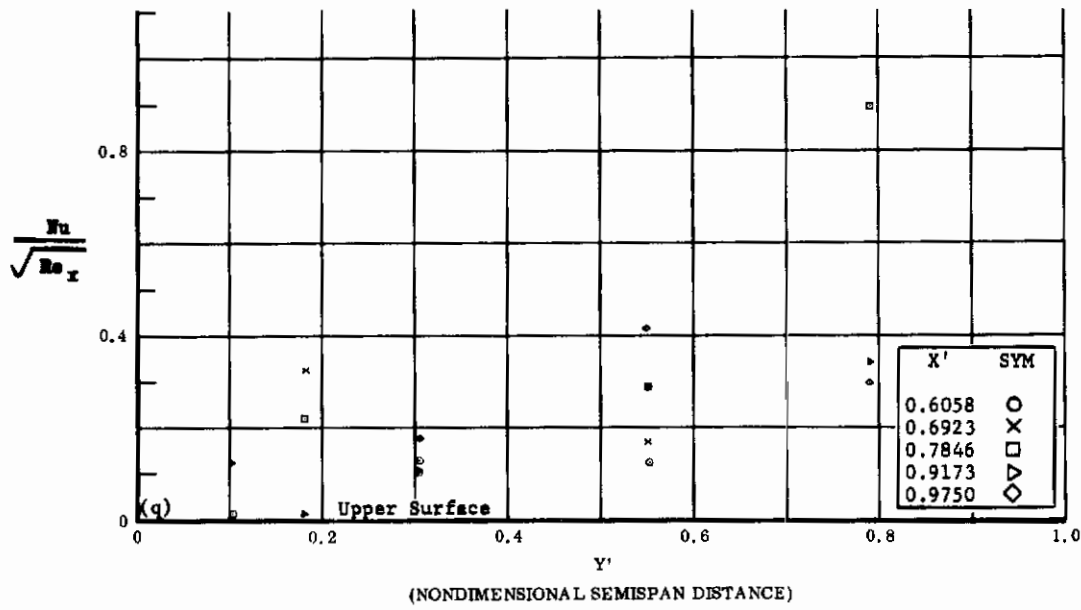


Fig. 19 Configuration IV, $\alpha = +20$, $\delta_2 = \delta_3 = +30$

q) $Nu/\sqrt{Re_x}$ vs. Y' upper surface

r) $Nu/\sqrt{Re_x}$ vs. X' upper surface

Contrails

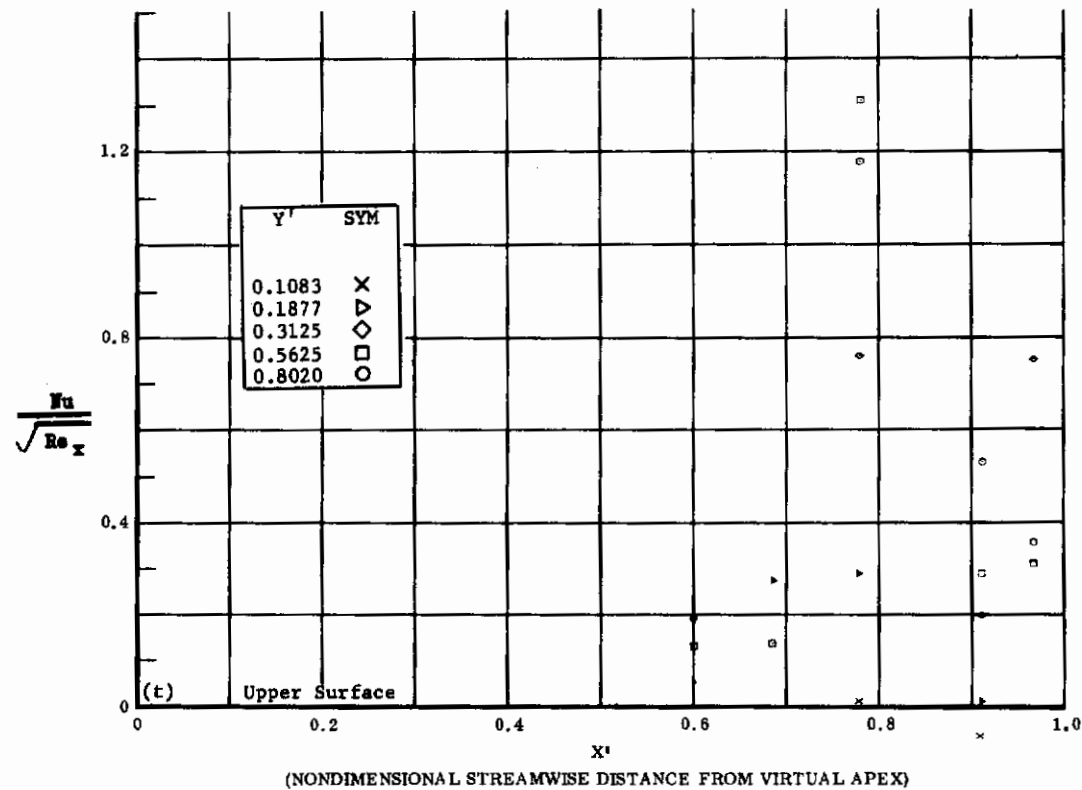
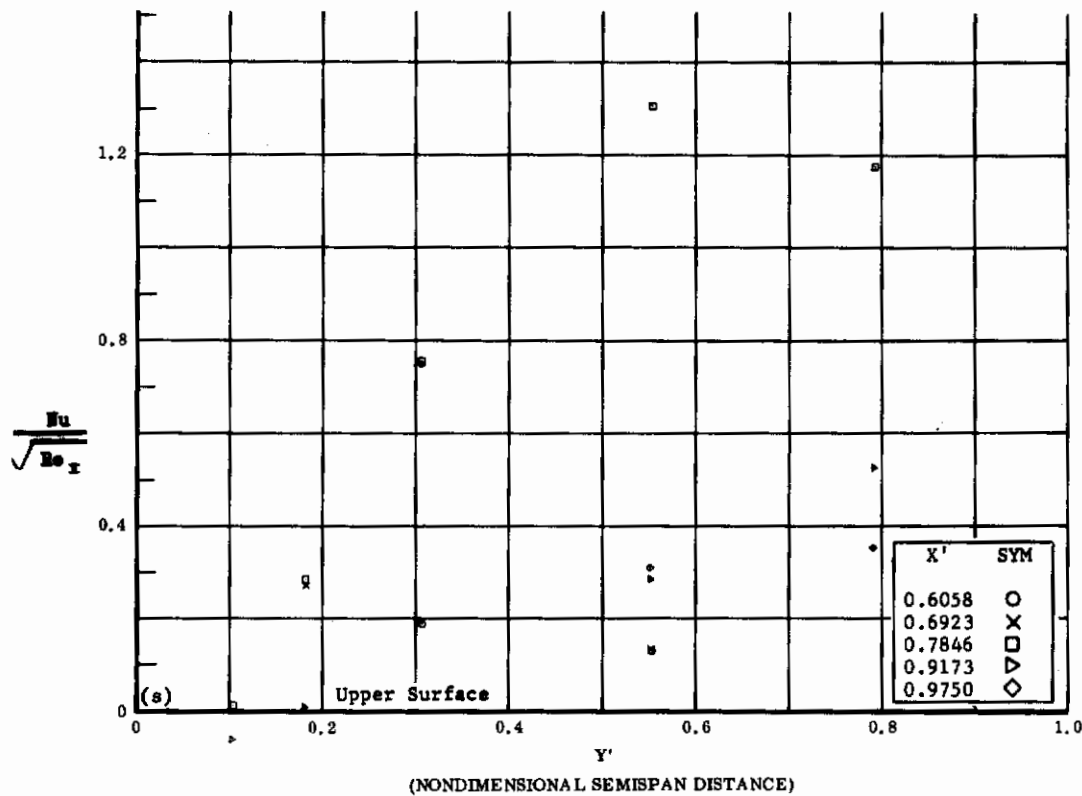


Fig. 19 Configuration IV, $\alpha = +20^\circ$, $\delta_2 = \delta_3 = +39^\circ$

s) $Nu/\sqrt{R_e x}$ vs. Y' upper surface

t) $Nu/\sqrt{R_e x}$ vs. X' upper surface

Contrails

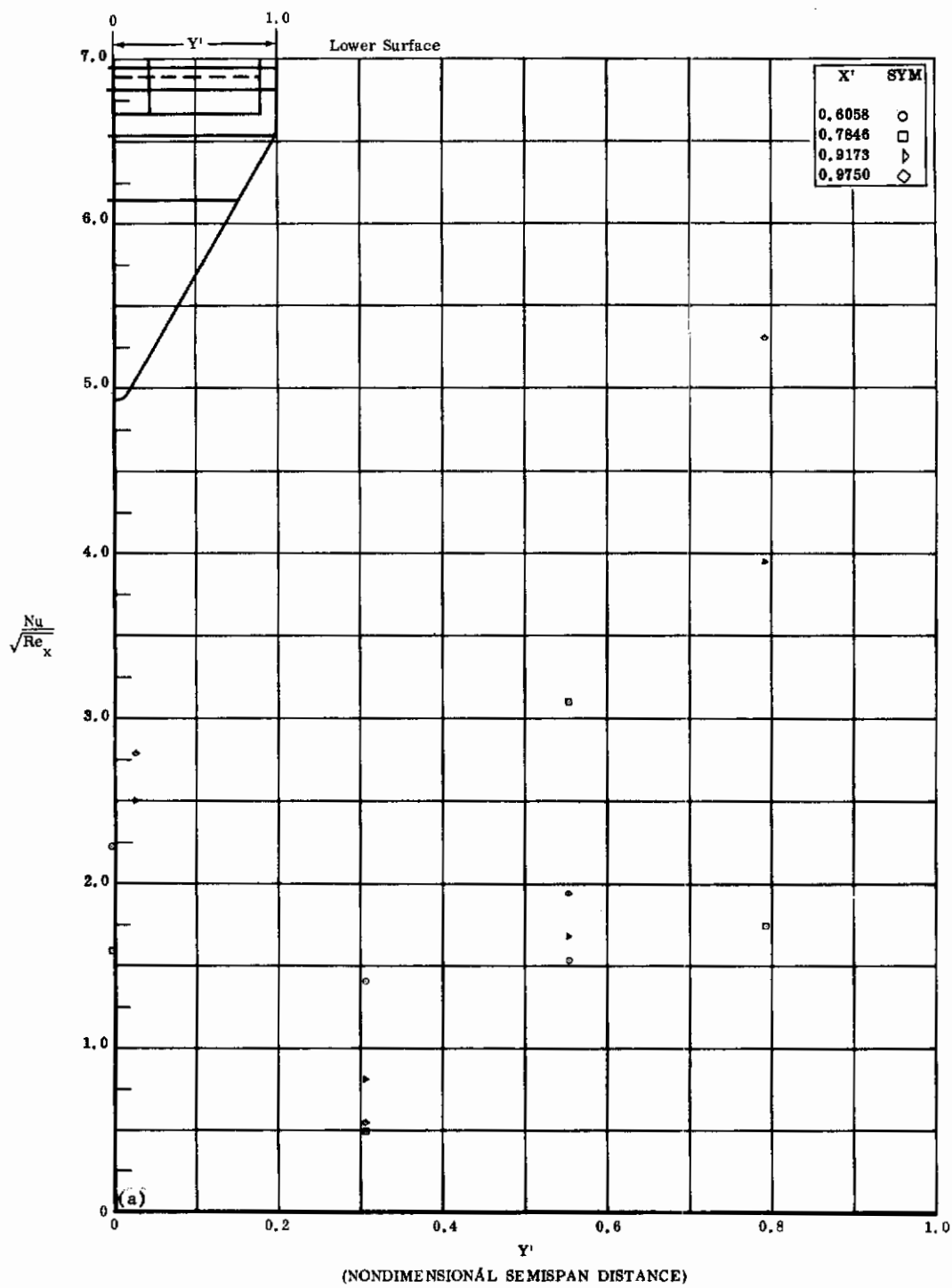


Fig. 20a Configuration IV, $\alpha = +20^\circ$; $\delta_2 = \delta_3 = -10^\circ$
 $\frac{Nu}{\sqrt{Re_x}}$ vs. Y' lower surface

Contrails

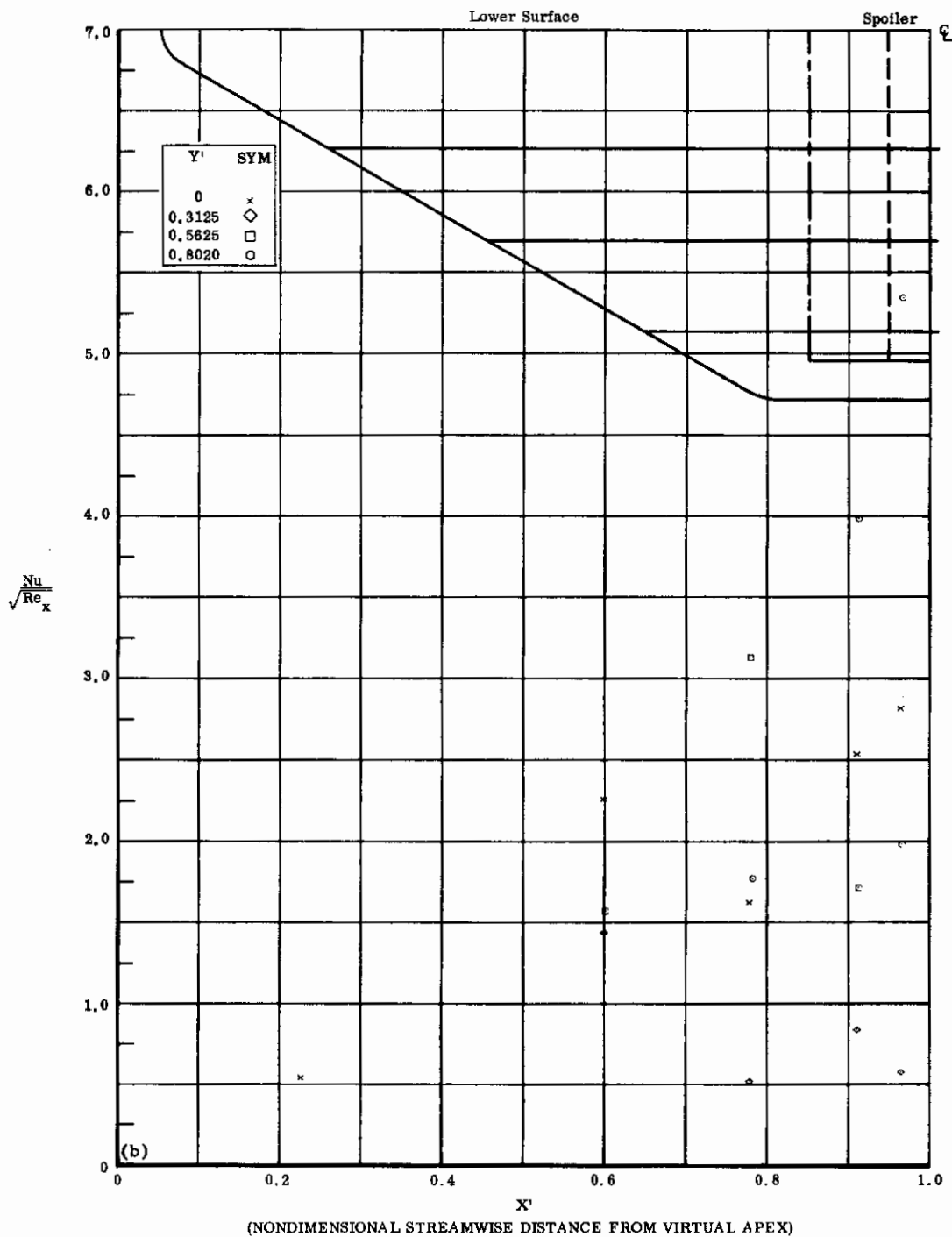


Fig. 20b Configuration IV, $\alpha = +20^\circ$, $\delta_2 = \delta_3 = -10^\circ$
 $\frac{Nu}{\sqrt{Re_x}}$ vs. X' lower surface

Contrails

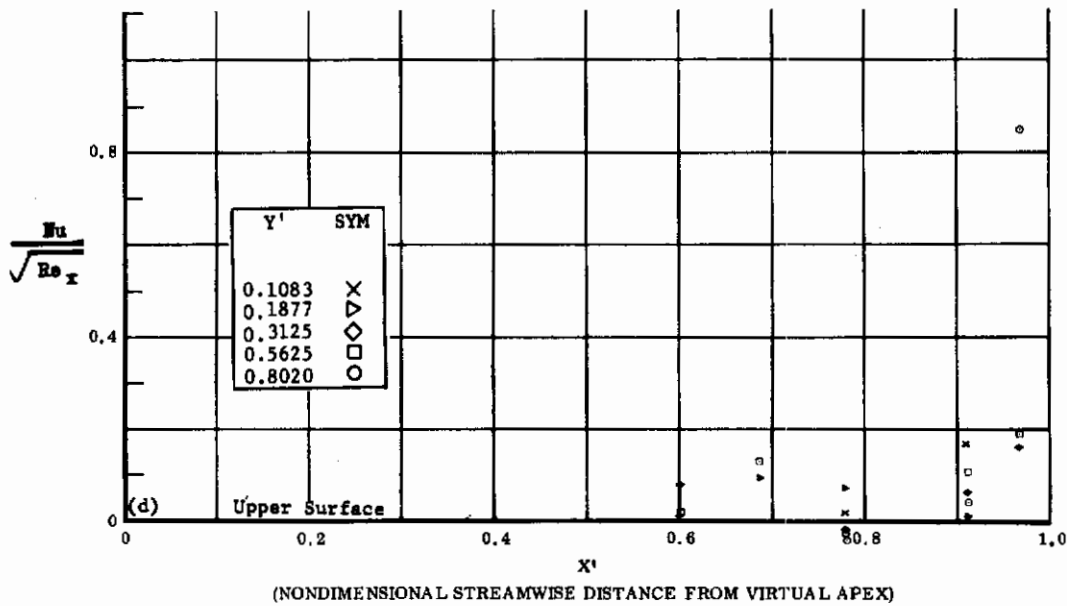
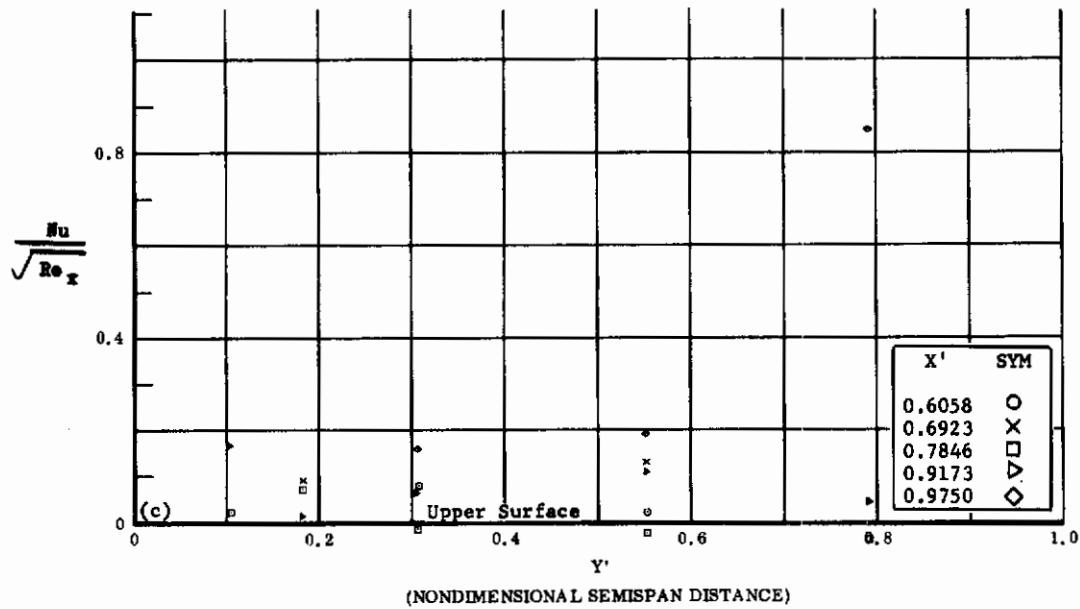


Fig. 20 Configuration IV, $\alpha = +20$, $\delta_2 = \delta_3 = -10$

- c) $Nu/\sqrt{Re_x}$ vs. Y' upper surface
- d) $Nu/\sqrt{Re_x}$ vs. X' upper surface

Contrails

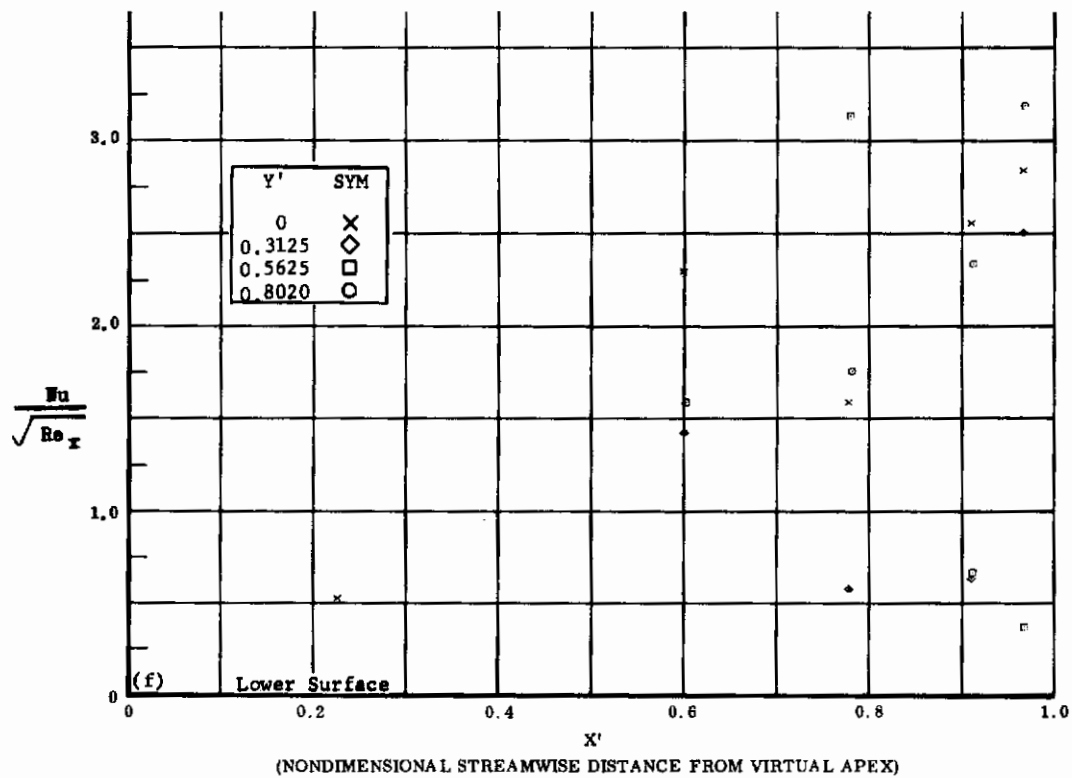
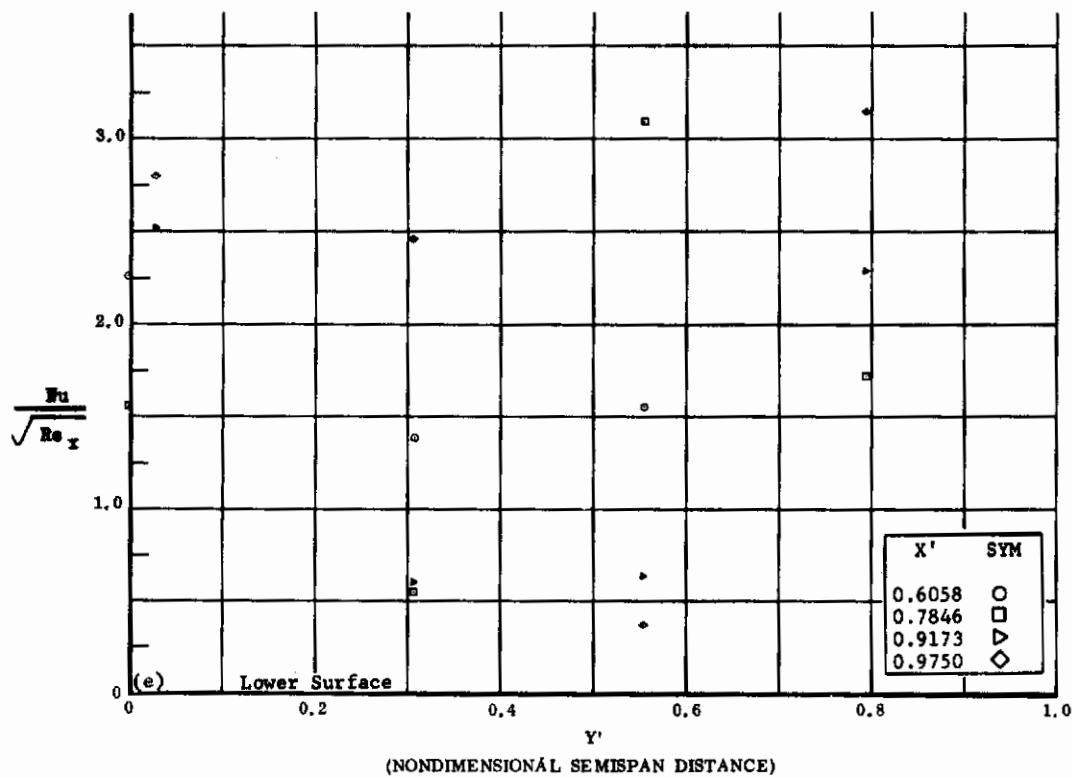


Fig. 20 Configuration IV, $\alpha = +20$, $\delta_2 = \delta_3 = -20$

e) $Nu/\sqrt{Re_x}$ vs. Y' lower surface

f) $Nu/\sqrt{Re_x}$ vs. X' lower surface

Contrails

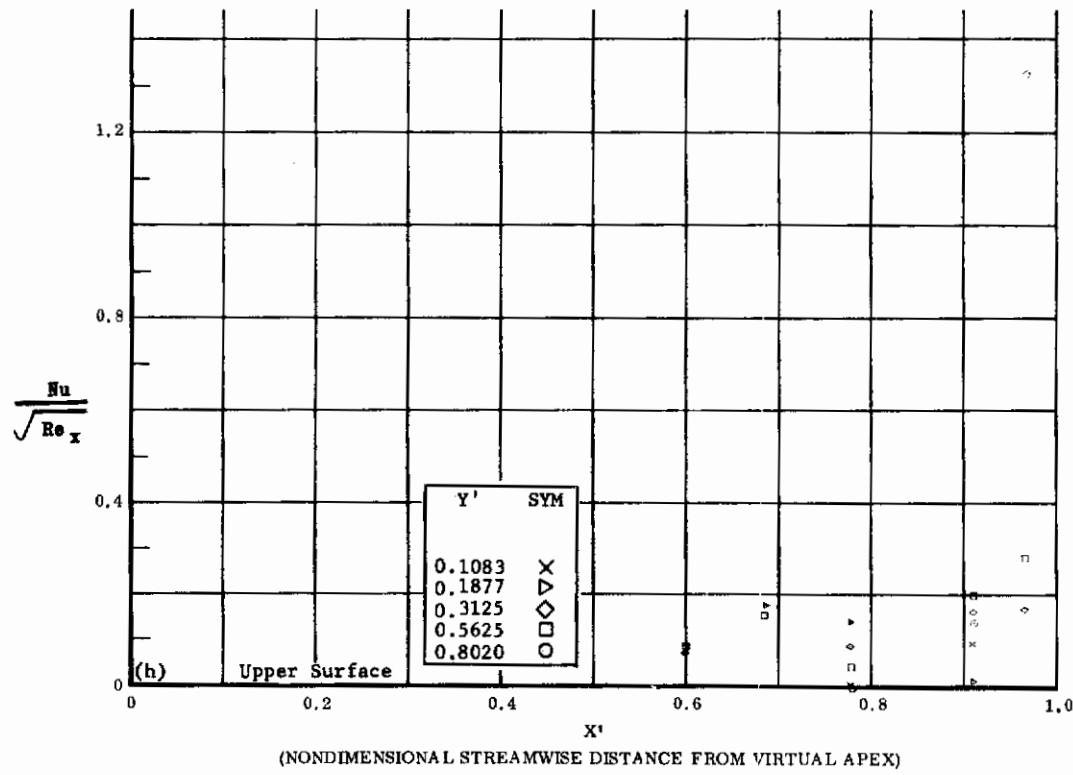
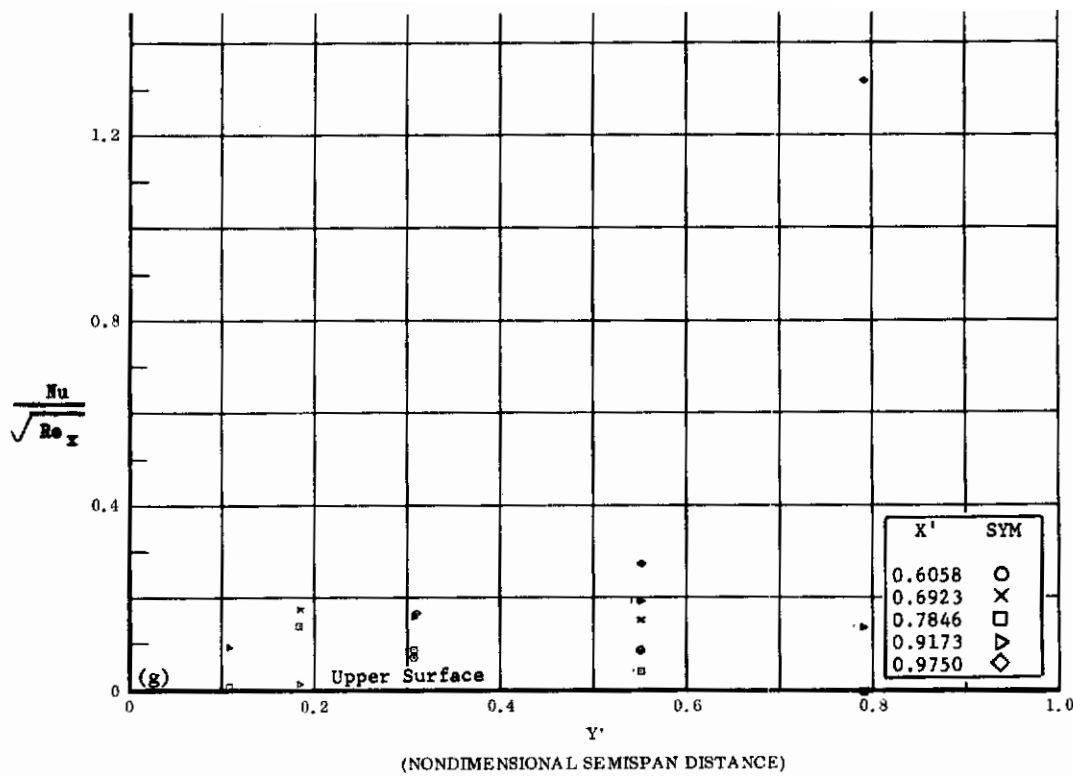


Fig. 20 Configuration IV, $\alpha = +20$, $\delta_2 = \delta_3 = -20$

g) $Nu/\sqrt{Re_x}$ vs. Y' upper surface

h) $Nu/\sqrt{Re_x}$ vs. X' upper surface

Contrails

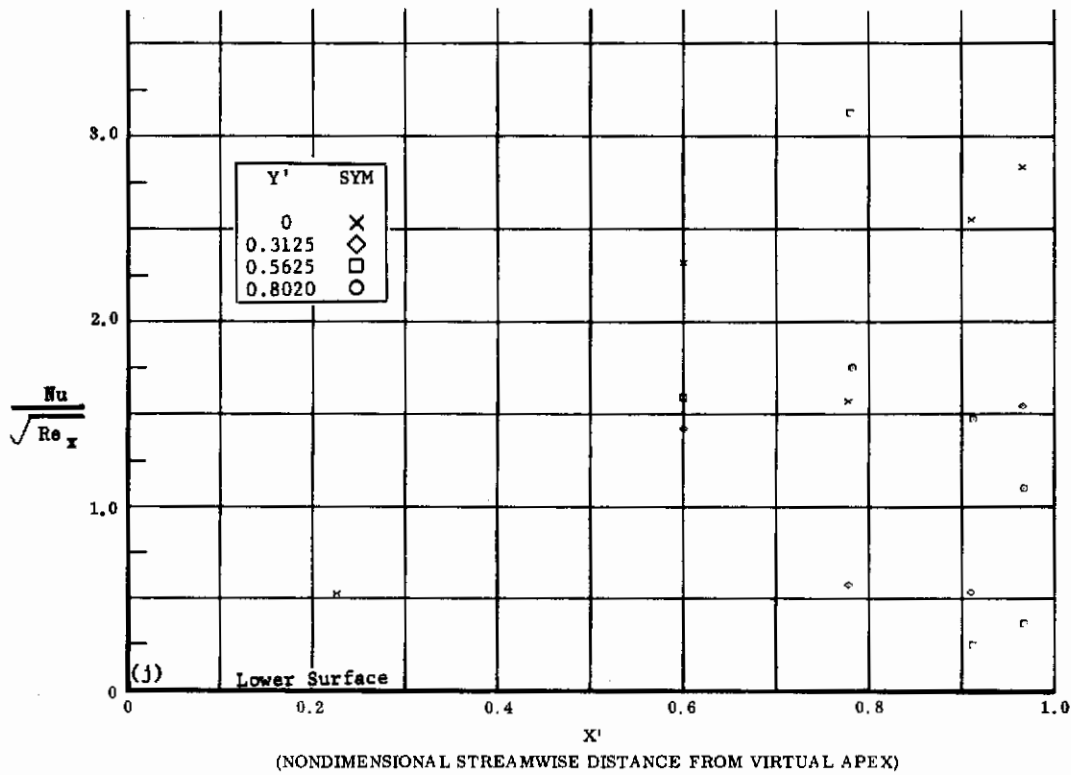
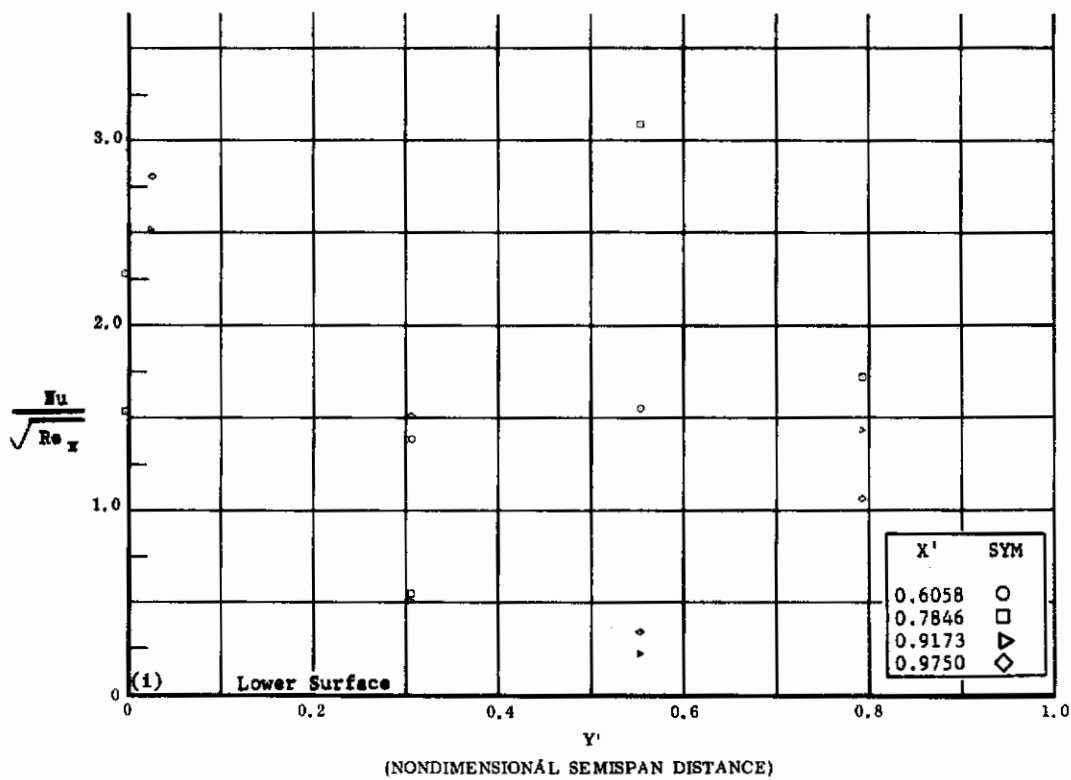


Fig. 20 Configuration IV, $\alpha = +20$, $\delta_2 = \delta_3 = -30$

i) $\text{Nu}/\sqrt{\text{Re}_x}$ vs. Y' lower surface

j) $\text{Nu}/\sqrt{\text{Re}_x}$ vs. X' lower surface

Contrails

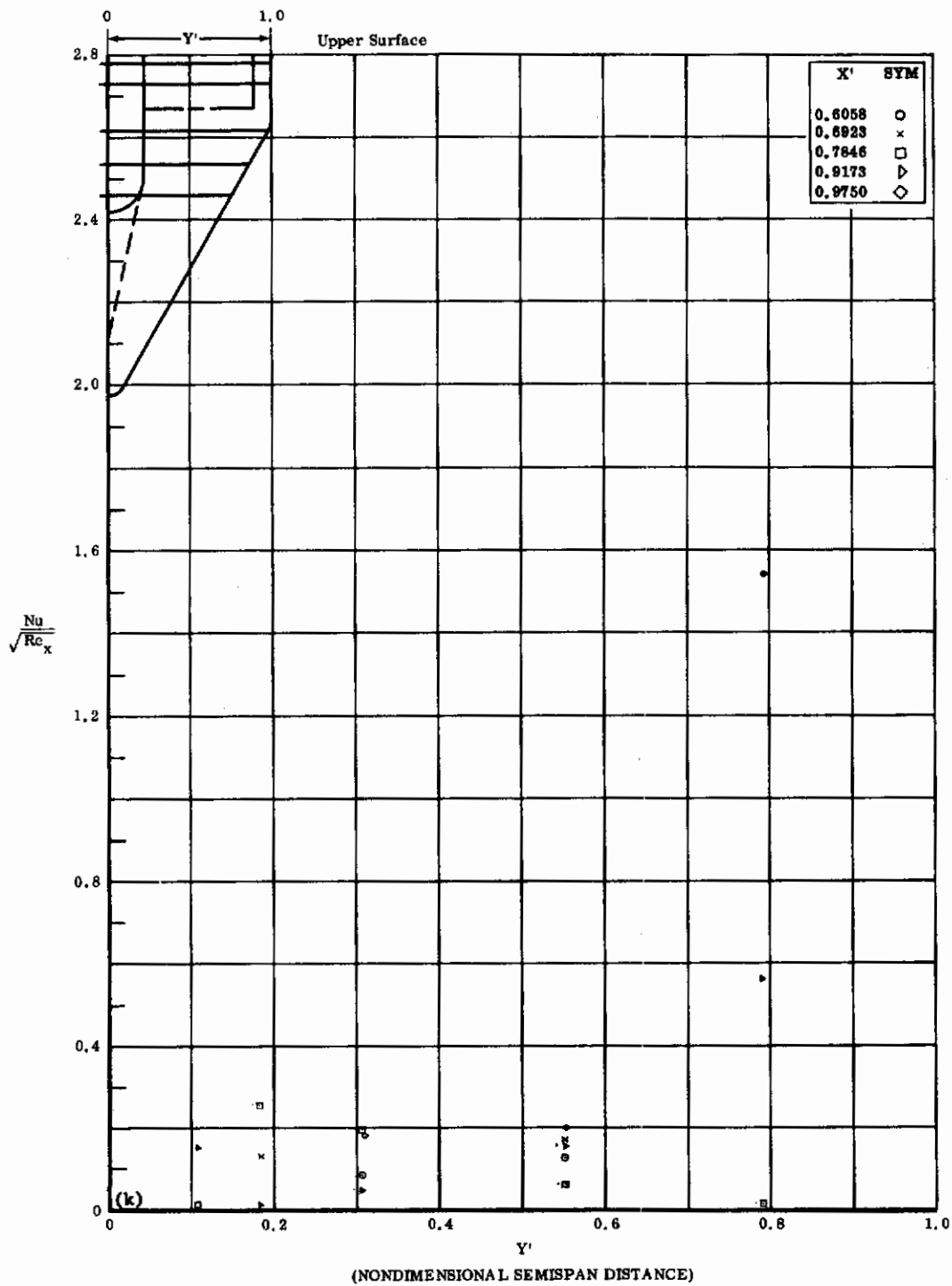


Fig. 20k Configuration IV, $\alpha = +20$, $b_2 = b_3 = -30$
 $\frac{Nu}{\sqrt{Re_x}}$ vs. Y' upper surface

Contrails

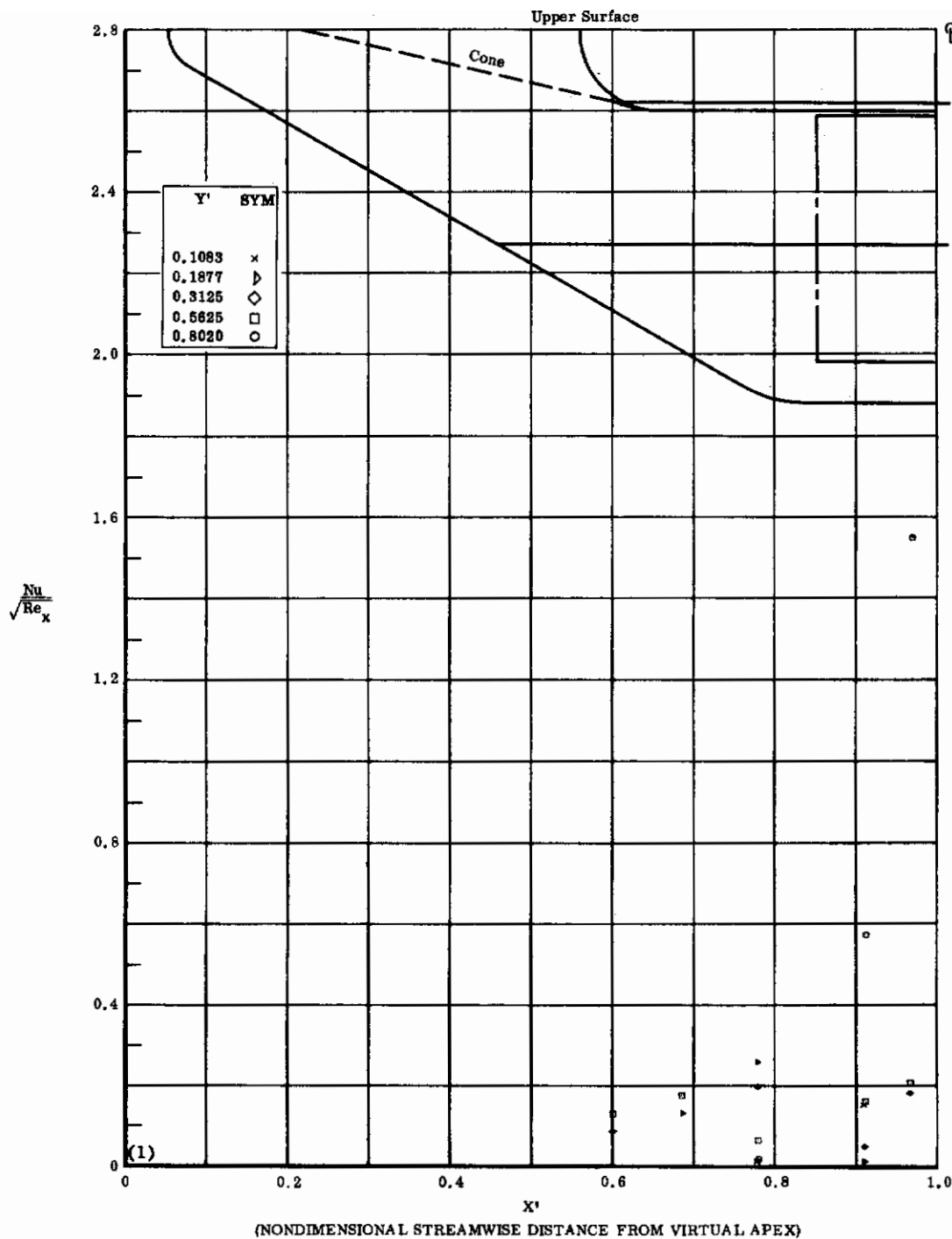


Fig. 20/ Configuration IV, $\alpha = +20^\circ$, $\delta_2 = \delta_3 = -30^\circ$

$Nu/\sqrt{Re_x}$ vs. X' upper surface

Contrails

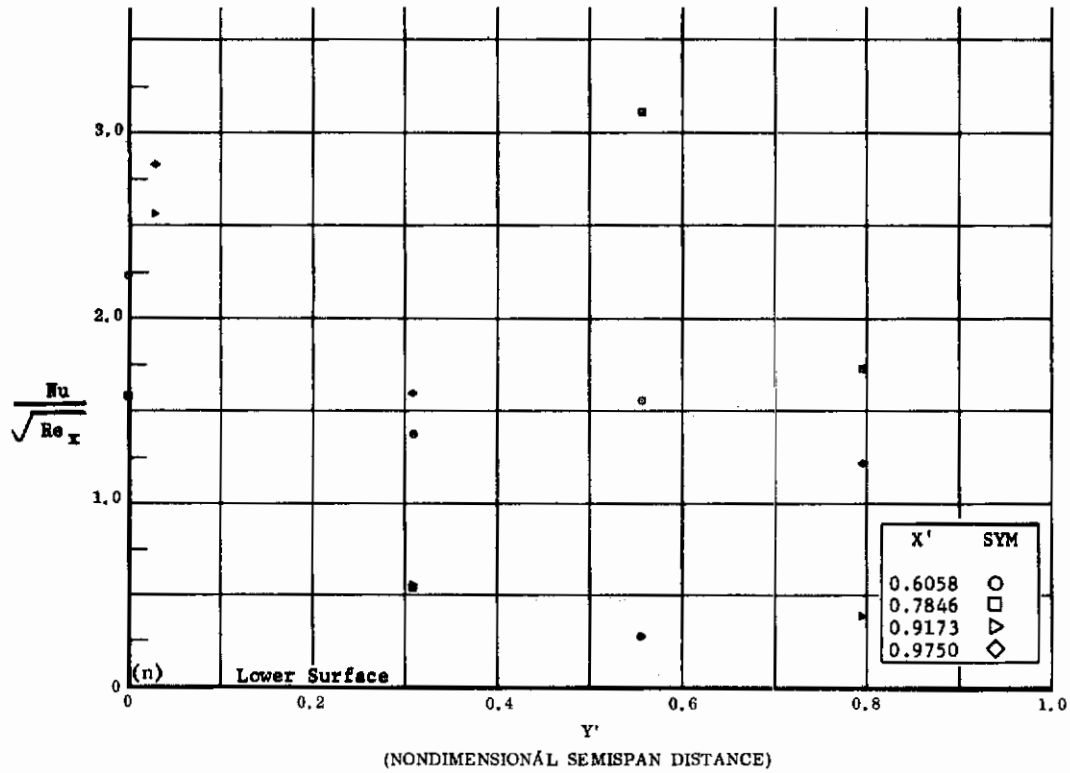
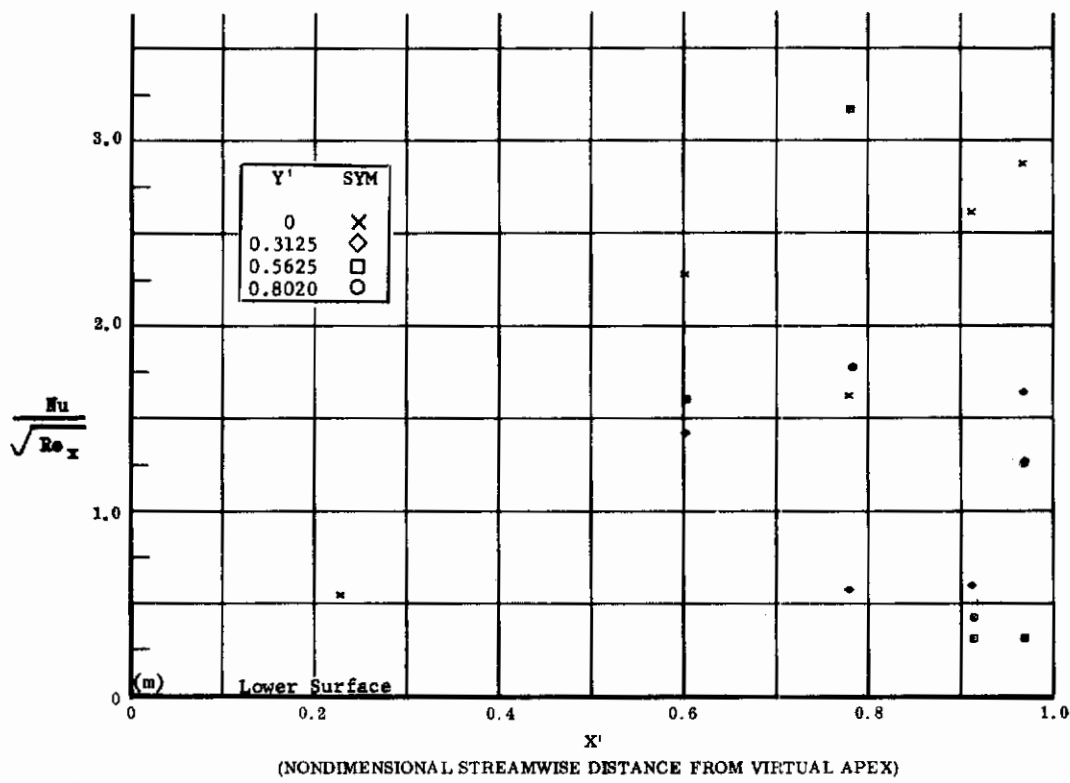


Fig. 20 Configuration IV, $\alpha = +20$, $\delta_2 = \delta_3 = -39$

m) $\text{Nu}/\sqrt{\text{Re}_x}$ vs. Y' lower surface

n) $\text{Nu}/\sqrt{\text{Re}_x}$ vs. X' lower surface

Contrails

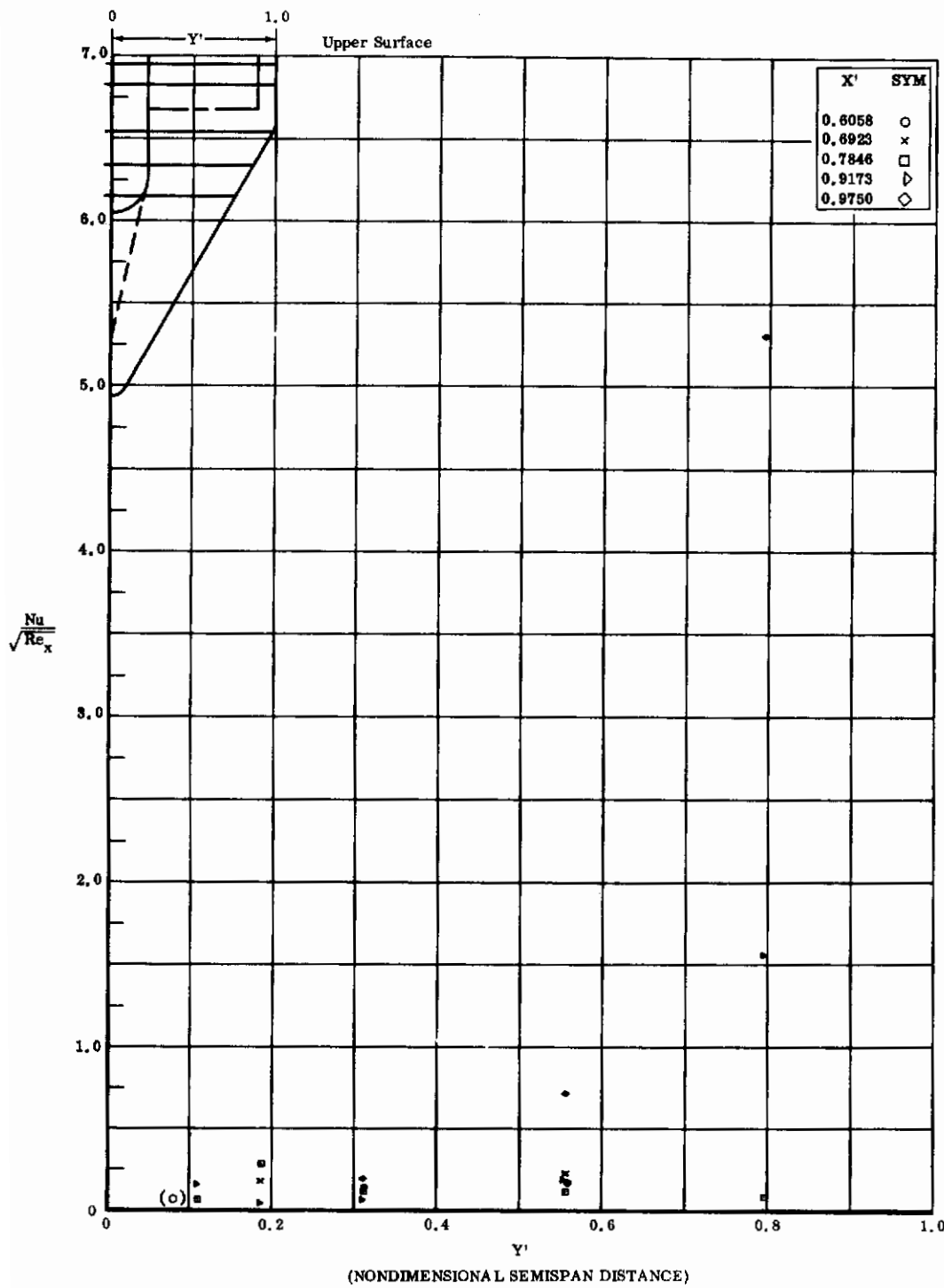


Fig. 20o Configuration IV, $\alpha = +20$, $\delta_2 = \delta_3 = -39$
 $Nu/\sqrt{Re_x}$ vs. Y' upper surface

Contrails

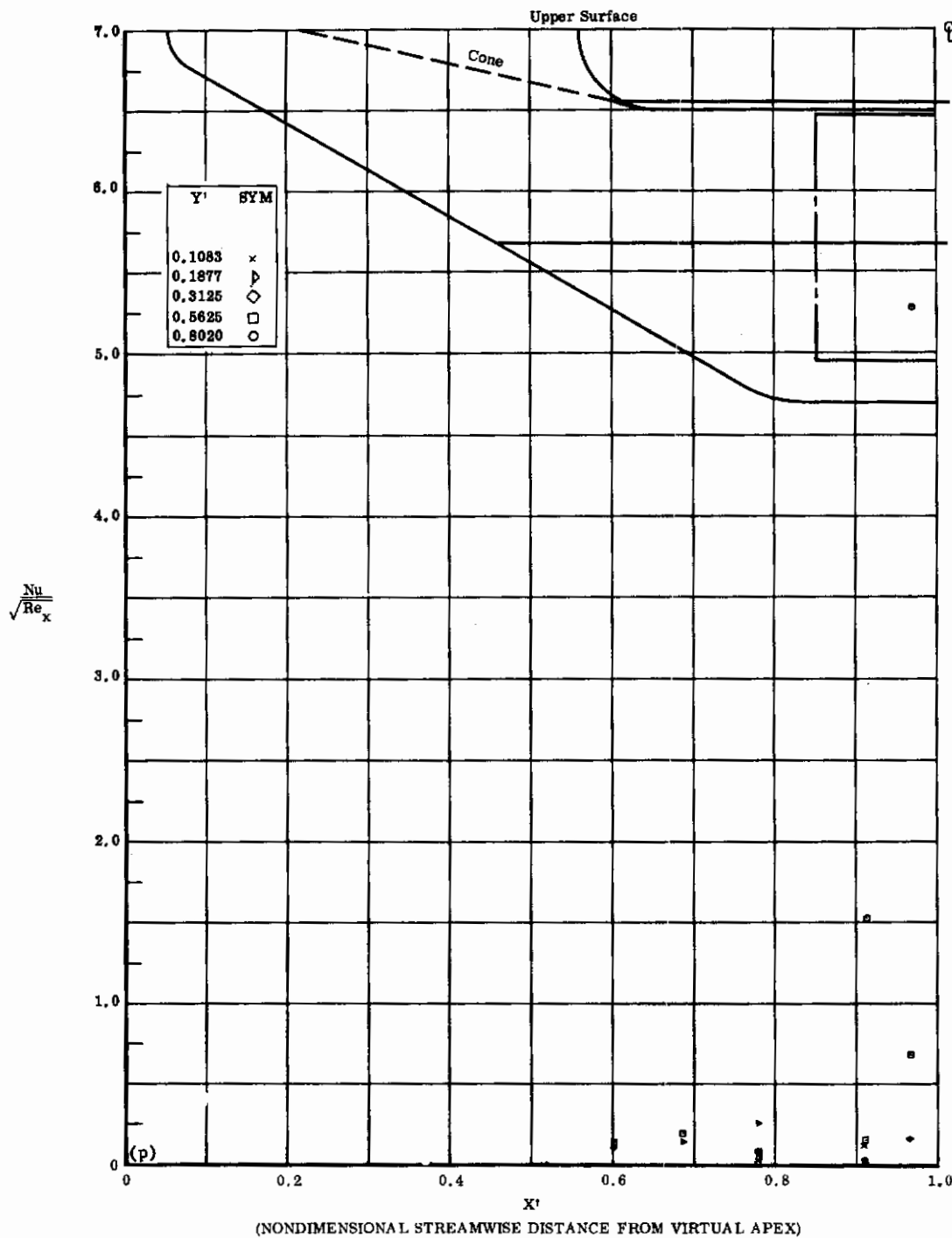


Fig. 20p Configuration IV, $\alpha = +20$, $b_2 = b_3 = -39$
 $Nu/\sqrt{Re_x}$ vs. X' upper surface

Contrails

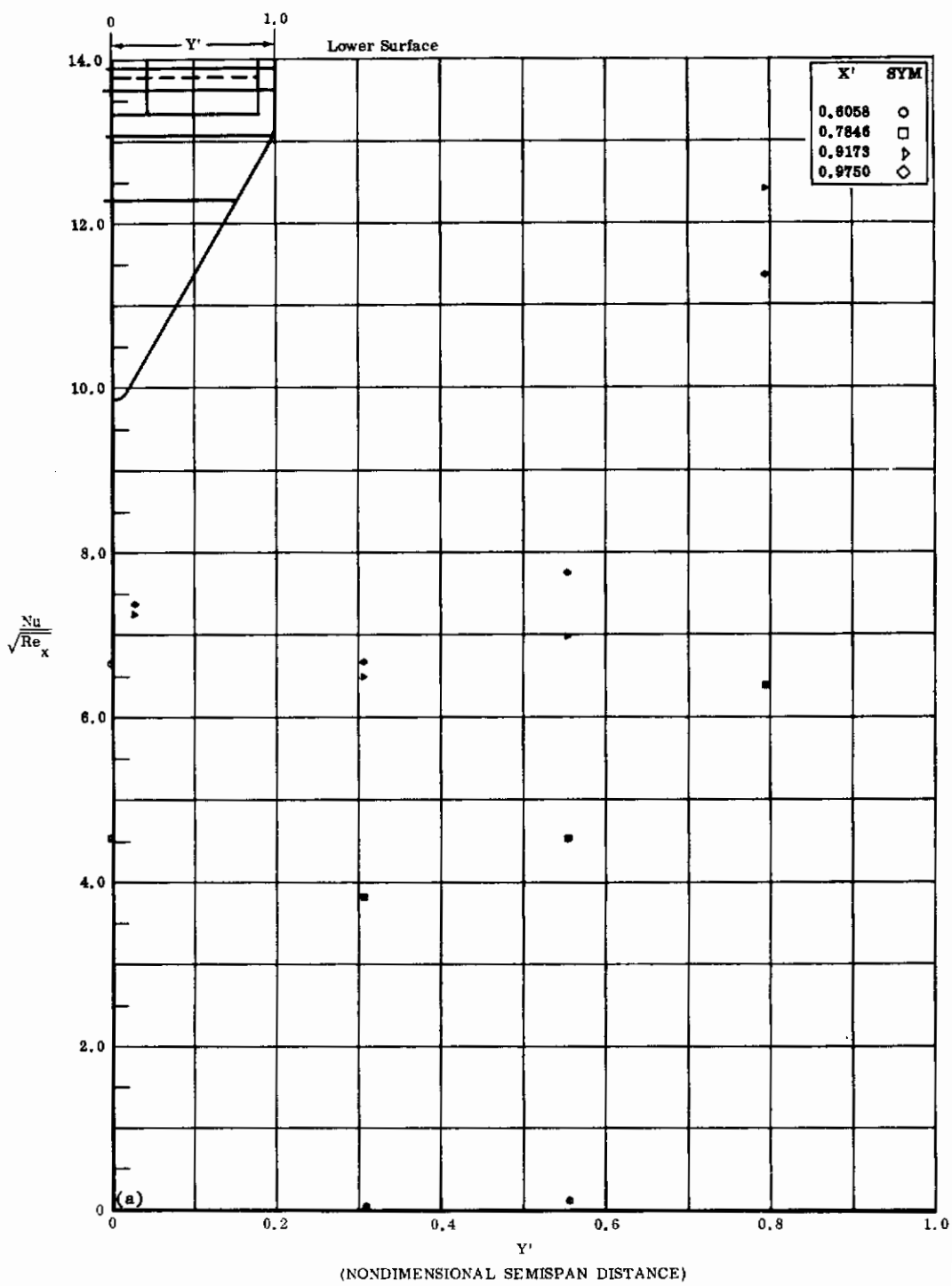


Fig. 21a Configuration IV, $\alpha = +35^\circ$, $\delta_2 = \delta_3 = 0$
 $Nu/\sqrt{Re_x}$ vs. Y' lower surface

Contrails

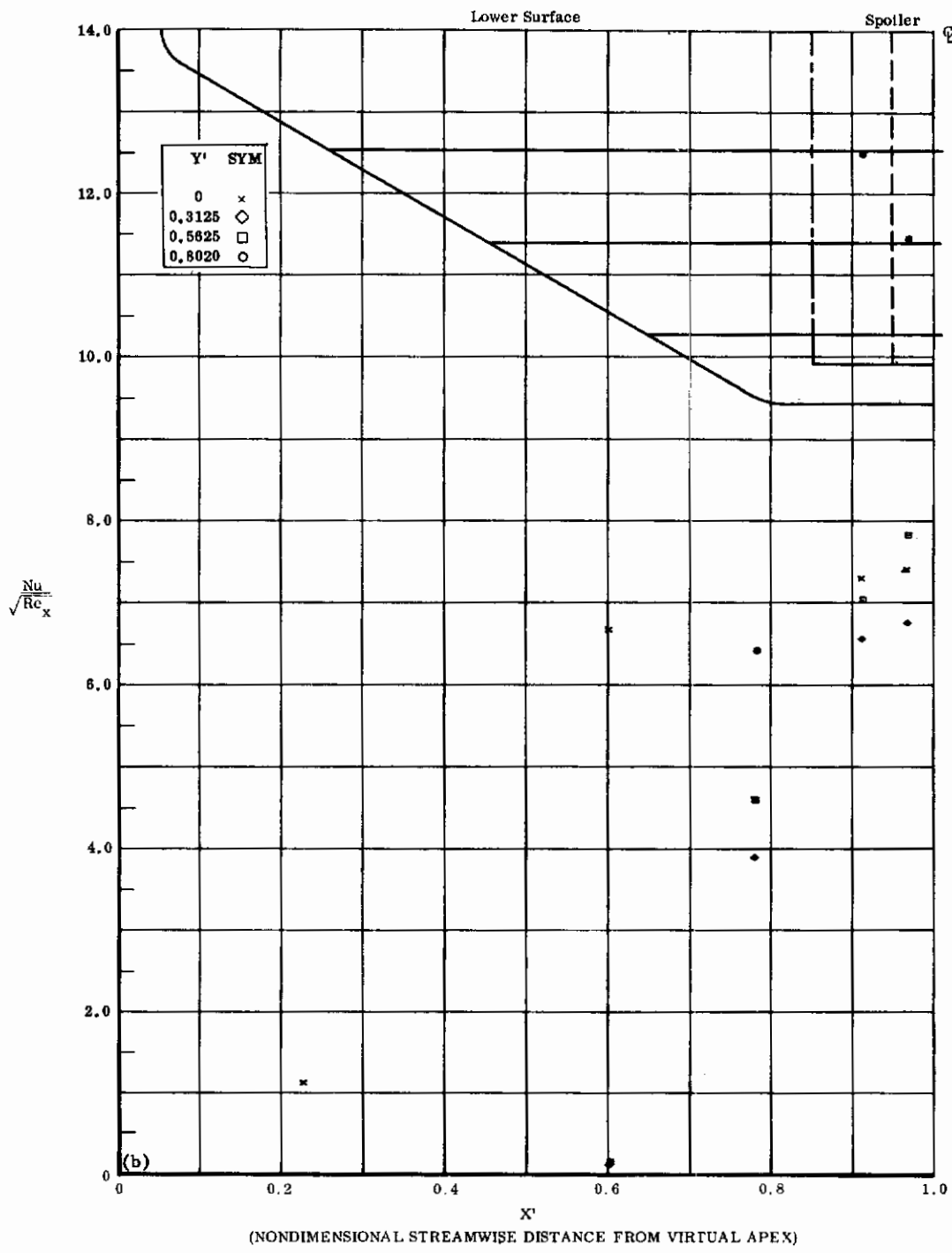


Fig. 21b Configuration IV, $\alpha = +35^\circ$, $\delta_2 = \delta_3 = 0$
 $\text{Nu}/\sqrt{\text{Re}_x}$ vs. X' lower surface

Contrails

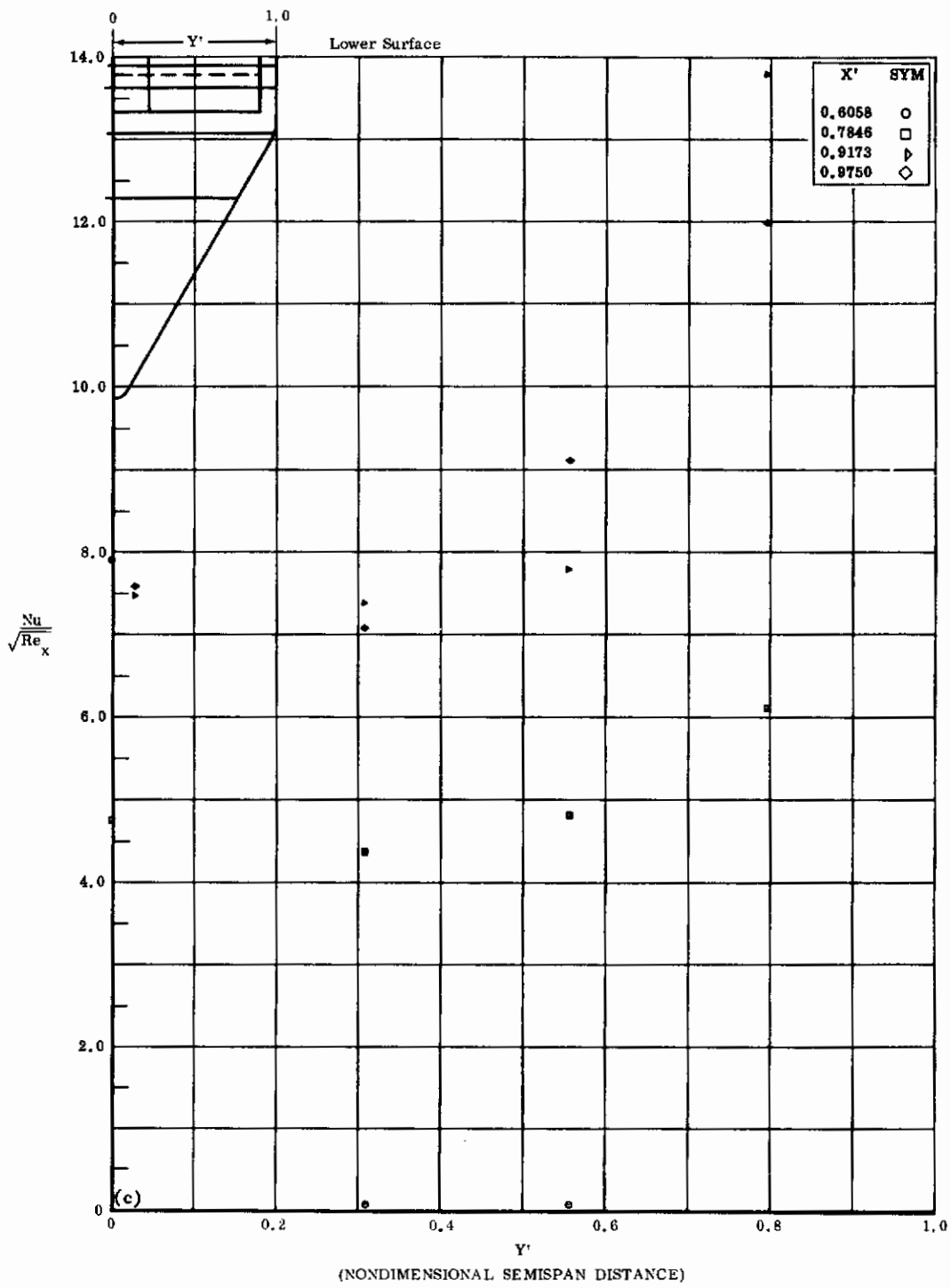


Fig. 2lc Configuration IV, $\alpha = +40^\circ$, $\delta_2 = \delta_3 = 0$
 $Nu/\sqrt{Re_x}$ vs. Y' lower surface

Contrails

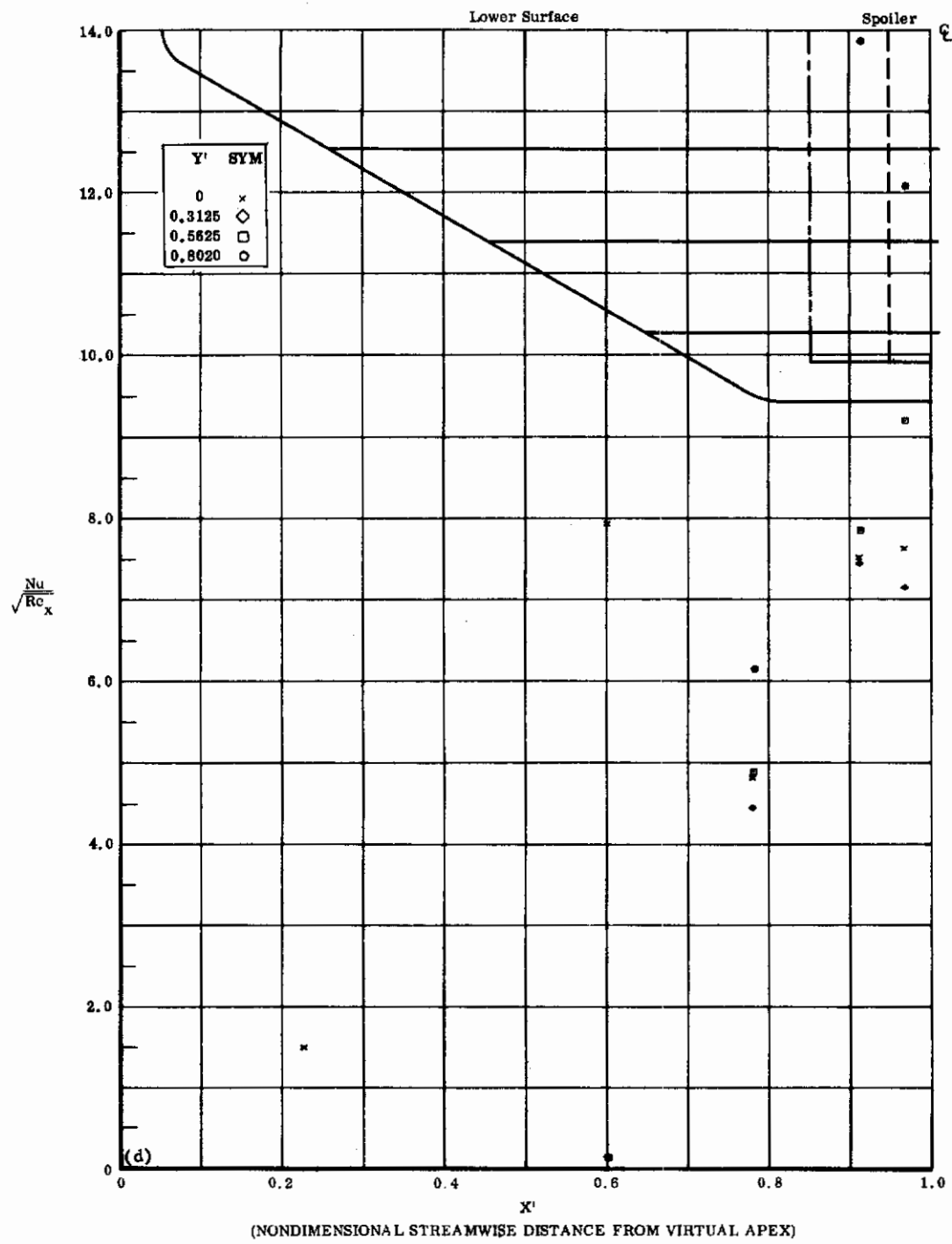
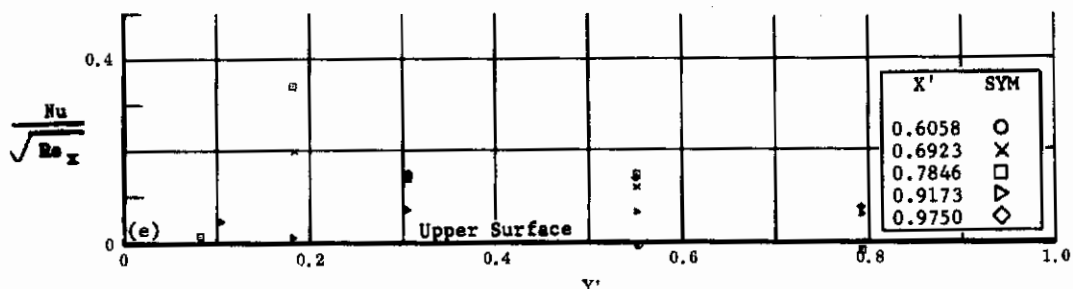


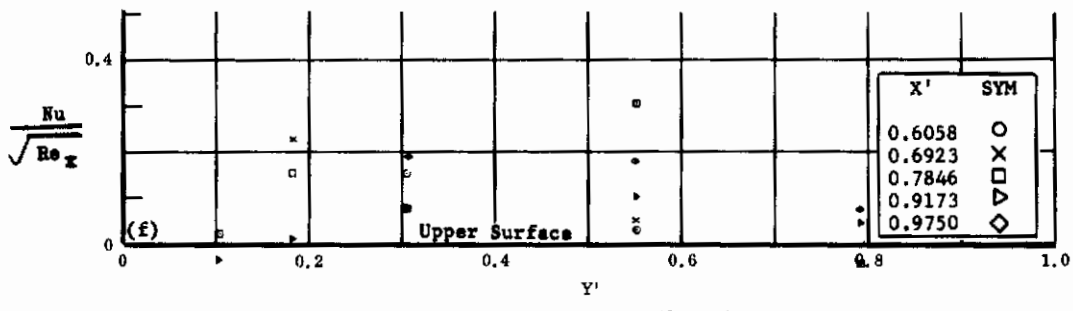
Fig. 21d Configuration IV, $\alpha = +40^\circ$, $\delta_2 = \delta_3 = 0$

$\text{Nu}/\sqrt{\text{Re}_x}$ vs. X' lower surface

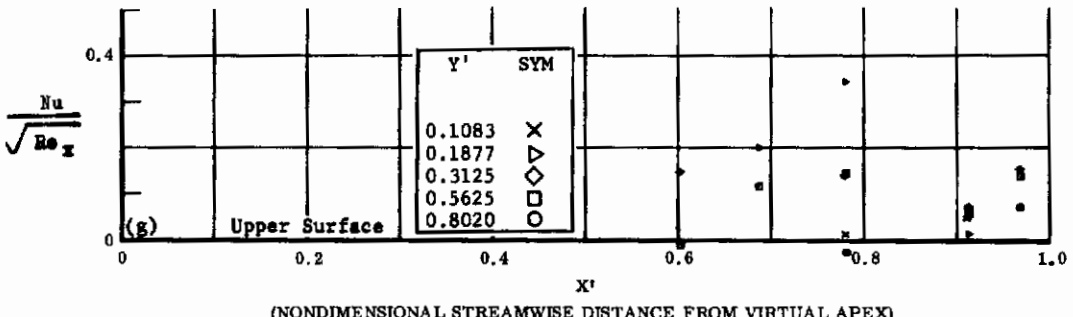
Controls



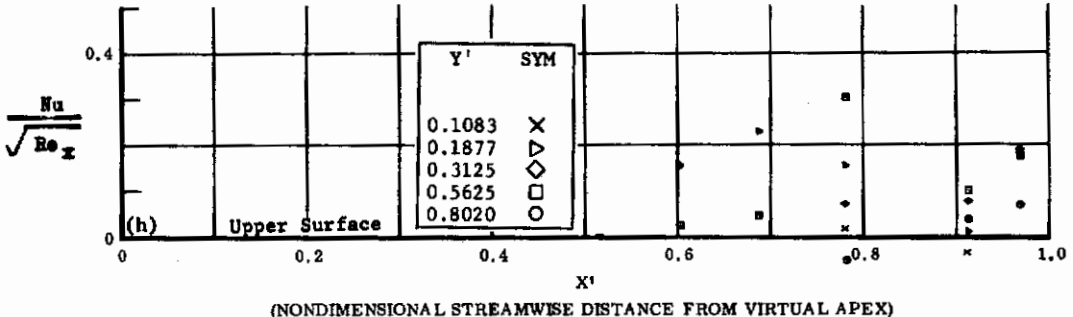
(NONDIMENSIONAL SEMISPAN DISTANCE)



(NONDIMENSIONAL SEMISPAN DISTANCE)



(NONDIMENSIONAL STREAMWISE DISTANCE FROM VIRTUAL APEX)



(NONDIMENSIONAL STREAMWISE DISTANCE FROM VIRTUAL APEX)

Fig. 21 Configuration IV, $\delta_2 = \delta_3 = 0$, upper surface

e) $\frac{Nu}{\sqrt{Re_x}}$ vs. Y' , $\alpha = +35$

f) $\frac{Nu}{\sqrt{Re_x}}$ vs. Y' , $\alpha = +40$

g) $\frac{Nu}{\sqrt{Re_x}}$ vs. X' , $\alpha = +35$

h) $\frac{Nu}{\sqrt{Re_x}}$ vs. X' , $\alpha = +40$

Contrails

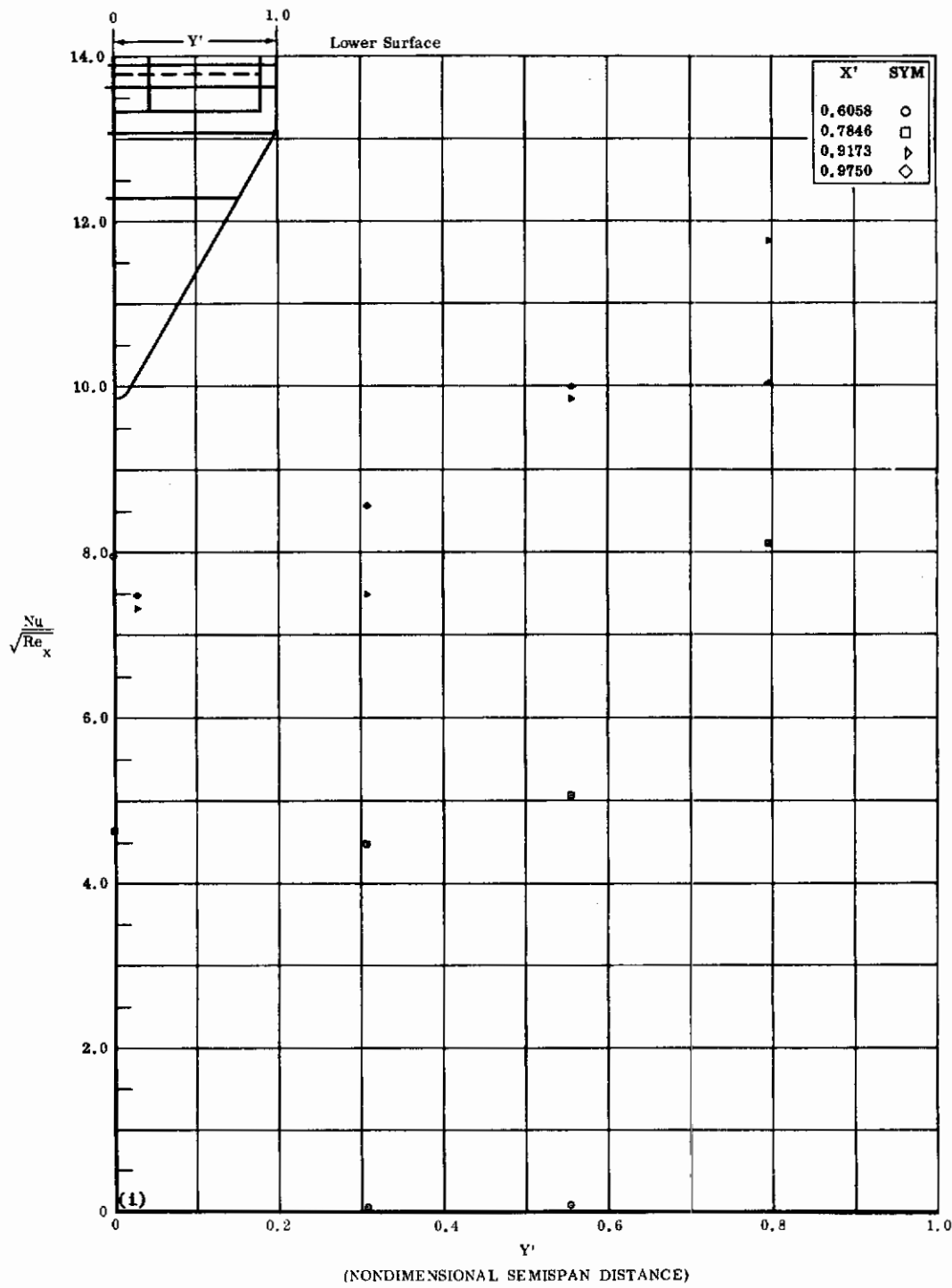


Fig. 21i Configuration IV, $\alpha = +45^\circ$, $\delta_2 = \delta_3 = 0$

$Nu/\sqrt{Re_x}$ vs. Y' lower surface

Contrails

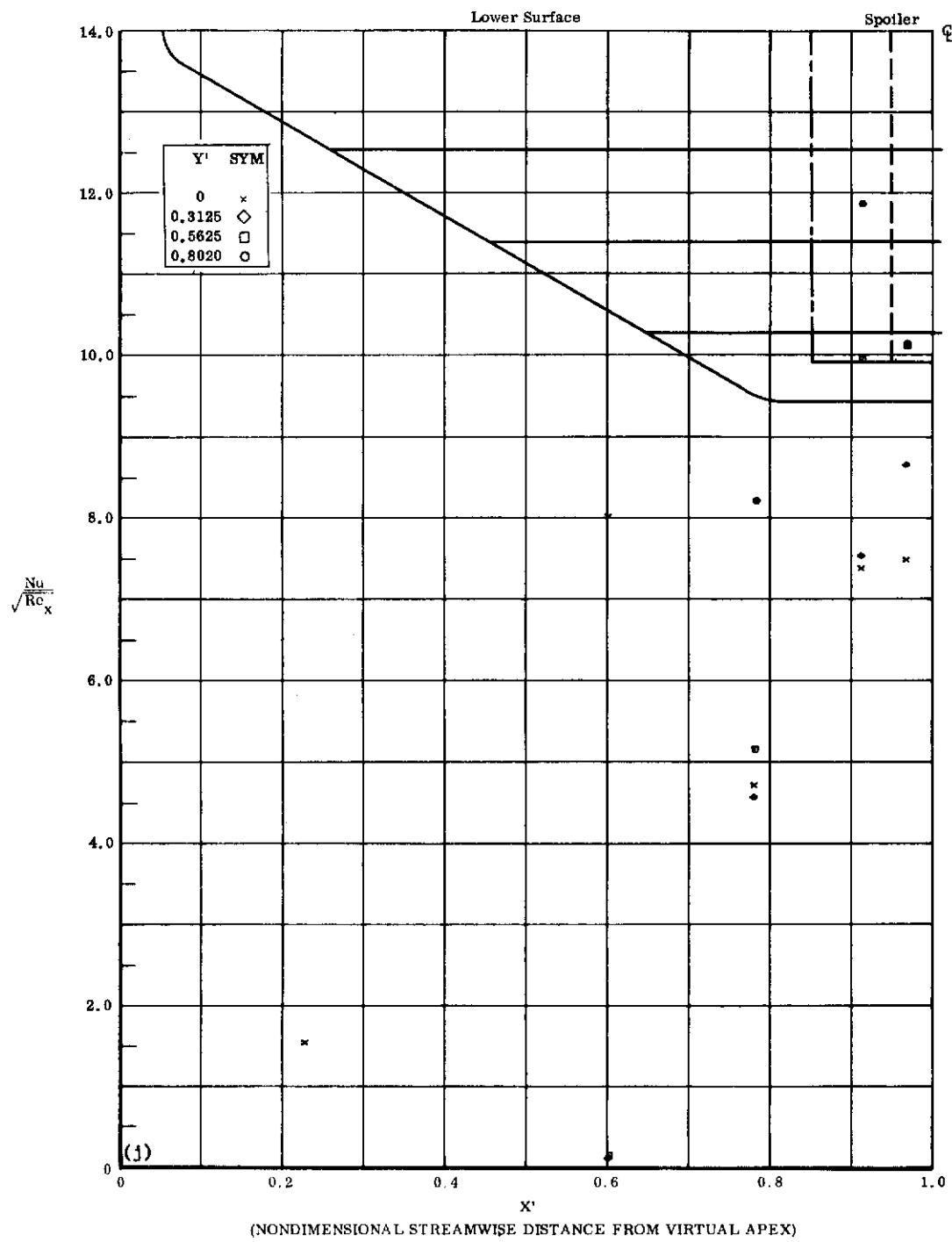


Fig. 21j Configuration IV, $\alpha = +45^\circ$, $\delta_2 = \delta_3 = 0$
 $\text{Nu}/\sqrt{\text{Re}_x}$ vs. X' lower surface

Contrails

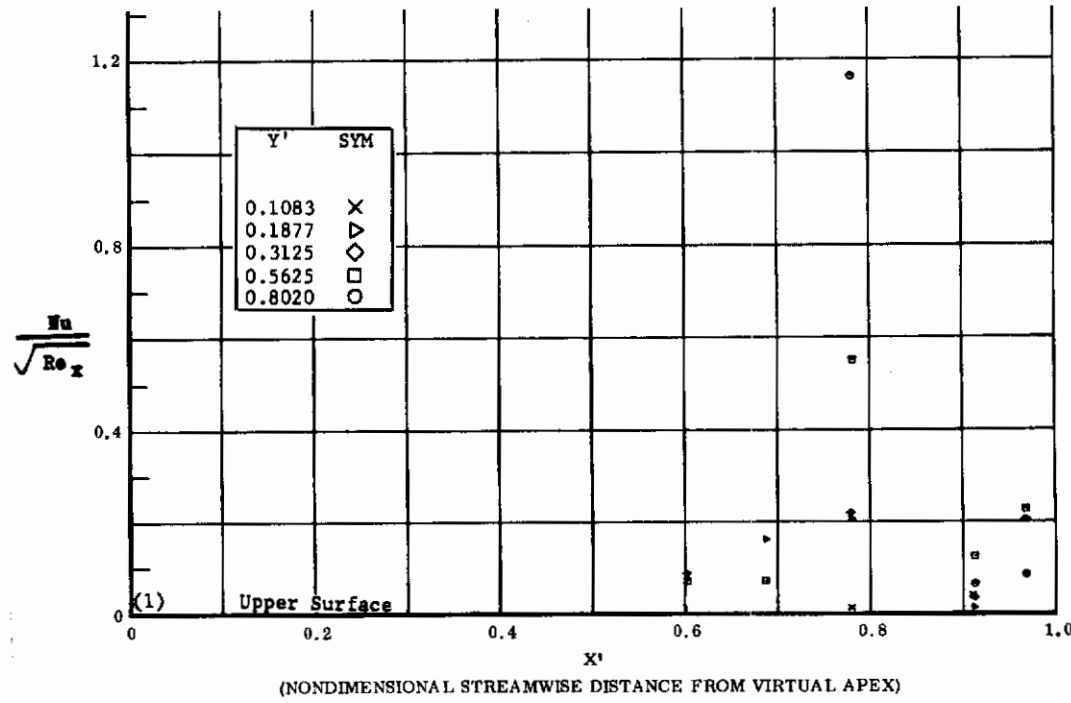
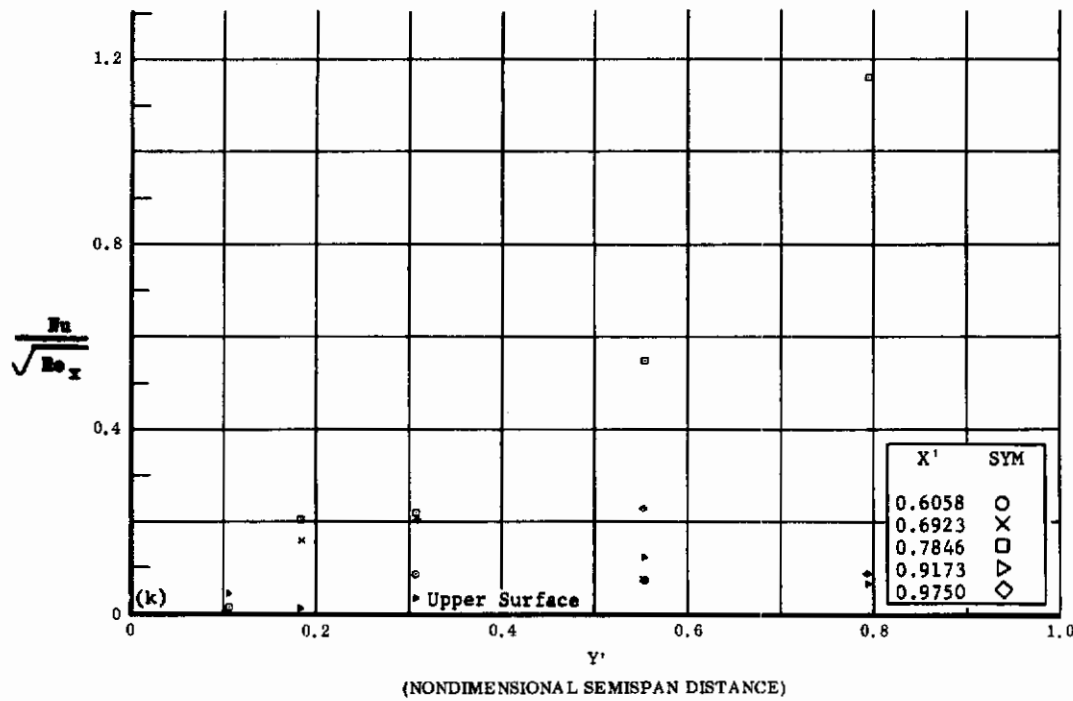


Fig. 21 Configuration IV, $\alpha = +45^\circ$, $\delta_2 = \delta_3 = 0$

k) $\bar{N}_u/\sqrt{Re_x}$ vs. Y' upper surface

l) $\bar{N}_u/\sqrt{Re_x}$ vs. X^1 upper surface

Contrails

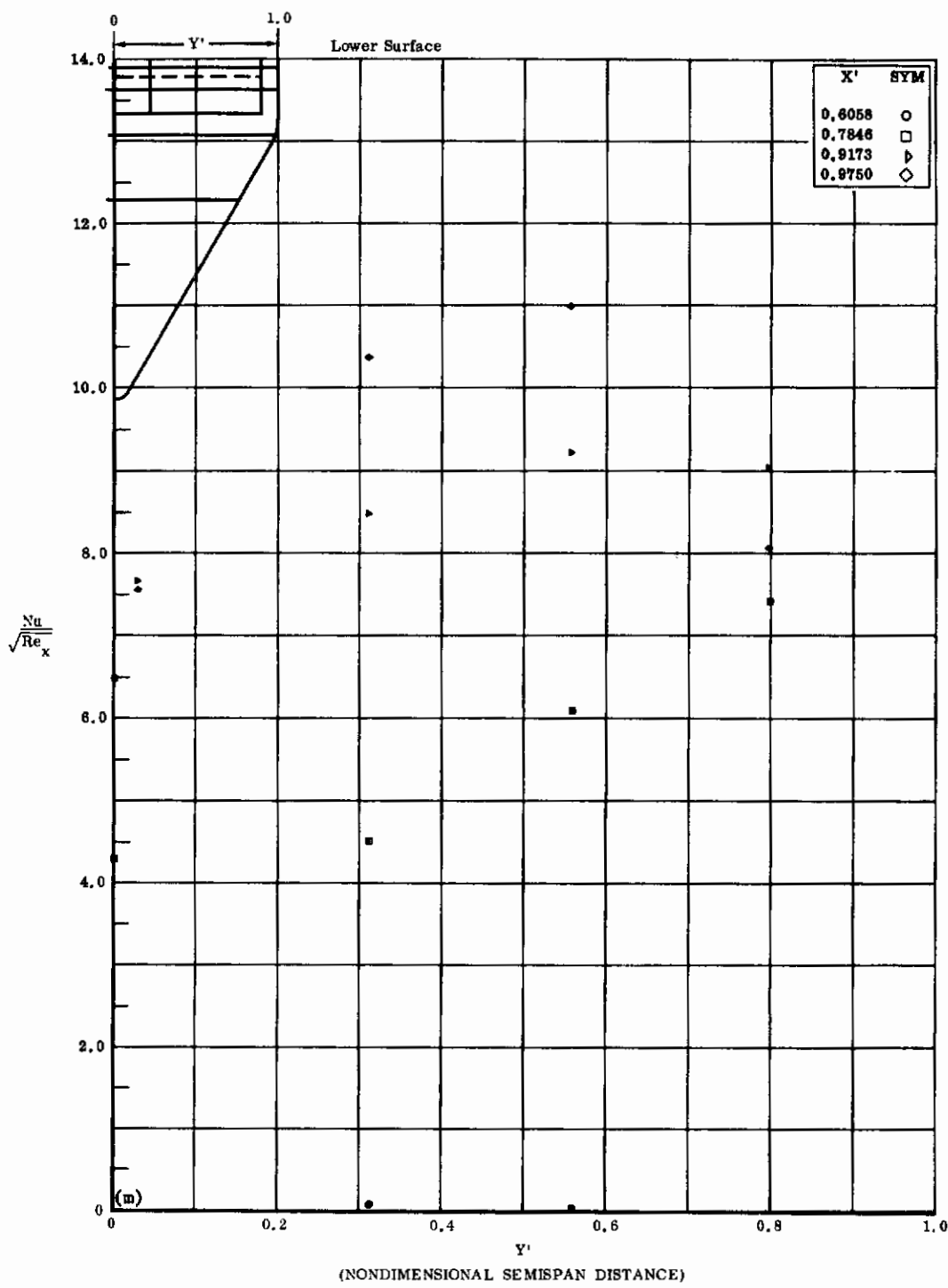


Fig. 21m Configuration IV, $\alpha = +50^\circ$, $\delta_2 = \delta_3 = 0$
 $Nu/\sqrt{Re_x}$ vs. Y' lower surface

Contrails

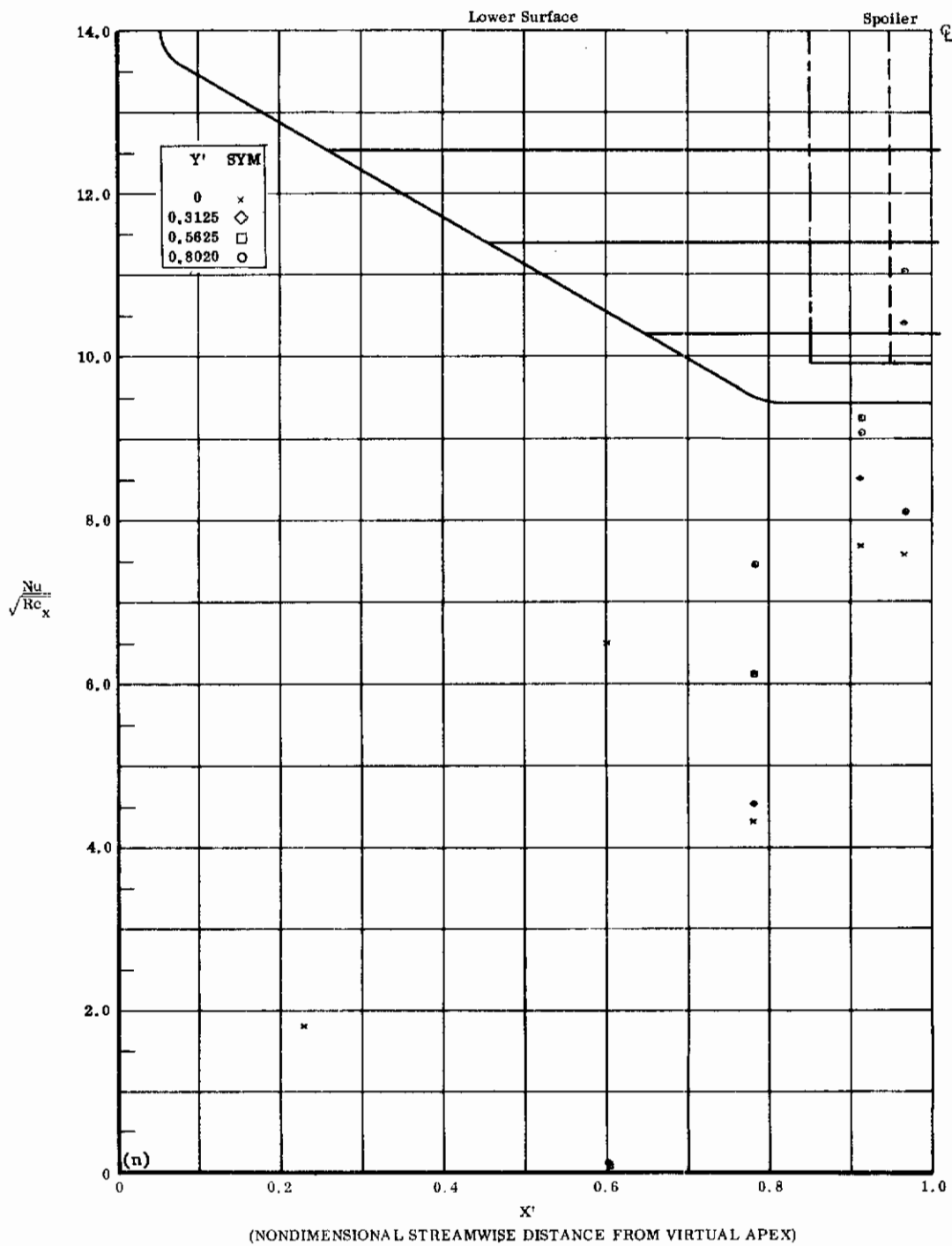


Fig. 21n Configuration IV, $\alpha = +50^\circ$, $\delta_2 = \delta_3 = 0$

$\text{Nu}/\sqrt{\text{Re}_x}$ vs. X' lower surface

Contrails

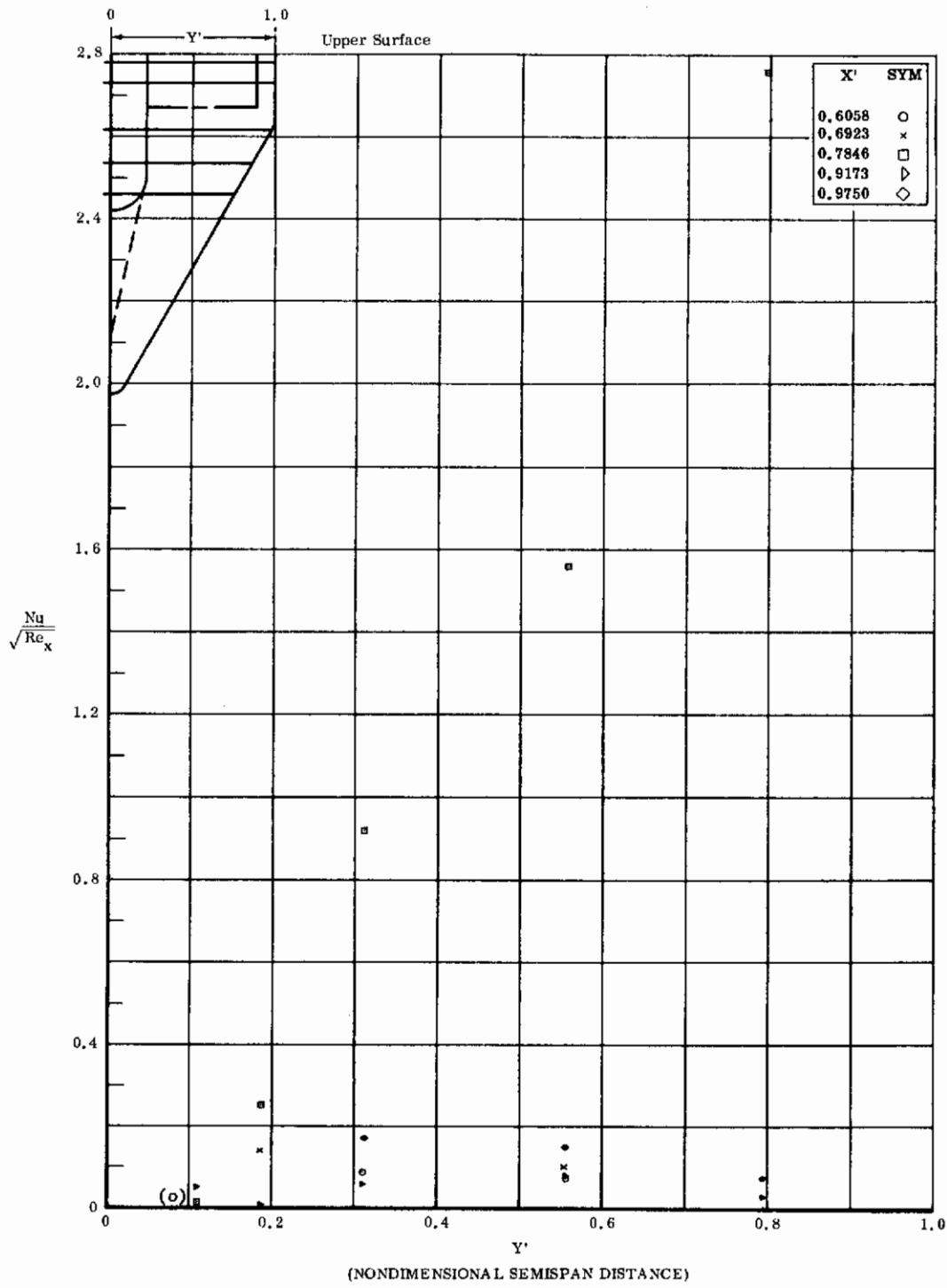


Fig. 21o Configuration IV, $\alpha = +50$, $\delta_2 = \delta_3 = 0$
 $\text{Nu}/\sqrt{\text{Re}_x}$ vs. Y' upper surface

Contrails

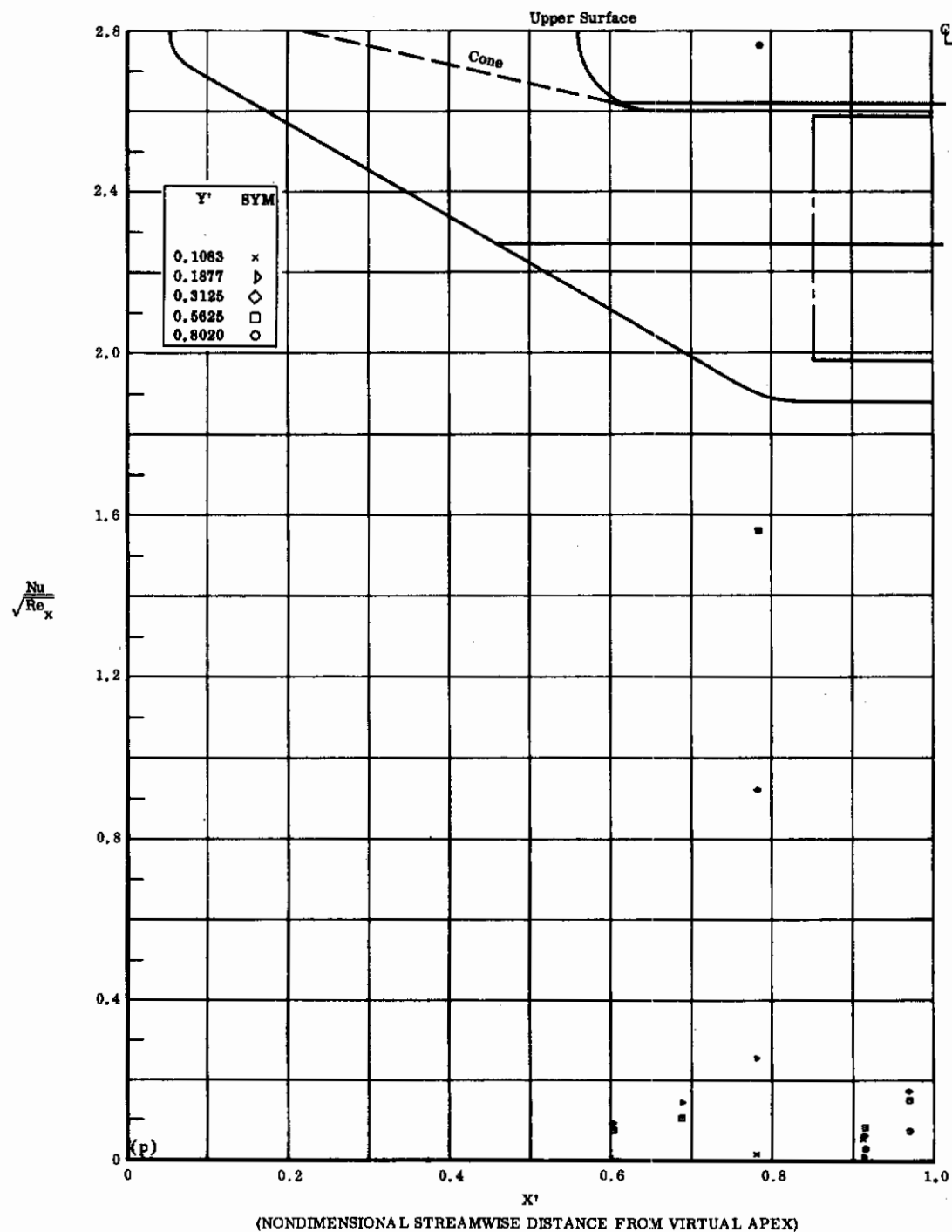


Fig. 21p Configuration IV, $\alpha = +50^\circ$, $\delta_2 = \delta_3 = 0$

$Nu/\sqrt{Re_x}$ vs. X' upper surface

Contrails

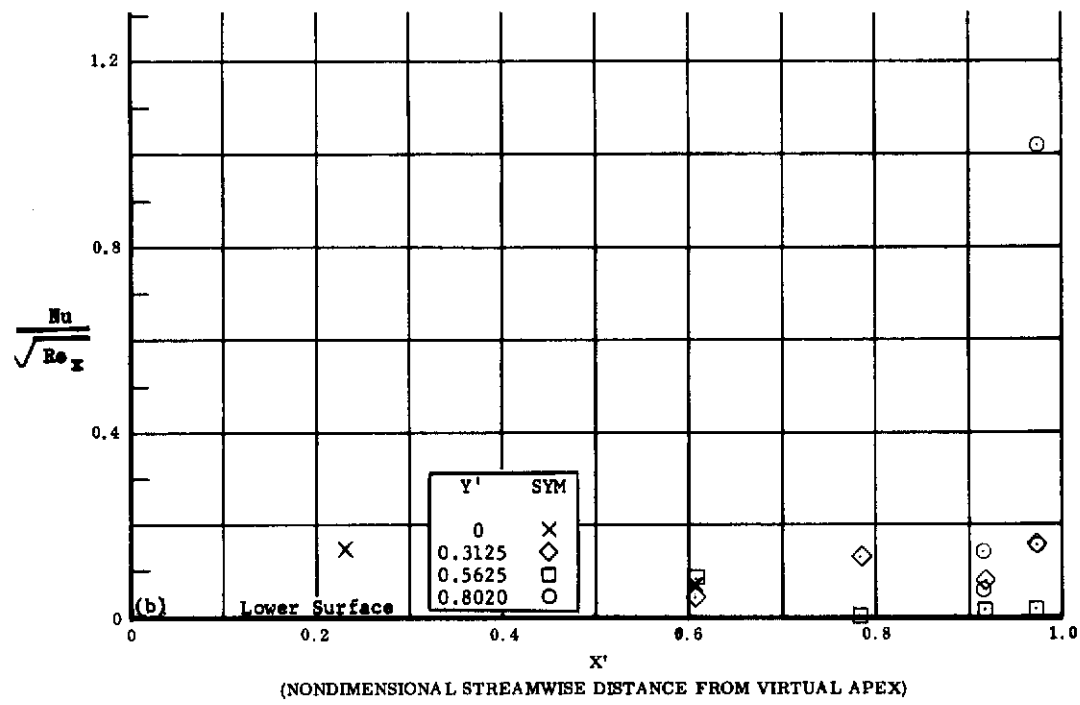
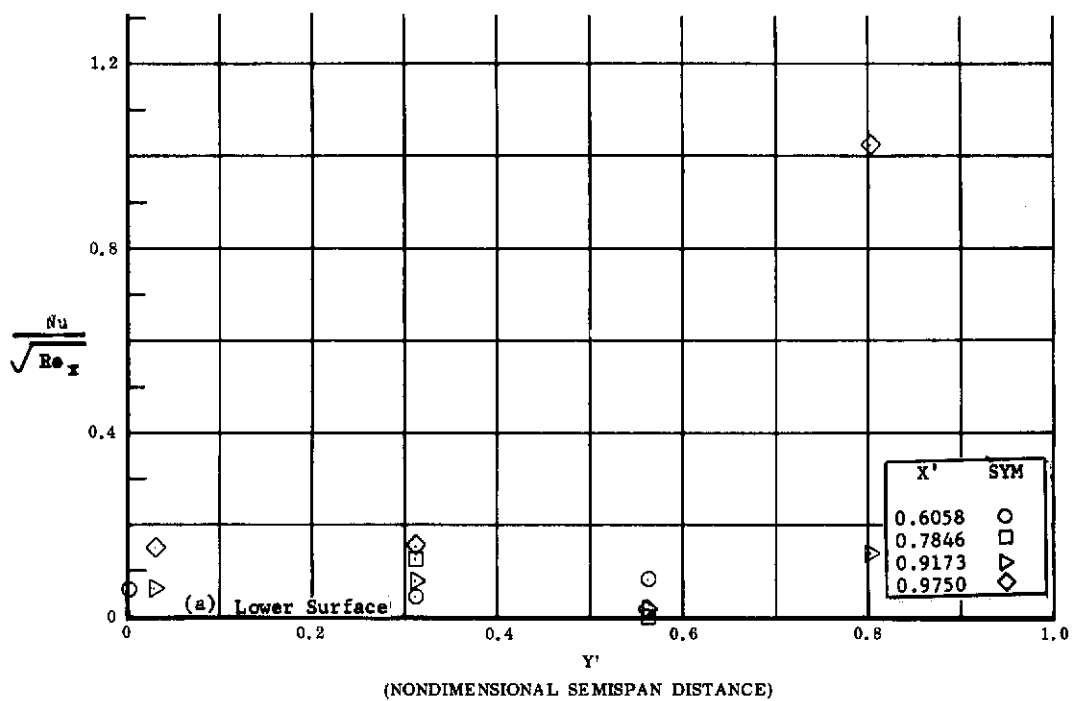


Fig. 22 Configuration IV, $\alpha = -10$, $\delta_2 = \delta_3 = 0$

- a) $Nu/\sqrt{Re_x}$ vs. Y' lower surface
- b) $Nu/\sqrt{Re_x}$ vs. X' lower surface

Contrails

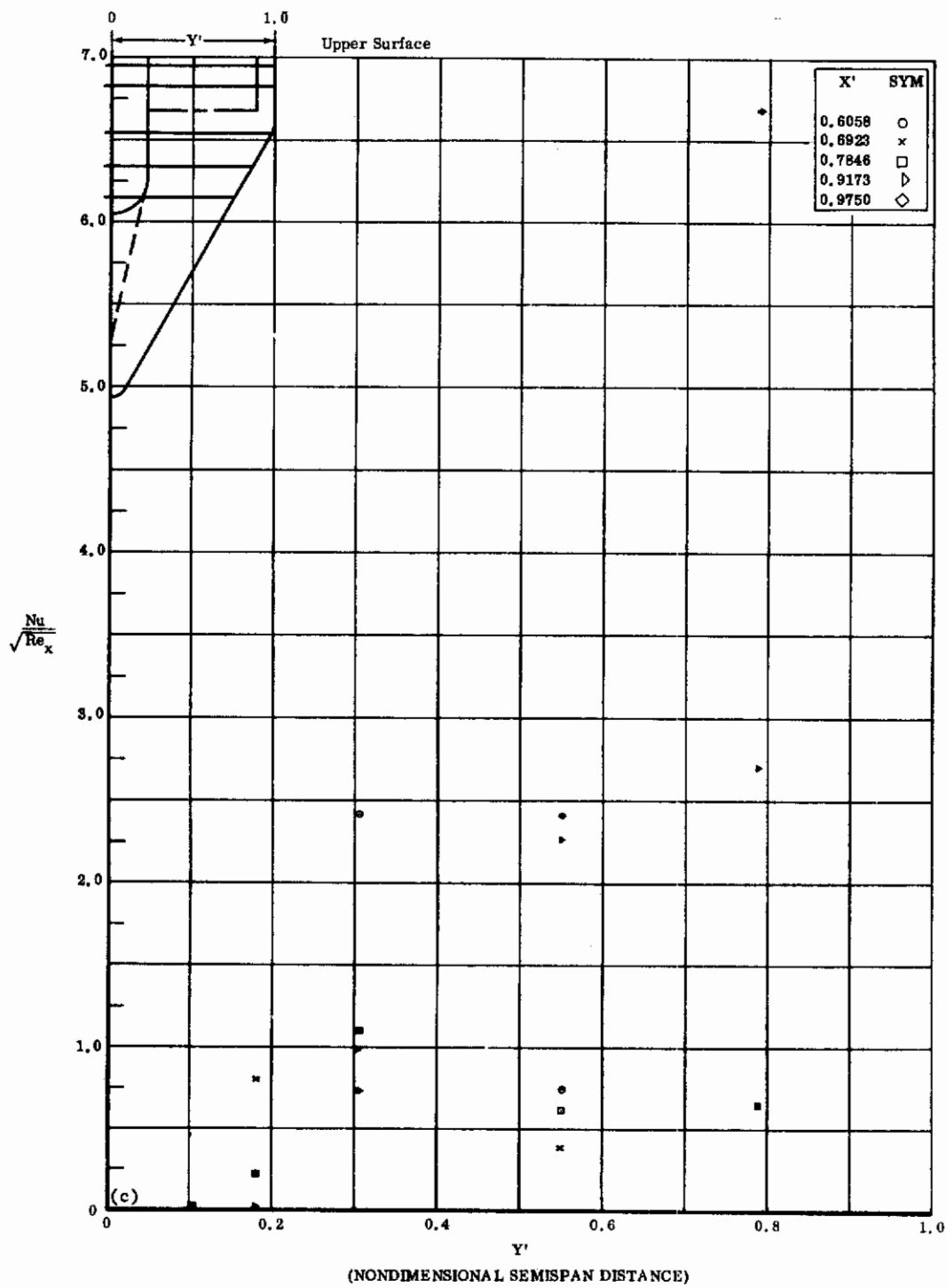


Fig. 22c Configuration IV, $\alpha = -10$, $\delta_2 = \delta_3 = 0$
 $Nu/\sqrt{Re_x}$ vs. Y' upper surface

Contrails

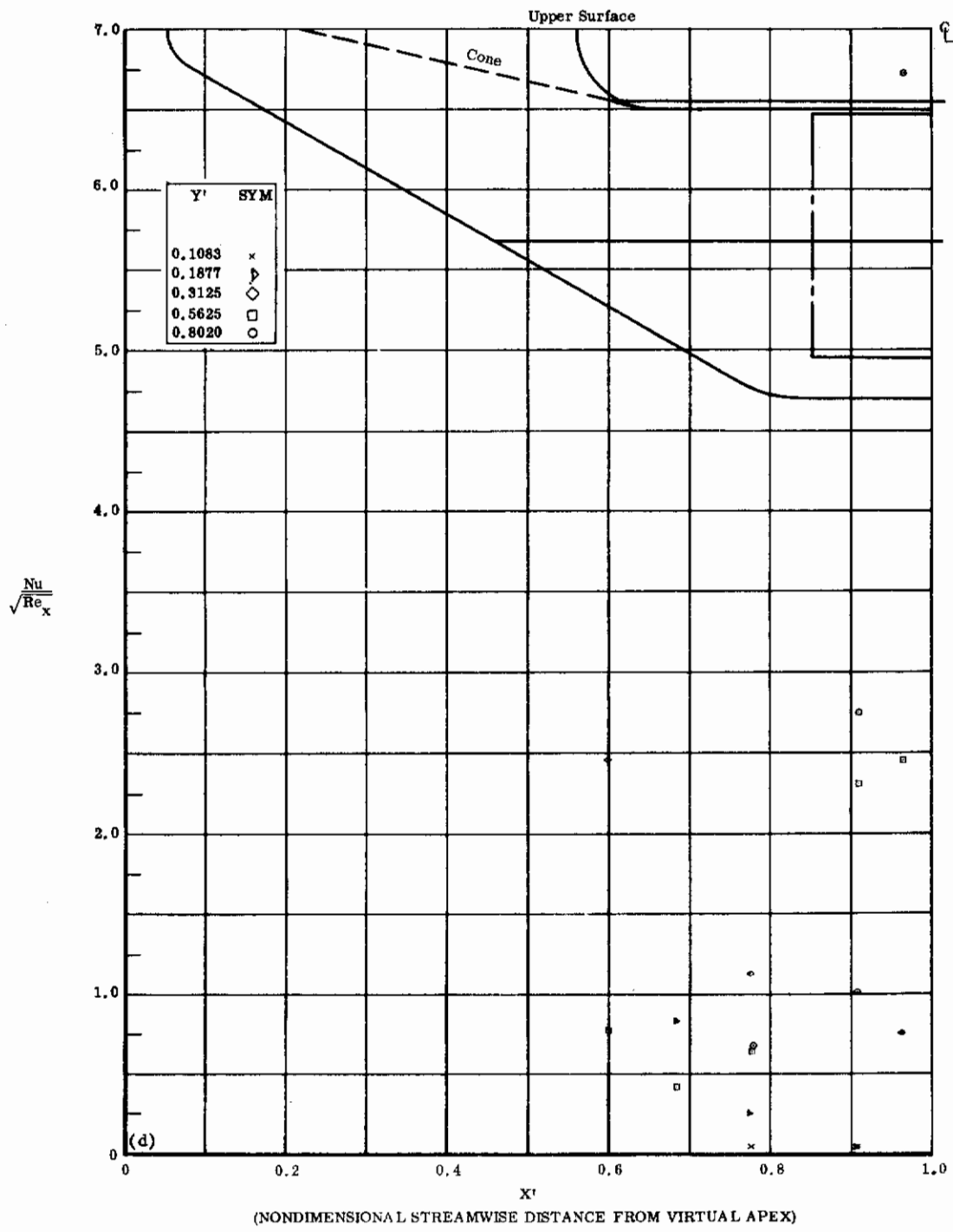


Fig. 22d Configuration IV, $\alpha = -10$, $\delta_2 = \delta_3 = 0$

$Nu/\sqrt{Re_x}$ vs. X' upper surface

Contrails

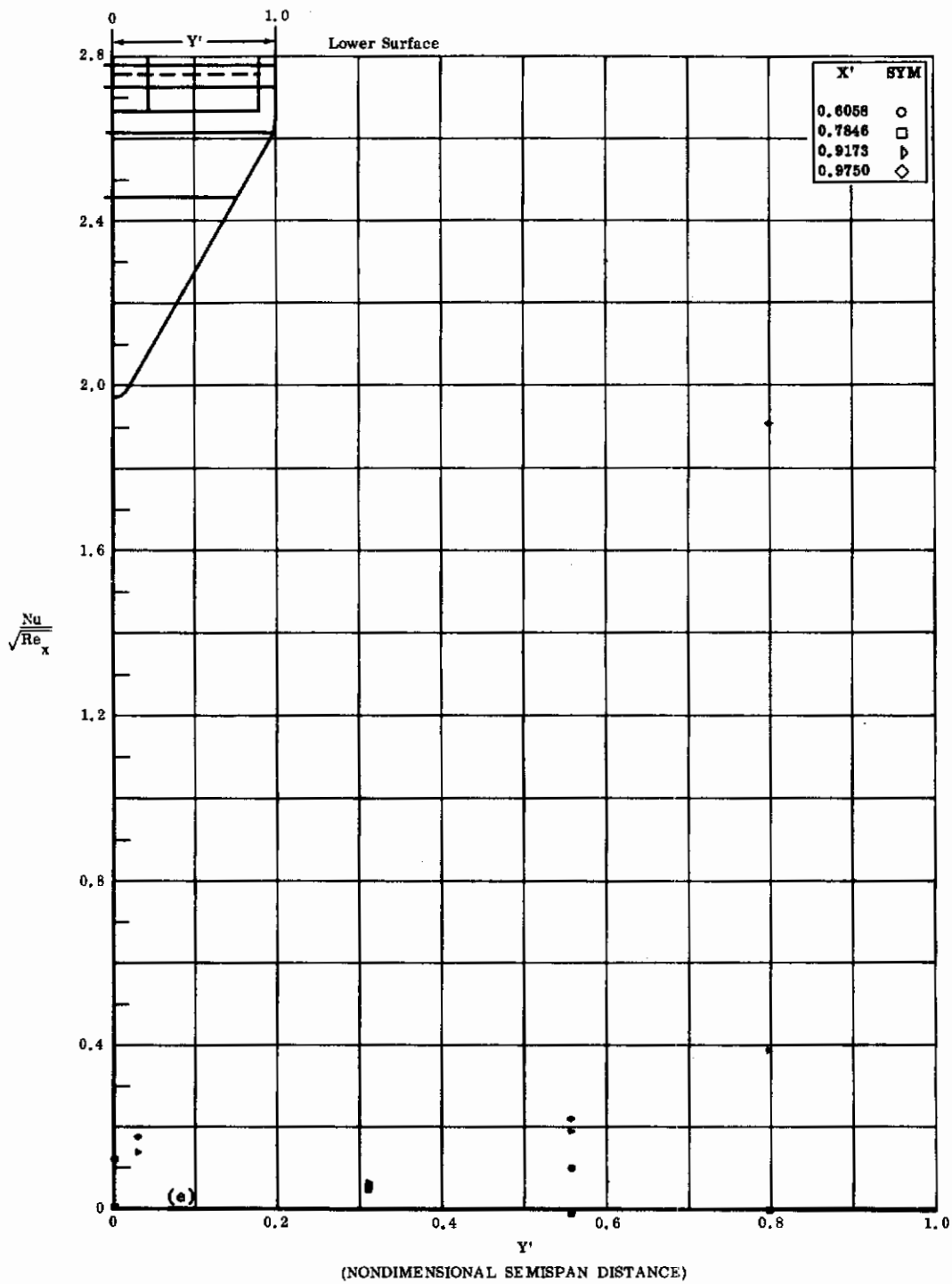


Fig. 22e Configuration IV, $\alpha = -10$, $\delta_2 = \delta_3 = +10$
 $.Nu/\sqrt{Re_x}$ vs. Y' lower surface

Contrails

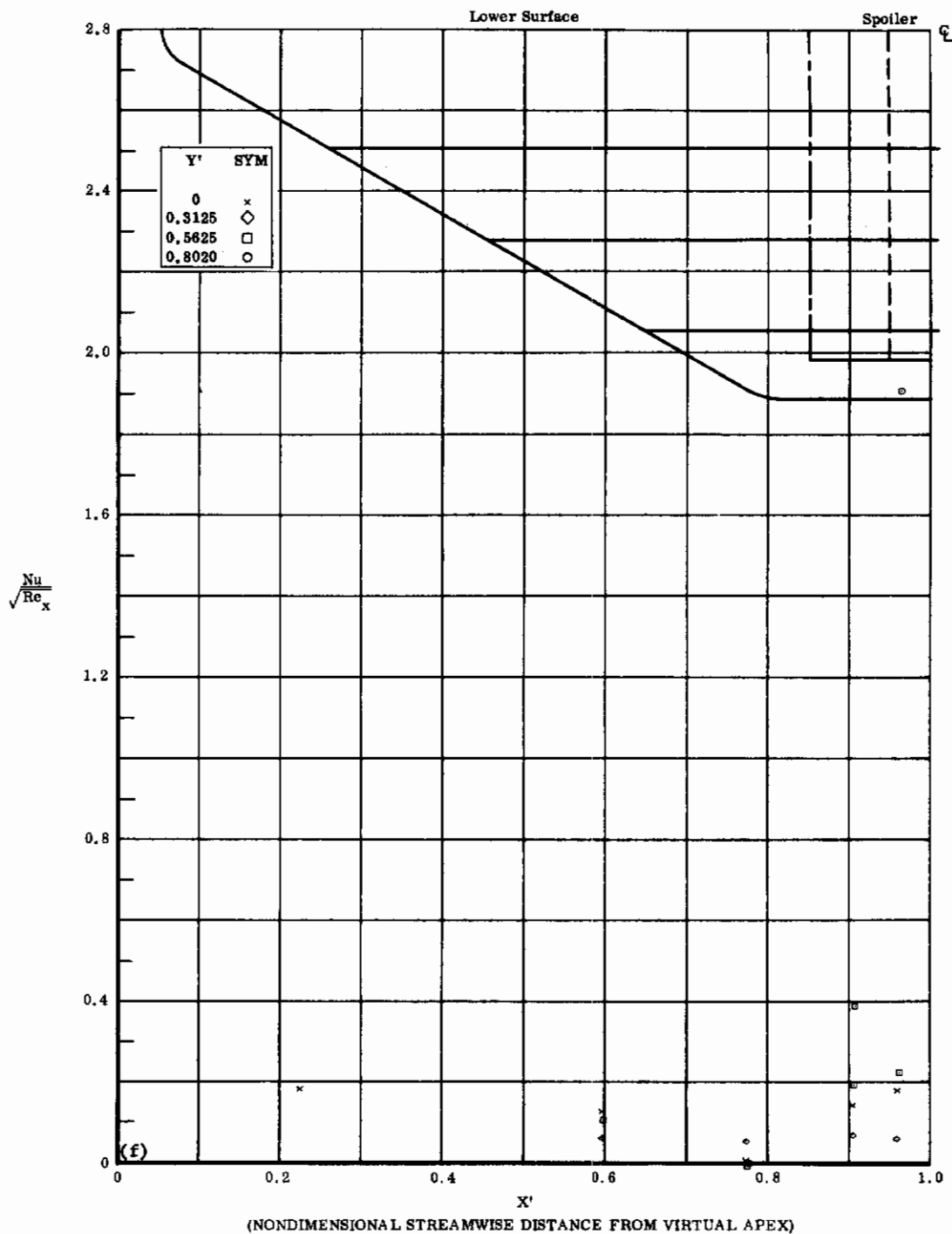


Fig. 22f Configuration IV, $\alpha = -10$, $\delta_2 = \delta_3 = +10$
 $Nu/\sqrt{Re_x}$ vs. X' lower surface

Contrails

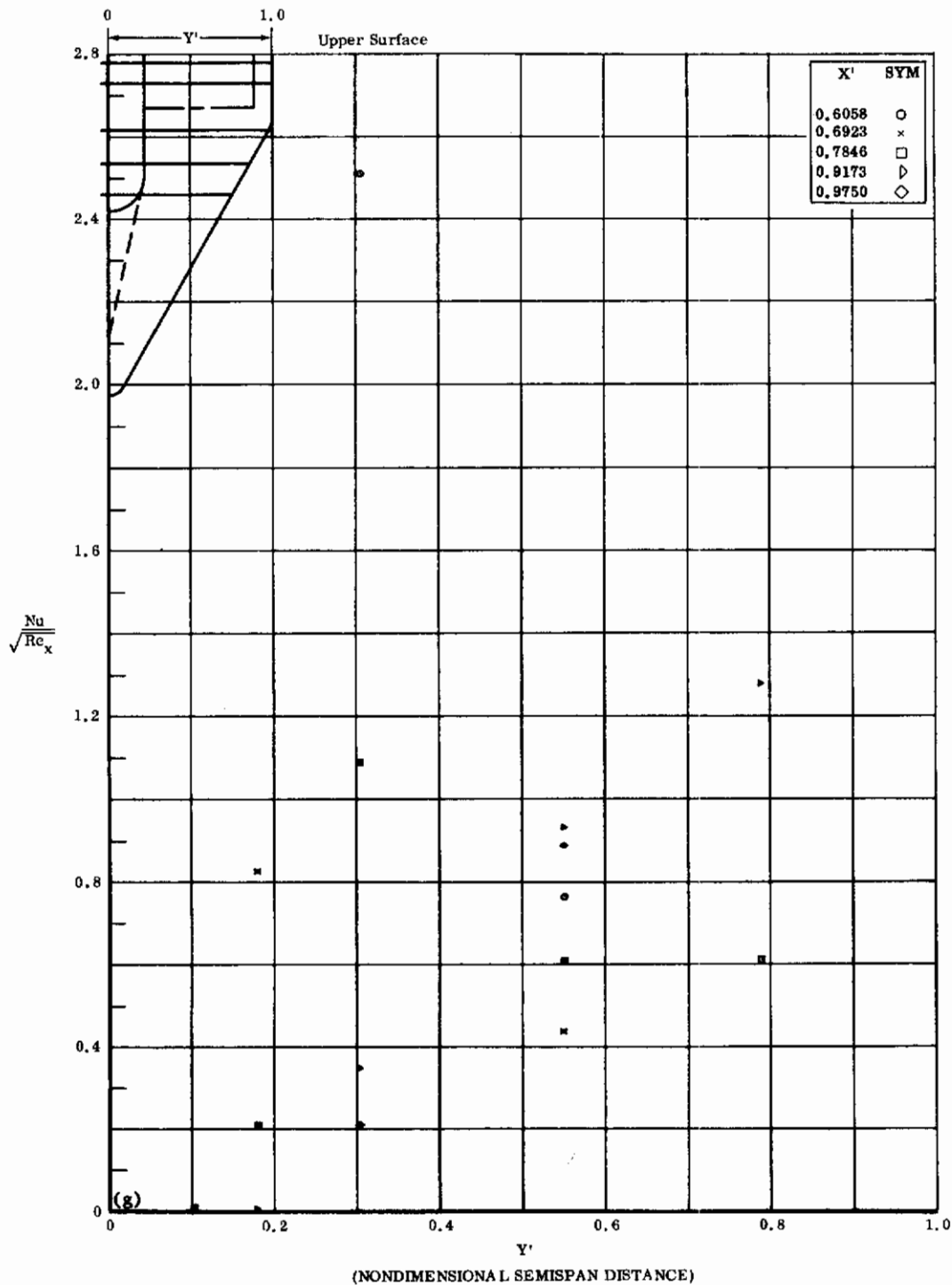


Fig. 22g Configuration IV, $\alpha = -10$, $\delta_2 = \delta_3 = +10$

$Nu/\sqrt{Re_x}$ vs. Y' upper surface

Contrails

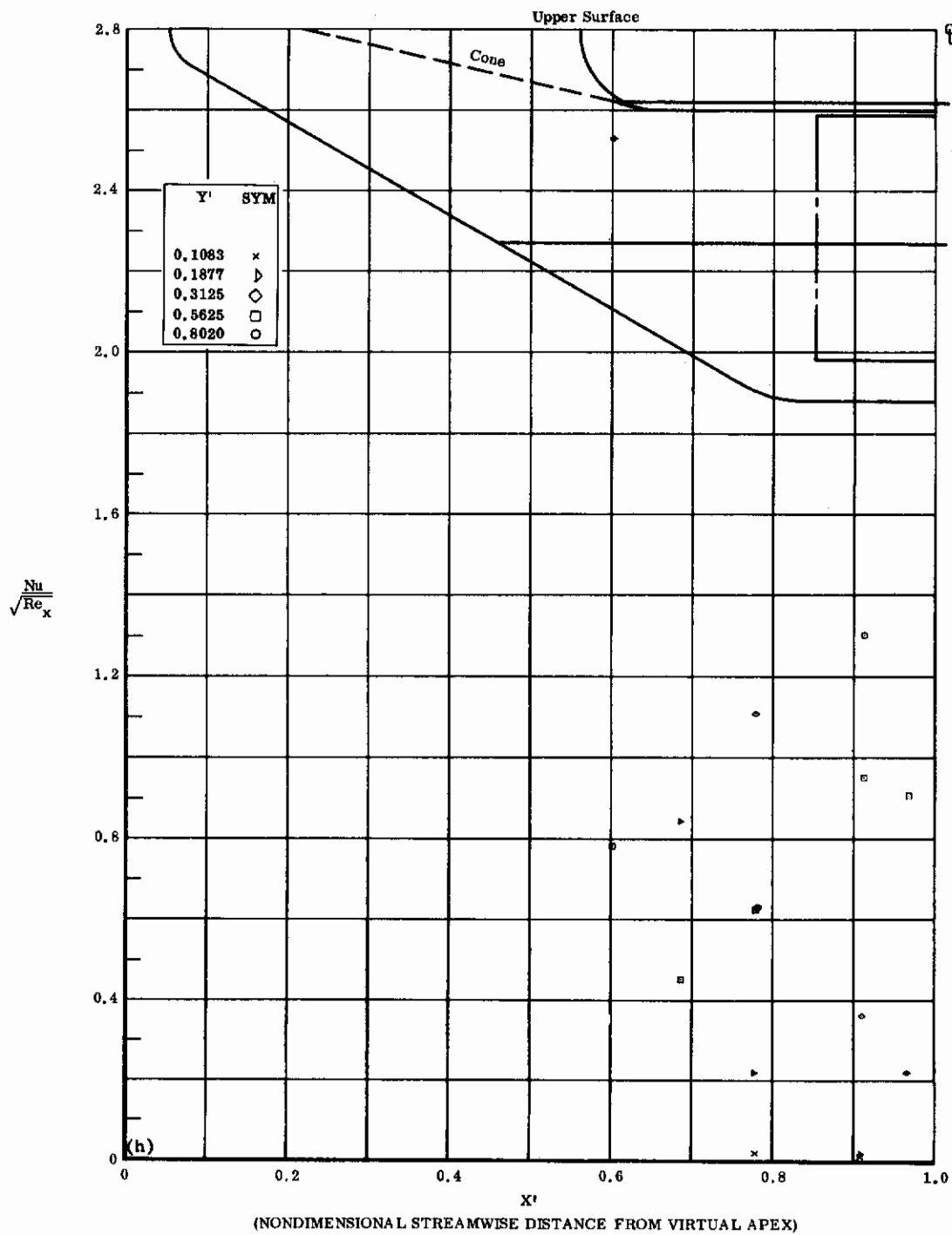


Fig. 22h Configuration IV, $\alpha = -10$, $\delta_2 = \delta_3 = +10$
 $\text{Nu}/\sqrt{\text{Re}_x}$ vs. X' upper surface

Contrails

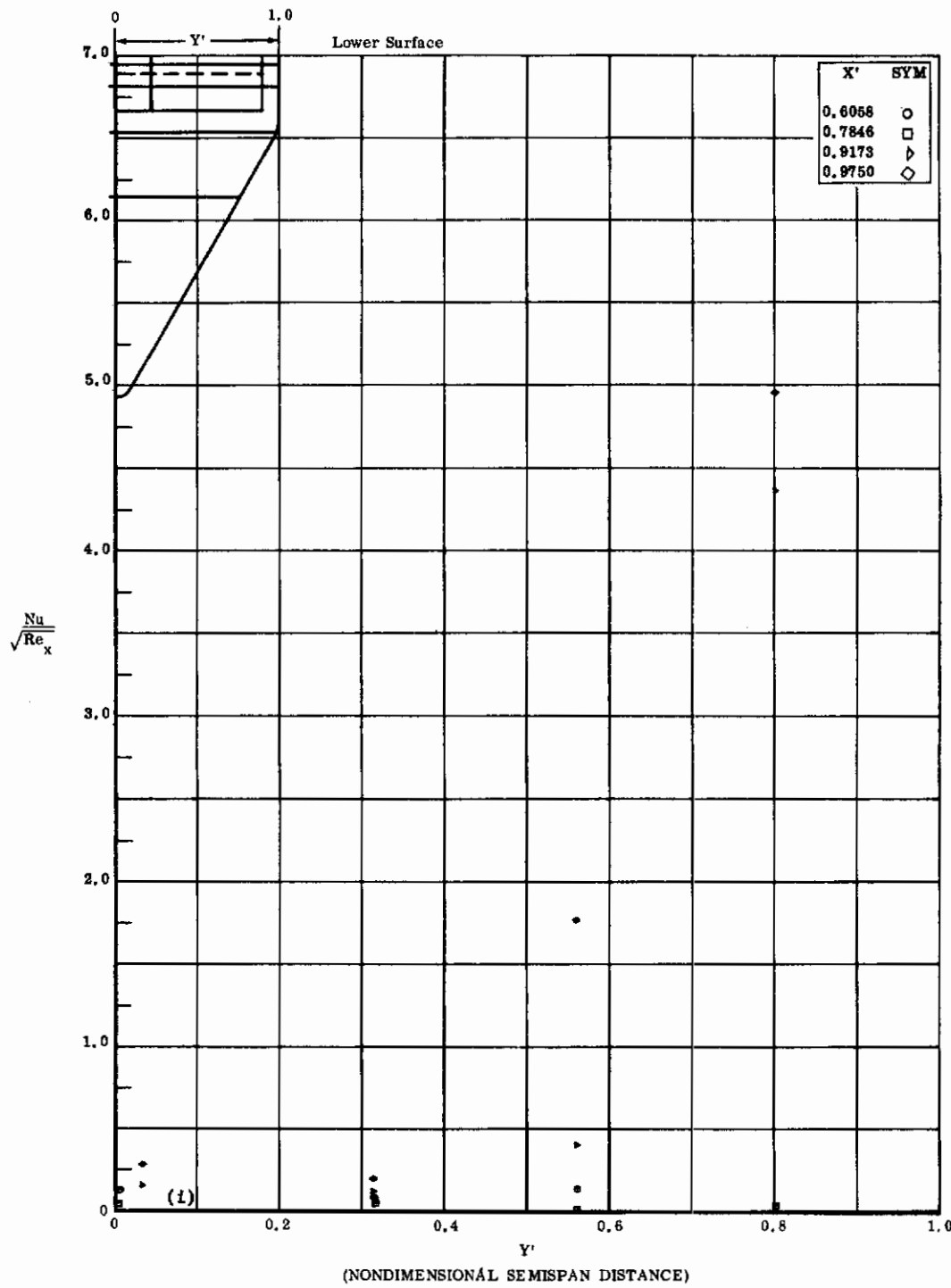


Fig. 22i Configuration IV, $\alpha = -10$, $\delta_2 = \delta_3 = +20$
 $Nu/\sqrt{Re_x}$ vs. Y' lower surface

Contrails

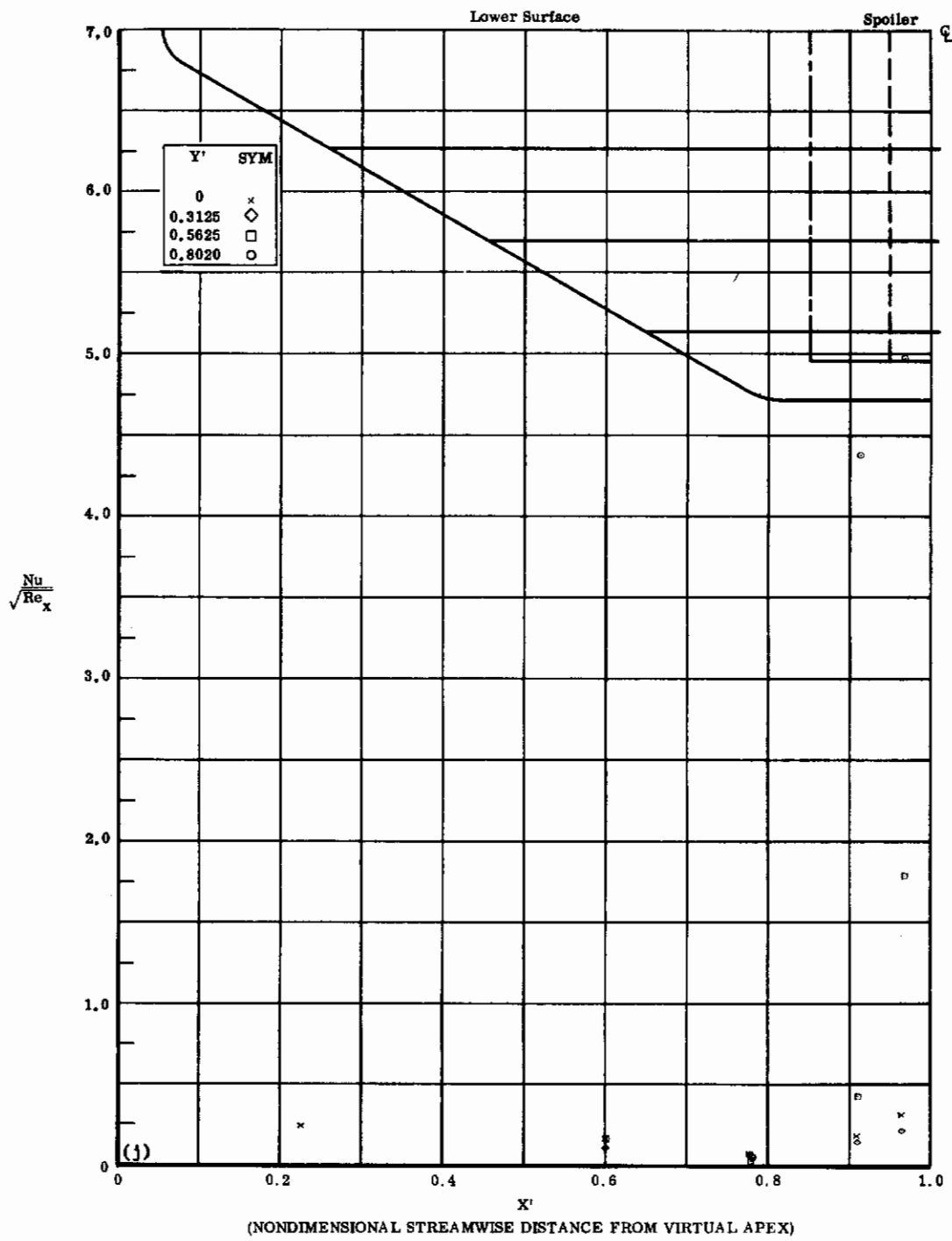


Fig. 22j Configuration IV, $\alpha = -10$, $\delta_2 = \delta_3 = +20$
 $\text{Nu}/\sqrt{\text{Re}_x}$ vs. X' lower surface

Contrails

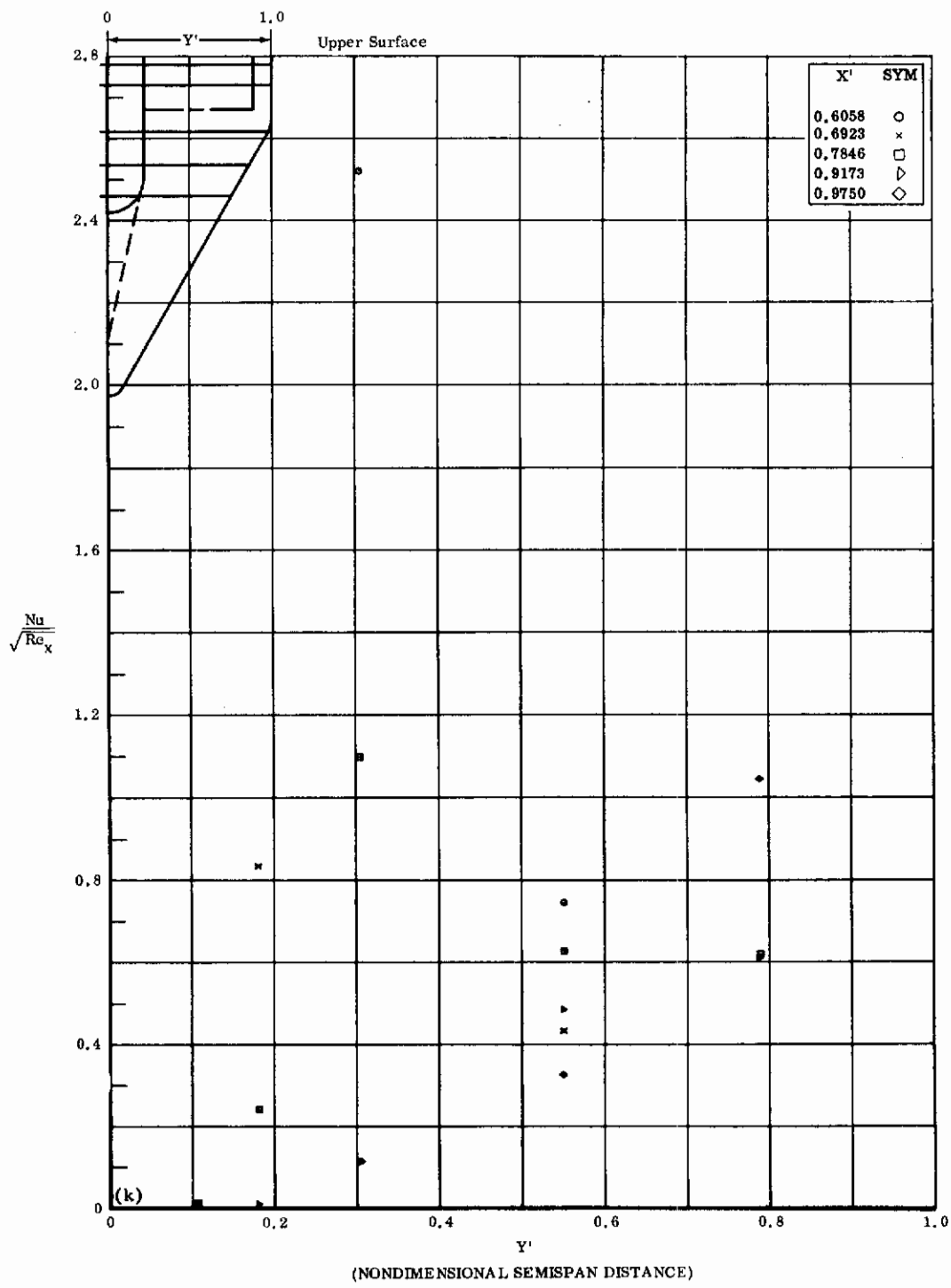


Fig. 22k Configuration IV, $\alpha = -10$, $\delta_2 = \delta_3 = +20$
 $\frac{Nu}{\sqrt{Re_x}}$ vs. Y' upper surface

Contrails

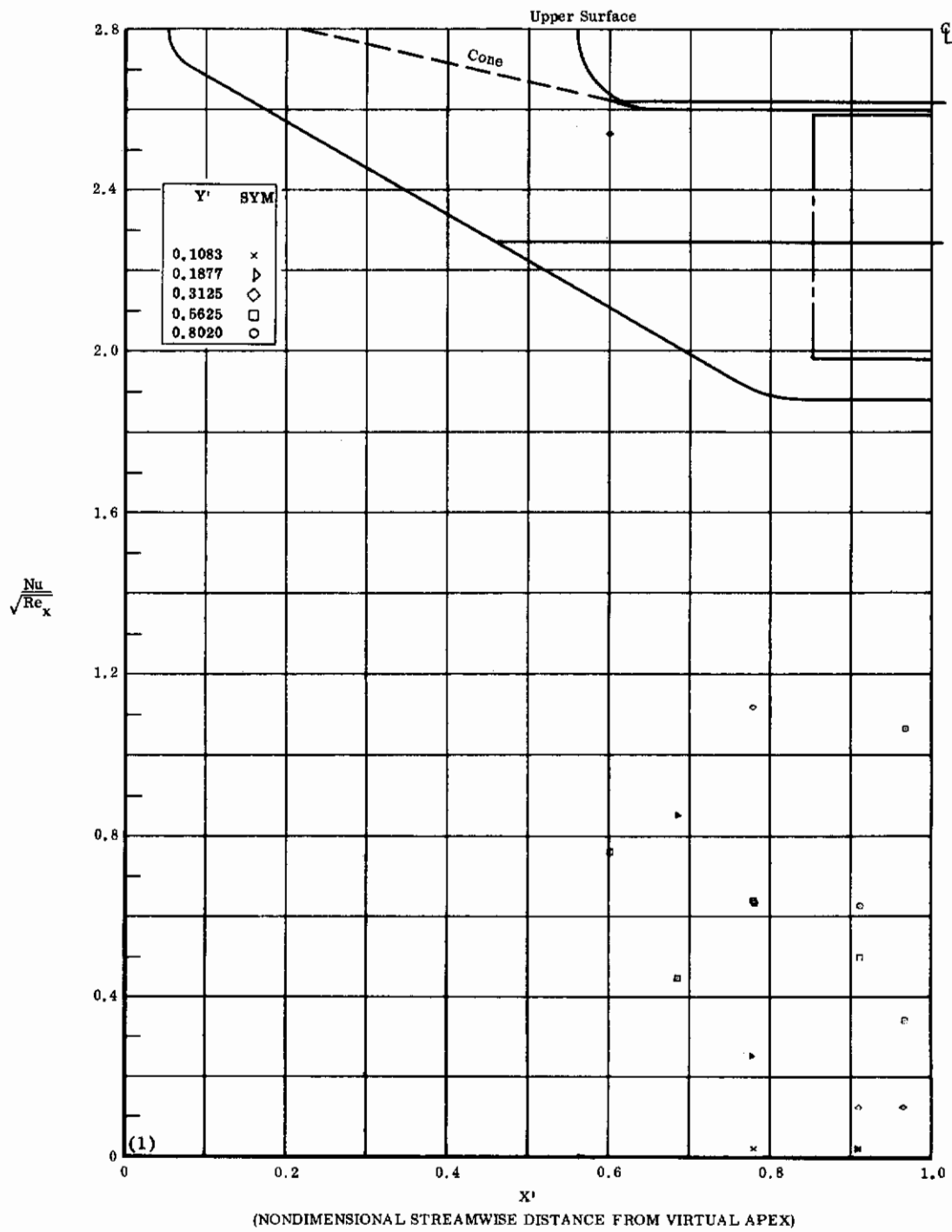


Fig. 22 ℓ Configuration IV, $\alpha = -10^\circ$, $\delta_2 = \delta_3 = +20^\circ$
 $\text{Nu}/\sqrt{\text{Re}_x}$ vs. X' upper surface

Contrails

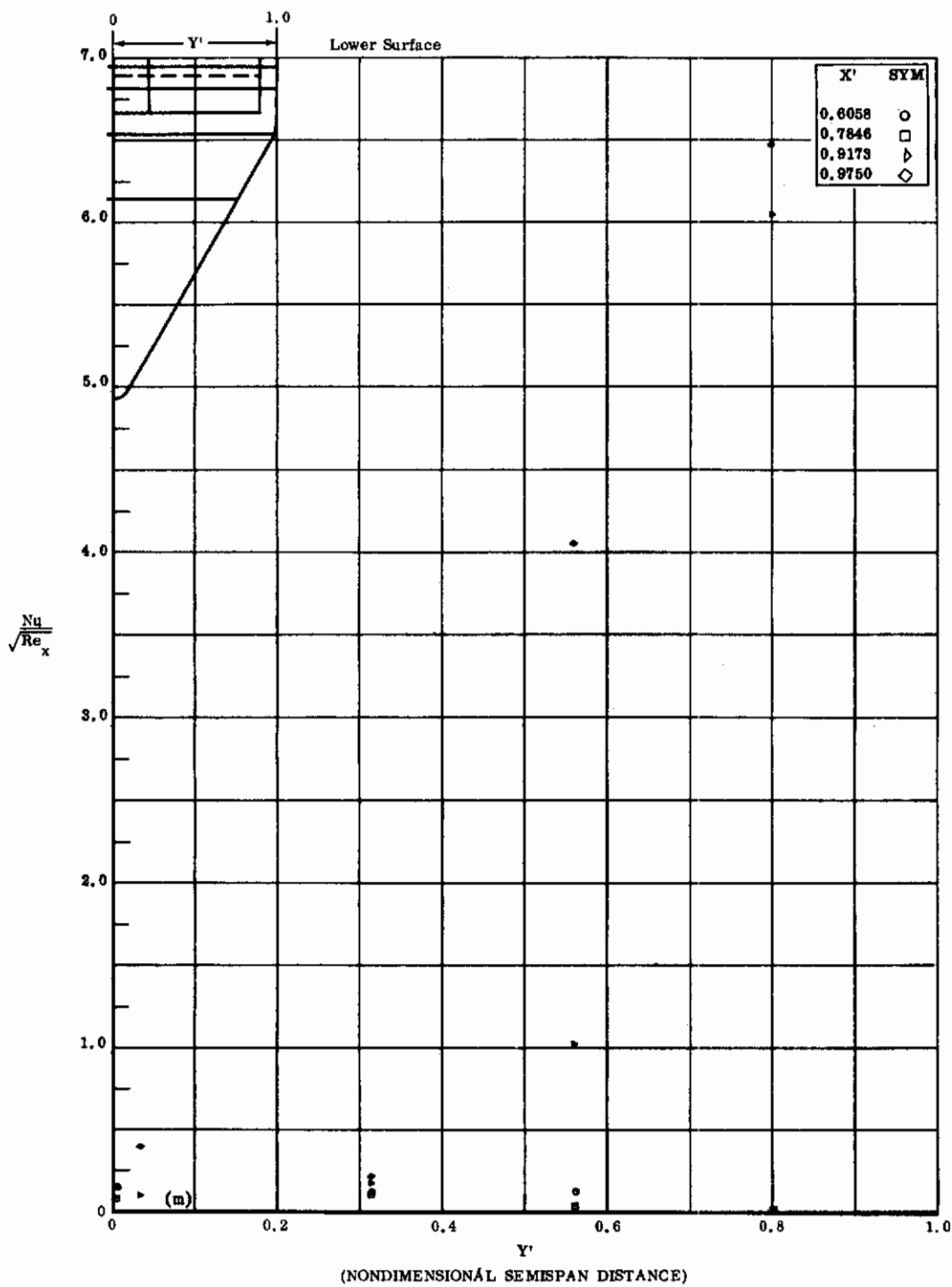


Fig. 22m Configuration IV, $\alpha = -10$, $\delta_2 = \delta_3 = +30$
 $Nu/\sqrt{Re_x}$ vs. Y' lower surface

Contrails

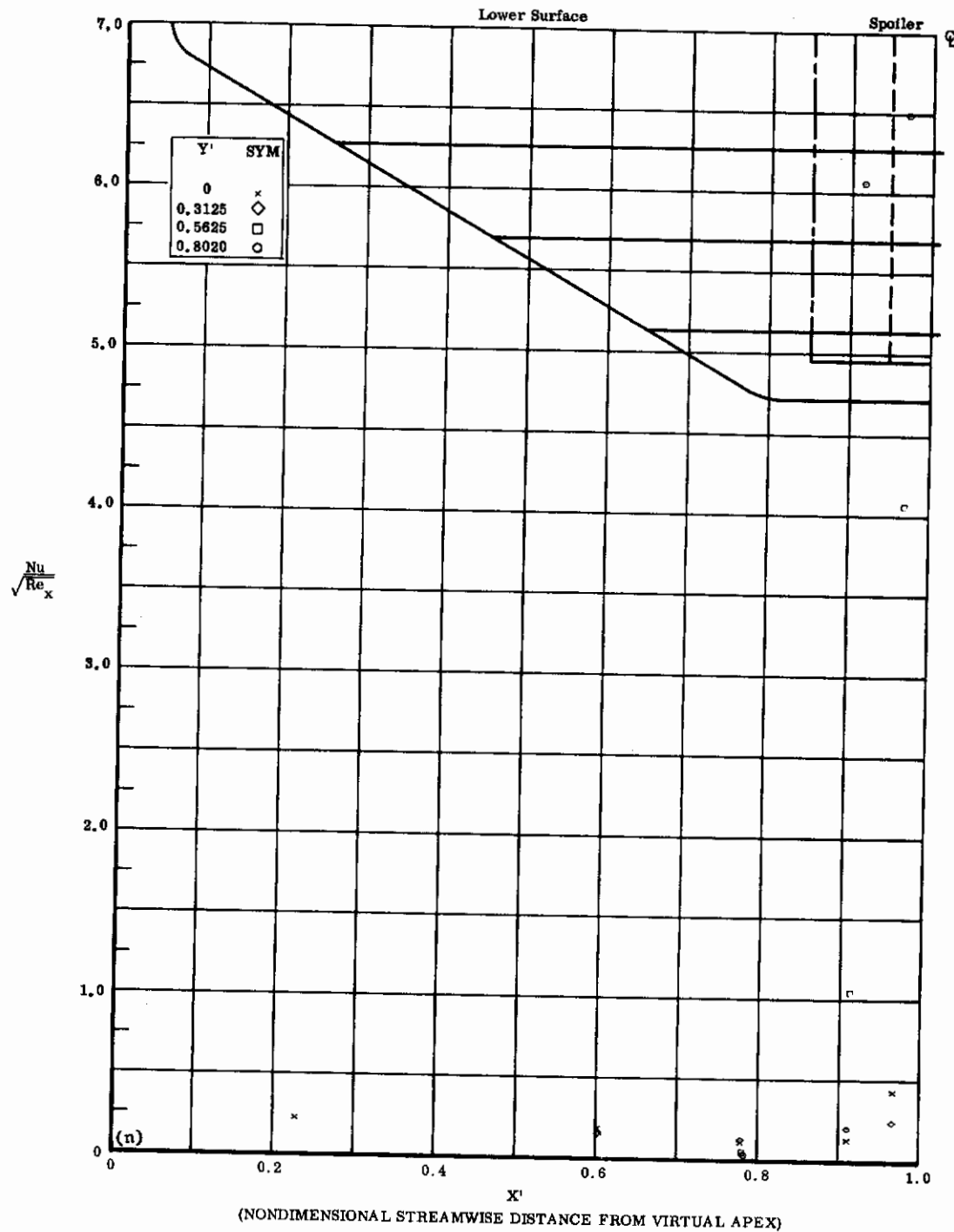


Fig. 22n Configuration IV, $\alpha = -10$, $\delta_2 = \delta_3 = +30$
 $Nu/\sqrt{Re_x}$ vs. X' lower surface

Contrails

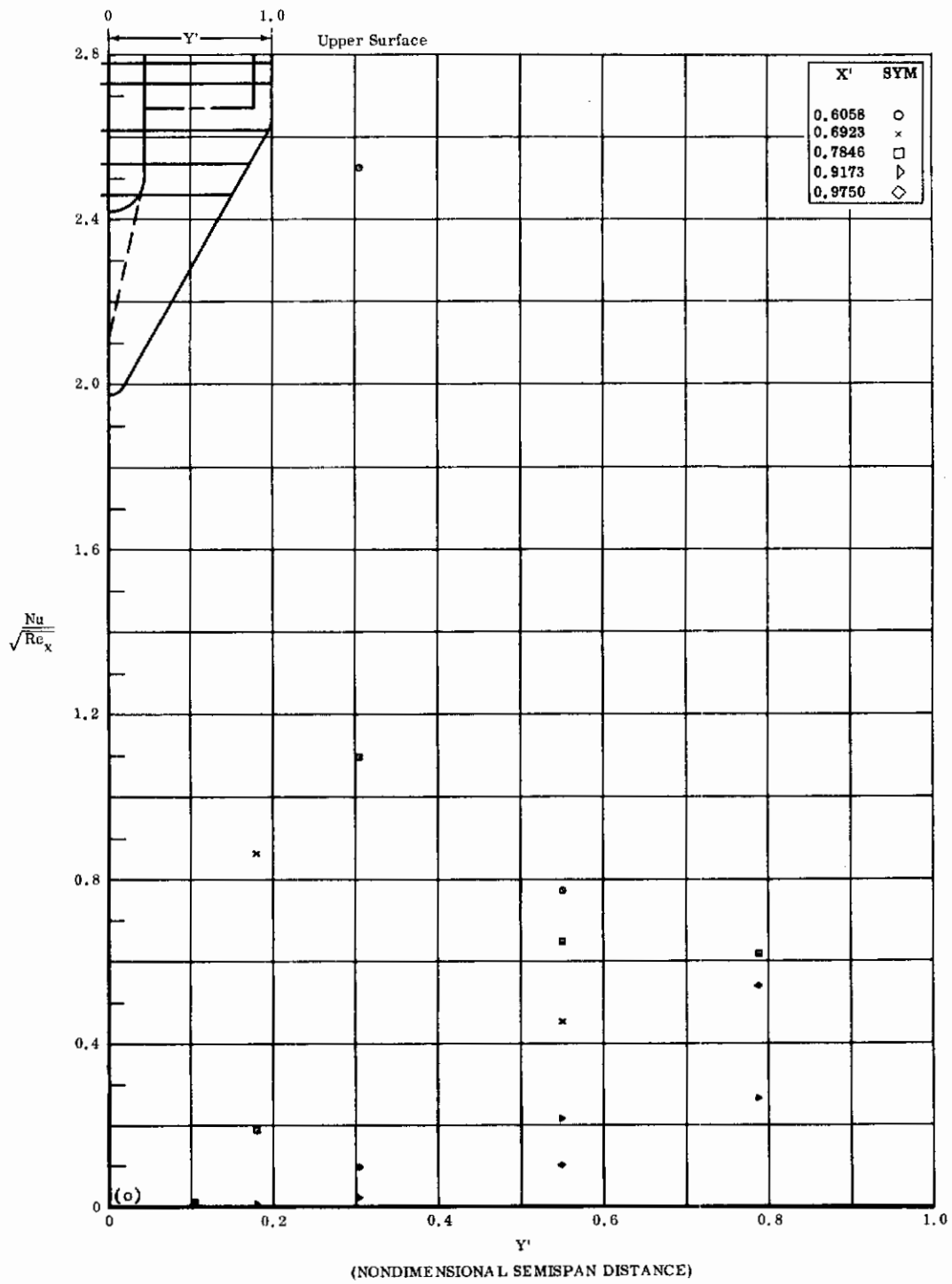


Fig. 22o Configuration IV, $\alpha = -10$, $\delta_2 = \delta_3 = +30$
 $\frac{Nu}{\sqrt{Re_x}}$ vs. Y^* upper surface

Contrails

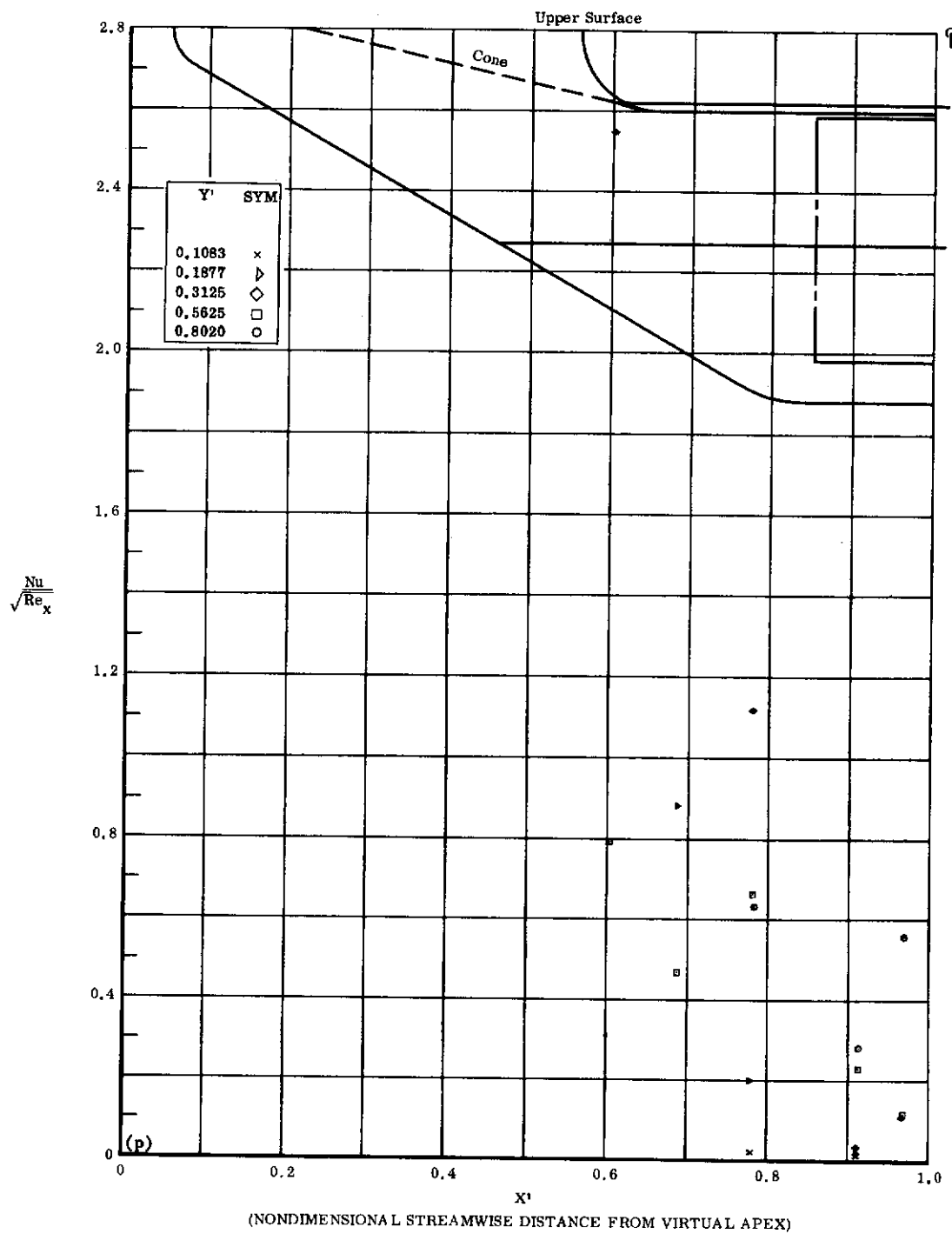


Fig. 22p Configuration IV, $\alpha = -10$, $\delta_2 = \delta_3 = +30$

$\text{Nu}/\sqrt{\text{Re}_x}$ vs. X' upper surface

Contrails

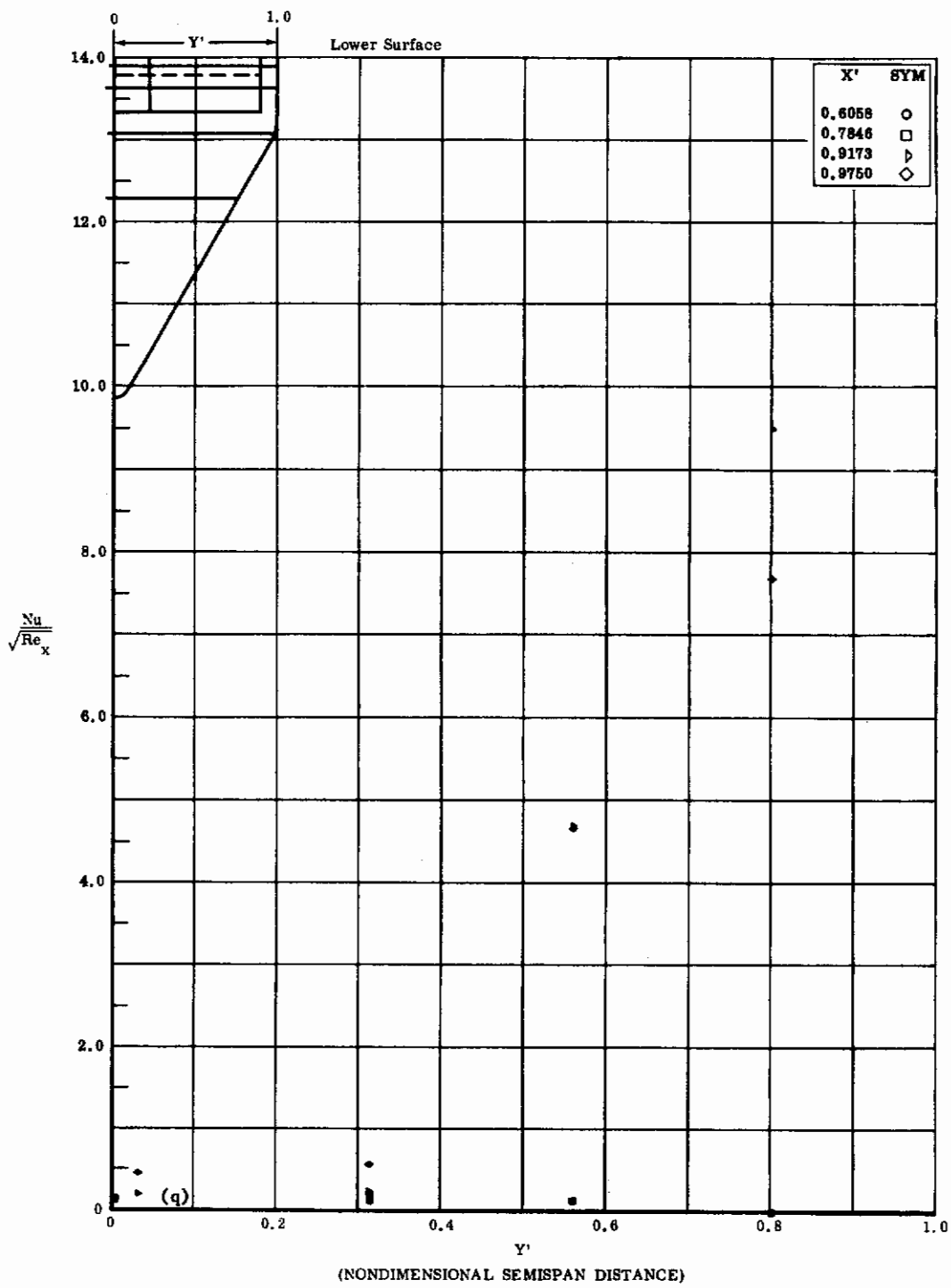


Fig. 22q Configuration IV, $\alpha = -10$, $\delta_2 = \delta_3 = +39$
 $Nu/\sqrt{Re_x}$ vs. Y' lower surface

Contrails

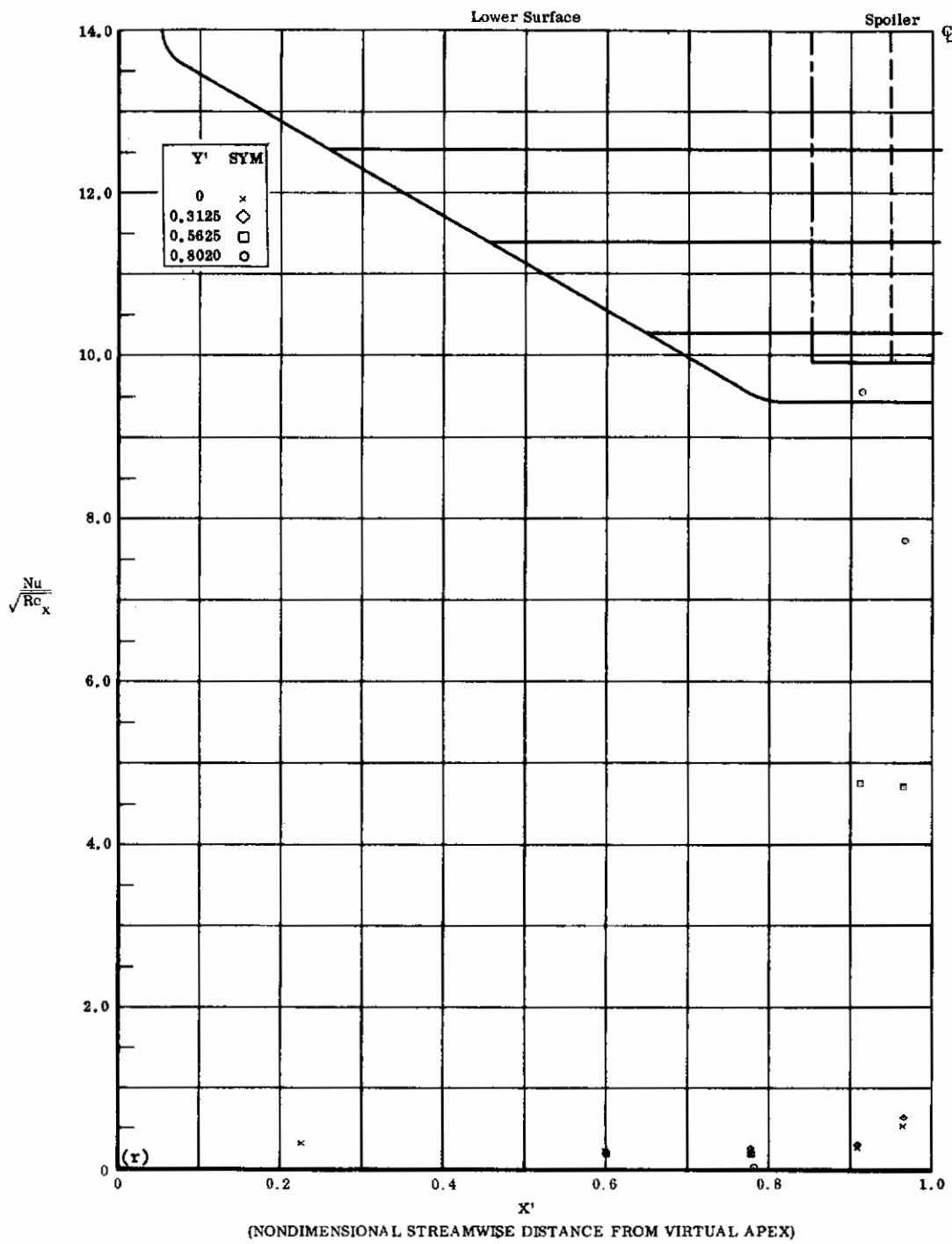


Fig. 22r Configuration IV, $\alpha = -10$, $\delta_2 = \delta_3 = +39$
 $Nu/\sqrt{Re_x}$ vs. X' lower surface

Contrails

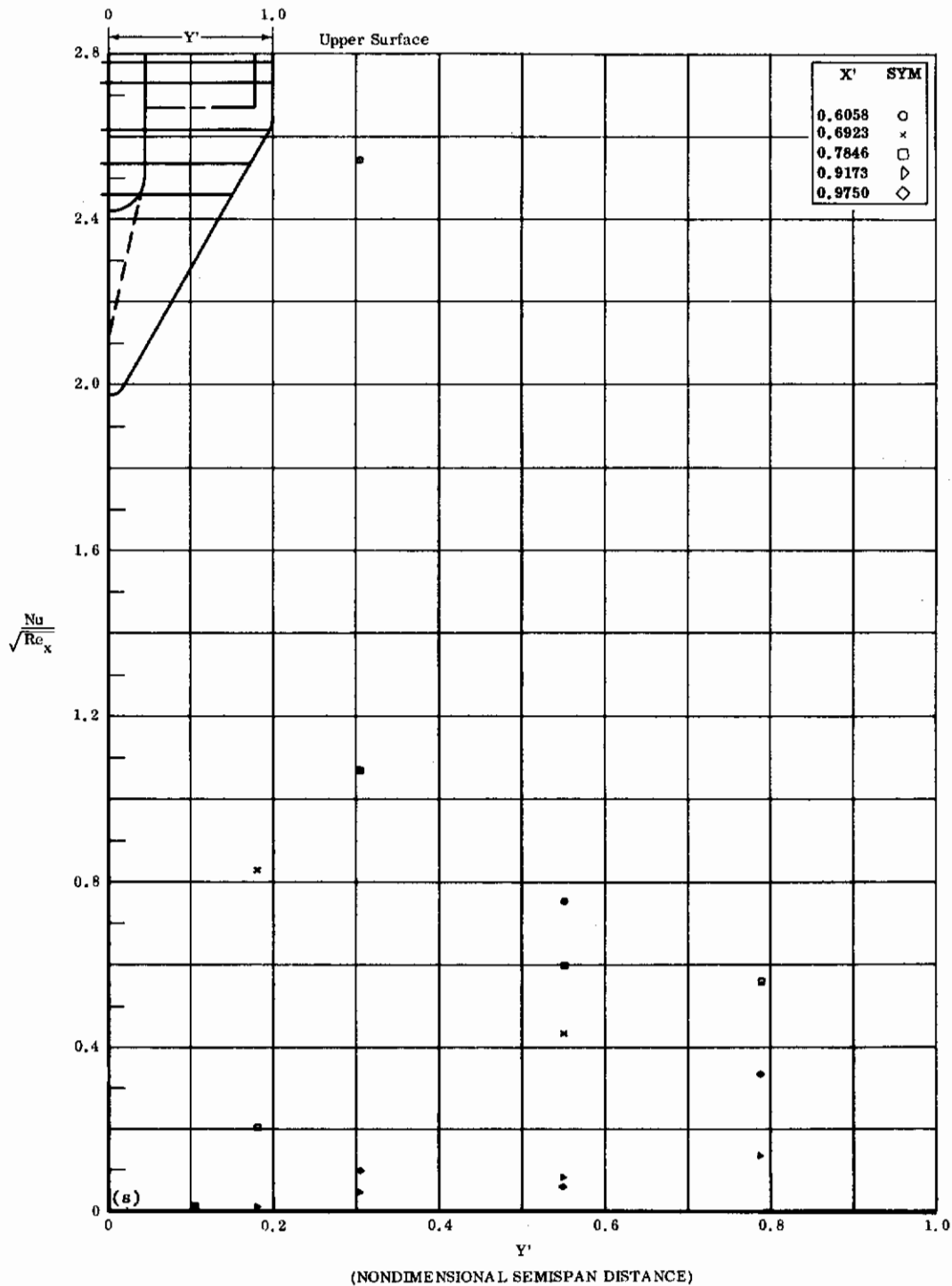


Fig. 22s Configuration IV, $\alpha = -10$, $\delta_2 = \delta_3 = +39$
 $Nu/\sqrt{Re_x}$ vs. Y' upper surface

Contrails

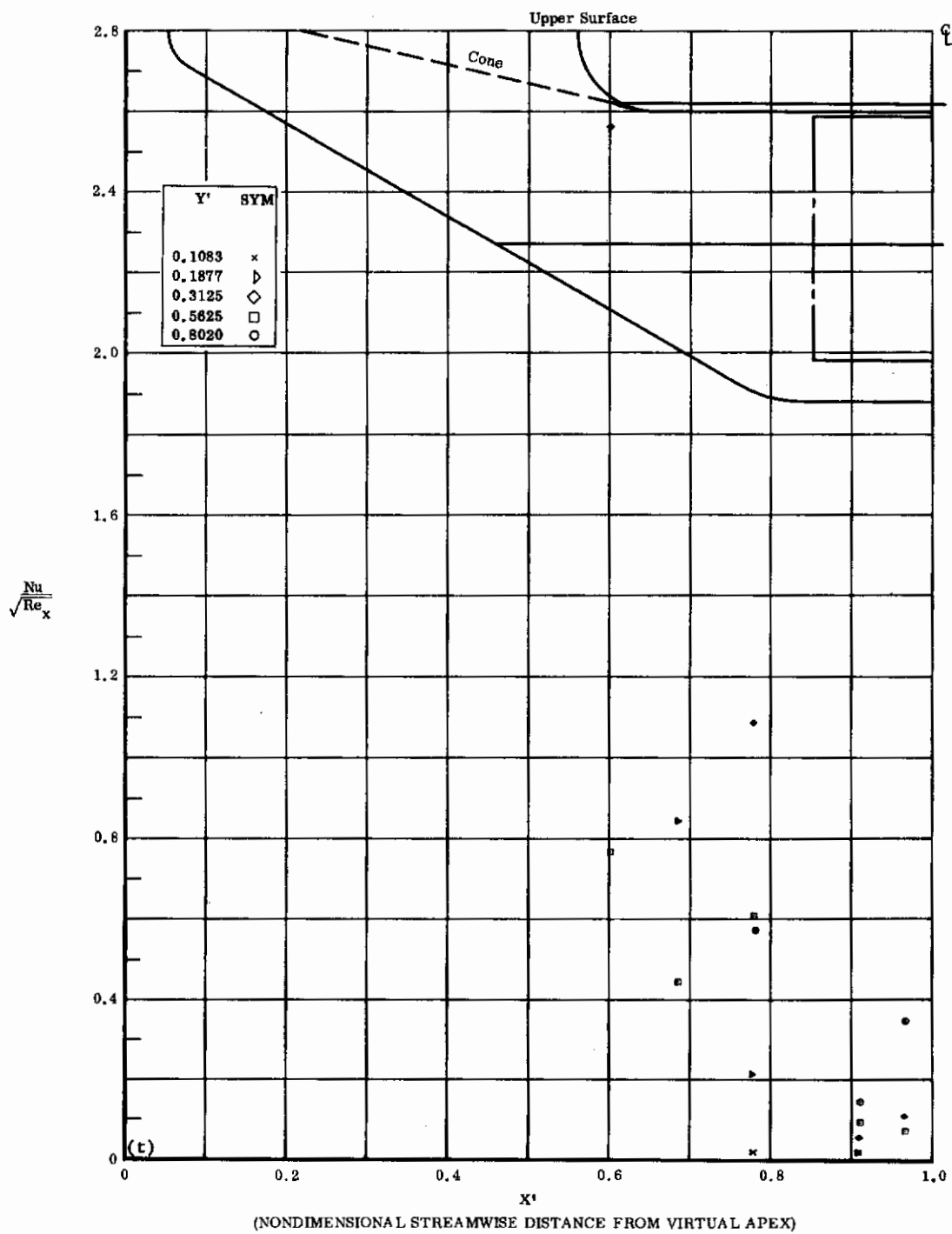
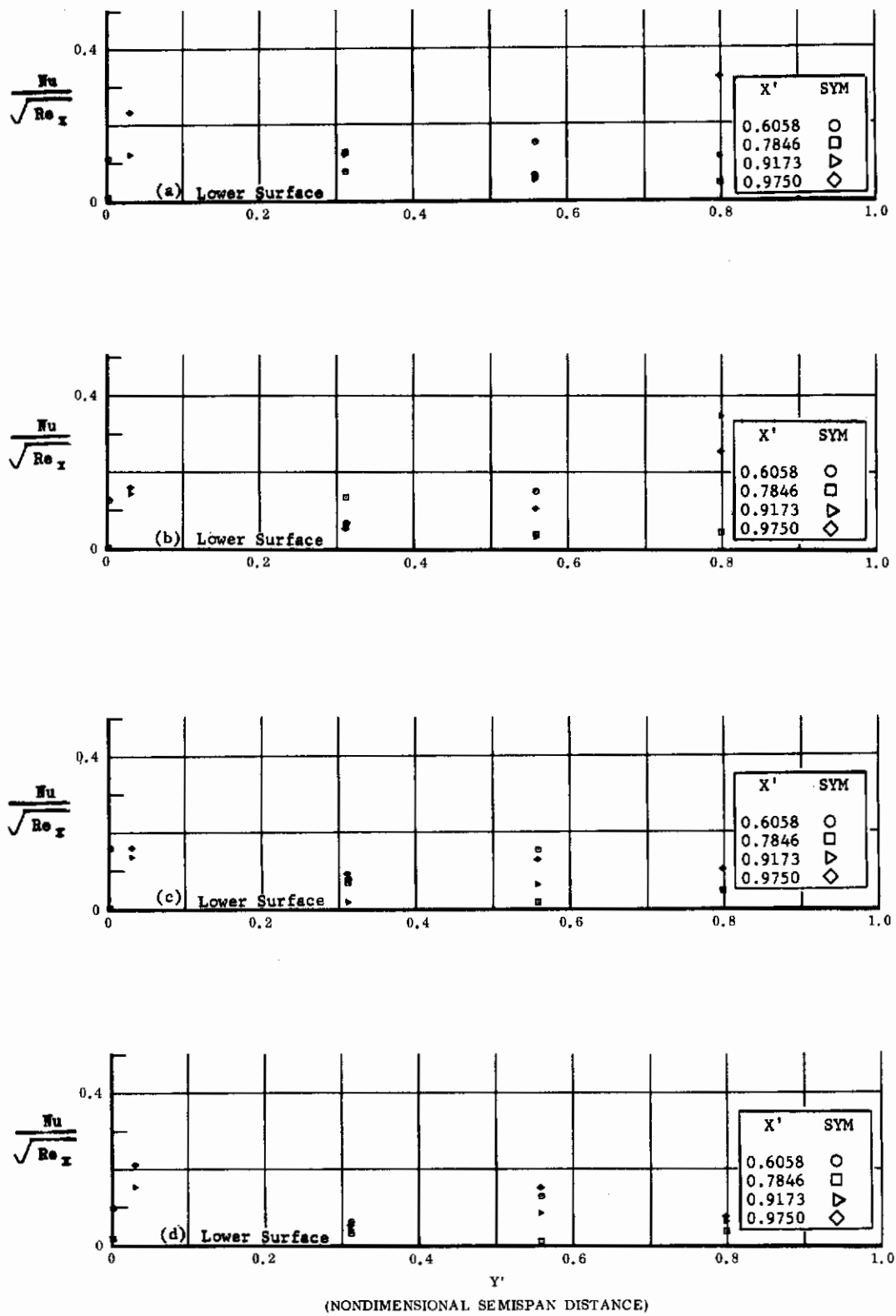


Fig. 22t Configuration IV, $\alpha = -10$, $\delta_2 = \delta_3 = +39$
 $Nu/\sqrt{Re_x}$ vs. X' upper surface

Contrails



(NONDIMENSIONAL SEMISPAN DISTANCE)

Fig. 23 Configuration IV, $\alpha = -10$, $Nu/\sqrt{Re_x}$ vs. Y' , lower surface

- a) $\delta_2 = \delta_3 = -10$
- b) $\delta_2 = \delta_3 = -20$
- c) $\delta_2 = \delta_3 = -30$
- d) $\delta_2 = \delta_3 = -39$

Contrails

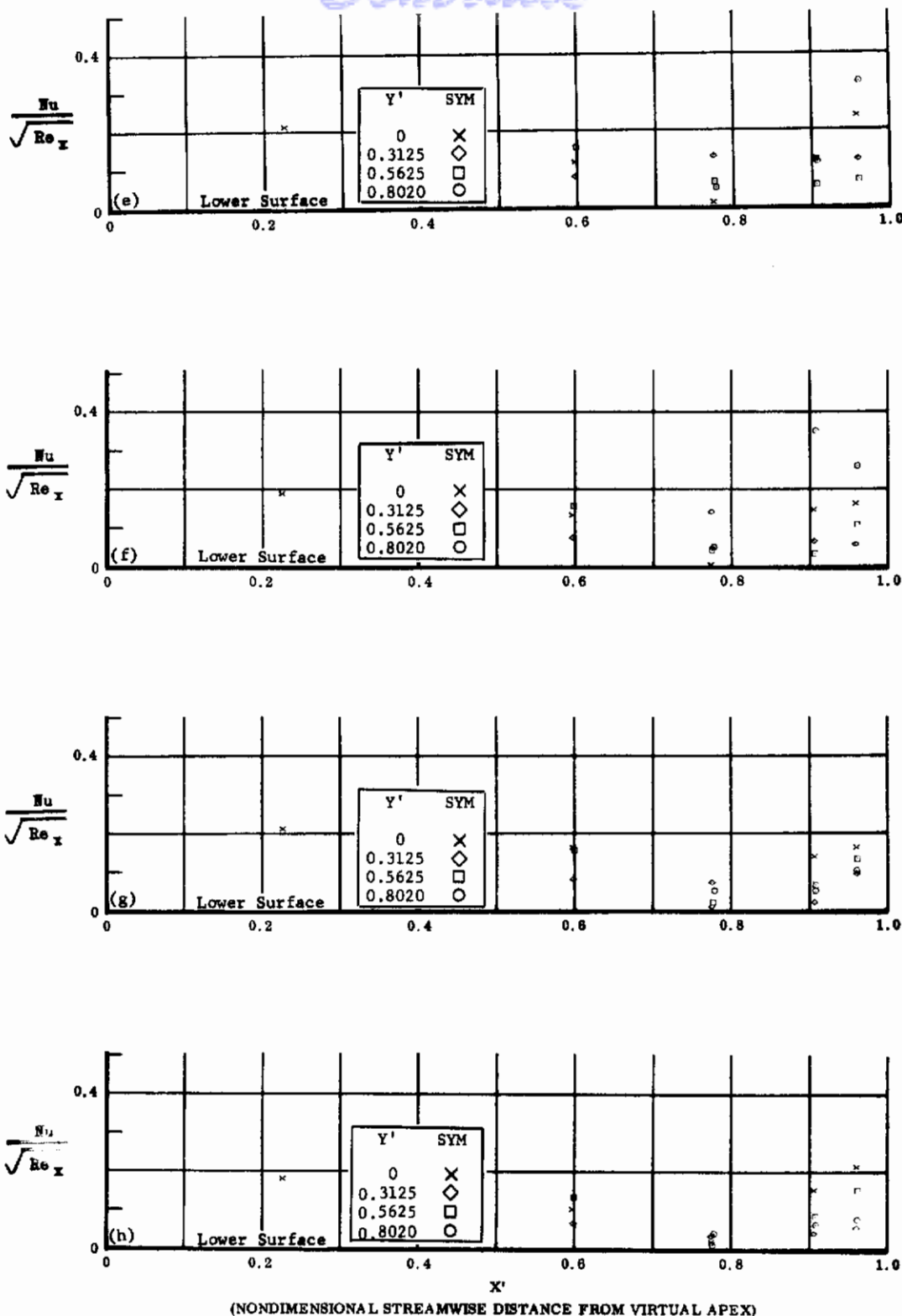


Fig. 23 Configuration IV, $\alpha = -10$, $Nu/\sqrt{Re_x}$ vs. X' , lower surface

e) $b_2 = b_3 = -10$

f) $b_2 = b_3 = -20$

g) $b_2 = b_3 = -30$

h) $b_2 = b_3 = -39$

Contrails

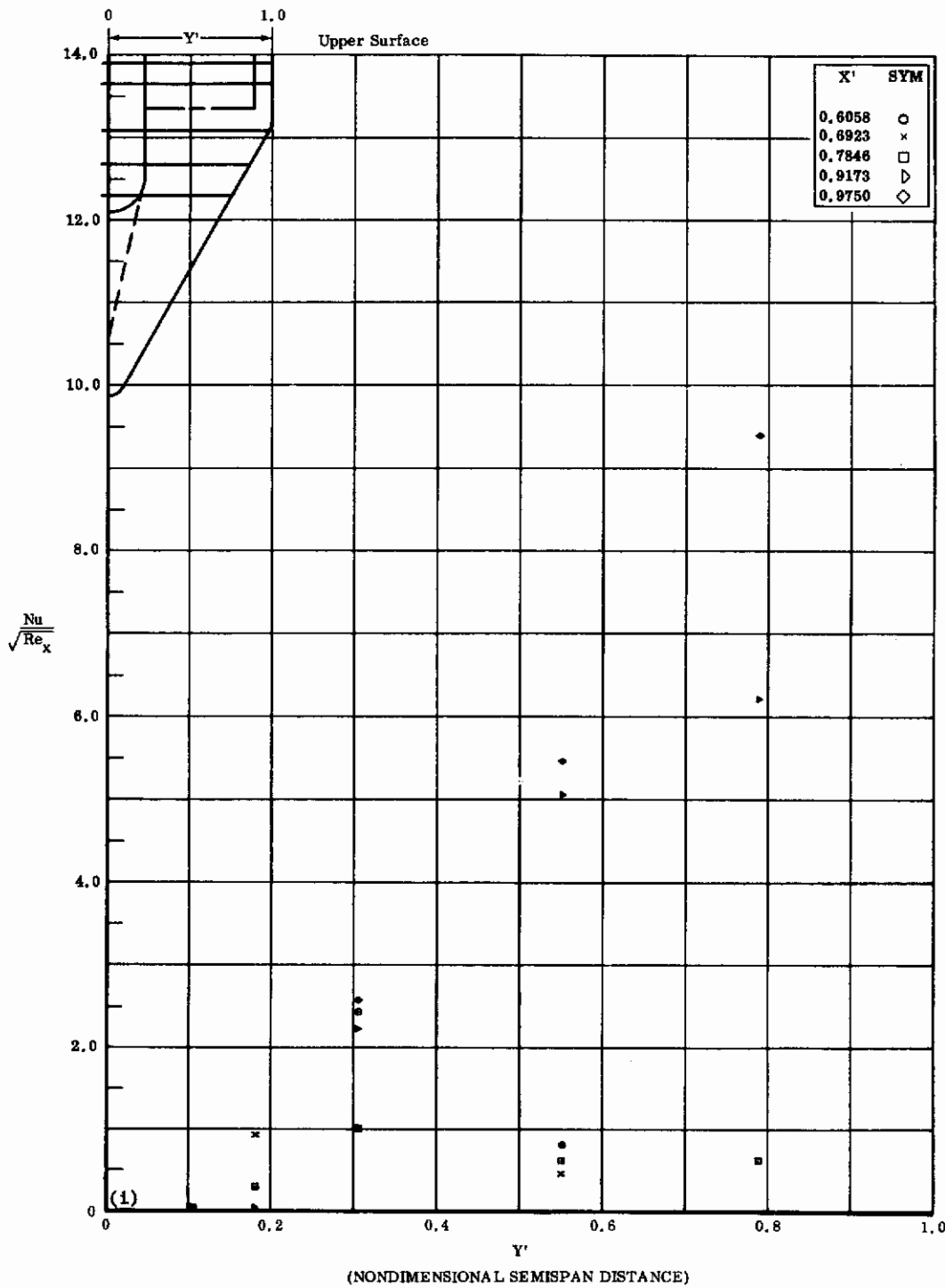


Fig. 23i Configuration IV, $\alpha = -10$, $b_2 = b_3 = -10$
 $\frac{Nu}{\sqrt{Re_x}}$ vs. Y' upper surface

Contrails

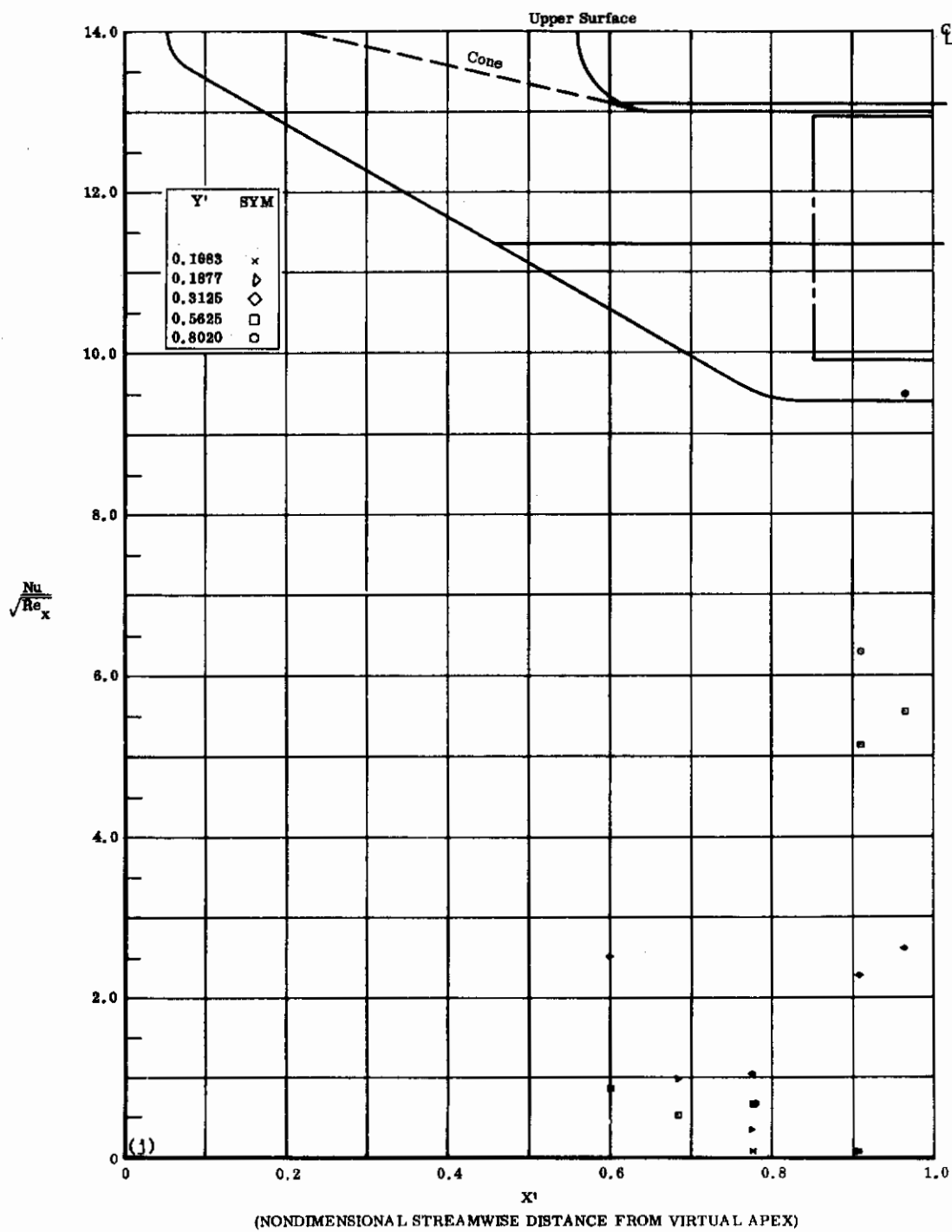


Fig. 23j Configuration IV, $\alpha = -10$, $b_2 = b_3 = -10$
 $Nu/\sqrt{Re_x}$ vs. X' upper surface

Contrails

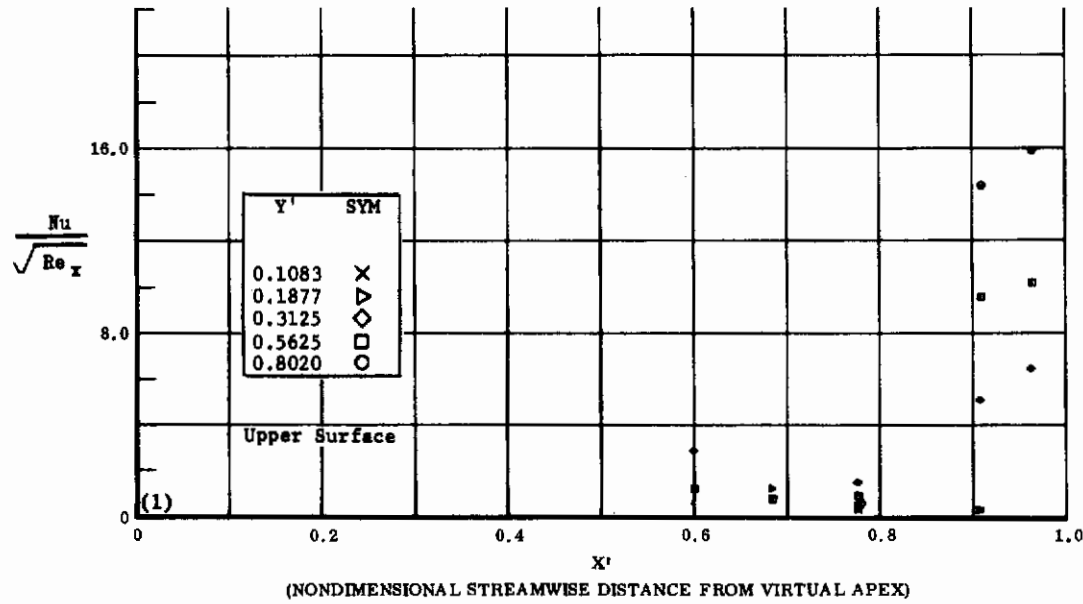
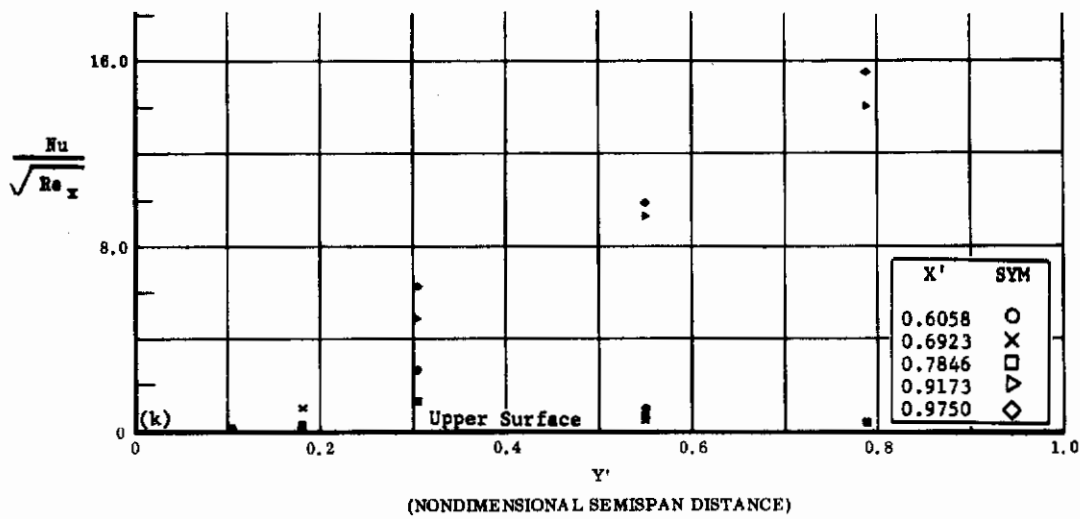


Fig. 23 Configuration IV, $\alpha = -10$, $\delta_2 = \delta_3 = -20$

k) $Nu/\sqrt{Re_x}$ vs. Y' upper surface

l) $Nu/\sqrt{Re_x}$ vs. X' upper surface

Contrails

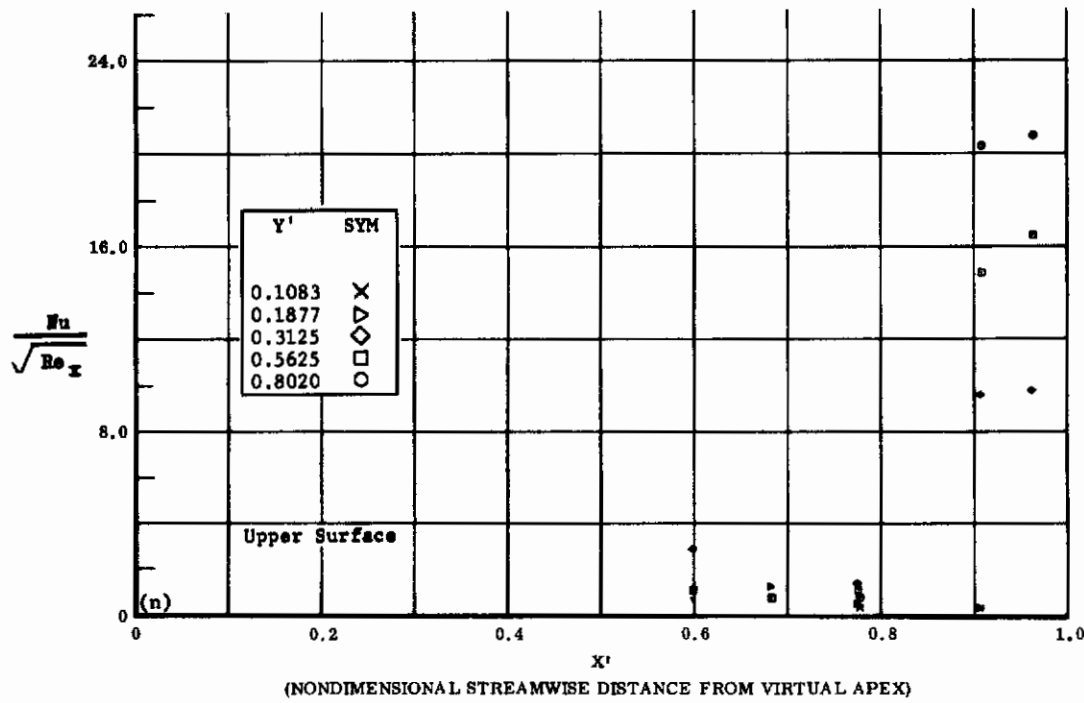
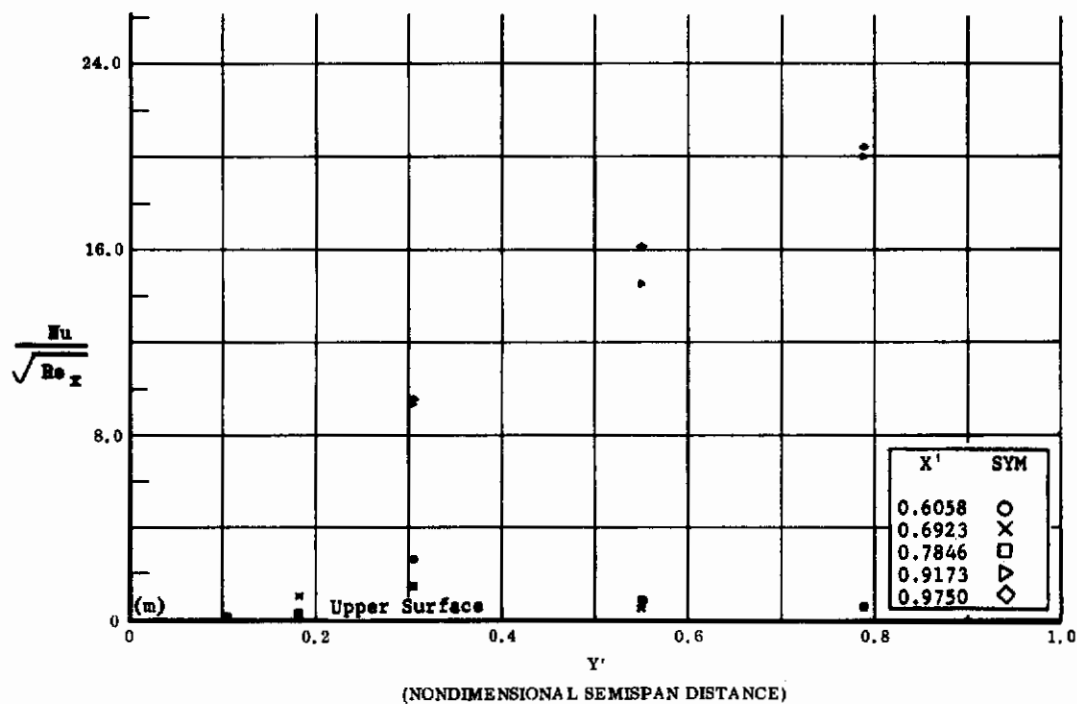


Fig. 23 Configuration IV, $\alpha = -10$, $\delta_2 = \delta_3 = -30$

m) $Nu/\sqrt{Re_x}$ vs. Y' upper surface

n) $Nu/\sqrt{Re_x}$ vs. X' upper surface

Contrails

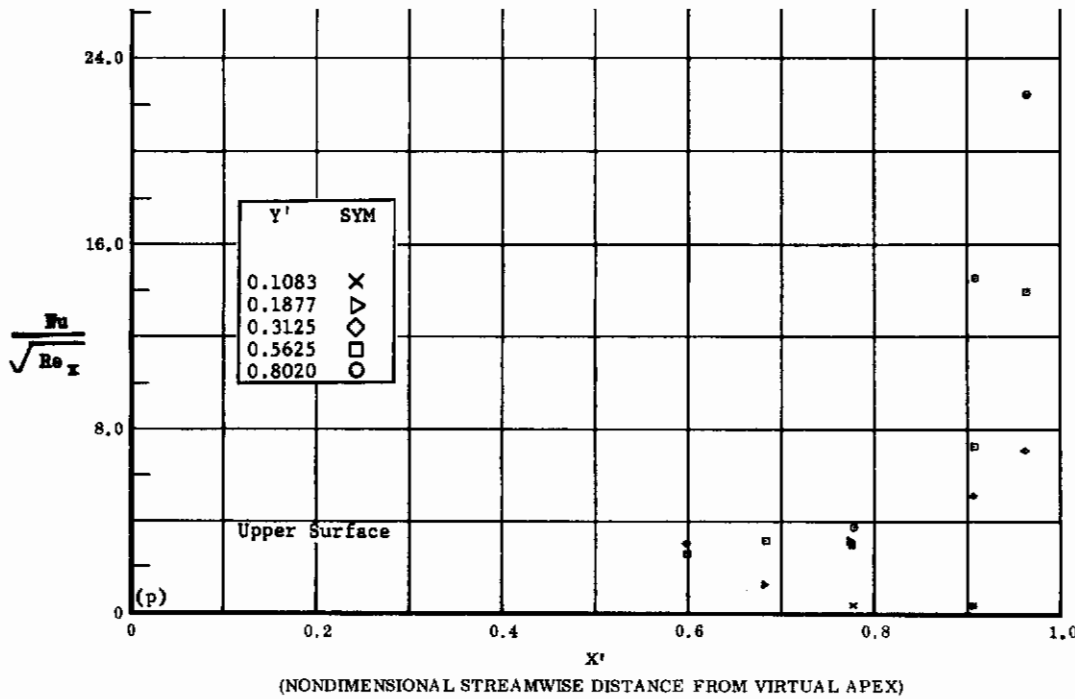
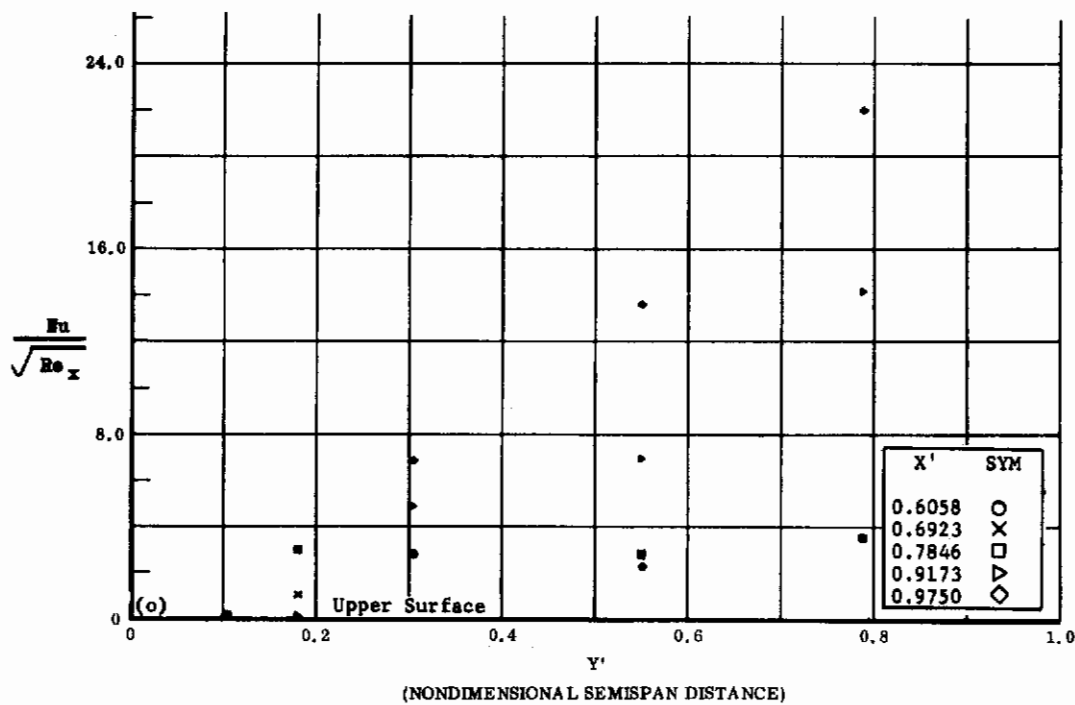


Fig. 23 Configuration IV, $\alpha = -10$, $\delta_2 = \delta_3 = -39$

o) $Nu/\sqrt{Re_x}$ vs. Y' upper surface

p) $Nu/\sqrt{Re_x}$ vs. X' upper surface

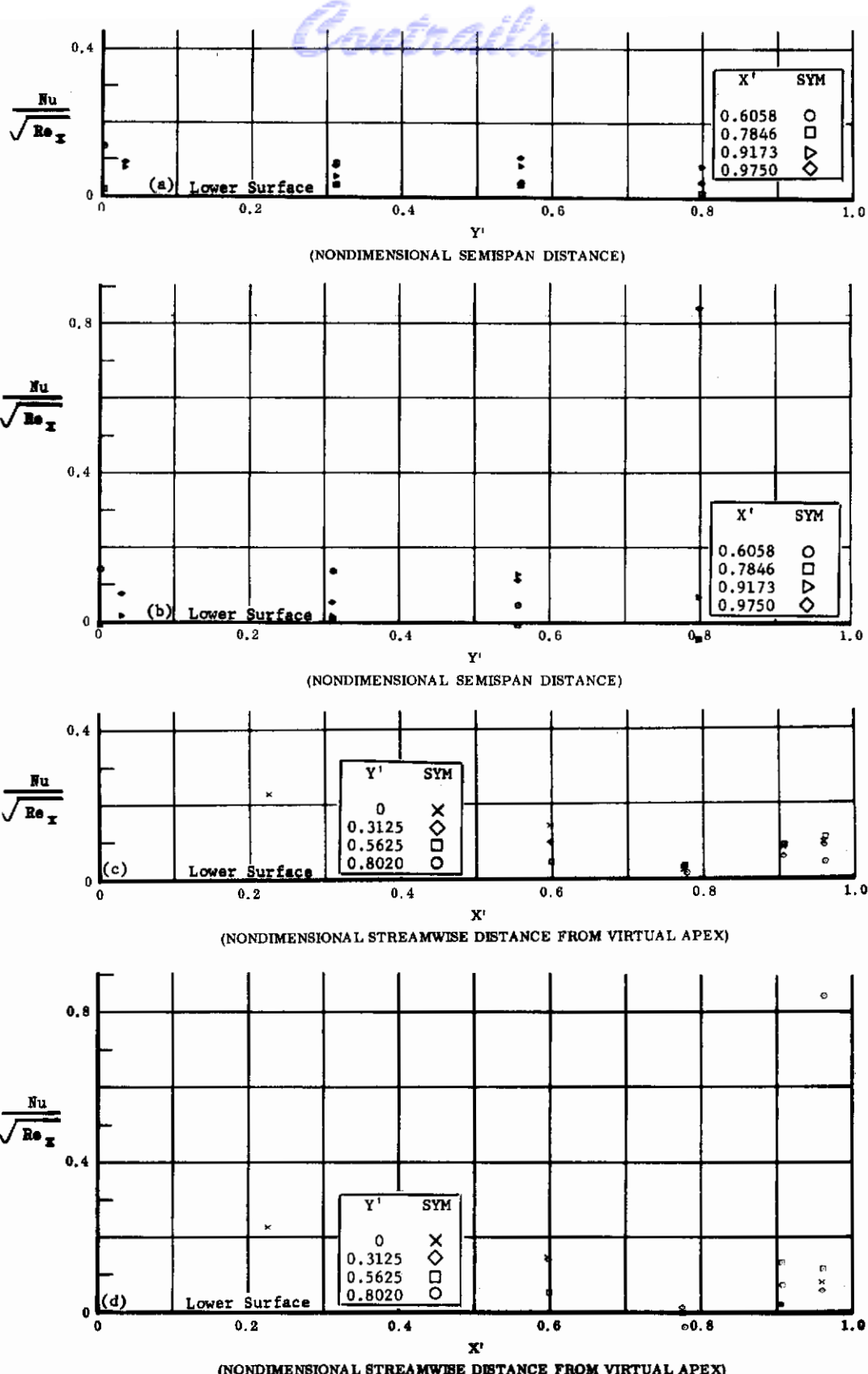


Fig. 24 Configuration IV, $\alpha = -20$, lower surface

- a) $Nu/\sqrt{Re_x}$ vs. Y' , $\delta_2 = \delta_3 = 0$
- b) $Nu/\sqrt{Re_x}$ vs. Y' , $\delta_2 = \delta_3 = +10$
- c) $Nu/\sqrt{Re_x}$ vs. X' , $\delta_2 = \delta_3 = 0$
- d) $Nu/\sqrt{Re_x}$ vs. X' , $\delta_2 = \delta_3 = +10$

Contrails

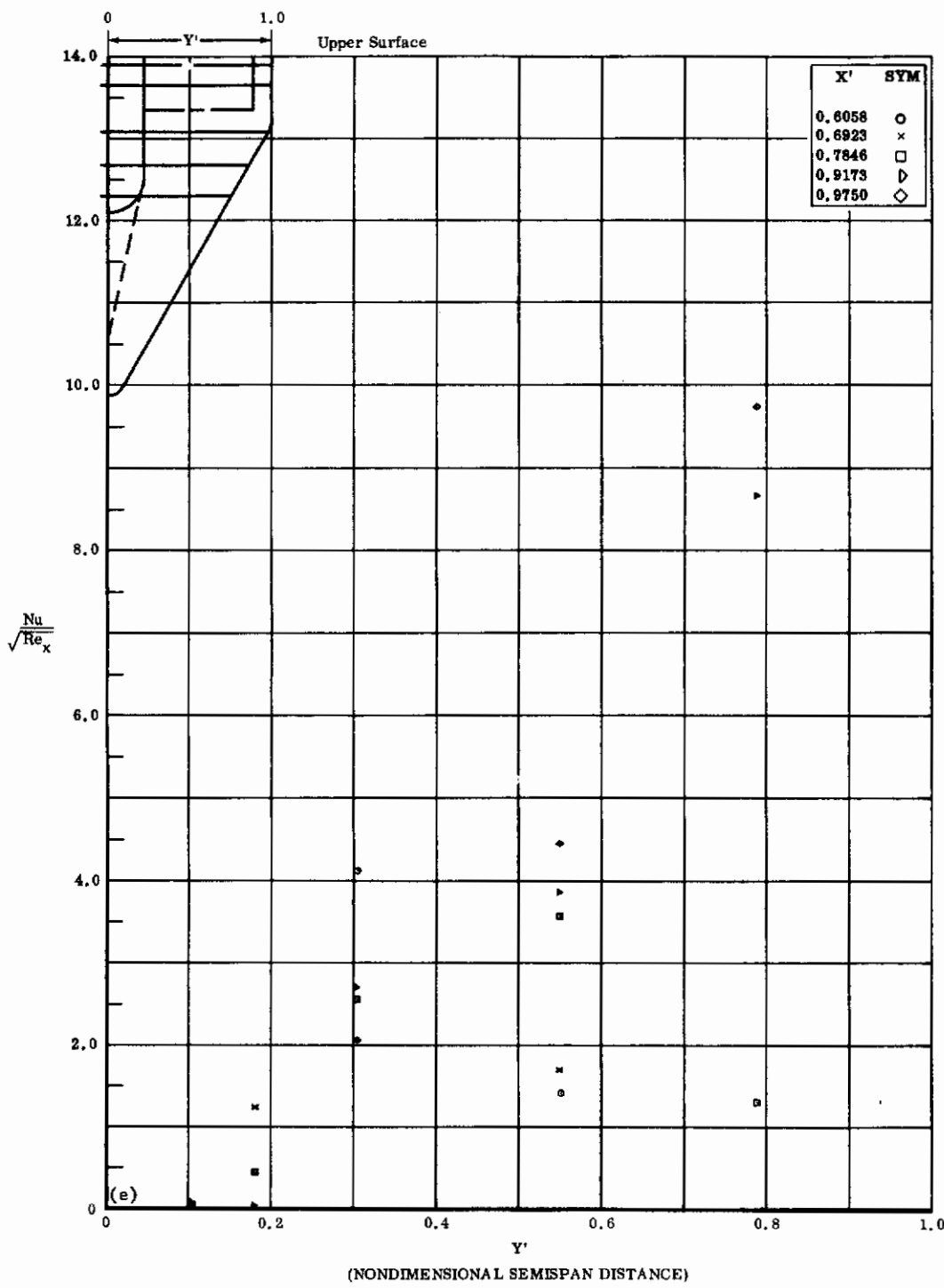


Fig. 24e Configuration IV, $\alpha = -20$, $b_2 = b_3 = 0$

$Nu/\sqrt{Re_x}$ vs. Y' upper surface

Contrails

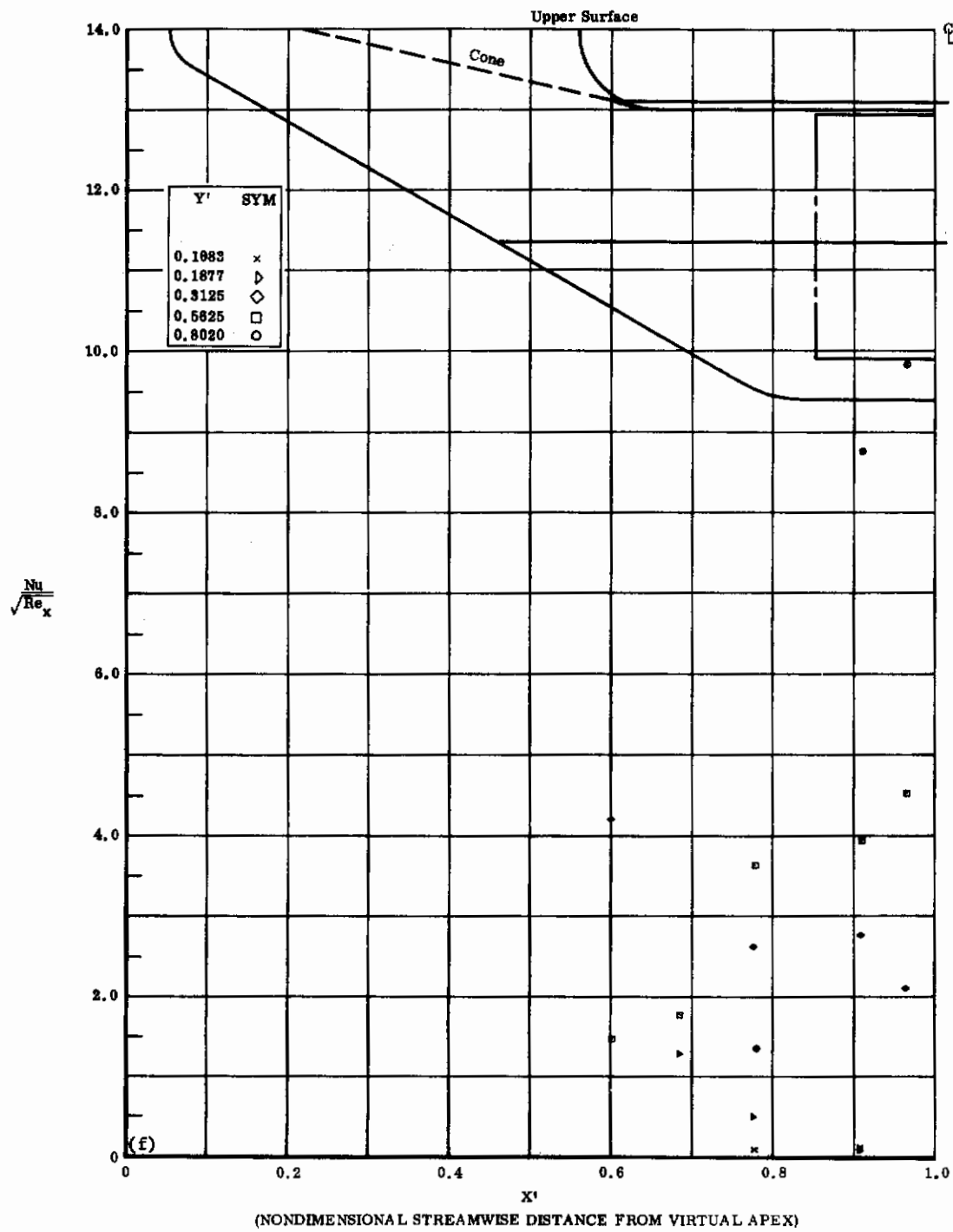


Fig. 24f Configuration IV, $\alpha = -20$, $\delta_2 = \delta_3 = 0$

$\text{Nu}/\sqrt{\text{Re}_x}$ vs. X' upper surface

Contrails

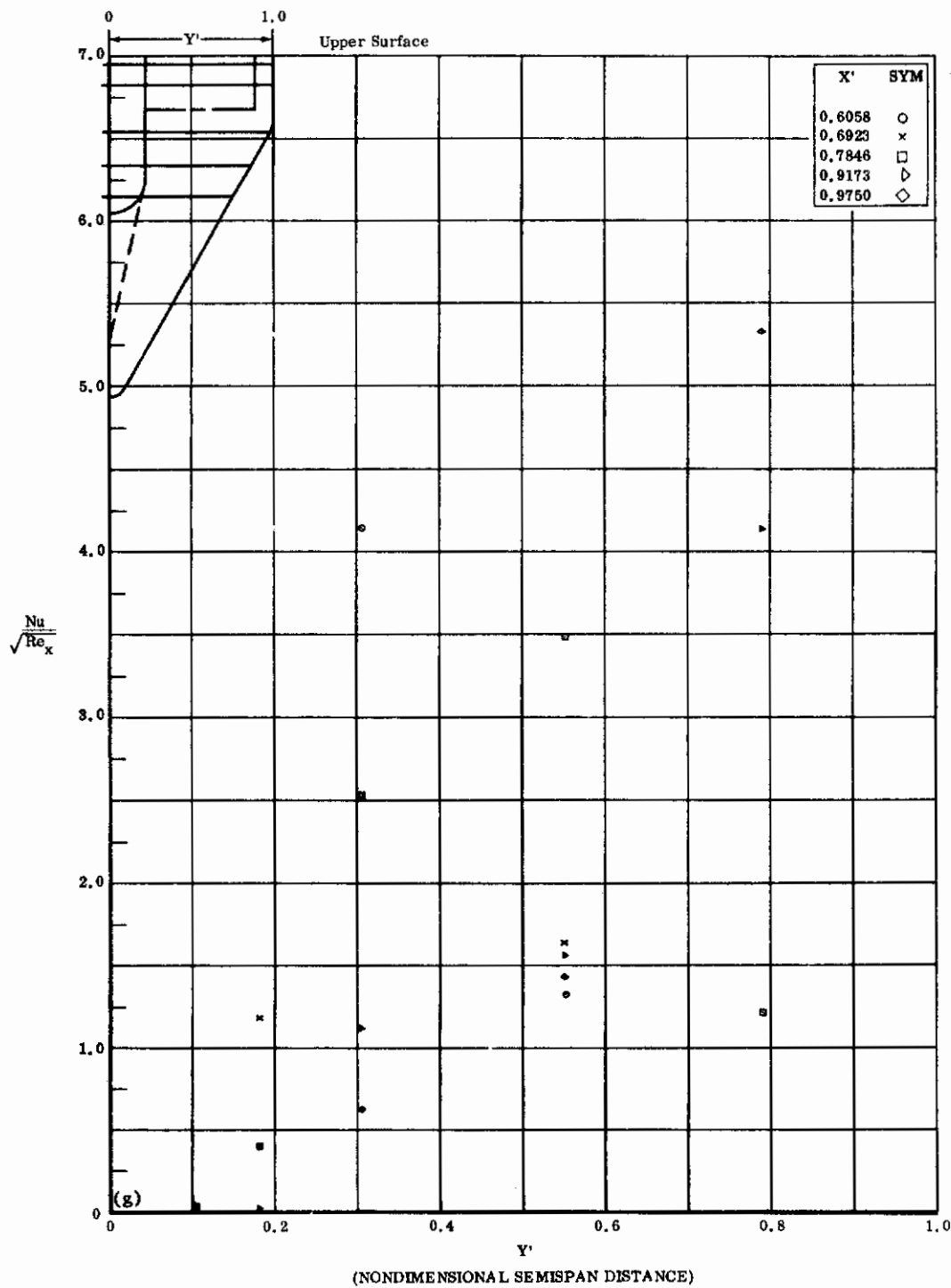


Fig. 24g Configuration IV, $\alpha = -20$, $\delta_2 = \delta_3 = +10$
 $Nu/\sqrt{Re_x}$ vs. Y' upper surface

Contrails

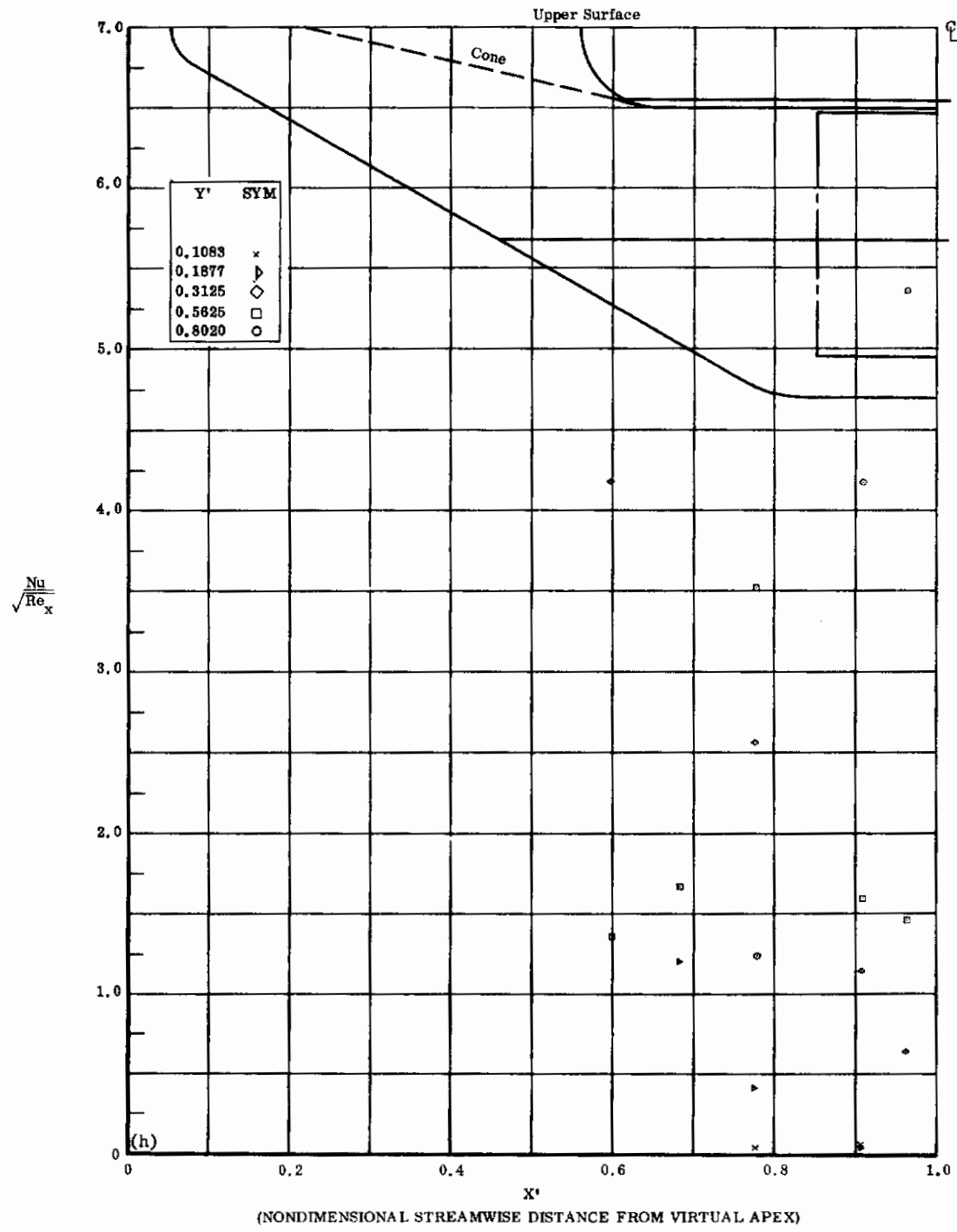


Fig. 24h Configuration IV, $\alpha = -20$, $s_2 = s_3 = +10$

$\text{Nu}/\sqrt{\text{Re}_x}$ vs. X^* upper surface

Contrails

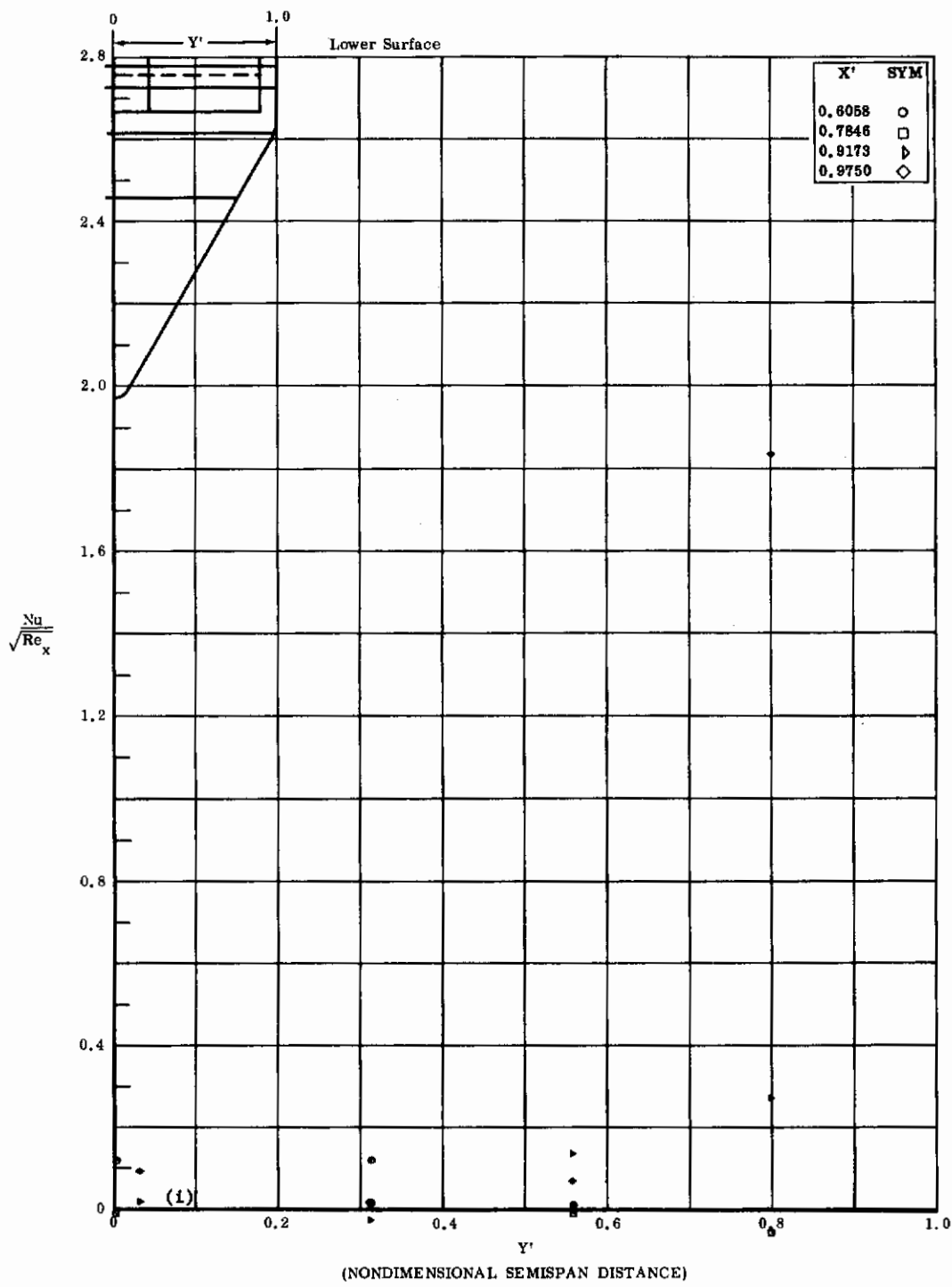


Fig. 24i Configuration IV, $\alpha = -20$, $\delta_2 = \delta_3 = +20$
 $Nu/\sqrt{Re_x}$ vs. Y' lower surface

Contrails

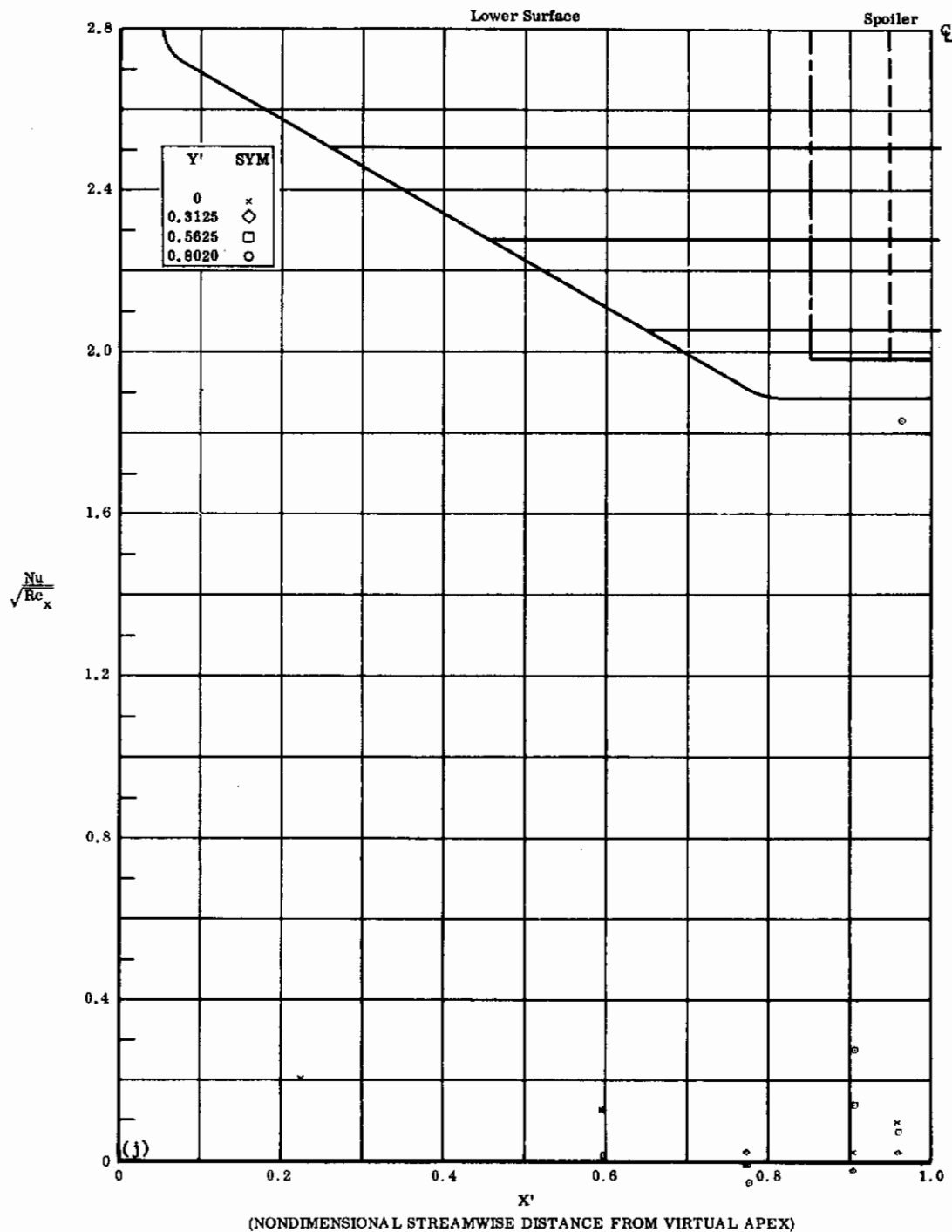


Fig. 24j Configuration IV, $\alpha = -20$, $b_2 = b_3 = +20$
 $Nu/\sqrt{Re_x}$ vs. X' lower surface

Contrails

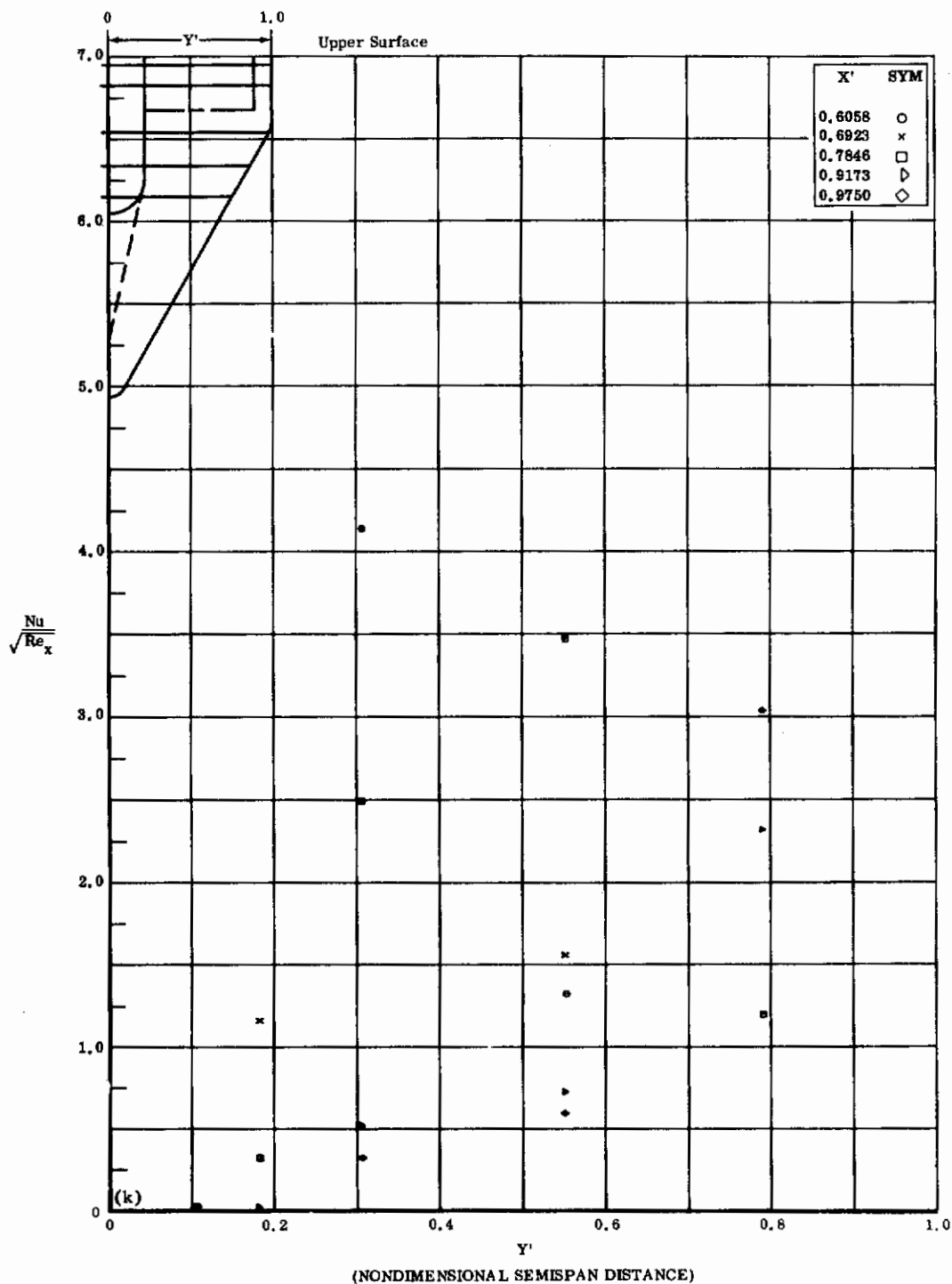


Fig. 24k Configuration IV, $\alpha = -20$, $\delta_2 = \delta_3 = +20$

$Nu/\sqrt{Re_x}$ vs. Y' upper surface

Contrails

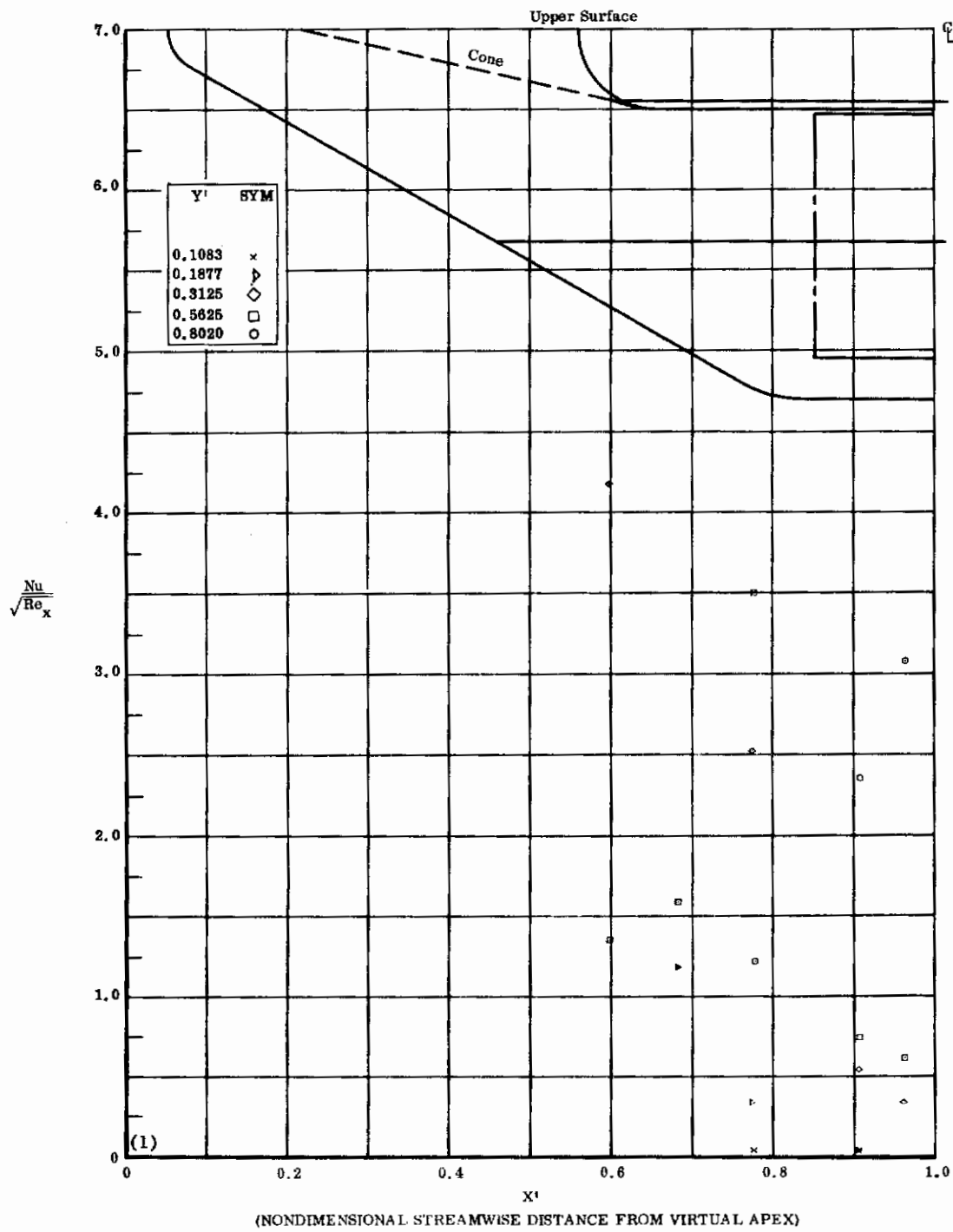


Fig. 24 ℓ Configuration IV, $\alpha = -20$, $\delta_2 = \delta_3 = +20$
 $Nu/\sqrt{Re_x}$ vs. X' upper surface

Contrails

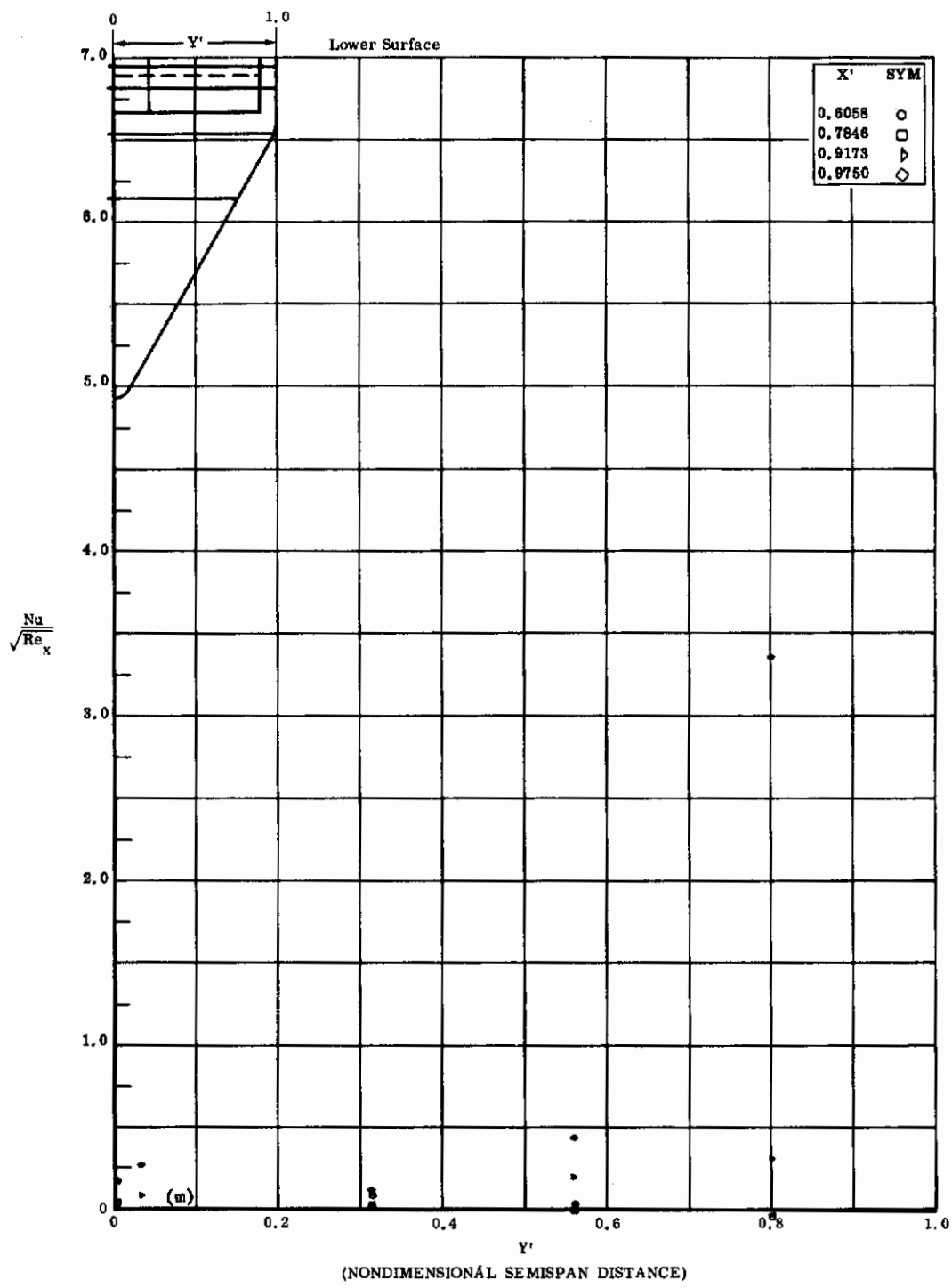


Fig. 24m *Configuration IV, $\alpha = -20$, $\delta_2 = \delta_3 = +30$
 $\frac{Nu}{\sqrt{Re_x}}$ vs. Y' lower surface

Contrails

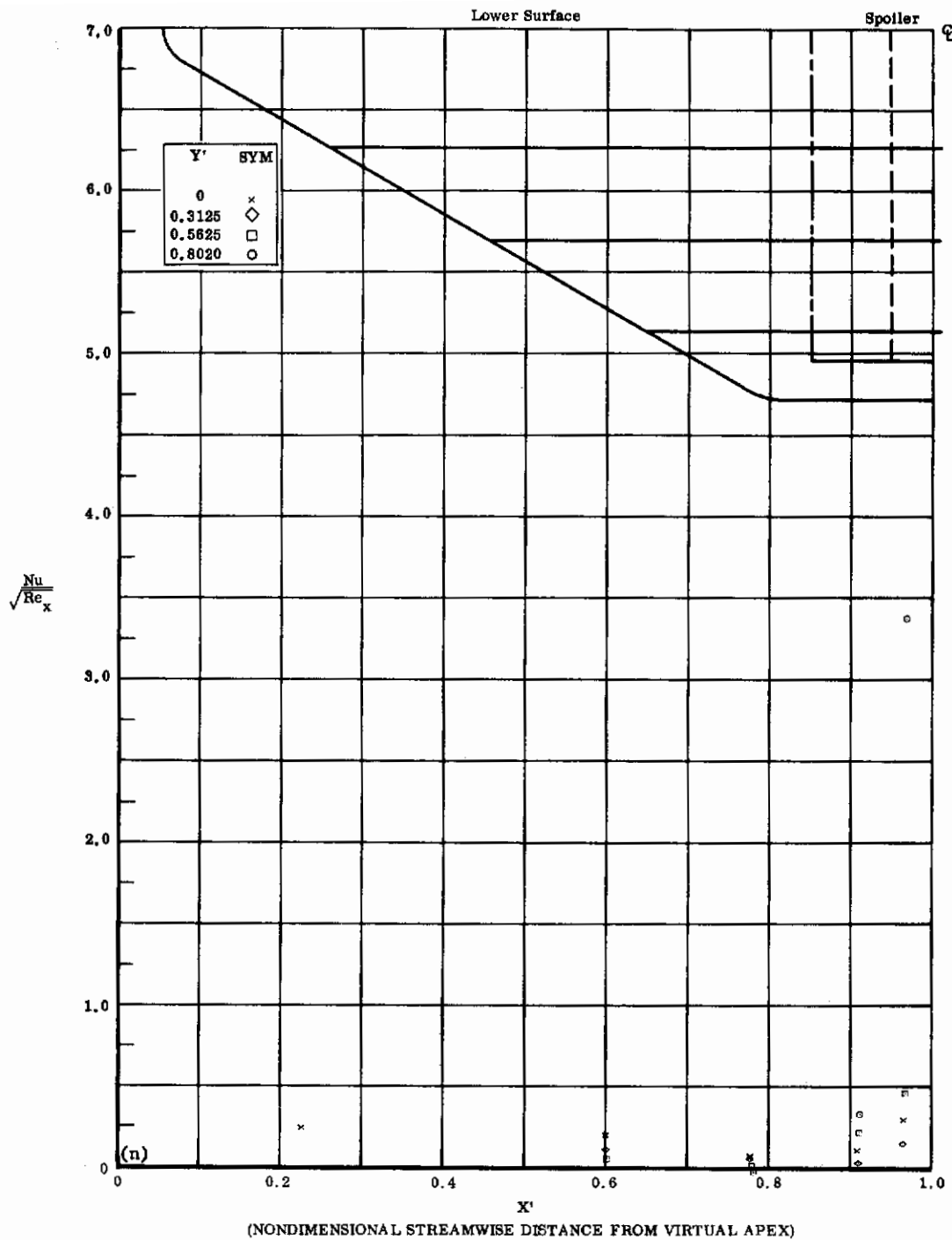


Fig. 24n Configuration IV, $\alpha = -20$, $\delta_2 = \delta_3 = +30$
 $\text{Nu}/\sqrt{\text{Re}_x}$ vs. X' lower surface

Contrails

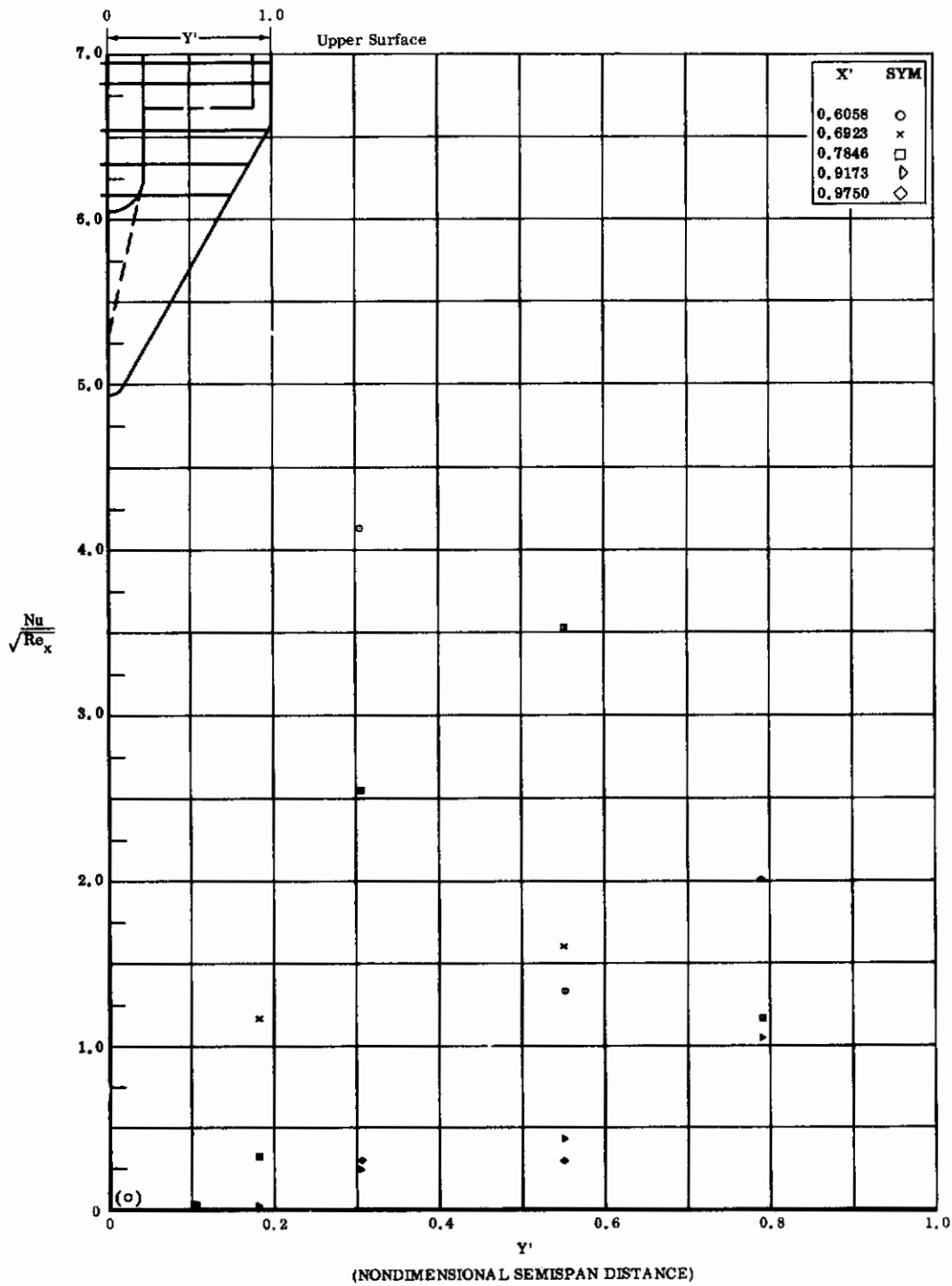


Fig. 24o Configuration IV, $\alpha = -20$, $b_2 = b_3 = +30$
 $\text{Nu}/\sqrt{\text{Re}_x}$ vs. Y' upper surface

Contrails

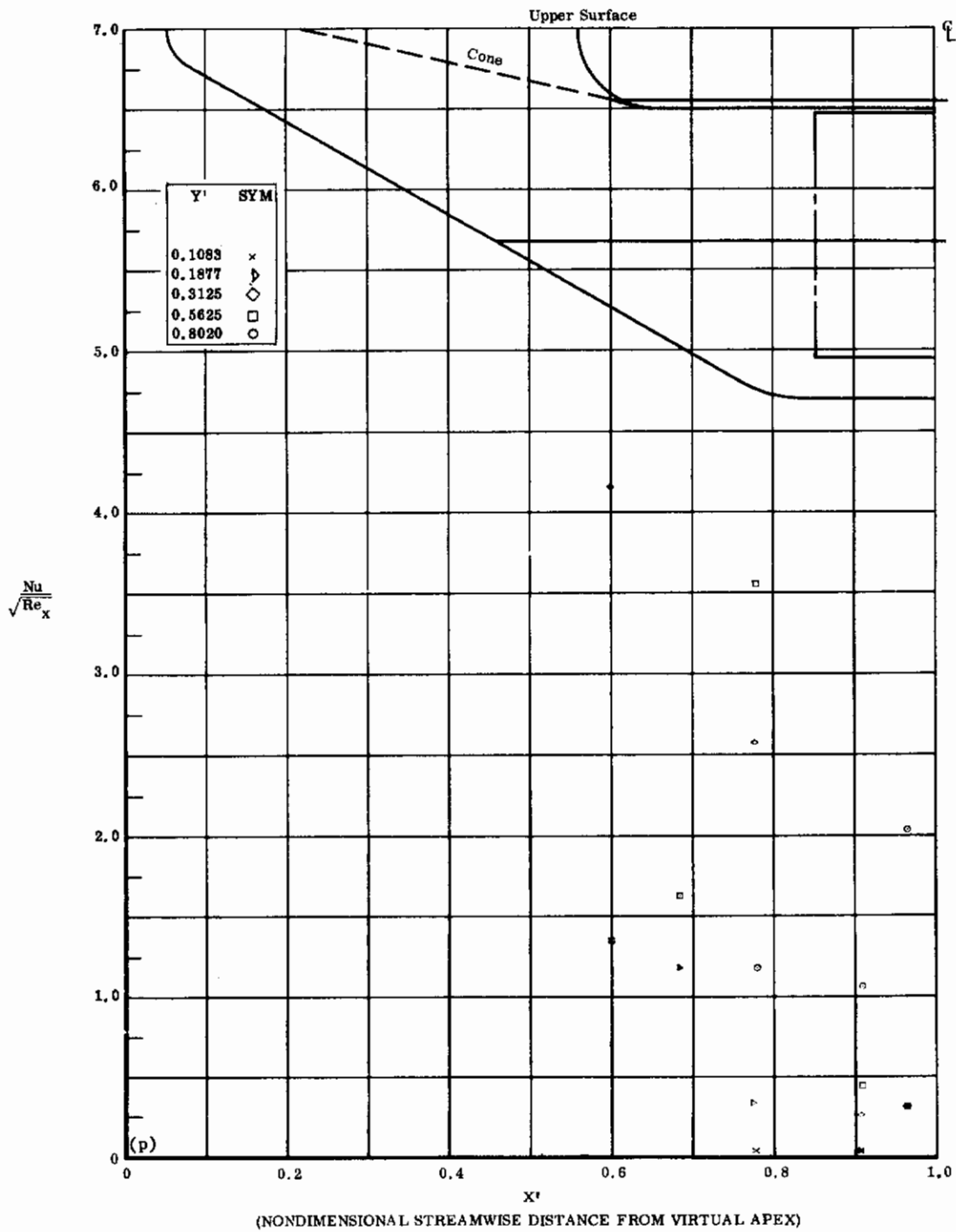


Fig. 24p Configuration IV, $\alpha = -20$, $\delta_2 = \delta_3 = +30$
 $Nu/\sqrt{Re_x}$ vs. X^1 upper surface

Contrails

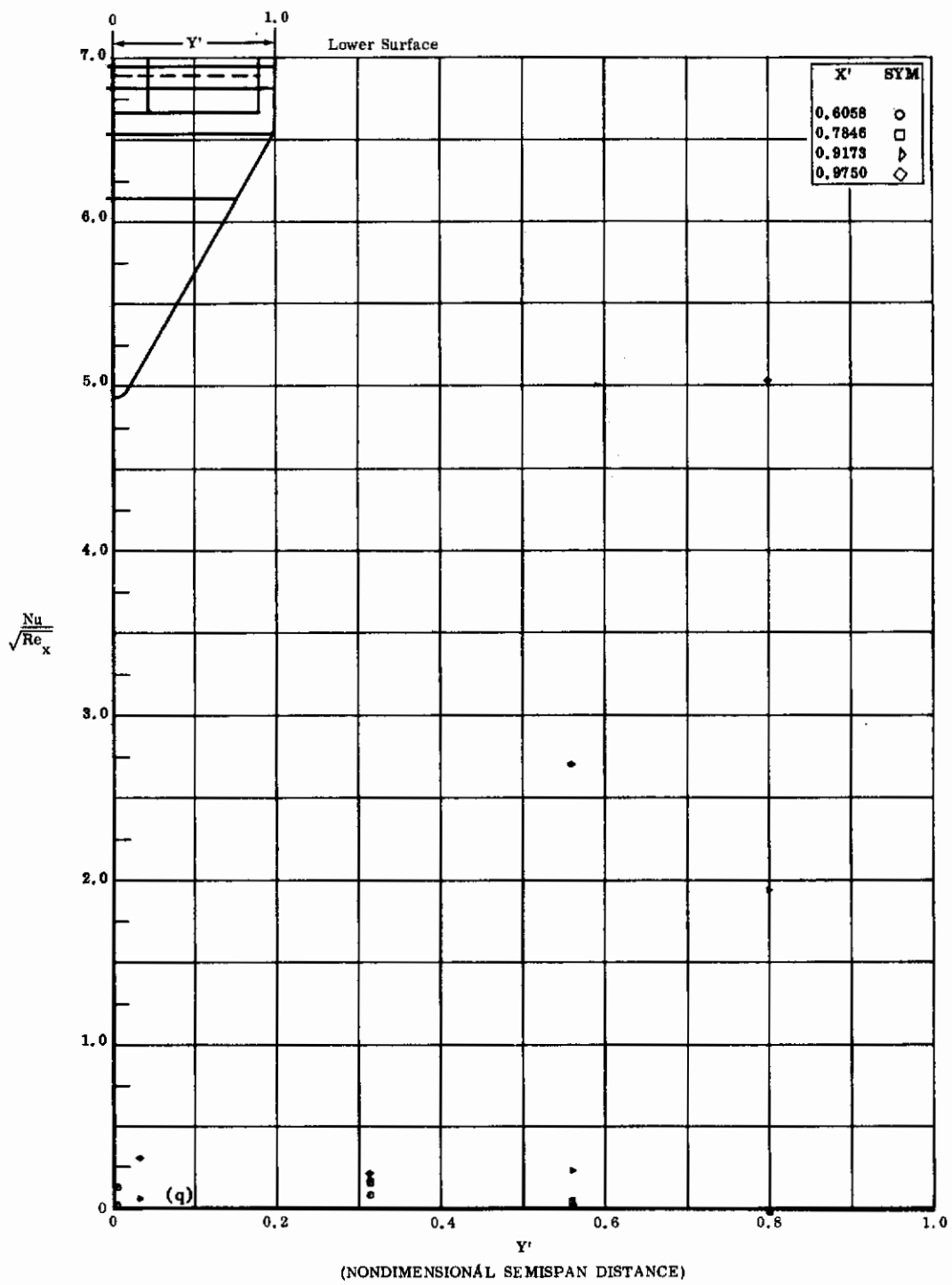


Fig. 24q Configuration IV, $\alpha = -20$, $\delta_2 = \delta_3 = +39$
 $Nu/\sqrt{Re_x}$ vs. Y' lower surface

Contrails

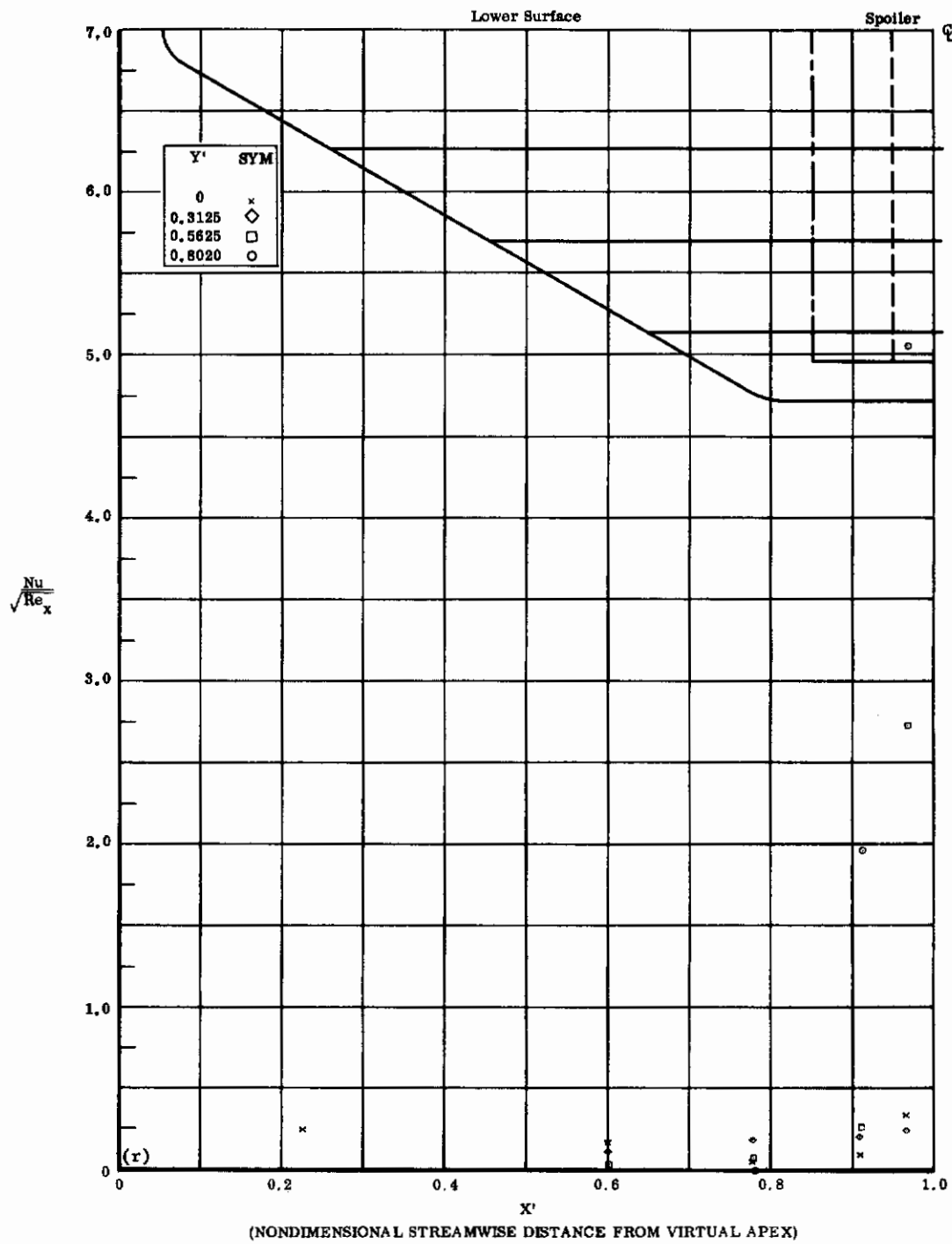


Fig. 24r Configuration IV, $\alpha = -20$, $\delta_2 = \delta_3 = +39$
 $Nu/\sqrt{Re_x}$ vs. X' lower surface

Contrails

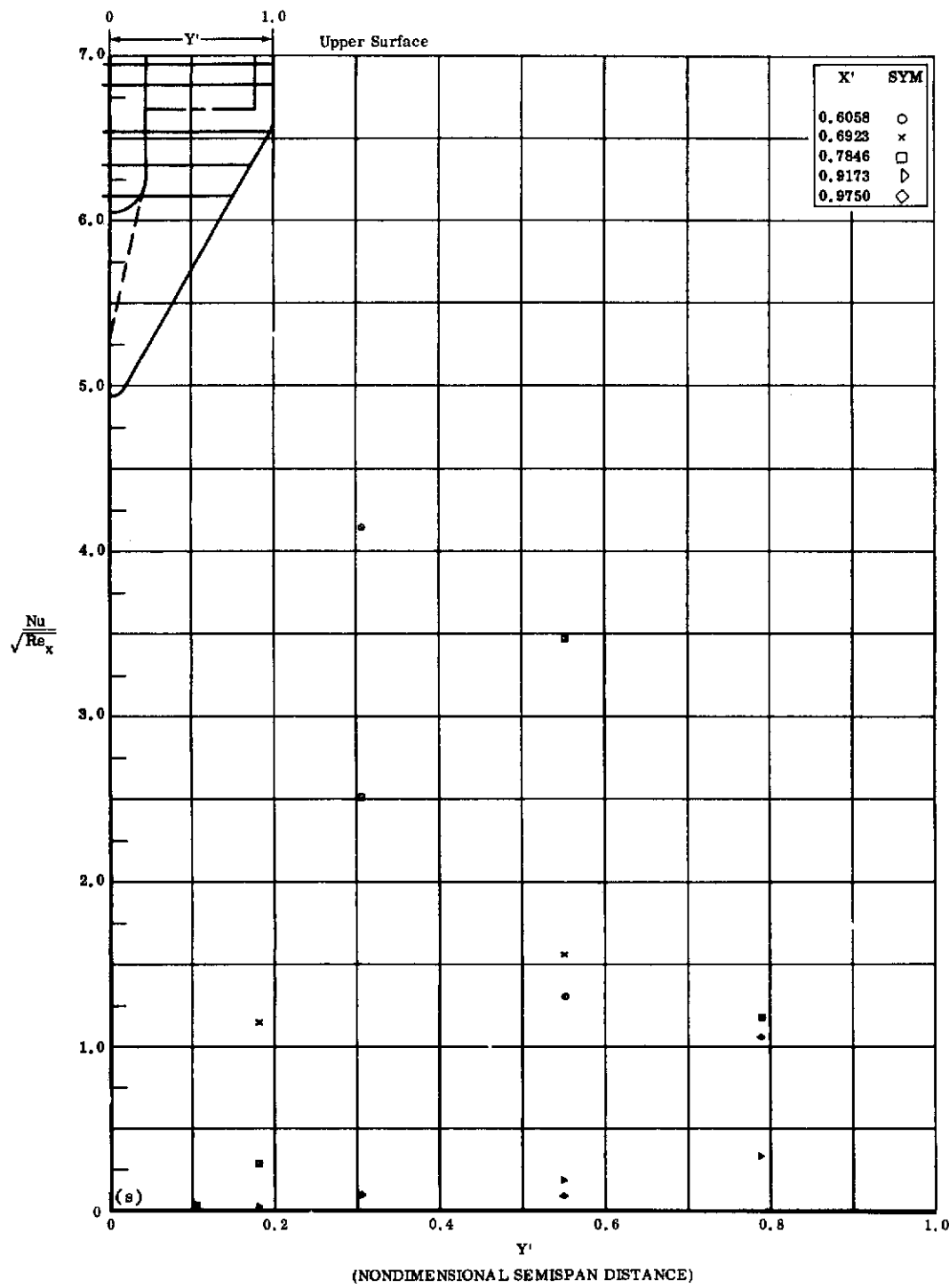


Fig. 24s Configuration IV, $\alpha = -20$, $s_2 = s_3 = +39$

$Nu/\sqrt{Re_x}$ vs. Y' upper surface

Contrails

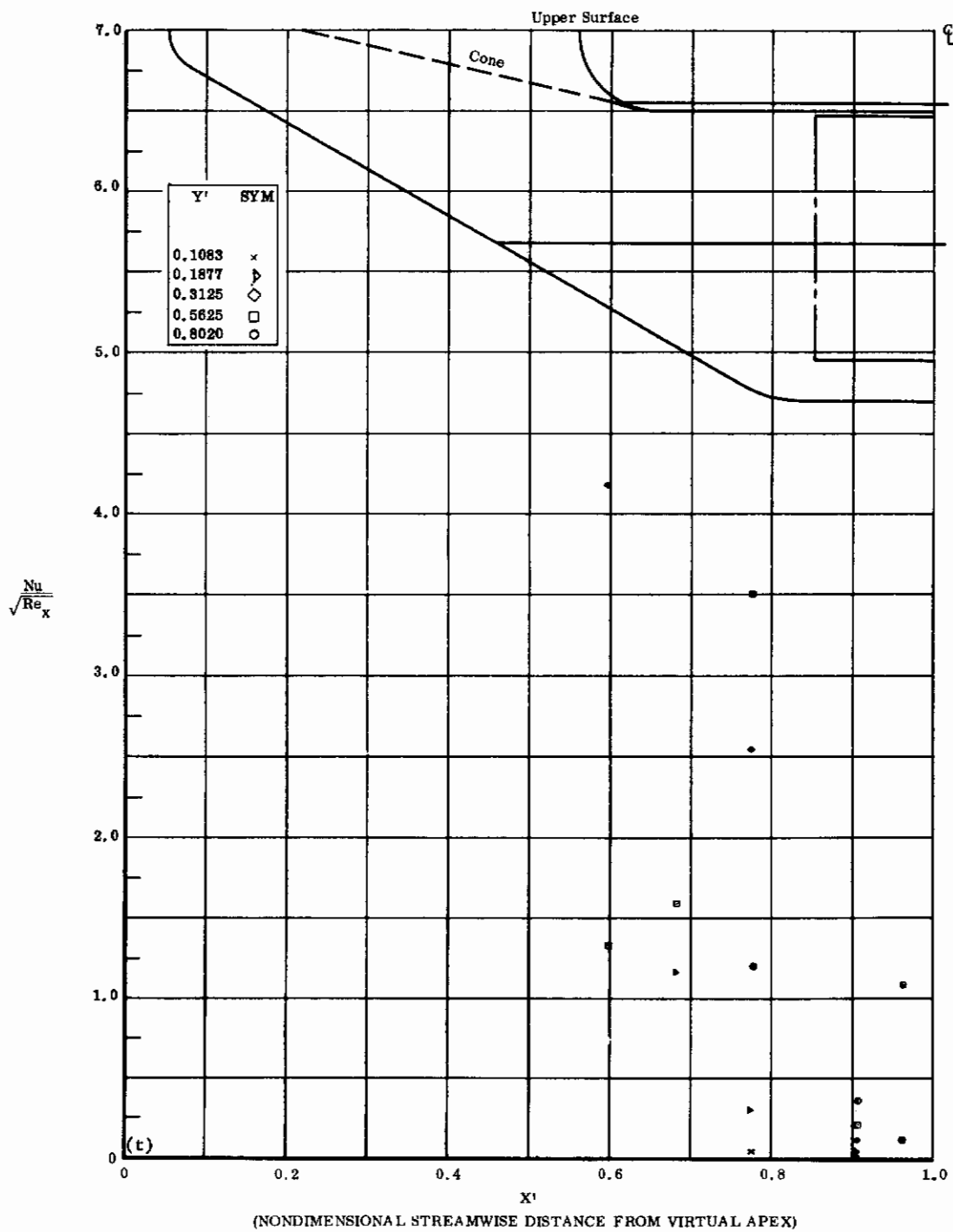


Fig. 24t Configuration IV, $\alpha = -20$, $\delta_2 = \delta_3 = +39$
 $Nu/\sqrt{Re_x}$ vs. X' upper surface

Contrails

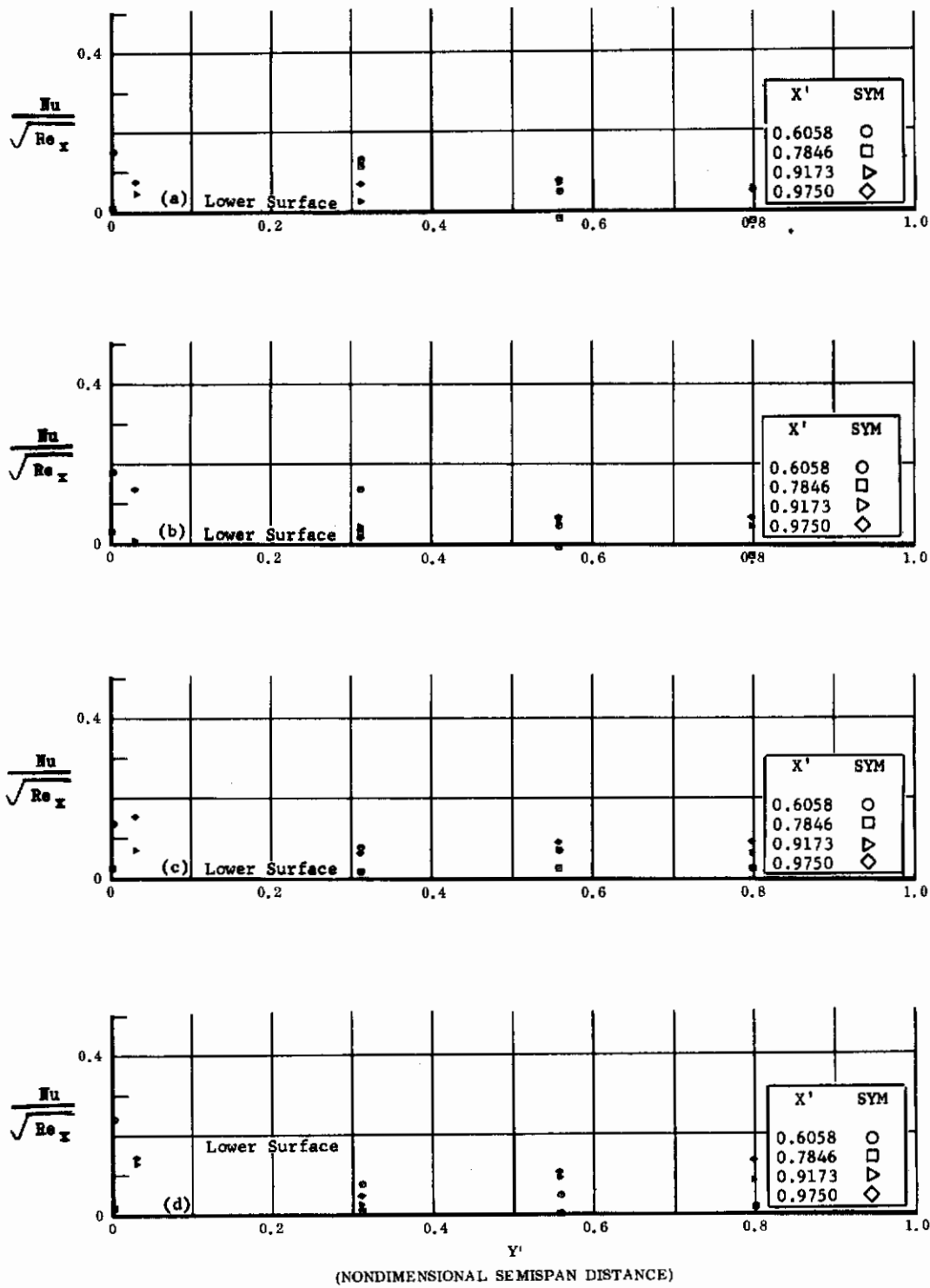


Fig. 25 Configuration IV, $\alpha = -20$, $Nu/\sqrt{Re_x}$ vs. Y' , lower surface

- a) $\delta_2 = \delta_3 = -10$
- b) $\delta_2 = \delta_3 = -20$
- c) $\delta_2 = \delta_3 = -30$
- d) $\delta_2 = \delta_3 = -39$

Contrails

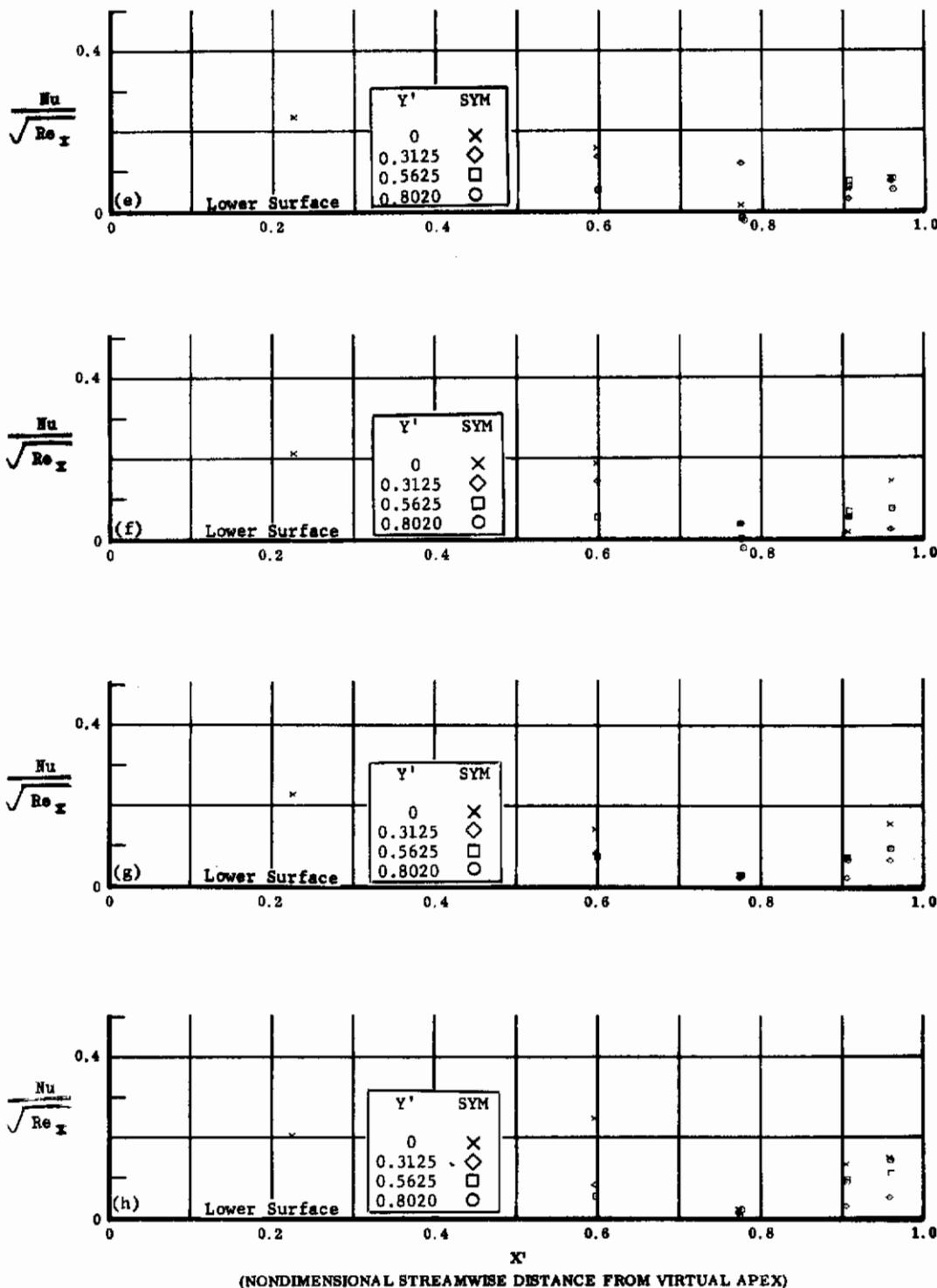


Fig. 25 Configuration IV, $\alpha = -20$, $Nu/\sqrt{Re_x}$ vs. X' , lower surface

e) $\delta_2 = \delta_3 = -10$

f) $\delta_2 = \delta_3 = -20$

g) $\delta_2 = \delta_3 = -30$

h) $\delta_2 = \delta_3 = -39$

Contrails

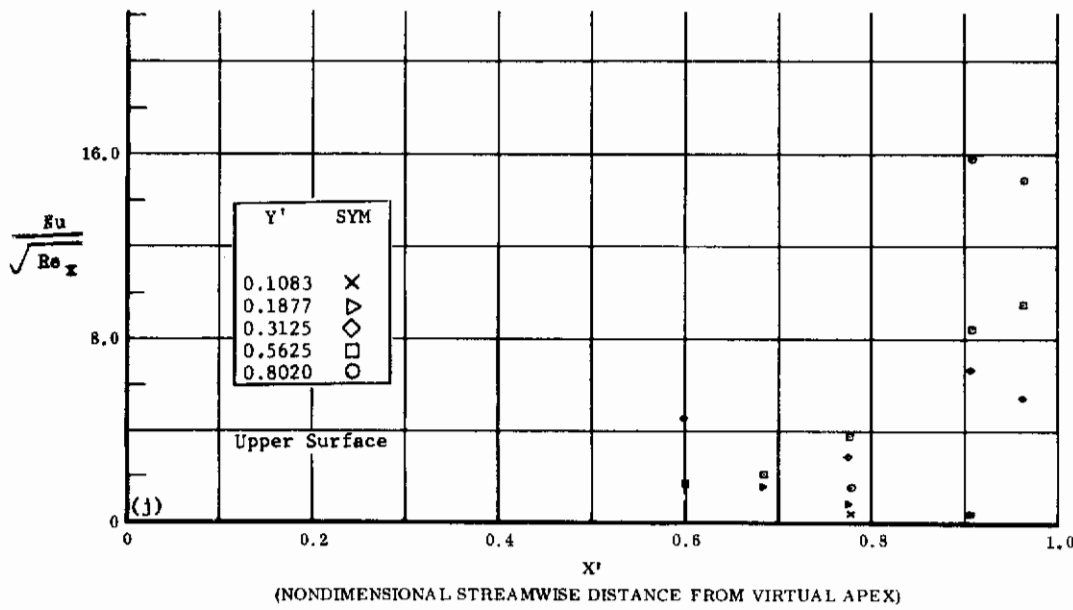
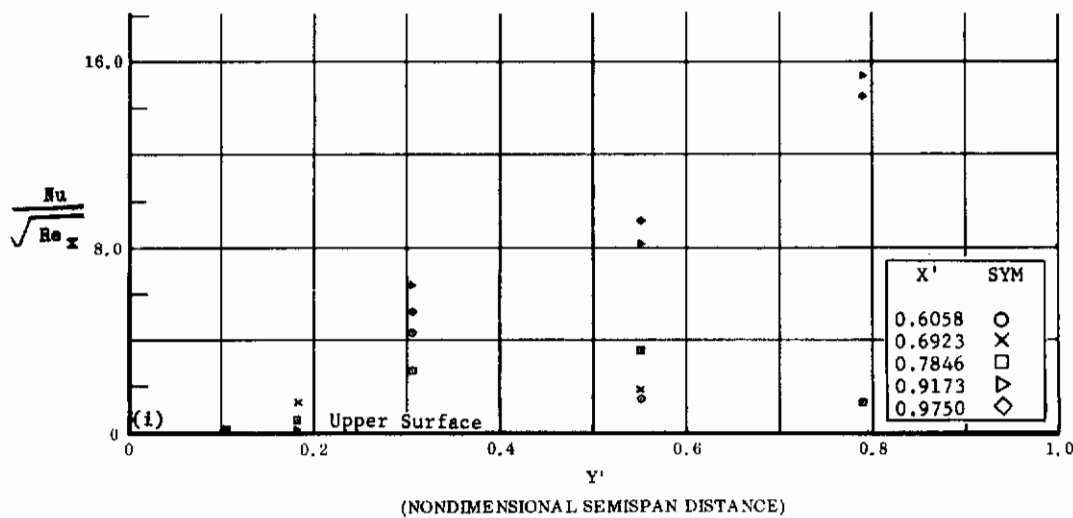
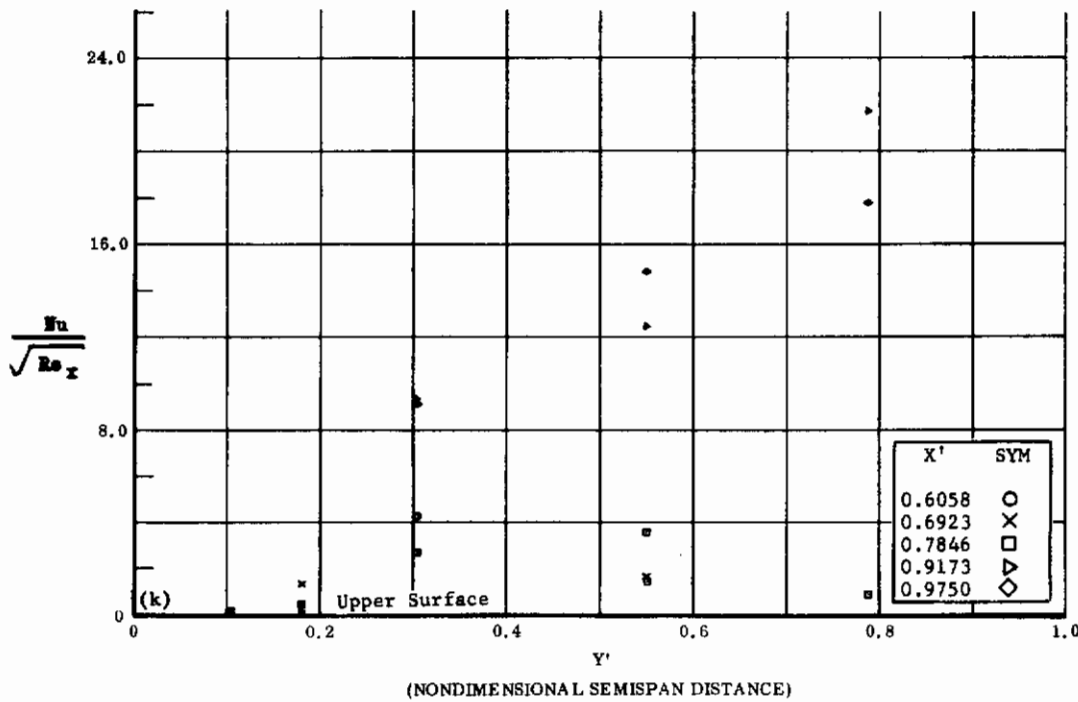


Fig. 25 Configuration IV, $\alpha = -20$, $\delta_2 = \delta_3 = -10$

i) $Nu/\sqrt{Re_x}$ vs. Y' upper surface

j) $Nu/\sqrt{Re_x}$ vs. X' upper surface

Contrails



(NONDIMENSIONAL SEMISPAN DISTANCE)

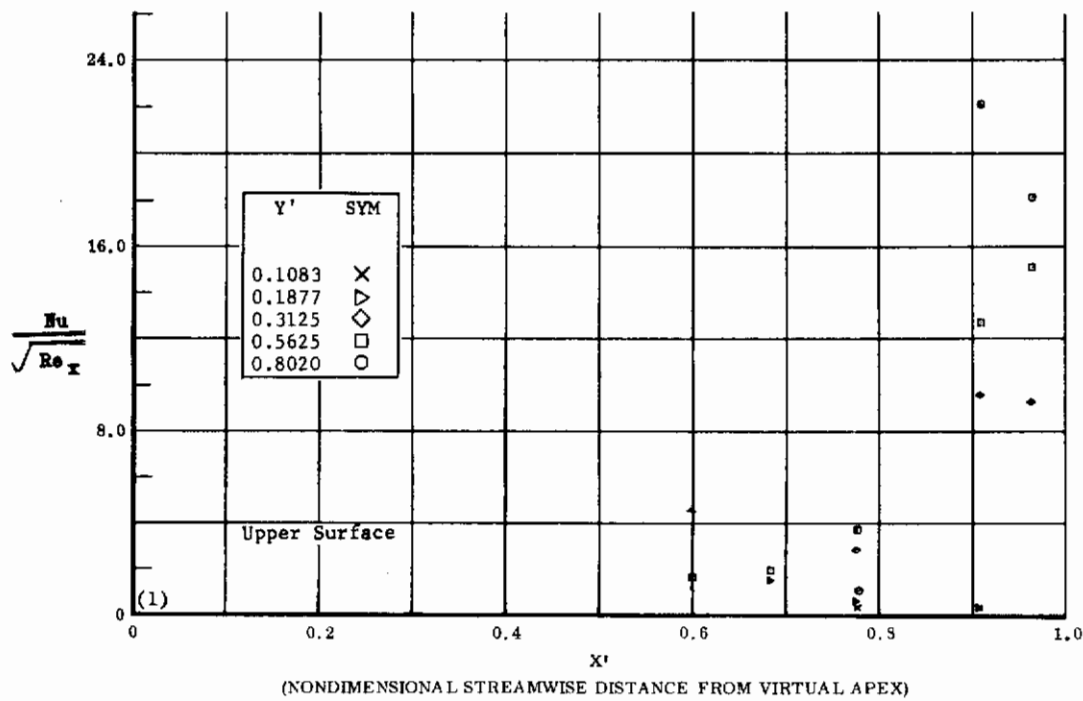


Fig. 25 Configuration IV, $\alpha = -20$, $\delta_2 = \delta_3 = -20$

k) $Nu/\sqrt{Re_x}$ vs. Y' upper surface

l) $Nu/\sqrt{Re_x}$ vs. X' upper surface

Contrails

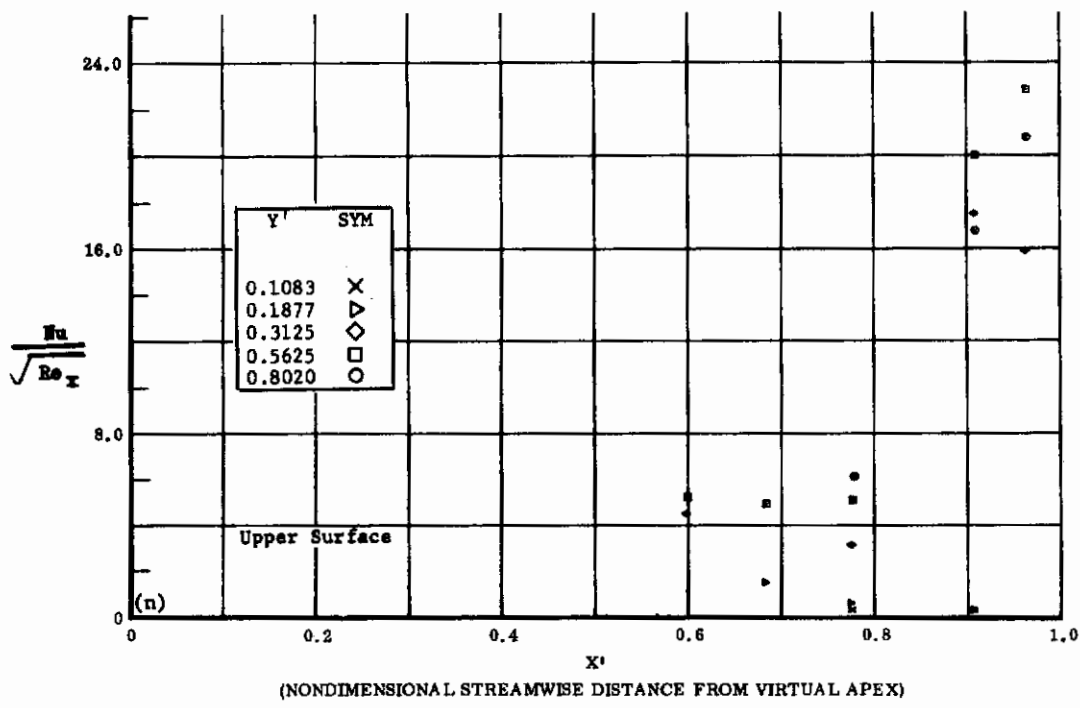
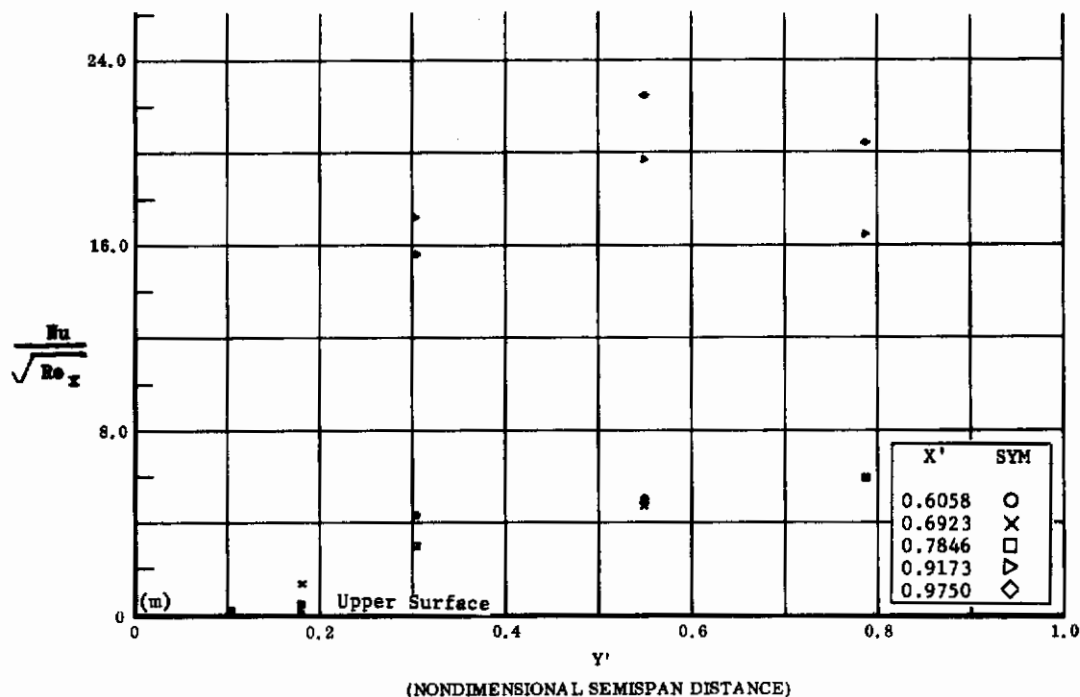


Fig. 25 Configuration IV, $\alpha = -20$, $\delta_2 = \delta_3 = -30$

m) $Nu/\sqrt{Re_x}$ vs. Y' upper surface

n) $Nu/\sqrt{Re_x}$ vs. X' upper surface

Contrails

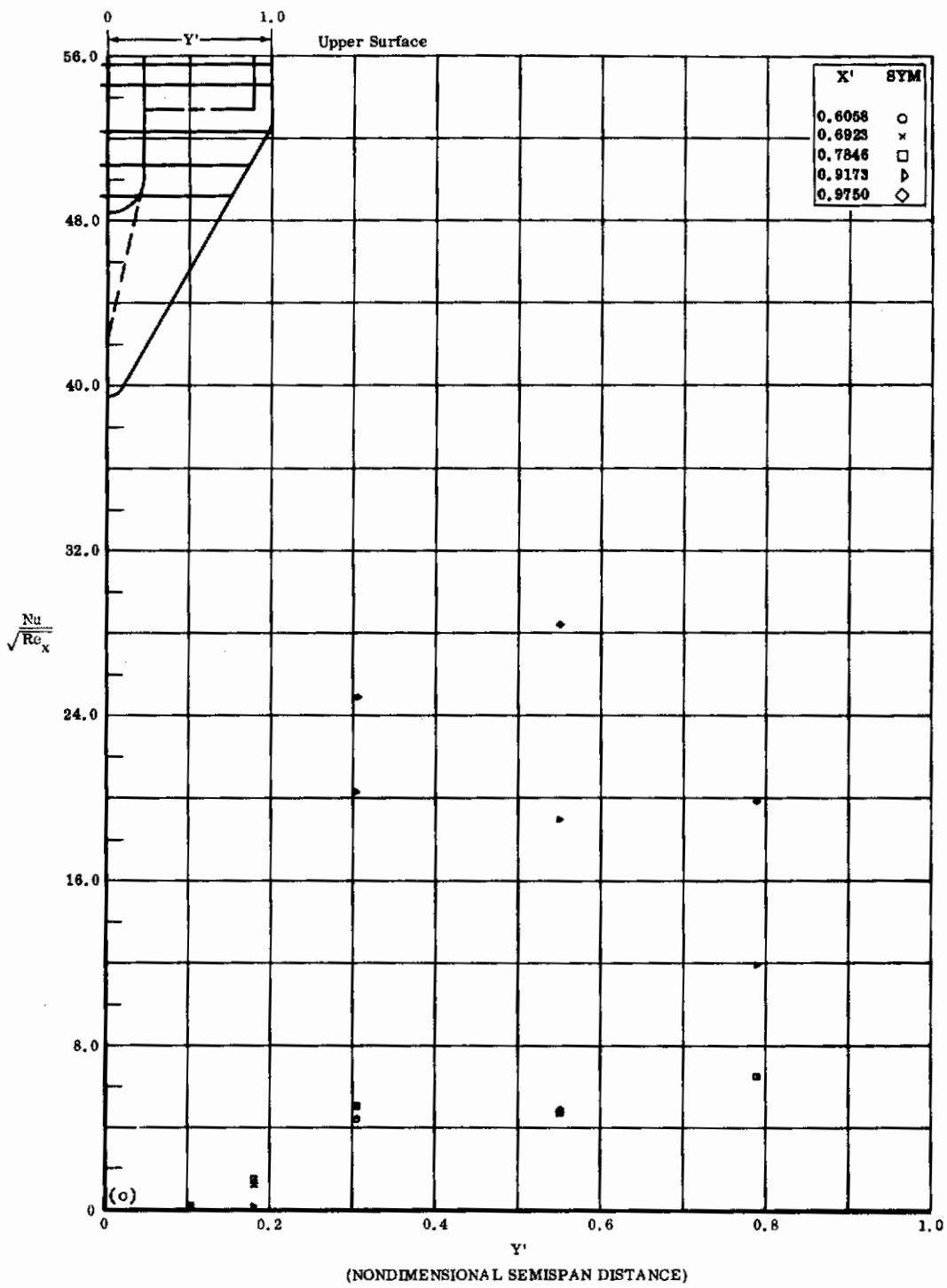


Fig. 25o Configuration IV, $\alpha = -20$, $\delta_2 = \delta_3 = -39$
 $Nu/\sqrt{Re_x}$ vs. Y' upper surface

Contrails

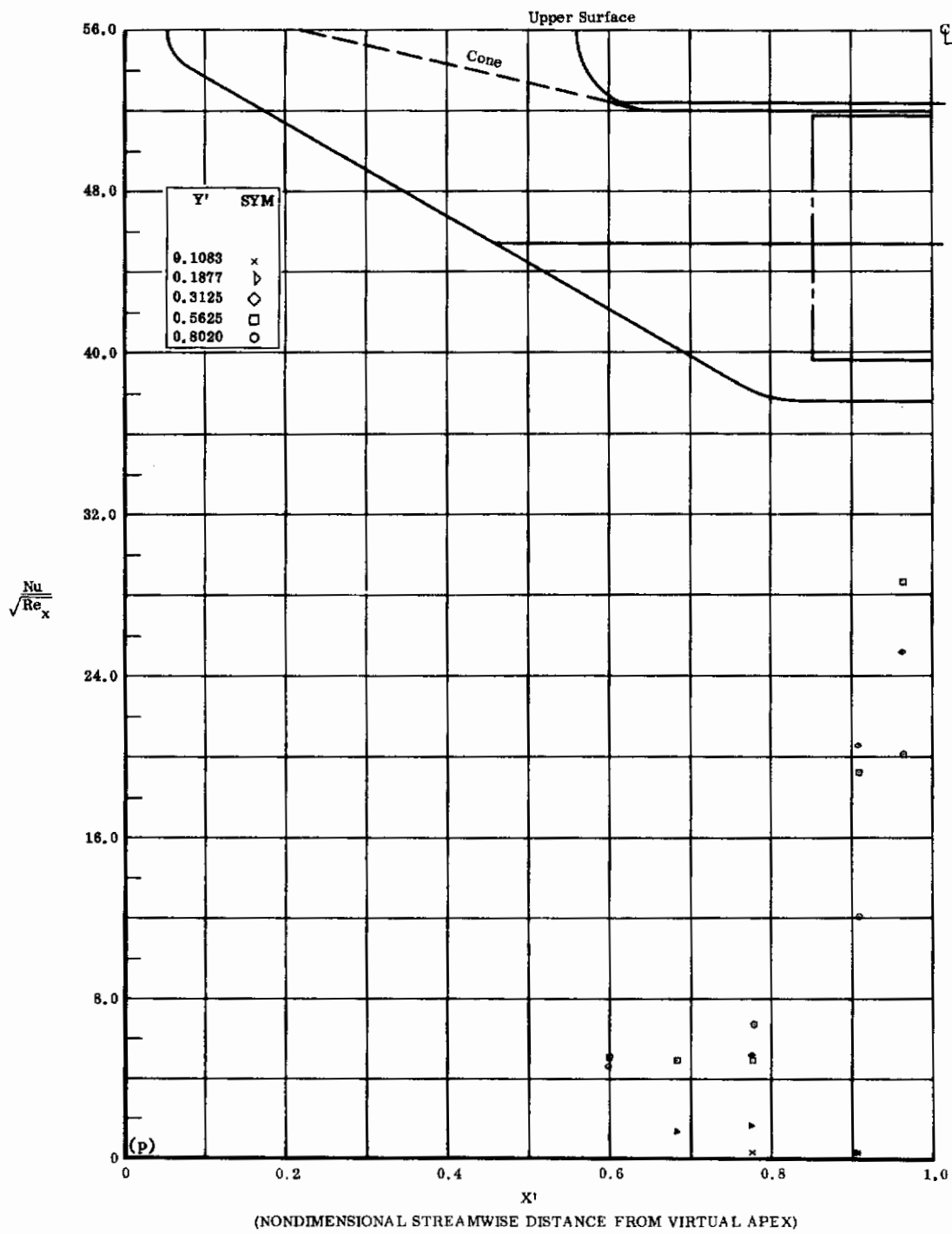


Fig. 25p Configuration IV, $\alpha = -20$, $\delta_2 = \delta_3 = -39$

$\text{Nu}/\sqrt{\text{Re}_x}$ vs. X' upper surface

Contrails

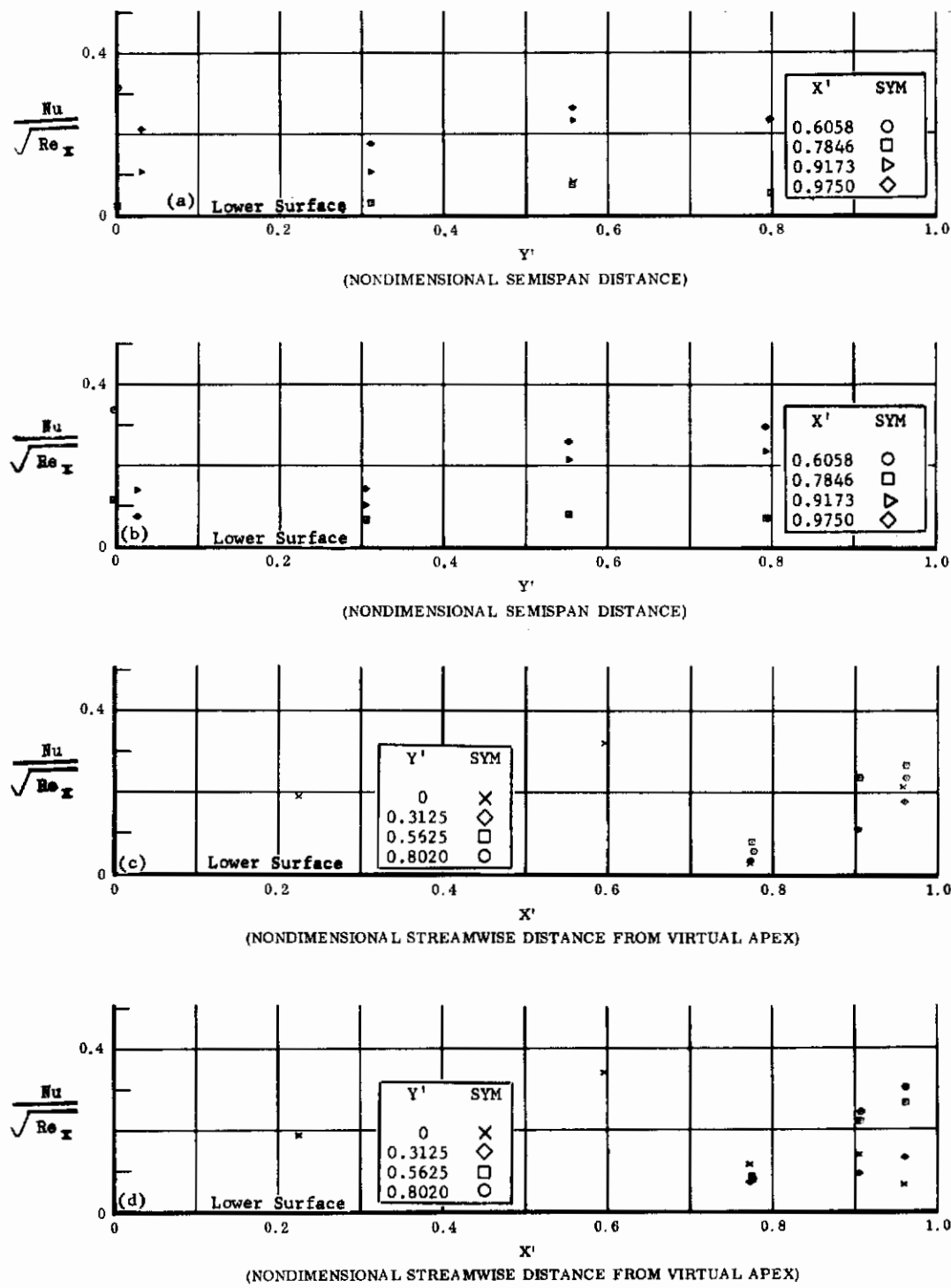


Fig. 26 Configuration IV, $\alpha = -30$, lower surface

- a) $Nu/\sqrt{Re_x}$ vs. Y' , $\delta_2 = \delta_3 = 0$
- b) $Nu/\sqrt{Re_x}$ vs. Y' , $\delta_2 = \delta_3 = +39$
- c) $Nu/\sqrt{Re_x}$ vs. X' , $\delta_2 = \delta_3 = 0$
- d) $Nu/\sqrt{Re_x}$ vs. X' , $\delta_2 = \delta_3 = +39$

Contrails

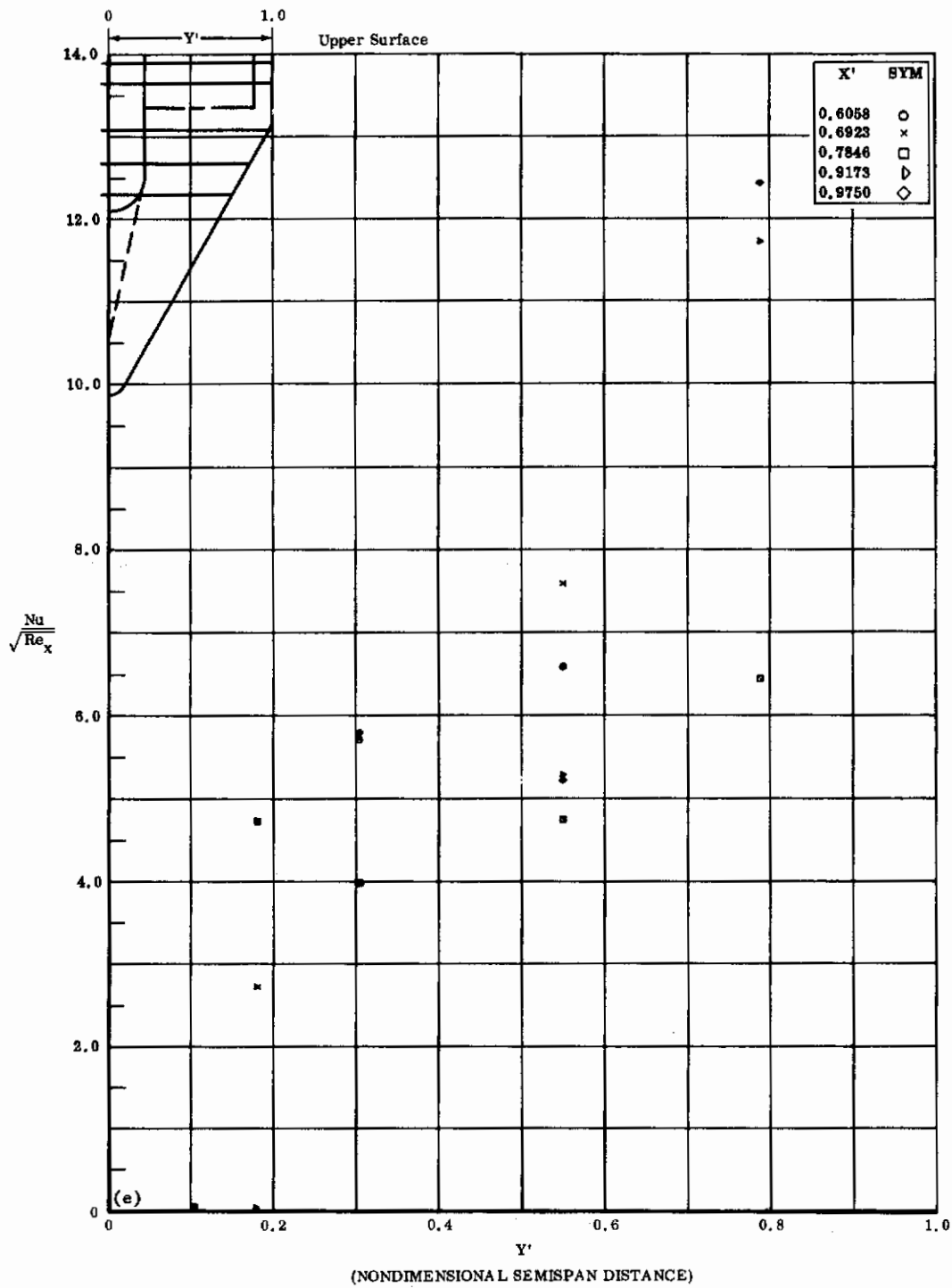


Fig. 26e Configuration IV, $\alpha = -30$, $\delta_2 = \delta_3 = 0$
 $Nu/\sqrt{Re_x}$ vs. Y' upper surface

Contrails

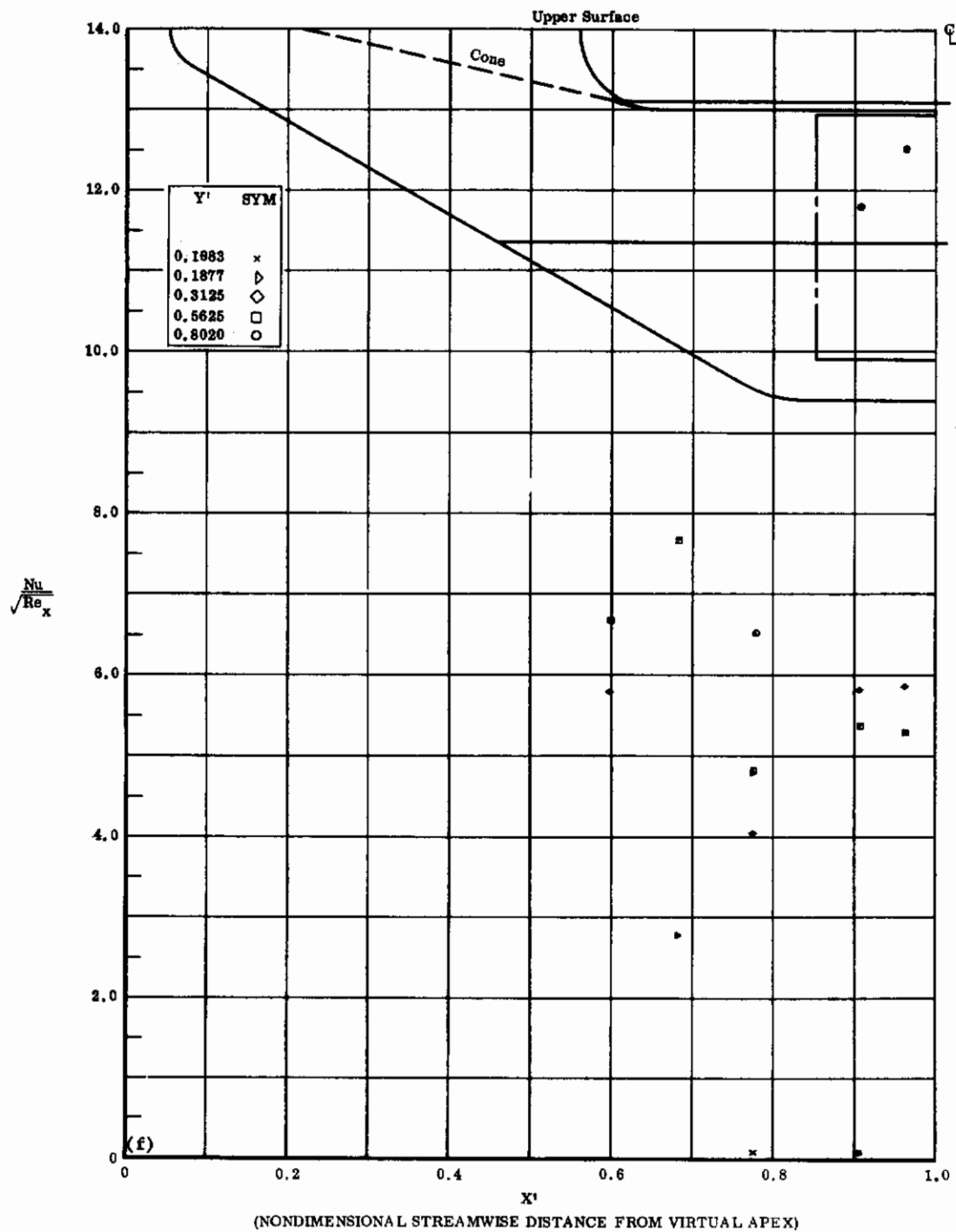


Fig. 26f Configuration IV, $\alpha = -30$, $\delta_2 = \delta_3 = 0$
 $Nu/\sqrt{Re_x}$ vs. X' upper surface

Contrails

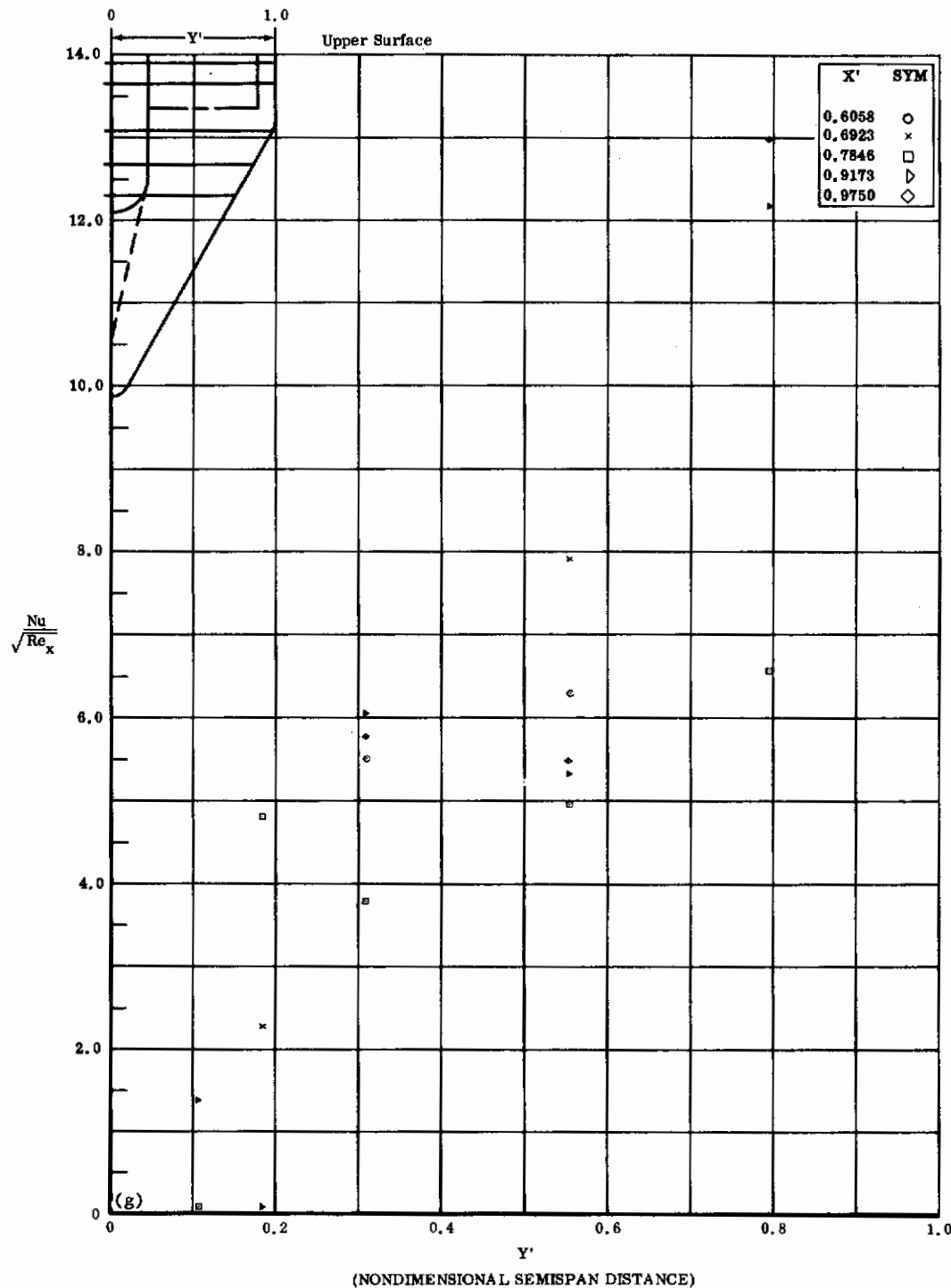


Fig. 26g Configuration IV, $\alpha = -30^\circ$, $\delta_2 = \delta_3 = +39^\circ$
 $\text{Nu}/\sqrt{\text{Re}_x}$ vs. Y' upper surface

Contrails

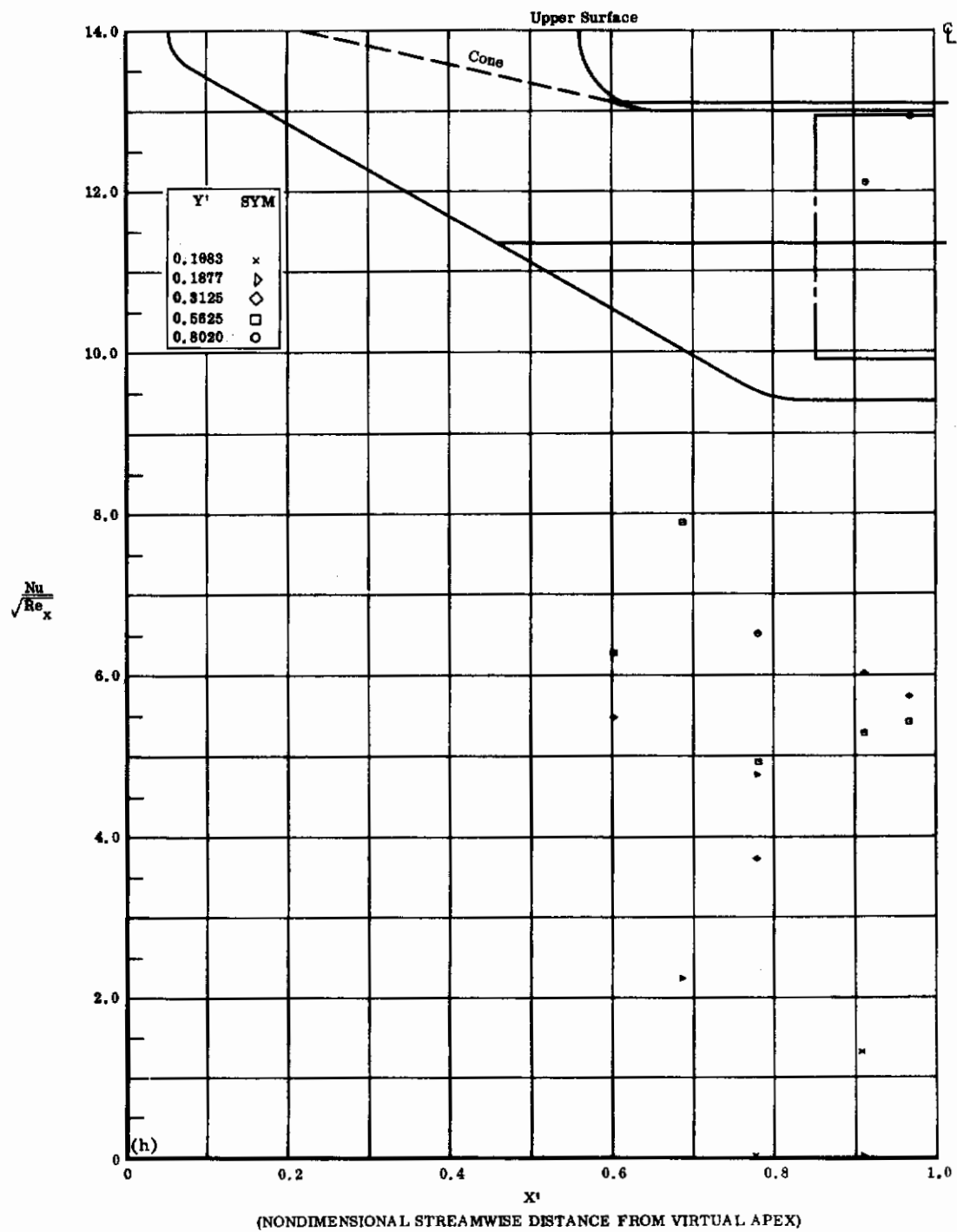


Fig. 26h Configuration IV, $\alpha = -30^\circ$, $\delta_2 = \delta_3 = +39^\circ$
 $Nu/\sqrt{Re_x}$ vs. X^i upper surface

Contrails

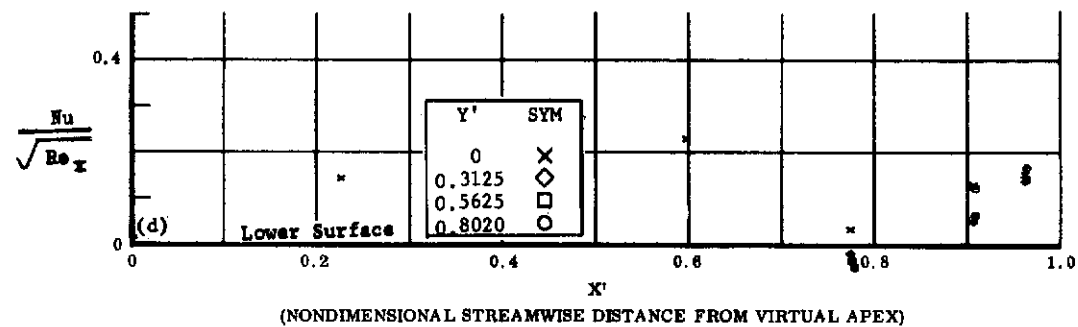
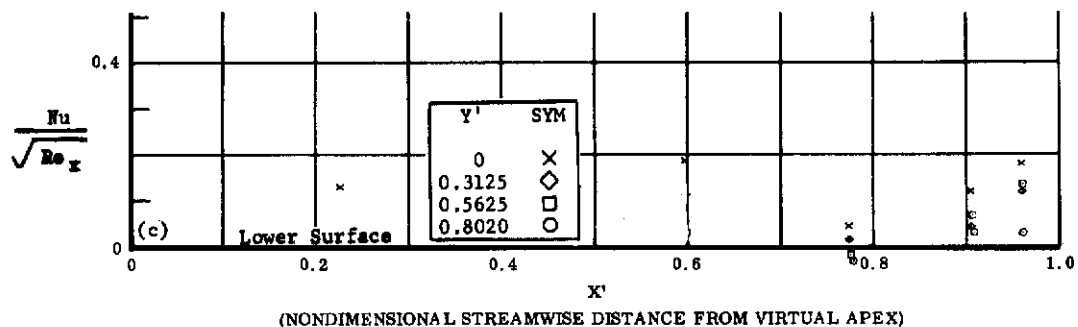
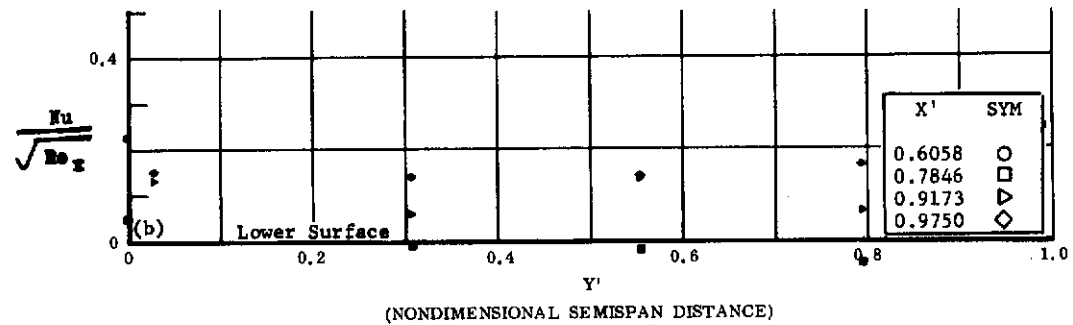
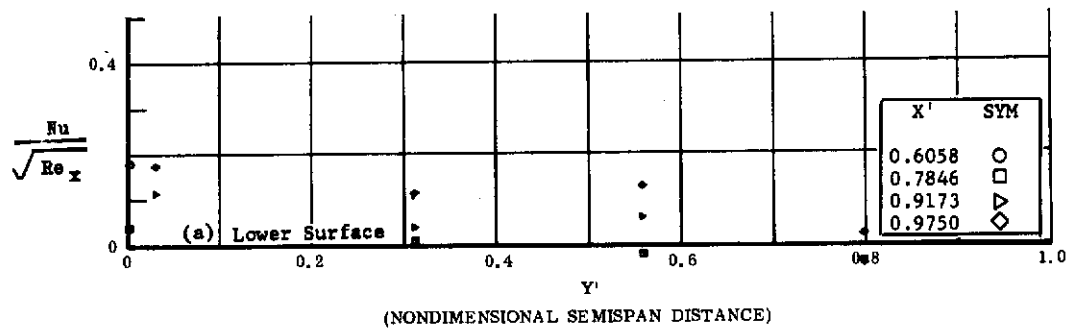


Fig. 27 Configuration IV, $\alpha = -40$, lower surface

a) $Nu/\sqrt{Re_x}$ vs. Y' , $\delta_2 = \delta_3 = 0$

b) $Nu/\sqrt{Re_x}$ vs. Y' , $\delta_2 = \delta_3 = +39$

c) $Nu/\sqrt{Re_x}$ vs. X' , $\delta_2 = \delta_3 = 0$

d) $Nu/\sqrt{Re_x}$ vs. X' , $\delta_2 = \delta_3 = +39$

Contrails

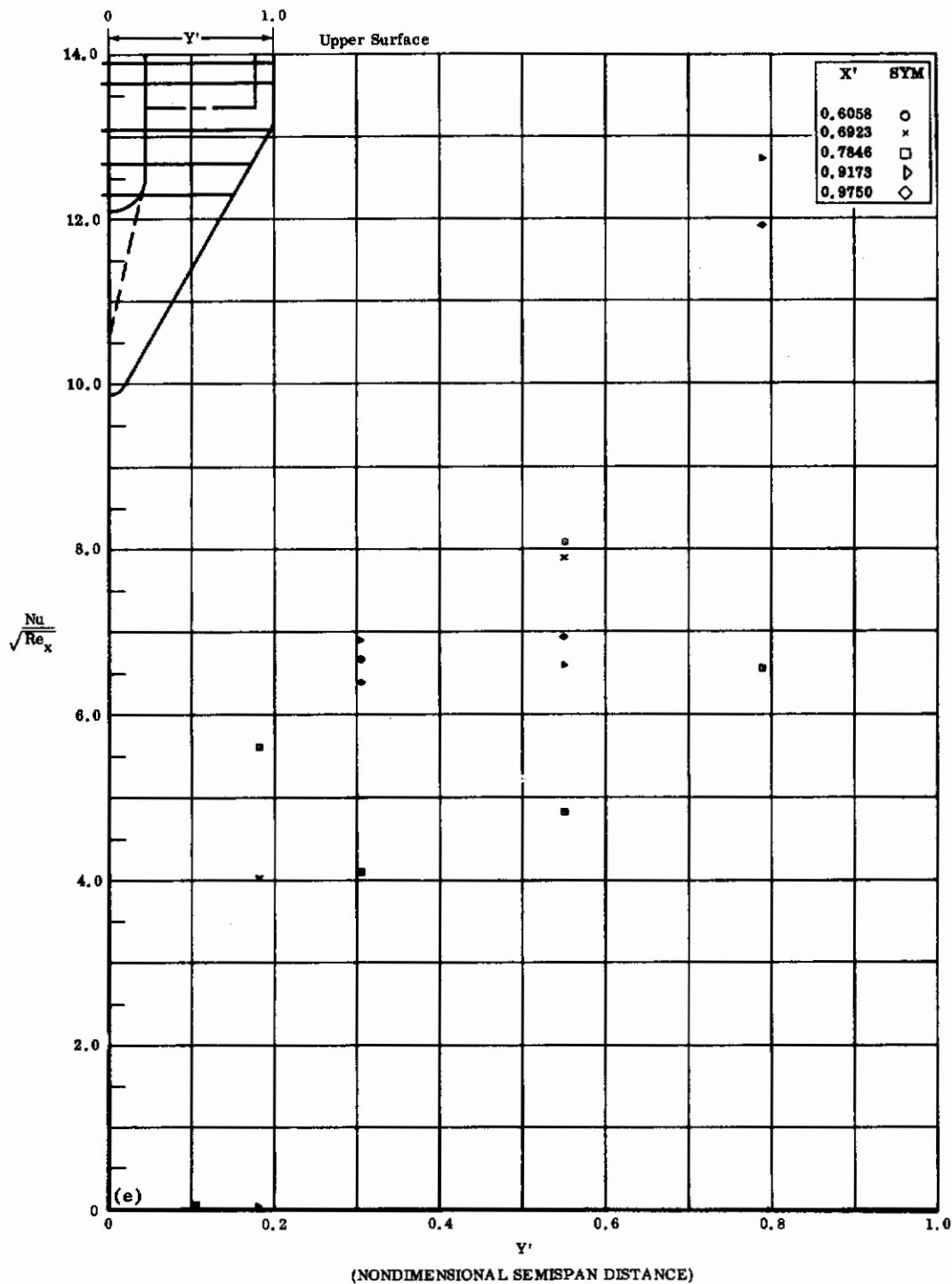


Fig. 27e Configuration IV, $\alpha = -40$, $b_2 = b_3 = 0$
 $Nu/\sqrt{Re_x}$ vs. Y' upper surface

Contrails

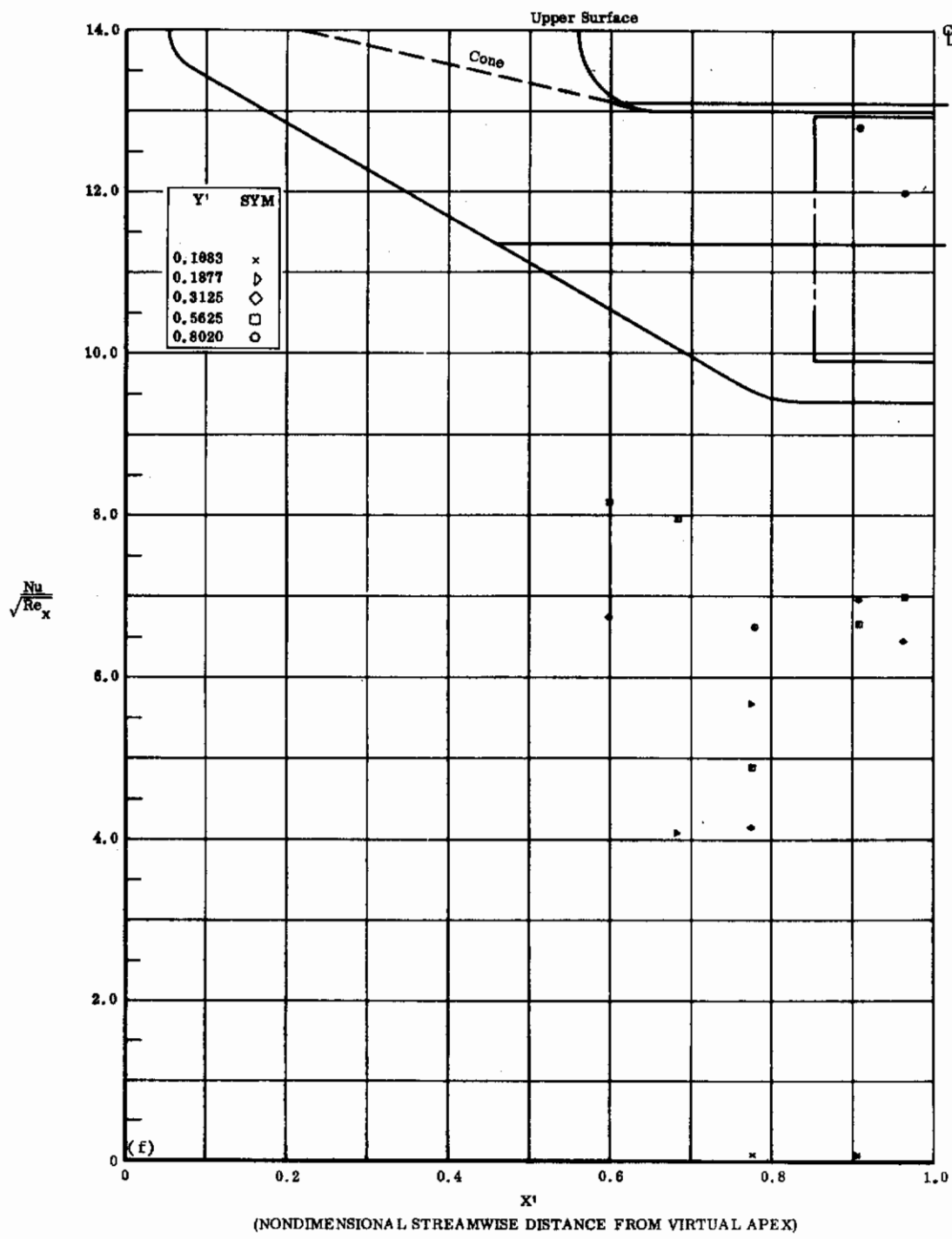


Fig. 27f Configuration IV, $\alpha = -40$, $b_2 = b_3 = 0$

$Nu/\sqrt{Re_x}$ vs. X^1 upper surface

Contrails

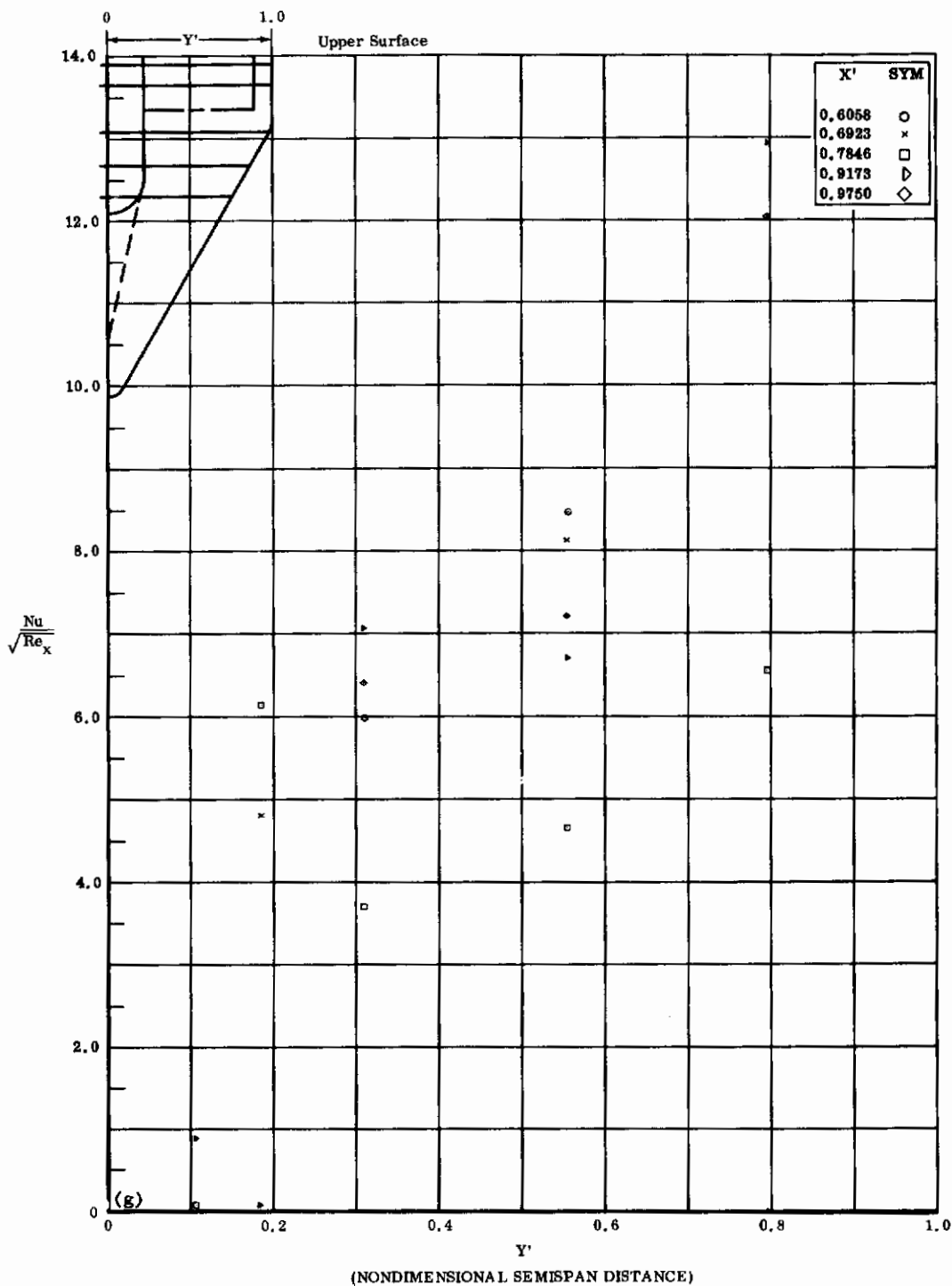


Fig. 27g Configuration IV, $\alpha = -40$, $\delta_2 = \delta_3 = +39$
 $\text{Nu}/\sqrt{\text{Re}_x}$ vs. Y' upper surface

Contrails

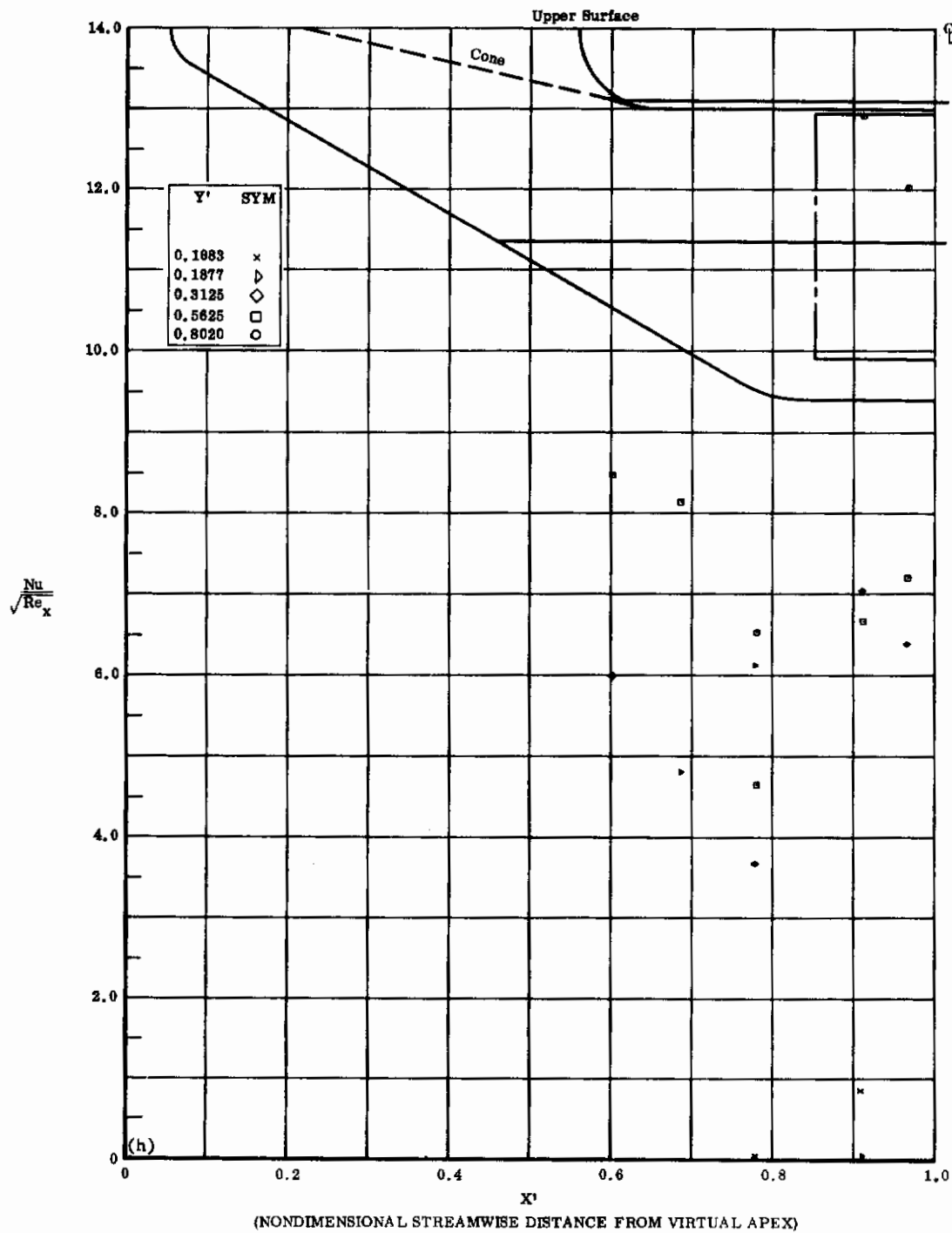


Fig. 27h Configuration IV, $\alpha = -40$, $\delta_2 = \delta_3 = +39$
 $Nu/\sqrt{Re_x}$ vs. X' upper surface

Contrails

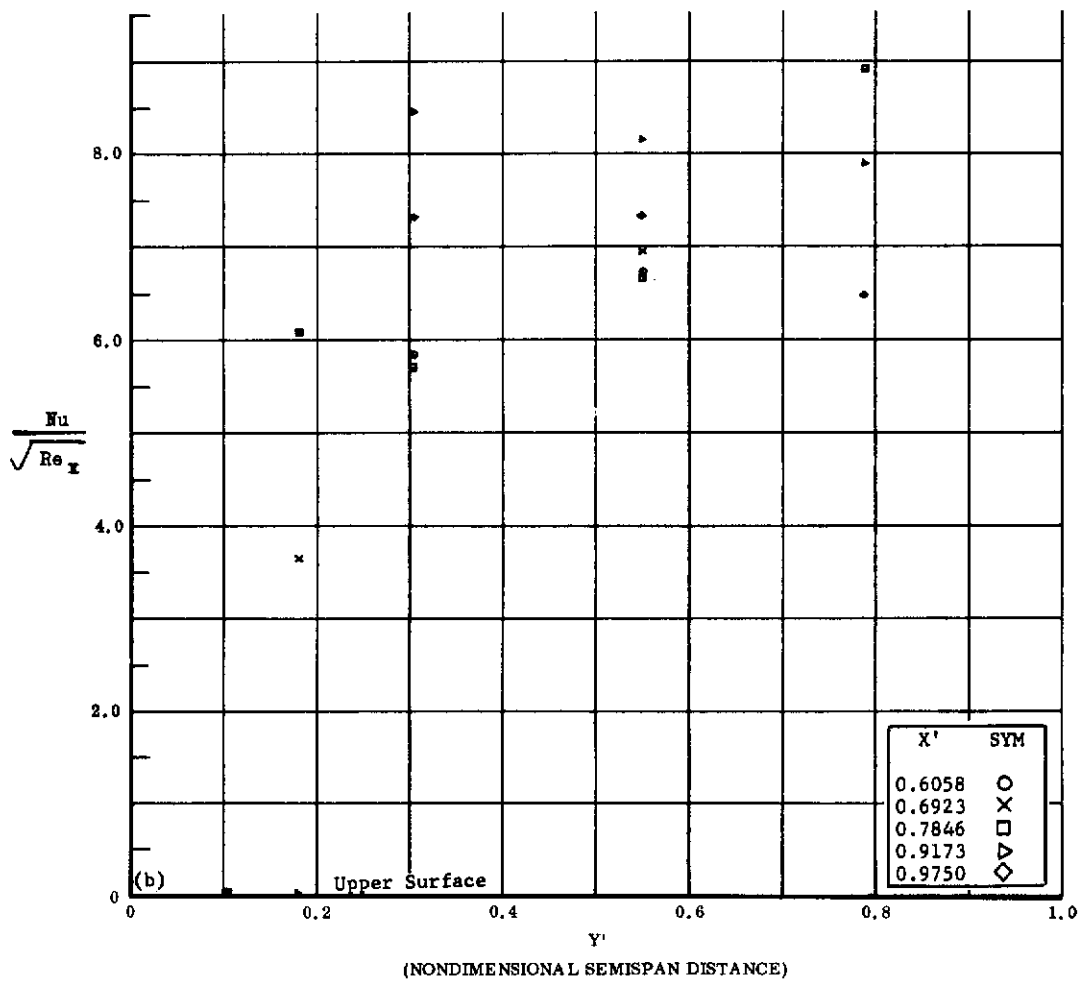
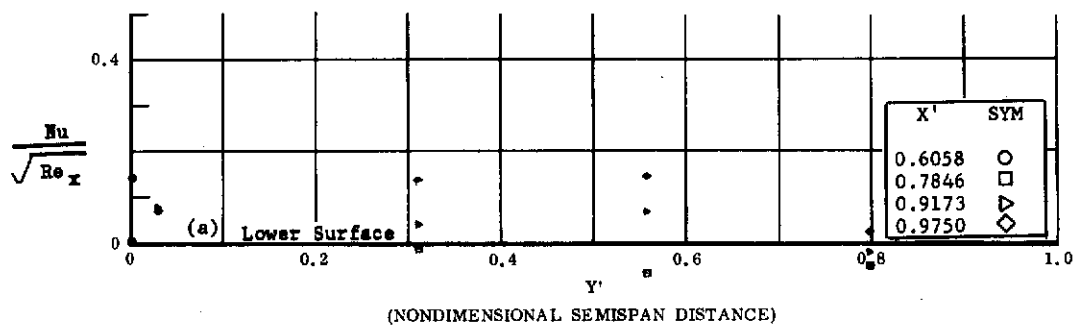


Fig. 28 Configuration IV, $\alpha = -50$, $\delta_2 = \delta_3 = 0$

a) $Nu/\sqrt{Re_x}$ vs. Y' lower surface

b) $Nu/\sqrt{Re_x}$ vs. Y' upper surface

Controls

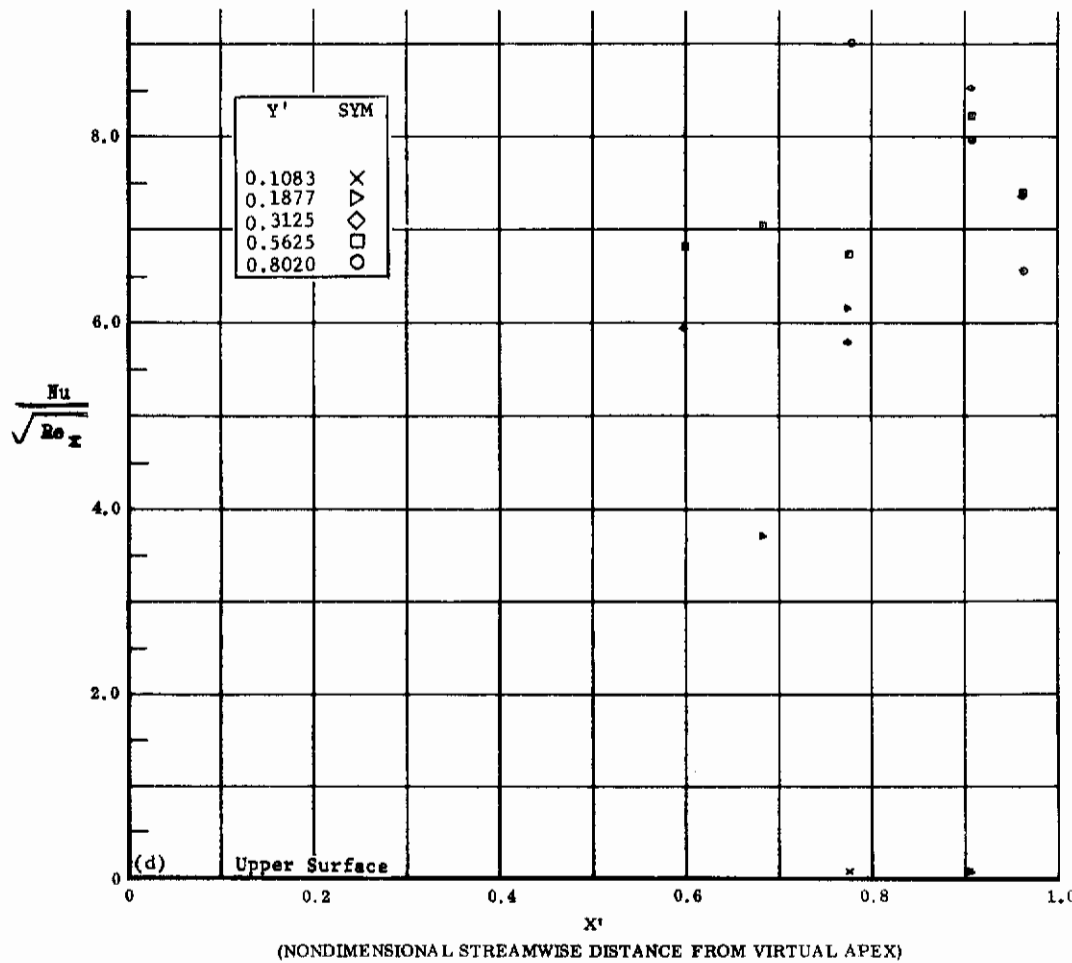
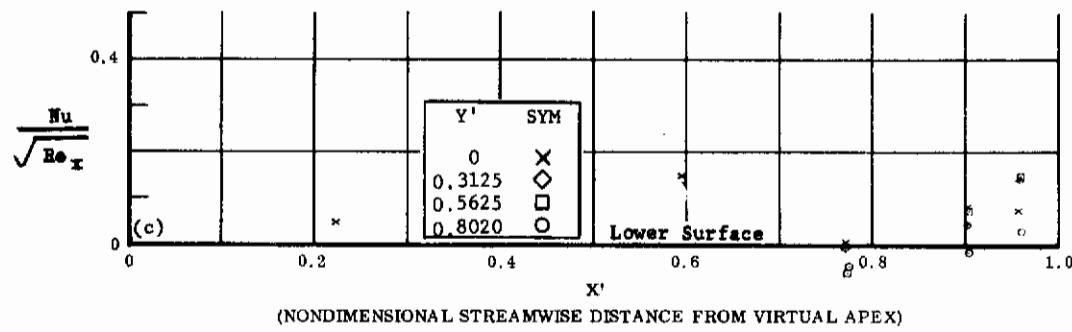


Fig. 28 Configuration IV, $\alpha = -50$, $s_2 = s_3 = 0$

c) $Nu/\sqrt{Re_x}$ vs. X' lower surface

d) $Nu/\sqrt{Re_x}$ vs. X' upper surface

Contrails

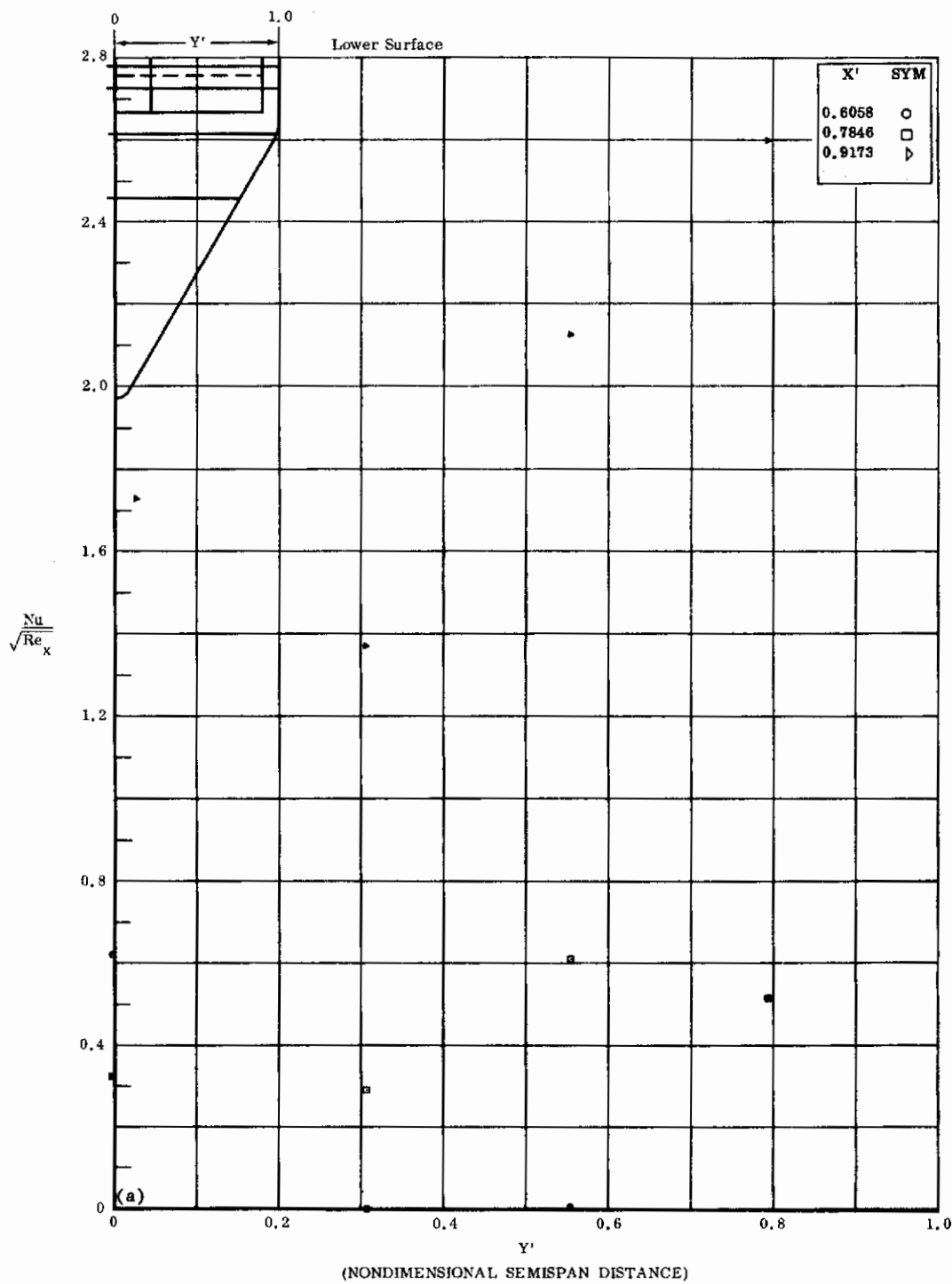


Fig. 29a Configuration VII, $\alpha = 0$, Spoiler on

$Nu/\sqrt{Re_x}$ vs. Y^i , lower surface, $Re_\infty/\text{ft} \times 10^{-6} = 3.3$

Contrails

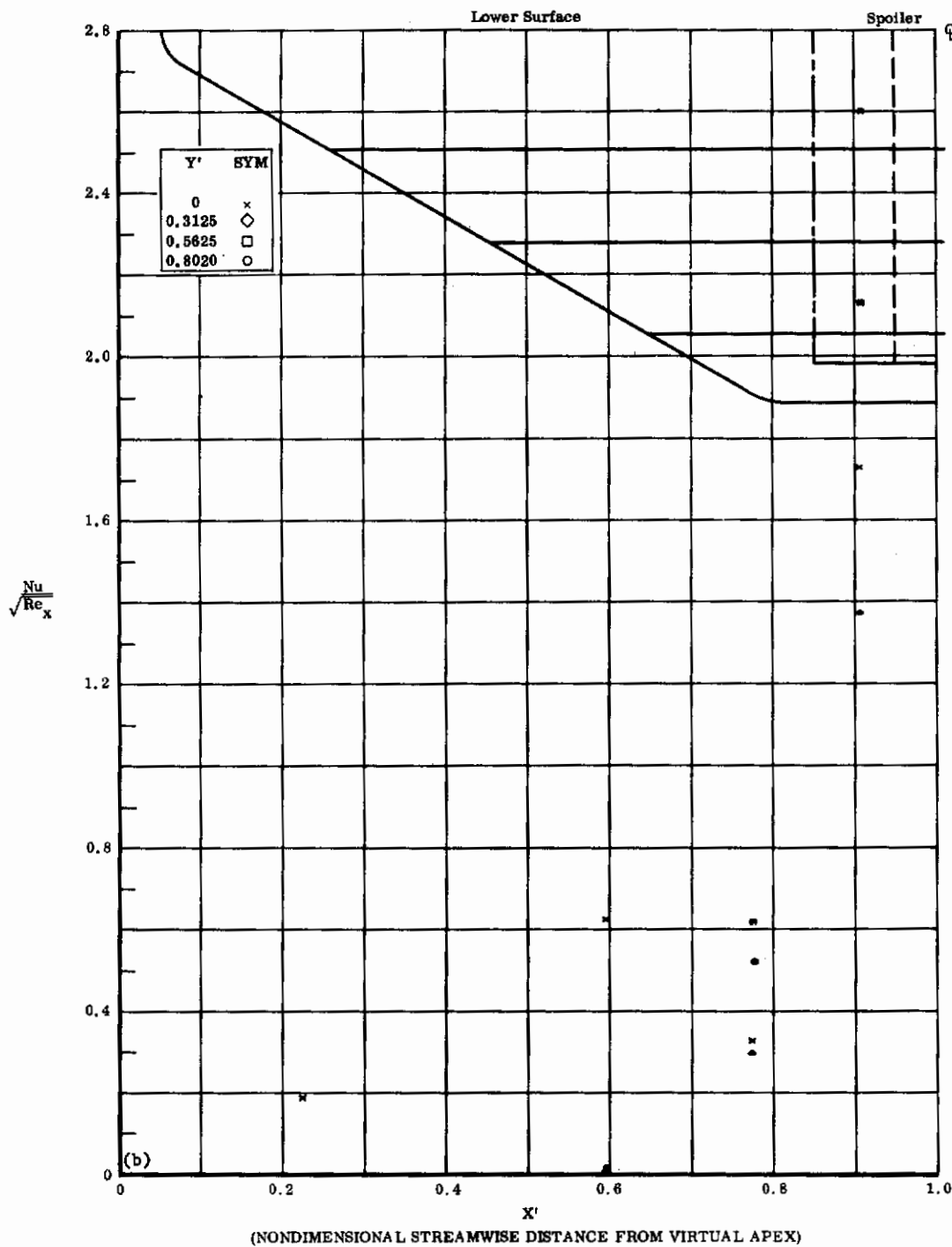


Fig. 29b Configuration VII, $\alpha = 0$, Spoiler on

$Nu/\sqrt{Re_x}$ vs. X' , lower surface, $Re_\infty/\text{ft} \times 10^{-6} = 3.3$

Contrails

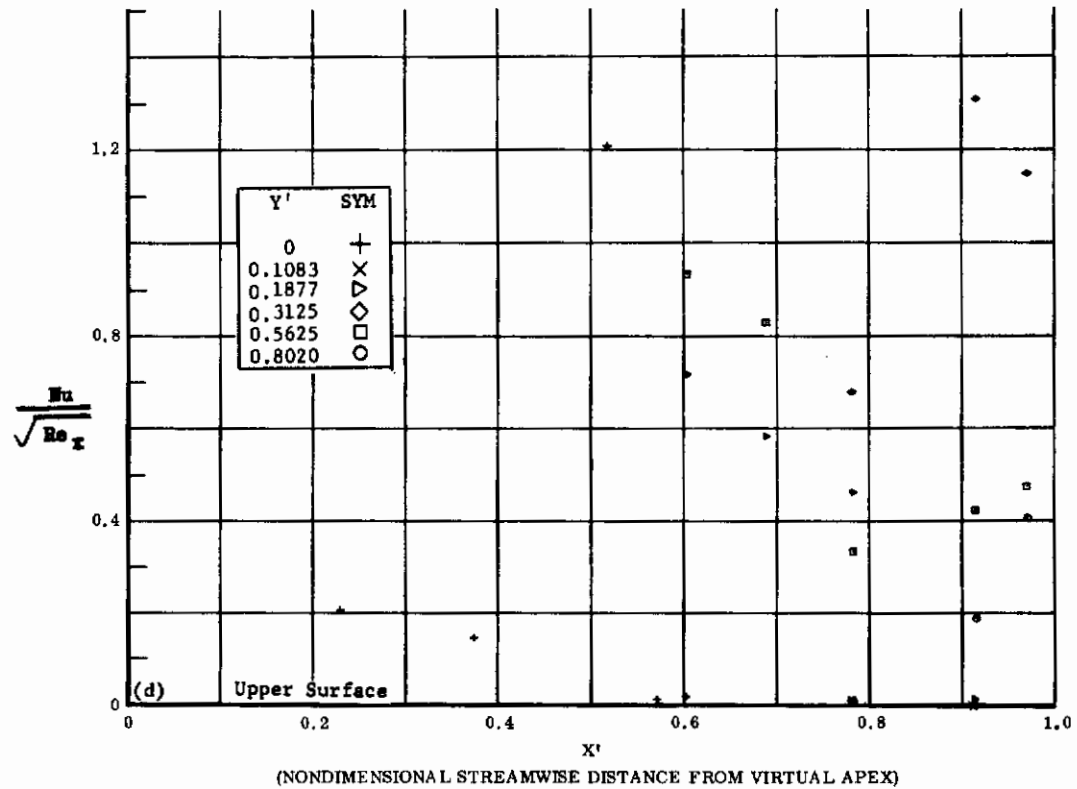
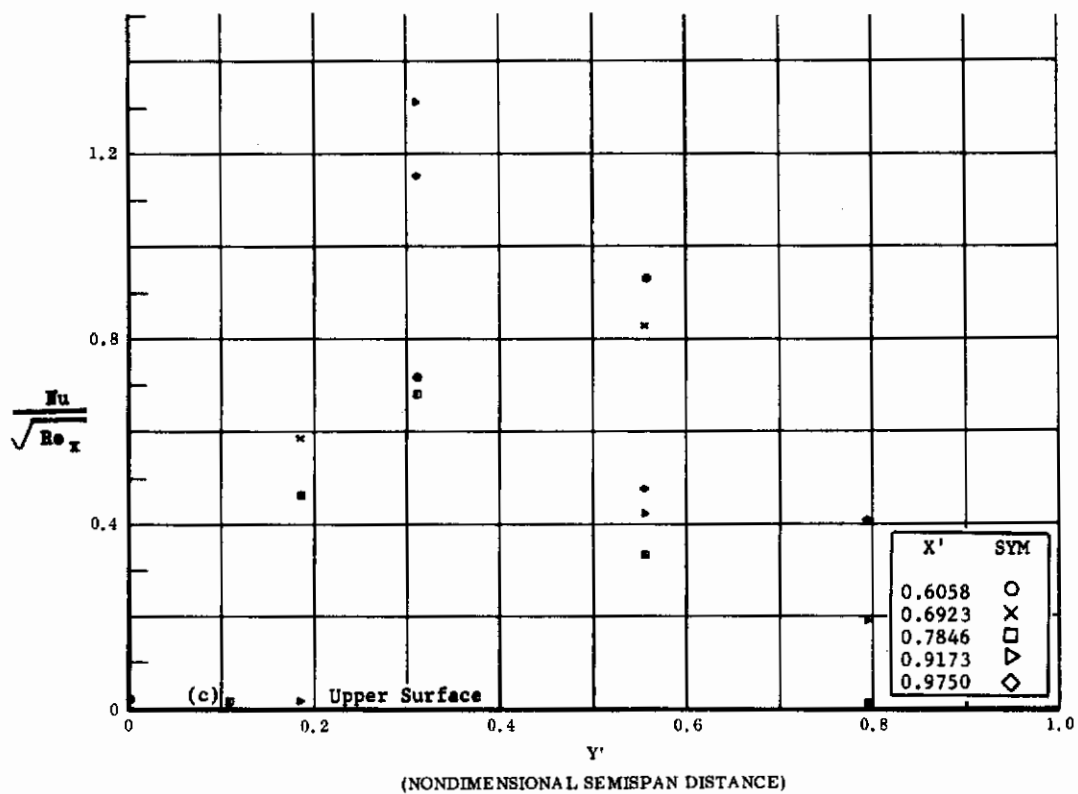


Fig. 29 Configuration VII, $\alpha = 0$, Spoiler on

c) $\text{Nu}/\sqrt{\text{Re}_x}$ vs. Y' , upper surface, $\text{Re}_{\infty}/\text{ft} \times 10^{-6} = 3,3$

d) $\text{Nu}/\sqrt{\text{Re}_x}$ vs. X' , upper surface, $\text{Re}_{\infty}/\text{ft} \times 10^{-6} = 3,3$

Contrails

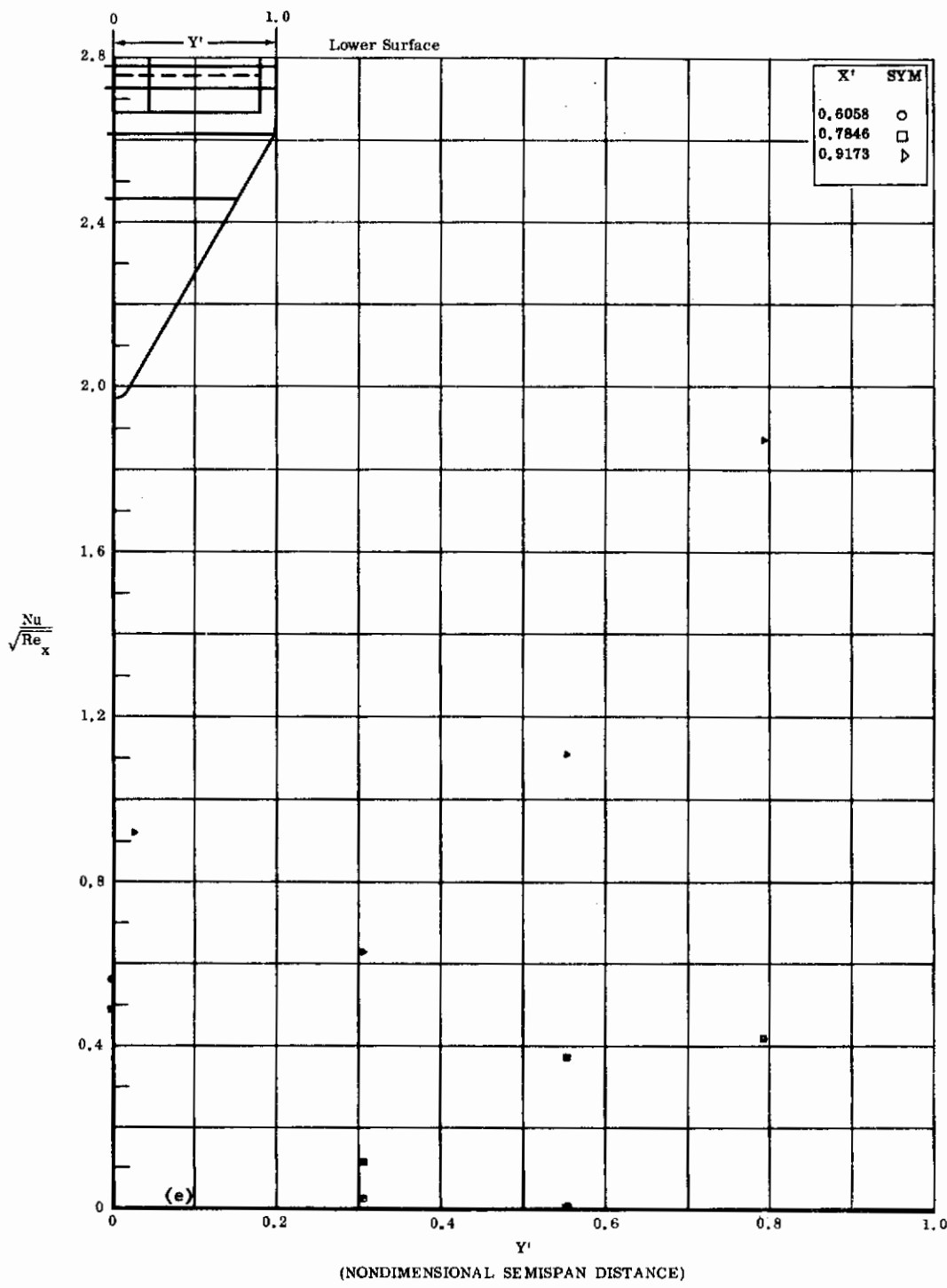


Fig. 29e Configuration VII, $\alpha = 0$, Spoiler on

$Nu/\sqrt{Re_x}$ vs. Y' , lower surface, $Re_\infty/\text{ft} \times 10^{-6} = 1.1$

Contrails

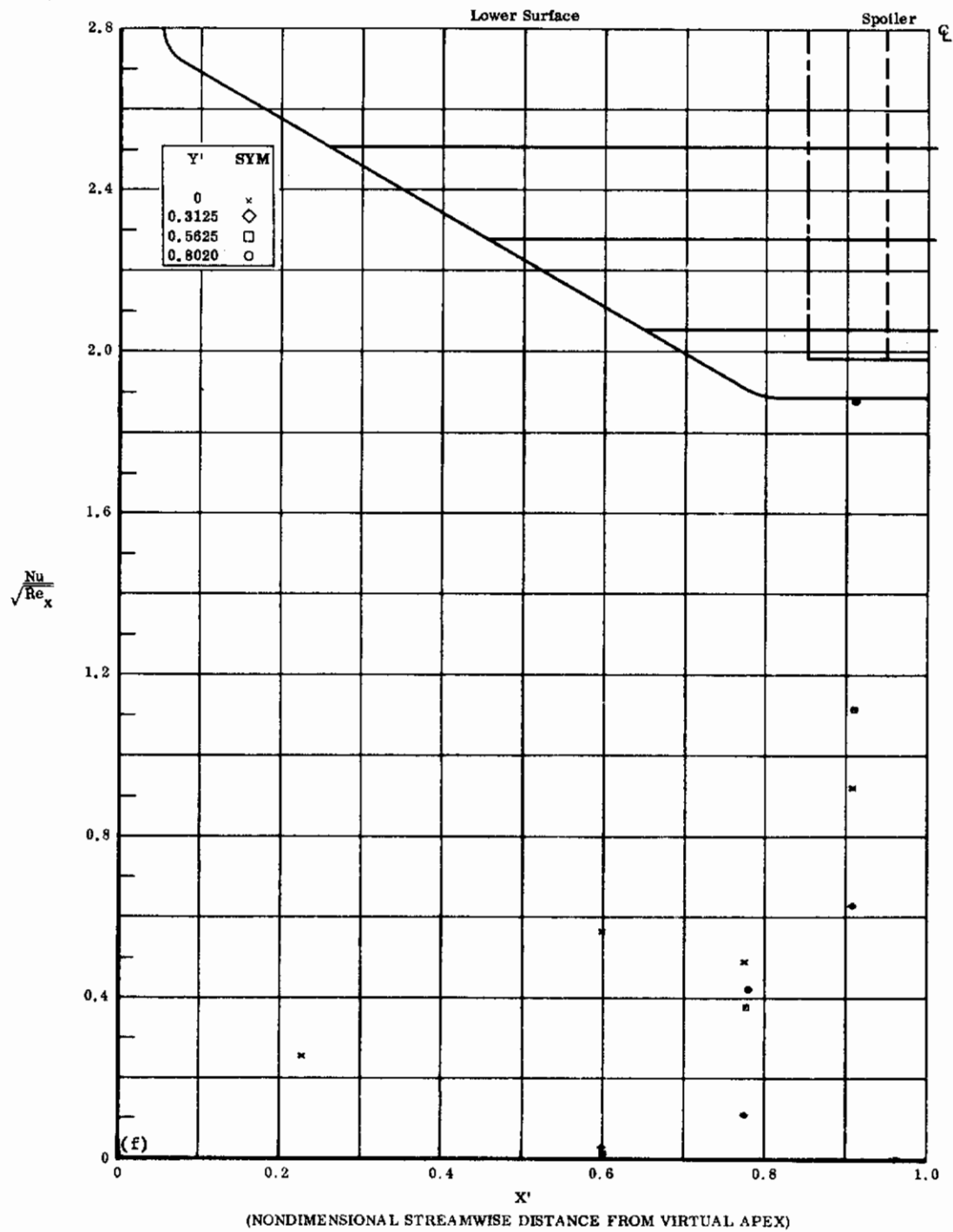


Fig. 29f Configuration VII, $\alpha = 0$, Spoiler on

$\text{Nu}/\sqrt{\text{Re}_x}$ vs. X' , lower surface, $\text{Re}_m/\text{ft} \times 10^{-6} = 1.1$

Contrails

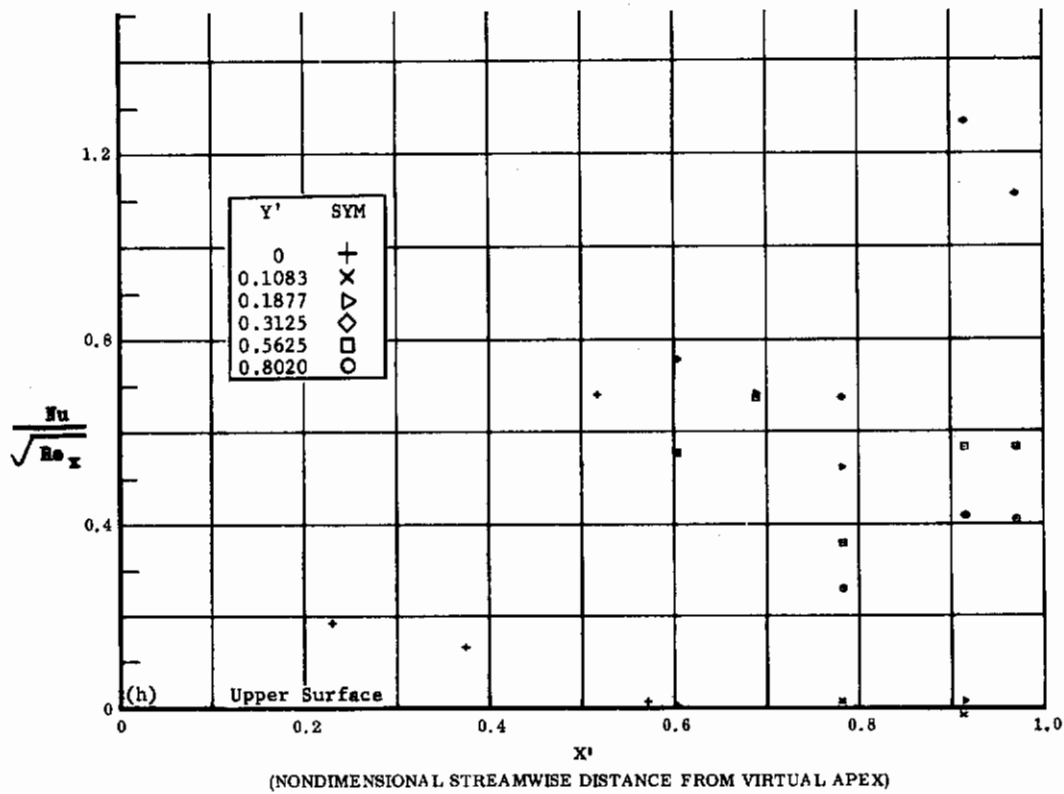
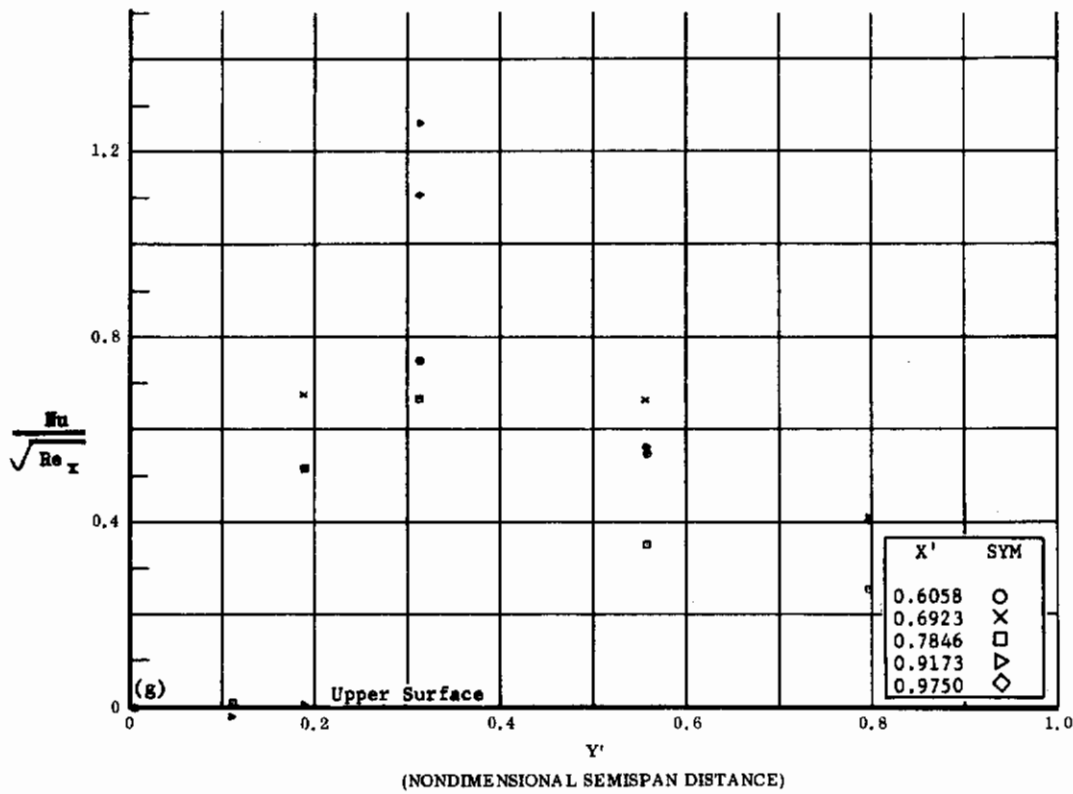


Fig. 29 Configuration VII, $\alpha = 0$, Spoiler on

g) $Nu/\sqrt{Re_x}$ vs. Y' , upper surface, $Re_\infty/\text{ft} \times 10^{-6} = 1.1$

h) $Nu/\sqrt{Re_x}$ vs. X' , upper surface, $Re_\infty/\text{ft} \times 10^{-6} = 1.1$

Contrails

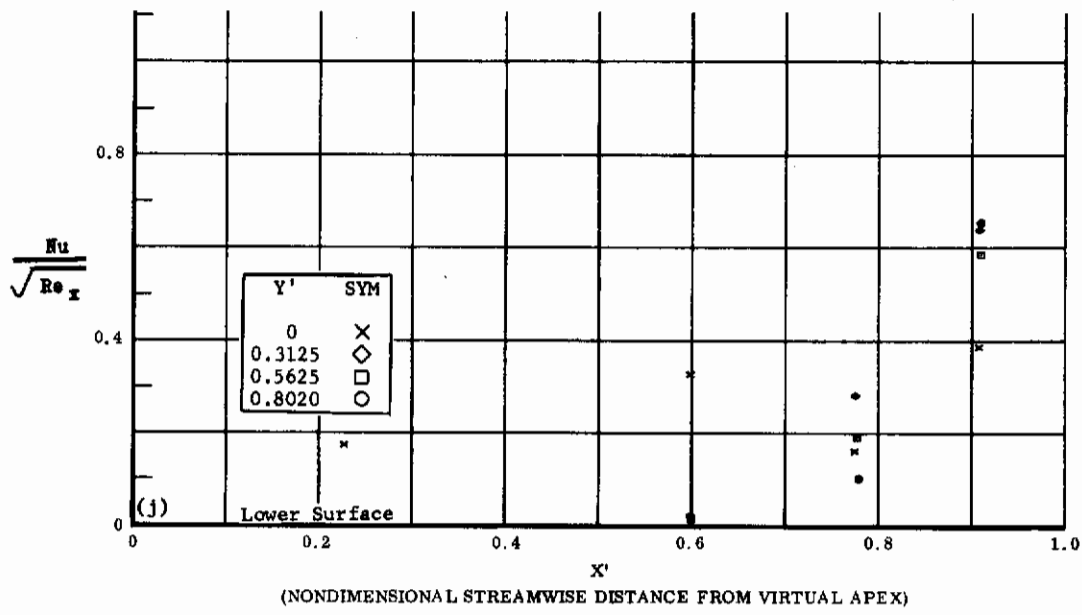
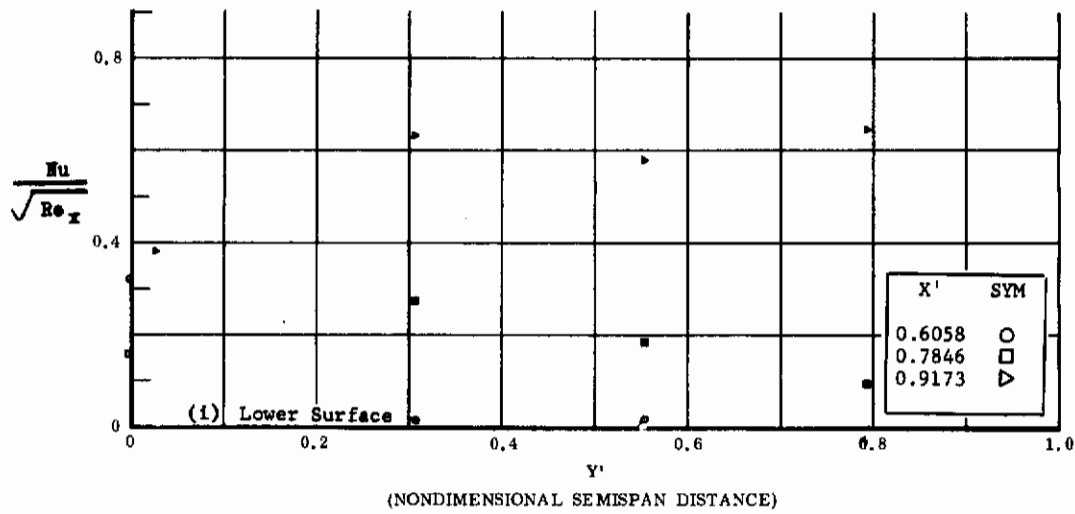


Fig. 29 Configuration VII, $\alpha = -10$, Spoiler on

- i) $Nu/\sqrt{Re_x}$ vs. Y' lower surface, $Re_\infty/\text{ft} \times 10^{-6} = 3.3$
- j) $Nu/\sqrt{Re_x}$ vs. X' lower surface, $Re_\infty/\text{ft} \times 10^{-6} = 3.3$

Contrails

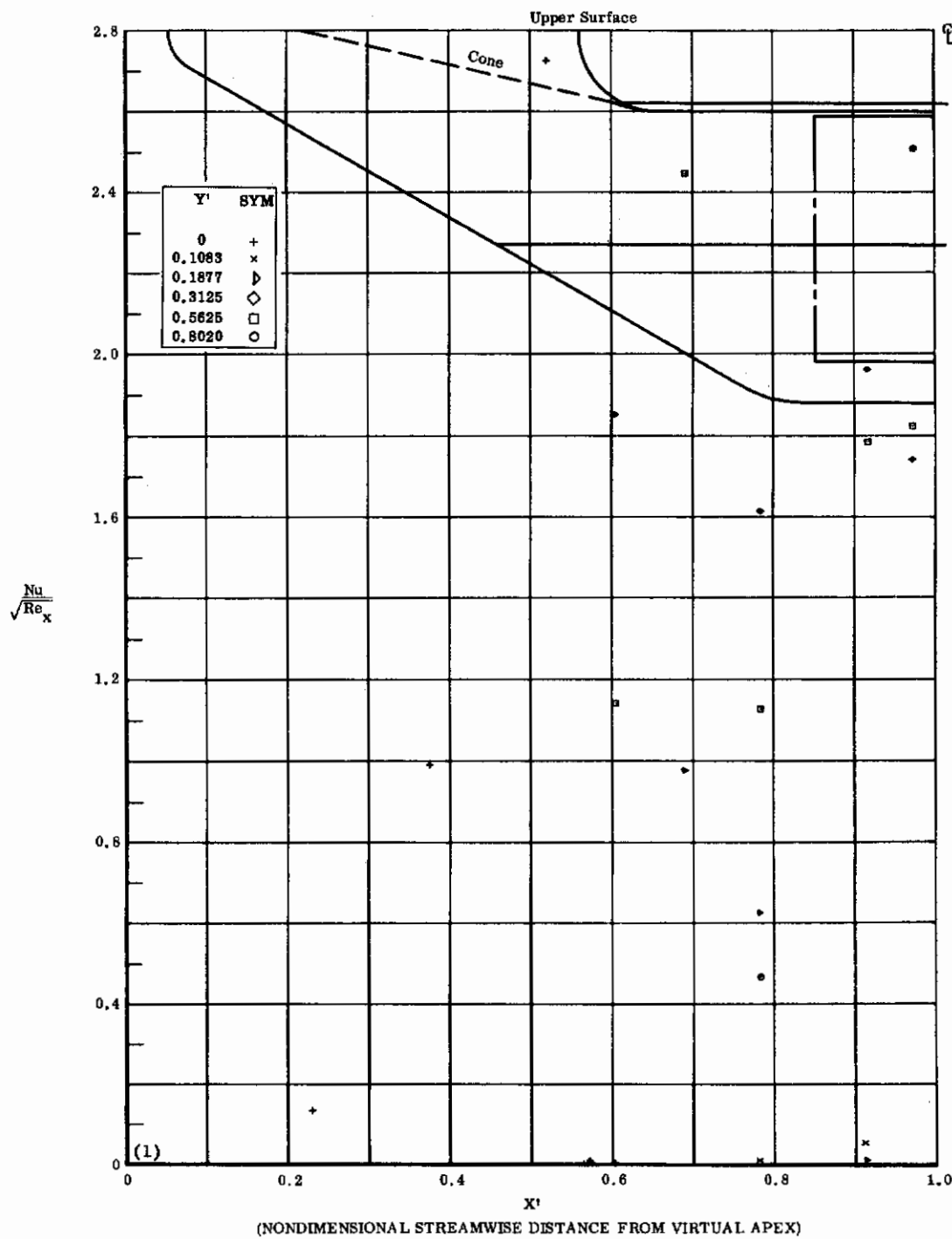


Fig. 29k Configuration VII, $\alpha = -10$, Spoiler on
 $Nu/\sqrt{Re_x}$ vs. Y' upper surface, $Re_\infty/\text{ft} \times 10^{-6} = 3.3$

Contrails

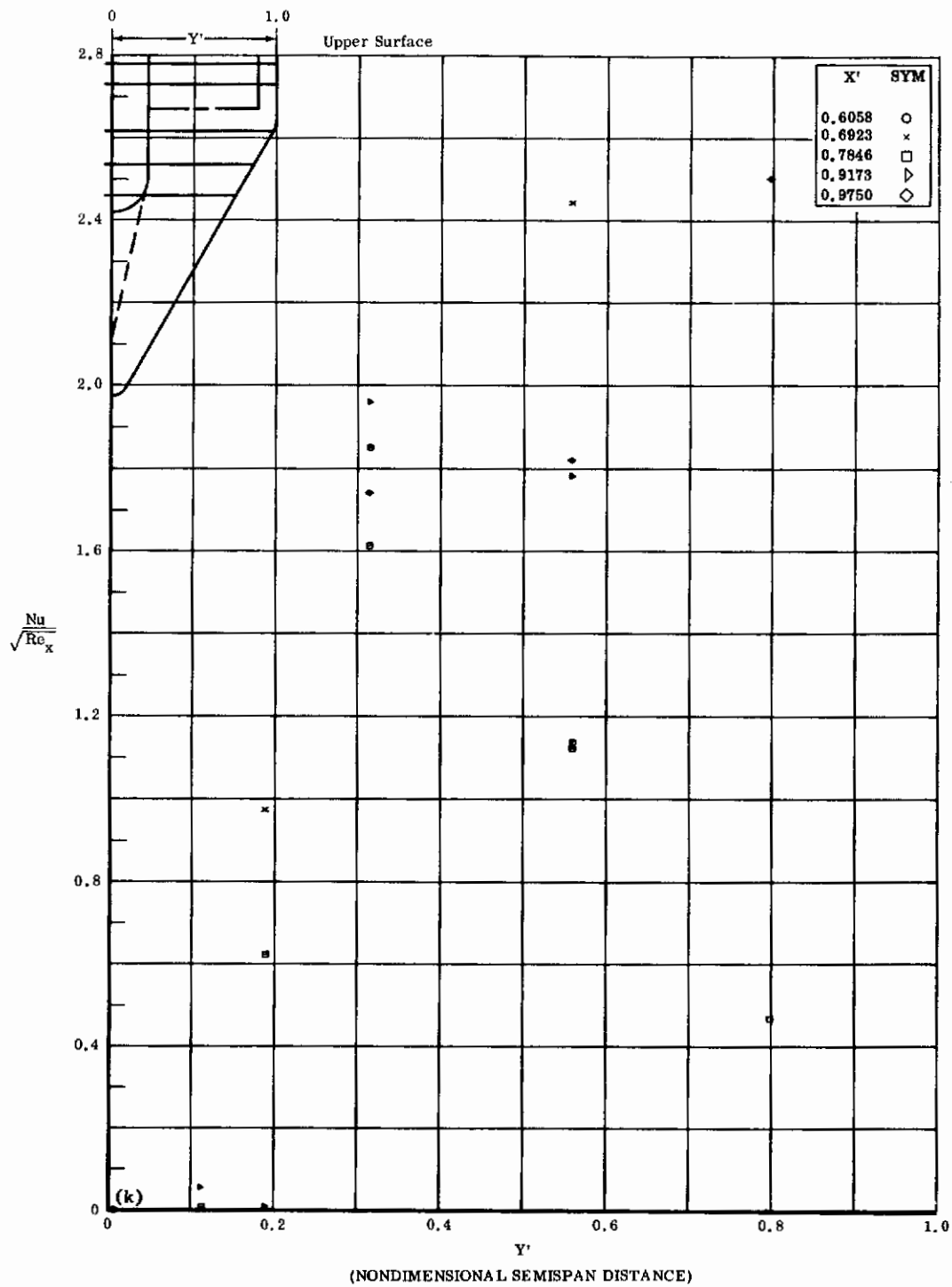


Fig. 29*f* Configuration VII, $\alpha = -10$, Spoiler on
 $Nu/\sqrt{Re_x}$ vs. X' upper surface, $Re_\infty/\text{ft} \times 10^{-6} = 3.3$

Controls

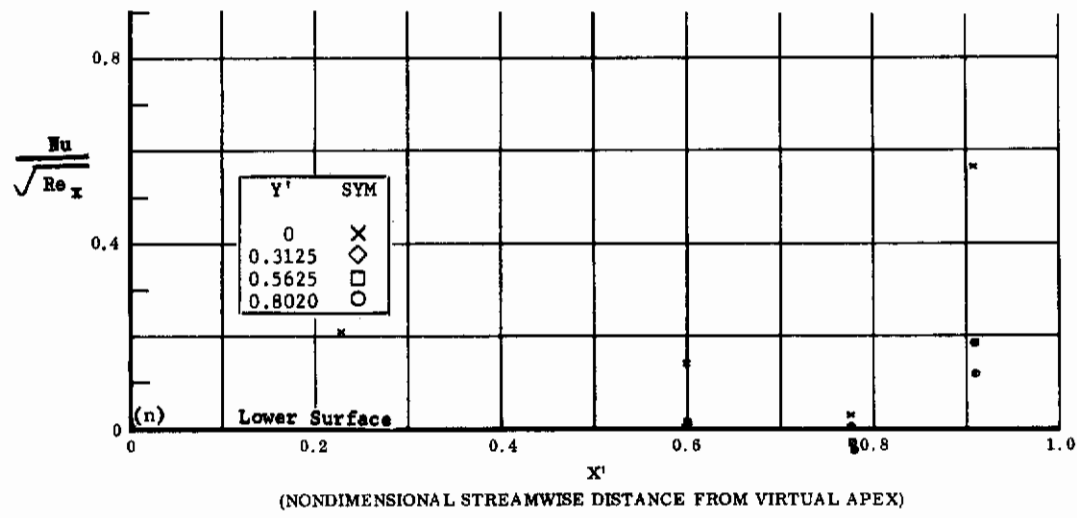
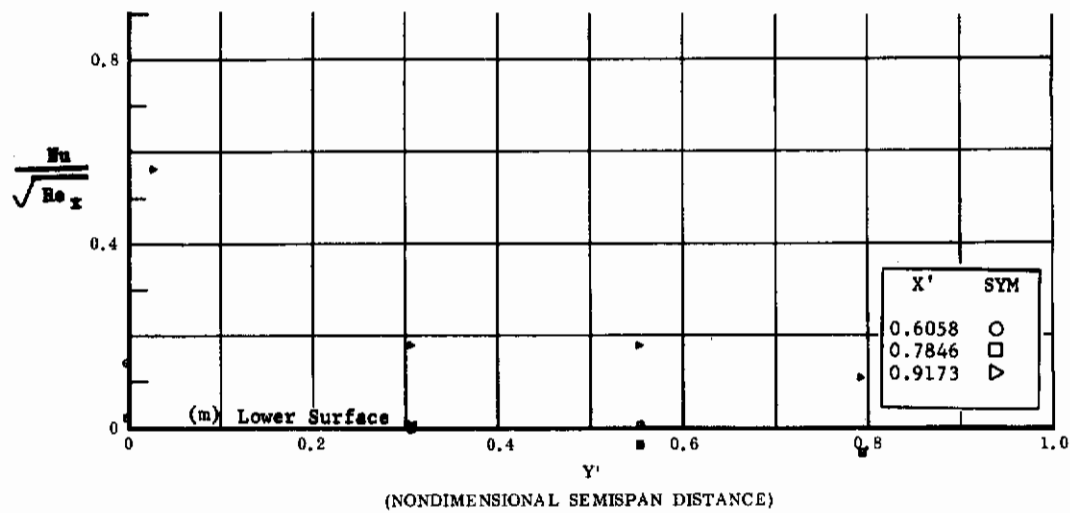


Fig. 29 Configuration VII, $\alpha = -20$, Spoiler on

- m) $\text{Nu}/\sqrt{\text{Re}_x}$ vs. Y' lower surface, $\text{Re}_{\infty}/\text{ft} \times 10^{-6} = 3.3$
- n) $\text{Nu}/\sqrt{\text{Re}_x}$ vs. X' lower surface, $\text{Re}_{\infty}/\text{ft} \times 10^{-6} = 3.3$

Contrails

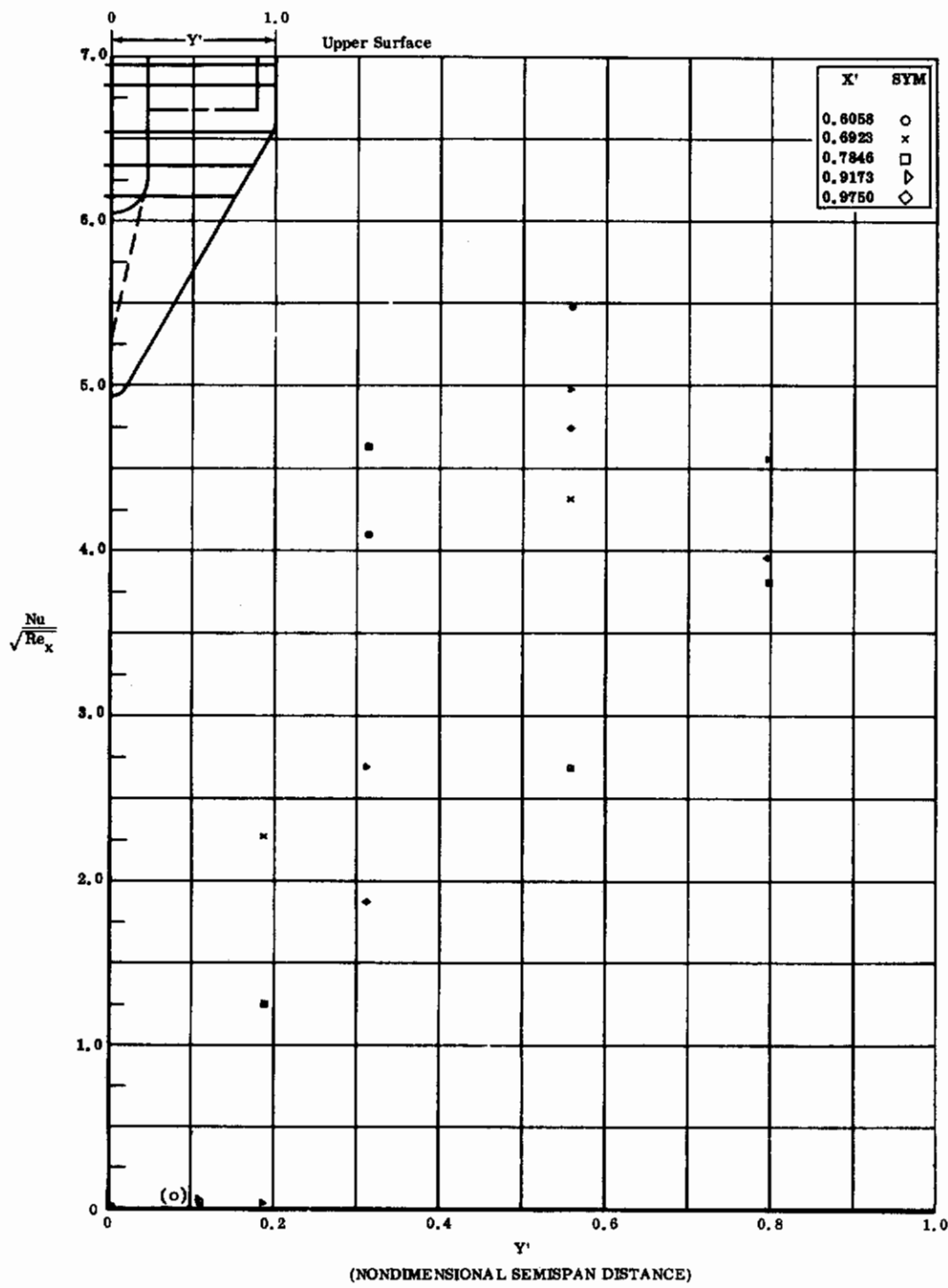


Fig. 29o Configuration VII, $\alpha = -20$, Spoiler on

$Nu/\sqrt{Re_x}$ vs. Y' upper surface, $Re_\infty/\text{ft} \times 10^{-6} = 3.3$

Contrails

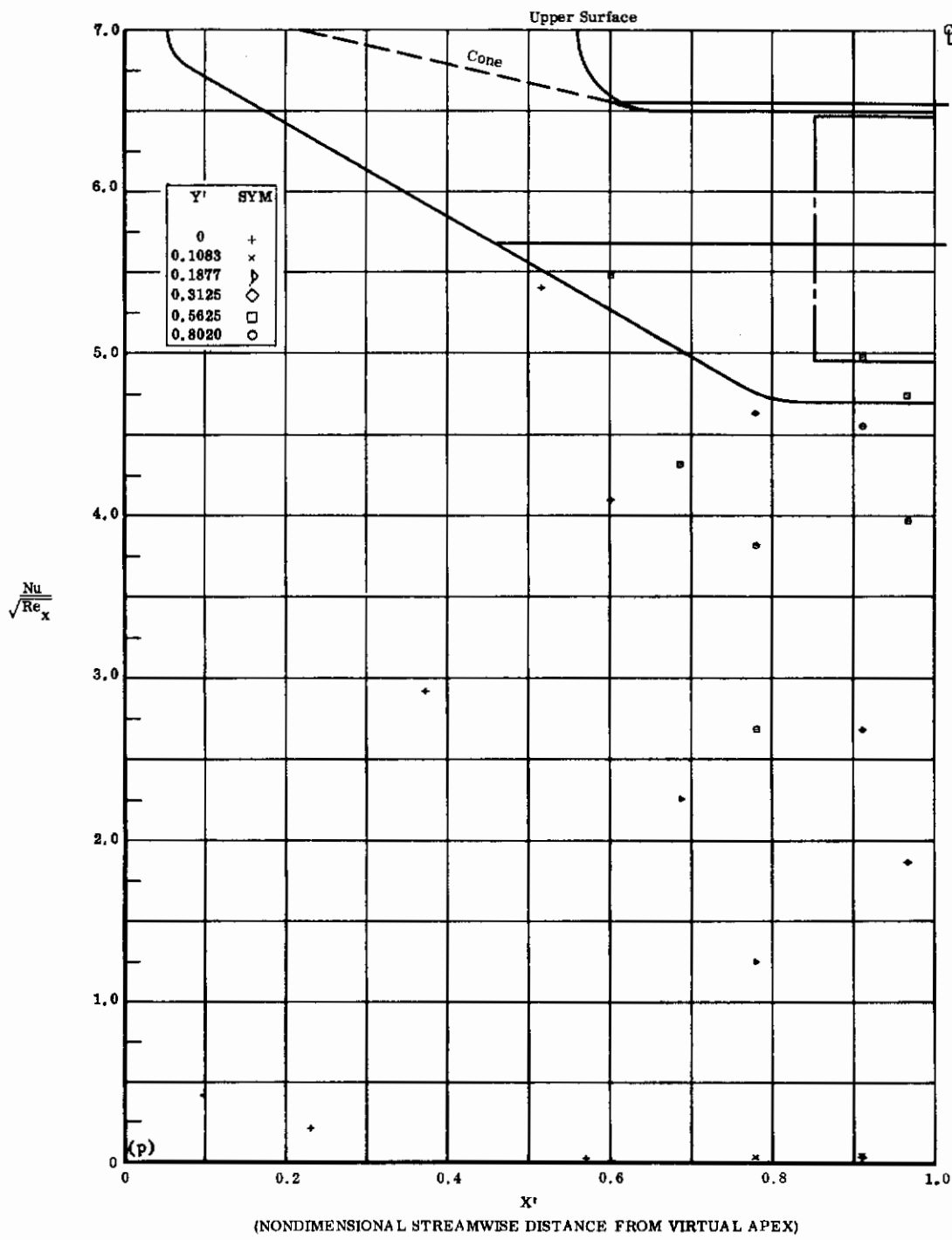


Fig. 29p Configuration VII, $\alpha = -20$, Spoiler on

$\text{Nu}/\sqrt{\text{Re}_x}$ vs. X' upper surface, $\text{Re}_{\infty}/\text{ft} \times 10^{-6} = 3.3$

Contrails

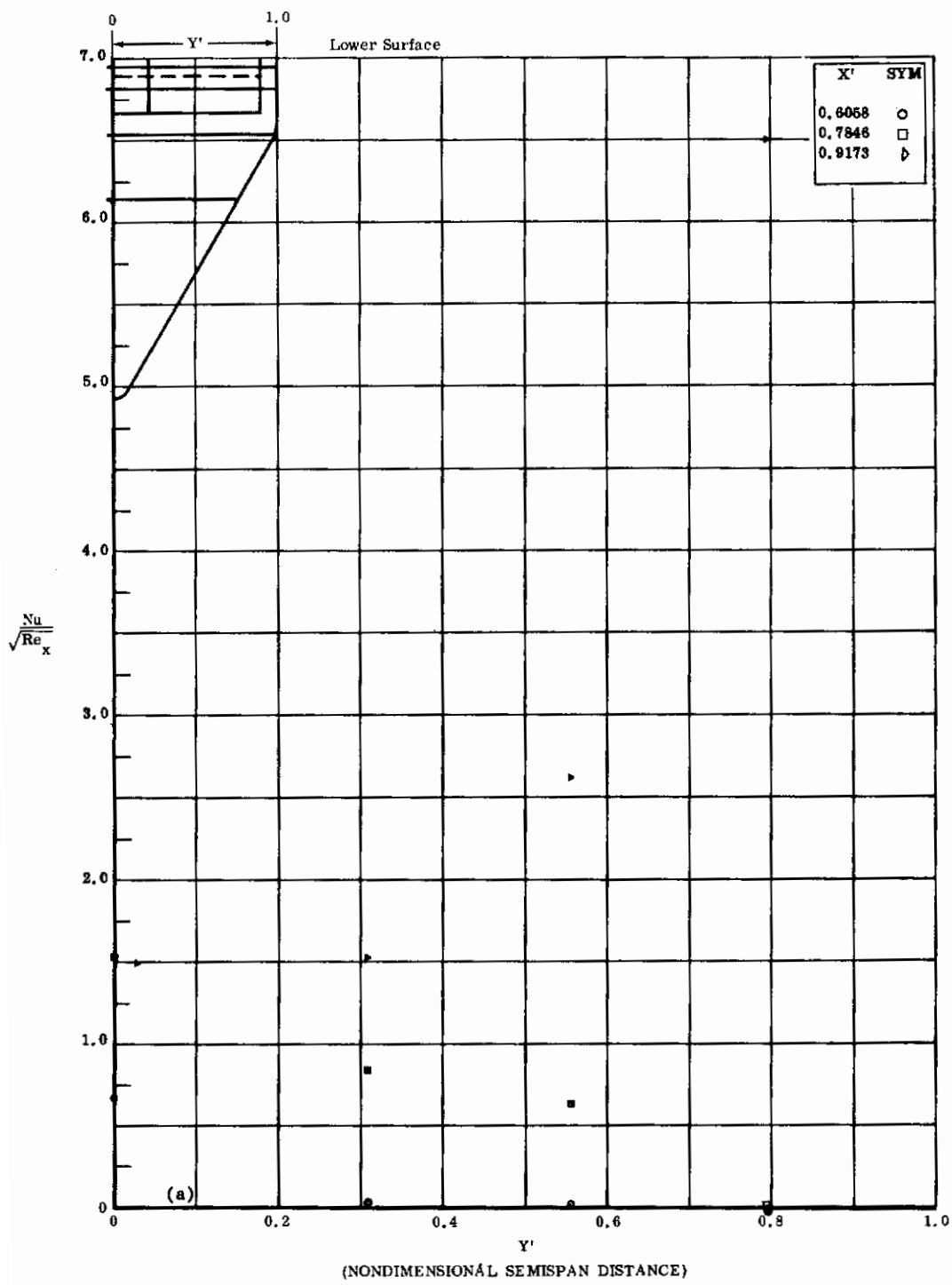


Fig. 30a Configuration VIII, $\alpha = 0$, Spoiler on, Fins on
 $Nu/\sqrt{Re_x}$ vs. Y' , lower surface, $Re_\infty/\text{ft} \times 10^{-6} = 3.3$

Contrails

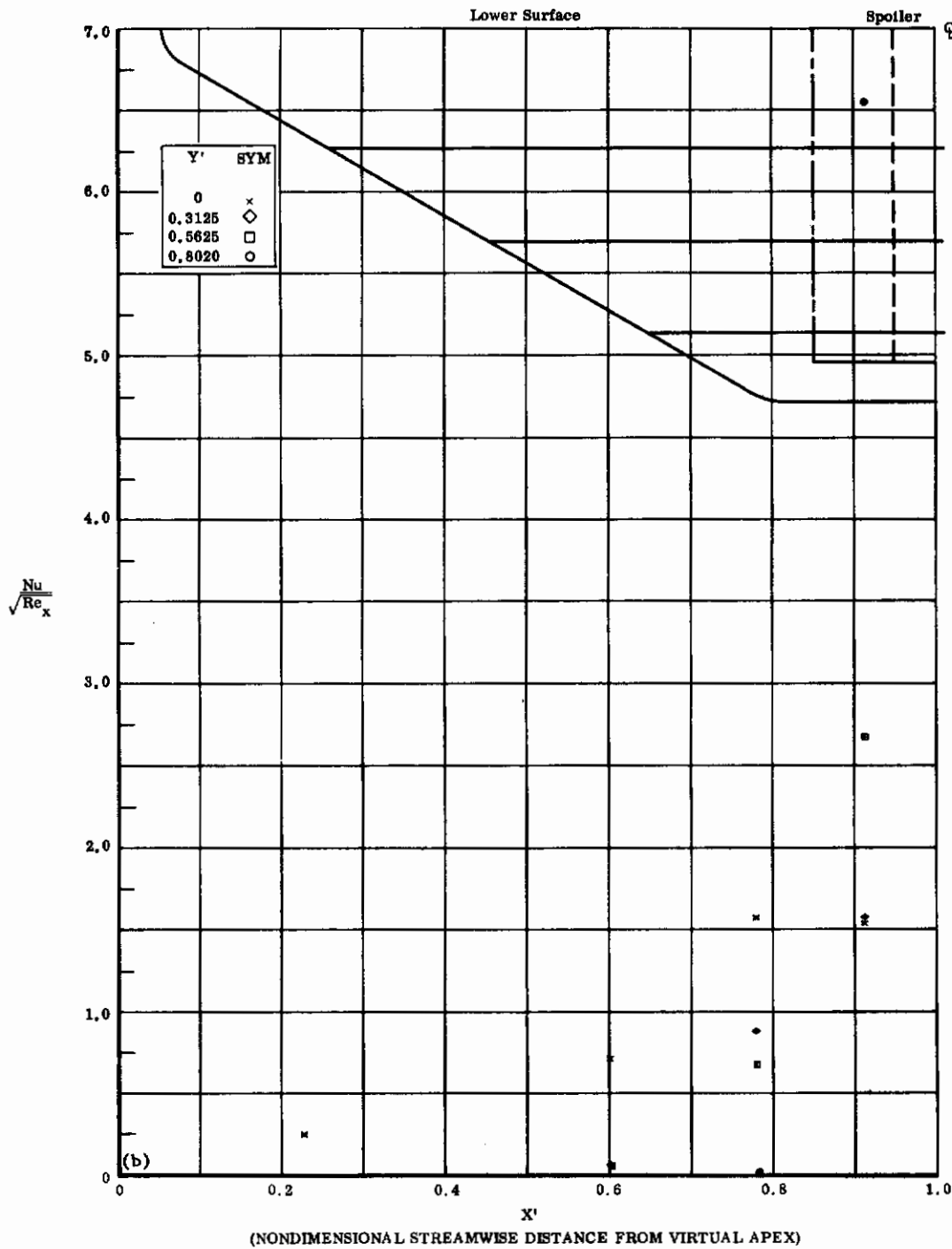


Fig. 30b Configuration VIII, $\alpha = 0$, Spoiler on, Fins on
 $Nu/\sqrt{Re_x}$ vs. X' , lower surface, $Re_\infty/\text{ft} \times 10^{-6} = 3.3$

Contrails

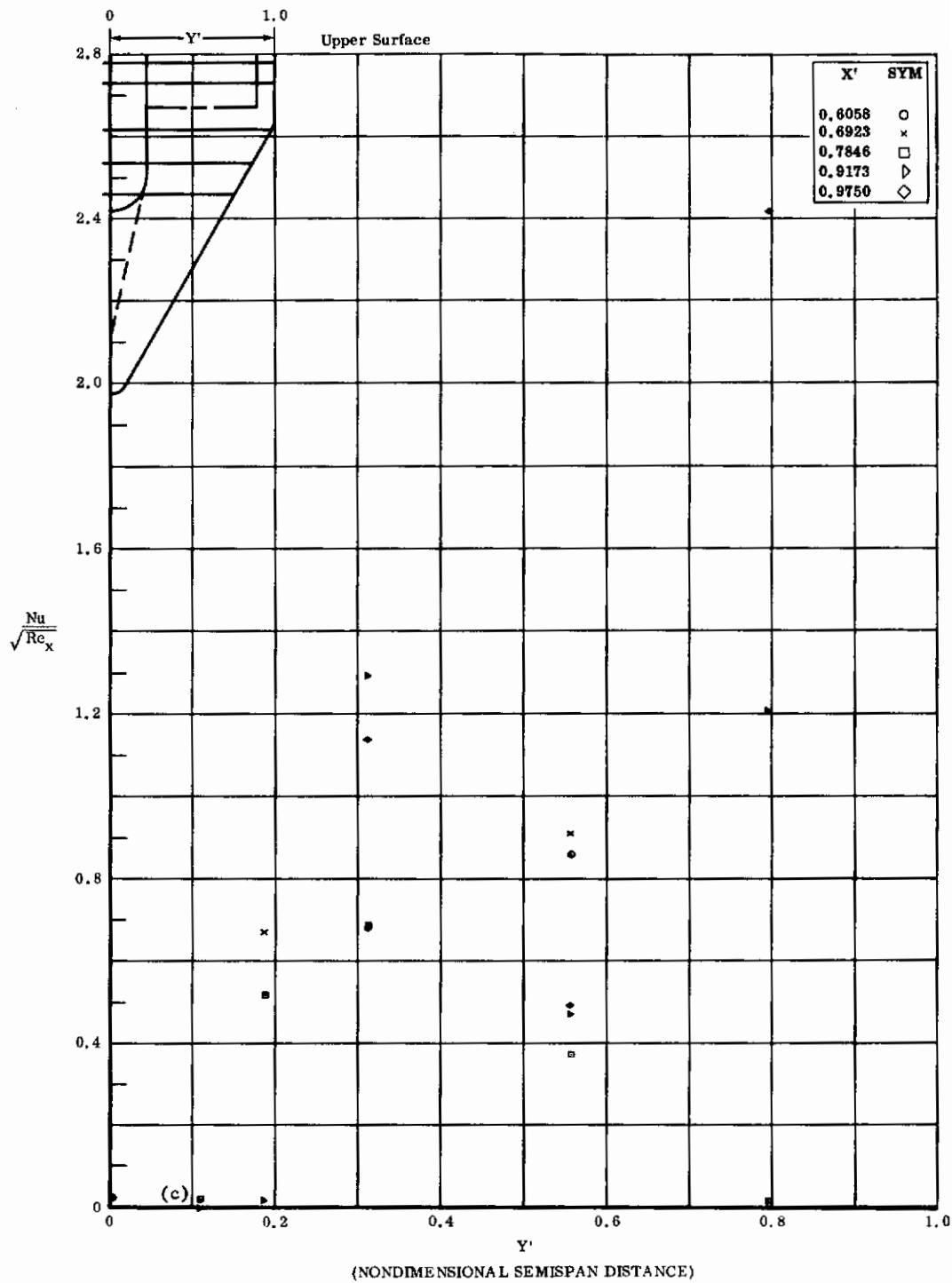


Fig. 30c Configuration VIII, $\alpha = 0$, Spoiler on, Fins on
 $\text{Nu}/\sqrt{\text{Re}_x}$ vs. Y' , upper surface, $\text{Re}_{\infty}/\text{ft} \times 10^{-6} = 3.3$

Contrails

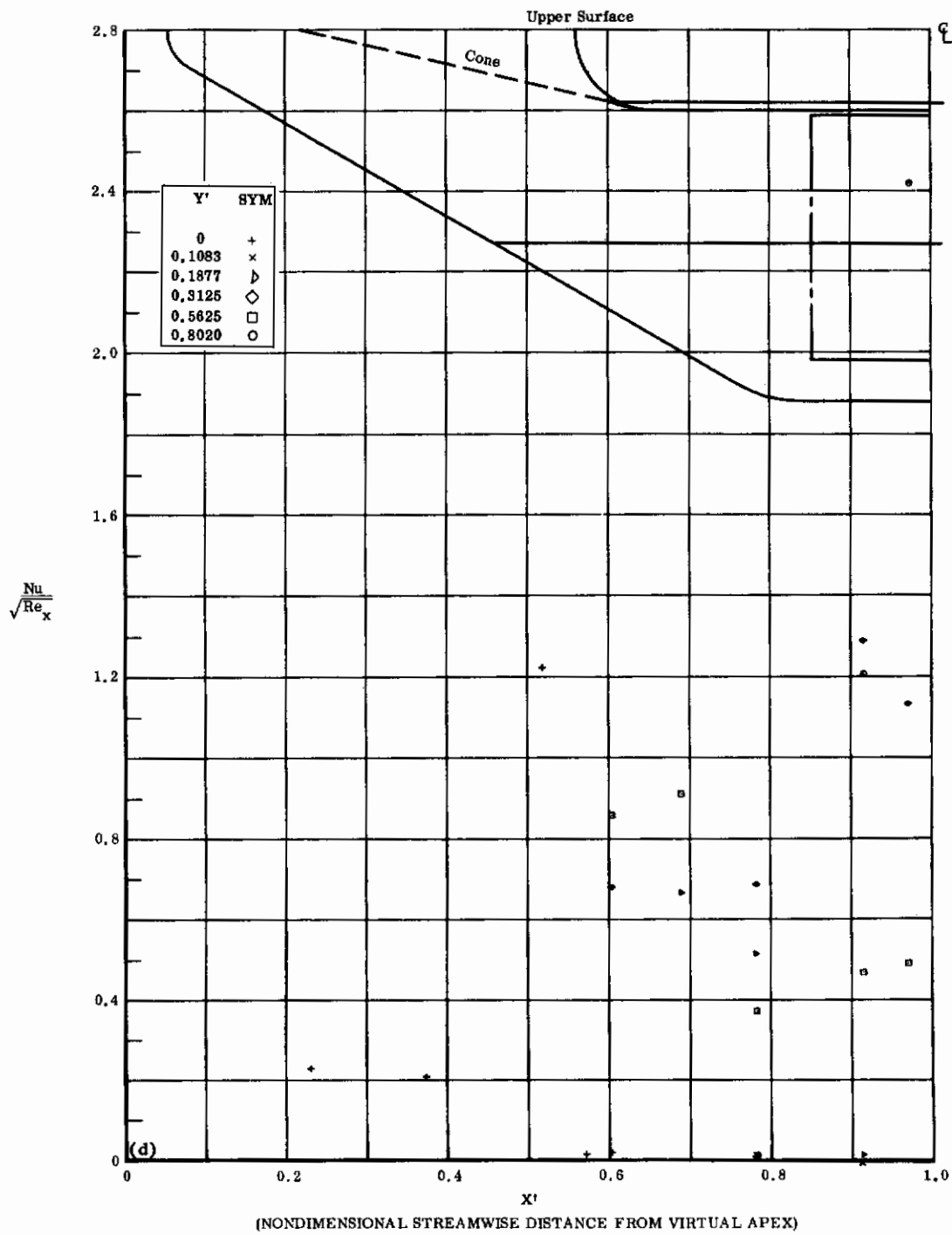


Fig. 30d Configuration VIII, $\alpha = 0$, Spoiler on, Fins on
 $Nu/\sqrt{Re_x}$ vs. X' , upper surface, $Re_\infty/\text{ft} \times 10^{-6} = 3.3$

Contrails

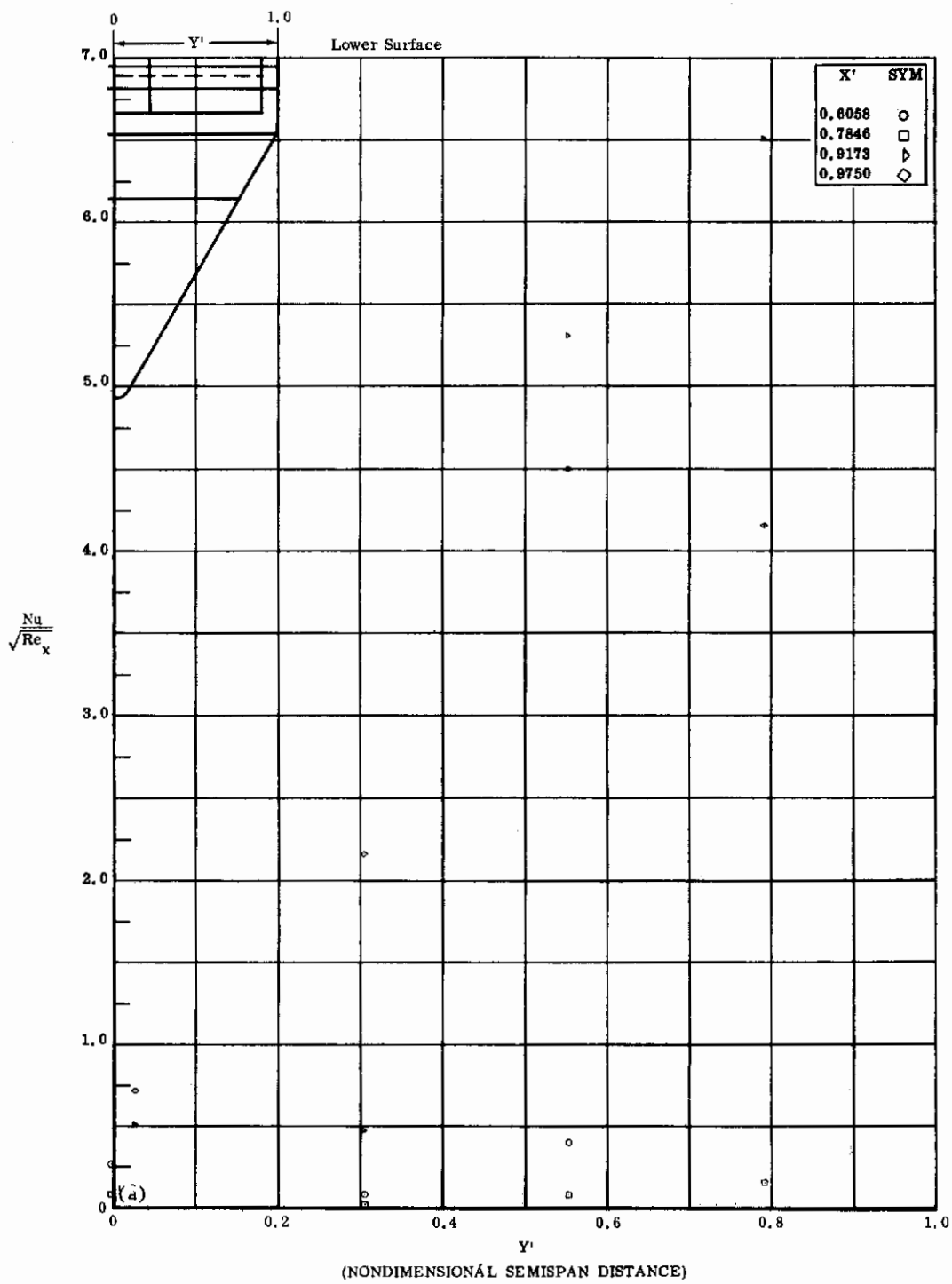


Fig. 31a Configuration IX, $\alpha = 0$, $\delta_2 = \delta_3 = +20$

$Nu/\sqrt{Re_x}$ vs. Y' lower surface $Re_\infty/ft \times 10^{-6} = 3.3$

Contrails

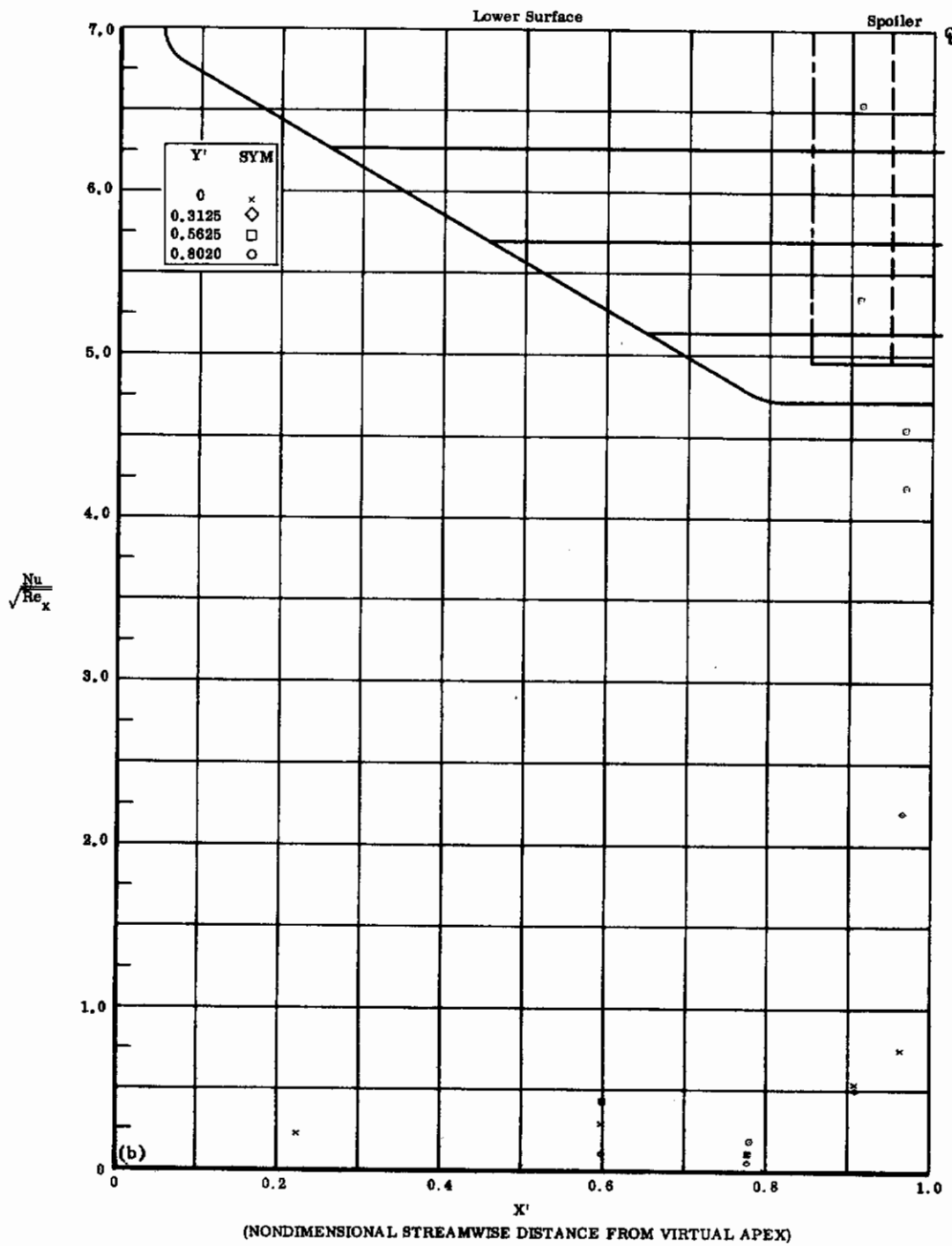


Fig. 31b Configuration IX, $\alpha = 0$, $\delta_2 = \delta_3 = +20$

$Nu/\sqrt{Re_x}$ vs. X' lower surface $Re_\infty/\text{ft} \times 10^{-6} = 3.3$

Contrails

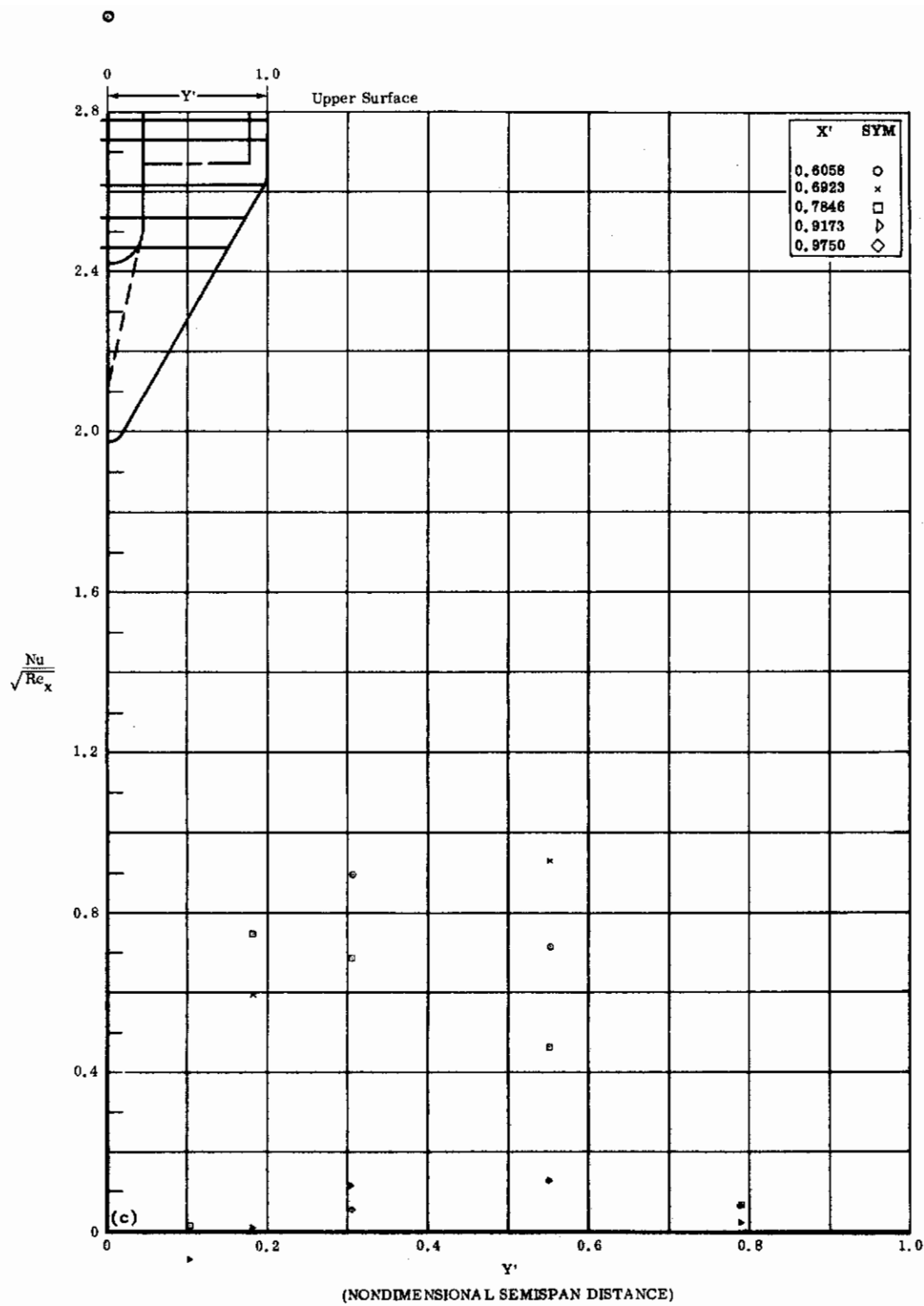


Fig. 31c Configuration IX, $\alpha = 0$, $b_2 = b_3 = +20$
 $Nu/\sqrt{Re_x}$ vs. Y' upper surface $Re_\infty/ft \times 10^{-6} = 3.3$

Contrails

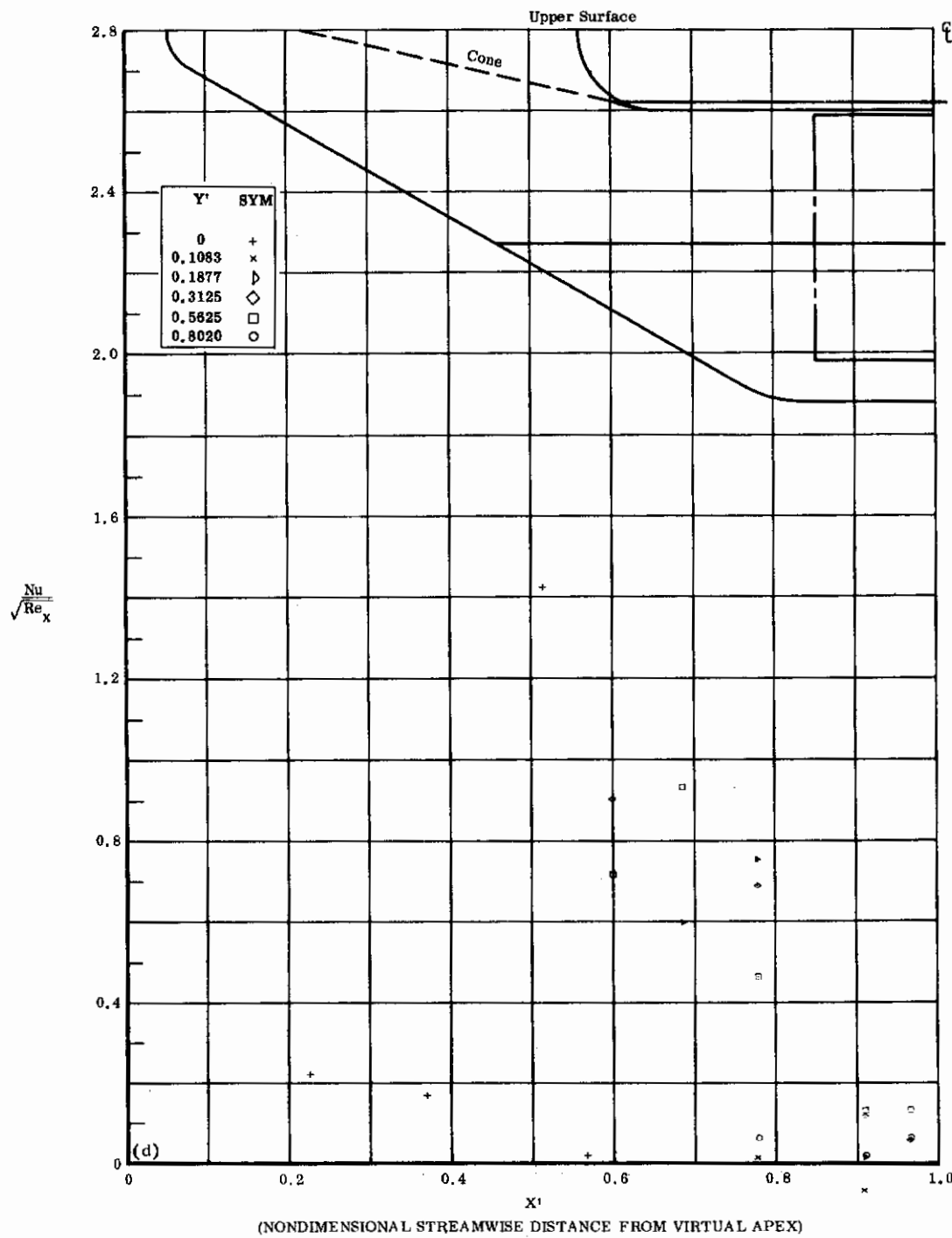


Fig. 31d Configuration IX, $\alpha = 0$, $\delta_2 = \delta_3 = +20$

$Nu/\sqrt{Re_x}$ vs. X' upper surface $Re_\infty/\text{ft} \times 10^{-6} = 3.3$

Contrails

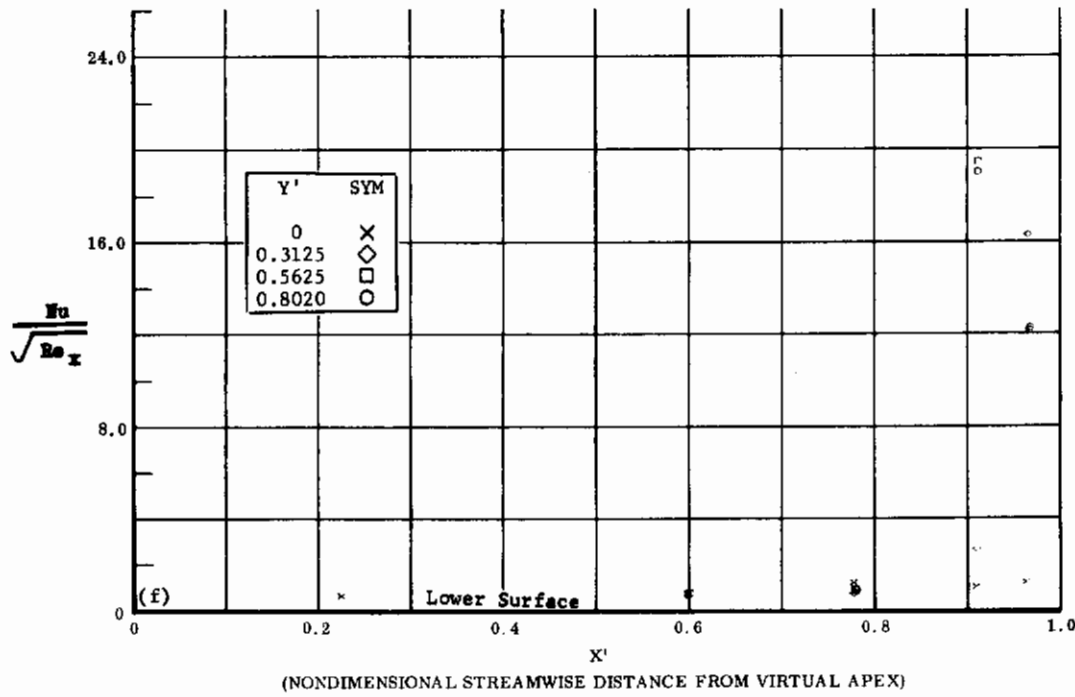
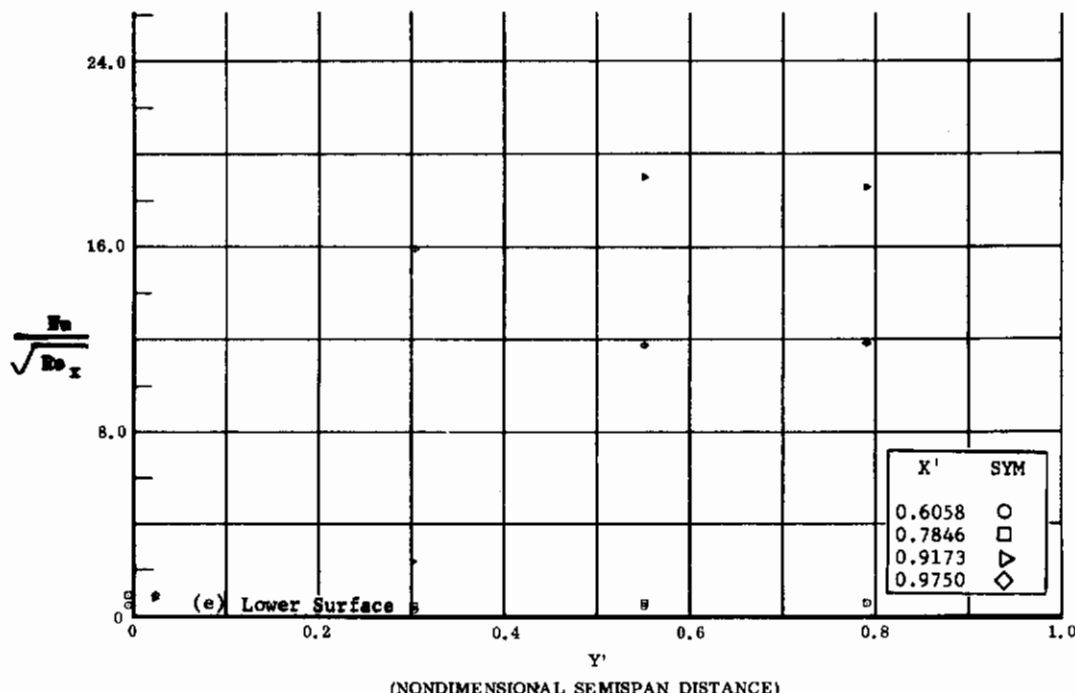


Fig. 31 Configuration IX, $\alpha = 0$, $\delta_2 = \delta_3 = +39$

e) $Nu/\sqrt{Re_x}$ vs. Y' lower surface $Re_\infty/\text{ft} \times 10^{-6} = 3.3$

f) $Nu/\sqrt{Re_x}$ vs. X' lower surface

Contrails

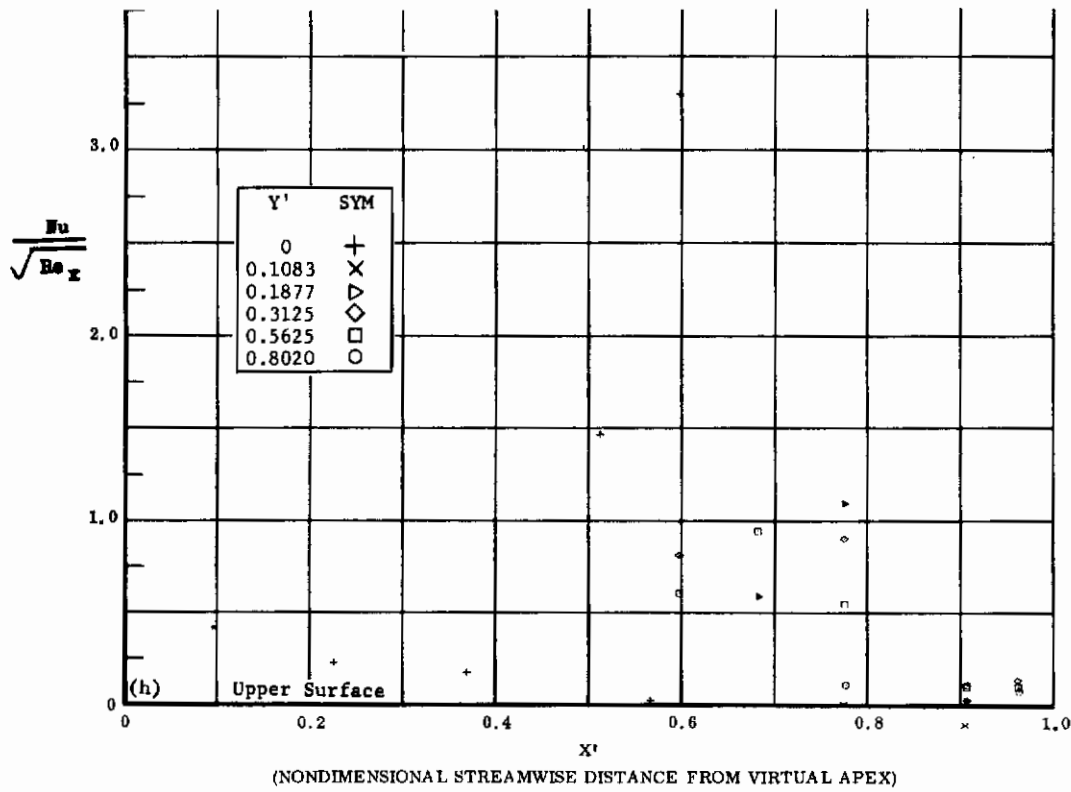
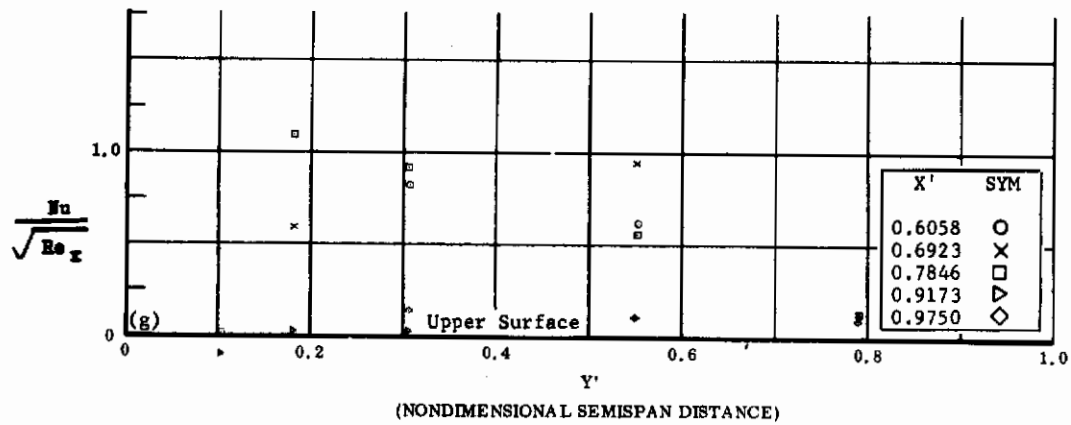


Fig. 31 Configuration IX, $\alpha = 0$, $\delta_2 = \delta_3 = +39$

g) $\text{Nu}/\sqrt{\text{Re}_x}$ vs. Y' upper surface $\text{Re}_{\infty}/\text{ft} \times 10^{-6} = 3.3$
 h) $\text{Nu}/\sqrt{\text{Re}_x}$ vs. X' upper surface

Contrails

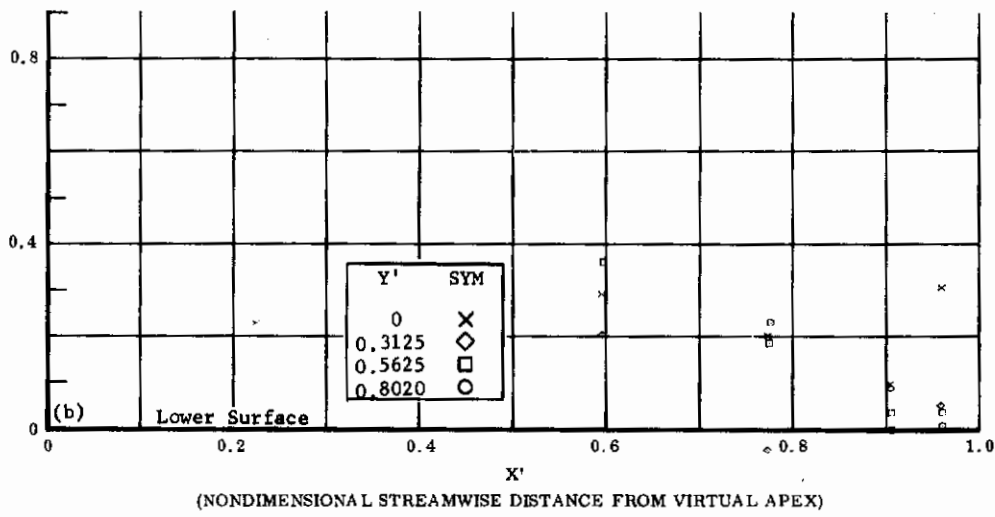
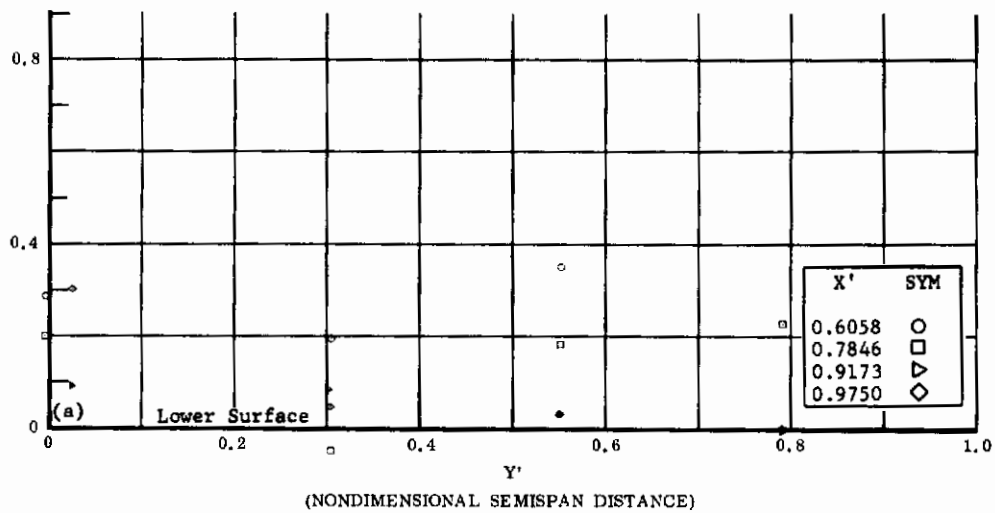


Fig. 32 Configuration IX, $\alpha = 0$, $s_2 = s_3 = -20$

- a) $Nu/\sqrt{Re_x}$ vs. Y' lower surface $Re_\infty/ft \times 10^{-6} = 3.3$
- b) $Nu/\sqrt{Re_x}$ vs. X' lower surface

Contrails

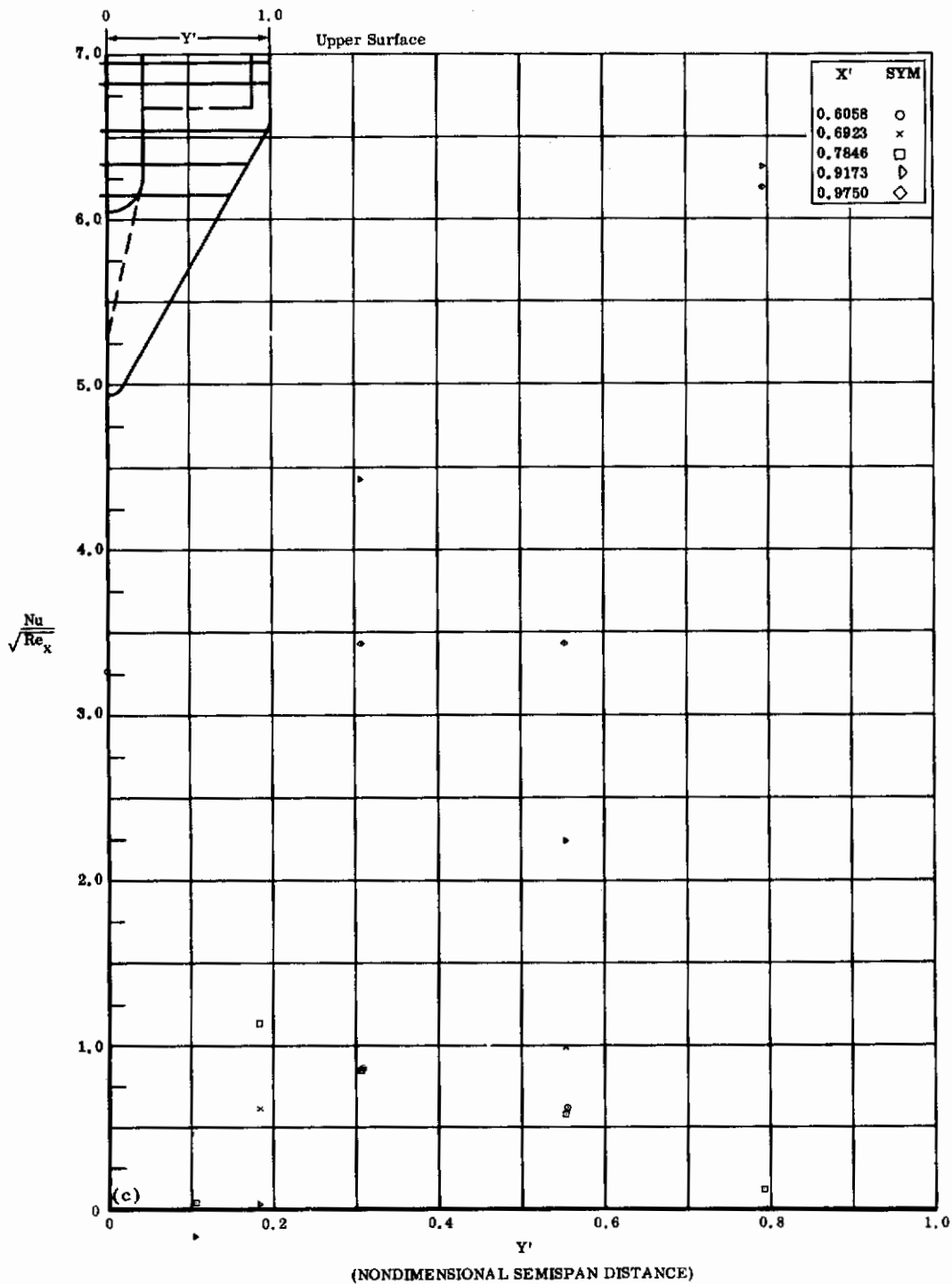


Fig. 32c Configuration IX, $\alpha = 0$, $\delta_2 = \delta_3 = -20$

$Nu/\sqrt{Re_x}$ vs. Y' upper surface $Re_\infty/\text{ft} \times 10^{-6} = 3.3$

Contrails

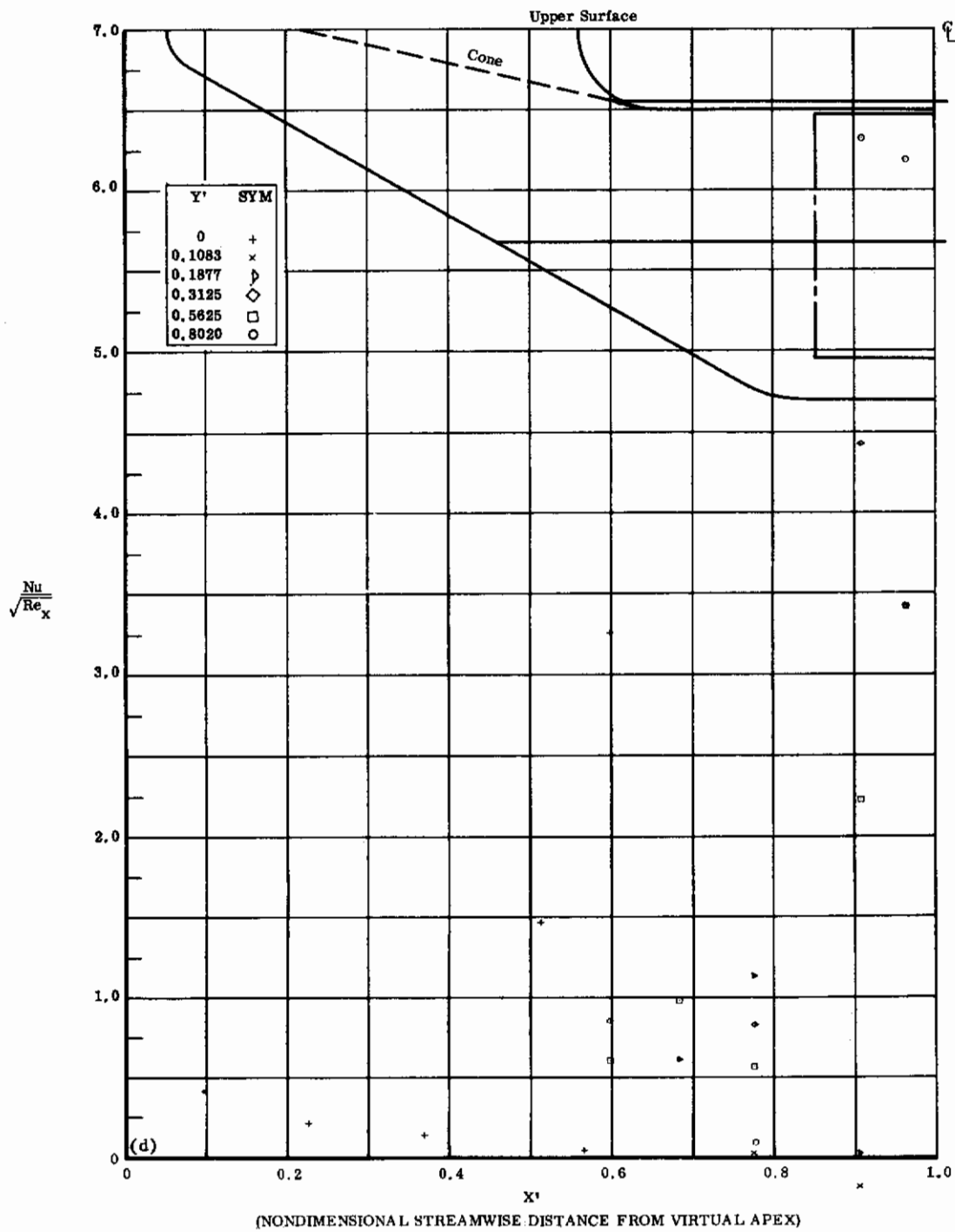


Fig. 32d Configuration IX, $\alpha = 0$, $\delta_2 = \delta_3 = -20$

$Nu/\sqrt{Re_x}$ vs. X' upper surface $Re_\infty / ft \times 10^{-6} = 3.3$

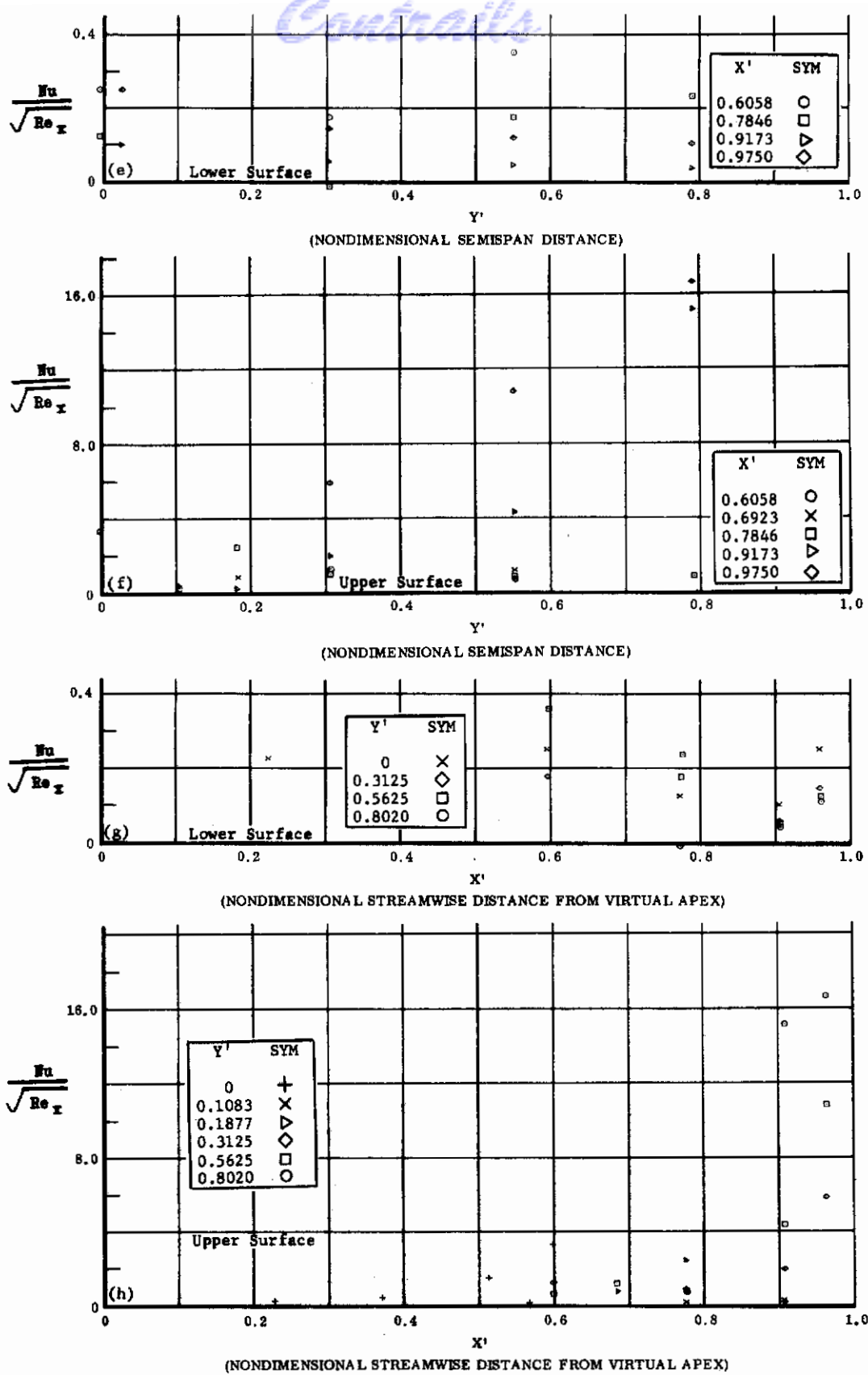


Fig. 32 Configuration IX, $\alpha = 0$, $\delta_2 = \delta_3 = -39$

e) $Nu/\sqrt{Re_x}$ vs. Y' lower surface

f) $Nu/\sqrt{Re_x}$ vs. Y' upper surface

g) $Nu/\sqrt{Re_x}$ vs. X' lower surface $Re_\infty/ft \times 10^{-6} = 3.3$

h) $Nu/\sqrt{Re_x}$ vs. X' upper surface

Contrails

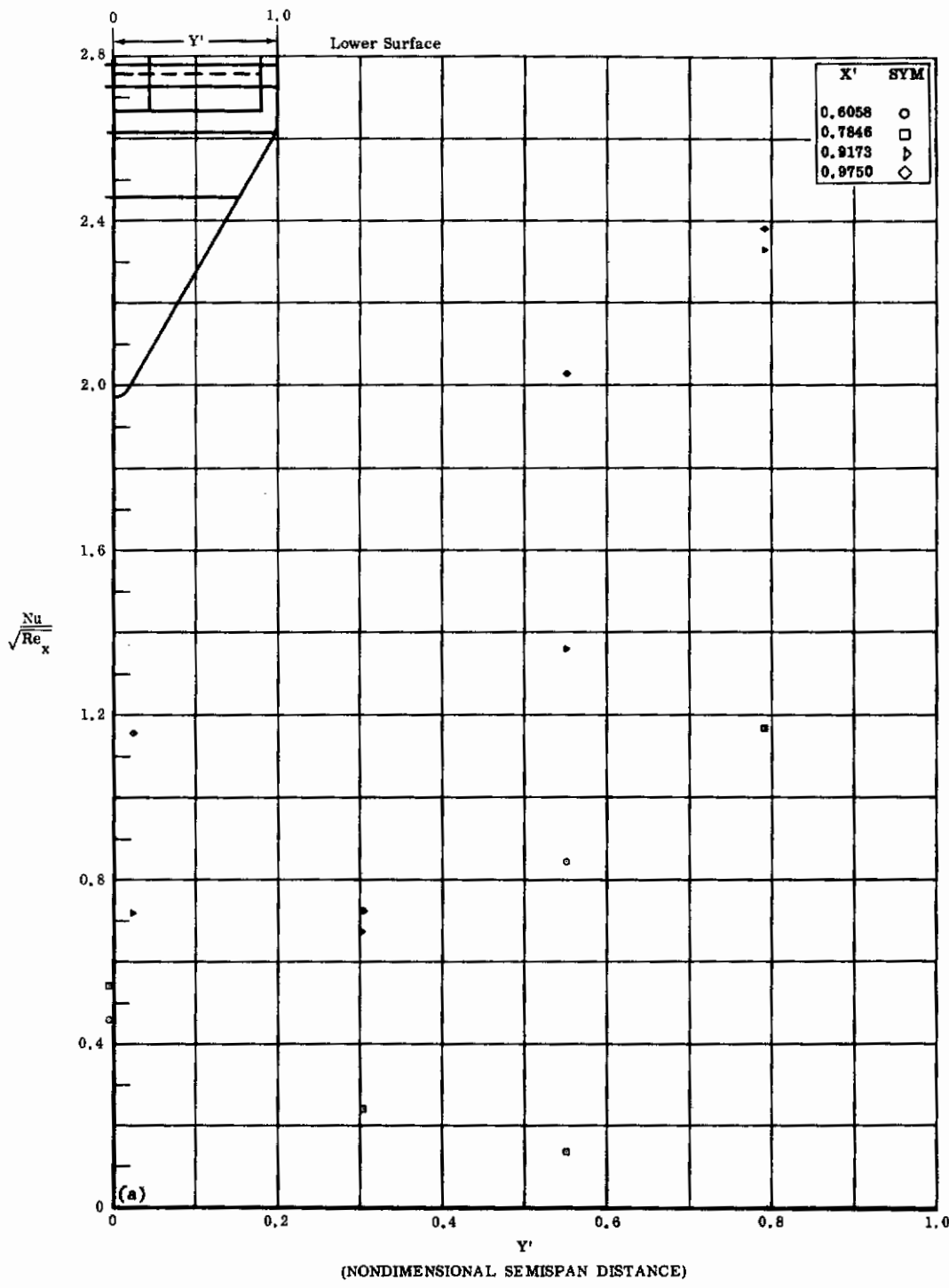


Fig. 33a Configuration IX, $\alpha = +10$, $\delta_2 = \delta_3 = 0$

$Nu/\sqrt{Re_x}$ vs. Y' lower surface $Re_\infty/\text{ft} \times 10^{-6} = 3.3$

Contrails

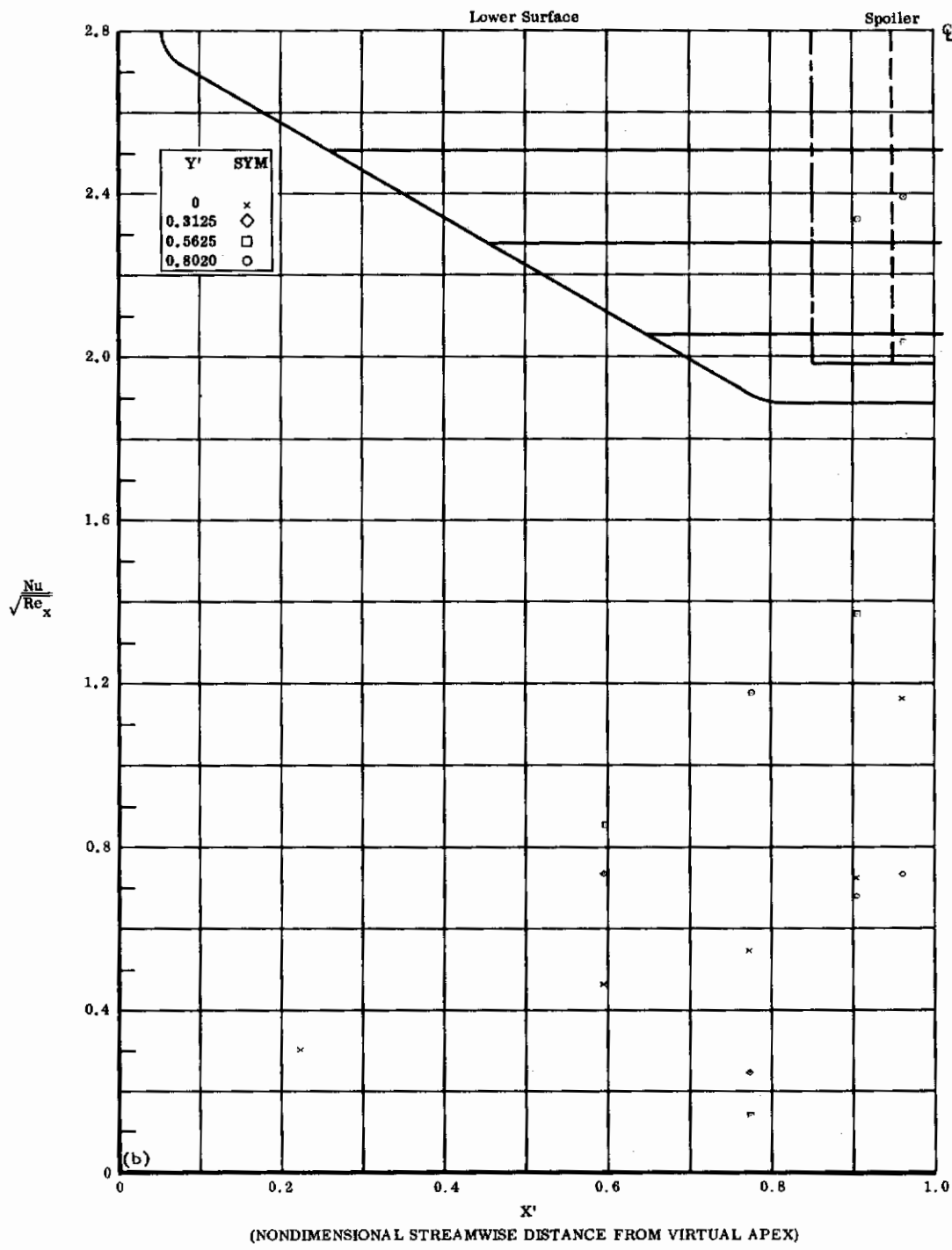


Fig. 33b Configuration IX, $\alpha = +10$, $\delta_2 = \delta_3 = 0$

$\text{Nu}/\sqrt{\text{Re}_x}$ vs. X' lower surface $\text{Re}_{\infty}/\text{ft} \times 10^{-6} = 3.3$

Contrails

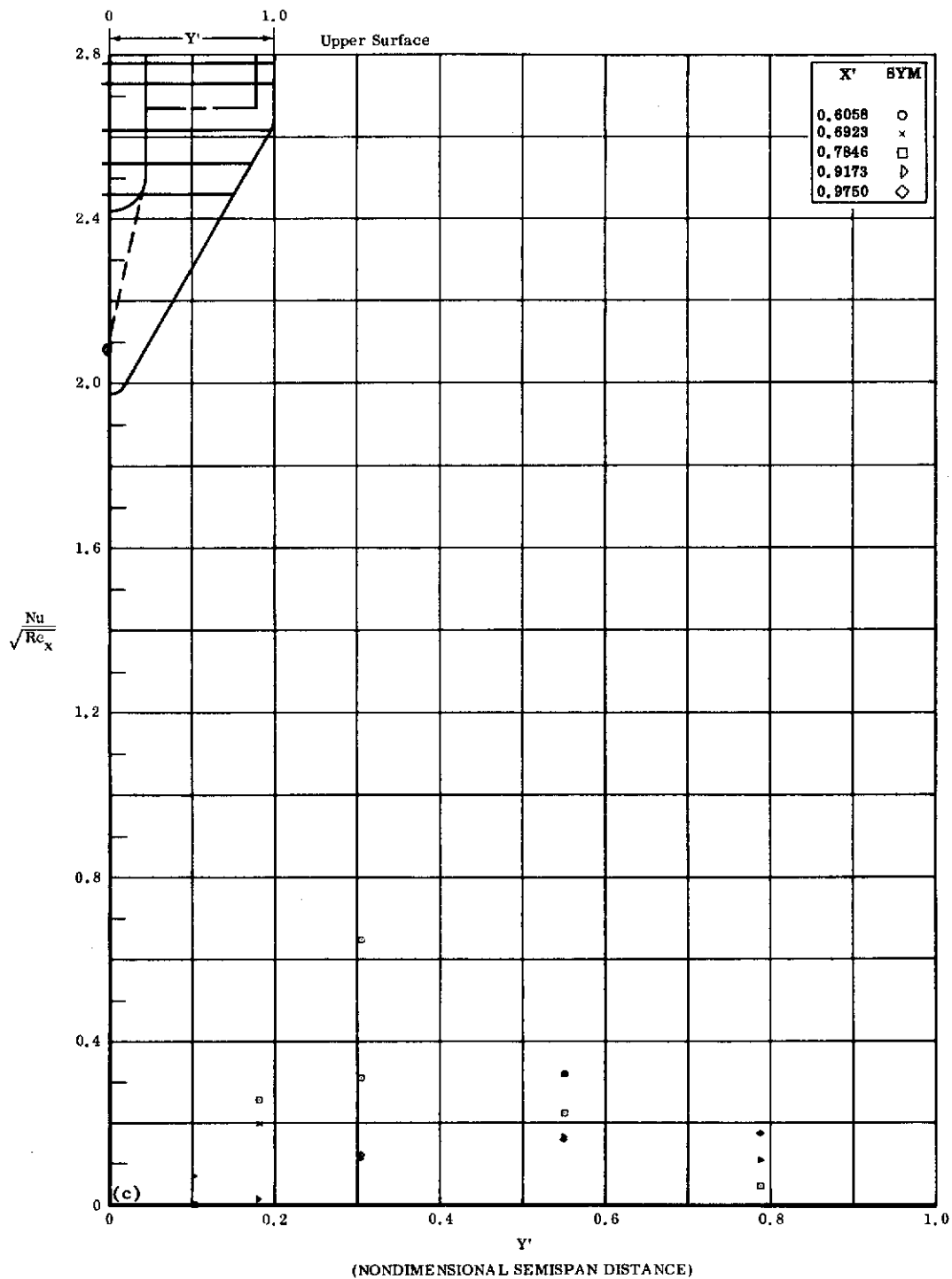


Fig. 33c Configuration IX, $\alpha = +10$, $\delta_2 = \delta_3 = 0$

$Nu/\sqrt{Re_x}$ vs. Y^* upper surface $Re_\infty/ft \times 10^{-6} = 3.3$

Contrails

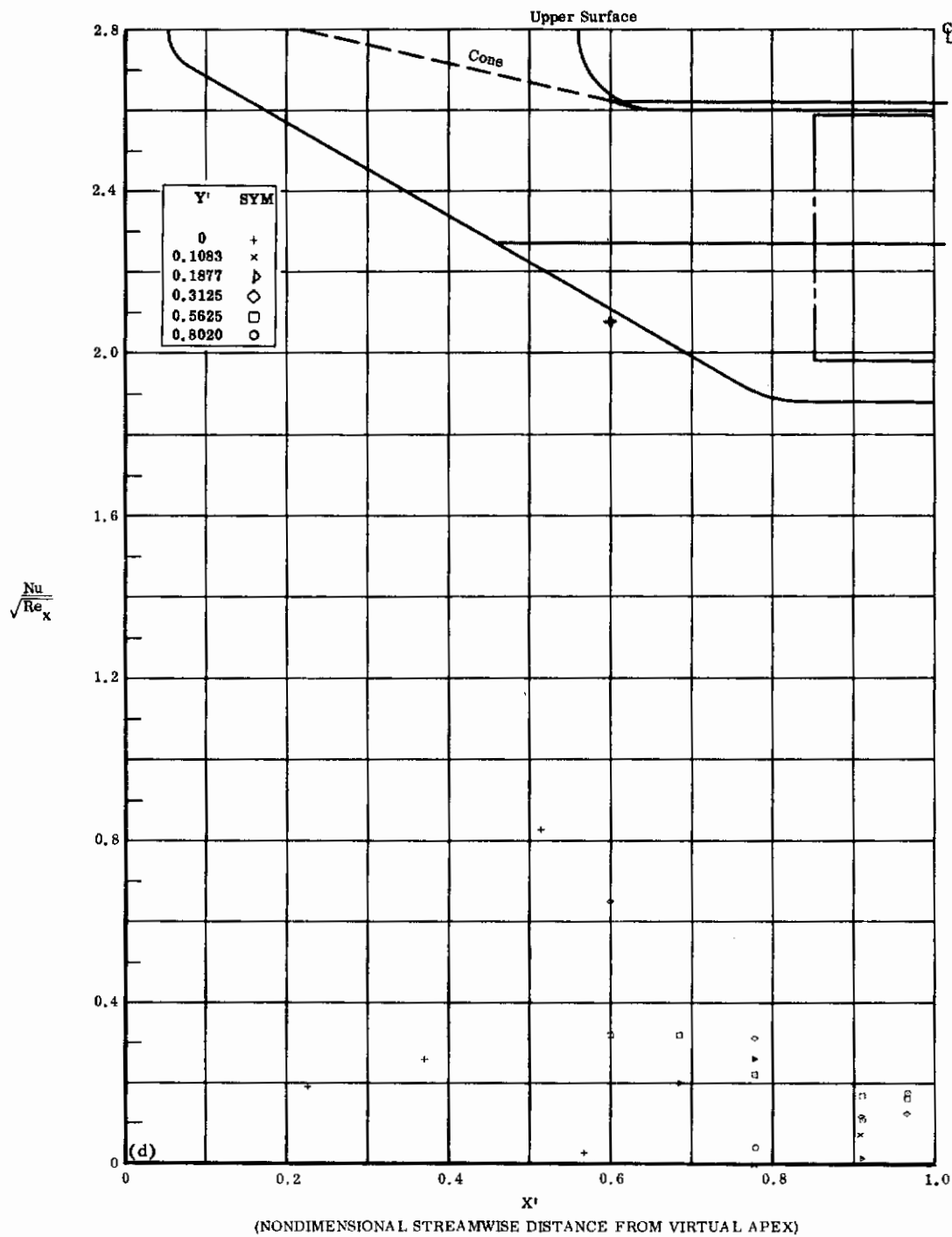


Fig. 33d Configuration IX, $\alpha = +10$, $\delta_2 = \delta_3 = 0$

$\text{Nu}/\sqrt{\text{Re}_x}$ vs. X' upper surface $\text{Re}_{\infty}/\text{ft} \times 10^{-6} = 3.3$

Contrails

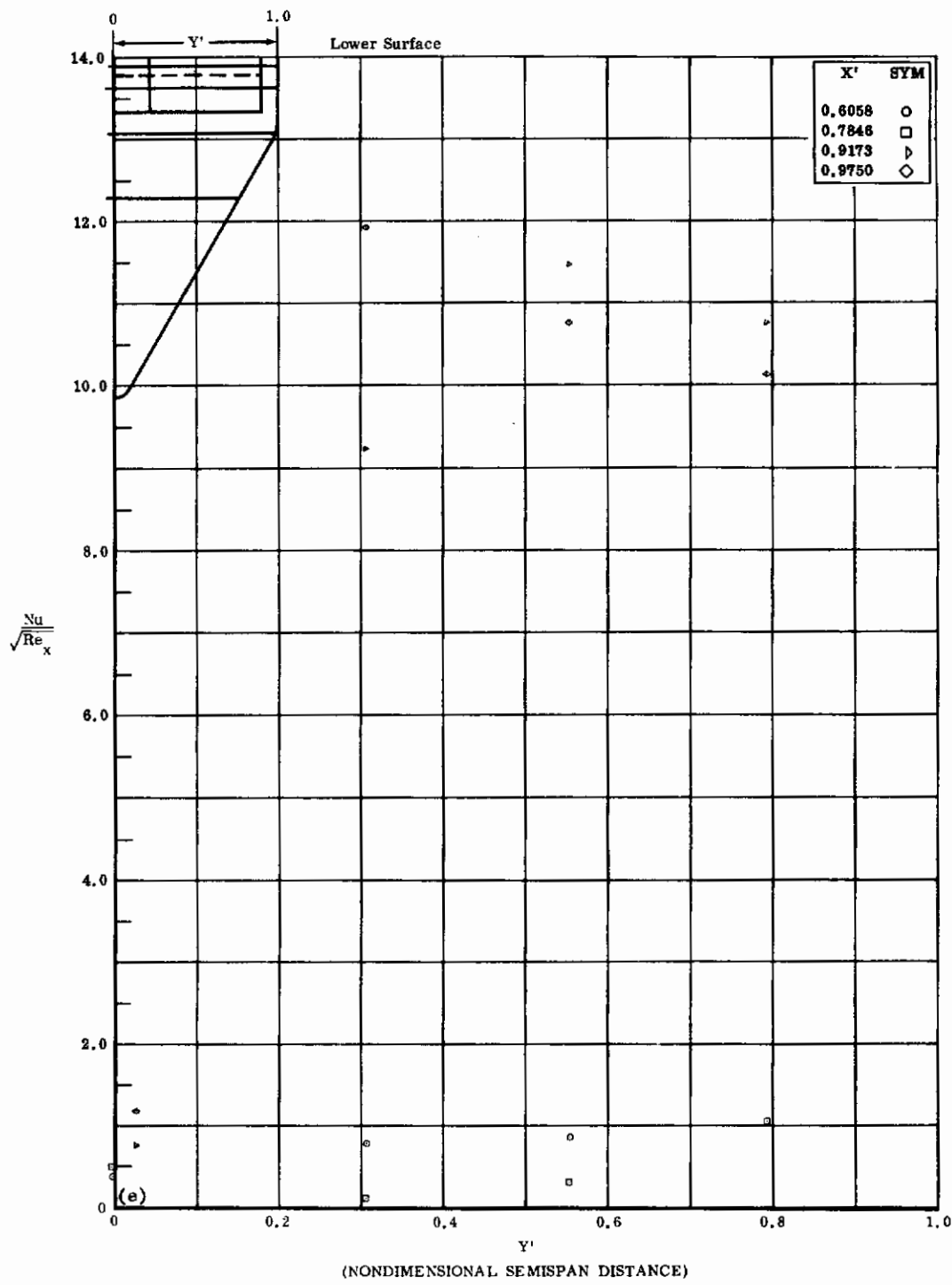


Fig. 33e Configuration IX, $\alpha = +10$, $\delta_2 = \delta_3 = +20$

$Nu/\sqrt{Re_x}$ vs. Y' lower surface $Re_\infty/\text{ft} \times 10^{-6} = 3.3$

Contrails

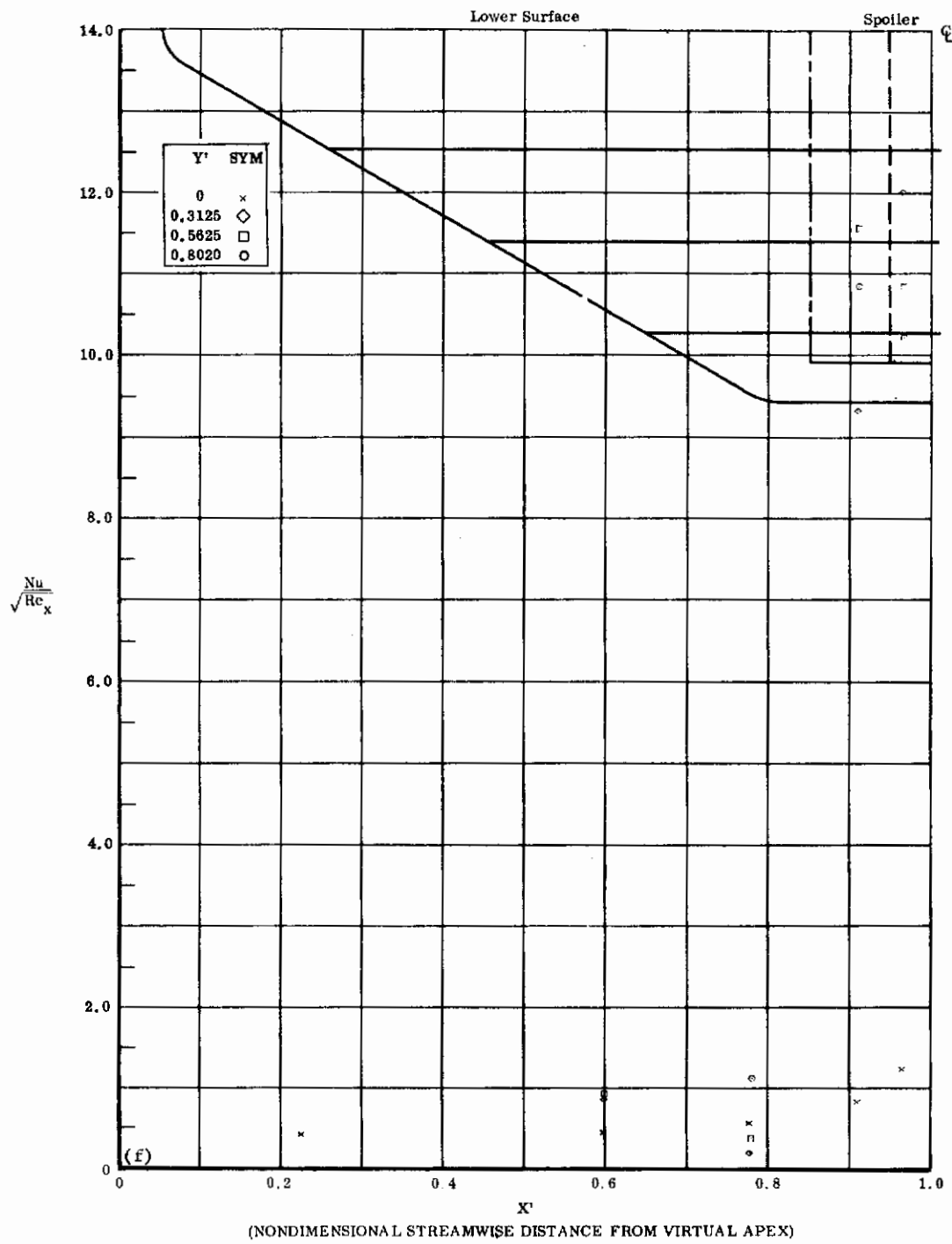


Fig. 33f Configuration IX, $\alpha = +10$, $\delta_2 = \delta_3 = +20$
 $Nu/\sqrt{Re_x}$ vs. X' lower surface $Re_\infty/\text{ft} \times 10^{-6} = 3.3$

Contrails

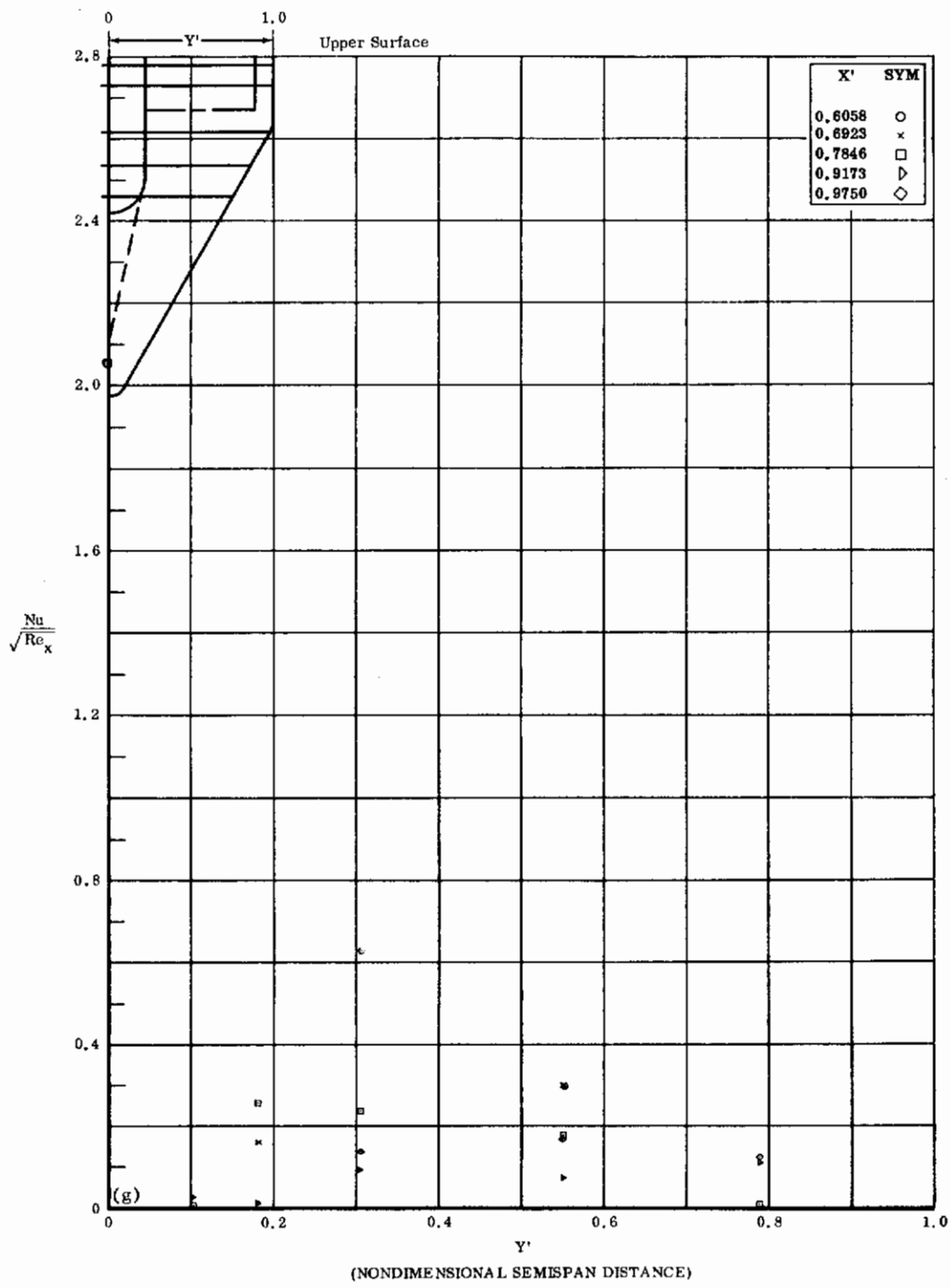


Fig. 33g Configuration IX, $\alpha = +10$, $s_2 = s_3 = +20$

$Nu/\sqrt{Re_x}$ vs. Y' upper surface $Re_\infty/\text{ft} \times 10^{-6} = 3.3$

Contrails

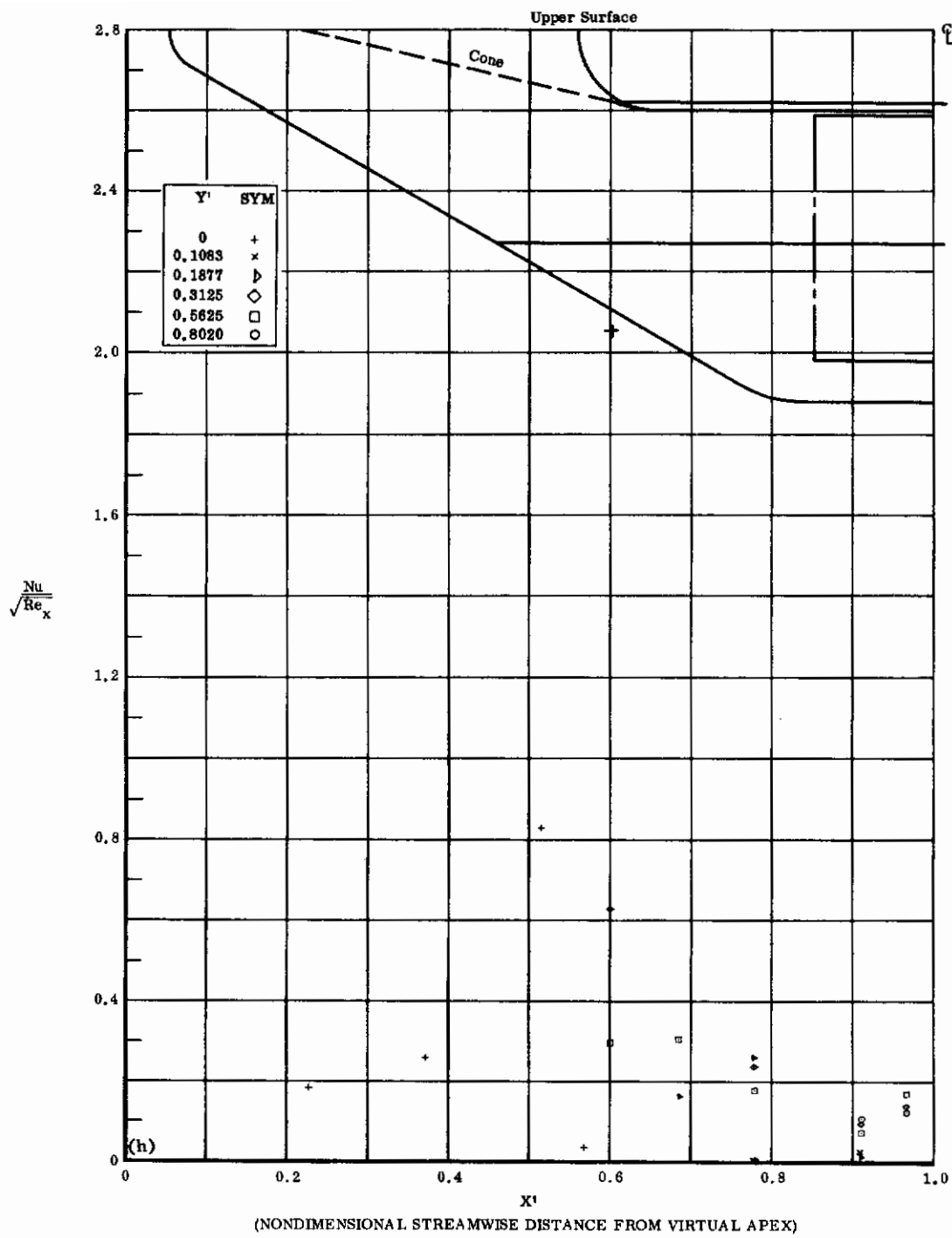


Fig. 33h Configuration IX, $\alpha = +10$, $\delta_2 = \delta_3 = +20$

$\text{Nu}/\sqrt{\text{Re}_x}$ vs. X^i upper surface $\text{Re}_\infty/\text{ft} \times 10^{-6} = 3.3$

Contrails

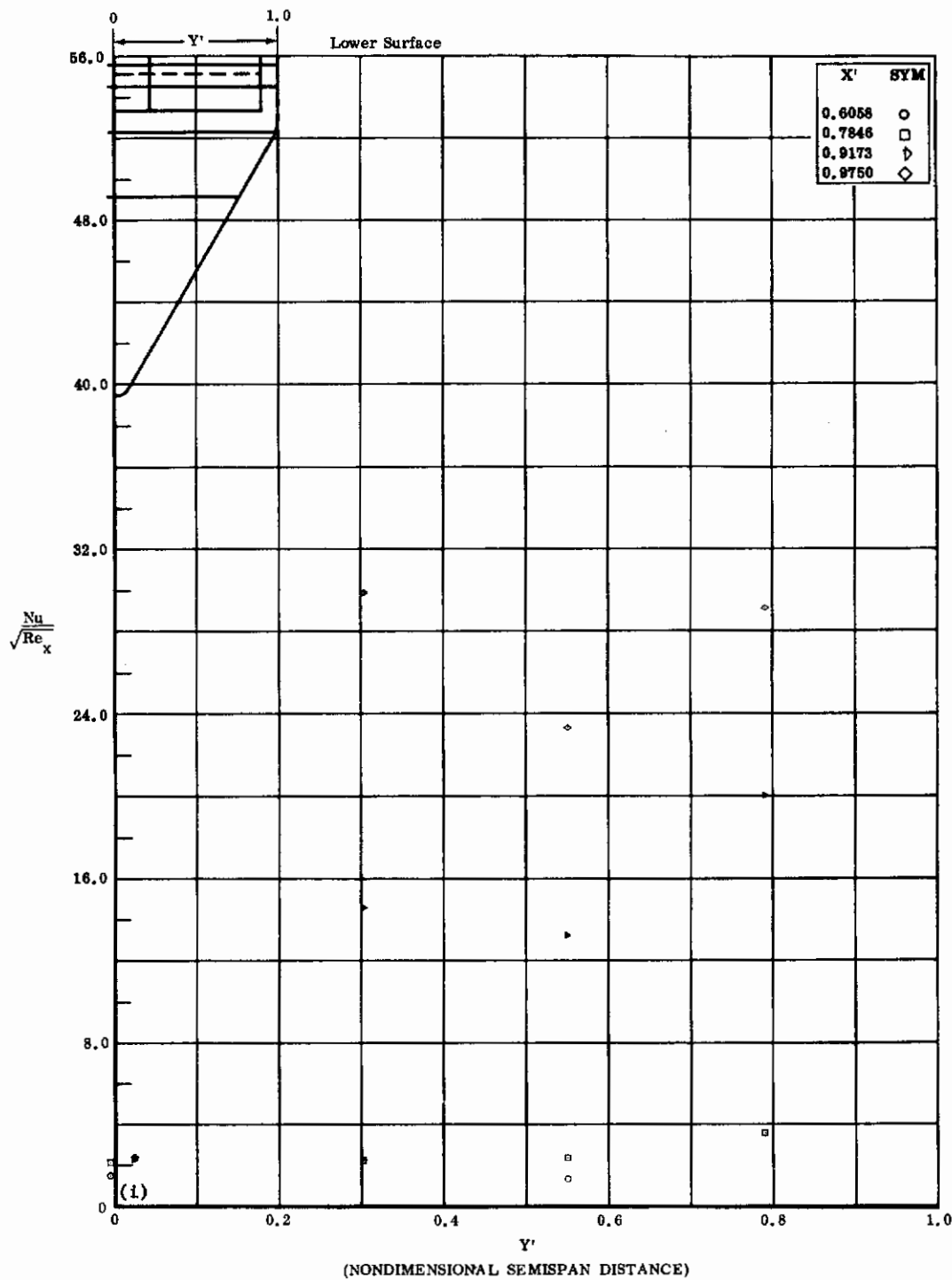


Fig. 33i Configuration IX, $\alpha = +10$, $\delta_2 = \delta_3 = +39$

$Nu/\sqrt{Re_x}$ vs. Y' lower surface $Re_\infty/\text{ft} \times 10^{-6} = 3.3$

Contrails

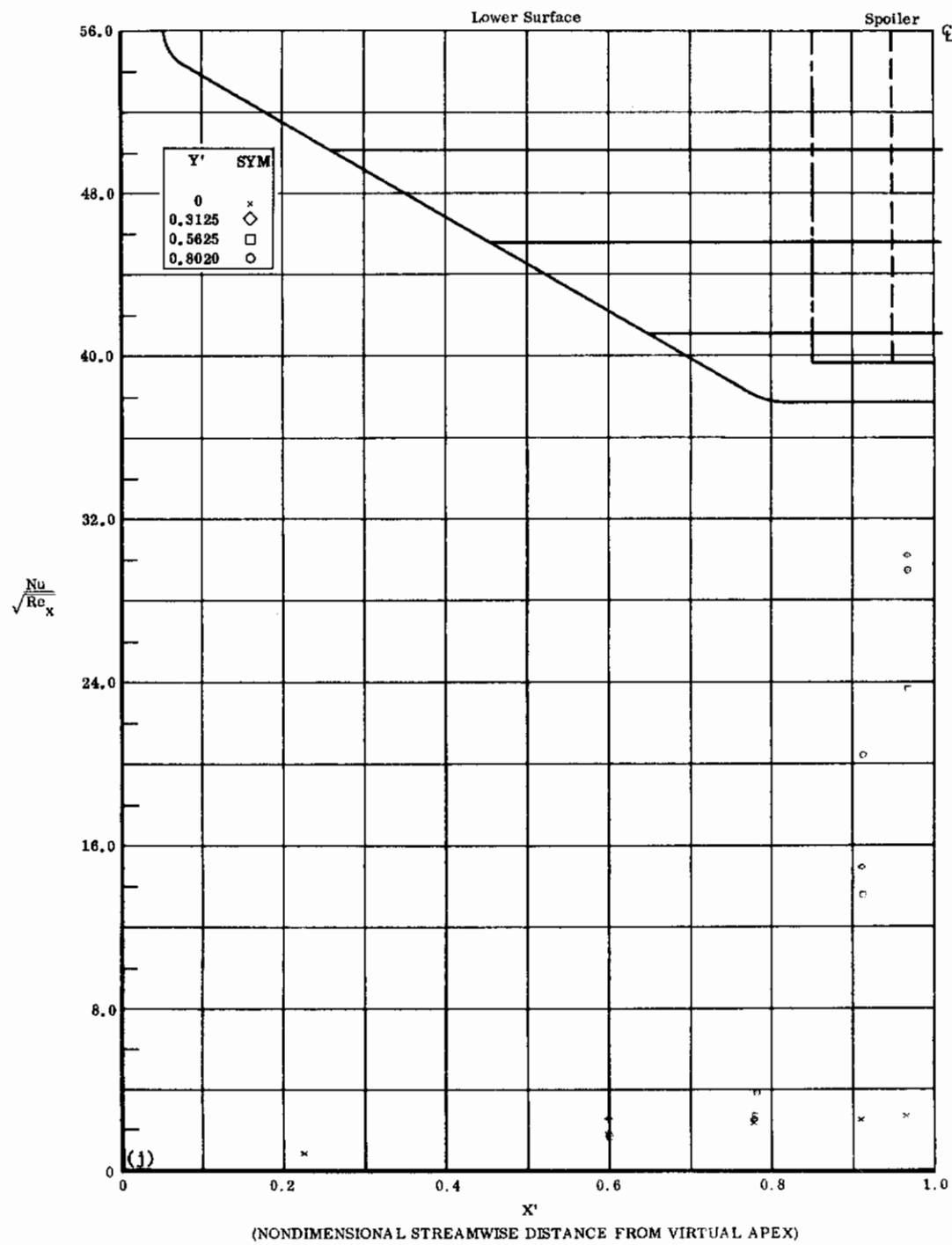


Fig. 33j Configuration IX, $\alpha = +10$, $s_2 = s_3 = +39$

$\text{Nu}/\sqrt{\text{Re}_x}$ vs. X' lower surface $\text{Re}_\infty/\text{ft} \times 10^{-6} = 3.3$

Contrails

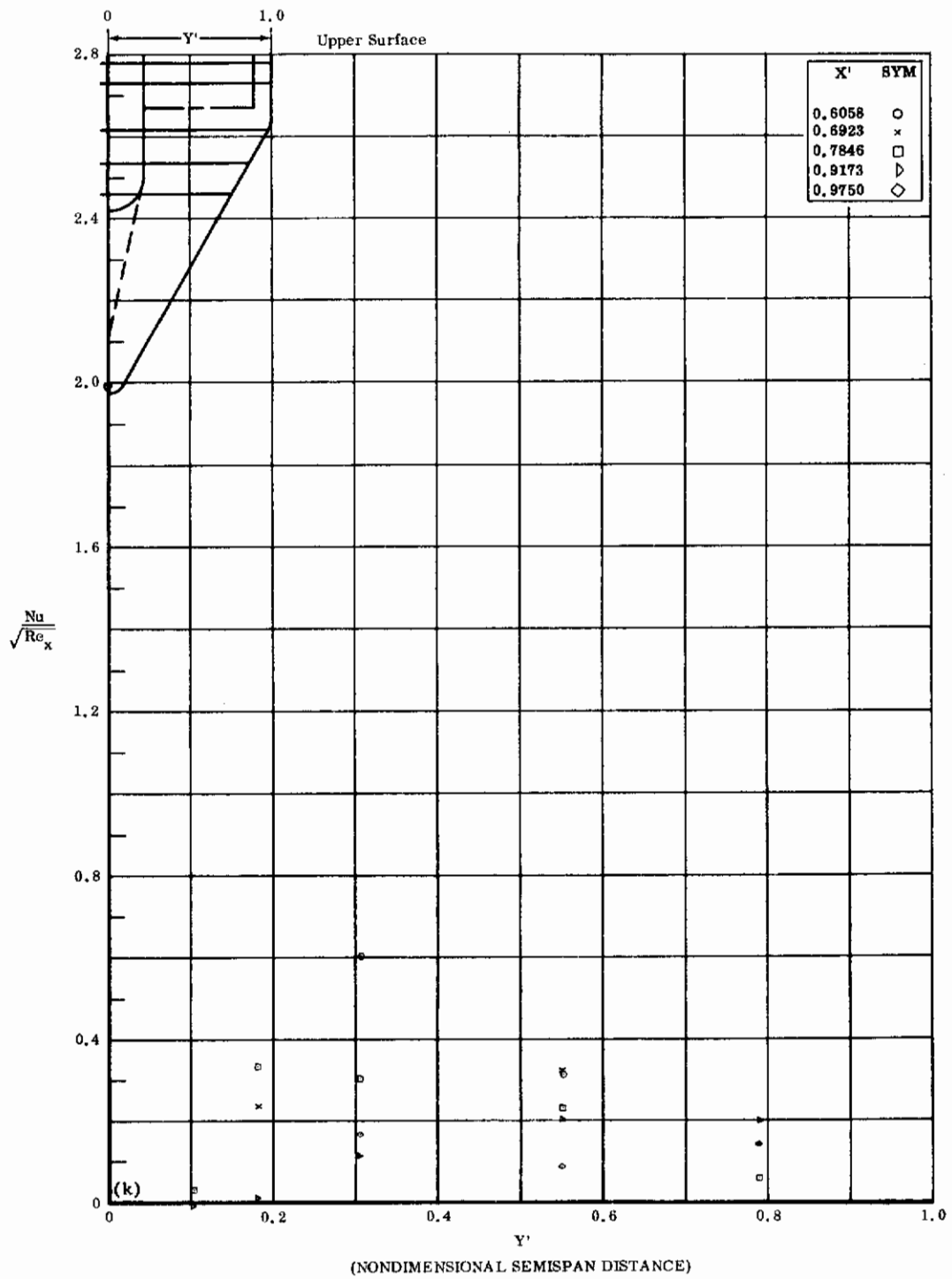


Fig. 33k Configuration IX, $\alpha = +10$, $\delta_2 = \delta_3 = +39$
 $Nu/\sqrt{Re_x}$ vs. Y' upper surface $Re_\infty/ft \times 10^{-6} = 3.3$

Contrails

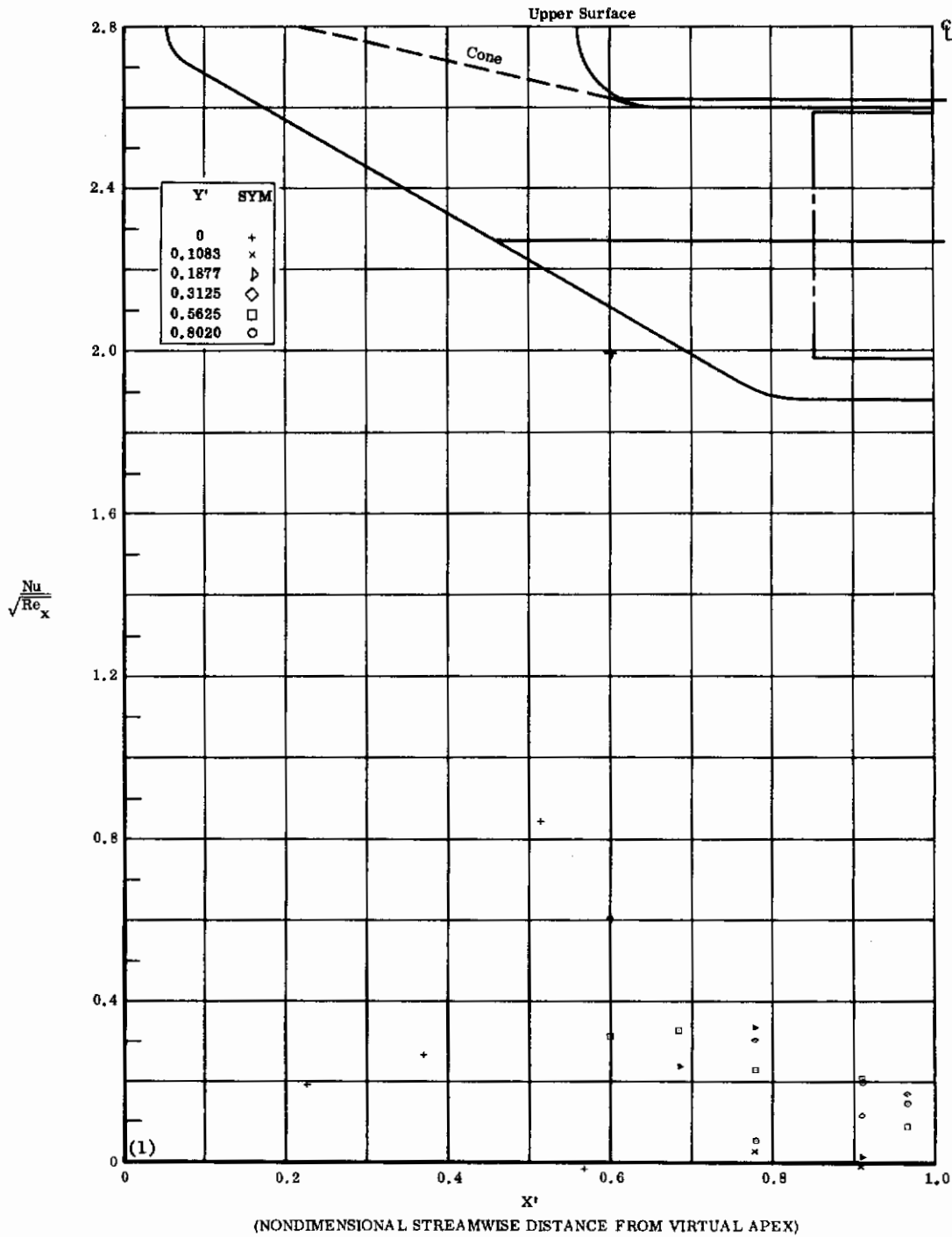


Fig. 33& Configuration IX, $\alpha = +10$, $\delta_2 = \delta_3 = +39$

$Nu/\sqrt{Re_x}$ vs. X' upper surface $Re_\infty/ft \times 10^{-6} = 3.3$

Contrails

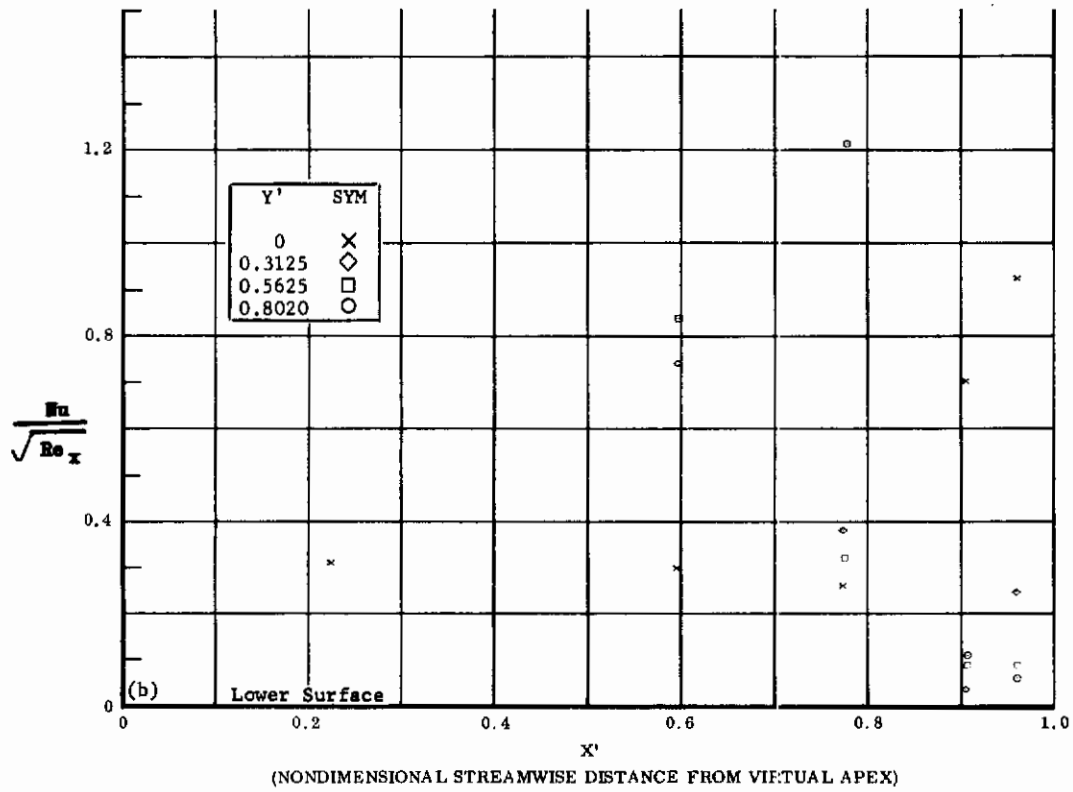
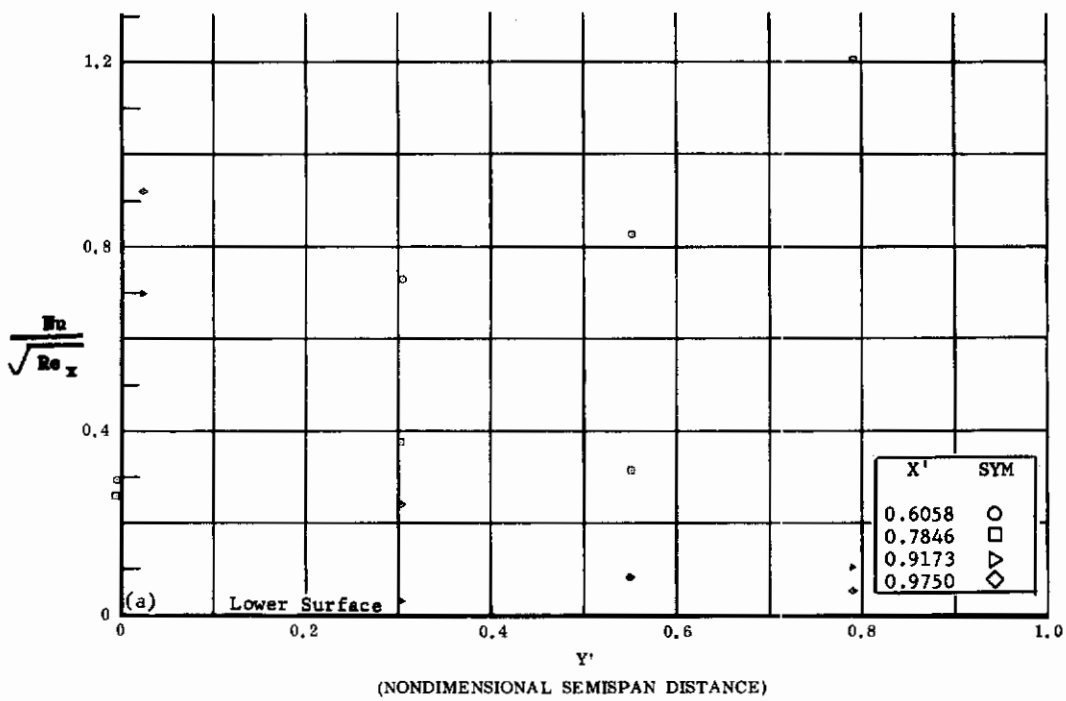


Fig. 34 Configuration IX, $\alpha = +10$, $\delta_2 = \delta_3 = -20$

- a) $Nu/\sqrt{Re_x}$ vs. Y' lower surface $Re_\infty/\text{ft} \times 10^{-6} = 3.3$
- b) $Nu/\sqrt{Re_x}$ vs. X' lower surface

Contrails

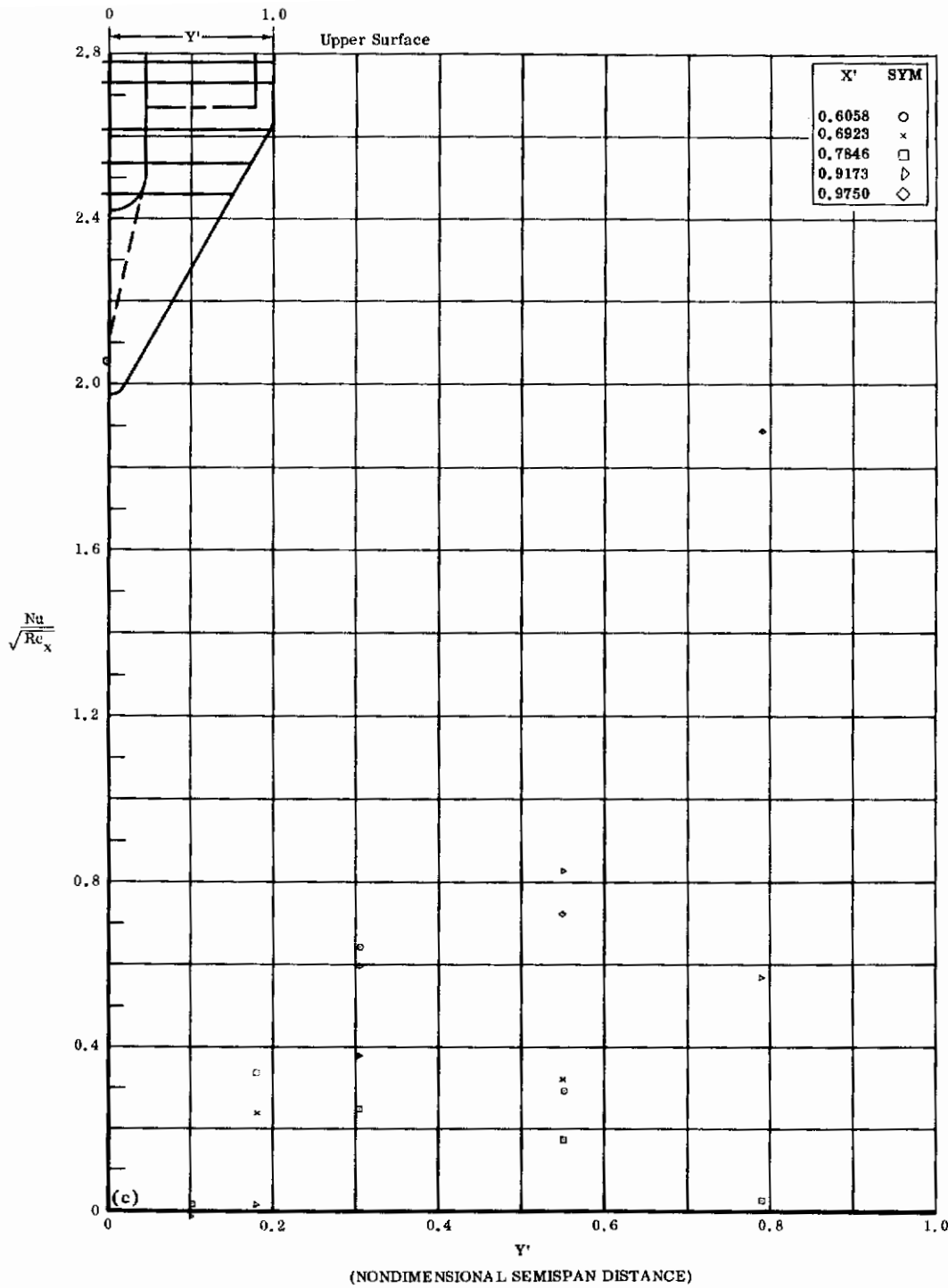


Fig. 34c Configuration IX, $\alpha = +10$, $b_2 = b_3 = -20$
 $Nu/\sqrt{Re_x}$ vs. Y' upper surface $Re_\infty/ft \times 10^{-6} = 3.3$

Contrails

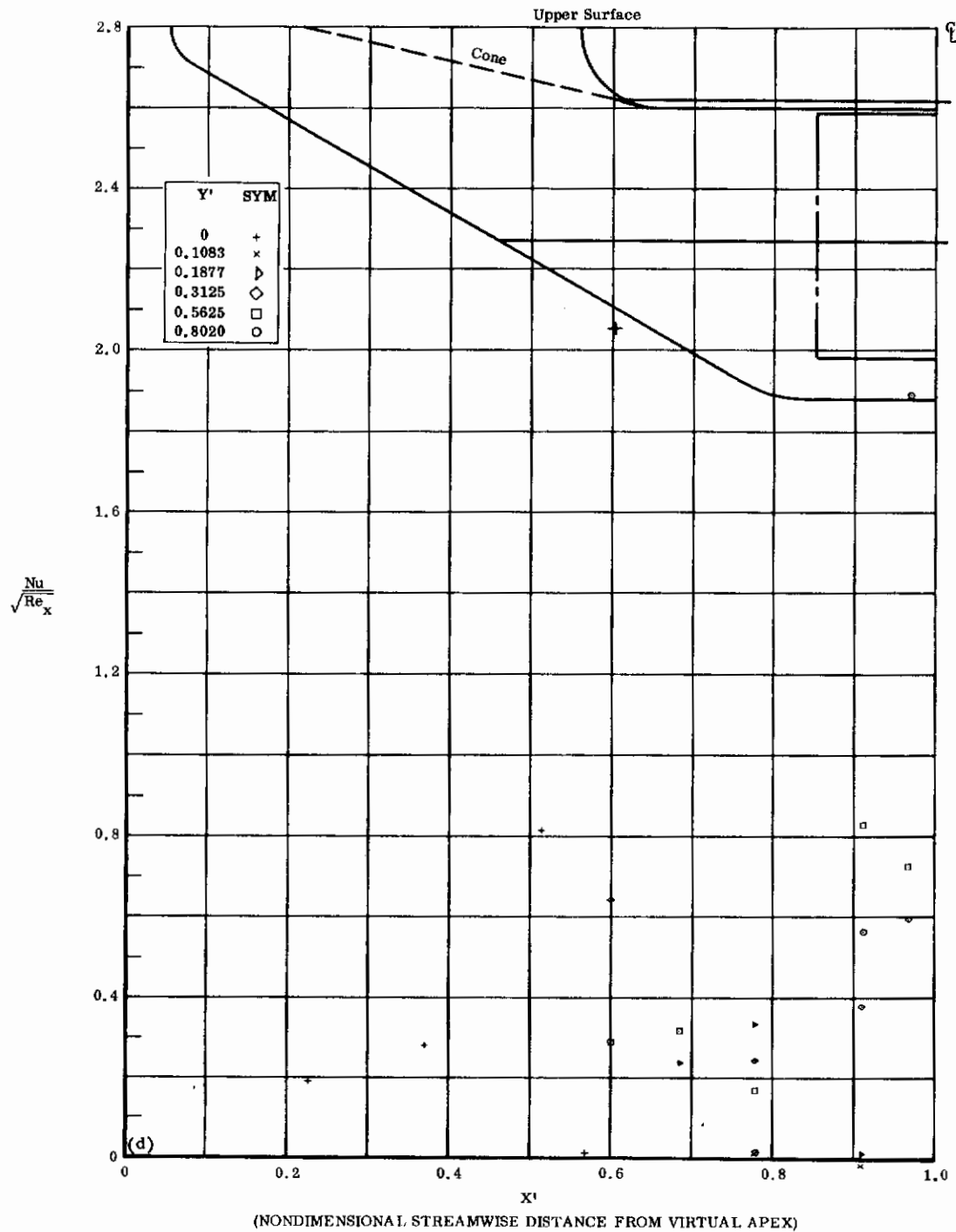


Fig. 34d Configuration IX, $\alpha = +10$, $b_2 = b_3 = -20$
 $Nu/\sqrt{Re_x}$ vs. X' upper surface $Re_\infty/\text{ft} \times 10^{-6} = 3.3$

Contrails

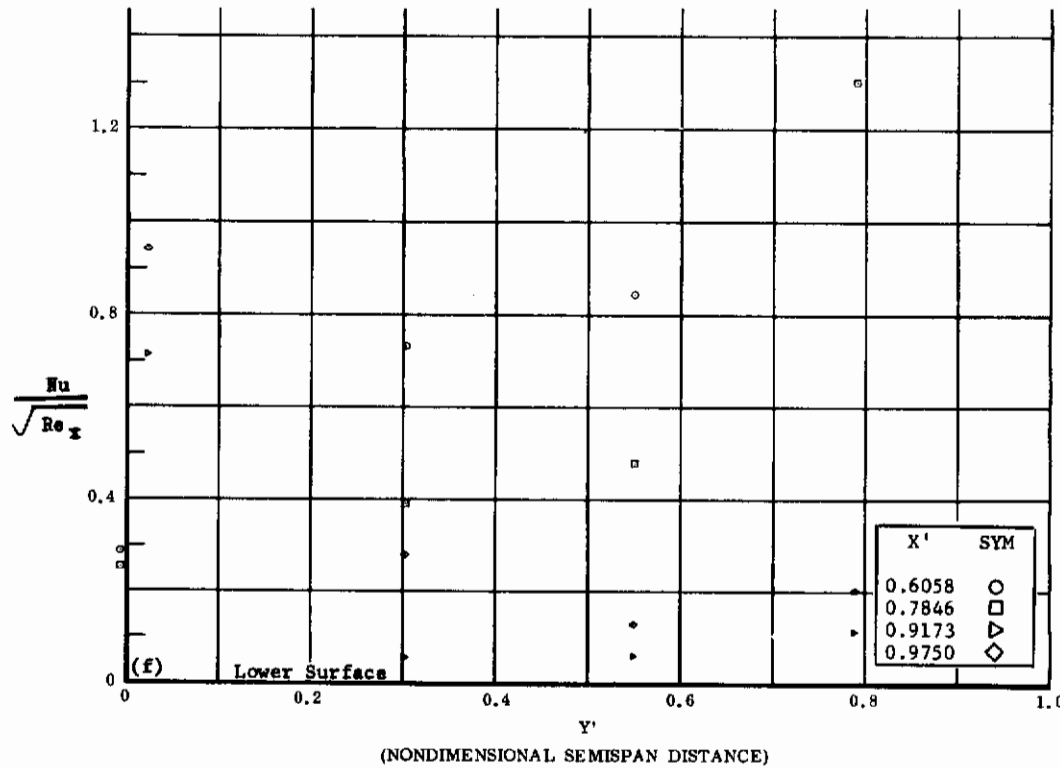
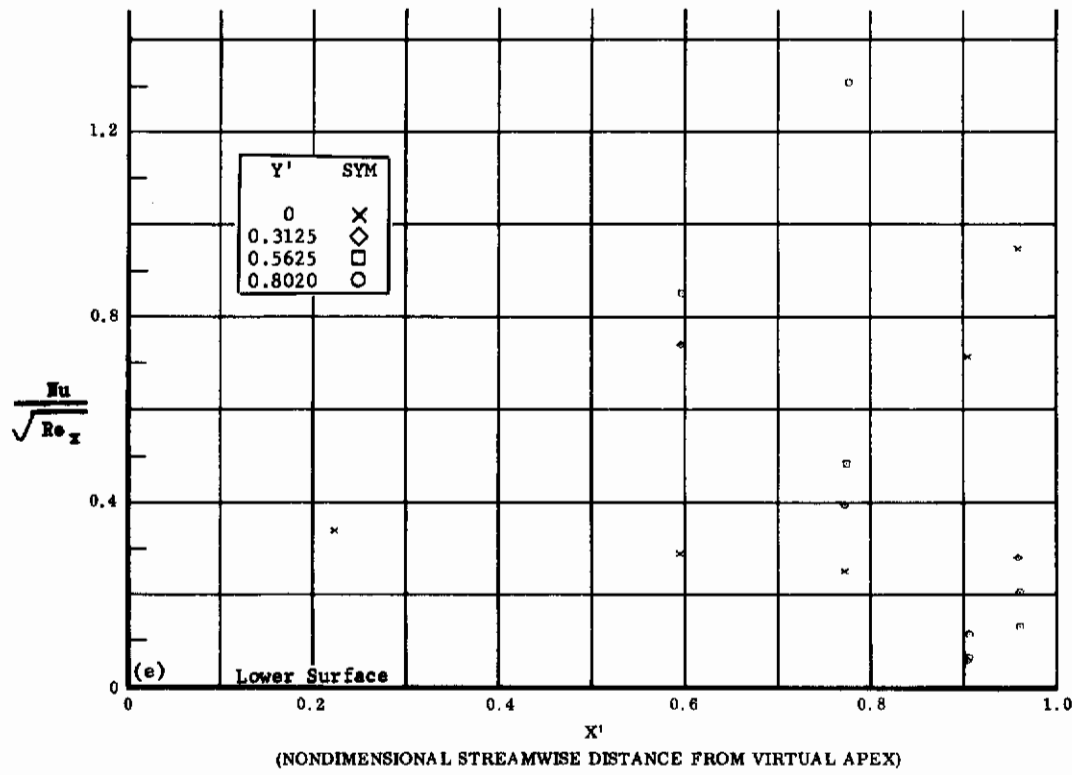


Fig. 34 Configuration IX, $\alpha = +10$, $b_2 = b_3 = -39$

e) $Nu/\sqrt{Re_x}$ vs. X^1 lower surface $Re_\infty/\text{ft} \times 10^{-6} = 3.3$

f) $Nu/\sqrt{Re_x}$ vs. Y^1 lower surface

Contrails

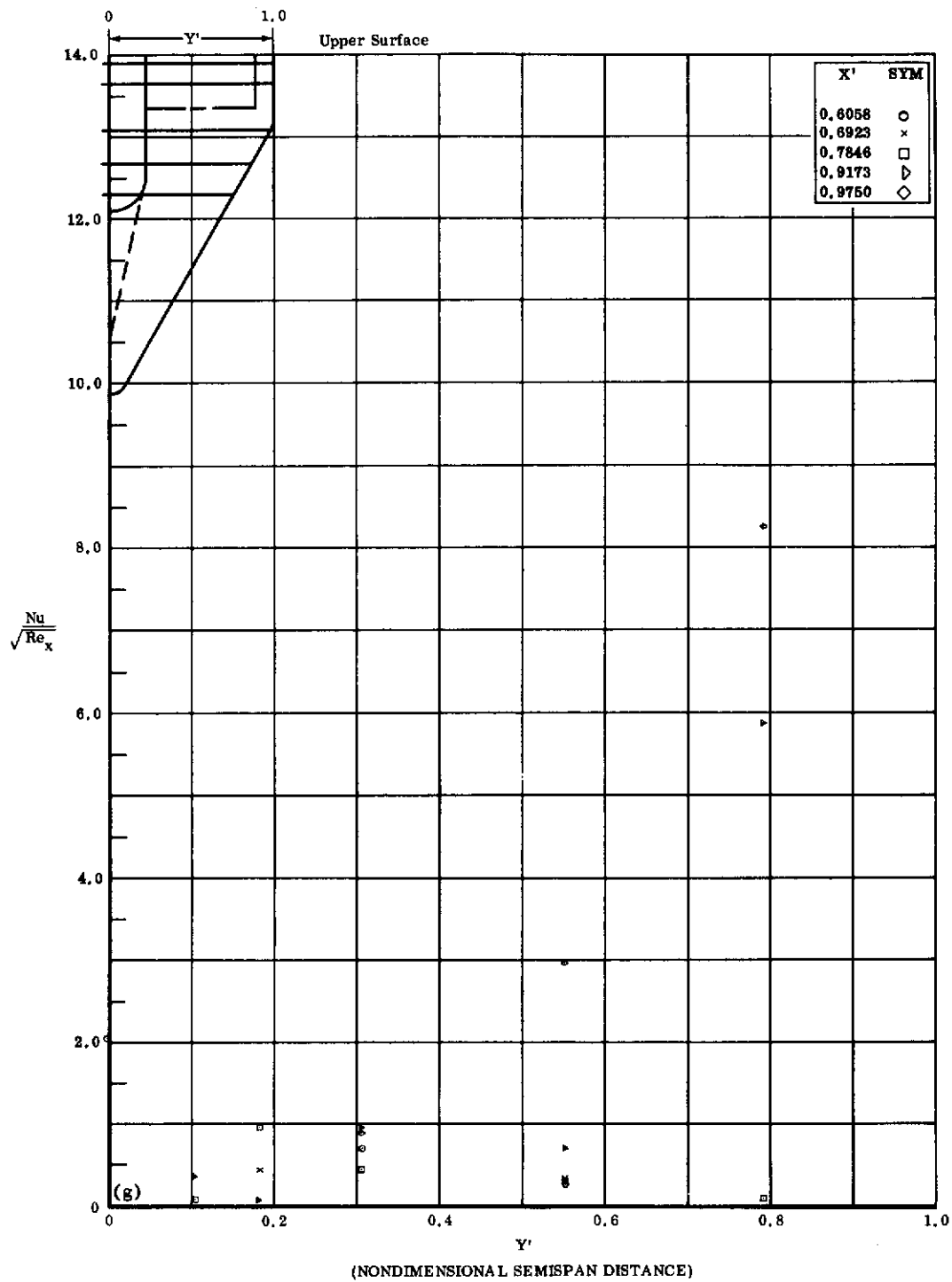


Fig. 34g Configuration IX, $\alpha = +10$, $\delta_2 = \delta_3 = -39$

$Nu/\sqrt{Re_x}$ vs. Y' upper surface $Re_\infty/\text{ft} \times 10^{-6} = 3.3$

Contrails

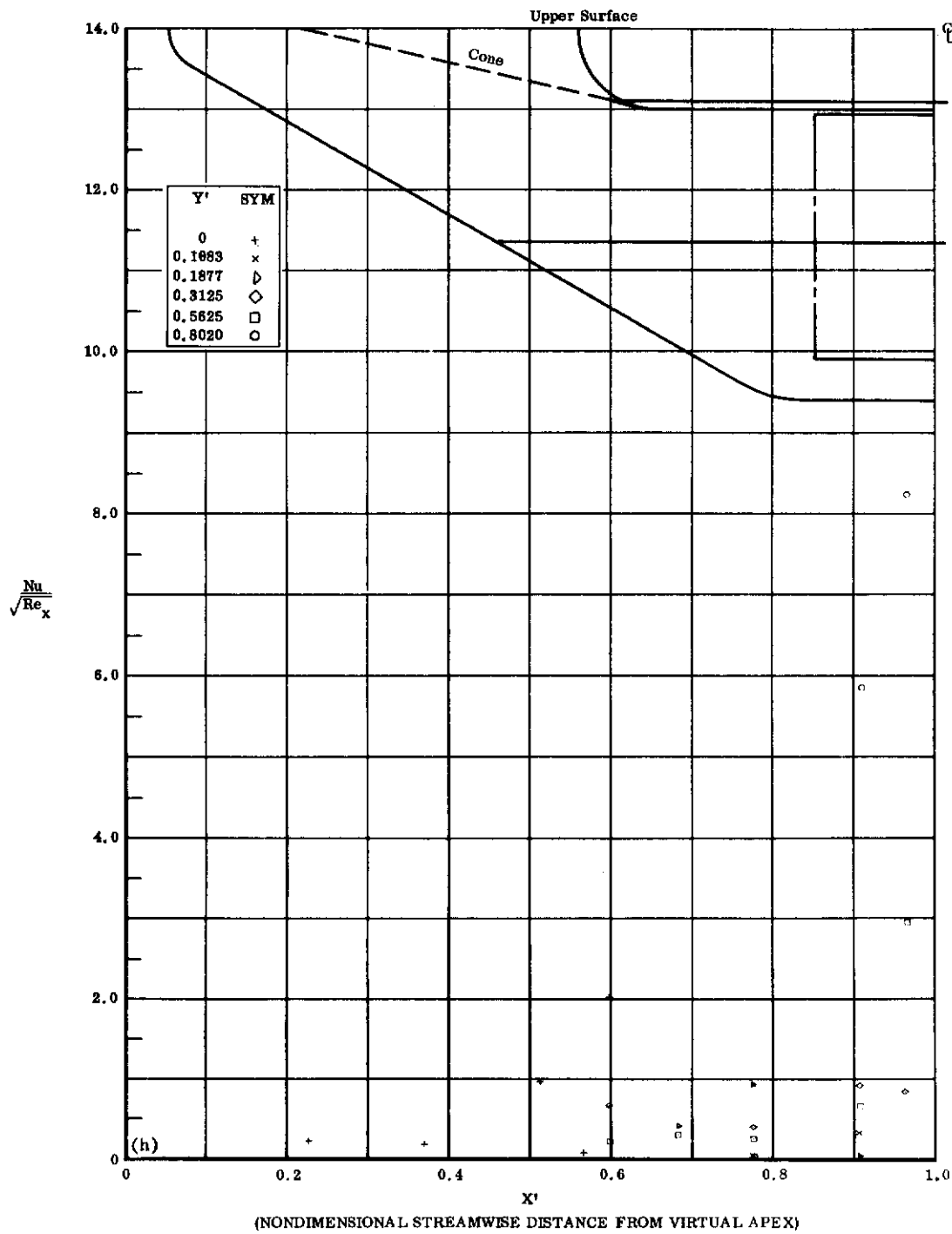


Fig. 34b Configuration IX, $\alpha = +10$, $b_2 = b_3 = -39$

$Nu/\sqrt{Re_x}$ vs. X' upper surface $Re_\infty/\text{ft} \times 10^{-6} = 3.3$

Contrails

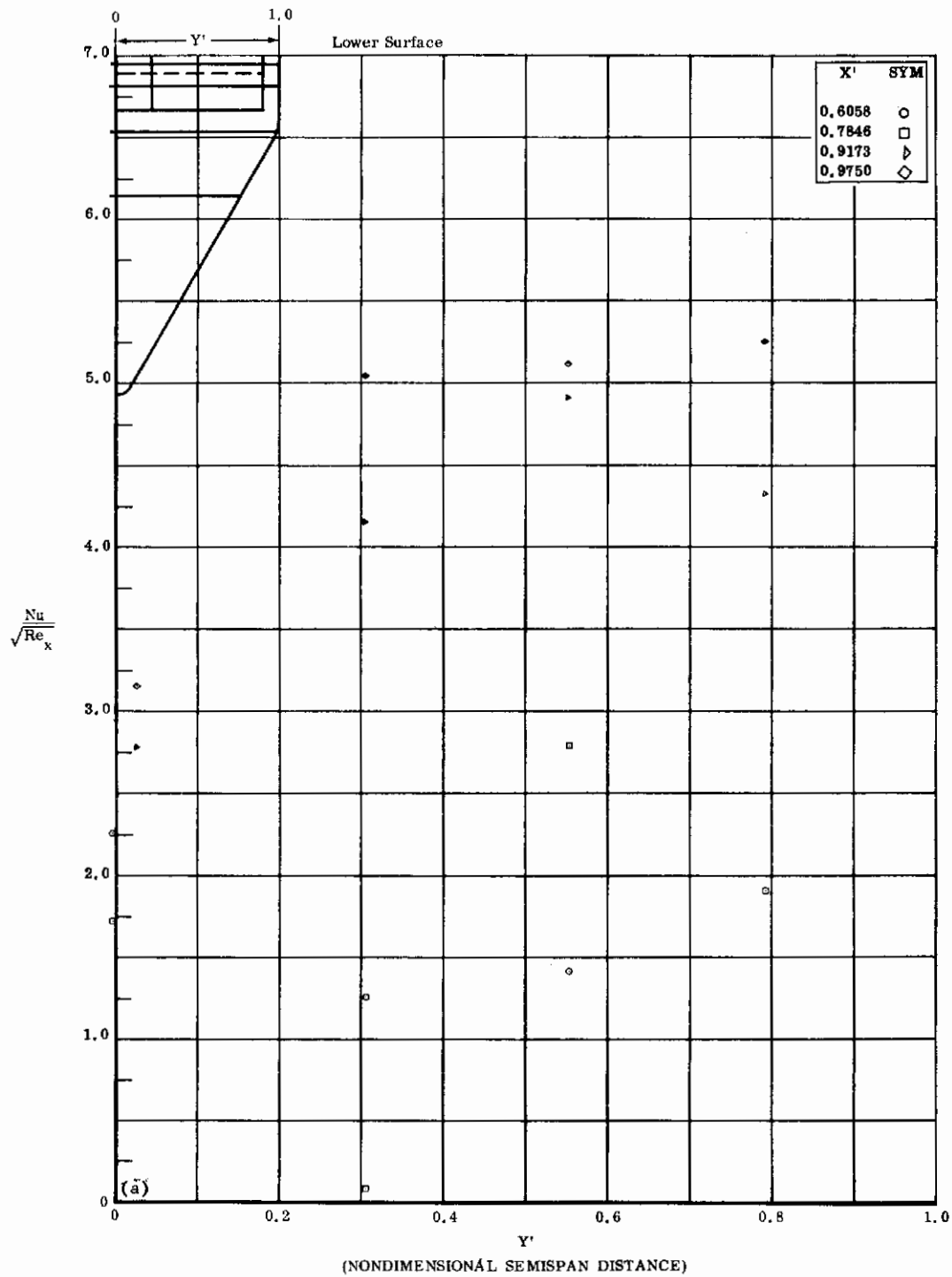


Fig. 35a Configuration IX, $\alpha = +20$, $\delta_2 = \delta_3 = 0$

$\text{Nu}/\sqrt{\text{Re}_x}$ vs. Y' lower surface $\text{Re}_\infty/\text{ft} \times 10^{-6} = 3.3$

Contrails

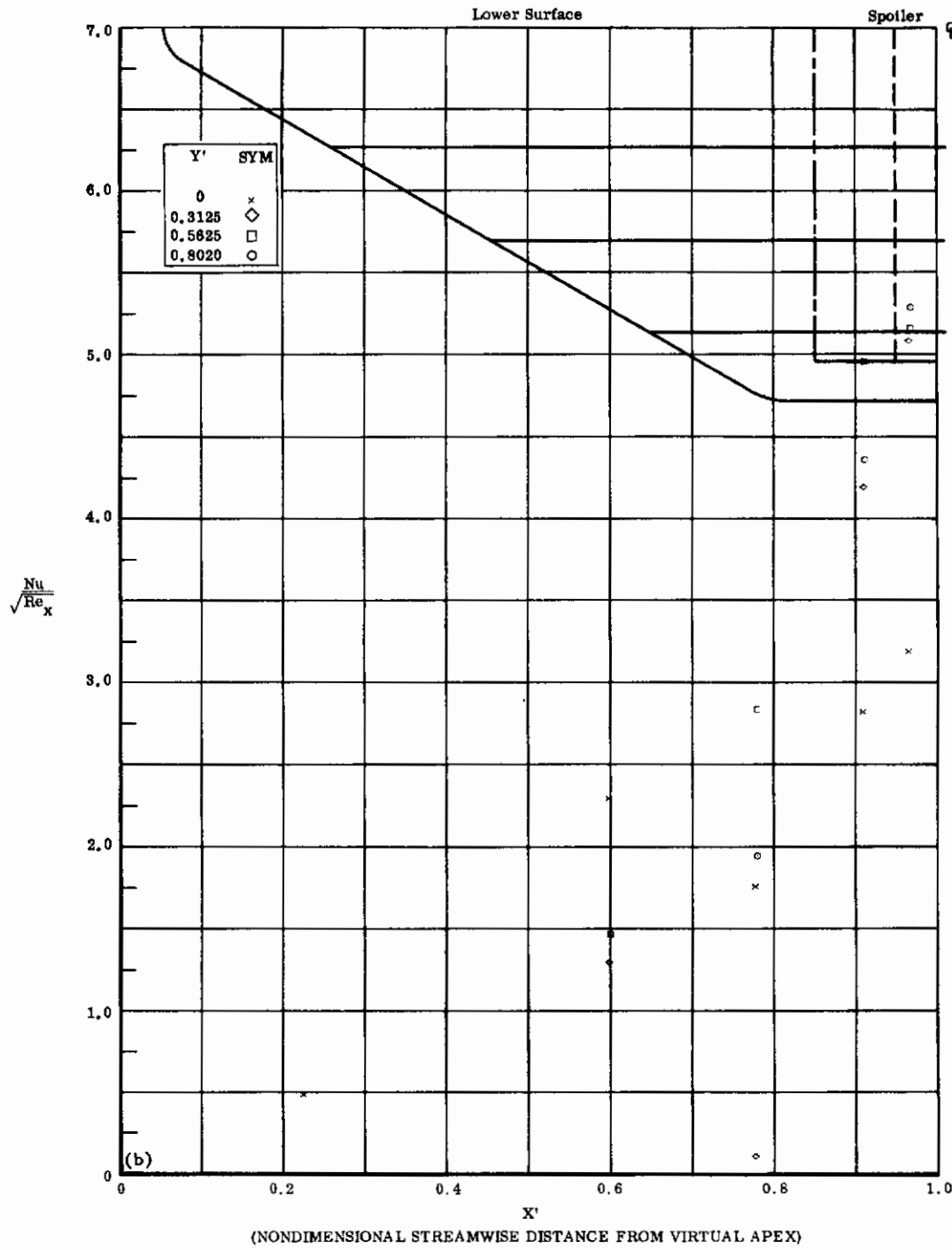


Fig. 35b Configuration IX, $\alpha = +20$, $\delta_2 = \delta_3 = 0$

$Nu/\sqrt{Re_x}$ vs. X' lower surface $Re_\infty/ft \times 10^{-6} = 3.3$

Contrails

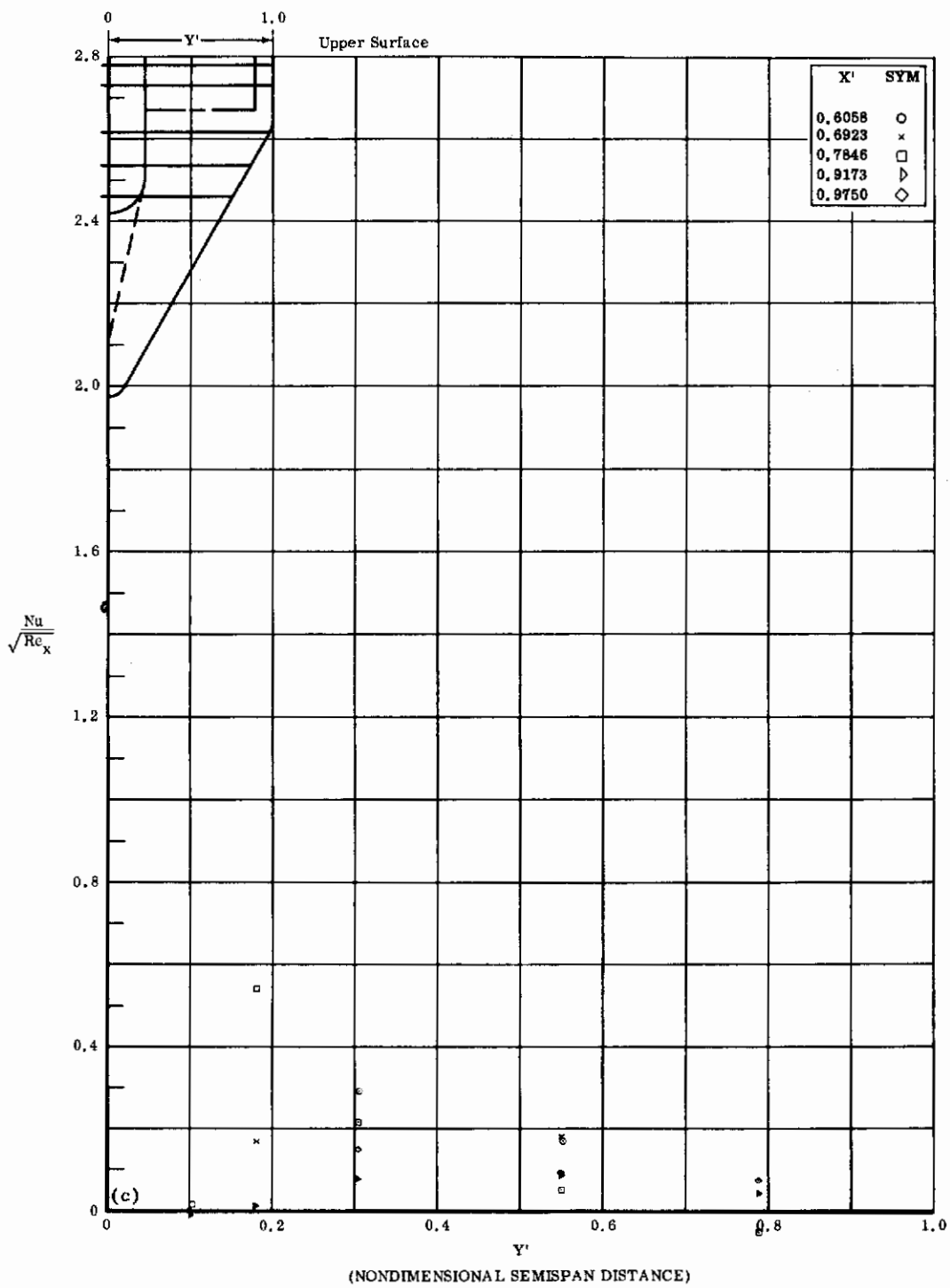


Fig. 35c Configuration IX, $\alpha = +20^\circ$, $s_2 = s_3 = 0$

$Nu/\sqrt{Re_x}$ vs. Y' upper surface $Re_\infty/\text{ft} \times 10^{-6} = 3.3$

Contrails

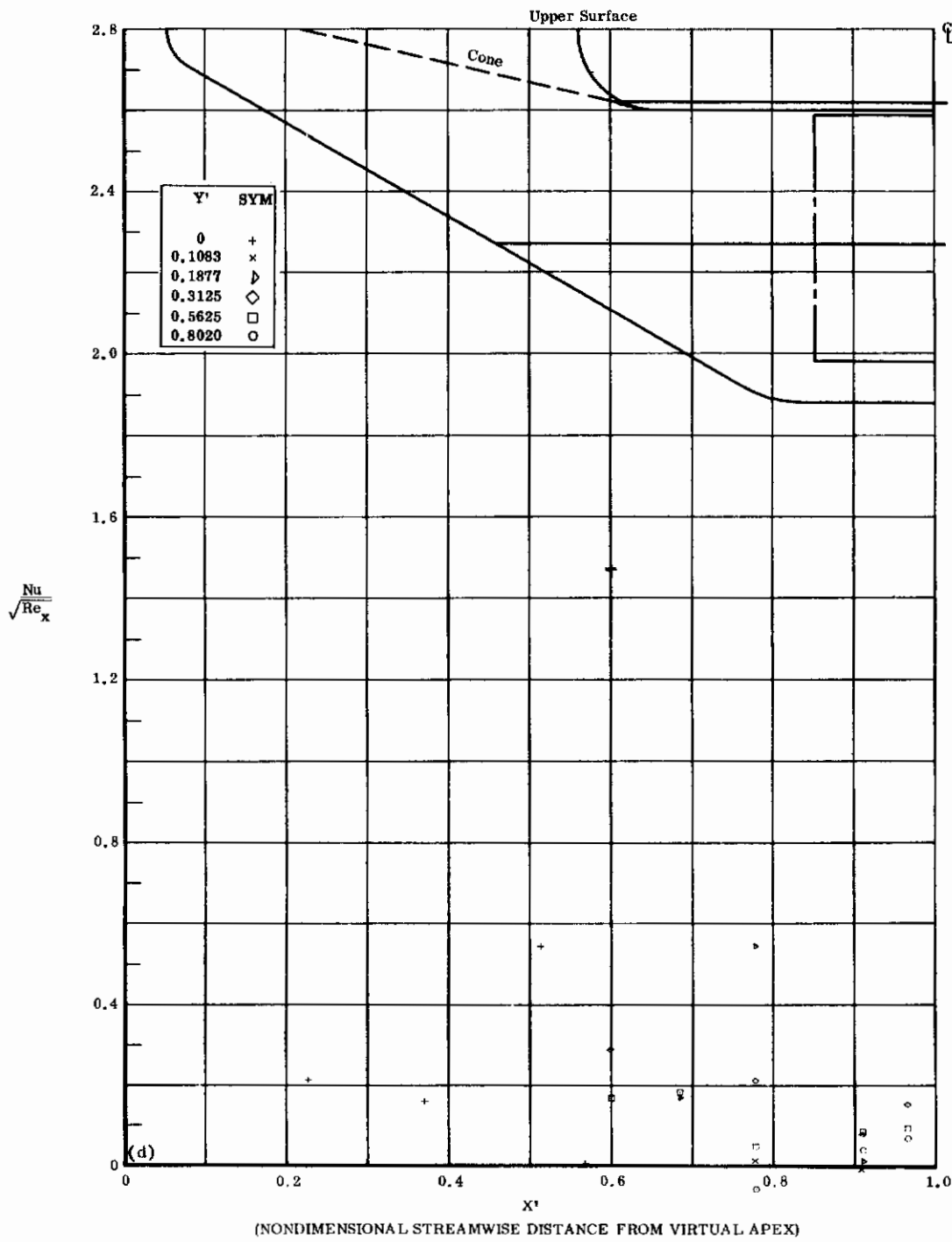


Fig. 35d Configuration IX, $\alpha = +20^\circ$, $\delta_2 = \delta_3 = 0$

$Nu/\sqrt{Re_x}$ vs. X' upper surface $Re_\infty/\text{ft} \times 10^{-6} = 3.3$

Contrails

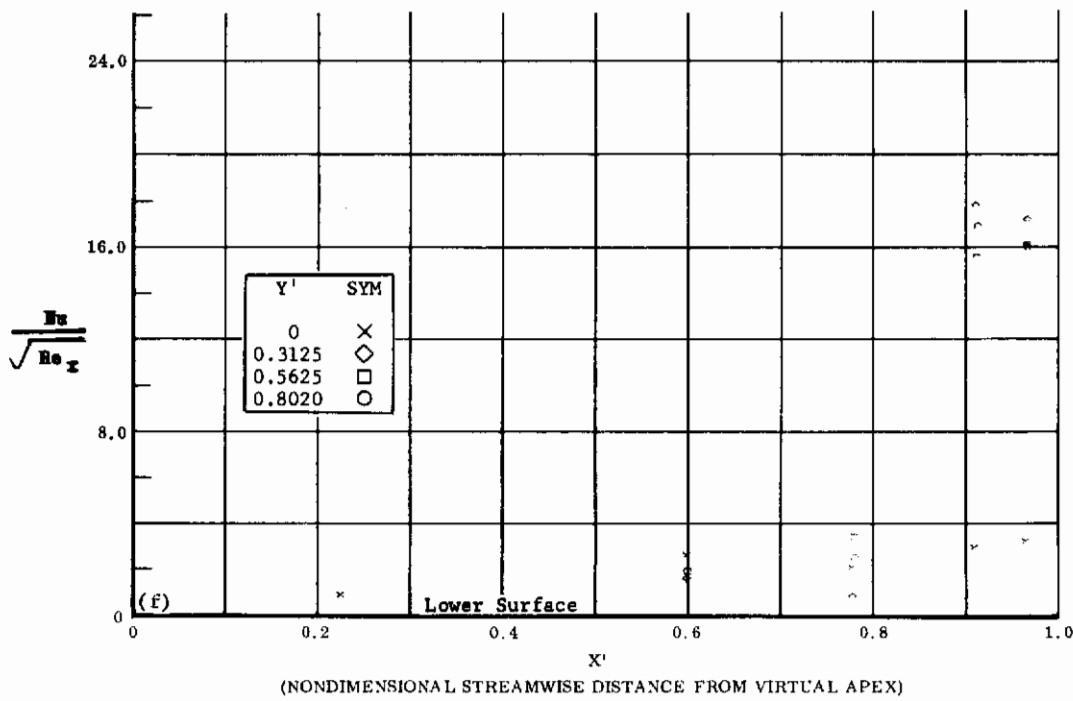
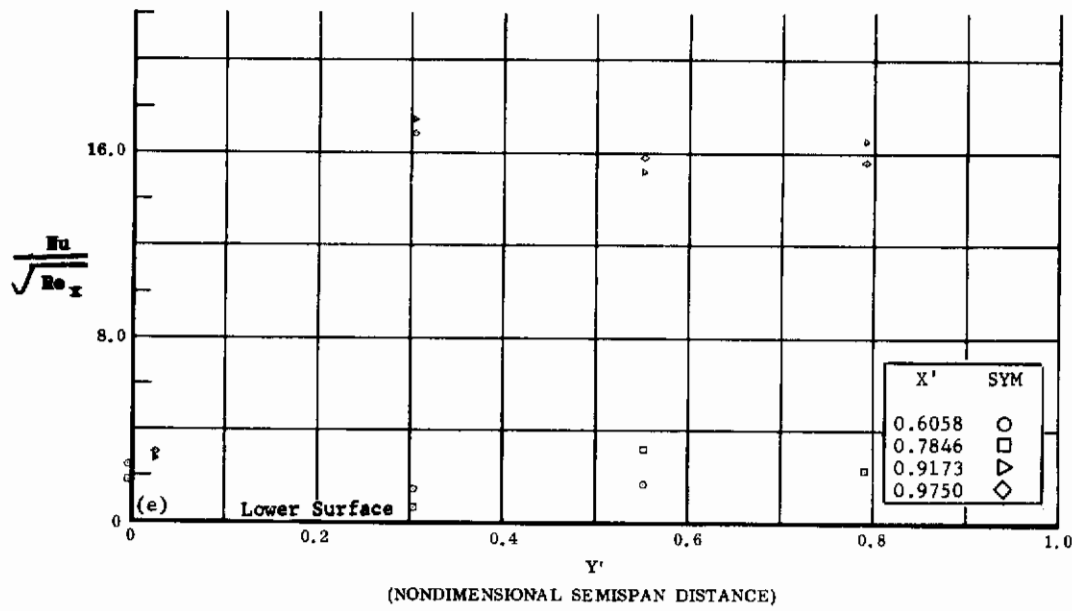


Fig. 35 Configuration IX, $\alpha = +20$, $b_2 = b_3 = +20$

e) $Nu/\sqrt{Re_x}$ vs. Y' lower surface $Re_\infty/\text{ft} \times 10^{-6} = 3.3$
 f) $Nu/\sqrt{Re_x}$ vs. X' lower surface

Contrails

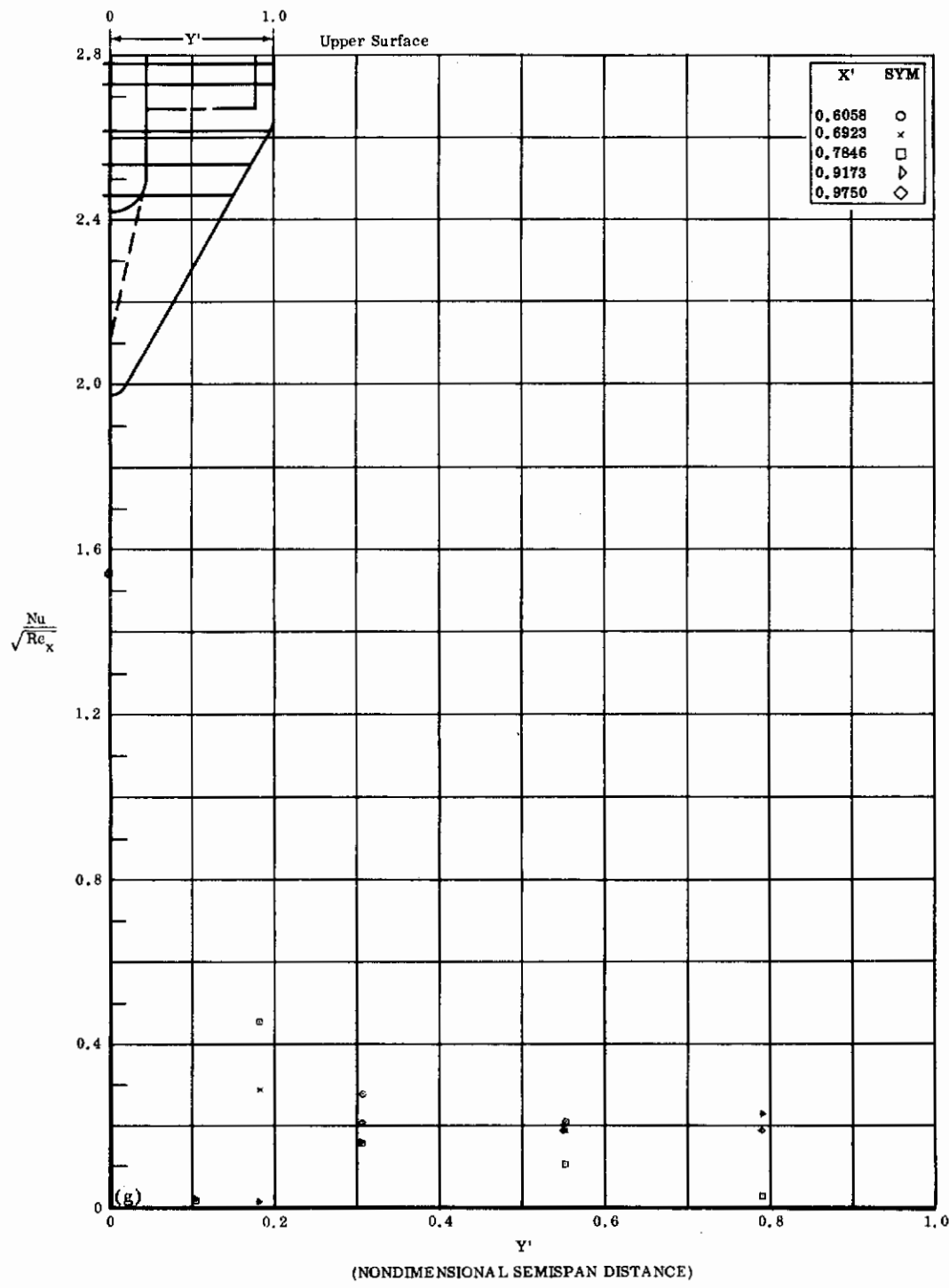


Fig. 35g Configuration IX, $\alpha = +20$, $b_2 = b_3 = +20$

$Nu/\sqrt{Re_x}$ vs. Y^* upper surface $Re_\infty/\text{ft} \times 10^{-6} = 3.3$

Contrails

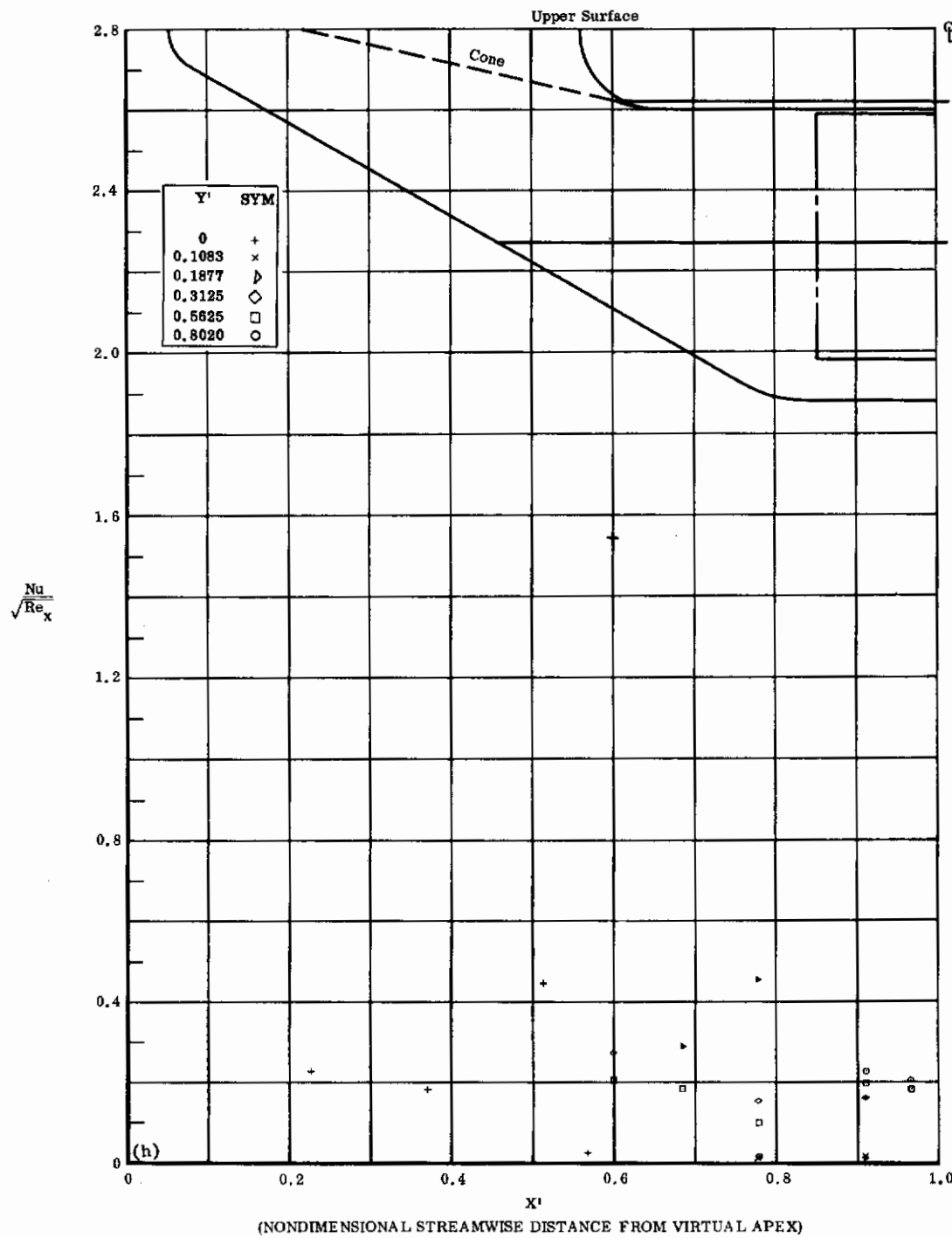


Fig. 35b Configuration IX, $\alpha = +20^\circ$, $\delta_2 = \delta_3 = +20^\circ$

$Nu/\sqrt{Re_x}$ vs. X' upper surface $Re_\infty/\text{ft} \times 10^{-6} = 3.3$

Contrails

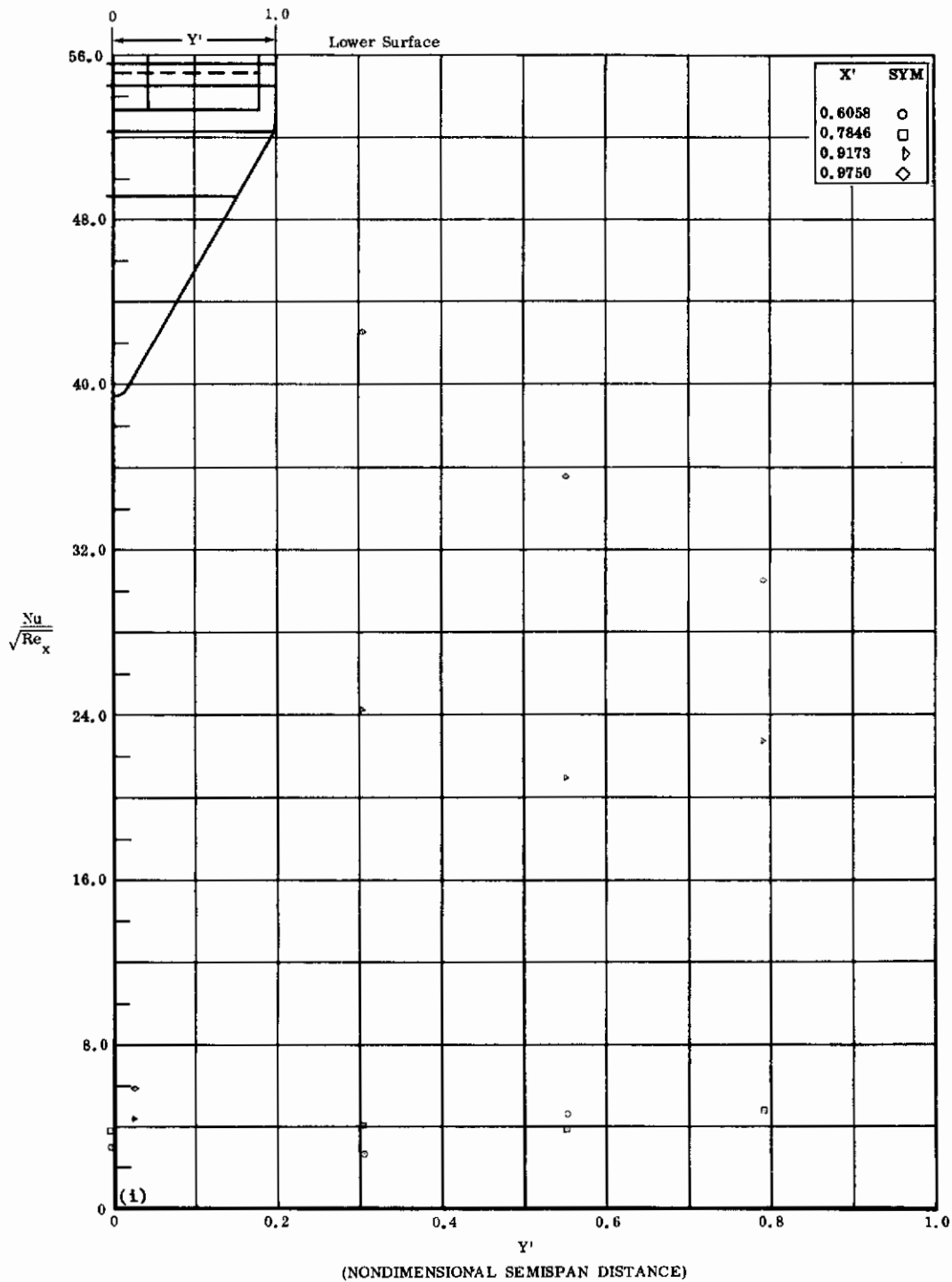


Fig. 35i Configuration IX, $\alpha = +20$, $\delta_2 = \delta_3 = +39$
 $Nu/\sqrt{Re_x}$ vs. Y' lower surface $Re_\infty/ft \times 10^{-6} = 3.3$

Contrails

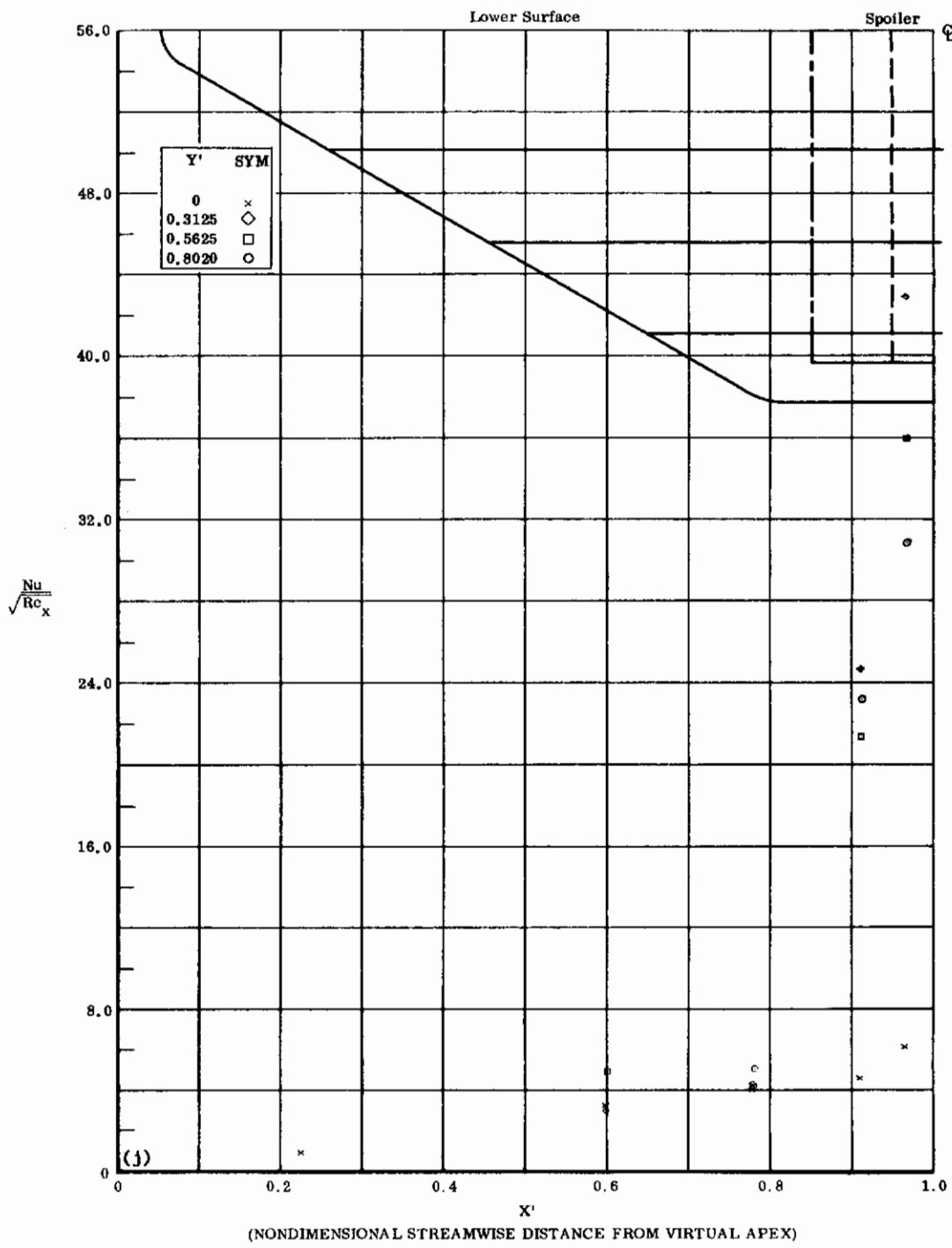


Fig. 35j Configuration IX, $\alpha = +20$, $\delta_2 = \delta_3 = +39$

$Nu/\sqrt{Re_x}$ vs. X' lower surface $Re_\infty/\text{ft} \times 10^{-6} = 3.3$

Contrails

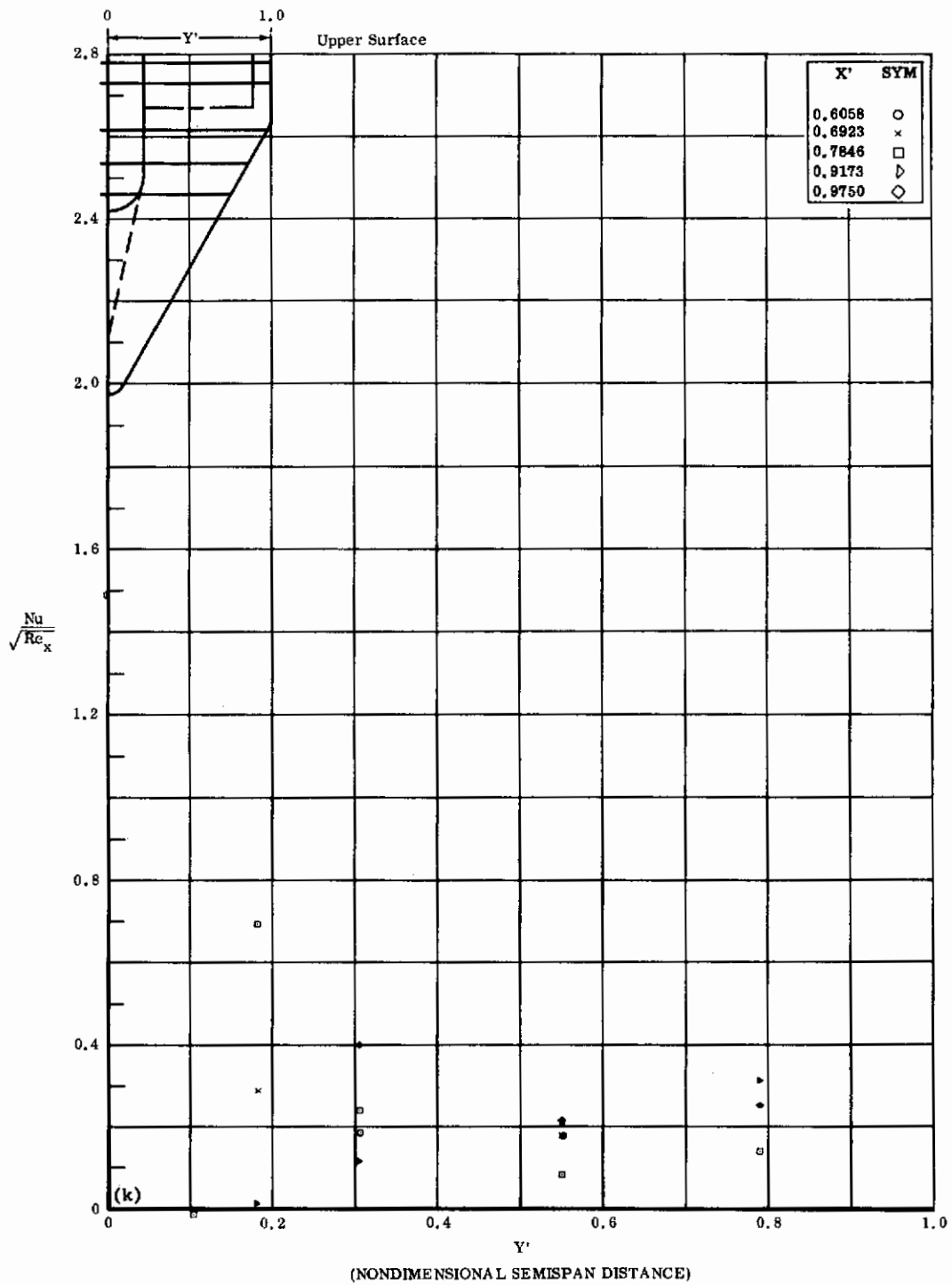


Fig. 35k Configuration IX, $\alpha = +20$, $\delta_2 = \delta_3 = +39$

$Nu/\sqrt{Re_x}$ vs. Y' upper surface $Re_\infty/ft \times 10^{-6} = 3.3$

Contrails

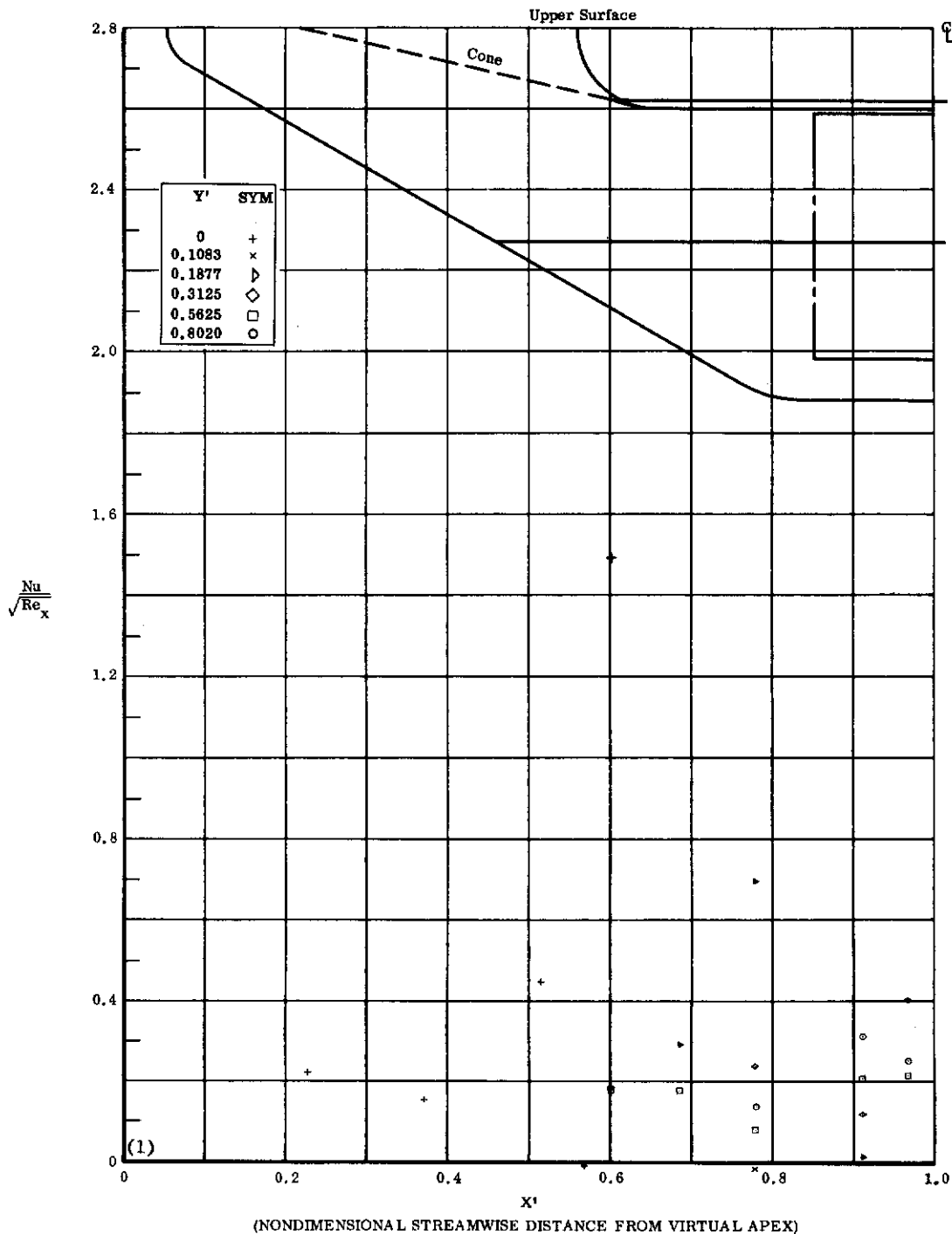


Fig. 35 ℓ Configuration IX, $\alpha = +20^\circ$, $\delta_2 = \delta_3 = +39^\circ$
 $\frac{Nu}{\sqrt{Re_x}}$ vs. X^* upper surface $Re_\infty/\text{ft} \times 10^{-6} = 3.3$

Contrails

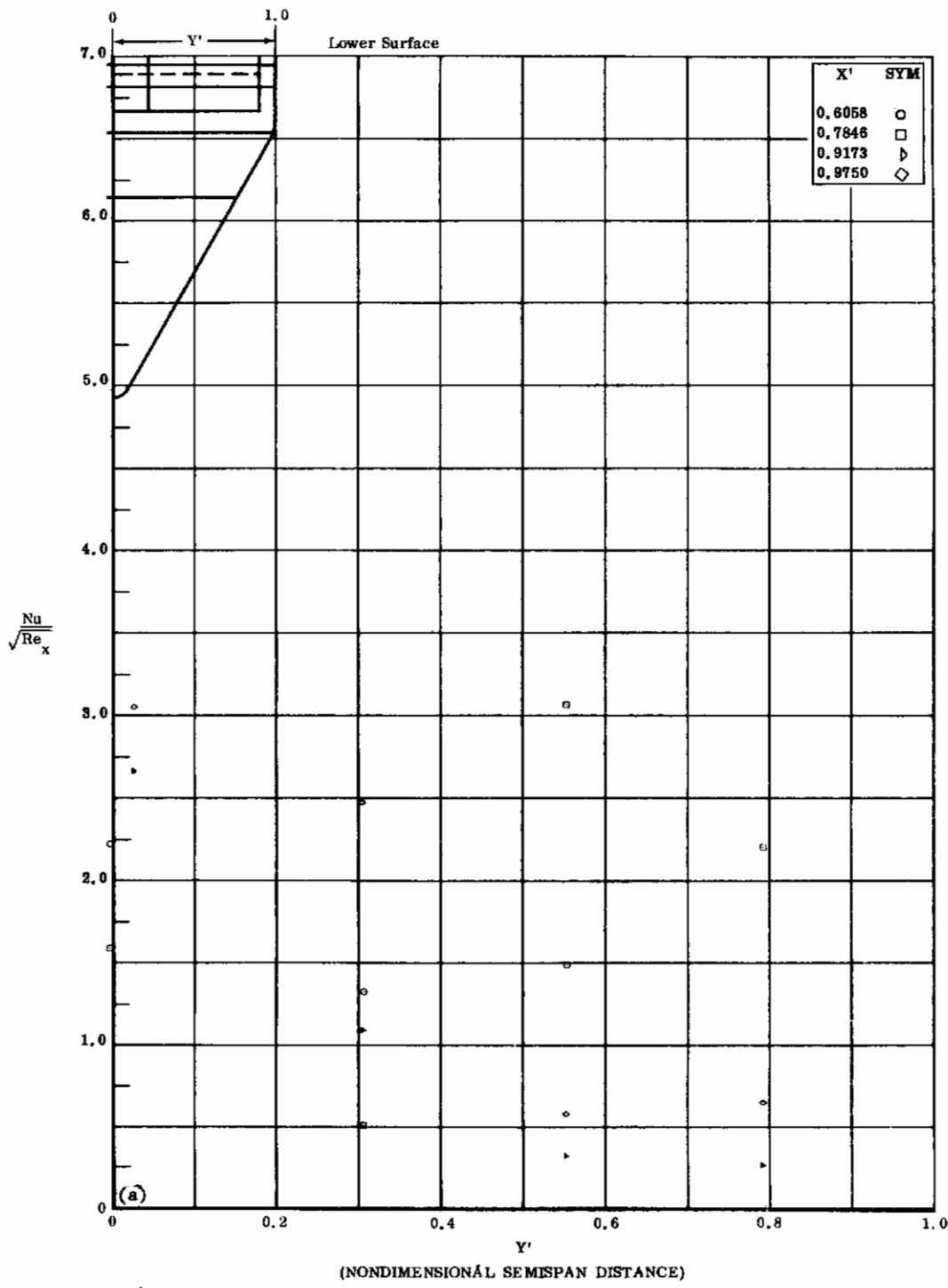


Fig. 36a Configuration IX, $\alpha = +20$, $b_2 = b_3 = -20$
 $Nu/\sqrt{Re_x}$ vs. Y' lower surface $Re_\infty/ft \times 10^{-6} = 3.3$

Contrails

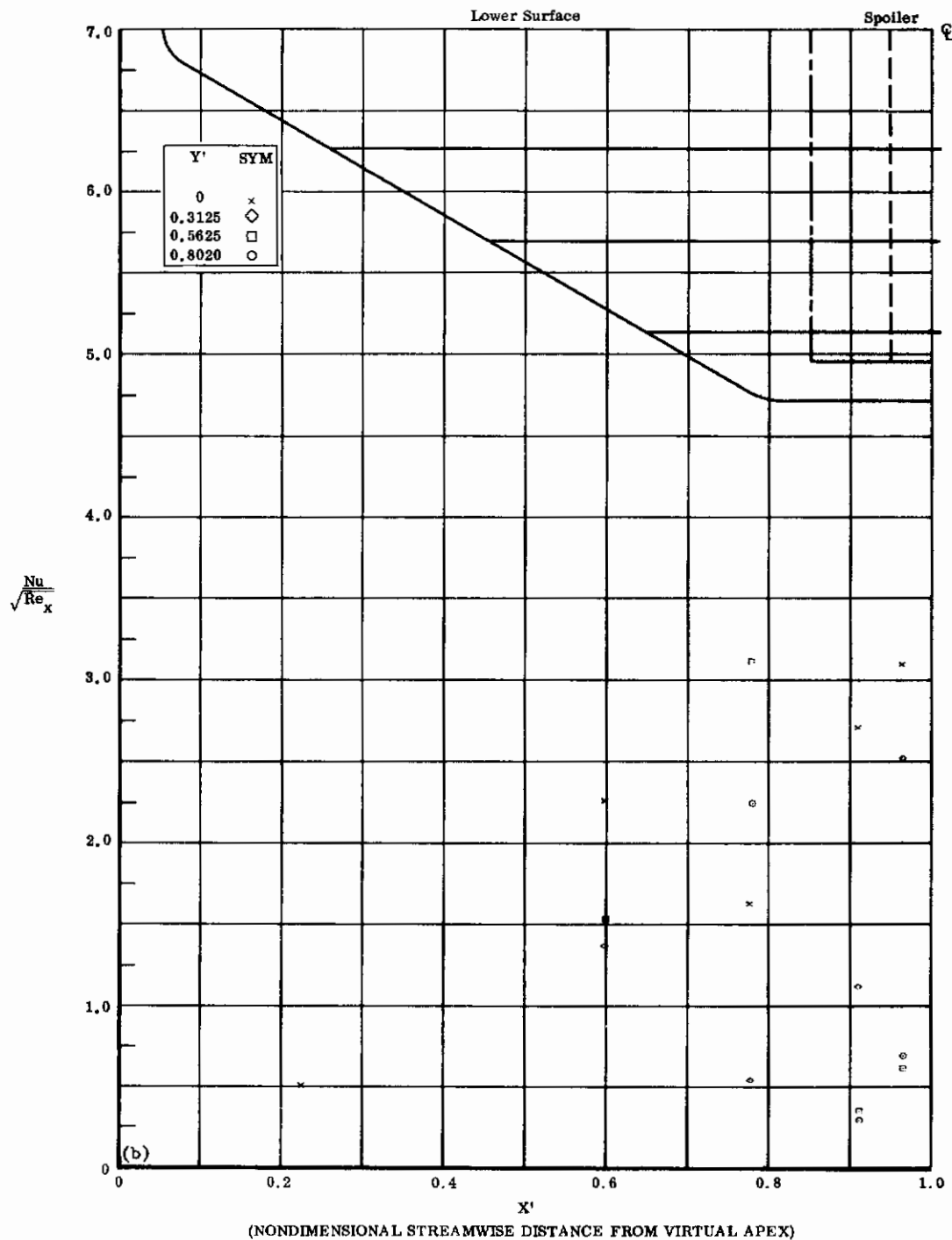


Fig. 36b Configuration IX, $\alpha = +20$, $\delta_2 = \delta_3 = -20$

$$Nu/\sqrt{Re_x} \text{ vs. } X' \text{ lower surface } Re_\infty/\text{ft} \times 10^{-6} = 3.3$$

Contrails

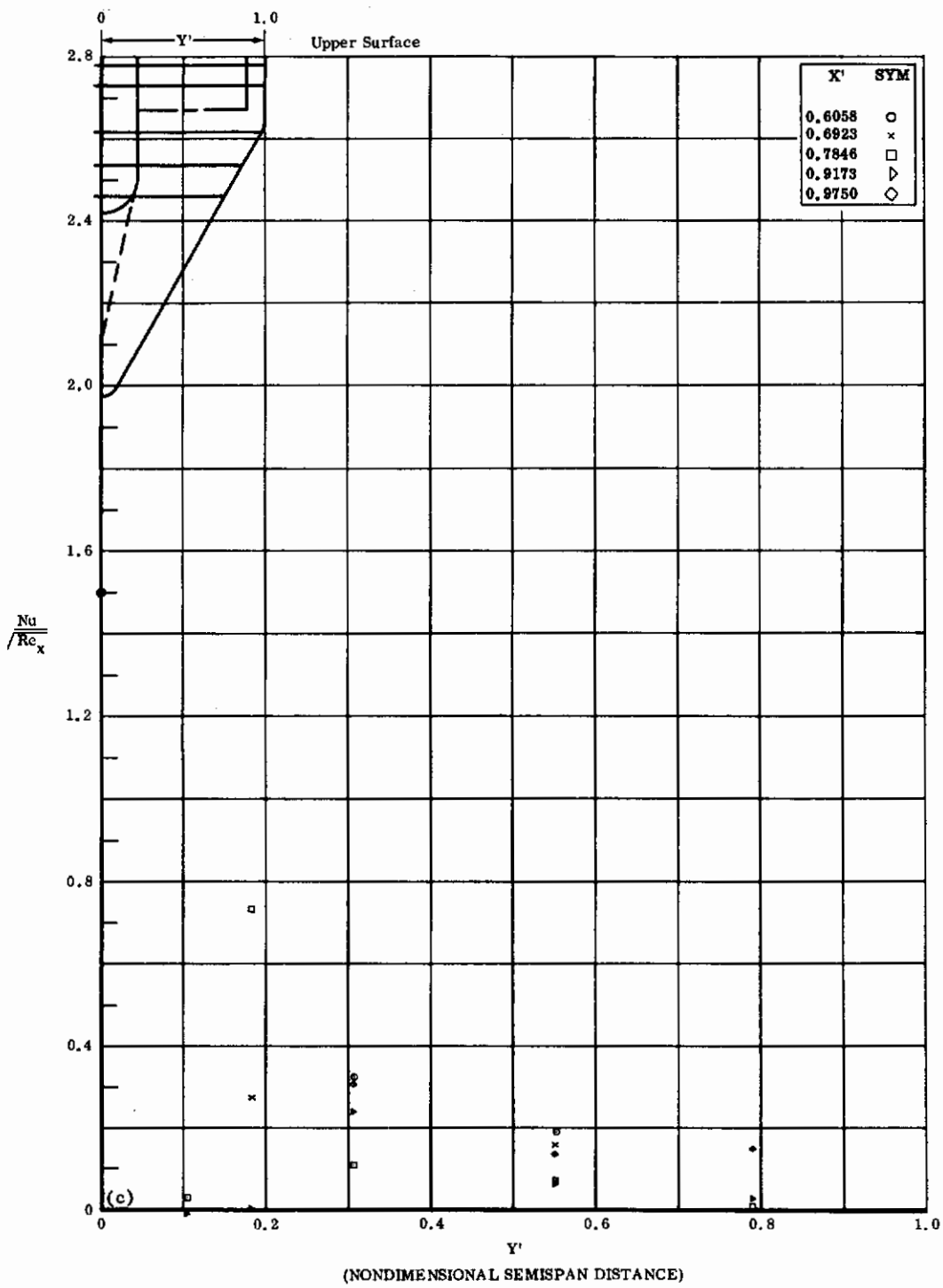


Fig. 36c Configuration IX, $\alpha = +20$, $\delta_2 = \delta_3 = -20$
 $\frac{Nu}{Re_x}$ vs. Y' upper surface $Re_\infty/ft \times 10^{-6} = 3.3$

Contrails

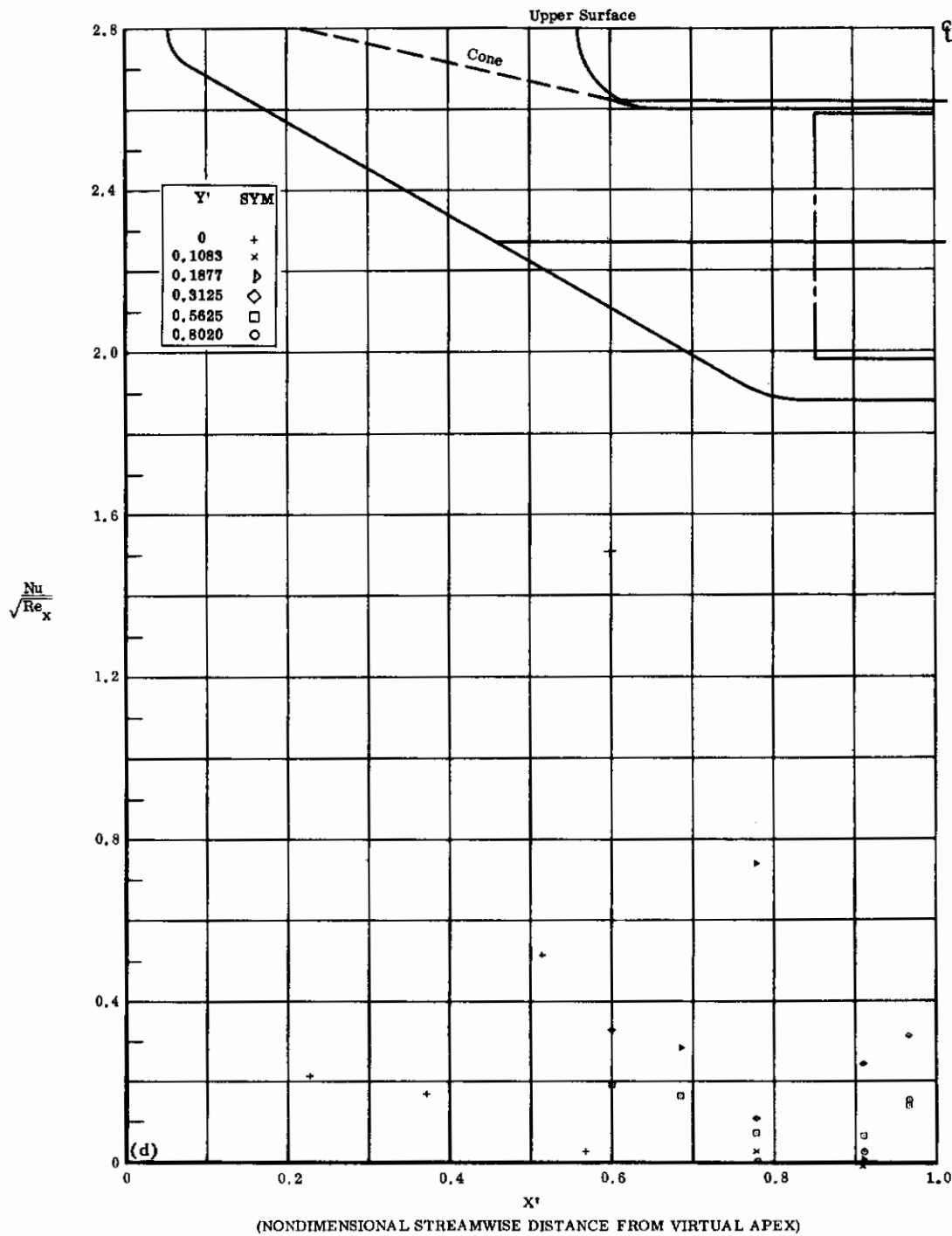


Fig. 36d Configuration IX, $\alpha = +20^\circ$, $\delta_2 = \delta_3 = -20^\circ$

$Nu/\sqrt{Re_x}$ vs. X' upper surface $Re_\infty/\text{ft} \times 10^{-6} = 3.3$

Contrails

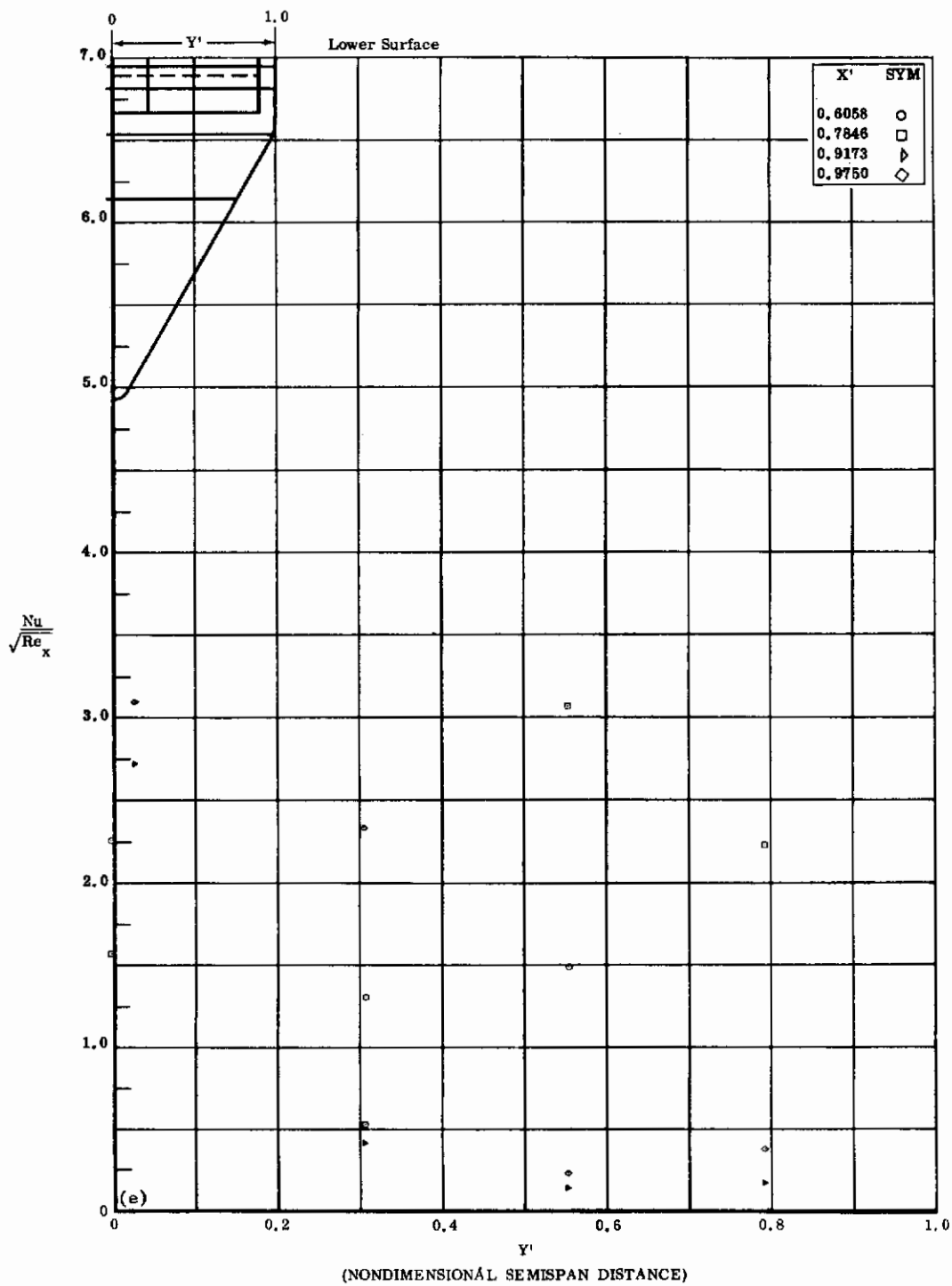


Fig. 36e Configuration IX, $\alpha = +20$, $\delta_2 = \delta_3 = -39$

$Nu/\sqrt{Re_x}$ vs. Y' lower surface $Re_\infty/ft \times 10^{-6} = 3.3$

Contrails

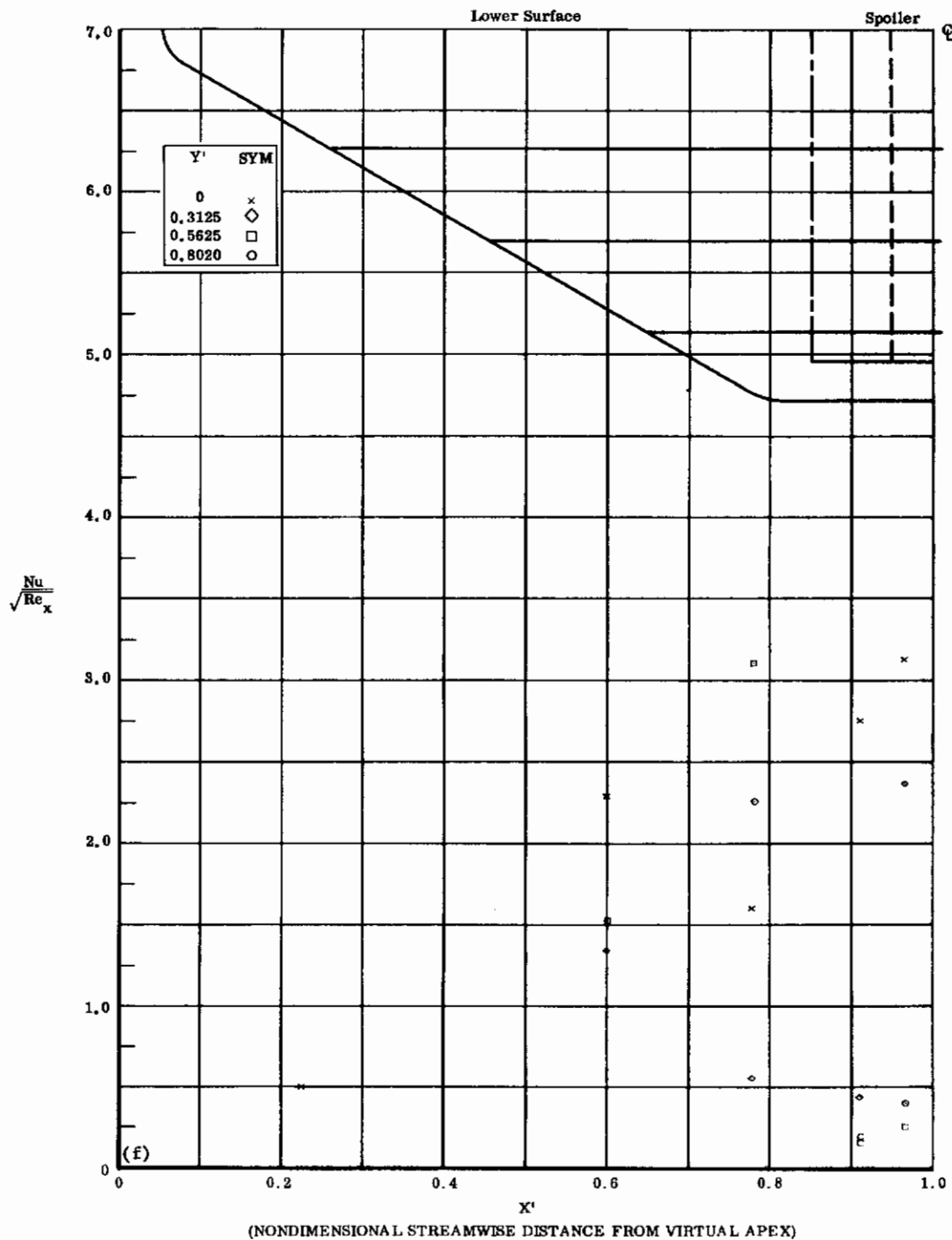


Fig. 36f Configuration IX, $\alpha = +20^\circ$, $b_2 = b_3 = -39^\circ$
 $Nu/\sqrt{Re_x}$ vs. X^1 lower surface $Re_\infty/\text{ft} \times 10^{-6} = 3.3$

Contrails

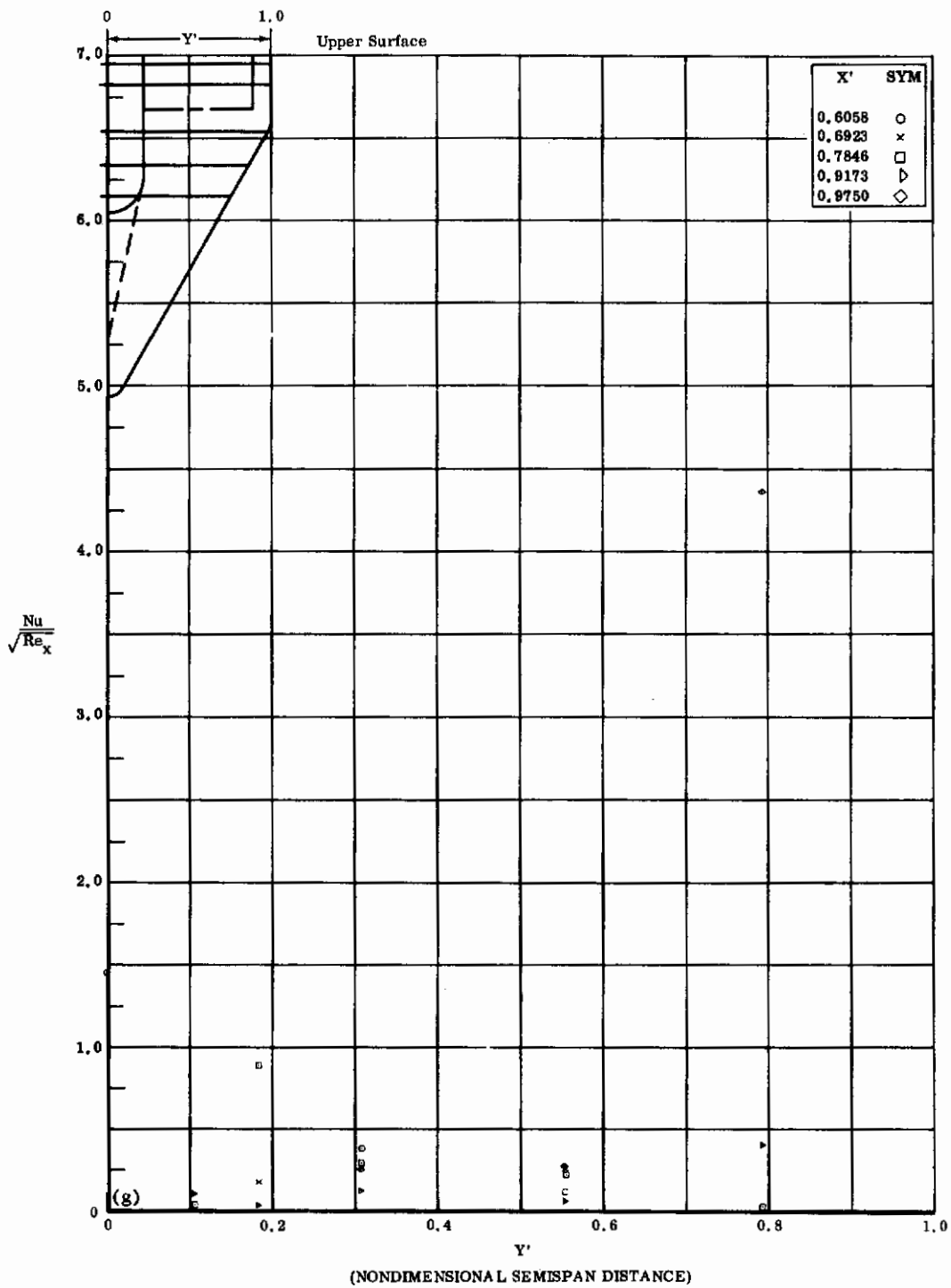


Fig. 36g Configuration IX, $\alpha = +20$, $\delta_2 = \delta_3 = -39$
 $\text{Nu}/\sqrt{\text{Re}_x}$ vs. Y' upper surface $\text{Re}_{\infty}/\text{ft} \times 10^{-6} = 3.3$

Contrails

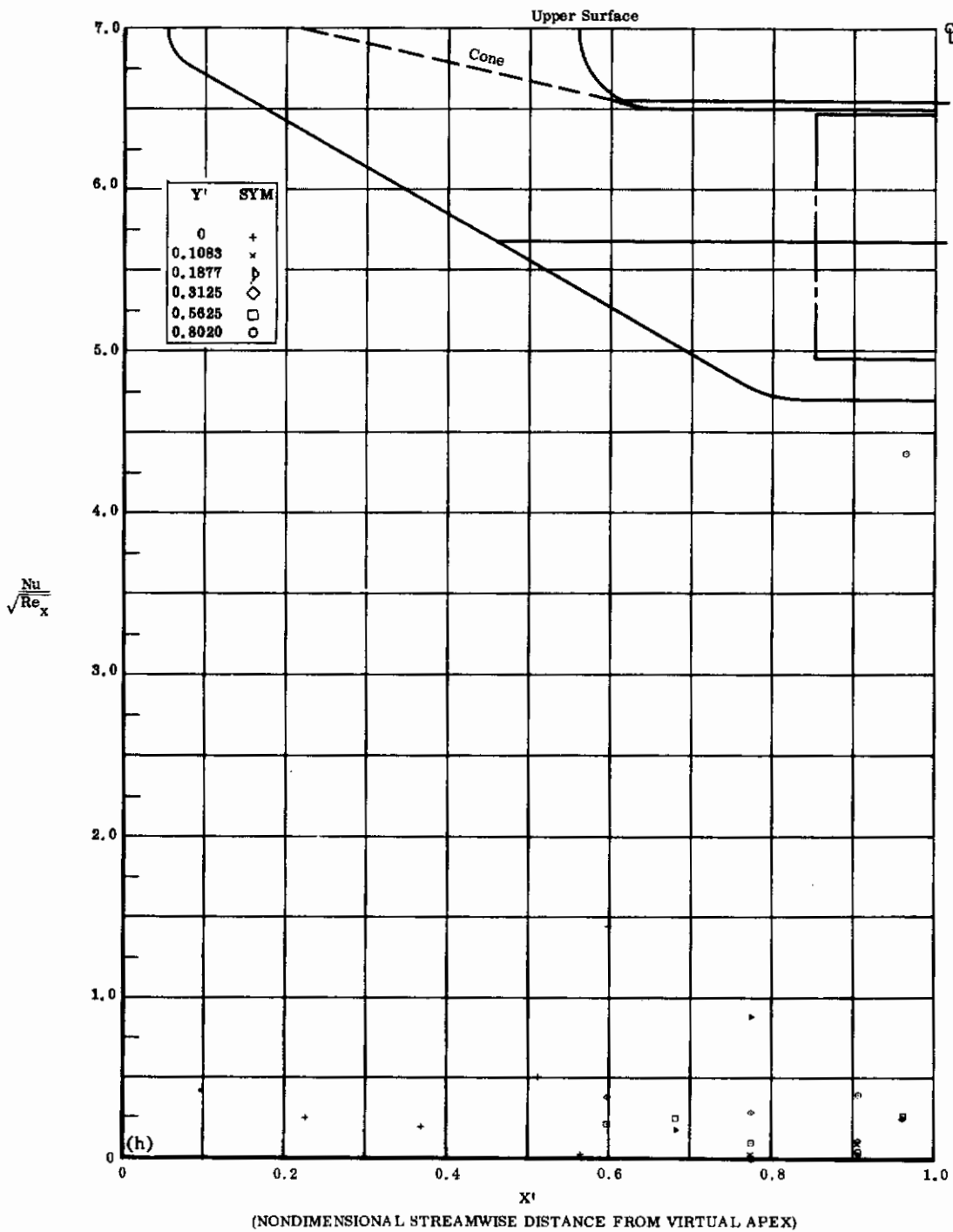


Fig. 36h Configuration IX, $\alpha = +20^\circ$, $\delta_2 = \delta_3 = -39^\circ$

$Nu/\sqrt{Re_x}$ vs. X' upper surface $Re_\infty/ft \times 10^{-6} = 3.3$

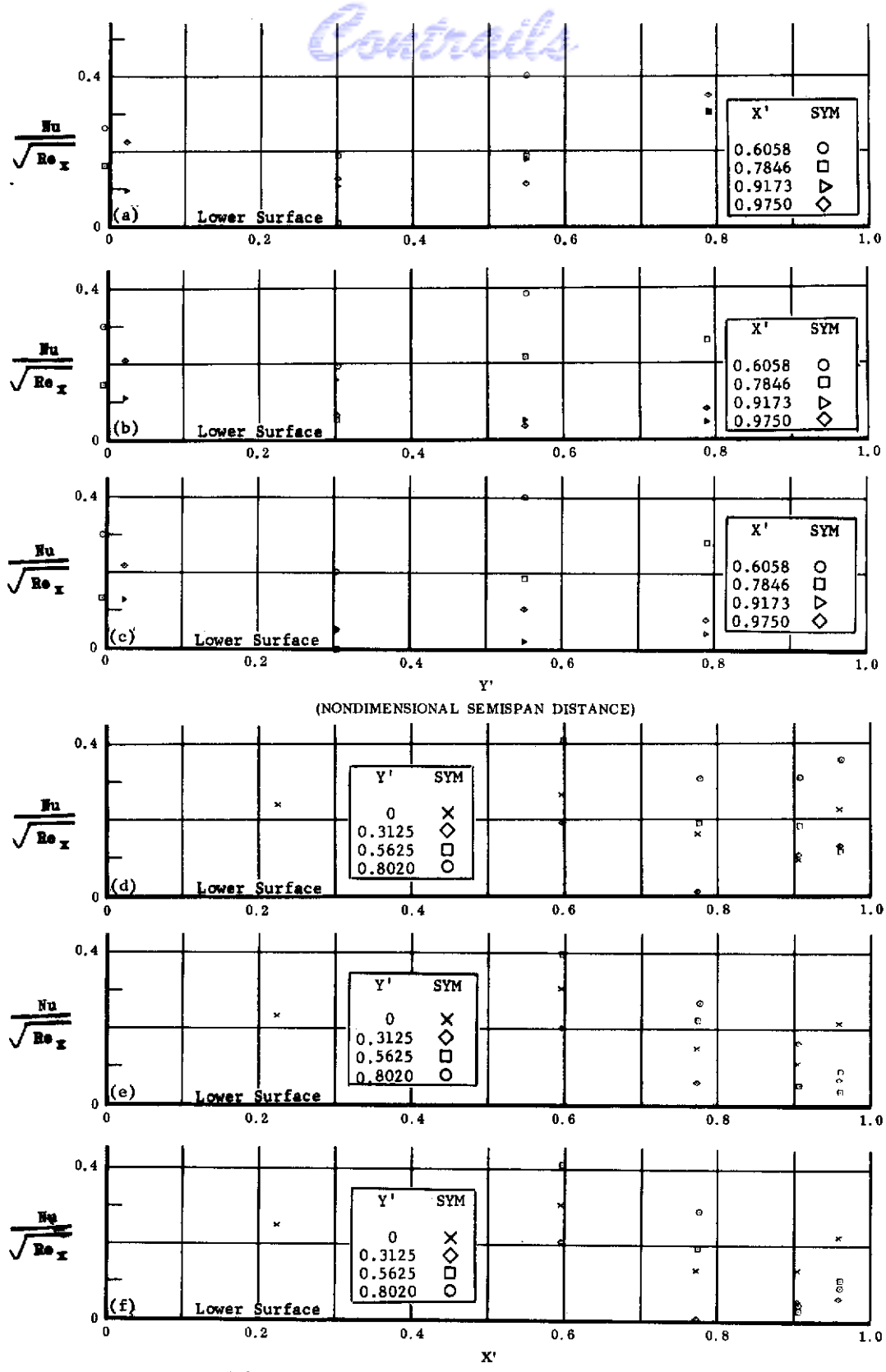


Fig. 37 Configuration IX, $\alpha = 0$, lower surface
a) $Nu/\sqrt{Re_x}$ vs. Y' , $\delta_2 = \delta_3 = 0$

b) $Nu/\sqrt{Re_x}$ vs. Y' , $\delta_2 = \delta_3 = -20$

c) $Nu/\sqrt{Re_x}$ vs. Y' , $\delta_2 = \delta_3 = -39$

d) $Nu/\sqrt{Re_x}$ vs. X' , $\delta_2 = \delta_3 = 0$ $Re_\infty/\text{ft} \times 10^{-6} = 1.1$

e) $Nu/\sqrt{Re_x}$ vs. X' , $\delta_2 = \delta_3 = -20$

f) $Nu/\sqrt{Re_x}$ vs. X' , $\delta_2 = \delta_3 = -39$

Contrails

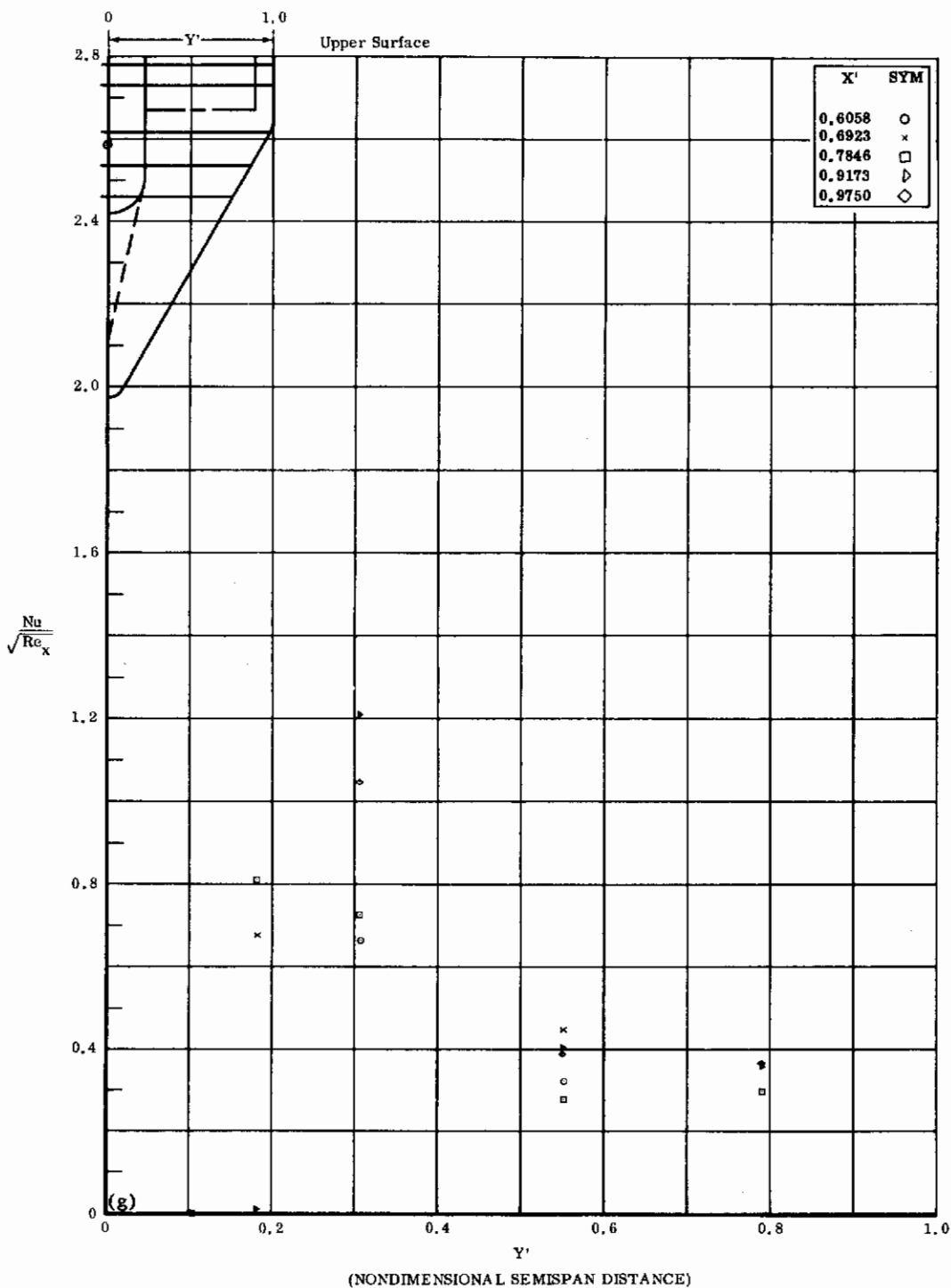


Fig. 37g Configuration IX, $\alpha = 0$, $\delta_2 = \delta_3 = 0$

$Nu/\sqrt{Re_x}$ vs. Y' upper surface $Re_\infty/ft \times 10^{-6} = 1.1$

Contrails

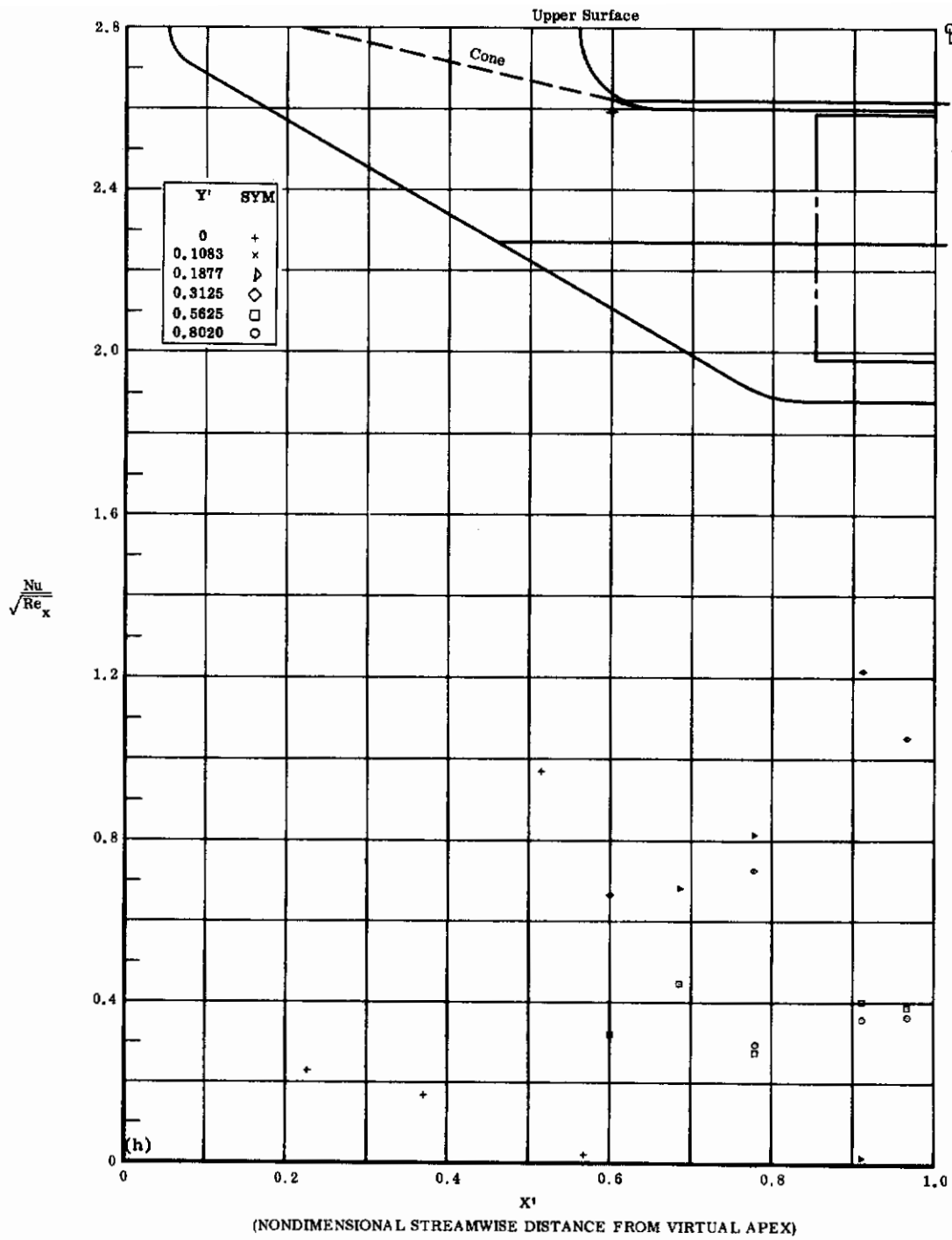


Fig. 37h Configuration IX, $\alpha = 0$, $\delta_2 = \delta_3 = 0$

$Nu/\sqrt{Re_x}$ vs. X' upper surface $Re_\infty/\text{ft} \times 10^{-6} = 1.1$

Contrails

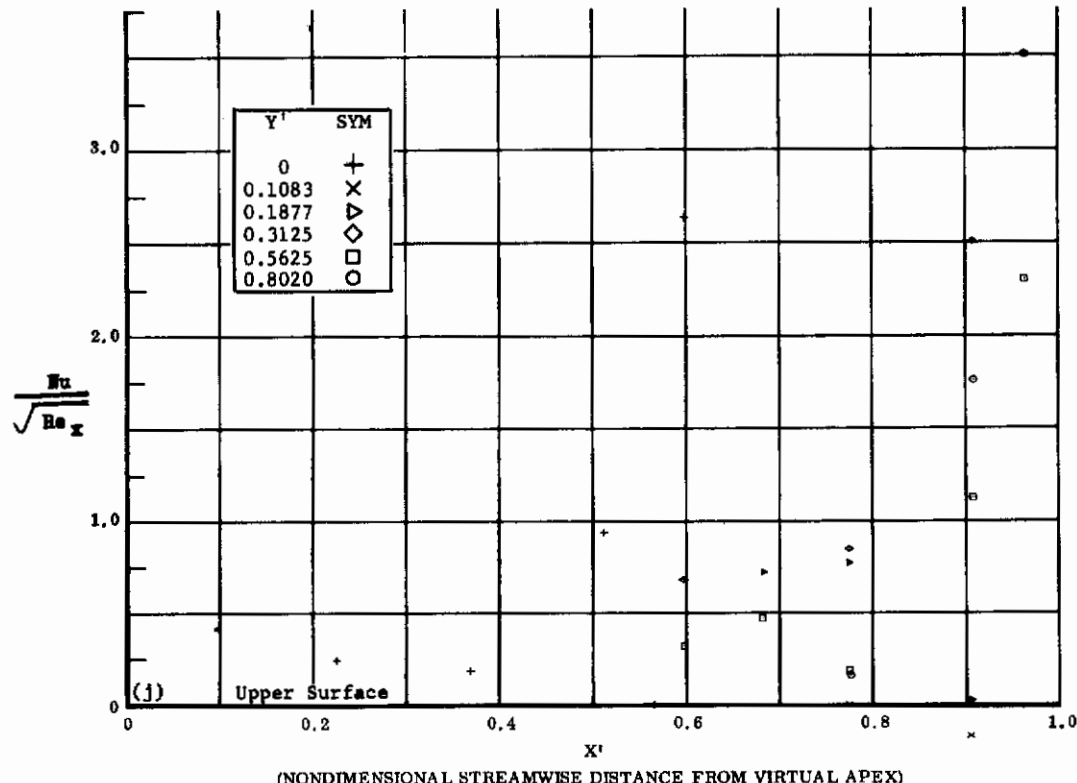
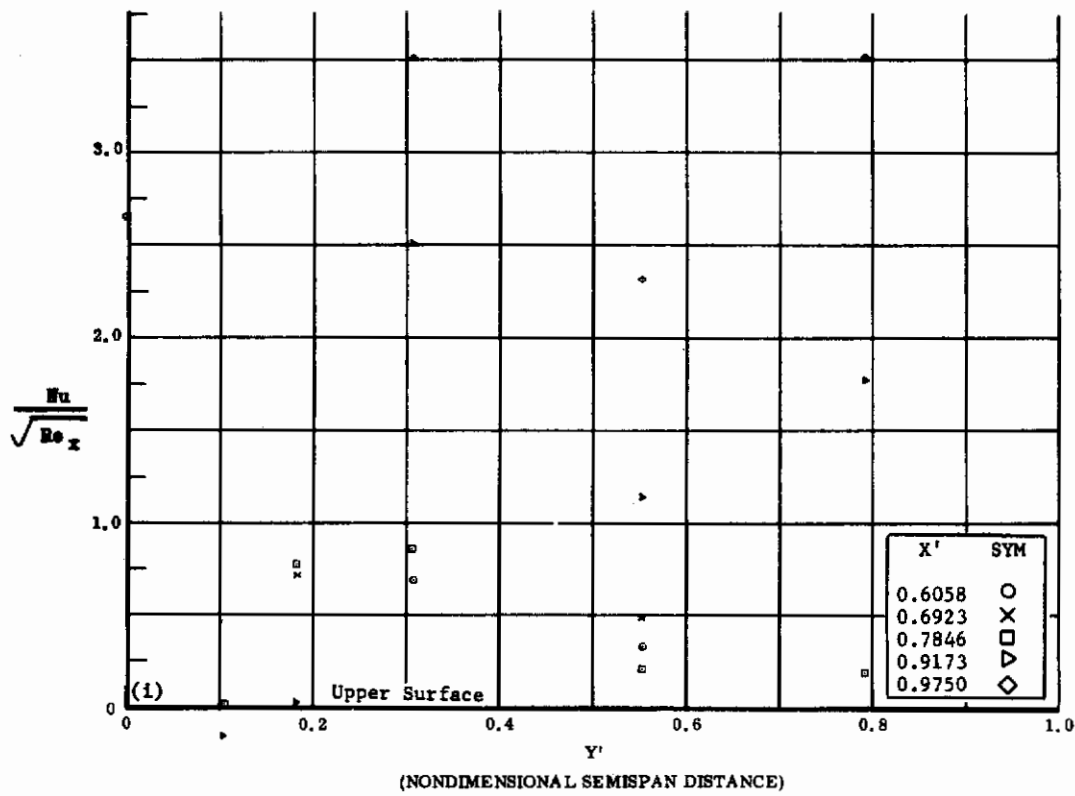


Fig. 37 Configuration IX, $\alpha = 0$, $b_2 = b_3 = -20$

i) $Nu/\sqrt{Re_x}$ vs. Y' upper surface

$Re_\infty/\text{ft} \times 10^{-6} = 1.1$

j) $Nu/\sqrt{Re_x}$ vs. X' upper surface

Contrails

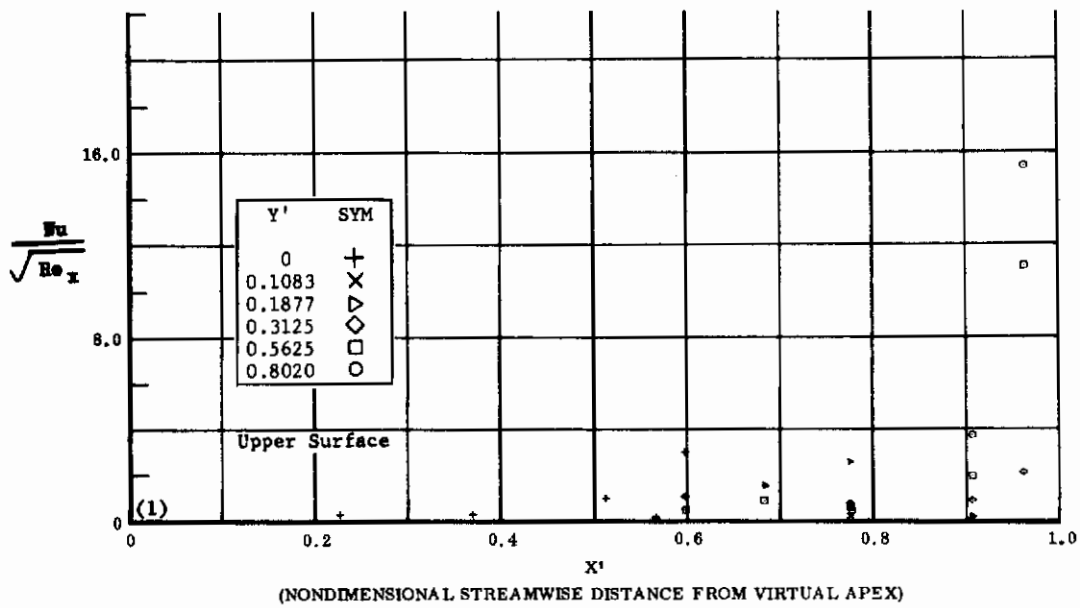
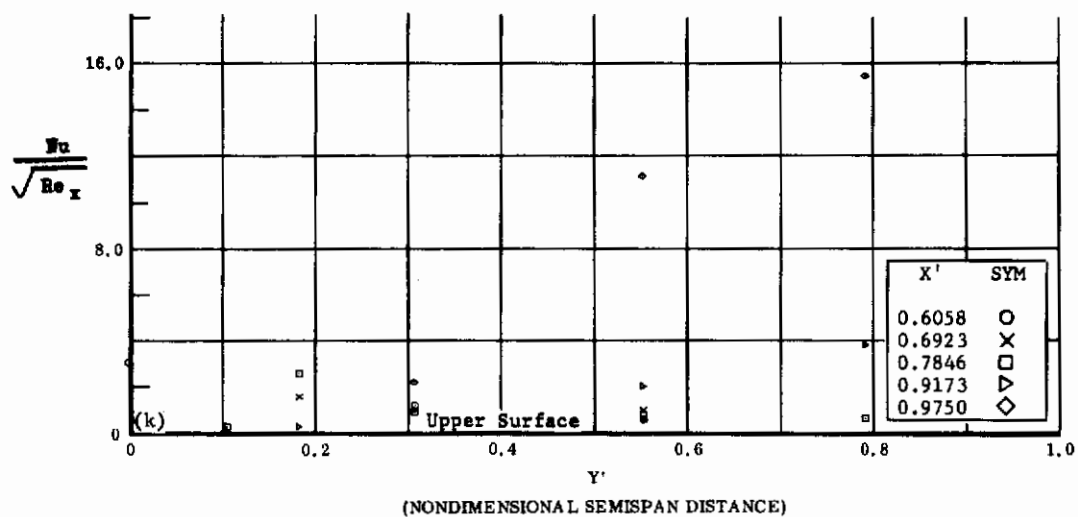


Fig. 37 Configuration IX, $\alpha = 0$, $b_2 = b_3 = -39$

k) $\text{Nu}/\sqrt{\text{Re}_x}$ vs. Y' upper surface $\text{Re}_{\infty}/\text{ft} \times 10^{-6} = 1.1$

l) $\text{Nu}/\sqrt{\text{Re}_x}$ vs. X' upper surface

Contrails

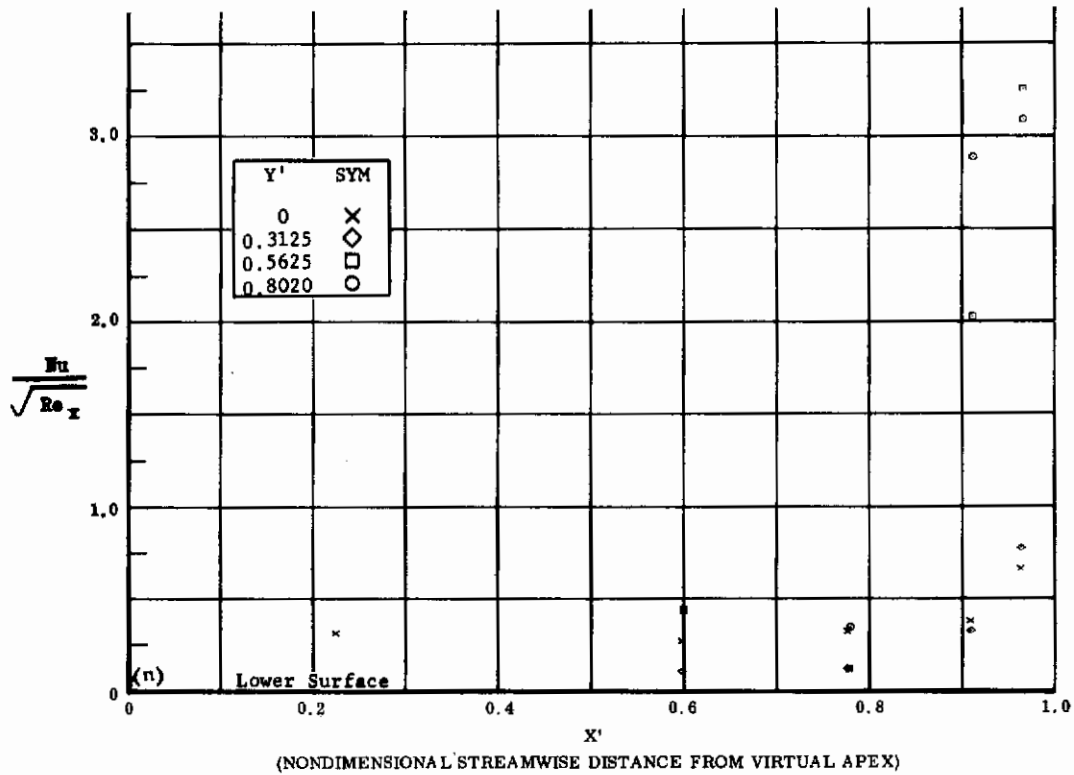
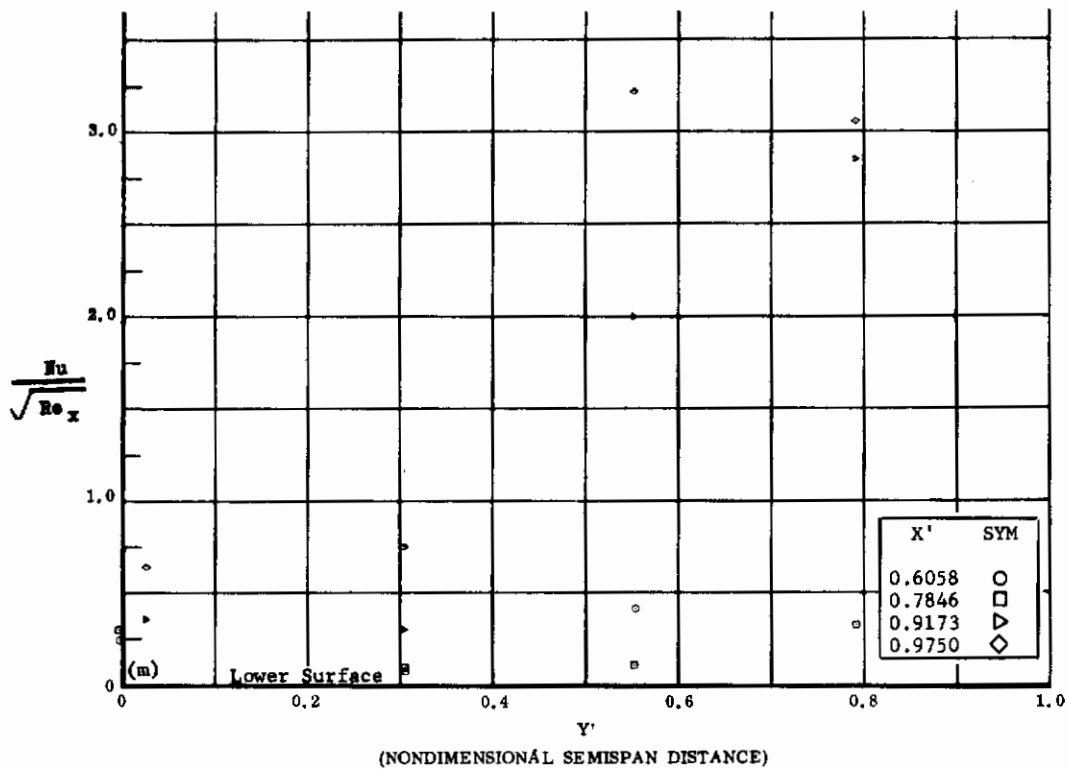


Fig. 37 Configuration IX, $\alpha = 0$, $\delta_2 = \delta_3 = +20$

- m) $Nu/\sqrt{Re_x}$ vs. Y' lower surface $Re_\infty/\text{ft} \times 10^{-6} = 1.1$
- n) $Nu/\sqrt{Re_x}$ vs. X' lower surface

Contrails

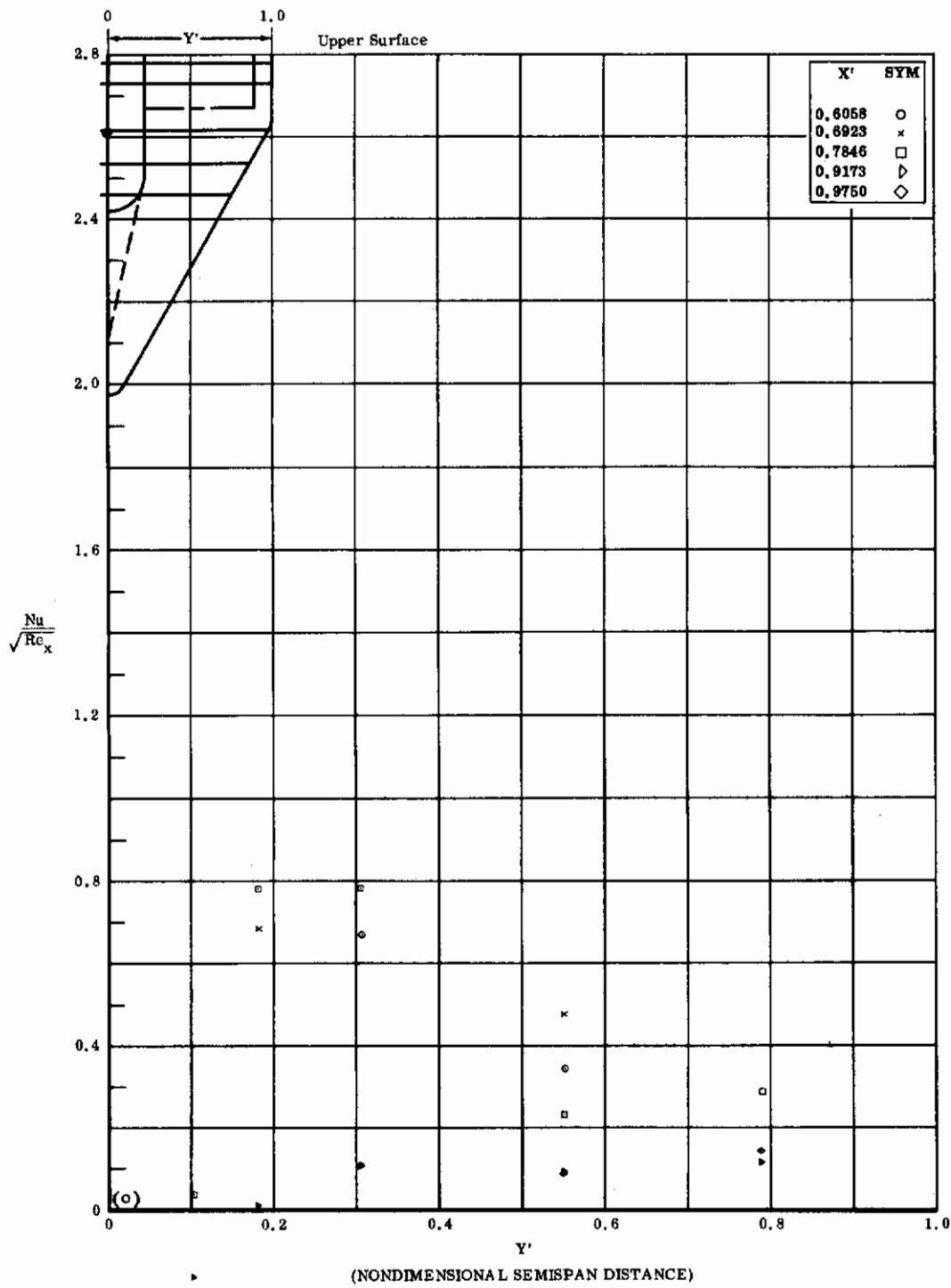


Fig. 37a Configuration IX, $\alpha = 0$, $\delta_2 = \delta_3 = +20$

$Nu/\sqrt{Re_x}$ vs. Y' upper surface $Re_\infty/ft \times 10^{-6} = 1.1$

Contrails

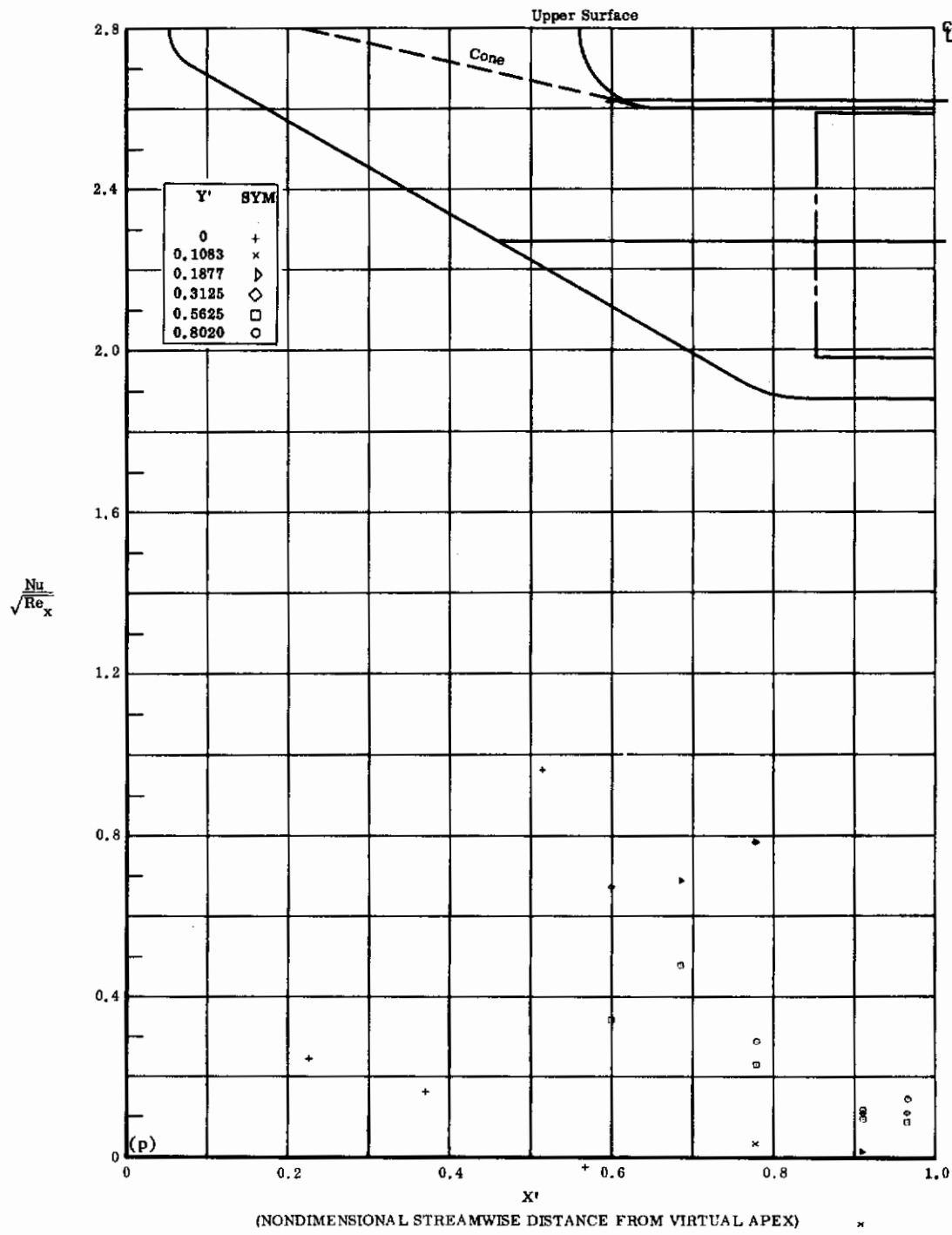


Fig. 37p Configuration IX, $\alpha = 0$, $\delta_2 = \delta_3 = +20$
 $\text{Nu}/\sqrt{\text{Re}_x}$ vs. X' upper surface $\text{Re}_\infty/\text{ft} \times 10^{-6} = 1.1$

Contrails

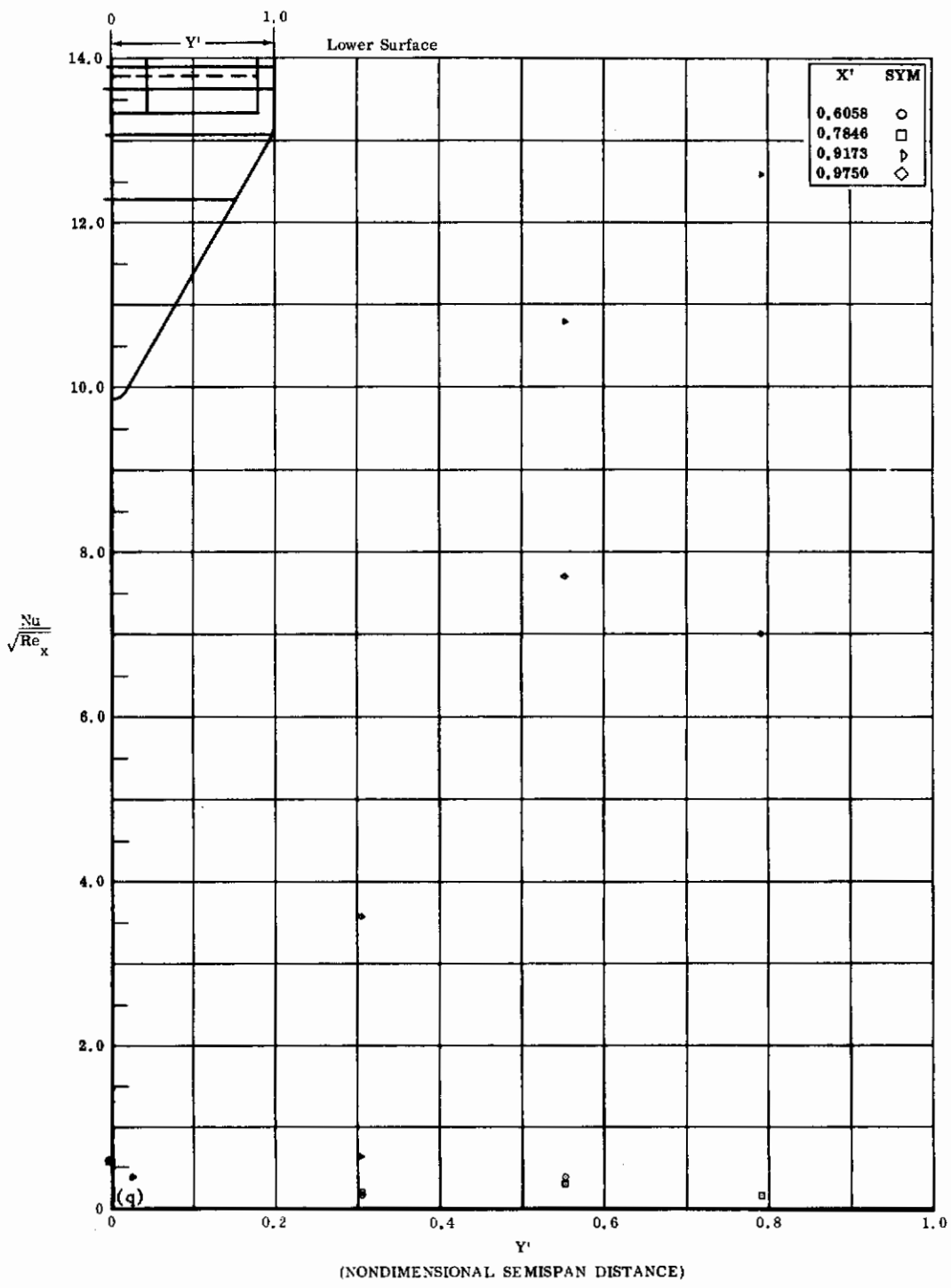


Fig. 37q Configuration IX, $\alpha = 0$, $\delta_2 = \delta_3 = +39$
 $Nu/\sqrt{Re_x}$ vs. Y^i lower surface $Re_\infty/\text{ft} \times 10^{-6} = 1.1$

Contrails

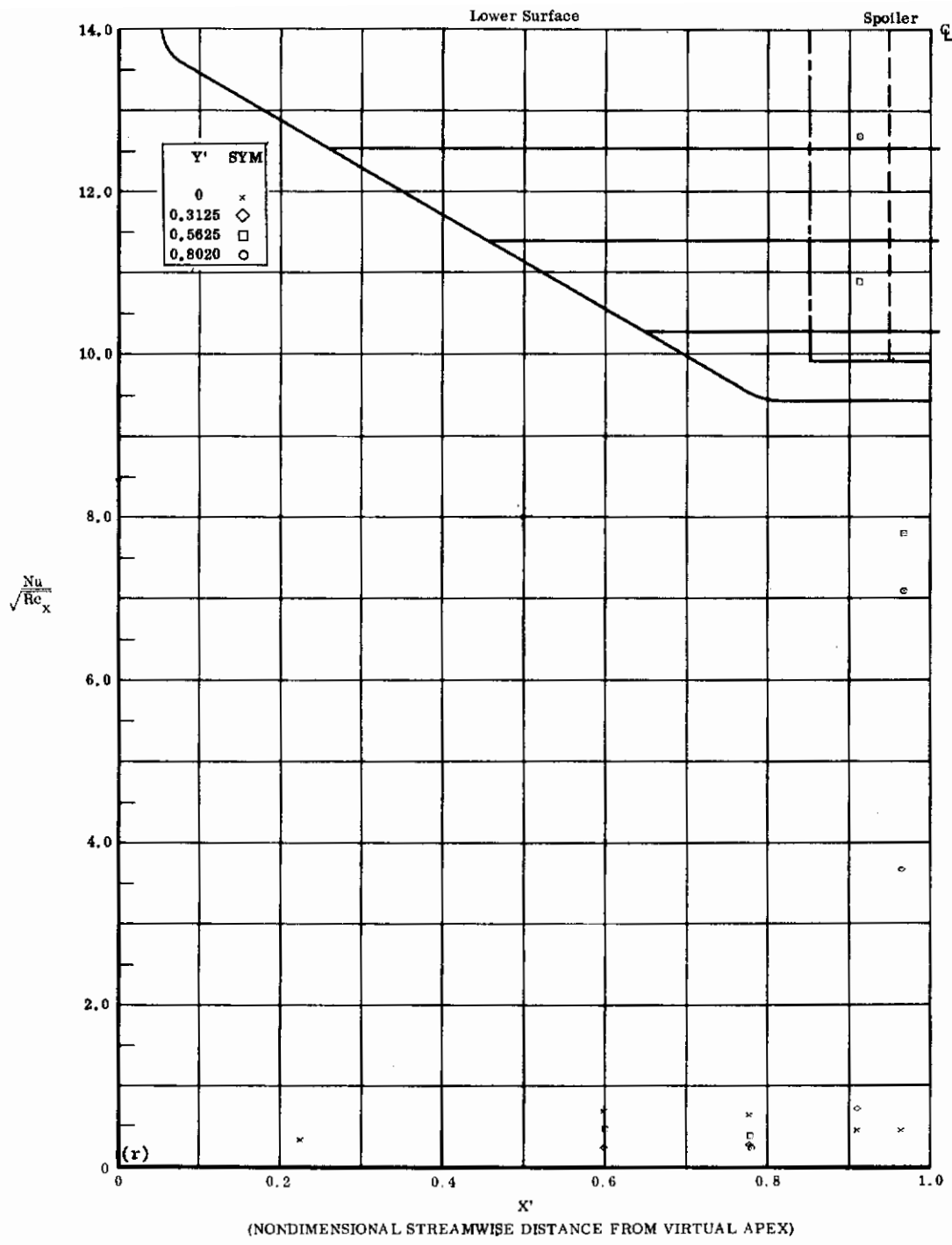


Fig. 37r Configuration IX, $\alpha = 0$, $\delta_2 = \delta_3 = +39$
 $\text{Nu}/\sqrt{\text{Re}_x}$ vs. X' lower surface $\text{Re}_\infty/\text{ft} \times 10^{-6} = 1.1$

Contrails

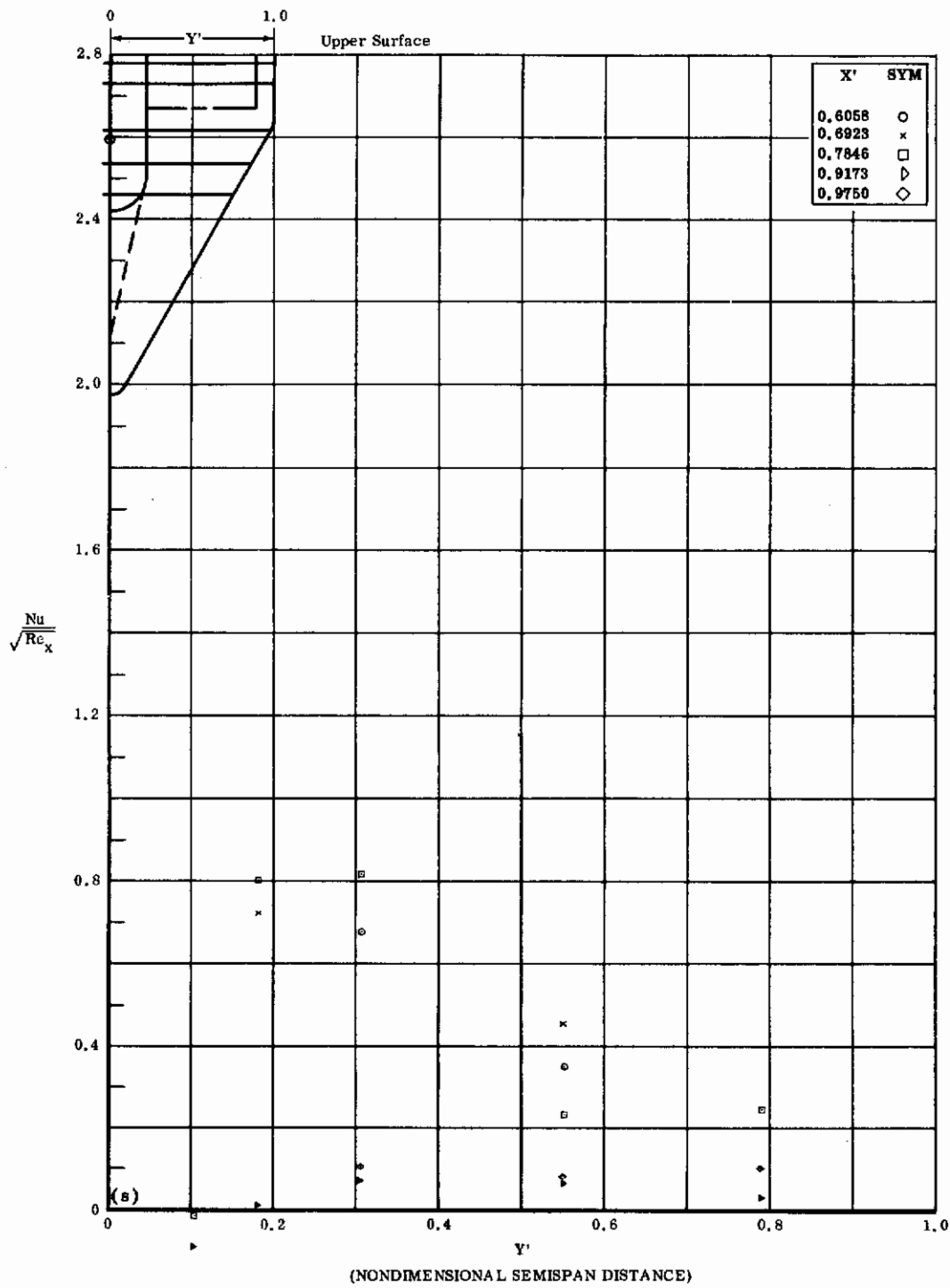


Fig. 37s Configuration IX, $\alpha = 0$, $\delta_2 = \delta_3 = +39$
 $Nu/\sqrt{Re_x}$ vs. Y' upper surface $Re_\infty/ft \times 10^{-6} = 1.1$

Contrails

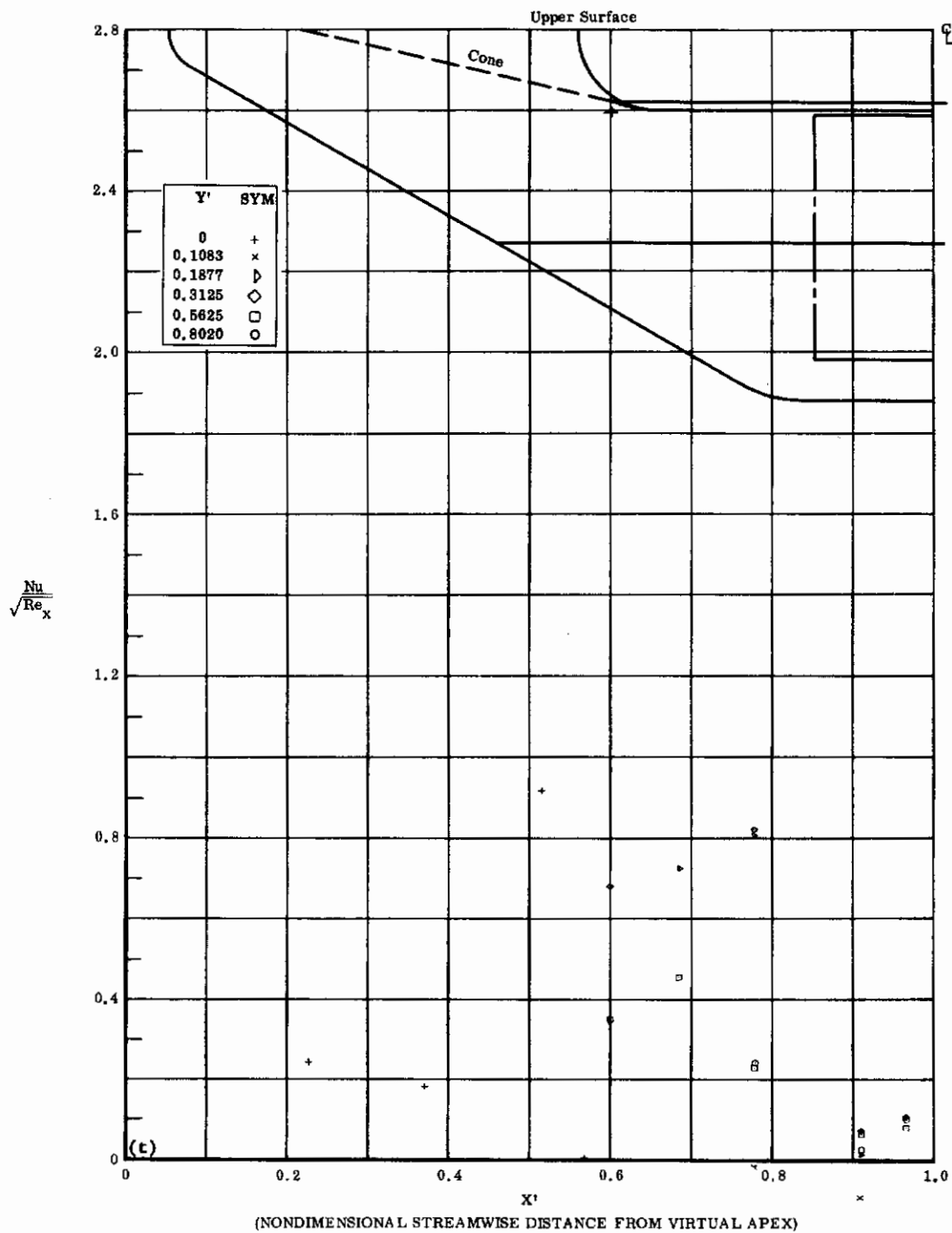


Fig. 37t Configuration IX, $\alpha = 0$, $\delta_2 = \delta_3 = +39$

$Nu/\sqrt{Re_x}$ vs. X' upper surface $Re_\infty/ft \times 10^{-6} = 1.1$

Contrails

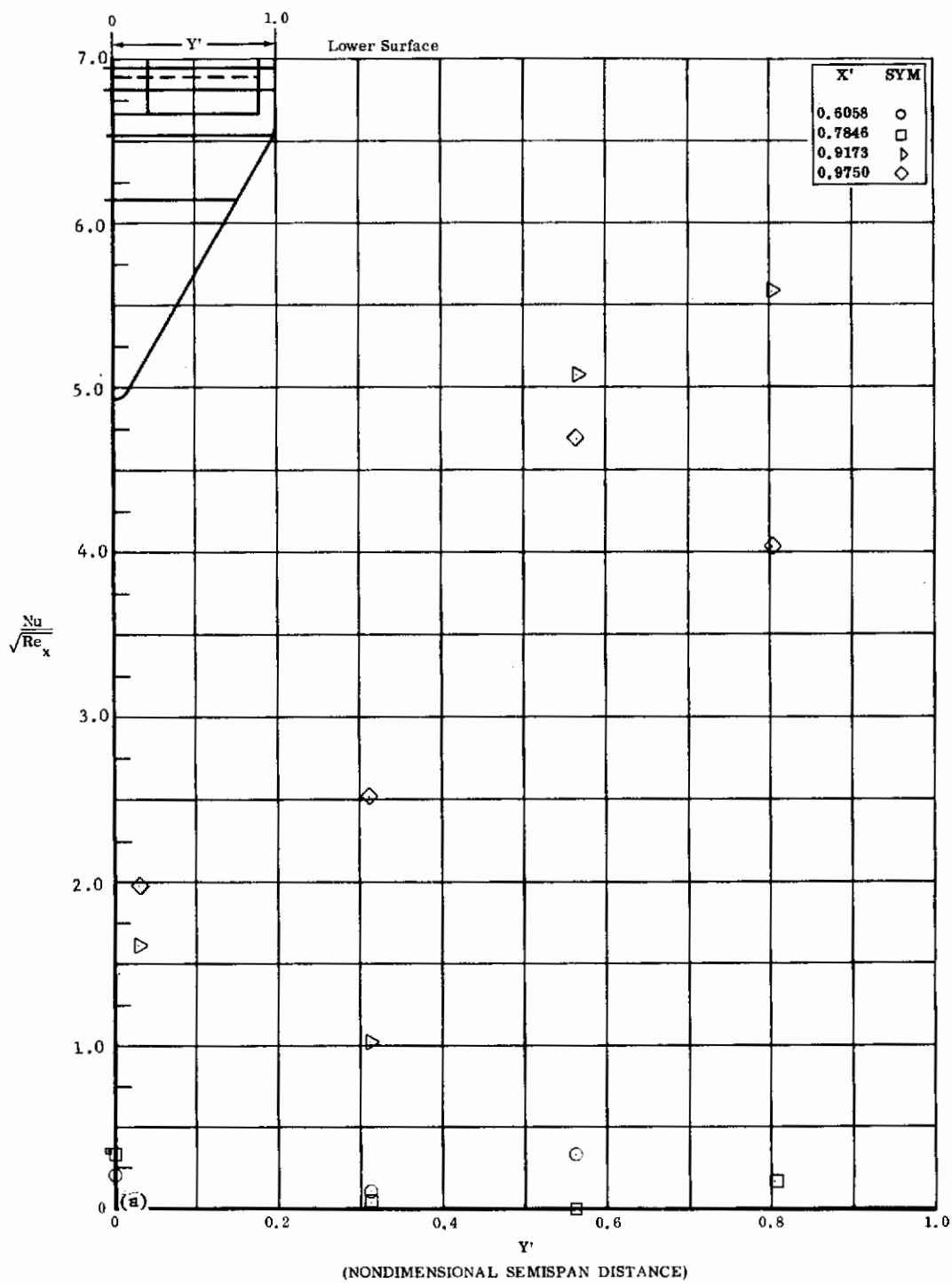


Fig. 38a Configuration X, $\alpha = 0$, $b_1 = b_2 = b_3 = +20$, $Re_\infty/\text{ft} \times 10^{-6} = 3.3$
 $Nu/\sqrt{Re_x}$ vs. Y' lower surface

Contrails

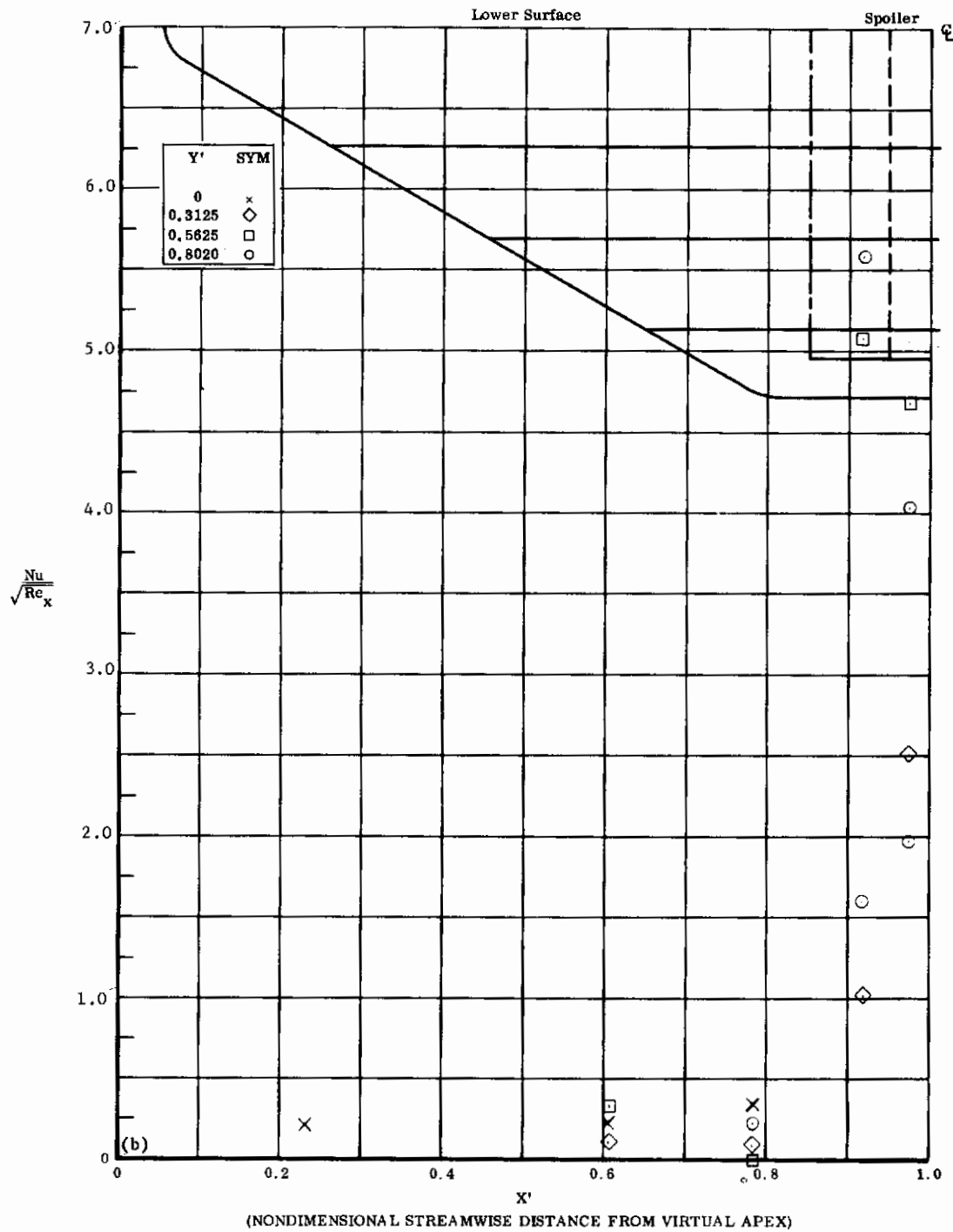


Fig. 38b Configuration X, $\alpha = 0$, $\delta_1 = \delta_2 = \delta_3 = +20$, $\text{Re}_{\infty}/ft \times 10^{-6} = 3.3$
 $\text{Nu}/\sqrt{\text{Re}_x}$ vs. X' lower surface

Contrails

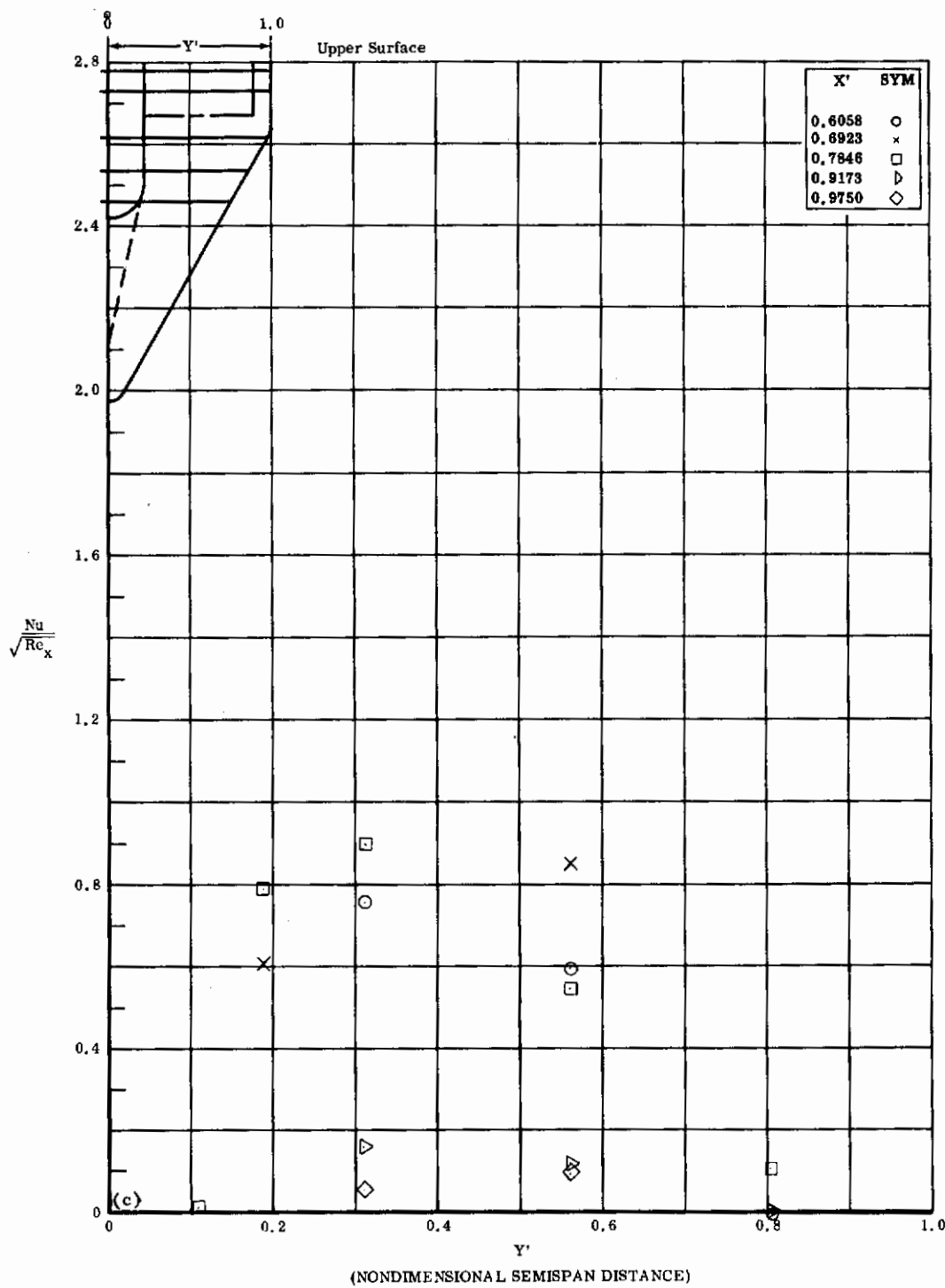


Fig. 38c Configuration X, $\alpha = 0$, $\delta_1 = \delta_2 = \delta_3 = +20$, $Re_\infty / ft \times 10^{-6} = 3.3$
 $Nu/\sqrt{Re_x}$ vs. Y' upper surface

Contrails

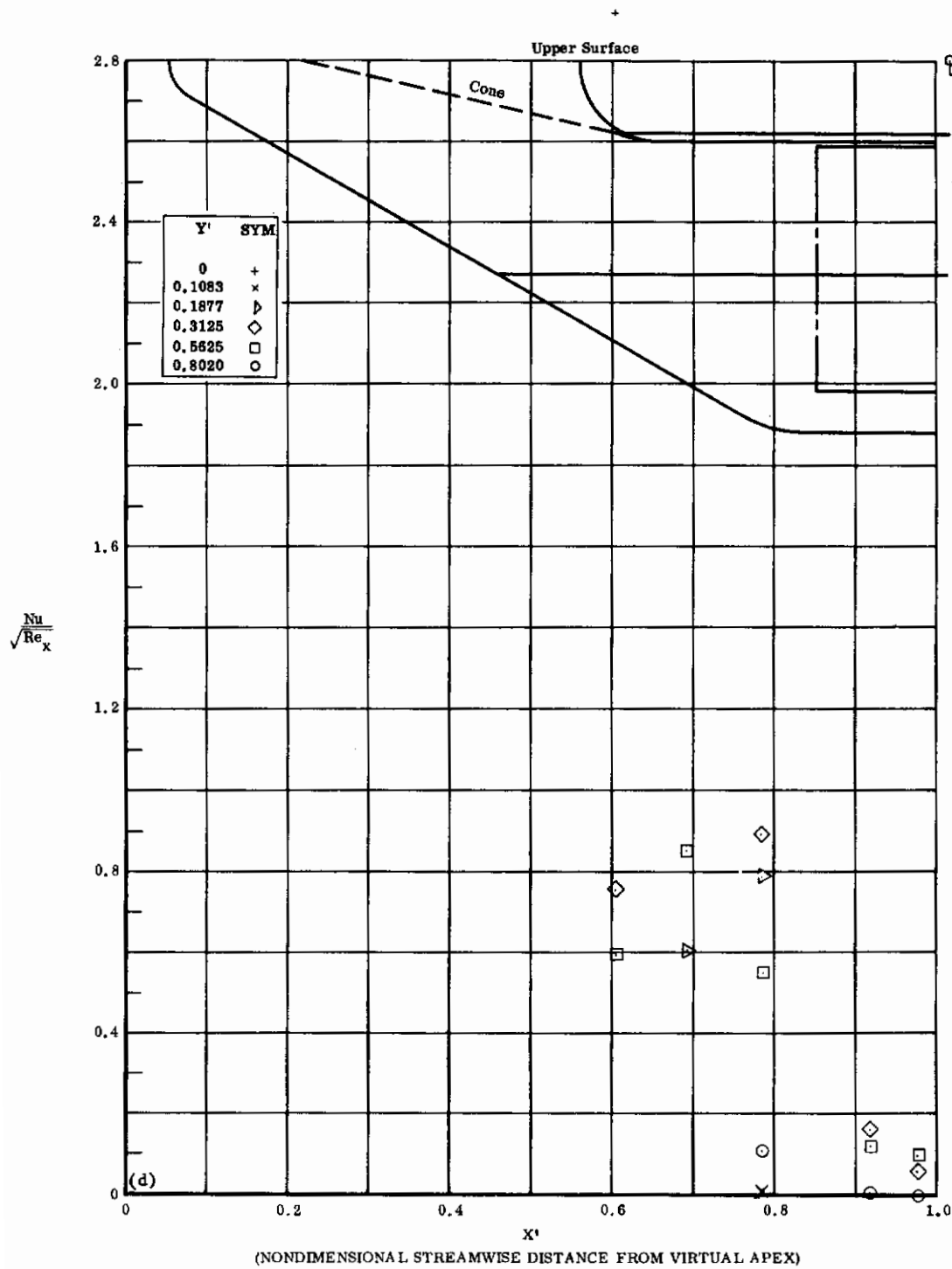


Fig. 38d Configuration X, $\alpha = 0$, $b_1 = b_2 = b_3 = +20$, $\text{Re}_{\infty}/\text{ft} \times 10^{-6} = 3.3$
 $\text{Nu}/\sqrt{\text{Re}_x}$ vs. X^* upper surface

Contrails

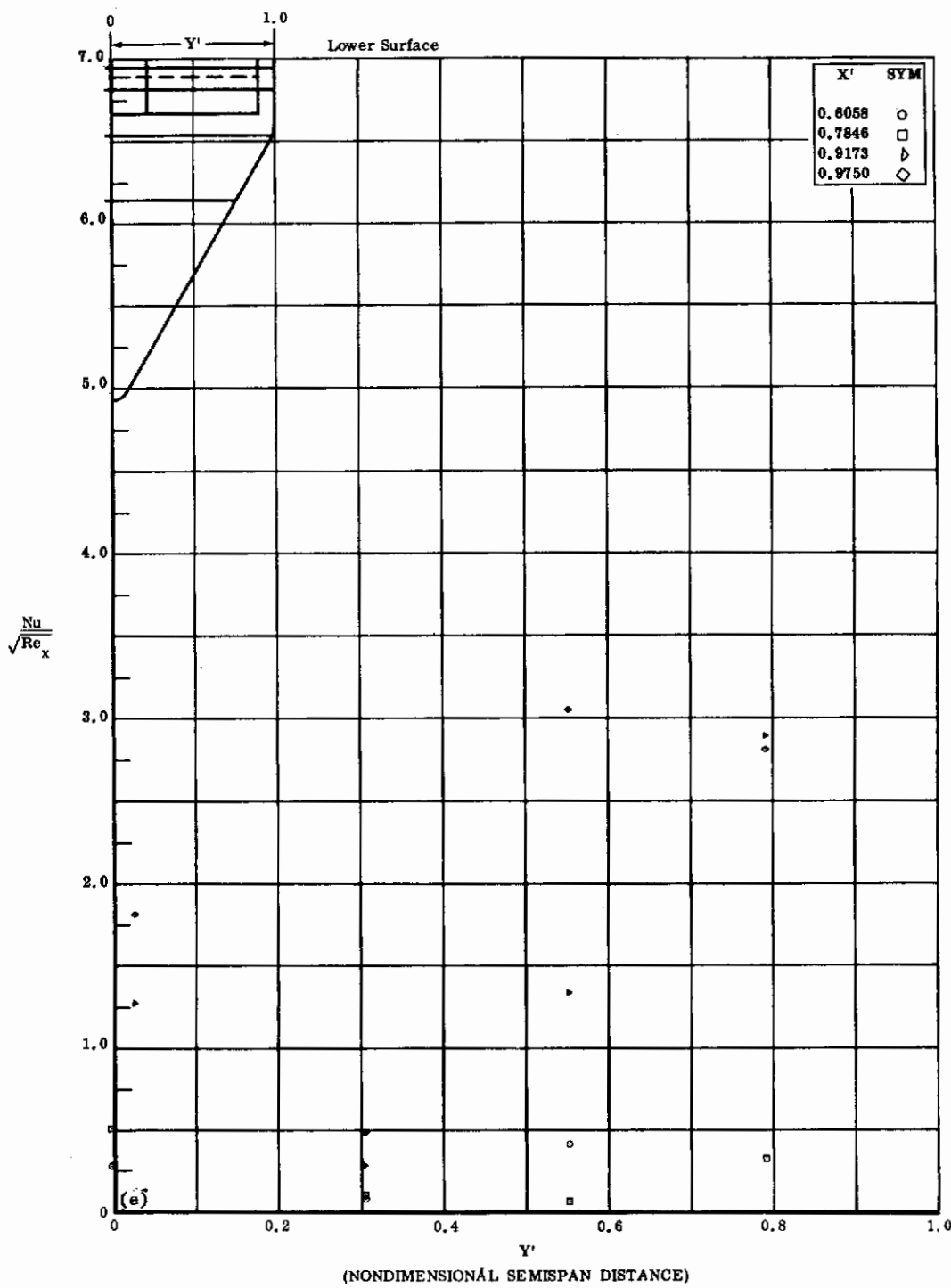


Fig. 38e Configuration X, $\alpha = 0$, $b_1 = b_2 = b_3 = +20$, $Re_\infty/\text{ft} \times 10^{-6} = 1.1$
 $\frac{Nu}{\sqrt{Re_x}}$ vs. Y' lower surface

Contrails

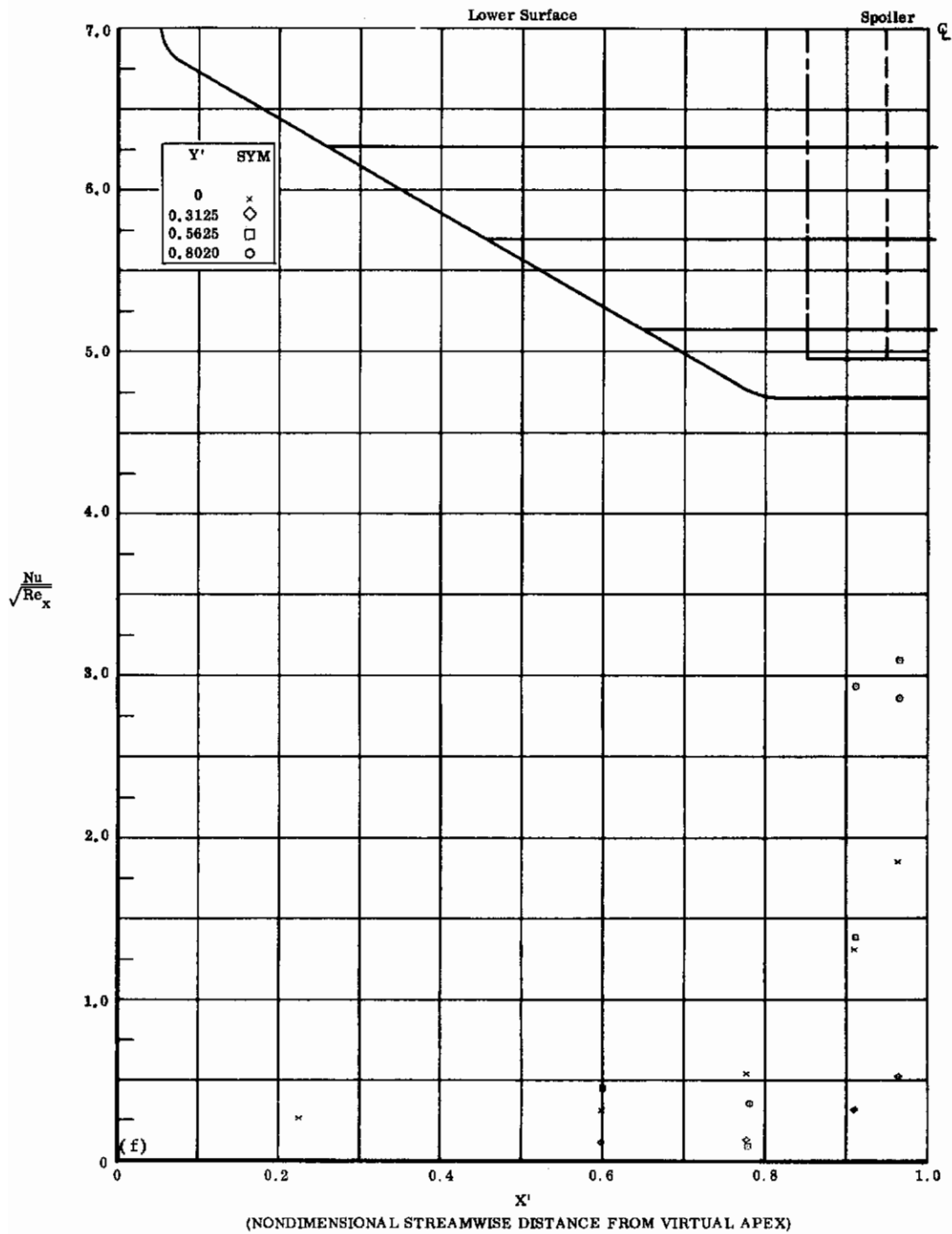


Fig. 38f Configuration X, $\alpha = 0$, $b_1 = b_2 = b_3 = +20$, $Re_\infty / \text{ft} \times 10^{-6} = 1.1$
 $Nu/\sqrt{Re_x}$ vs. X' lower surface

Contrails

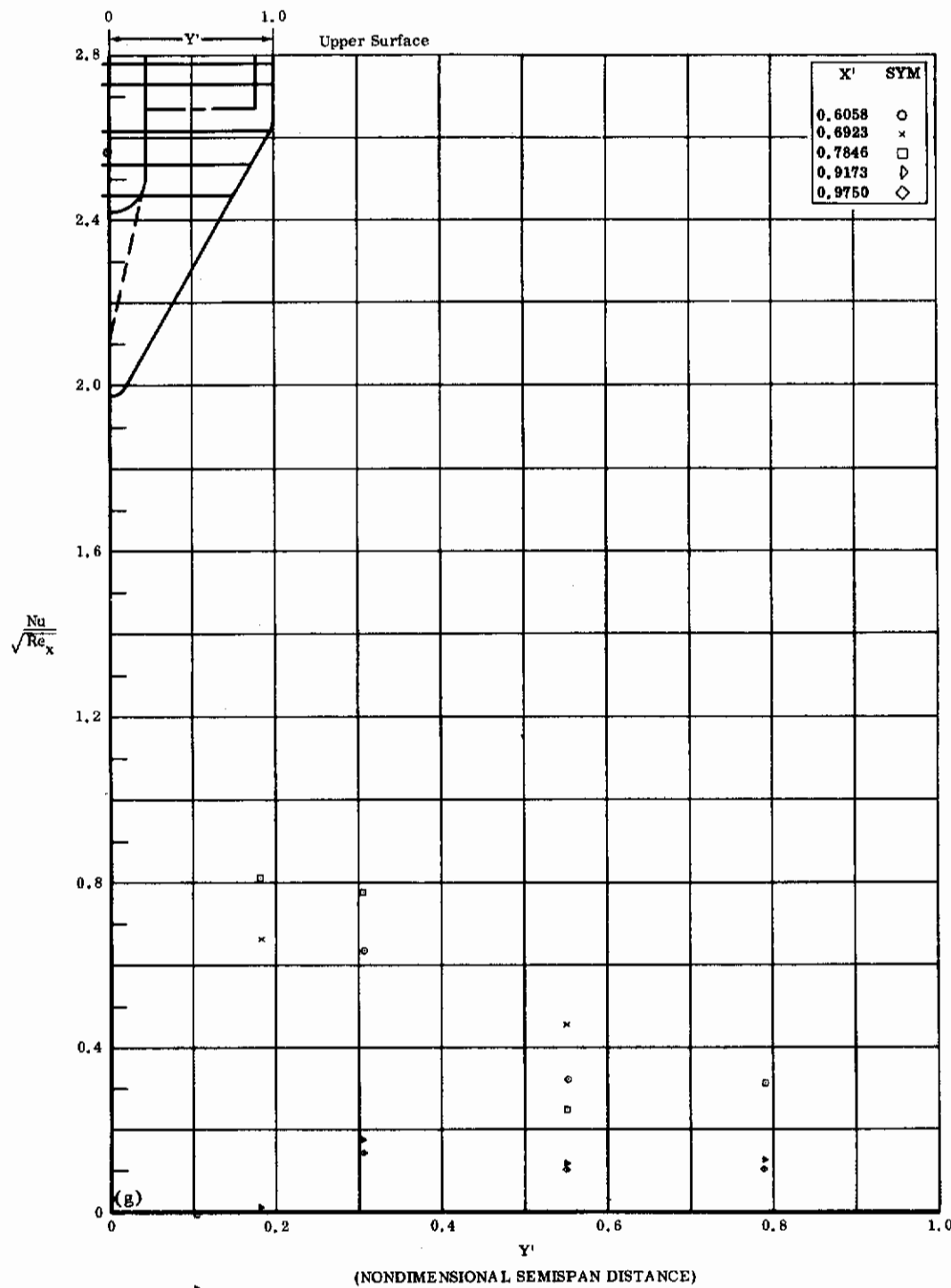


Fig. 38g Configuration X, $\alpha = 0$, $\delta_1 = \delta_2 = \delta_3 = +20$, $Re_\infty / ft \times 10^{-6} = 1.1$
 $Nu/\sqrt{Re_x}$ vs. Y' upper surface

Contrails

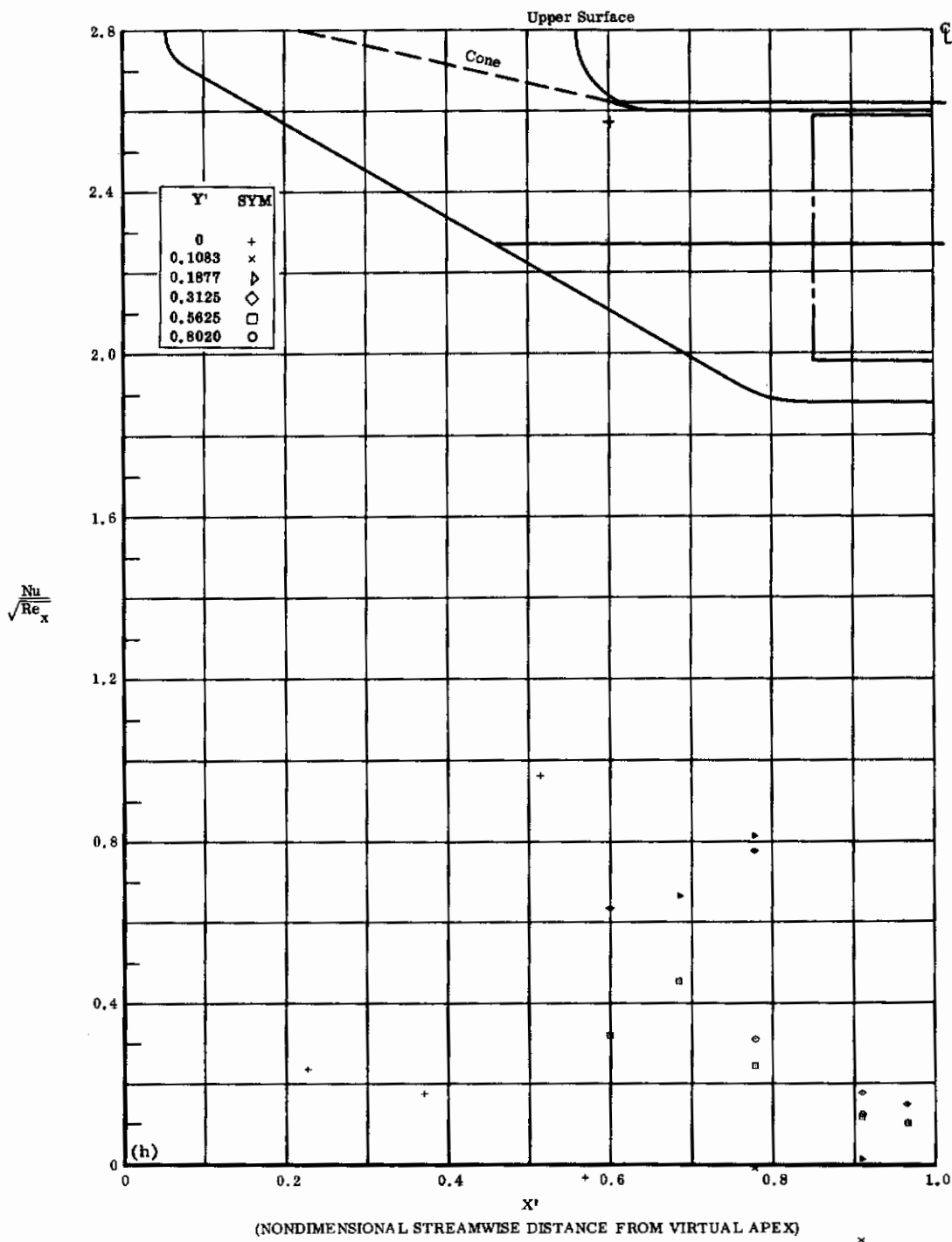


Fig. 38h Configuration X, $\alpha = 0$, $\delta_1 = \delta_2 = \delta_3 = +20$, $Re_\infty/\text{ft} \times 10^{-6} = 1.1$
 $Nu/\sqrt{Re_x}$ vs. X' upper surface

Contrails

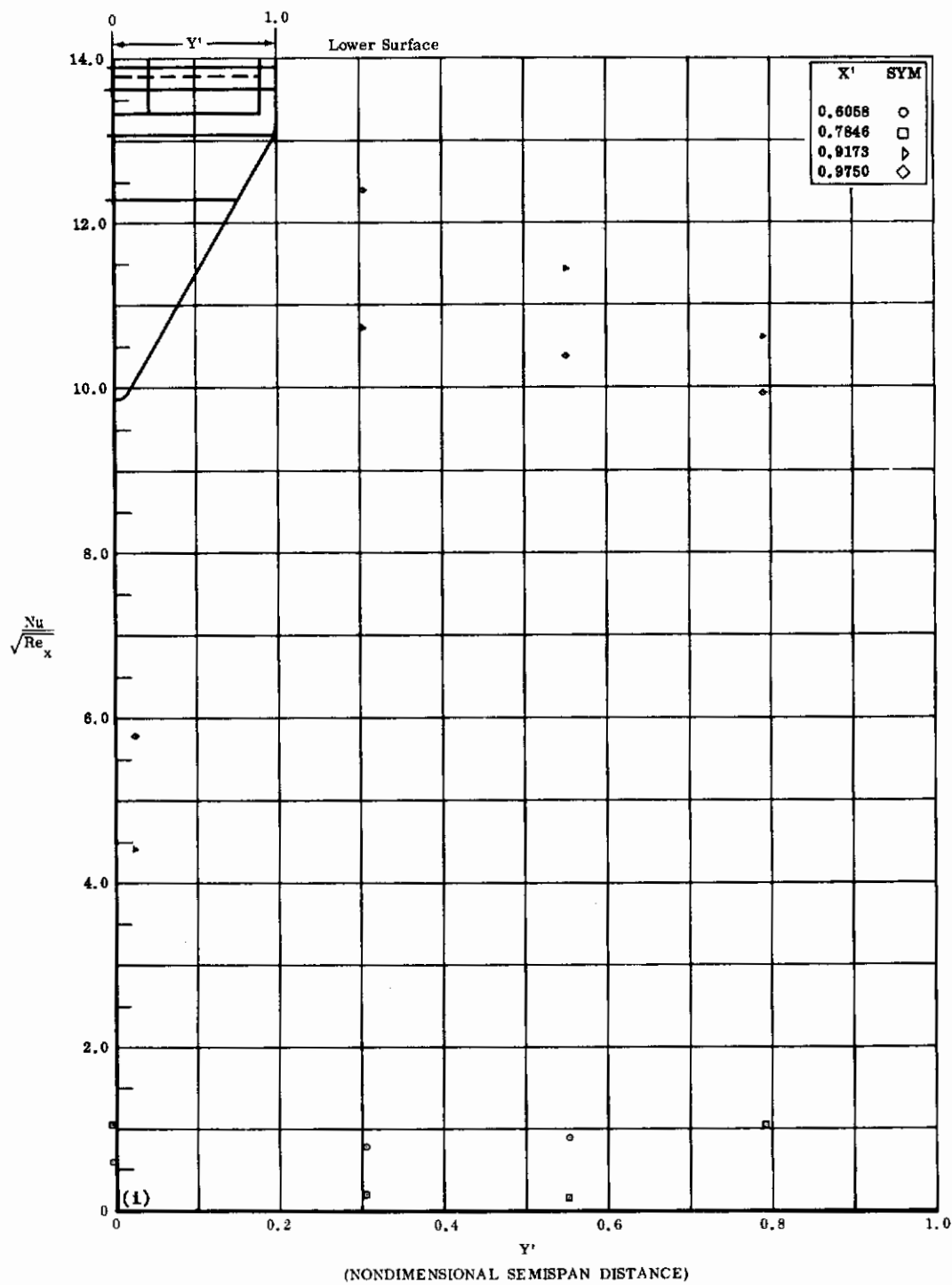


Fig. 38i Configuration X, $\alpha = +10$, $\delta_1 = \delta_2 = \delta_3 = +20$, $Re_\infty / ft \times 10^{-6} = 3.3$
 $Nu/\sqrt{Re_x}$ vs. Y' lower surface

Contrails

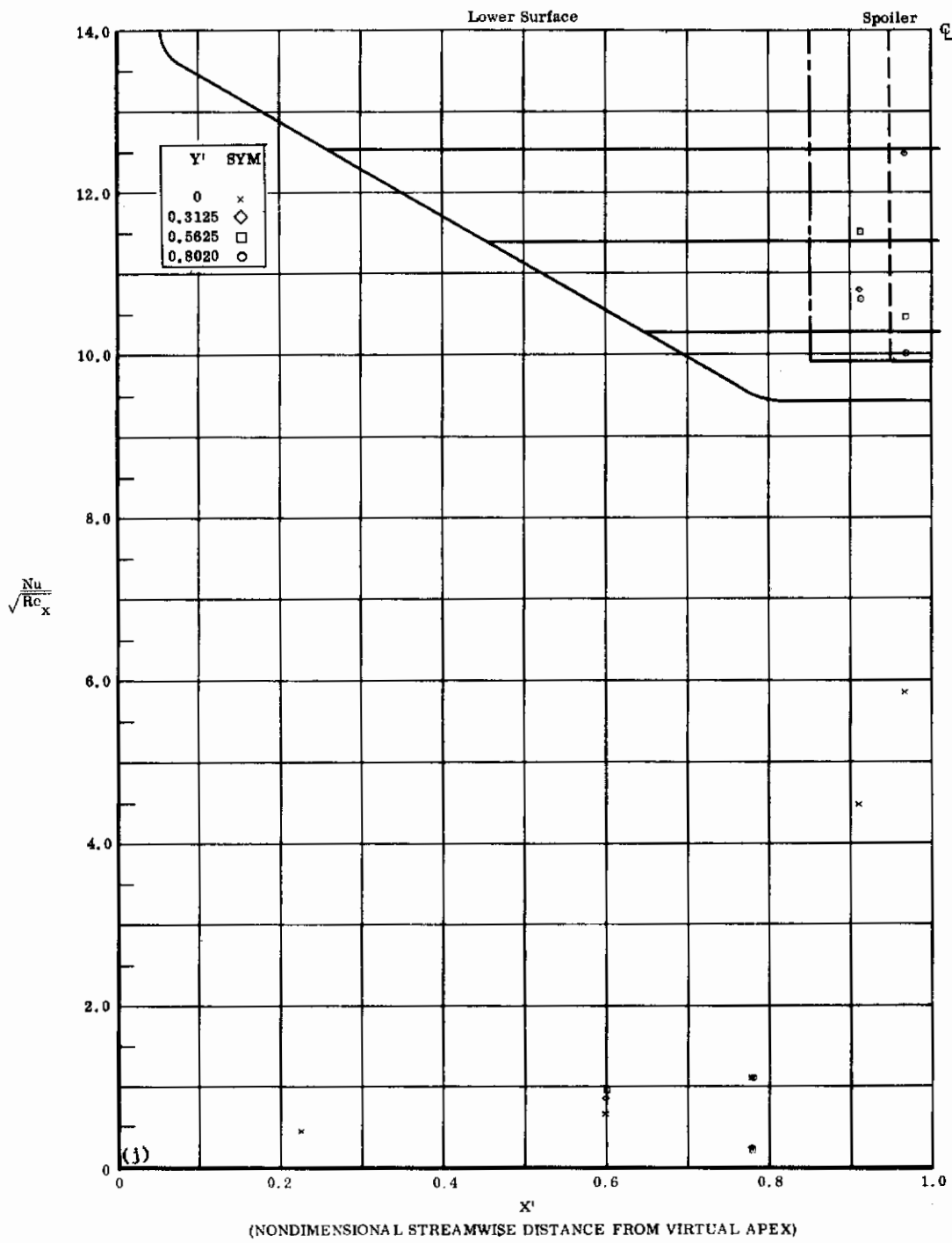


Fig. 38j Configuration X, $\alpha = +10$, $\delta_1 = \delta_2 = \delta_3 = +20$, $\text{Re}_{\infty}/\text{ft} \times 10^{-6} = 3.3$
 $\text{Nu}/\sqrt{\text{Re}_x}$ vs. X' lower surface

Contrails

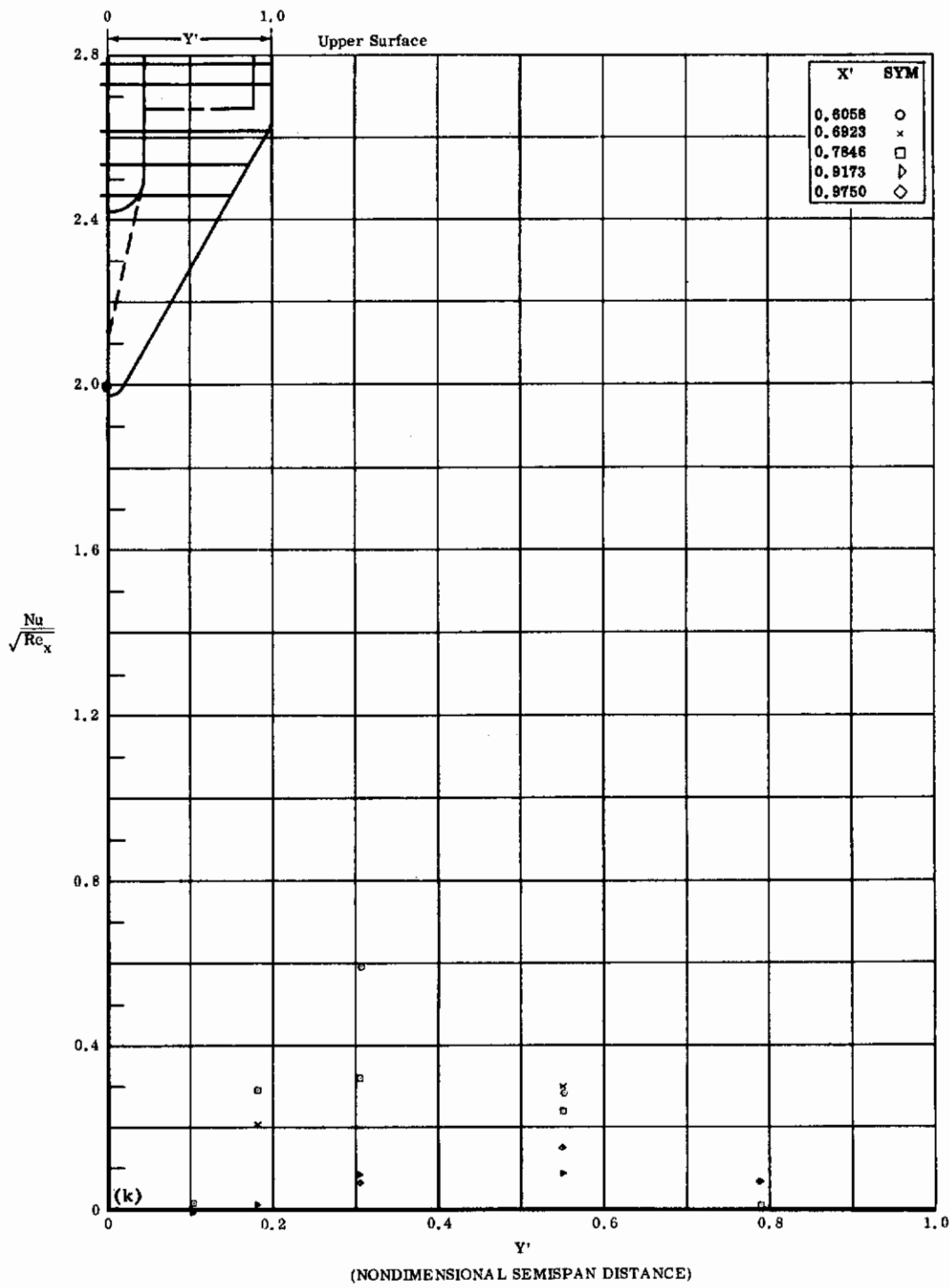


Fig. 38k Configuration X, $\alpha = +10$, $\delta_1 = \delta_2 = \delta_3 = +20$, $\text{Re}_{\infty}/\text{ft} \times 10^{-6} = 3.3$
 $\text{Nu}/\sqrt{\text{Re}_x}$ vs. Y' upper surface

Contrails

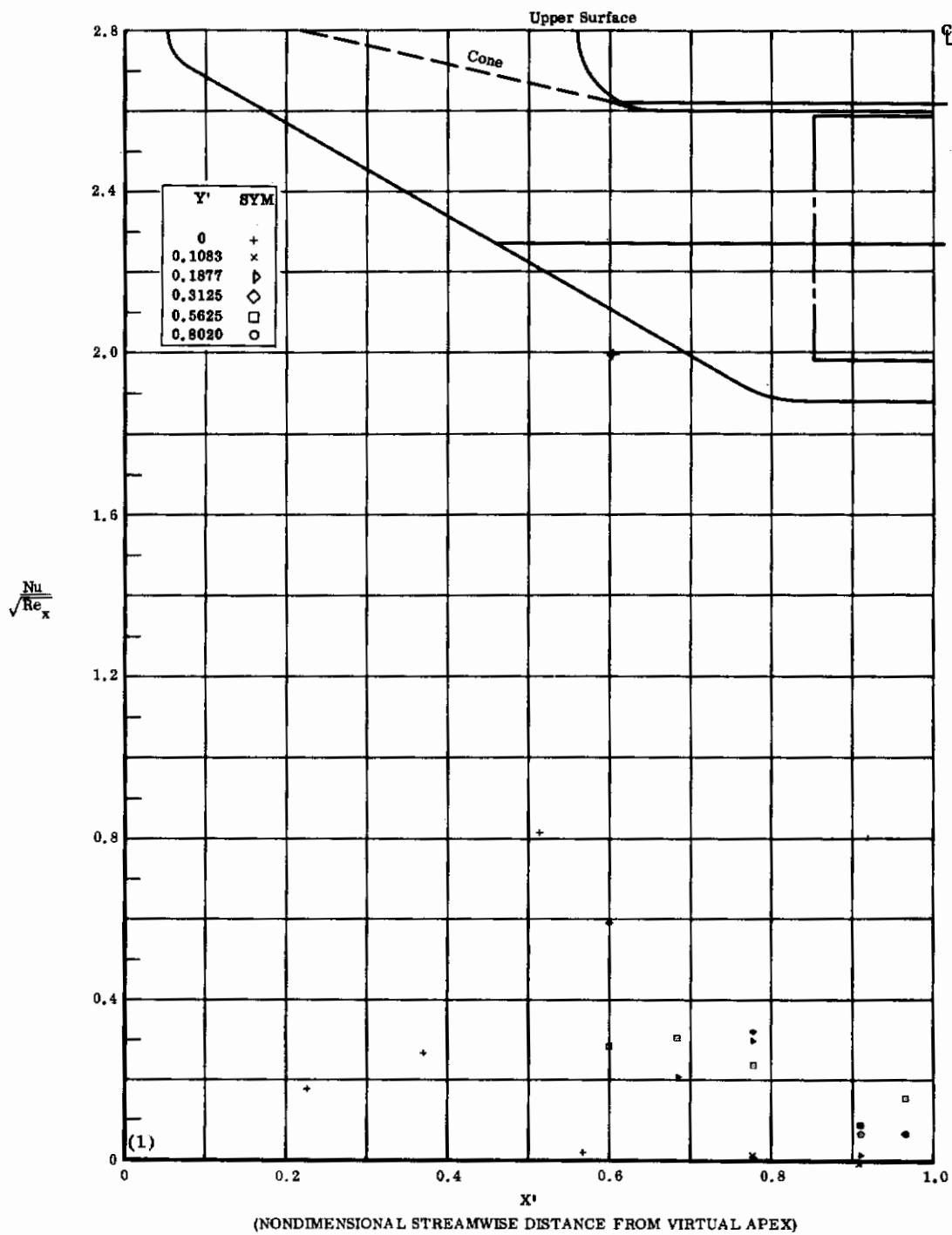


Fig. 38f Configuration X, $\alpha = +10$, $\delta_1 = \delta_2 = \delta_3 = +20$, $\text{Re}_{\infty}/\text{ft} \times 10^{-6} = 3.3$
 $\text{Nu}/\sqrt{\text{Re}_x}$ vs. X' upper surface

Contrails

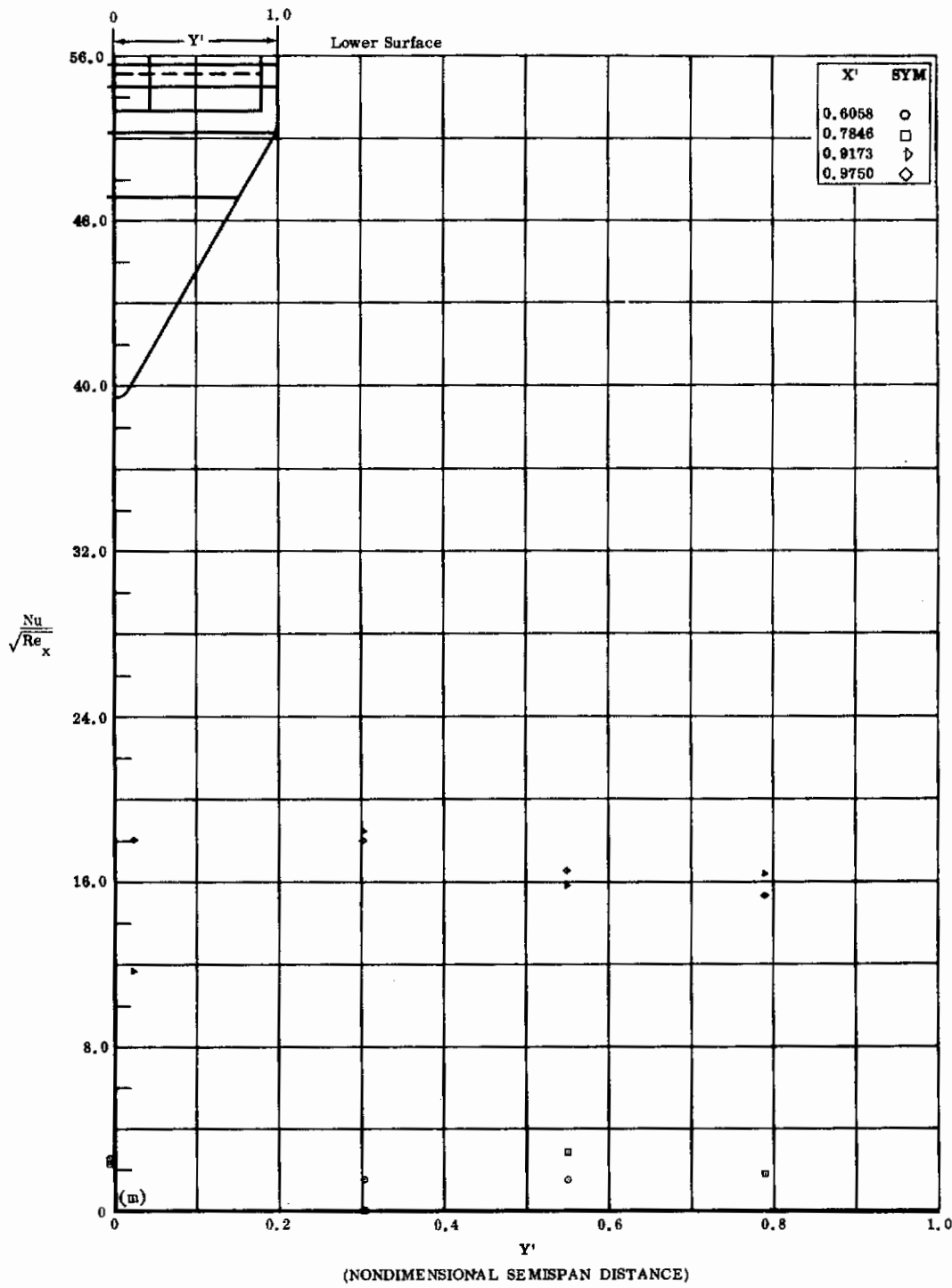


Fig. 38m Configuration X, $\alpha = +20$, $s_1 = s_2 = s_3 = +20$, $Re_\infty / \text{ft} \times 10^{-6} = 3.3$
 $Nu/\sqrt{Re_x}$ vs. Y' lower surface

Contrails

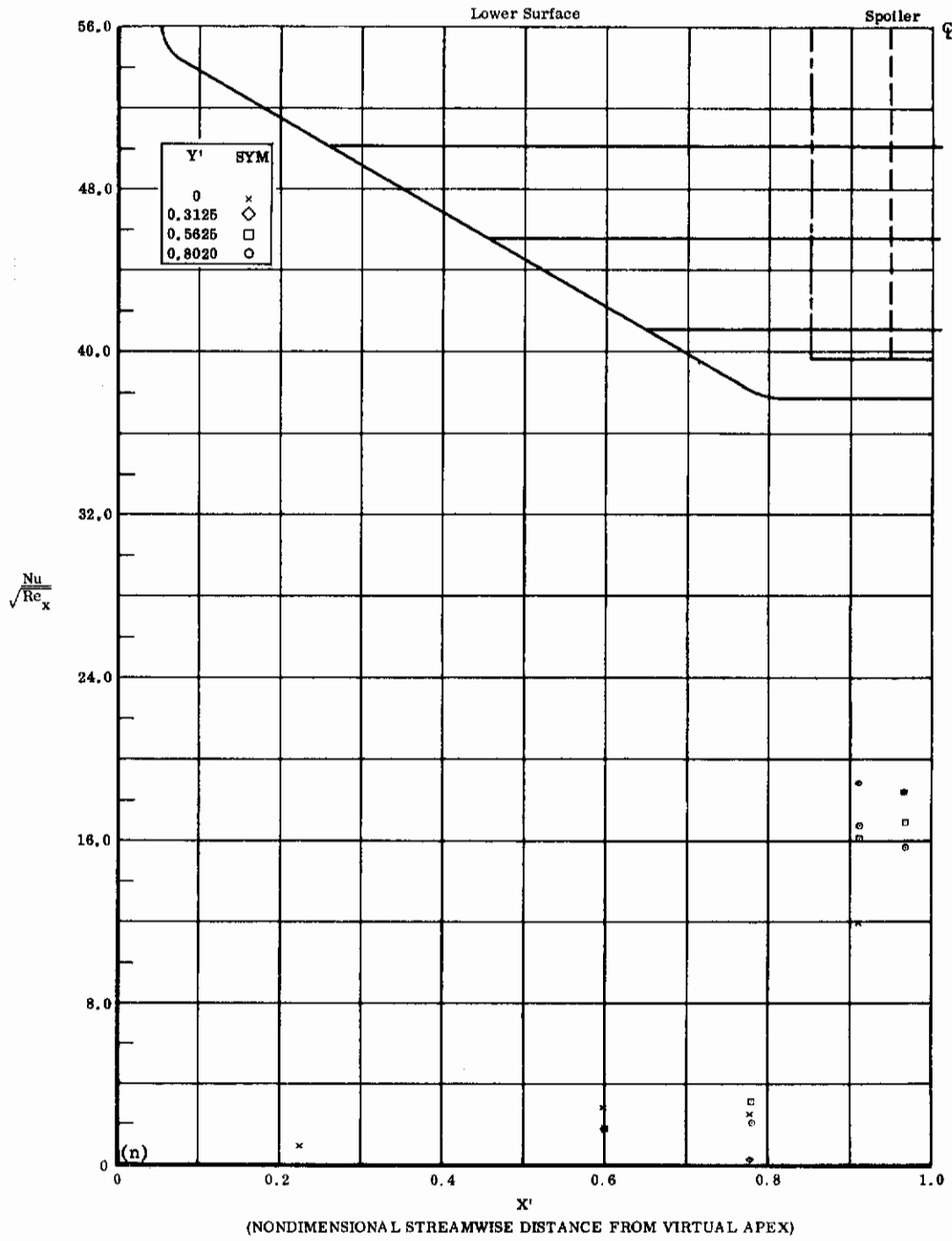


Fig. 38n Configuration X, $\alpha = +20^\circ$, $s_1 = s_2 = s_3 = +20^\circ$, $Re_\infty/\text{ft} \times 10^{-6} = 3.3$
 $\frac{Nu}{\sqrt{Re_x}}$ vs. X' lower surface

Contrails

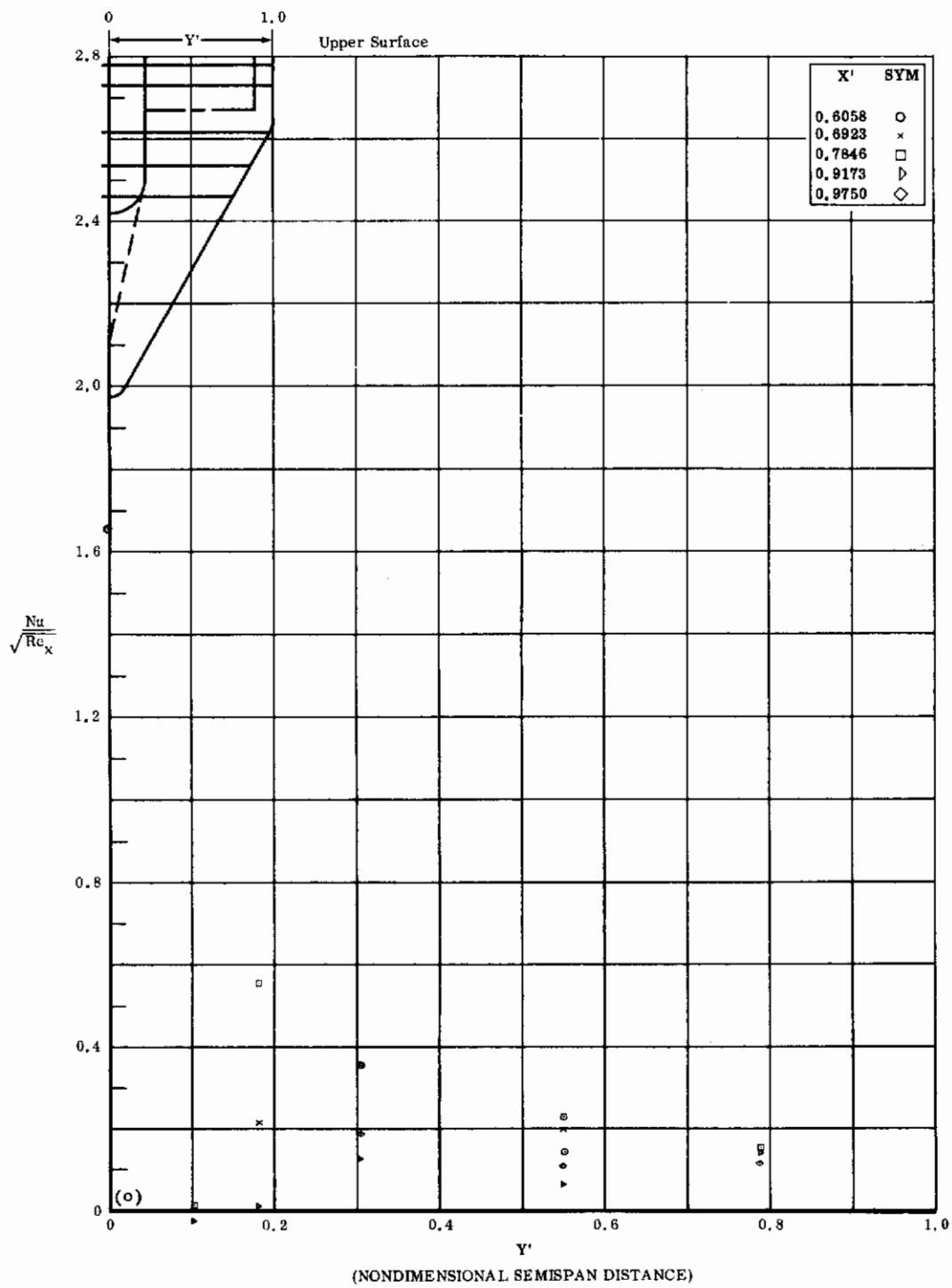


Fig. 38o Configuration X, $\alpha = +20$, $\delta_1 = \delta_2 = \delta_3 = +20$, $Re_\infty/\text{ft} \times 10^{-6} = 3.3$
 $Nu/\sqrt{Re_x}$ vs. Y' upper surface

Contrails

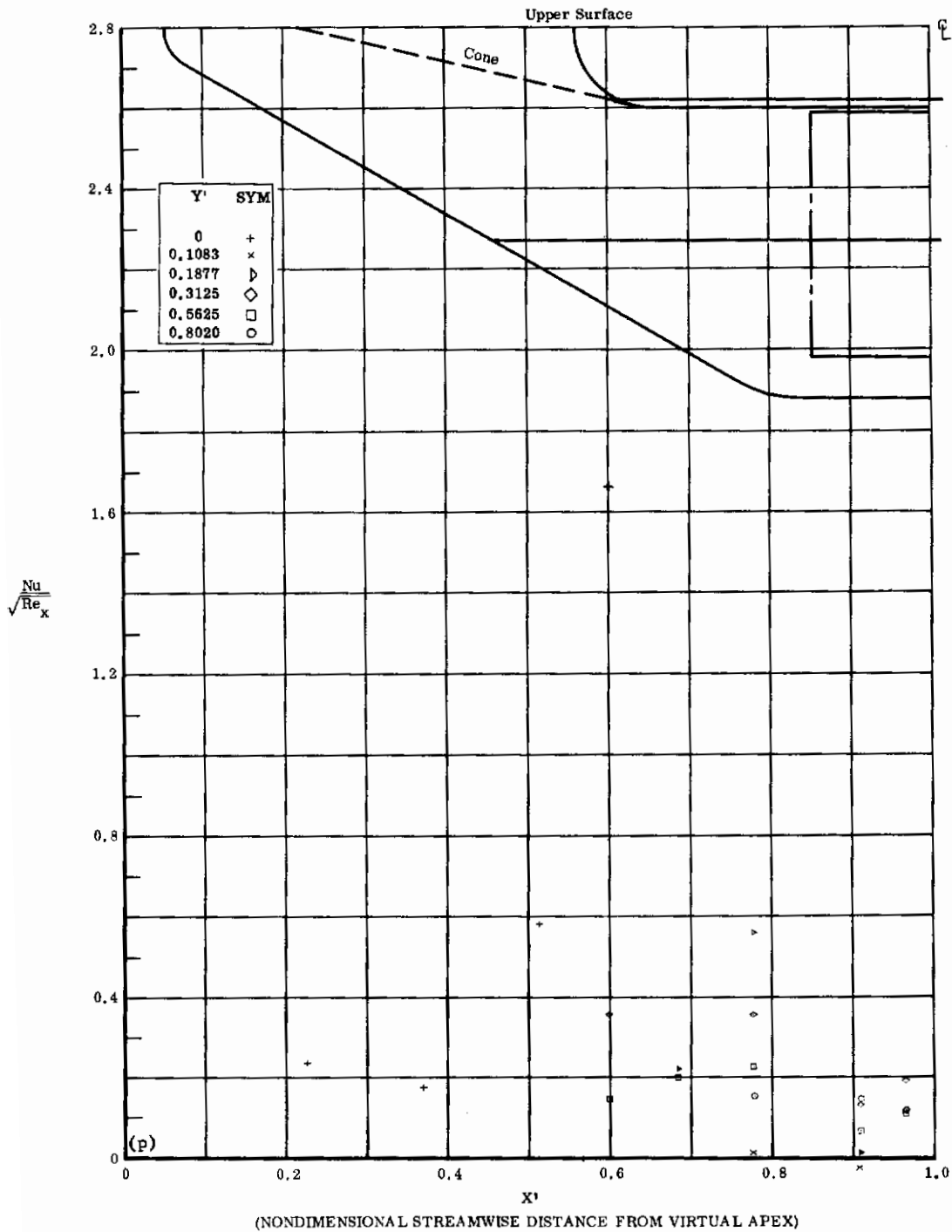


Fig. 38p Configuration X, $\alpha = +20^\circ$, $\delta_1 = \delta_2 = \delta_3 = +20^\circ$, $Re_\infty / ft \times 10^{-6} = 3,3$
 $Nu/\sqrt{Re_x}$ vs. X' upper surface

Contracts